

Advances

in Clinical and Experimental Medicine

MONTHLY ISSN 1899-5276 (PRINT) ISSN 2451-2680 (ONLINE)

advances.umw.edu.pl

2025, Vol. 34, No. 12 (December)

Impact Factor (IF) – 1.9
Ministry of Science and Higher Education – 70 pts
Index Copernicus (ICV) – 161.00 pts



WROCLAW
MEDICAL UNIVERSITY

Advances
in Clinical and Experimental
Medicine



Advances in Clinical and Experimental Medicine

ISSN 1899-5276 (PRINT)

ISSN 2451-2680 (ONLINE)

advances.umw.edu.pl

MONTHLY 2025
Vol. 34, No. 12
(December)

Advances in Clinical and Experimental Medicine (*Adv Clin Exp Med*) publishes high-quality original articles, research-in-progress, research letters and systematic reviews and meta-analyses of recognized scientists that deal with all clinical and experimental medicine.

Editorial Office

ul. Marcinkowskiego 2–6
50-368 Wrocław, Poland
Tel.: +48 71 784 12 05
E-mail: redakcja@umw.edu.pl

Editor-in-Chief

Prof. Donata Kurpas

Deputy Editor

Prof. Robert Śmigiel

Managing Editor

Marek Misiak, MA

Statistical Editors

Wojciech Bombała, MSc
Assoc. Prof. Andrzej Paweł
Karpiński
Anna Kopszak, MSc
Dr. Krzysztof Kujawa
Prof. Łukasz Łaczmański

Jakub Wronowicz, MSc
Maciej Wuczyński, MSc

Manuscript editing

Marek Misiak, MA
Paulina Piątkowska, MA

Publisher

Wrocław Medical University
Wybrzeże L. Pasteura 1
50-367 Wrocław, Poland

Online edition is the original version
of the journal

Scientific Committee

Prof. Sabine Bährer-Kohler
Prof. Sandra Maria Barbalho
Prof. Antonio Cano
Prof. Chong Chen
Prof. Breno Diniz
Prof. Erwan Donal
Prof. Chris Fox
Prof. Yuko Hakamata
Prof. Carol Holland

Prof. Markku Kurkinen
Prof. Christopher S. Lee
Prof. Christos Lionis
Prof. Leszek Lisowski
Prof. Raimundo Mateos
Prof. Zbigniew W. Raś
Prof. Dorota Religa
Prof. Jerzy W. Rozenblit
Prof. Silvina Santana

Prof. Sajee Sattayut
Prof. Barbara Schneider
Prof. James Sharman
Prof. Jamil Shibli
Prof. Luca Testarelli
Prof. Michał J. Toborek
Prof. László Vécsei
Prof. Cristiana Vitale
Prof. Ming Yi
Prof. Hao Zhang

Section Editors

Basic Sciences

Prof. Iwona Bil-Lula
Prof. Dorota Danuta Diakowska
Prof. Bartosz Kempisty
Dr. Wiesława Kranc
Dr. Anna Lebedeva
Dr. Piotr Chmielewski
Dr. Phuc Van Pham
Dr. Sławomir Woźniak

Clinical Anatomy, Legal Medicine, Innovative Technologies

Prof. Rafael Boscolo-Berto

Dentistry

Prof. Marzena Dominiak
Prof. Tomasz Gedrange

Prof. Jamil Shibli

Prof. Luca Testarelli

Laser Dentistry

Prof. Kinga Grzech-Leśniak

Dermatology

Prof. Jacek Szepietowski
Assoc. Prof. Marek Konop

Emergency Medicine, Innovative Technologies

Prof. Jacek Smereka

Evidence-Based Healthcare

Assoc. Prof. Aleksandra Królikowska
Dr. Robert Prill

Gynecology and Obstetrics

Assoc. Prof. Tomasz Fuchs
Dr. Christopher Kobierzycki
Dr. Jakub Staniczek

Histology and Embryology

Dr. Mateusz Olbromski

Internal Medicine

Angiology

Dr. Angelika Chachaj

Cardiology

Dr. Daniel Morris
Assoc. Prof. Joanna Popiołek-Kalisz
Prof. Pierre François Sabouret

Endocrinology

Prof. Marek Bolanowski
Assoc. Prof. Agnieszka Zubkiewicz-Kucharska

Gastroenterology

Dr. Anna Kofla-Dłubacz
Assoc. Prof. Katarzyna Neubauer

Hematology

Prof. Andrzej Deptała
Prof. Dariusz Wołowicz

Nephrology and Transplantology

Prof. Mirosław Banasik
Prof. Krzysztof Letachowicz
Assoc. Prof. Tomasz Gołębiowski

Rheumatology

Assoc. Prof. Agata Sebastian
Dr. Sylwia Szafraniec-Buryło

Lifestyle Medicine, Nutrition and Health Promotion

Assoc. Prof. Michał Czapla
Prof. Raúl Juárez-Vela
Dr. Anthony Dissen

Microbiology

Dr. Malwina Brożyna
Assoc. Prof. Adam Junka

Molecular Biology

Dr. Monika Bielecka
Prof. Dorota Danuta Diakowska
Dr. Phuc Van Pham

Neurology

Assoc. Prof. Magdalena Koszewicz
Dr. Nasrollah Moradikor
Assoc. Prof. Anna Pokryszko-Dragan
Dr. Masaru Tanaka

Neuroscience

Dr. Simone Battaglia
Dr. Francesco Di Gregorio
Dr. Nasrollah Moradikor

Omics, Bioinformatics and Genetics

Assoc. Prof. Izabela Łaczmarska
Prof. Łukasz Łaczmarski
Prof. Mariusz Fleszar
Assoc. Prof. Paweł Andrzej Karpiński

Oncology

Prof. Andrzej Deptała
Prof. Adam Maciejczyk
Prof. Hao Zhang

Gynecological Oncology

Dr. Marcin Jędryka

Ophthalmology

Dr. Małgorzata Gajdzis
Prof. Marta Misiuk-Hojło

Orthopedics

Prof. Paweł Reichert

Otolaryngology

Prof. Tomasz Zatoński

Pediatrics

Pediatrics, Metabolic Pediatrics, Clinical Genetics, Neonatology, Rare Disorders

Dr. Anna Kofla-Dłubacz
Prof. Robert Śmigiel

Pediatric Nephrology

Prof. Katarzyna Kiliś-Pstrusińska

Pediatric Oncology and Hematology

Assoc. Prof. Marek Ussowicz

Pharmaceutical Sciences

Assoc. Prof. Marta Kepinska
Prof. Adam Matkowski

Pharmacoeconomics

Dr. Sylwia Szafraniec-Buryło

Psychiatry

Dr. Melike Küçükrapınar
Prof. Jerzy Leszek
Assoc. Prof. Bartłomiej Stańczykiewicz

Public Health

Prof. Monika Sawhney
Prof. Izabella Uchmanowicz

Pulmonology

Prof. Anna Brzecka

Qualitative Studies, Quality of Care

Prof. Ludmiła Marcinowicz
Assoc. Prof. Anna Rozensztrauch

Radiology

Prof. Paweł Gać

Rehabilitation

Assoc. Prof. Aleksandra Królikowska
Dr. Robert Prill

Surgery

Assoc. Prof. Mariusz Chabowski

Telemedicine, Geriatrics, Multimorbidity

Assoc. Prof. Maria Magdalena
Bujnowska-Fedak
Prof. Ferdinando Petrazzuoli

Editorial Policy

Advances in Clinical and Experimental Medicine (Adv Clin Exp Med) is an independent multidisciplinary forum for exchange of scientific and clinical information, publishing original research and news encompassing all aspects of medicine, including molecular biology, biochemistry, genetics, biotechnology and other areas. During the review process, the Editorial Board conforms to the "Uniform Requirements for Manuscripts Submitted to Biomedical Journals: Writing and Editing for Biomedical Publication" approved by the International Committee of Medical Journal Editors (www.ICMJE.org). The journal publishes (in English only) original papers and reviews. Short works considered original, novel and significant are given priority. Experimental studies must include a statement that the experimental protocol and informed consent procedure were in compliance with the Helsinki Convention and were approved by an ethics committee.

For all subscription-related queries please contact our Editorial Office: redakcja@umw.edu.pl

For more information visit the journal's website: advances.umw.edu.pl

Pursuant to the ordinance of the Rector of Wrocław Medical University No. 37/XVI R/2024, from March 1, 2024, authors are required to pay a fee for each manuscript accepted for publication in the journal Advances in Clinical and Experimental Medicine. The fee amounts to 1600 EUR for all types of papers.

Indexed in: MEDLINE, Science Citation Index Expanded, Journal Citation Reports/Science Edition, Scopus, EMBASE/Excerpta Medica, Ulrich'sTM International Periodicals Directory, Index Copernicus

Typographic design: Piotr Gil, Monika Kołęda

DTP: Wydawnictwo UMW

Cover: Monika Kołęda

Printing and binding: Drukarnia I-BiS Bierorący Sp.k.

Contents

Editorials

- 1995 Sabine Bährer-Köhler
Access to services. Mental health in catastrophes and emergencies: Aspects
- 1999 Chong Chen, Shin Nakagawa
Recent advances in the study of perinatal mental health: Epidemiology, psychopathology and intervention
- 2005 Rafał Matkowski, Aleksandra Simiczyjew, Marcin Ziętek, Dorota Nowak
Stromal cells as a part of tumor microenvironment of melanoma: Their role in cancer progression and drug resistance
- 2011 Martyna Biała, Brygida Knysz
Community-acquired pneumonia in HIV-infected patients: Updated insights on epidemiology and etiology

Meta-analysis

- 2017 Zhenhao Fei, Xingfu Duan, Junhua Liang, Zhiwei Sun, Jianzhong Tang
Traumatic complications linked to prophylactic drain placement after hepatectomy: A meta-analysis
- 2025 Liang Zhang
Relative qualities of telerehabilitation compared to traditional in-person speech and language treatment for individuals with aphasia: A meta-analysis
- 2035 Xiang Wen, Fuliang Qi, Hailong Qian, Rancen Tao, Jie Li, Liang Wang
Effectiveness of sorafenib in combination with physical thermal ablation for hepatocellular carcinoma: A meta-analysis

Original papers

- 2045 Ju-Cun Huang, Yu-Wei Feng, Kang Zhao, Dan Dai
Revealing the causal relationship between HBV and HCV infection and liver cirrhosis by Mendelian randomization
- 2055 Yun Yang, Dan Li, Lu Sun, Shasha Liu
MALAT1 modulates granulosa cells ferroptosis and apoptosis through PAK2 upregulation in polycystic ovary syndrome
- 2067 Heng Zhang, Xiao Yang, Leilei Yuan, Haibo Zhao, Pei Jiang, Qing-Qing Yu
YOLO algorithm improves diagnostic performance of mammography: More than eyes
- 2077 Antonio Martínez-Sabater, Elena Chover-Sierra, Pablo Del Pozo-Herce, Alberto Tovar-Reinoso, Natalia Cano-Ruiz, Marta Araujo-Blesa, Javier Curto-Ramos, Gustavo Mora-Navarro, Raquel Martínez-Pascual, Raúl Juárez-Vela, Eva García Carpintero-Blas
Gender identity stories: Experiences and perspectives of transgender people about healthcare system in Spain
- 2091 Ewa Brzozowska, Wiesław Świętnicki, Jordan Sycz, Monika Kołodziejczak, Łukasz Stachowicz, Anna Wzorek, Agnieszka Korzeniowska-Kowal, Michał Skowicki, Tomasz Lipiński
Reconstruction of outer glycolipid synthesis pathways from *Porphyromonas gingivalis* in *Escherichia coli* for production of a vaccine candidate
- 2105 Łukasz Rogowski, Joanna Kowalska, Katarzyna Bulińska, Małgorzata Stefańska, Agnieszka Zembron-Łacny, Andrea Mahrová, Jitka Marenčáková, Weronika Pawlaczyk, Tomasz Gołębiowski, Witold Wnukiewicz, Mariusz Kusztal, Wioletta Dziubek
Assessment of physical performance and muscle function in hemodialysis patients participating in an exercise regimen: A cluster-randomized, single-center study
- 2119 Krzysztof Siemion, Joanna Kiśluk, Natalia Wasilewska, Joanna Reszec-Giełazyn, Anna Korzyńska, Tomasz Łysoń, Zenon Mariak
Next-generation sequencing study of inflammatory spindle cell lesions focused on receptor tyrosine kinase gene rearrangements most frequently occurring in inflammatory myofibroblastic tumor

- 2137 Muhammed Talha Karadogan, Bulent Yavuzer, Cebrail Gursul, Gulbaniz Huseynova, Gulce Naz Yazici, Mine Gulaboglu, Furkan Yilmaz, Ali Sefa Mendil, Halis Suleyman
Comparative study of the protective effects of adenosine triphosphate and resveratrol against amiodarone-induced potential liver damage and dysfunction in rats
- 2153 Adam Fabisiak, Maria R. Wołyniak, Fabiana Piscitelli, Roberta Verde, Vincenzo Di Marzo, Marta Zielińska, Weronika Machelak, Ewa Małecka-Wojcieszko
Combined CB1 antagonist AM6545 and NOP agonist SCH221510 worsen DSS-induced colitis in mice
- 2163 Piotr Karniej, Raúl Juárez-Vela, Anthony Dissen, Antonio Martinez-Sabater, Pablo Del Pozo-Herce, Vicente Gea-Caballero, Emmanuel Echániz-Serrano, Elena Chover-Sierra, Ruben Perez-Elvira, Michał Czapla
Psychometric properties and cultural adaptation of the Spanish version of the Lesbian, Gay, Bisexual, and Transgender Development of Clinical Skills Scale (LGBT-DOCSS-ES)

Reviews

- 2175 Weidong Yao, Xinyi Yu, Yameng Wang, Liang Xia
Progress in stem cells mitochondrial proteomics research: A review
- 2187 Sara Lauricella, Francesco Brucchi, Roberto Cirocchi
The evolution of transanal approaches in rectal cancer surgery

Access to services. Mental health in catastrophes and emergencies: Aspects

Sabine Bährer-Kohler^{1,2,A–F}

¹ World Federation For Mental Health, USA

² Association for Global Mental Health, Basel, Switzerland

A – research concept and design; B – collection and/or assembly of data; C – data analysis and interpretation;

D – writing the article; E – critical revision of the article; F – final approval of the article

Advances in Clinical and Experimental Medicine, ISSN 1899–5276 (print), ISSN 2451–2680 (online)

Adv Clin Exp Med. 2025;34(12):1995–1998

Address for correspondence

Sabine Bährer-Kohler

E-mail: sabine.baehrer@datacomm.ch

Funding sources

None declared

Conflict of interest

None declared

Received on September 6, 2025

Accepted on September 23, 2025

Published online on October 31, 2025

Abstract

Disasters, wars and health emergencies profoundly affect mental health, with nearly 1/3 of affected populations developing conditions such as posttraumatic stress disorder (PTSD), depression or anxiety, particularly among vulnerable groups like children, the elderly and the chronically ill. Access to mental health and psychosocial support (MHPSS) is often limited by conflict-related disruptions, stigma or resource shortages, while healthcare workers themselves face immense psychological strain and inadequate protection. Long-term strategies integrating disaster preparedness, mental health services and professional support are essential to safeguard both affected populations and frontline workers during emergencies.

Key words: mental health, catastrophes, access to services, emergencies

Cite as

Bährer-Kohler S. Access to services. Mental health in catastrophes and emergencies: Aspects.

Adv Clin Exp Med. 2025;34(12):1995–1998.

doi:10.17219/acem/211237

DOI

10.17219/acem/211237

Copyright

Copyright by Author(s)

This is an article distributed under the terms of the Creative Commons Attribution 3.0 Unported (CC BY 3.0)

(<https://creativecommons.org/licenses/by/3.0/>)

Highlights

- Disasters, wars, and public health emergencies have a profound impact on mental health, with up to 1/3 of affected individuals developing PTSD, depression, anxiety, or related disorders.
- Limited access to mental health and psychosocial support (MHPSS) – due to stigma, resource shortages, and disrupted health systems – worsens outcomes among vulnerable populations.
- Integrating mental health care into disaster preparedness and emergency response frameworks is essential to improve resilience and recovery in crisis-affected communities.

Introduction

The term “emergency” is often used interchangeably with “disaster” in global contexts, such as biological and technological hazards, health emergencies, and other crises – a catastrophe or sudden event that causes widespread suffering, hardship, or destruction.¹ Millions of people worldwide were and are affected by such events, which profoundly impact both physical and mental health.

Mental health is a state of wellbeing that enables individuals to cope with life’s stresses, realize their abilities, learn and work well, and contribute to their communities. It is an integral component of health and wellbeing, supporting both individual and collective capacity to make decisions, build relationships, and shape the world we live in. Mental health is a fundamental human right for everybody and is essential for personal, community and socioeconomic development.²

The implications of disasters, including armed conflicts, for both civilian and military populations have long been the subject of research.^{3–6} In disaster situations, vulnerable groups often experience intense stress, face major challenges and may develop mental disorders. Nearly 1/3 of disaster-affected individuals may suffer significant mental health consequences. While wars, disasters, emergencies, and catastrophes differ in nature, they share many common features.

What these situations have in common is that people often struggle to move on and adapt to change. Particularly vulnerable groups, such as the elderly, individuals who are ill or injured, pregnant women, young children, and infants, are especially dependent on support. Mesa-Vieira et al. documented that younger individuals are at a higher risk of developing mental health disorders such as post-traumatic stress disorder (PTSD), major depressive disorder and generalized anxiety disorder.⁷

Emergency medicine research has repeatedly emphasized that help and support must effectively reach those in need – and that people must be able to reach support services as well.⁸ Traumatized individuals, especially those from vulnerable groups, depend on specialized assistance. Access to support always has to do with forms of access and availability, but also with information about it. Outreach support is therefore essential. However, this requires

appropriate frameworks to ensure the safety and protection of both helpers and recipients – conditions that are not always guaranteed in emergencies and catastrophes.

Mental health in catastrophes and emergencies

Mental health disorders resulting from disasters and emergencies require specialized skills and effective communication abilities, particularly in trauma-informed care.^{9,10} Training and continuing education in this area are essential. Conditions such as PTSD, anxiety disorders, depression, and suicidal ideation are among the most common challenges, while others may experience panic attacks, delusions, or impulsive behaviors.¹¹ Nearly all individuals affected by emergencies experience some form of psychological distress, which, in most cases, tends to improve over time.

However, approx. 1 in 5 people (22%) who have experienced war or conflict within the past 10 years suffer from depression, anxiety, PTSD, bipolar disorder, or schizophrenia.¹² Individuals may experience traumatic losses, and women consistently show higher rates of anxiety, depression and PTSD symptoms compared to those without such experiences or to men, across all time points.^{6,13}

Meta-analyses estimate that approx. 15.3–36.0% of war-affected adult populations experience PTSD, compared to 3.9–7.8% in the general population.^{5,14} Other surveys suggest that 26% and 27% of war survivors suffer from PTSD and/or depression, respectively.¹³ Studies further indicate that factors such as life uncertainty, individual helplessness, and dependence on others or external circumstances can cause significant psychological distress.¹⁵

Access and support: Access to services

International guidelines and reports recommend a range of activities and interventions to provide mental health and psychosocial support (MHPSS) during emergencies – from self-help and community-based support to effective communication, psychological first aid and clinical mental

health care. Preparedness and integration with disaster risk reduction are essential to mitigating measurable impacts. Countries can also use emergencies as opportunities to invest in mental health services, leveraging the increased aid and attention they receive to build stronger and more sustainable care systems for the long term.¹² Nevertheless, damage to medical and social systems caused by disasters, wars, conflicts, and violence has multiple consequences. For instance, in areas affected by armed conflict, people often cannot access essential services due to ongoing violence, infrastructure destruction, stigma, legal restrictions, financial barriers, or other obstacles.¹¹ Additionally, mental health and psychosocial support professionals remain scarce in conflict settings.¹⁶

Mental health care in emergencies often requires “a major rethink.”¹⁷ What previously applied may no longer be effective or available. The Inter-Agency Standing Committee (IASC) Reference Group on Mental Health and Psychosocial Support in Emergency Settings plays a pivotal and active role in promoting mental health care and ensuring access to psychosocial support during conflicts.¹⁸ They have developed specific guidelines on MHPSS in emergency settings through an inclusive process involving input from United Nations (UN) agencies, non-governmental institutions (NGOs) and universities. These guidelines, available in several languages, help plan, establish and coordinate a set of minimum multi-sectoral responses to protect, support and improve people’s mental health and psychosocial wellbeing during emergencies.¹⁹

Aspects of professionals: Healthcare workers

Zavyalova, an emergency physician, emphasized that being a doctor in wartime means returning home after each shift, wishing the war had never happened and praying for its swift end. People are exhausted – the clients, patients and healthcare workers alike. Yet, as social and medical professionals, they do not have the luxury of fatigue. The clients and patients need the professionals to keep going and they must push through the fatigue to continue delivering the care they deserve.²⁰

The immense need for treatment and counseling, combined with the often-limited number of helpers, places great strain and risk of overload on professionals in these situations. At the same time, it is essential to focus on protecting and supporting these professionals and ensuring that employers conduct proper risk assessments. The International Committee of the Red Cross (ICRC) has repeatedly emphasized that the failure to protect professionals in war zones is one of the most critical yet frequently overlooked humanitarian issues today.^{21,22} As already noted by Javed,¹¹ other factors can exacerbate these challenging conditions. The harmful effects of operating in war zones extend to material and

supply shortages, including disruptions in essential services such as electricity, medicines, equipment, water and nutrition, all of which further increase the stress experienced by health professionals.^{22,23}

Furthermore, the mental health of professionals can be profoundly affected by their work during disasters and catastrophes. Abed Alah emphasized that constant exposure to trauma, combined with the pressure of providing care and counseling under extreme conditions, places an immense burden on the mental wellbeing of professionals, making their situation in conflict zones both critical and often overlooked.²⁴

Conclusions

The effects of war, catastrophes and disasters are varied and multifaceted – for both affected populations and deployed helpers. Ultimately, it is recommended that long-term policies, strategies, and actions be developed to address the medical and psychosocial impacts of conflict, trauma, mental health disorders, and access to support and services.

While national health policies must incorporate disaster management and analysis, priority should also be given to reshaping local, regional, and global structures. This includes emphasizing resource allocation, needs assessment, and strengthening infrastructure to meet requirements, as well as ensuring ongoing evaluation, training and continuing education in this context.¹¹ However, professionals also need protection to ensure access to facilities that support both physical and mental health. The World Federation for Mental Health calls on all responsible parties to safeguard access and strengthen facilities for people affected by catastrophes and emergencies.

Use of AI and AI-assisted technologies

Not applicable.

References

1. United Nations (UN), United Nations Office for Disaster Risk Reduction (UNDRR). The Sendai Framework Terminology on Disaster Risk Reduction: Disaster. New York, USA: United Nations (UN); 2017. <https://www.undrr.org/terminology/disaster>. Accessed August 15, 2025.
2. World Health Organization (WHO). Mental Health: Key facts. Geneva, Switzerland: World Health Organization (WHO); 2022. <https://www.who.int/news-room/fact-sheets/detail/mental-health-strengthening-our-response>. Accessed August 15, 2025.
3. Nordstrand AE, Anyan F, Bøe HJ, et al. Problematic anger among military personnel after combat deployment: Prevalence and risk factors. *BMC Psychol*. 2024;12(1):451. doi:10.1186/s40359-024-01955-8
4. Hitch C, Spikol E, Toner P, Armour C. The relationship between co-occurring traumatic experiences and co-occurring mental health domains for veterans resident in Northern Ireland. *BMC Psychol*. 2024; 12(1):523. doi:10.1186/s40359-024-01991-4
5. Williamson V, Murphy D. Psychological consequences of global armed conflict. *BMC Psychol*. 2025;13(1):197. doi:10.1186/s40359-024-02305-4

6. Amsalem D, Haim-Nachum S, Lazarov A, et al. The effects of war-related experiences on mental health symptoms of individuals living in conflict zones: A longitudinal study. *Sci Rep.* 2025;15(1):889. doi:10.1038/s41598-024-84410-3
7. Mesa-Vieira C, Haas AD, Buitrago-Garcia D, et al. Mental health of migrants with pre-migration exposure to armed conflict: A systematic review and meta-analysis. *Lancet Public Health.* 2022;7(5):e469–e481. doi:10.1016/S2468-2667(22)00061-5
8. World Health Organization (WHO). The frontline responders in health emergencies. Geneva, Switzerland: World Health Organization (WHO); 2024. www.who.int/europe/news-room/feature-stories/item/the-frontline-responders-in-health-emergencies. Accessed August 15, 2025.
9. Papageorgiou A, Loke YK, Fromage M. Communication skills training for mental health professionals working with people with severe mental illness. *Cochrane Database Syst Rev.* 2017;2017(6):CD010006. doi:10.1002/14651858.CD010006.pub2
10. Kumar YS, Kamath JS. Healthcare workers on the frontlines of war: Essential roles and responsibilities. *Am J Med Open.* 2024;11:100064. doi:10.1016/j.ajmo.2024.100064
11. Javed A. Wars, conflicts & mental health. *Pak J Med Sci.* 2024;40(5):797–799. doi:10.12669/pjms.40.5.9505
12. World Health Organization (WHO). Mental health in emergencies. Geneva, Switzerland: World Health Organization (WHO); 2025. <https://www.who.int/news-room/fact-sheets/detail/mental-health-in-emergencies>. Accessed August 15, 2025.
13. Morina N, Stam K, Pollet TV, Priebe S. Prevalence of depression and posttraumatic stress disorder in adult civilian survivors of war who stay in war-afflicted regions. A systematic review and meta-analysis of epidemiological studies. *J Affect Disord.* 2018;239:328–338. doi:10.1016/j.jad.2018.07.027
14. Hoppen TH, Priebe S, Vetter I, Morina N. Global burden of post-traumatic stress disorder and major depression in countries affected by war between 1989 and 2019: A systematic review and meta-analysis. *BMJ Glob Health.* 2021;6(7):e006303. doi:10.1136/bmjgh-2021-006303
15. Porter M, Haslam N. Predisplacement and postdisplacement factors associated with mental health of refugees and internally displaced persons: A meta-analysis. *JAMA.* 2005;294(5):602. doi:10.1001/jama.294.5.602
16. International Committee of the Red Cross (ICRC); Serafini M. Ensuring access to Mental Health and Psychosocial Support in Conflict, Post-conflict and Humanitarian Settings. Geneva, Switzerland: International Committee of the Red Cross (ICRC); 2022. <https://www.icrc.org/en/document/mental-health-psychosocial-support-conflict-post-conflict-humanitarian-settings>. Accessed August 15, 2025.
17. Zarocostas J. Mental health in emergencies requires a major rethink. *Lancet.* 2024;403(10444):2582. doi:10.1016/S0140-6736(24)01241-8
18. Inter-Agency Standing Committee (IASC). IASC Guidelines on Mental Health and Psychosocial Support in Emergency Settings, 2007. Geneva, Switzerland: Inter-Agency Standing Committee (IASC); 2007. <https://interagencystandingcommittee.org/mental-health-and-psychosocial-support-emergency-settings-0/documents-public/iasc-guidelines-mental>. Accessed August 15, 2025.
19. Mental Health Europe. The impact of wars and armed conflicts on mental health. Brussels, Belgium: Mental Health Europe; 2023. <https://www.mentalhealtheurope.org/impact-of-wars-and-armed-conflicts-on-mental-health>. Accessed August 15, 2025.
20. World Health Organization (WHO). Three years of war: Rising demand for mental health support, trauma care and rehabilitation. Geneva, Switzerland: World Health Organization (WHO); 2025. <https://www.who.int/europe/news/item/24-02-2025-three-years-of-war-rising-demand-for-mental-health-support-trauma-care-and-rehabilitation>. Accessed August 15, 2025.
21. International Committee of the Red Cross (ICRC). Health-Care Workers Suffer Attacks Every Single Week. Geneva, Switzerland: International Committee of the Red Cross (ICRC); 2018. <https://www.icrc.org/en/document/icrc-health-care-workers-suffer-attacks-every-single-week>. Accessed August 15, 2025.
22. Vuorio A, Bor R. Safety of health care workers in a war zone: A European issue. *Front Public Health.* 2022;10:886394. doi:10.3389/fpubh.2022.886394
23. The PLOS Medicine Editors. Health care in danger: Deliberate attacks on health care during armed conflict. *PLoS Med.* 2014;11(6):e1001668. doi:10.1371/journal.pmed.1001668
24. Abed Alah M. Echoes of conflict: The enduring mental health struggle of Gaza's healthcare workers. *Confl Health.* 2024;18(1):21. doi:10.1186/s13031-024-00577-6

Recent advances in the study of perinatal mental health: Epidemiology, psychopathology and intervention

Chong Chen^{A,D–F}, Shin Nakagawa^{E,F}

Division of Neuropsychiatry, Department of Neuroscience, Yamaguchi University Graduate School of Medicine, Ube, Japan

A – research concept and design; B – collection and/or assembly of data; C – data analysis and interpretation;

D – writing the article; E – critical revision of the article; F – final approval of the article

Advances in Clinical and Experimental Medicine, ISSN 1899–5276 (print), ISSN 2451–2680 (online)

Adv Clin Exp Med. 2025;34(12):1999–2003

Address for correspondence

Chong Chen

Email: cchen@yamaguchi-u.ac.jp

Funding sources

This work was supported by Japan Society for the Promotion of Science KAKENHI grant No. JP25K10835.

Conflict of interest

Chong Chen is the author of *Psychology for Pregnancy*. Shin Nakagawa declares no conflicts of interest.

Received on October 14, 2025

Accepted on October 15, 2025

Published online on November 6, 2025

Abstract

Perinatal mental health has been increasingly recognized as one of the most prevalent and consequential complications of pregnancy and childbirth. Approximately 1 in 5 women experience depression during or after pregnancy, and up to 1 in 4 encounter difficulties in establishing an emotional bond with their infants – a condition known as mother-to-infant bonding difficulties (MIBD). Pooled global estimates from meta-analyses indicate that these conditions are more prevalent than major obstetric complications such as gestational diabetes and preeclampsia. They also represent the leading cause of maternal mortality, particularly in high-income countries. For example, suicidal ideation (SI) is approx. 16 times more common among women with postpartum depression (PPD) than among those without. Moreover, SI occurring alongside PPD is often associated with prior depressive episodes and a lack of social support, whereas SI in the absence of depression tends to be linked to first-time motherhood, infection during pregnancy, or loneliness. Postpartum depression and MIBD are also closely interconnected, exhibiting a bidirectional relationship and sharing major risk factors such as prenatal depression, limited family support, and adverse childhood experiences. When left untreated, perinatal depression and MIBD can impair maternal functioning and delay infants' emotional, cognitive and social development. Emerging integrative approaches that combine psychotherapy with bonding-focused, lifestyle and psychosocial components show promise in improving outcomes. Future research should focus on developing comprehensive, multimodal interventions that integrate psychotherapy with lifestyle and psychosocial elements within a preventive, family-centered framework, promoting sustained recovery beyond active treatment.

Key words: perinatal depression, mother-to-infant bonding, suicidal ideation, adverse childhood experiences, infant development

Cite as

Chen C, Nakagawa S. Recent advances in the study of perinatal mental health: Epidemiology, psychopathology and intervention. *Adv Clin Exp Med.* 2025;34(12):1999–2003. doi:10.17219/acem/212646

DOI

10.17219/acem/212646

Copyright

Copyright by Author(s)

This is an article distributed under the terms of the Creative Commons Attribution 3.0 Unported (CC BY 3.0) (<https://creativecommons.org/licenses/by/3.0/>)

Highlights

- Perinatal mental health conditions affect up to 1 in 5 women and are more common than major obstetric complications.
- Suicidal ideation is 16 times more likely in women with postpartum depression, especially when social support is lacking.
- Mother–infant bonding difficulties and perinatal depression share risk factors and can hinder child development if untreated.
- Integrative therapies combining psychotherapy, lifestyle, and family support offer promising outcomes for maternal recovery.

Introduction

Perinatal mental health refers to the psychological well-being of women during pregnancy and the 1st year after childbirth. Recognized as common and consequential for mothers, infants and families,^{1–3} this field has gained global attention. This overview summarizes recent advances in perinatal depression, including prenatal and postpartum, and mother-to-infant bonding difficulties (MIBD), highlighting progress in epidemiology, psychopathology and intervention.

Prevalence and epidemiological trends

Perinatal mental disorders are among the most frequent complications of pregnancy and childbirth, often surpassing major obstetric complications. Meta-analyses reported a pooled global prevalence of 20.7% (95% confidence interval (95% CI): 19.4–21.9%) for prenatal depression⁴ and 17.7% (95% CI: 16.6–18.8%) for postpartum depression (PPD).⁵ While global estimates for MIBD are unavailable, community-based surveys report prevalence rates ranging from 3%⁶ to 24%,⁷ based on cutoff scores from the Postpartum Bonding Questionnaire (PBQ)⁸ or the Mother-to-Infant Bonding Scale (MIBS).⁹

In contrast, major obstetric complications typically occur at lower frequencies: gestational diabetes mellitus – 14.0% (95% CI: 13.97–14.04%)¹⁰; preeclampsia – 4.6% (95% CI: 2.7–8.2%)¹¹; preterm birth – 10.6% (95% CI: 9.0–12.0%)¹²; and postpartum hemorrhage – 10.8% (95% CI: 9.6–12.1).¹³

Therefore, perinatal mental disorders represent leading morbidities during pregnancy and the postpartum period, and they are also major contributors to maternal mortality.¹⁴ In UK surveillance data, suicide was the leading direct cause of death from 6 weeks to 12 months postpartum, accounting for 39% of late maternal deaths.¹⁵ Similar findings have been reported in other high-income countries, such as the Netherlands, where suicide accounts for 28% of maternal deaths.¹⁶ This mortality pattern underscores the critical importance of assessing and managing suicidal thoughts and behaviors during the perinatal period.

Importantly, during the COVID-19 pandemic, the prevalence of perinatal depression and MIBD increased markedly across different populations.^{17–19} For example, the pooled global prevalence of prenatal depression and PPD has been estimated at 29% (95% CI: 25–33%) and 26% (95% CI: 23–30%), respectively,²⁰ consistent with findings from another meta-analysis reporting similar estimates.²¹ This increase likely reflects heightened social isolation, fear of infection, and reduced access to perinatal care and support services.

Psychopathology and clinical features

Perinatal depression shares core symptoms with major depressive disorder, including low mood and anhedonia.²² The uniqueness of perinatal depression is that it manifests in the specific context of pregnancy, childbirth and childbearing, where biological influences, including genetic vulnerability and hormonal fluctuations, play a prominent role.²³ Consistent with the mortality data described above, severe cases of perinatal depression may involve thoughts of suicide^{14–16} or harming the infant,²⁴ which requires urgent response.

A key concern is the strong association between perinatal depression and suicidal ideation (SI),^{25–27} in which SI primarily occurs in women with perinatal depression, be it prenatal or postpartum. For instance, it has been estimated that SI is about 16 times more common in women with PPD.²⁷ When SI occurs without PPD, it shows distinct predictors.²⁷ In women with PPD, SI links to prior depressive episodes and lack of support (e.g., being single, canceled family visits). Without PPD, SI relates to first-time motherhood, infections during pregnancy, or loneliness aggravated by COVID-19. These distinctions underscore the need for context-sensitive risk assessment.

Another robust finding is that prenatal depression represents a strong predictor of PPD. A meta-analysis of 88 cohort studies found that about 37% of women with prenatal depression later developed PPD, representing a 4.6-fold higher risk compared with those without prenatal depression.²⁸

Finally, the close interrelationship between PPD and MIBD has been increasingly documented. Cross-sectional data indicate that more than half of women with PPD experience MIBD, while up to 40% of those with MIBD also have PPD.¹⁹ The 2 conditions not only show reciprocal influences on each other,¹⁹ but also share major risk factors such as prenatal depression,^{28,29} poor family support^{30,31} and adverse childhood experiences.^{32,33} Network analyses identify overlapping “bridge symptoms” (e.g., fear, overwhelm, insomnia) that vary across postpartum stages,¹⁹ which emphasizes the need for dynamic, stage-sensitive care. Moving forward, adopting dimensional and biologically informed analytic frameworks^{34,35} may help disentangle the shared and distinct mechanisms underlying this high comorbidity, paving the way toward more personalized preventive and therapeutic interventions for mothers and infants.

Impact on mothers and infants

Untreated perinatal depression affects not only the mother but also her overall health and caregiving capacity. Women with depression often experience difficulties in daily functioning and are more likely to develop physical conditions such as hypertension.^{36–38} Beyond the impact on their own wellbeing, they may also struggle to respond sensitively to their infants.^{1,39,40}

They may display flat or negative affect, breastfeed less frequently, adopt unsafe sleep practices, and neglect preventive healthcare measures such as vaccinations. Depressed mothers are also more likely to use harsh discipline or engage in abusive behavior.^{1,39,41–43} These challenges contribute to suboptimal caregiving environments that can hinder infant development.

Evidence consistently links maternal depression to cognitive, language, and socioemotional delays, as well as an increased risk of mental health problems in offspring.^{44–46} Likewise, unresolved MIBD the risk of emotional abuse and perpetuates maternal depression,^{19,47} leading to disrupted infant emotional^{48,49} and cognitive development.⁵⁰

Limitations of current screening tools

Given these profound impacts, early detection of perinatal mental health issues through routine screening, using tools such as the Edinburgh Postnatal Depression Scale (EPDS)⁵¹ and the PBQ⁸ or MIBS,⁹ has become standard practice in many healthcare systems.

However, these tools have important limitations. The EPDS, developed nearly 4 decades ago, has been criticized for outdated and occasionally confusing wording,^{26,52} as well as for limited cultural adaptation prior to translation and validation in non-UK populations.⁵³ Its inclusion

of anxiety-related items, while useful for identifying anxiety, can blur distinctions between depression, anxiety and trauma.⁵⁴ These concerns have prompted calls for updated, multidimensional screening tools that assess depression, anxiety and trauma as distinct but related constructs.

Similarly, the MIBS, despite its widespread use, has been criticized for the absence of validated cutoff thresholds, partly due to methodological limitations.⁵⁵ Recent studies have begun refining this measure, contributing to the development of more reliable tools for assessing perinatal mental health difficulties.

Toward tailored and integrated interventions

Encouragingly, effective treatment of perinatal depression has been shown not only to prevent its progression to chronic depression but also to improve mother–infant interactions and enhance infants’ cognitive and emotional development.^{56–58}

The most promising strategies appear to be integrated interventions addressing maternal depression, bonding, and parenting simultaneously.^{59,60} Yet in practice, treatment remains fragmented: cognitive-behavioral therapy (CBT) is the standard for depression,⁶¹ while bonding-focused approaches remain in the pilot stages.⁶²

Future research should aim to develop comprehensive, multimodal models that integrate psychotherapy with lifestyle and psychosocial components, such as physical activity,^{63,64} nature-based interventions,^{65,66} and positive psychological techniques like positive memory recall.^{67,68} These modalities can be further enhanced through the integration of wearable technologies, advanced sensors and video- or artificial intelligence-powered applications.^{69,70}


These approaches can enhance maternal and infant wellbeing within a preventive, family-centered framework.^{71,72} Moreover, given their distinct mechanisms of action, combining them may produce synergistic effects that foster sustainable behavioral and emotional changes extending beyond the period of active treatment.

Use of AI and AI-assisted technologies

Not applicable.

ORCID iDs

Chong Chen  <https://orcid.org/0000-0002-3189-7397>

Shin Nakagawa  <https://orcid.org/0000-0002-7502-5734>

References

1. Chen C. *Psychology for Pregnancy: How Your Mental Health During Pregnancy Programs Your Baby's Developing Brain*. London, UK: Brain & Life Publishing; 2017. ISBN:978-1-9997601-9-9.
2. Howard LM, Khalifeh H. Perinatal mental health: A review of progress and challenges. *World Psychiatry*. 2020;19(3):313–327. doi:10.1002/wps.20769
3. Stowe ZN. Perinatal mental health: Advances and opportunities. *Am J Psychiatry*. 2023;180(12):874–877. doi:10.1176/appi.ajp.20230822

4. Yin X, Sun N, Jiang N, et al. Prevalence and associated factors of antenatal depression: Systematic reviews and meta-analyses. *Clin Psychol Rev*. 2021;83:101932. doi:10.1016/j.cpr.2020.101932
5. Hahn-Holbrook J, Cornwell-Hinrichs T, Anaya I. Economic and health predictors of national postpartum depression prevalence: A systematic review, meta-analysis, and meta-regression of 291 studies from 56 countries. *Front Psychiatry*. 2018;8:248. doi:10.3389/fpsy.2017.00248
6. Garcia-Esteve L, Torres A, Lasheras G, et al. Assessment of psychometric properties of the Postpartum Bonding Questionnaire (PBQ) in Spanish mothers. *Arch Womens Ment Health*. 2016;19(2):385–394. doi:10.1007/s00737-015-0589-x
7. Vengadavaradan A, Bharadwaj B, Sathyanarayanan G, Durairaj J. Frequency and correlates of mother-infant bonding disorders among postpartum women in India. *Asian J Psychiatry*. 2019;44:72–79. doi:10.1016/j.ajp.2019.07.004
8. Brockington IF, Fraser C, Wilson D. The Postpartum Bonding Questionnaire: A validation. *Arch Womens Ment Health*. 2006;9(5):233–242. doi:10.1007/s00737-006-0132-1
9. Taylor A, Atkins R, Kumar R, Adams D, Glover V. A new Mother-to-Infant Bonding Scale: Links with early maternal mood. *Arch Womens Ment Health*. 2005;8(1):45–51. doi:10.1007/s00737-005-0074-z
10. Wang H, Li N, Chivese T, et al. IDF Diabetes Atlas: Estimation of global and regional gestational diabetes mellitus prevalence for 2021 by International Association of Diabetes in Pregnancy Study Group's Criteria. *Diabetes Res Clin Pract*. 2022;183:109050. doi:10.1016/j.diabres.2021.109050
11. Abalos E, Cuesta C, Grosso AL, Chou D, Say L. Global and regional estimates of preeclampsia and eclampsia: A systematic review. *Eur J Obstet Gynecol Reprod Biol*. 2013;170(1):1–7. doi:10.1016/j.ejogrb.2013.05.005
12. Chawanpaiboon S, Vogel JP, Moller AB, et al. Global, regional, and national estimates of levels of preterm birth in 2014: A systematic review and modelling analysis. *Lancet Global Health*. 2019;7(1):e37–e46. doi:10.1016/S2214-109X(18)30451-0
13. Calvert C, Thomas SL, Ronsmans C, Wagner KS, Adler AJ, Filippi V. Identifying regional variation in the prevalence of postpartum haemorrhage: A systematic review and meta-analysis. *PLoS One*. 2012;7(7):e41114. doi:10.1371/journal.pone.0041114
14. Yu H, Shen Q, Bränn E, et al. Perinatal depression and risk of suicidal behavior. *JAMA Netw Open*. 2024;7(1):e2350897. doi:10.1001/jamanetworkopen.2023.50897
15. Knight M, Bunch K, Felker A, et al. *Saving Lives, Improving Mothers' Care Lessons Learned to Inform Maternity Care from the UK and Ireland Confidential Enquiries into Maternal Deaths and Morbidity 2019–2021*. London, UK: EMBRACE-UK: Mothers and Babies: Reducing Risk through Audits and Confidential Enquiries across the UK; Maternal, Newborn and Infant Clinical Outcome Review Programme; 2023. https://www.npeu.ox.ac.uk/assets/downloads/mbrrace-uk/reports/maternal-report-2023/MBRRACE-UK_Maternal_Report_2023.pdf.
16. Lommerse KM, Mérelle S, Rietveld AL, Berkemans G, Van Den Akker T; The Netherlands Audit Committee Maternal Mortality and Morbidity. The contribution of suicide to maternal mortality: A nationwide population-based cohort study. *BJOG*. 2024;131(10):1392–1398. doi:10.1111/1471-0528.17784
17. Chen C, Okubo R, Okawa S, Higuchi N, Nakagawa S, Tabuchi T. The prevalence and risk factors of suicidal ideation in pregnancy and postpartum under the COVID-19 pandemic in Japan. *Psychiatry Clin Neurosci*. 2023;77(5):300–301. doi:10.1111/pcn.13538
18. Chen C, Mochizuki Y, Okawa S, Okubo R, Nakagawa S, Tabuchi T. Postpartum loneliness predicts future depressive symptoms: A nationwide Japanese longitudinal study. *Arch Womens Ment Health*. 2024;27(3):447–457. doi:10.1007/s00737-024-01424-6
19. Harasawa N, Chen C, Okawa S, et al. A network analysis of postpartum depression and mother-to-infant bonding shows common and unique symptom-level connections across three postpartum periods. *Commun Psychol*. 2025;3(1):7. doi:10.1038/s44271-024-00171-9
20. Caffieri A, Gómez-Gómez I, Barquero-Jimenez C, De-Juan-Iglesias P, Margherita G, Motrico E. Global prevalence of perinatal depression and anxiety during the COVID-19 pandemic: An umbrella review and meta-analytic synthesis. *Acta Obstet Gynecol Scand*. 2024;103(2):210–224. doi:10.1111/aogs.14740
21. Sahebi A, Kheiry M, Abdi K, Qomi M, Golitaleb M. Postpartum depression during the COVID-19 pandemic: An umbrella review and meta-analyses. *Front Psychiatry*. 2024;15:1393737. doi:10.3389/fpsy.2024.1393737
22. Radoš SN, Akik BK, Žutić M, et al. Diagnosis of peripartum depression disorder: A state-of-the-art approach from the COST Action Riseup-PPD. *Compr Psychiatry*. 2024;130:152456. doi:10.1016/j.comppsych.2024.152456
23. Batt MM, Duffy KA, Novick AM, Metcalf CA, Epperson CN. Is postpartum depression different from depression occurring outside of the perinatal period? A review of the evidence. *Focus (Am Psychiatr Publ)*. 2020;18(2):106–119. doi:10.1176/appi.focus.20190045
24. Donahue Jennings K, Ross S, Popper S, Elmore M. Thoughts of harming infants in depressed and nondepressed mothers. *J Affect Disord*. 1999;54(1–2):21–28. doi:10.1016/S0165-0327(98)00185-2
25. Arditi-Arbel B, Hamdan S, Winterman M, Gvion Y. Suicidal ideation and behavior among perinatal women and their association with sleep disturbances, medical conditions, and known risk factors. *Front Psychiatry*. 2023;13:987673. doi:10.3389/fpsy.2022.987673
26. Chen C, Okubo R, Okawa S, Nakagawa S, Tabuchi T. The diagnostic accuracy of the Edinburgh Postnatal Depression Scale without the self-harm item. *J Psychiatr Res*. 2023;165:70–76. doi:10.1016/j.jpsychires.2023.07.015
27. Chen C, Okubo R, Okawa S, et al. The prevalence and risk factors of suicidal ideation in women with and without postpartum depression. *J Affect Disord*. 2023;340:427–434. doi:10.1016/j.jad.2023.08.051
28. Dlamini LP, Amelia VL, Shongwe MC, Chang PC, Chung MH. Antenatal depression across trimesters as a risk for postpartum depression and estimation of the fraction of postpartum depression attributable to antenatal depression: A systematic review and meta-analysis of cohort studies. *Gen Hosp Psychiatry*. 2023;85:35–42. doi:10.1016/j.genhosppsy.2023.09.005
29. Chen C, Okawa S, Okubo R, Nakagawa S, Tabuchi T. Risk factors for mother-to-infant bonding difficulties and maternal anger/rejection towards the infant in a Japanese longitudinal study. *Asian J Psychiatry*. 2023;89:103778. doi:10.1016/j.ajp.2023.103778
30. Cho H, Lee K, Choi E, et al. Association between social support and postpartum depression. *Sci Rep*. 2022;12(1):3128. doi:10.1038/s41598-022-07248-7
31. Chen C, Okawa S, Okubo R, Nakagawa S, Tabuchi T. Risk factors for persistent versus episodic mother-to-infant bonding difficulties in postpartum women in a nationwide Japanese longitudinal study. *J Affect Disord*. 2024;349:370–376. doi:10.1016/j.jad.2024.01.001
32. Chen C, Okubo R, Okawa S, et al. Broad impact of adverse childhood experiences on postpartum maternal mental health, child-rearing behaviors, and child development in Japan. *Psychiatry Clin Neurosci*. 2023;77(10):569–571. doi:10.1111/pcn.13581
33. Hirai T, Hagiwara K, Chen C, et al. The impact of adverse childhood experiences on adult physical, mental health, and abuse behaviors: A sex-stratified nationwide latent class analysis in Japan. *J Affect Disord*. 2025;369:1071–1081. doi:10.1016/j.jad.2024.10.074
34. Tanaka M. Beyond the boundaries: Transitioning from categorical to dimensional paradigms in mental health diagnostics. *Adv Clin Exp Med*. 2024;33(12):1295–1301. doi:10.17219/acem/197425
35. Tanaka M, Szabó Á, Vécsei L. Preclinical modeling in depression and anxiety: Current challenges and future research directions. *Adv Clin Exp Med*. 2023;32(5):505–509. doi:10.17219/acem/165944
36. Qiu C, Williams MA, Calderon-Margalit R, Cripe SM, Sorensen TK. Preeclampsia risk in relation to maternal mood and anxiety disorders diagnosed before or during early pregnancy. *Am J Hypertens*. 2009;22(4):397–402. doi:10.1038/ajh.2008.366
37. Duman H, Duman H, Puşuroğlu M, Yılmaz AS. Anxiety disorders and depression are associated with resistant hypertension. *Adv Clin Exp Med*. 2023;33(2):111–118. doi:10.17219/acem/166304
38. Grabek-Kujawa H, Lubiński W, Mularczyk M, Kucharska-Mazur J, Dańczura E, Samochowiec J. Visual pathway function in untreated individuals with major depression. *Adv Clin Exp Med*. 2023;32(1):117–123. doi:10.17219/acem/158483
39. Field T, Diego M, Hernandez-Reif M, et al. Comorbid depression and anxiety effects on pregnancy and neonatal outcome. *Infant Behav Dev*. 2010;33(1):23–29. doi:10.1016/j.infbeh.2009.10.004

40. Brookman R, Kalashnikova M, Levickis P, et al. Effects of maternal depression on maternal responsiveness and infants' expressive language abilities. *PLoS One*. 2023;18(1):e0277762. doi:10.1371/journal.pone.0277762
41. Ahmadienezhad GS, Karimi FZ, Abdollahi M, NaviPour E. Association between postpartum depression and breastfeeding self-efficacy in mothers: A systematic review and meta-analysis. *BMC Pregnancy Childbirth*. 2024;24(1):273. doi:10.1186/s12884-024-06465-4
42. Taraban L, Shaw DS, Leve LD, et al. Maternal depression and parenting in early childhood: Contextual influence of marital quality and social support in two samples. *Dev Psychol*. 2017;53(3):436–449. doi:10.1037/dev0000261
43. Ayers S, Bond R, Webb R, Miller P, Bateson K. Perinatal mental health and risk of child maltreatment: A systematic review and meta-analysis. *Child Abuse Neglect*. 2019;98:104172. doi:10.1016/j.chiabu.2019.104172
44. Drury SS, Scaramella L, Zeanah CH. The neurobiological impact of postpartum maternal depression. *Child Adolesc Psychiatr Clin North Am*. 2016;25(2):179–200. doi:10.1016/j.chc.2015.11.001
45. Slomian J, Honvo G, Emonts P, Reginster JY, Bruyère O. Consequences of maternal postpartum depression: A systematic review of maternal and infant outcomes. *Womens Health (Lond Engl)*. 2019;15:1745506519844044. doi:10.1177/1745506519844044
46. Rogers A, Obst S, Teague SJ, et al. Association between maternal perinatal depression and anxiety and child and adolescent development: A meta-analysis. *JAMA Pediatr*. 2020;174(11):1082. doi:10.1001/jamapediatrics.2020.2910
47. Chen C, Okawa S, Okubo R, et al. Mother-to-infant bonding difficulties are associated with future maternal depression and child-maltreatment behaviors: A Japanese nationwide longitudinal study. *Psychiatry Res*. 2024;334:115814. doi:10.1016/j.psychres.2024.115814
48. Le Bas GA, Youssef GJ, Macdonald JA, et al. The role of antenatal and postnatal maternal bonding in infant development: A systematic review and meta-analysis. *Soc Dev*. 2020;29(1):3–20. doi:10.1111/sode.12392
49. Le Bas GA, Youssef GJ, Macdonald JA, et al. Maternal bonding, negative affect, and infant social-emotional development: A prospective cohort study. *J Affect Disord*. 2021;281:926–934. doi:10.1016/j.jad.2020.11.031
50. Murakami K, Noda A, Ishikuro M, et al. Maternal postnatal bonding disorder and developmental delays in children: The Tohoku Medical Megabank Project Birth and Three-Generation Cohort Study. *Arch Womens Ment Health*. 2023;26(2):219–226. doi:10.1007/s00737-023-01298-0
51. Cox JL, Holden JM, Sagovsky R. Detection of postnatal depression: Development of the 10-item Edinburgh Postnatal Depression Scale. *Br J Psychiatry*. 1987;150(6):782–786. doi:10.1192/bjp.150.6.782
52. Moyer SW, Brown R, Jallo N, Kinser PA. Scoping review of the use of the Edinburgh Postnatal Depression Scale in the United States. *J Womens Health (Larchmt)*. 2023;32(7):767–778. doi:10.1089/jwh.2022.0520
53. Moyer SW, Ameringer S, Elswick RK, Nunziato JD, Kinser PA. Exploration of the psychometric properties of the EPDS-US: A validation study. *J Affect Disord*. 2024;352:193–198. doi:10.1016/j.jad.2024.02.025
54. Fellmeth G, Harrison S, McNeill J, Lynn F, Redshaw M, Alderdice F. Identifying postnatal anxiety: Comparison of self-identified and self-reported anxiety using the Edinburgh Postnatal Depression Scale. *BMC Pregnancy Childbirth*. 2022;22(1):180. doi:10.1186/s12884-022-04437-0
55. Chen C, Mochizuki Y, Asai Y, et al. Determining the optimal cutoff point for the Japanese Mother-to-Infant Bonding Scale: A data-driven approach. *Asian J Psychiatry*. 2024;91:103874. doi:10.1016/j.ajp.2023.103874
56. Amani B, Merza D, Savoy C, et al. Peer-delivered cognitive-behavioral therapy for postpartum depression: A randomized controlled trial. *J Clin Psychiatry*. 2021;83(1):21m13928. doi:10.4088/JCP.21m13928
57. Stein A, Netsi E, Lawrence PJ, et al. Mitigating the effect of persistent postnatal depression on child outcomes through an intervention to treat depression and improve parenting: A randomised controlled trial. *Lancet Psychiatry*. 2018;5(2):134–144. doi:10.1016/S2215-0366(18)30006-3
58. Hoffmann EV, Duarte CS, Matsuzaka CT, et al. The positive impact of maternal depression intervention on children's emotional and behavioral symptoms in a low-resource setting. *Braz J Psychiatry*. 2022;44(6):590–601. doi:10.47626/1516-4446-2022-2498
59. Aktar E, Qu J, Lawrence PJ, Tollenaar MS, Elzinga BM, Bögels SM. Fetal and infant outcomes in the offspring of parents with perinatal mental disorders: Earliest influences. *Front Psychiatry*. 2019;10:391. doi:10.3389/fpsy.2019.00391
60. Kumar D, Hameed W, Avan BI. Comparing the effectiveness of mother-focused interventions to that of mother-child focused interventions in improving maternal postpartum depression outcomes: A systematic review. *PLoS One*. 2023;18(12):e0295955. doi:10.1371/journal.pone.0295955
61. Li X, Laplante DP, Paquin V, Lafortune S, Elgbeili G, King S. Effectiveness of cognitive behavioral therapy for perinatal maternal depression, anxiety and stress: A systematic review and meta-analysis of randomized controlled trials. *Clin Psychol Rev*. 2022;92:102129. doi:10.1016/j.cpr.2022.102129
62. Loh AHY, Ong LL, Yong FSH, Chen HY. Improving mother-infant bonding in postnatal depression: The SURE MUMS study. *Asian J Psychiatry*. 2023;81:103457. doi:10.1016/j.ajp.2023.103457
63. Ji M, Li R, Xu Y. Meta-analysis of the effect of different exercise modalities in the prevention and treatment of perinatal depression. *J Affect Disord*. 2024;350:442–451. doi:10.1016/j.jad.2024.01.076
64. Chen C, Nakagawa S. Recent advances in the study of the neurobiological mechanisms behind the effects of physical activity on mood, resilience and emotional disorders. *Adv Clin Exp Med*. 2023;32(9):937–942. doi:10.17219/acem/171565
65. Hall K, Barnes C, Duggan L, et al. The applicability of nature-based interventions to support mothers' postnatal wellbeing: A conceptual review. *Wellbeing Space Society*. 2024;6:100187. doi:10.1016/j.wss.2024.100187
66. Mizumoto T, Ikei H, Hagiwara K, et al. Mood and physiological effects of visual stimulation with images of the natural environment in individuals with depressive and anxiety disorders. *J Affect Disord*. 2024;356:257–266. doi:10.1016/j.jad.2024.04.025
67. Watarai M, Hagiwara K, Mochizuki Y, et al. Toward a computational understanding of how reminiscing about positive autobiographical memories influences decision-making under risk. *Cogn Affect Behav Neurosci*. 2023;23(5):1365–1373. doi:10.3758/s13415-023-01117-0
68. Rohde J, Meine LE, Brown AD, Kleim B. The impact of momentary stress on autobiographical memory recall in a self-efficacy intervention. *Sci Rep*. 2024;14(1):29864. doi:10.1038/s41598-024-80896-z
69. Vinker S. Innovations in family medicine and the implication to rural and remote primary care. *Adv Clin Exp Med*. 2023;32(2):147–150. doi:10.17219/acem/158171
70. Cunningham K, Märginean V, Hylock R. Navigating promise and perils: applying artificial intelligence to the perinatal mental health care cascade. *NPJ Health Syst*. 2025;2(1):26. doi:10.1038/s44401-025-00030-7
71. Webb R, Uddin N, Ford E, et al. Barriers and facilitators to implementing perinatal mental health care in health and social care settings: A systematic review. *Lancet Psychiatry*. 2021;8(6):521–534. doi:10.1016/S2215-0366(20)30467-3
72. Parfitt Y, Pike A, Ayers S. Infant developmental outcomes: A family systems perspective. *Infant Child Dev*. 2014;23(4):353–373. doi:10.1002/icd.1830

Stromal cells as a part of tumor microenvironment of melanoma: Their role in cancer progression and drug resistance

Rafał Matkowski^{1,2,A–F}, Aleksandra Simiczjew^{3,A–F}, Marcin Ziętek^{1,2,A–F}, Dorota Nowak^{3,A–F}

¹ Department of Oncology, Faculty of Medicine, Wrocław Medical University, Poland

² Lower Silesian Oncology, Pulmonology and Hematology Center, Wrocław, Poland

³ Department of Cell Pathology, Faculty of Biotechnology, University of Wrocław, Poland

A – research concept and design; B – collection and/or assembly of data; C – data analysis and interpretation;

D – writing the article; E – critical revision of the article; F – final approval of the article

Advances in Clinical and Experimental Medicine, ISSN 1899–5276 (print), ISSN 2451–2680 (online)

Adv Clin Exp Med. 2025;34(12):2005–2009

Address for correspondence

Rafał Matkowski

E-mail: rafal.matkowski@umw.edu.pl

Funding sources

None declared

Conflict of interest

None declared

Acknowledgements

This work was supported by a Team Award for Scientific Achievements granted by the Minister of Science and Higher Education in 2025.

Received on August 25, 2025

Reviewed on October 2, 2025

Accepted on October 10, 2025

Published online on November 5, 2025

Abstract

Today, it is well established that the tumor microenvironment (TME), the tumor niche, along with melanoma cells, plays a crucial role in cancer dissemination and influences the effectiveness of anticancer therapies. Therefore, it may serve as a potential therapeutic target in melanoma treatment. In our research, we focused on the effects exerted by cells within the melanoma microenvironment on cancer progression and the development of therapy resistance. Specifically, we examined stromal cells accompanying melanoma cells in the tumor – cancer-associated fibroblasts (CAFs), cancer-associated keratinocytes (CAKs), and cancer-associated adipocytes (CAAs). Particular attention was given to keratinocytes, as their role in the melanoma microenvironment remains the least understood.

Key words: melanoma, drug resistance, stromal cells, microenvironment, signaling pathways

Cite as

Matkowski R, Simiczjew A, Ziętek M, Nowak D. Stromal cells as a part of tumor microenvironment of melanoma: Their role in cancer progression and drug resistance. *Adv Clin Exp Med.* 2025;34(12):2005–2009. doi:10.17219/acem/211897

DOI

10.17219/acem/211897

Copyright

Copyright by Author(s)

This is an article distributed under the terms of the Creative Commons Attribution 3.0 Unported (CC BY 3.0) (<https://creativecommons.org/licenses/by/3.0/>)

Highlights

- The melanoma tumor microenvironment (TME) plays a critical role in cancer progression, metastasis, and resistance to anticancer therapies.
- Stromal cells, including cancer-associated fibroblasts (CAFs), keratinocytes (CAKs), and adipocytes (CAAs), actively influence melanoma cell behavior and therapeutic outcomes.
- The study emphasizes the underexplored role of keratinocytes in the melanoma microenvironment and their contribution to tumor growth and drug resistance.
- Understanding cell–cell interactions within the melanoma niche may provide new molecular targets for personalized melanoma therapy.

Introduction

Melanoma originates from pigment-producing cells, melanocytes, and is characterized by the highest mortality rate among skin cancers. One of the most significant risk factors for melanoma is prolonged exposure to ultraviolet (UV) radiation. In healthy skin, melanocytes interact with keratinocytes and other neighboring cells to protect DNA from UV-induced damage, primarily through melanin-dependent mechanisms.¹

Mutations in genes encoding proteins associated with the mitogen-activated protein kinase (MAPK) pathway, such as serine/threonine-protein kinase B-Raf (BRAF) and NRAS, account for approx. 70% of genetic aberrations induced by UV irradiation.² A mutation in the BRAF gene (BRAF V600E) occurs in about 50% of melanoma patients and results in a constitutively active kinase.^{3,4} Several targeted therapies against melanoma-specific molecular markers, including mutated BRAF, are currently used in clinical practice. Nevertheless, resistance to these drugs often develops rapidly in treated patients.^{5,6} For all patients with invasive cutaneous melanoma, surgical excision of the primary tumor with 1–2 cm margins remains the standard of oncologic management. Sentinel lymph node biopsy (SLNB) is recommended for patients with T1b or more advanced melanoma (tumor thickness >0.8 mm or any tumor with ulceration).⁷ In patients with sentinel lymph node micrometastasis, complete lymph node dissection (CLND) is no longer performed, based on the findings of the DeCOG and MSLT-II clinical trials.⁸ Instead of extensive surgical intervention, systemic adjuvant therapy has proven more effective in improving disease-free survival (DFS) and overall survival (OS). High-risk stage IIB/C melanoma (T3b–T4b tumors with negative SLNB) is currently also an indication for 1 year of adjuvant immunotherapy with pembrolizumab or nivolumab (anti-PD-1 agents).^{9,10} In patients with clinically detected metastatic lymph nodes or skin in-transit metastases (resectable stage III), the standard of care includes therapeutic lymph node dissection (TLND) or resection of in-transit tumors, followed by 1 year of adjuvant systemic treatment with either targeted therapy (dabrafenib and trametinib

– BRAF/MEK inhibitors) or immunotherapy (pembrolizumab or nivolumab – anti-PD-1). New systemic adjuvant therapies improve OS and relapse-free survival (RFS) by approx. 20%.^{11–13}

Before the advent of immunotherapies and targeted therapies, chemotherapy was the only treatment option for patients with stage IV melanoma (disseminated disease) and was associated with very poor outcomes. Today, it is used only in patients who are resistant to modern systemic treatments.¹⁴ For patients with unresectable stage III melanoma (metastatic lymph nodes or skin metastases) or stage IV disease, several systemic treatment options are available, similar to those used in the adjuvant setting. In BRAF-mutated patients, either immunotherapy or targeted therapy may be employed, whereas in BRAF wild-type patients, immunotherapy remains the standard of care. The combination of nivolumab and ipilimumab has demonstrated superiority over either agent used as monotherapy, providing a durable survival benefit in terms of progression-free survival (PFS) and melanoma-specific survival (MSS).^{15,16} Radiotherapy may also be effective for melanoma patients with bone or brain metastases, although its use is limited to palliative settings.^{17,18}

Among the factors influencing the effectiveness of anticancer therapy is the tumor microenvironment (TME). Solid tumors are composed not only of malignant cells but also of various nonmalignant components within the tumor niche, including keratinocytes, cancer-associated fibroblasts (CAFs), immune cells, and adipocytes.^{19,20} Additional elements, such as the composition of the extracellular matrix (ECM) and physical factors like hypoxia, must also be considered.^{21–23} The TME exerts diverse effects on melanoma progression and the development of therapy resistance. Initially, the TME may act as a physical barrier that limits drug delivery to cancer cells.²⁴ In addition, stromal cells within the melanoma TME can promote tumor growth and enhance its invasive and angiogenic potential through paracrine signaling. These cells secrete growth factors, cytokines and chemokines that influence not only neighboring cells within the niche but also distant sites in the body.²⁵ Moreover, they produce matrix metalloproteinases (MMPs), which degrade ECM

components, thereby creating pathways that facilitate cancer cell invasion through surrounding tissues.²⁶ Cells within the TME can also secrete high-energy metabolites that are subsequently utilized by melanoma cells.²⁷ Finally, immune cells, while initially contributing to the elimination of malignantly transformed cells, begin, during tumor progression, to facilitate immune evasion by melanoma cells. This occurs through various mechanisms, including the secretion of proinflammatory factors, expression of inhibitory receptors and induction of pro-tumor immune cell phenotypes.²⁰

In our research, we focused on the effects of cells present in the melanoma microenvironment on cancer progression and the development of therapy resistance. In particular, we examined stromal cells accompanying melanoma cells in the tumor: CAFs, CAKs and CAAs. Special attention was given to keratinocytes, as their role in the melanoma microenvironment remains the least understood.

Keratinocytes play a protective role toward melanocytes in healthy skin; however, their interactions with cancer cells following melanomagenesis remain poorly understood. Under physiological conditions, keratinocytes regulate melanocyte proliferation through paracrine signaling and direct interactions mediated by E-cadherin-dependent cell–cell adhesion.^{19,28} During melanoma development, E-cadherin expression decreases, while N-cadherin expression increases, leading to the loss of keratinocyte-mediated control over melanocytes. As a result, melanocytes begin to interact with N-cadherin-expressing cells such as fibroblasts.¹⁶

The cadherin switch is regulated by transcription factors involved in the epithelial–mesenchymal transition (EMT), such as Snail, Twist and Slug, and may contribute to melanoma tumorigenesis.²⁹ Moreover, Hsu et al. demonstrated that restoring E-cadherin expression in melanoma cells reestablishes their connection with keratinocytes, thereby reducing melanoma cell growth.³⁰ In addition, keratinocytes exposed to UV radiation activate DNA repair pathways in melanocytes through the secretion of endothelin-1 (End-1) and α -melanocortin, thereby inhibiting melanocyte transformation into melanoma.³¹ Conversely, some studies suggest a pro-tumorigenic influence of keratinocytes on melanoma cells. It has been demonstrated that endothelin-1 secreted by keratinocytes activates caspase-8, which transiently binds to the E-cadherin/catenin complex in melanoma cells, leading to reduced E-cadherin expression and enhanced cancer cell invasion.³² Furthermore, extracellular End-1 has been shown to stimulate extracellular signal-regulated kinase (ERK) activation in melanoma cells treated with BRAF inhibitors. Moreover, End-1 expression is influenced by the level of melanocyte-inducing transcription factor (MITF). Overexpression of MITF enhances End-1 production, whereas its depletion is associated with End-1 downregulation. Furthermore, inhibition of endothelin receptor B increases the sensitivity of BRAF inhibitor-resistant melanoma

cells to treatment.^{19,33} Additionally, under the influence of fibroblast-derived keratinocyte growth factor (KGF), keratinocytes secrete the c-KIT ligand, stem cell factor (SCF), which subsequently activates the protein kinase B (AKT) and MAPK pathways, regulating cancer cell invasion and proliferation.³⁴ Reports on the effects of melanoma on keratinocytes are scarce. One such study demonstrated alterations in the levels of intermediate filament proteins – cytokeratins – associated with the differentiation status of keratinocytes.^{35,36} Cytokeratin 10 (CK10) is expressed in suprabasal keratinocytes undergoing cornification and desquamation, whereas cytokeratin 14 (CK14) is highly expressed in rapidly proliferating basal keratinocytes. Kodet et al. demonstrated that melanoma cells alter cytokeratin expression profiles in keratinocytes, leading to upregulation of CK14 and downregulation of CK10.³⁷ Our findings indicate that keratinocytes activated through indirect co-culture with melanoma cells or incubation with melanoma-conditioned medium exhibit characteristics of less differentiated cells, including decreased CK10 expression, and show a preference for interacting with cancer cells rather than with other keratinocytes, likely due to reduced E-cadherin levels. Activated keratinocytes secrete a wide range of proteases, several of which, such as matrix metalloproteinase 3 (MMP3), were first identified by our group as components of the activated keratinocyte secretome. These keratinocytes display high proteolytic activity, characterized by increased activity of MMP9 and MMP14 and decreased expression of tissue inhibitors of metalloproteinases (TIMPs). They also exhibit elevated ERK activity and increased levels of MMP expression regulators, including runt-related transcription factor 2 (RUNX2) and galectin-3. Furthermore, cancer-associated keratinocytes (CAKs) demonstrate enhanced migratory and invasive abilities following co-culture with melanoma cells in Transwell assays.³⁷

Fibroblasts represent the most abundant cell population within the melanoma niche, comprising up to 80% of the tumor mass.³⁸ In our study, we utilized 4 melanoma cell lines differing in invasiveness: 2 derived from primary tumors (WM1341D and A375) and 2 from lymph node metastases (WM9 and Hs294T). Importantly, when comparing the effects of these melanoma cells on fibroblast characteristics, we considered both their origin and invasive potential. An earlier study by Makowiecka et al.³⁹ demonstrated that A375, WM9 and Hs294T cells exhibit higher rates of migration, invasion and proteolytic activity, as well as greater invadopodia formation, compared with WM1341D cells. Therefore, we classified the WM1341D cell line as less aggressive, while A375, WM9 and Hs294T were considered highly aggressive melanoma cell lines. We observed that fibroblasts co-cultured with melanoma cells exhibited increased motility, enhanced proteolytic activity and elevated secretion of several cytokines, lactate and angiogenesis-related proteins. The observed alterations in CAF biology were primarily induced by the highly

aggressive melanoma cell lines (A375, WM9 and Hs294T), rather than by the less aggressive WM1341D line.⁴⁰ These CAF-associated features can promote melanoma invasion and contribute to angiogenesis, inflammation and acidification of the TME. Adipocytes, another cellular component of the melanoma niche, are located in the deepest layer of the skin. The interactions between adipocytes and melanoma cells remain poorly understood, and the influence of obesity on melanoma progression is still controversial.⁴¹ Cancer-associated adipocytes (CAAs) were obtained by differentiating 3T3-L1 preadipocytes into mature adipocytes according to the protocol described by Zebisch et al.⁴² Subsequently, mature adipocytes were co-cultured with melanoma cells using Transwell inserts. The transformation of adipocytes into CAAs was evaluated based on the expression of markers characteristic of differentiated adipocytes, which are typically reduced in CAAs. We also observed that melanoma-associated adipocytes exhibited decreased levels of adipogenesis markers and a reduced number of lipid droplets. Moreover, we observed that adipocytes exposed to melanoma cells undergo dedifferentiation into fibroblast-like cells. Cancer-associated adipocytes also exhibited significantly increased lactate release and upregulated expression of transporters for lactate, H⁺ ions and glucose, likely reflecting substantial metabolic reprogramming within the TME. The secreted lactate may serve as an energy source for melanoma cells, thereby promoting their proliferation. Concurrently, CAAs showed enhanced activation of specific signaling pathways, including extracellular signal-regulated kinase (ERK) and signal transducer and activator of transcription 3 (STAT3), along with decreased secretion of angiogenesis-related factors.⁴³


Conclusions

In the past, cancer cells were considered the sole target of anticancer therapy. Today, it is well recognized that cells within the tumor niche also play a crucial role in cancer dissemination. These cells influence cancer behavior both through paracrine signaling and direct cell–cell interactions. Notably, all of the described cell types contribute to the development of drug resistance and may therefore represent potential therapeutic targets in melanoma treatment.

Use of AI and AI-assisted technologies

Not applicable.

ORCID iDs

Rafał Matkowski  <https://orcid.org/0000-0002-1705-5097>
 Aleksandra Simiczyjew  <https://orcid.org/0000-0002-6060-2375>
 Marcin Ziętek  <https://orcid.org/0000-0002-7890-3483>
 Dorota Nowak  <https://orcid.org/0000-0002-6426-1686>

References

- Williams PF, Olsen CM, Hayward NK, Whiteman DC. Melanocortin 1 receptor and risk of cutaneous melanoma: A meta-analysis and estimates of population burden. *Int J Cancer*. 2011;129(7):1730–1740. doi:10.1002/ijc.25804
- Davis LE, Shalin SC, Tackett AJ. Current state of melanoma diagnosis and treatment. *Cancer Biol Ther*. 2019;20(11):1366–1379. doi:10.1080/15384047.2019.1640032
- Rebecca VW, Sondak VK, Smalley KSM. A brief history of melanoma: From mummies to mutations. *Melanoma Res*. 2012;22(2):114–122. doi:10.1097/CMR.0b013e328351fa4d
- Schreck KC, Grossman SA, Pratilas CA. BRAF mutations and the utility of RAF and MEK inhibitors in primary brain tumors. *Cancers (Basel)*. 2019;11(9):1262. doi:10.3390/cancers11091262
- Luebker SA, Koepsell SA. Diverse mechanisms of BRAF inhibitor resistance in melanoma identified in clinical and preclinical studies. *Front Oncol*. 2019;9:268. doi:10.3389/fonc.2019.00268
- Kim A, Cohen MS. The discovery of vemurafenib for the treatment of BRAF-mutated metastatic melanoma. *Exp Opin Drug Discov*. 2016;11(9):907–916. doi:10.1080/17460441.2016.1201057
- Garbe C, Amaral T, Peris K, et al. European consensus-based interdisciplinary guideline for melanoma. Part 2. Treatment: Update 2019. *Eur J Cancer*. 2020;126:159–177. doi:10.1016/j.ejca.2019.11.015
- Wong SL, Faries MB, Kennedy EB, et al. Sentinel lymph node biopsy and management of regional lymph nodes in melanoma: American Society of Clinical Oncology and Society of Surgical Oncology Clinical Practice Guideline Update. *J Clin Oncol*. 2018;36(4):399–413. doi:10.1200/JCO.2017.75.7724
- Kirkwood JM, Del Vecchio M, Weber J, et al. Adjuvant nivolumab in resected stage IIB/C melanoma: Primary results from the randomized, phase 3 CheckMate 76K trial. *Nat Med*. 2023;29(11):2835–2843. doi:10.1038/s41591-023-02583-2
- Luke JJ, Rutkowski P, Queirolo P, et al. Pembrolizumab versus placebo as adjuvant therapy in completely resected stage IIB or IIC melanoma (KEYNOTE-716): A randomised, double-blind, phase 3 trial. *Lancet*. 2022;399(10336):1718–1729. doi:10.1016/S0140-6736(22)00562-1
- Long GV, Hauschild A, Santinami M, et al. Adjuvant dabrafenib plus trametinib in stage III BRAF-mutated melanoma. *N Engl J Med*. 2017;377(19):1813–1823. doi:10.1056/NEJMoa1708539
- Eggermont AMM, Blank CU, Mandala M, et al. Adjuvant pembrolizumab versus placebo in resected stage III melanoma. *N Engl J Med*. 2018;378(19):1789–1801. doi:10.1056/NEJMoa1802357
- Weber J, Mandala M, Del Vecchio M, et al. Adjuvant nivolumab versus ipilimumab in resected stage III or IV melanoma. *N Engl J Med*. 2017;377(19):1824–1835. doi:10.1056/NEJMoa1709030
- Goldinger SM, Buder-Bakhaya K, Lo SN, et al. Chemotherapy after immune checkpoint inhibitor failure in metastatic melanoma: A retrospective multicentre analysis. *Eur J Cancer*. 2022;162:22–33. doi:10.1016/j.ejca.2021.11.022
- Hodi FS, Chiarion-Sileni V, Gonzalez R, et al. Nivolumab plus ipilimumab or nivolumab alone versus ipilimumab alone in advanced melanoma (CheckMate 067): 4-year outcomes of a multicentre, randomised, phase 3 trial. *Lancet Oncol*. 2018;19(11):1480–1492. doi:10.1016/S1470-2045(18)30700-9
- Wolchok JD, Chiarion-Sileni V, Rutkowski P, et al. Final, 10-year outcomes with nivolumab plus ipilimumab in advanced melanoma. *N Engl J Med*. 2025;392(1):11–22. doi:10.1056/NEJMoa2407417
- Rate WR, Solin LJ, Turrisi AT. Palliative radiotherapy for metastatic malignant melanoma: Brain metastases, bone metastases, and spinal cord compression. *Int J Radiat Oncol Biol Phys*. 1988;15(4):859–864. doi:10.1016/0360-3016(88)90118-6
- Garsa A, Jang JK, Baxi S, et al. Radiation therapy for brain metastases: A systematic review. *Pract Radiat Oncol*. 2021;11(5):354–365. doi:10.1016/j.prro.2021.04.002
- Mazurkiewicz J, Simiczyjew A, Dratkiewicz E, Ziętek M, Matkowski R, Nowak D. Stromal cells present in the melanoma niche affect tumor invasiveness and its resistance to therapy. *Int J Mol Sci*. 2021;22(2):529. doi:10.3390/ijms22020529
- Simiczyjew A, Dratkiewicz E, Mazurkiewicz J, Ziętek M, Matkowski R, Nowak D. The influence of tumor microenvironment on immune escape of melanoma. *Int J Mol Sci*. 2020;21(21):8359. doi:10.3390/ijms21218359

21. Dratkiewicz E, Simiczyjew A, Mazurkiewicz J, Ziętek M, Matkowski R, Nowak D. Hypoxia and extracellular acidification as drivers of melanoma progression and drug resistance. *Cells*. 2021;10(4):862. doi:10.3390/cells10040862
22. Ruiter D, Bogenrieder T, Elder D, Herlyn M. Melanoma-stroma interactions: Structural and functional aspects. *Lancet Oncol*. 2002;3(1):35–43. doi:10.1016/s1470-2045(01)00620-9
23. Gurzu S, Beleaua MA, Jung I. The role of tumor microenvironment in development and progression of malignant melanomas: A systematic review. *Rom J Morphol Embryol*. 2018;59(1):23–28. PMID:29940608.
24. Sriraman SK, Aryasomayajula B, Torchilin VP. Barriers to drug delivery in solid tumors. *Tissue Barriers*. 2014;2(3):e29528. doi:10.4161/tisb.29528
25. Labrousse AL, Ntayi C, Hornebeck W, Bernard P. Stromal reaction in cutaneous melanoma. *Crit Rev Oncol Hematol*. 2004;49(3):269–275. doi:10.1016/j.critrevonc.2003.10.007
26. Shiga K, Hara M, Nagasaki T, Sato T, Takahashi H, Takeyama H. Cancer-associated fibroblasts: Their characteristics and their roles in tumor growth. *Cancers (Basel)*. 2015;7(4):2443–2458. doi:10.3390/cancers7040902
27. Shu SL, Yang Y, Allen CL, et al. Metabolic reprogramming of stromal fibroblasts by melanoma exosome microRNA favours a pre-metastatic microenvironment. *Sci Rep*. 2018;8(1):12905. doi:10.1038/s41598-018-31323-7
28. Wang JX, Fukunaga-Kalabis M, Herlyn M. Crosstalk in skin: Melanocytes, keratinocytes, stem cells, and melanoma. *J Cell Commun Signal*. 2016;10(3):191–196. doi:10.1007/s12079-016-0349-3
29. Kuphal S, Bosserhoff AK. E-cadherin cell–cell communication in melanogenesis and during development of malignant melanoma. *Arch Biochem Biophys*. 2012;524(1):43–47. doi:10.1016/j.abb.2011.10.020
30. Hsu MY, Meier FE, Nesbit M, et al. E-cadherin expression in melanoma cells restores keratinocyte-mediated growth control and down-regulates expression of invasion-related adhesion receptors. *Am J Pathol*. 2000;156(5):1515–1525. doi:10.1016/S0002-9440(10)65023-7
31. Swope VB, Starner RJ, Rauck C, Abdel-Malek ZA. Endothelin-1 and α -melanocortin have redundant effects on global genome repair in UV-irradiated human melanocytes despite distinct signaling pathways. *Pigment Cell Melanoma Res*. 2020;33(2):293–304. doi:10.1111/pcmr.12823
32. Jamal S, Schneider RJ. UV-induction of keratinocyte endothelin-1 down-regulates E-cadherin in melanocytes and melanoma cells. *J Clin Invest*. 2002;110(4):443–452. doi:10.1172/JCI0213729
33. Smith MP, Rowling EJ, Miskolczi Z, et al. Targeting endothelin receptor signalling overcomes heterogeneity driven therapy failure. *EMBO Mol Med*. 2017;9(8):1011–1029. doi:10.15252/emmm.201607156
34. Belleudi F, Cardinali G, Kovacs D, Picardo M, Torrisi MR. KGF promotes paracrine activation of the SCF/c-KIT axis from human keratinocytes to melanoma cells. *Transl Oncol*. 2010;3(2):80–90. doi:10.1593/tlo.09196
35. Alam H, Sehgal L, Kundu ST, Dalal SN, Vaidya MM. Novel function of keratins 5 and 14 in proliferation and differentiation of stratified epithelial cells. *Mol Biol Cell*. 2011;22(21):4068–4078. doi:10.1091/mbc.e10-08-0703
36. Kodet O, Lacina L, Krejčí E, et al. Melanoma cells influence the differentiation pattern of human epidermal keratinocytes. *Mol Cancer*. 2015;14(1):1. doi:10.1186/1476-4598-14-1
37. Mazurkiewicz J, Simiczyjew A, Dratkiewicz E, et al. Melanoma stimulates the proteolytic activity of HaCaT keratinocytes. *Cell Commun Signal*. 2022;20(1):146. doi:10.1186/s12964-022-00961-w
38. Gascard P, Tlsty TD. Carcinoma-associated fibroblasts: Orchestrating the composition of malignancy. *Genes Dev*. 2016;30(9):1002–1019. doi:10.1101/gad.279737.116
39. Makowiecka A, Simiczyjew A, Nowak D, Mazur AJ. Varying effects of EGF, HGF and TGF β on formation of invadopodia and invasiveness of melanoma cell lines of different origin. *Eur J Histochem*. 2016;60(4):2728. doi:10.4081/ejh.2016.2728
40. Mazurkiewicz J, Simiczyjew A, Dratkiewicz E, et al. Melanoma cells with diverse invasive potential differentially induce the activation of normal human fibroblasts. *Cell Commun Signal*. 2022;20(1):63. doi:10.1186/s12964-022-00871-x
41. Smith LK, Arabi S, Lelliott EJ, McArthur GA, Sheppard KE. Obesity and the impact on cutaneous melanoma: Friend or foe? *Cancers (Basel)*. 2020;12(6):1583. doi:10.3390/cancers12061583
42. Zebisch K, Voigt V, Wabitsch M, Brandsch M. Protocol for effective differentiation of 3T3-L1 cells to adipocytes. *Anal Biochem*. 2012;425(1):88–90. doi:10.1016/j.ab.2012.03.005
43. Simiczyjew A, Wądryńska J, Pietraszek-Gremplewicz K, et al. Melanoma cells induce dedifferentiation and metabolic changes in adipocytes present in the tumor niche. *Cell Mol Biol Lett*. 2023;28(1):58. doi:10.1186/s11658-023-00476-3

Community-acquired pneumonia in HIV-infected patients: Updated insights on epidemiology and etiology

Martyna Biała^{A–F}, Brygida Knysz^{D–F}

Department of Infectious Diseases, Liver Diseases and Acquired Immune Deficiencies, Wrocław Medical University, Poland

A – research concept and design; B – collection and/or assembly of data; C – data analysis and interpretation;

D – writing the article; E – critical revision of the article; F – final approval of the article

Advances in Clinical and Experimental Medicine, ISSN 1899–5276 (print), ISSN 2451–2680 (online)

Adv Clin Exp Med. 2025;34(12):2011–2016

Address for correspondence

Martyna Biała

E-mail: martyna.biala@umw.edu.pl

Funding sources

None declared

Conflict of interest

None declared

Received on May 8, 2025

Reviewed on August 15, 2025

Accepted on September 4, 2025

Published online on October 29, 2025

Abstract

Bacterial pneumonia is a cause of HIV-associated morbidity and mortality. Recurrent pneumonia, defined as 2 or more episodes within a 12-month period, is an AIDS-defining illness. The prevalence of bacterial pulmonary infections in HIV-infected patients has been decreasing with the introduction and widespread use of antiretroviral therapy. In well-developed settings, the frequency of bacterial pneumonia in people living with HIV is comparable to that in the general population. Studies have shown that the cumulative incidence of pneumonia is higher in HIV-infected patients with advanced immunosuppression, airflow limitation, smoking, intravenous drug use, or in those from underdeveloped countries and urban areas. In HIV-infected patients with community-acquired bacterial pneumonia, *Streptococcus pneumoniae* and *Haemophilus* species are the most frequently isolated pathogens. However, in untreated or poorly adherent HIV-infected individuals, opportunistic infections may occur. Although the incidence of opportunistic infections among HIV-infected patients has declined in well-developed settings due to the widespread use of antiretroviral therapy, tuberculosis remains a serious threat and a major cause of morbidity and mortality among HIV-infected individuals worldwide. Early diagnosis of HIV infection, timely initiation of antiretroviral therapy with good adherence, and promotion of vaccination remain priorities. This editorial provides an overview of community-acquired pneumonia in HIV-infected patients and discusses recent changes in its epidemiology and etiology.

Key words: infection, HIV, community-acquired pneumonia

Cite as

Biała M, Knysz B. Community-acquired pneumonia in HIV-infected patients: Updated insights on epidemiology and etiology. *Adv Clin Exp Med.* 2025;34(12):2011–2016. doi:10.17219/acem/210307

DOI

10.17219/acem/210307

Copyright

Copyright by Author(s)

This is an article distributed under the terms of the Creative Commons Attribution 3.0 Unported (CC BY 3.0) (<https://creativecommons.org/licenses/by/3.0/>)

Highlights

- Bacterial pneumonia remains one of a major causes of morbidity and mortality among HIV-infected patients.
- The introduction of antiretroviral therapy (ART) has significantly lowered bacterial pulmonary infection rates in HIV-positive individuals, bringing them closer to those of the general population in developed regions.
- *Streptococcus pneumoniae* and *Haemophilus* species are the predominant bacterial pathogens, while opportunistic infections continue to pose serious risks in untreated or non-adherent HIV patients.
- Early HIV detection, prompt ART initiation, therapy adherence, and vaccination programs are essential strategies to reduce pneumonia incidence and improve clinical outcomes in HIV-related lung disease.

Introduction

The prevalence of bacterial pulmonary infections in HIV-infected patients has decreased with the introduction and widespread use of antiretroviral therapy. In well-developed settings, the frequency of bacterial pneumonia among people living with HIV is now comparable to that in the general population.¹

A study conducted in a Swiss cohort demonstrated that the incidence of bacterial pneumonia declined from 13.2 to 6.8 cases per 1,000 person-years between 2008 and 2018 in HIV-infected patients.² Another study reported an incidence rate of pneumonia of 5.5 cases per 1,000 person-years among people living with HIV in Denmark.³ In comparison, in the French adult population, the estimated incidence rate of outpatient community-acquired pneumonia was 4.7 cases per 1,000 inhabitants, rising to 6.7 cases per 1,000 among individuals aged 65 years or older.⁴ The reported annual incidence of community-acquired pneumonia in industrialized countries ranges from 1.19 to 8.7 cases per 1,000 inhabitants in general practice.⁴

This editorial provides an overview of community-acquired pneumonia in HIV-infected adult patients and discusses recent changes in its epidemiology and etiology. A comprehensive literature search was conducted across multiple databases (PubMed, Embase, Web of Science, Google Scholar, and UpToDate), including only peer-reviewed studies published in English.

Risk factors for community-acquired pneumonia in HIV-infected adults

The estimated global incidence of community-acquired pneumonia ranges from 1.5 to 14 cases per 1,000 person-years and is influenced by several factors, including geographical region, season, and population characteristics.^{5,6} However, studies have shown that the cumulative incidence of pneumonia is higher among HIV-infected patients with advanced immunosuppression, airflow limitation, smoking

habits, intravenous drug use, and among individuals from developing countries and urban areas.^{1,3,7}

Lower CD4 counts have been associated with a higher risk of bacterial pneumonia in people living with HIV. Kohli et al. reported that the incidence rates of bacterial pneumonia in HIV-infected patients with CD4 T-cell counts >500, 200–500 and <200 cells/mm³ were 4.9, 8.7 and 17.9 cases per 100 patient-years, respectively.⁸ Another study found that individuals with CD4 T cell counts of 350–499 cells/mm³ were at a higher risk of bacterial pneumonia compared with those whose CD4 T cell counts exceeded 500 cells/mm³.²

Compared with uninfected individuals, people living with HIV are more likely to develop chronic obstructive pulmonary disease (COPD) and to experience an earlier-than-expected decline in lung function.⁹ Factors contributing to these differences include higher smoking rates, chronic immune activation and inflammation, increased susceptibility to pulmonary infections associated with lower CD4 T-cell counts, accelerated aging, alterations in the lung and gut microbiome, and greater vulnerability to air pollution-related lung damage.⁹

Ronit et al. showed that HIV infection was independently associated with lower forced expiratory volume in 1 s (FEV₁) and forced vital capacity (FVC).¹⁰ Chronic obstructive pulmonary disease and lung function abnormalities are linked to an increased rate of severe pneumonia in HIV-infected patients.⁹ Drummond et al. evaluated spirometry results in individuals with HIV and found that nearly 40% of them exhibited abnormal spirometric patterns.¹¹ Airflow limitation was associated with a higher frequency of bacterial pneumonia and *Pneumocystis jirovecii* infection, as well as with smoking status and intensity, age, asthma diagnosis, and the presence of respiratory symptoms.¹¹ Smoking is more common among individuals with HIV, and HIV-infected smokers are more susceptible to smoking-induced lung damage compared with their uninfected counterparts.^{9,12–14}

It is estimated that smoking is associated with a 2- to 5-fold greater risk of bacterial pneumonia and invasive pneumococcal disease in individuals with HIV.¹ Intravenous drug users (IDUs) have a 10-fold higher risk of developing pneumonia compared to non-users.¹⁵ Among people

living with HIV, bacterial pneumonia is more common in those who are IDUs.¹⁶

Intravenous drug users have a substantially higher risk of pneumonia due to immunosuppression, poor nutrition, homelessness, and an increased risk of aspiration. Moreover, alcohol consumption, hazardous drinking, and alcohol dependence are associated with greater pneumonia severity among HIV-infected individuals.¹⁷ A summary of risk factors for community-acquired pneumonia in HIV-infected adults is presented in Table 1.

Table 1. Risk factors for community-acquired pneumonia in HIV-infected adults

Low CD4 T cell counts and unsuppressed HIV viral load
Coexisting airflow limitation (e.g., chronic obstructive pulmonary disease)
Other comorbidities affecting function of the immune system
Alterations which predispose to aspiration
Age over 65 years
Smoking
Intravenous drug use
Poor nutrition
Persons from undeveloped countries
City residents
Homelessness
Alcohol consumption
Lack of vaccinations
Poor dental hygiene

Epidemiology and etiologies of community-acquired pneumonia in HIV-infected patients

In people living with HIV who develop community-acquired bacterial pneumonia, *Streptococcus pneumoniae* and *Haemophilus* species are the most frequently isolated pathogens, similar to those found in the general population.^{1,18} Schleenvoigt et al. analyzed a German cohort with community-acquired pneumonia and found that *S. pneumoniae* was the most common pathogen isolated from both people living with HIV (21.3%) and the control group (17.2%), followed by *Haemophilus influenzae* (13.5% vs 12.6%, respectively).¹⁸

Interestingly, the same study found that *Staphylococcus aureus* was detected in 20.2% of samples from people living with HIV and in 19.2% of samples from the control group.¹⁸ However, distinguishing between *S. aureus* infection and colonization in this cohort was challenging, as positive sputum specimens and nasopharyngeal swabs were predominantly identified using multiplex polymerase chain reaction (PCR).¹⁸

The 6-month mortality rate in the German cohort was significantly higher among people living with HIV (6.8%) than in the control group (1.4%), although the authors noted that the number of cases was lower than previously reported.¹⁸ The opportunistic pathogen *P. jirovecii* was detected only rarely.¹⁸ Another study demonstrated that *S. pneumoniae* and *S. aureus* are among the most common bacterial coinfections in hospitalized patients with influenza.¹⁹

Previous studies from the early antiretroviral therapy era demonstrated that the prevalence of community-acquired pneumonia caused by *Pseudomonas aeruginosa* and *S. aureus* was higher among people living with HIV than among those without HIV infection.^{20,21} Risk factors associated with *P. aeruginosa* pneumonia include poorly controlled HIV infection, low CD4 T-cell counts, neutropenia, immunosuppression, malnutrition, coexisting lung disease, corticosteroid use, hospitalization within the past 90 days, mechanical ventilation or intensive care unit (ICU) admission, prior antimicrobial exposure, residence in a healthcare facility or nursing home, burns, malignancy, hemodialysis, organ transplantation, uncontrolled diabetes mellitus, and the presence of invasive devices such as indwelling catheters or endotracheal tubes.^{22,23}

Risk factors for *S. aureus* infection include IDUs, open wounds or sores, prior antimicrobial exposure, hospitalization within the past 90 days, ICU admission, immunosuppression, colonization with methicillin-resistant *S. aureus* (MRSA), invasive procedures, hemodialysis, corticosteroid use, residence in a healthcare facility or nursing home, diabetes mellitus, long-term central venous access or indwelling urinary catheter, and employment as a healthcare provider.^{23–25} Previous studies have also shown that community-acquired MRSA infections can be transmitted among men who have sex with men (MSM).²⁶

Globally, MSM are at greater risk of acquiring HIV and represent the main group of people living with HIV in many countries. A described community-acquired outbreak of MRSA infection among MSM most commonly manifested as infections of the buttocks, genitals or perineum.²⁶ However, skin and soft tissue infections caused by MRSA can progress to invasive diseases such as pneumonia and sepsis. Moreover, MRSA colonization is a known risk factor for the development of MRSA pneumonia, and studies have shown that MRSA nasal carriage and skin colonization occur more frequently in people living with HIV than in their seronegative counterparts.^{27,28}

Shet et al. indicated that cumulative prevalence of MRSA carriage was substantially higher in HIV-infected patients (16.8%) than among seronegative individuals (5.8%).²⁷ However, little up-to-date data are available on MRSA and *P. aeruginosa* as etiologic agents of community-acquired pneumonia in people living with HIV. Community outbreaks of MRSA, usually harboring Panton–Valentine leukocidin and associated with high morbidity and mortality, appear to be relatively rare.

In HIV-infected individuals without additional risk factors for *P. aeruginosa* or *S. aureus* infection, antibiotic regimens provide broad coverage against MRSA and *P. aeruginosa* does not seem to be obligatory. The most common pathogens cause community-acquired pneumonia in HIV-infected individuals in well-developed settings are the same as in seronegative counterparts and the antibiotic regimens in HIV-infected patients are also the same as those without HIV.²⁹

Compared with historical data, people living with HIV who have achieved virological suppression and maintain CD4 T-cell counts above 350 cells/mm³ are less likely to develop invasive pneumococcal disease. Moreover, they are now more likely to be vaccinated against *S. pneumoniae*.

Cillóniz et al. reported that people living with HIV who developed pneumonia caused by *S. pneumoniae* were more likely to have been vaccinated against influenza (14% vs 2%) and pneumococcal disease (10% vs 1%) compared with HIV-negative individuals with pneumococcal pneumonia.³⁰ Both groups (HIV-positive and HIV-negative) had similar rates of ICU admission (18% vs 27%), need for mechanical ventilation (12% vs 8%), length of hospital stay (7 days vs 7 days), and 30-day mortality (0%).³⁰

These data indicate that the need for hospitalization and clinical outcomes of pneumococcal pneumonia in virologically suppressed people living with HIV who have CD4 T-cell counts above 350 cells/mm³ are similar to those in the general population.³⁰ However, Mamani et al. reported a high incidence of invasive pneumococcal disease among people living with HIV with median CD4 T-cell counts below 350 cells/mm³ and found that alcoholism, hepatic cirrhosis and lower nadir CD4 T-cell count were associated with an increased risk of death.³¹ Moreover, the rate of vaccination against *S. pneumoniae* was low in this group.³¹ These findings emphasize that early diagnosis of HIV infection, adherence to antiretroviral therapy and promotion of vaccination remain priorities.

Atypical bacteria are intracellular organisms that are difficult to culture and not visible on Gram stain. The true incidence of pneumonia caused by atypical bacteria such as *Mycoplasma pneumoniae* and *Chlamydophila* spp. is unknown; however, these pathogens appear to be uncommon causes of community-acquired pneumonia in people living with HIV. In a Brazilian study examining the etiologic agents of community-acquired pulmonary infections in people living with HIV, *M. pneumoniae* was detected in 8% and *Chlamydophila pneumoniae* in 5% of cases.³² The majority of participants in this study had never used antiretroviral therapy, had discontinued treatment, or reported poor adherence. CD4 T-cell counts were available for 90% of these patients, and 73% had counts below 200 cells/mm³.³²

It is worth noting that the diagnosis of atypical pneumonia is particularly challenging in people living with HIV with advanced immunosuppression and may often go unrecognized. *Legionella* spp. infection is infrequent

and presents with a similar clinical course in people living with HIV and in seronegative individuals.³³ Respiratory viruses have been detected by molecular methods in approx. 1/3 of the general adult population with community-acquired pneumonia. However, the extent to which viral respiratory pathogens act as single causative agents, cofactors in the progression of bacterial pneumonia or triggers of a dysregulated immune response remains unclear.²⁹

Viruses are also frequently detected in people living with HIV, and some studies suggest that the mortality rate from influenza or COVID-19 may be higher in this population.^{34,35} Furthermore, the prevalence of severe acute respiratory infections caused by respiratory syncytial virus (RSV) is higher among people living with HIV and among individuals aged 65 years or older.³⁶

The prevalence of opportunistic pulmonary infections in people living with HIV has decreased with the use of antiretroviral therapy and varies across regions. Moreover, it depends on individual risk factors such as advanced immunosuppression related to HIV, malignancies, use of immunosuppressive agents, and long-term corticosteroid therapy. The incidence of *P. jirovecii* pneumonia has been significantly reduced by antiretroviral therapy and prophylaxis with trimethoprim–sulfamethoxazole.³⁷

However, Figueiredo-Mello et al. reported that among 143 people living with HIV who were untreated, had discontinued therapy, or demonstrated poor adherence to antiretroviral treatment, *P. jirovecii* was the most frequently detected pathogen (36%), followed by *Mycobacterium tuberculosis* (20%).³² Another study conducted in Cape Town, South Africa, included 284 people living with HIV (64% women) and found that 148 had culture-confirmed tuberculosis (TB), 100 had community-acquired pneumonia, and 26 had *P. jirovecii* pneumonia.³⁸

The median CD4 T-cell count in this cohort was 97 cells/mm³, and 38% of participants were receiving antiretroviral therapy.³⁸ Aspergillosis can also occur in people living with HIV, and many of these cases are associated with high mortality.³⁹

Although the incidence of opportunistic infections among people living with HIV has declined, particularly in well-developed countries, due to the widespread use of antiretroviral therapy, TB remains a serious threat and a leading cause of morbidity and mortality worldwide.⁴⁰ It is estimated that people living with HIV are 14 times more likely to develop TB and experience poorer treatment outcomes.⁴⁰ Moreover, people living with HIV are at higher risk of developing multidrug-resistant tuberculosis (MDR-TB).⁴¹ In 2020 and 2021, the COVID-19 pandemic slowed global TB control efforts due to widespread disruptions in healthcare and TB diagnostic services. In Europe, TB is more common among migrants from regions with high TB incidence and among individuals affected by social determinants such as poverty and homelessness, with the disease burden remaining particularly high in Eastern Europe.⁴²

Given the increased risk of TB in people living with HIV, TB should always be considered when assessing a patient's medical history, potential exposure, risk factors, and chest X-ray findings. Establishing the etiology of community-acquired pneumonia is essential to ensure appropriate therapy and to prevent the overuse of antibiotics.

Moreover, people living with HIV who have low CD4 T-cell counts are at higher risk of developing polymicrobial pneumonia, defined as infection caused by more than one pathogen.⁴³ Recent advances in microbiological diagnostics, particularly molecular techniques and MALDI-TOF mass spectrometry, have improved microorganism identification by reducing testing time and increasing sensitivity and specificity, thereby enabling faster, more accurate diagnosis and targeted treatment. However, interpretation of these results must always take the clinical context into account, as a positive test does not necessarily indicate an active infection.

Conclusions


In well-developed settings, the frequency of bacterial pneumonia among people living with HIV is comparable to that in the general population, and HIV infection alone does not appear to be a risk factor for increased mortality in community-acquired pneumonia, owing to effective antiretroviral therapy. However, in untreated individuals or those with poor adherence to antiretroviral therapy, opportunistic infections may still occur. Early diagnosis of HIV infection, timely initiation of antiretroviral therapy with good adherence, and promotion of vaccination remain key priorities.

Use of AI and AI-assisted technologies

Not applicable.

ORCID iDs

Martyna Biała  <https://orcid.org/0000-0002-5772-7839>

Brygida Knysz  <https://orcid.org/0000-0003-2605-1079>

References

- Lucas GM. Bacterial pulmonary infections in patients with HIV. Alphen aan den Rijn, the Netherlands: UpToDate (Wolters Kluwer Health); 2024. <https://www.uptodate.com/contents/bacterial-pulmonary-infections-in-patients-with-hiv>. Accessed April 18, 2025.
- Balakrishna S, Wolfensberger A, Kachalov V, et al. Decreasing incidence and determinants of bacterial pneumonia in people with HIV: The Swiss HIV Cohort Study. *J Infect Dis*. 2022;225(9):1592–1600. doi:10.1093/infdis/jiab573
- Heidari SL, Hove-Skovsgaard M, Arentoft NS, et al. Incidence of bacterial respiratory infection and pneumonia in people with HIV with and without airflow limitation. *Int J Infect Dis*. 2024;139:183–191. doi:10.1016/j.ijid.2023.12.009
- Partouche H, Lepoutre A, Vaure CBD, Poisson T, Toubiana L, Gilberg S. Incidence of all-cause adult community-acquired pneumonia in primary care settings in France. *Med Mal Infect*. 2018;48(6):389–395. doi:10.1016/j.medmal.2018.02.012
- Regunath H, Oba Y. Community-acquired pneumonia. In: *StatPearls*. Treasure Island, USA: StatPearls Publishing; 2025. <http://www.ncbi.nlm.nih.gov/books/NBK430749>. Accessed September 4, 2025.
- Tsoumani E, Carter JA, Salomonsson S, Stephens JM, Bencina G. Clinical, economic, and humanistic burden of community acquired pneumonia in Europe: A systematic literature review. *Expert Rev Vaccines*. 2023; 22(1):876–884. doi:10.1080/14760584.2023.2261785
- Islam S, Piggott DA, Moriggia A, et al. Reducing injection intensity is associated with decreased risk for invasive bacterial infection among high-frequency injection drug users. *Harm Reduct J*. 2019; 16(1):38. doi:10.1186/s12954-019-0312-8
- Kohli R, Lo Y, Homel P, et al. Bacterial pneumonia, HIV therapy, and disease progression among HIV-infected women in the HIV Epidemiologic Research (HER) Study. *Clin Infect Dis*. 2006;43(1):90–98. doi:10.1086/504871
- Byanova K, Abelman R, North C, Christenson S, Huang L. COPD in people with HIV: Epidemiology, pathogenesis, management, and prevention strategies. *Int J Chron Obstruct Pulmon Dis*. 2023;18:2795–2817. doi:10.2147/COPD.S388142
- Ronit A, Lundgren J, Afzal S, et al. Airflow limitation in people living with HIV and matched uninfected controls. *Thorax*. 2018;73(5): 431–438. doi:10.1136/thoraxjnl-2017-211079
- Drummond MB, Huang L, Diaz PT, et al. Factors associated with abnormal spirometry among HIV-infected individuals. *AIDS*. 2015;29(13): 1691–1700. doi:10.1097/QAD.0000000000000750
- Mdodo R, Frazier EL, Dube SR, et al. Cigarette smoking prevalence among adults with HIV compared with the general adult population in the United States: Cross-sectional surveys. *Ann Intern Med*. 2015;162(5):335–344. doi:10.7326/M14-0954
- Mdege ND, Shah S, Ayo-Yusuf OA, Hakim J, Siddiqui K. Tobacco use among people living with HIV: Analysis of data from Demographic and Health Surveys from 28 low-income and middle-income countries. *Lancet Global Health*. 2017;5(6):e578–e592. doi:10.1016/S2214-109X(17)30170-5
- Johnston PI, Wright SW, Orr M, et al. Worldwide relative smoking prevalence among people living with and without HIV. *AIDS*. 2021; 35(6):957–970. doi:10.1097/QAD.00000000000002815
- Lavender TW, McCarron B. Acute infections in intravenous drug users. *Clin Med (Lond)*. 2013;13(5):511–513. doi:10.7861/clinmedicine.13-5-511
- Selwyn PA, Feingold AR, Hartel D, et al. Increased risk of bacterial pneumonia in HIV-infected intravenous drug users without AIDS. *AIDS*. 1988;2(4):267–272. doi:10.1097/00002030-198808000-00005
- Jolley SE, Alkhafaf Q, Hough C, Welsh DA. Presence of an alcohol use disorder is associated with greater pneumonia severity in hospitalized HIV-infected patients. *Lung*. 2016;194(5):755–762. doi:10.1007/s00408-016-9920-1
- Schleenvoigt BT, Ankert J, Barten-Neiner G, et al. Pathogen spectrum of community acquired pneumonia in people living with HIV (PLWH) in the German CAPNETZ-Cohort. *Infection*. 2024;52(1):129–137. doi:10.1007/s15010-023-02070-3
- Klein EY, Monteforte B, Gupta A, et al. The frequency of influenza and bacterial coinfection: A systematic review and meta-analysis. *Influenza Other Respir Viruses*. 2016;10(5):394–403. doi:10.1111/irv.12398
- Afessa B, Green B. Bacterial pneumonia in hospitalized patients with HIV infection: The Pulmonary Complications, ICU Support, and Prognostic Factors of Hospitalized Patients with HIV (PIP) Study. *Chest*. 2000;117(4):1017–1022. doi:10.1378/chest.117.4.1017
- Levine SJ, White DA, Fels AO. The incidence and significance of *Staphylococcus aureus* in respiratory cultures from patients infected with the human immunodeficiency virus. *Am Rev Respir Dis*. 1990;141(1): 89–93. doi:10.1164/ajrccm/141.1.89
- Wilson MG, Pandey S. *Pseudomonas aeruginosa*. In: *StatPearls*. Treasure Island, USA: StatPearls Publishing; 2025:Bookshelf ID: NBK557831. <http://www.ncbi.nlm.nih.gov/books/NBK557831/>. Accessed September 4, 2025.
- Office of AIDS Research, National Institutes of Health (NIH). Guidelines for the Prevention and Treatment of Opportunistic Infections in Adults and Adolescents with HIV. Rockville, USA: Office of AIDS Research National Institutes of Health (NIH); 2022. <https://clinicalinfo.hiv.gov/en/guidelines/hiv-clinical-guidelines-adult-and-adolescent-opportunistic-infections/community-acquired>. Accessed May 2, 2025.
- Siddiqui AH, Koirala J. Methicillin-resistant *Staphylococcus aureus*. In: *StatPearls*. Treasure Island, USA: StatPearls Publishing; 2025:Bookshelf ID: NBK482221. <http://www.ncbi.nlm.nih.gov/books/NBK482221>. Accessed September 4, 2025.

25. Taylor TA, Unakal CG. *Staphylococcus aureus* infection. In: *StatPearls*. Treasure Island, USA: StatPearls Publishing; 2025:Bookshelf ID: NBK441868. <http://www.ncbi.nlm.nih.gov/books/NBK441868>. Accessed September 4, 2025.
26. Diep BA, Chambers HF, Graber CJ, et al. Emergence of multidrug-resistant, community-associated, methicillin-resistant *Staphylococcus aureus* clone USA300 in men who have sex with men. *Ann Intern Med*. 2008;148(4):249–257. doi:10.7326/0003-4819-148-4-200802190-00204
27. Shet A, Mathema B, Mediavilla JR, et al. Colonization and subsequent skin and soft tissue infection due to methicillin-resistant *Staphylococcus aureus* in a cohort of otherwise healthy adults infected with HIV type 1. *J Infect Dis*. 2009;200(1):88–93. doi:10.1086/599315
28. Lowy FD, Miller M, Cespedes C, Vavagiakis P, Klein RS. *Staphylococcus aureus* colonization in a community sample of HIV-infected and HIV-uninfected drug users. *Eur J Clin Microbiol Infect Dis*. 2003;22(8):463–469. doi:10.1007/s10096-003-0969-4
29. Ramirez JA. Overview of community-acquired pneumonia in adults. Alphen aan den Rijn, the Netherlands: UpToDate (Wolters Kluwer Health); 2024. <https://www.uptodate.com/contents/overview-of-community-acquired-pneumonia-in-adults>. Accessed May 2, 2025.
30. Cillóniz C, Torres A, Manzardo C, et al. Community-acquired pneumococcal pneumonia in virologically suppressed HIV-infected adult patients. *Chest*. 2017;152(2):295–303. doi:10.1016/j.chest.2017.03.007
31. Mamani RF, López TDA, Jalo WM, et al. Invasive pneumococcal disease in people living with HIV: A retrospective case-control study in Brazil. *Trop Med Infect Dis*. 2023;8(6):328. doi:10.3390/tropicalmed8060328
32. Figueiredo-Mello C, Naucler P, Negra MD, Levin AS. Prospective etiological investigation of community-acquired pulmonary infections in hospitalized people living with HIV. *Medicine (Baltimore)*. 2017;96(4):e5778. doi:10.1097/MD.00000000000005778
33. Cillóniz C, Miguel-Escuder L, Pedro-Bonet ML, et al. Community-acquired *Legionella* pneumonia in human immunodeficiency virus-infected adult patients: A matched case-control study. *Clin Infect Dis*. 2018;67(6):958–961. doi:10.1093/cid/ciy314
34. Kenmoe S, Bigna JJ, Fatawou Modiyingi A, et al. Case fatality rate and viral aetiologies of acute respiratory tract infections in HIV positive and negative people in Africa: The VARIAFRICA-HIV systematic review and meta-analysis. *J Clin Virol*. 2019;117:96–102. doi:10.1016/j.jcv.2019.06.006
35. Danwang C, Noubiap JJ, Robert A, Yombi JC. Outcomes of patients with HIV and COVID-19 co-infection: A systematic review and meta-analysis. *AIDS Res Ther*. 2022;19(1):3. doi:10.1186/s12981-021-00427-y
36. Moyes J, Walaza S, Pretorius M, et al. Respiratory syncytial virus in adults with severe acute respiratory illness in a high HIV prevalence setting. *J Infect*. 2017;75(4):346–355. doi:10.1016/j.jinf.2017.06.007
37. McDonald EG, Afshar A, Assiri B, et al. *Pneumocystis jirovecii* pneumonia in people living with HIV: A review. *Clin Microbiol Rev*. 2024;37(1):e00101-22. doi:10.1128/cmr.00101-22
38. Maartens G, Griesel R, Dube F, Nicol M, Mendelson M. Etiology of pulmonary infections in human immunodeficiency virus-infected inpatients using sputum multiplex real-time polymerase chain reaction. *Clin Infect Dis*. 2020;70(6):1147–1152. doi:10.1093/cid/ciz332
39. Denning DW, Morgan EF. Quantifying deaths from aspergillosis in HIV positive people. *J Fungi*. 2022;8(11):1131. doi:10.3390/jof8111131
40. World Health Organization (WHO). *WHO Consolidated Guidelines on Tuberculosis. Module 6: Tuberculosis and Comorbidities*. Geneva, Switzerland: World Health Organization (WHO); 2024. ISBN:978-92-4-008700-2.
41. Song Y, Jin Q, Qiu J, Ye D. A systematic review and meta-analysis on the correlation between HIV infection and multidrug-resistance tuberculosis. *Heliyon*. 2023;9(11):e21956. doi:10.1016/j.heliyon.2023.e21956
42. Ahmed R, Zumla A, Taylor E, Aklillu E, Ippolito G, Satta G. Perspectives on tuberculosis in migrants, refugees, and displaced populations in Europe. *IJID Reg*. 2025;14:100576. doi:10.1016/j.ijregi.2025.100576
43. Cillóniz C, García-Vidal C, Moreno A, Miro JM, Torres A. Community-acquired bacterial pneumonia in adult HIV-infected patients. *Exp Rev Anti Infect Ther*. 2018;16(7):579–588. doi:10.1080/14787210.2018.1495560

Traumatic complications linked to prophylactic drain placement after hepatectomy: A meta-analysis

*Zhenhao Fei^C, Xingfu Duan^B, Junhua Liang^D, *Zhiwei Sun^A, Jianzhong Tang^{E,F}

Department of Hepatobiliary Pancreatic Surgery, The First People Hospital of Yunnan Province, Kunming, China

A – research concept and design; B – collection and/or assembly of data; C – data analysis and interpretation;

D – writing the article; E – critical revision of the article; F – final approval of the article

Advances in Clinical and Experimental Medicine, ISSN 1899–5276 (print), ISSN 2451–2680 (online)

Adv Clin Exp Med. 2025;34(12):2017–2024

Address for correspondence

Zhiwei Sun

E-mail: zwsun6345@163.com

Funding sources

None declared

Conflict of interest

None declared

*Zhenhao Fei and Zhiwei Sun contributed equally to this article

Received on August 9, 2024

Reviewed on January 24, 2025

Accepted on February 10, 2025

Published online on July 31, 2025

Abstract

Background. Research documenting the results of liver trauma surgery revealed a connection between prophylactic drainage (PD) and escalating infections or septic consequences.

Objectives. Meta-analysis research was conducted to review the wound complications (WCs) frequency of PD in liver resections (LRs).

Materials and methods. Up until June 2024, comprehensive literature study was completed, and 757 related studies were reviewed. The 10 selected studies included 5,459 LRs at the beginning; 2,918 of them were drained and 2,541 were not. The dichotomous approaches and a fixed or random model were used to assess the WCs frequency of PD in LRs using odds ratios (ORs) and 95% confidence intervals (95% CIs).

Results. Prophylactic drainage had significantly higher surgical site wound infection rate (OR = 1.97; 95% CI: 1.09–3.55, $p = 0.02$) compared to non-PD in LR patients, though no significant difference was found among PD and non-PD in LR patients in infected intra-abdominal collections (IIACs; OR = 3.17; 95% CI: 0.93–10.80, $p = 0.07$).

Conclusions. Prophylactic drainage had a considerably greater surgical site wound infection rate, and there was no discernible difference between IIACs and non-PD in LR individuals. Nevertheless, because there were not many studies nominated for comparison in the meta-analysis, care must be used when working with its outcomes, and further research is warranted to confirm these findings.

Key words: liver resections, prophylactic drainage, infected intra-abdominal collections, surgical site wound infection

Cite as

Fei Z, Duan X, Liang J, Sun Z, Tang J. Meta-analysis of the incidence of traumatic complications of prophylactic drainage in hepatectomy. *Adv Clin Exp Med.* 2025;34(12):2017–2024. doi:10.17219/acem/201227

DOI

10.17219/acem/201227

Copyright

Copyright by Author(s)

This is an article distributed under the terms of the Creative Commons Attribution 3.0 Unported (CC BY 3.0) (<https://creativecommons.org/licenses/by/3.0/>)

Highlights

- Meta-analysis of liver resections shows prophylactic drainage (PD) markedly increases surgical-site infection (SSI) risk compared to no drain placement.
- PD does not significantly alter intra-abdominal abscess rates compared with non-PD approaches.
- Limited trial pool and borderline p-values (~ 0.05) temper confidence and signal the need for larger, high-quality studies.
- Surgeons should balance routine PD use against elevated SSI risk when planning liver-resection aftercare.

Background

Franco et al. confirmed in 1989 that prophylactic drainage (PD) was not required following simple liver resections (LRs) and suggested a no-drainage treatment in elective LRs.¹ Patients may experience an accumulation of fluid in the abdominal cavity, referred to as ascites. This may occur due to various factors, including elevated pressure in one of the primary hepatic blood arteries (portal vein).² A physician can prescribe medications to alleviate fluid retention.

The predominant reason for a biliary drain is an obstruction or constriction (stricture) of a bile duct. This results in cholestasis, characterized by the deceleration or cessation of bile flow from the liver.³ Various disorders may lead to bile duct obstruction and cholestasis, including pancreatitis (inflammation of the pancreas). Abdominal drainage is a technique designed to remove fluid from the peritoneal cavity, the area between the abdominal wall and the organs.² Traditionally, in patients undergoing hepatic resection, an abdominal drain is typically placed in the subphrenic or subhepatic space next to the resection surface. This facilitates the alleviation of intra-abdominal pressure caused by ascitic fluid accumulation and enables the observation of postoperative intra-abdominal hemorrhage, in addition to the identification and drainage of any bile leakage. Research documenting the results of liver trauma surgery revealed a connection among PD and escalating infections or septic consequences.² Fang et al. found that there was no indication to support the usual utilization of PD in elective LRs in their meta-analysis of 6 randomized controlled trials (RCTs) comprising 465 persons.³ The studies included in that meta-analysis showed no significant variations in postoperative illness between patients with or without PD.³ Drainage after elective LRs is still frequently utilized in existing practice and appears to be more based on experience than on scientific research. A multi-institutional investigation of 1,041 persons found that 564 of them had drains put at the operator's discretion, with a frequency of utilization of 54%. When compared to the non-drained cohort, the drained cohort showed higher rates of complications, bile leaks and 30-day readmissions.

Objectives

Our goal was to review the routine utilization of PD after LRs by reviewing the most recent research. To compare drained with non-drained patients, a meta-analysis was conducted with the aim to evaluate the wound complications (WCs) frequency of PD in LRs.

Materials and methods

We conducted a meta-analysis to assess studies demonstrating the frequency of WC in PD cases involving LR.⁴

Information sources

Figure 1 characterizes the study selection process. When the inclusion criteria were satisfied, the following literature was included in the study^{5,6}:

1. The investigation was prospective, observational, RCT, or retrospective research.
2. Persons with LRs were the investigated patients.
3. The intervention was PD.
4. The research appraised the effect of PD and non-PD in the management of LRs on surgical site wound infection (SSWI) and infected intra-abdominal collections (IIACs)

Studies that did not evaluate the effect of PD and non-PD in the management of LRs on SSWI and IIACs, and studies with no comparison were also excluded.^{7–9}

Search strategy

Based on the PICOS approach, we identified a search protocol operation and described it as follows: PD was the “intervention” or “exposure”, SSWI and IIACs were the “outcome” and “research design”, and PD was the “population” for people with LRs. The planned research was not restricted in any way.¹⁰

A comprehensive literature search was conducted through June 2024 across the following databases: Google Scholar, Embase, Cochrane Library, PubMed, and Ovid. We used a keyword organization and additional keywords for LRs, PD, IIAC, and SSWI, as shown in Table 1. Duplicate records were removed, and the remaining studies were

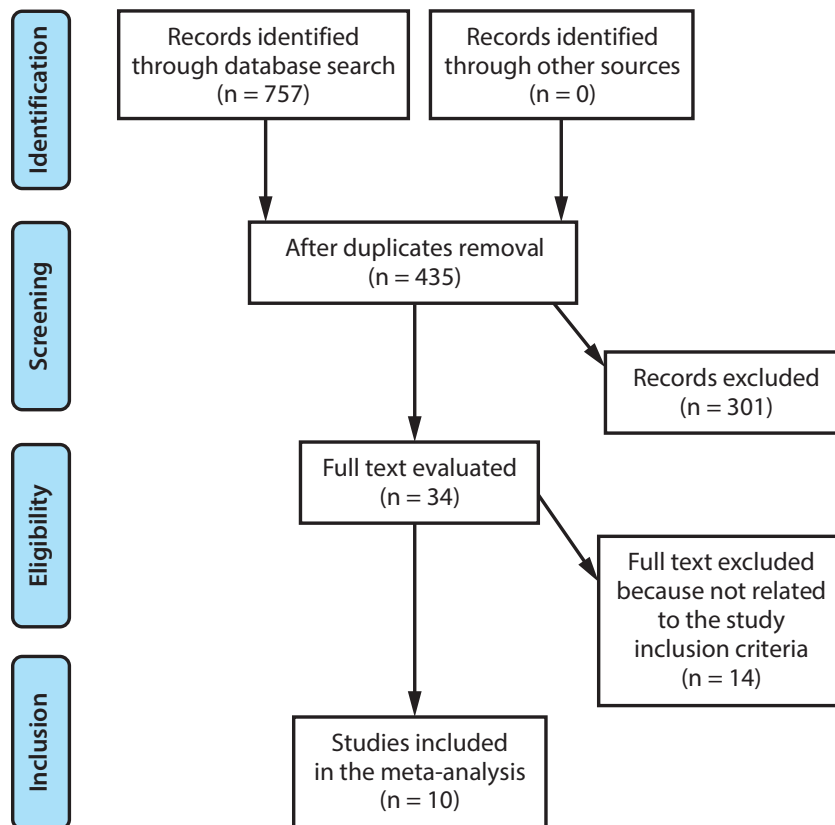


Fig. 1. Flow diagram illustrating the study selection process used in the meta-analysis

Table 1. Search strategy used for each database

Database	Search strategy
PubMed	#1 "liver resections"[MeSH Terms] OR "surgical site wound infection"[MeSH Terms] [All Fields] #2 "infected intra-abdominal collections"[MeSH Terms] OR "prophylactic drainage"[MeSH Terms] [All Fields] #3 #1 AND #2
Embase	#1 'liver resections'/exp OR 'surgical site wound infection' #2 'infected intra-abdominal collections'/exp OR 'prophylactic drainage' #3 #1 AND #2
Cochrane Library	#1 (liver resections):ti,ab,kw (surgical site wound infection):ti,ab,kw (Word variations have been searched) #2 (infected intra-abdominal collections):ti,ab,kw OR (prophylactic drainage):ti,ab,kw (Word variations have been searched) #3 #1 AND #2

compiled into an EndNote library (Clarivate, London, UK). Titles and abstracts were re-evaluated to exclude studies unlikely to contribute meaningfully to the assessment of the association between the frequency of PD in LRs and WCs.¹¹

Selection process

The procedure that followed the epidemiological announcement was then arranged and evaluated using the meta-analysis method.^{12–19}

Data collection process

The data collection criteria included authors' names, study date and year, geographical location, population type, medical and treatment characteristics, study categories,

methods of quantitative and qualitative assessment, data sources, outcome evaluation, and statistical analysis. When the study yielded different results, we separately gathered the data depended on an estimation of the WCs frequency of PD in LRs.

Research risk of bias assessment

We evaluated the methodology of the chosen publications to determine the potential for bias in each analyzed study. The technical quality was assessed utilizing the "risk of bias instrument" from the Cochrane Handbook for Systematic Reviews of Interventions, v. 5.1.0.²⁰ Each study was classified according to the assessment criteria and assigned a corresponding level of risk of bias. The research was classified as having a medium bias risk if 1 or more quality criteria were unmet and as having a low bias risk

if all criteria were satisfied. The research was considered to have a substantial risk of bias if several quality requirements were either completely or partially met.

Effect estimates

Sensitivity analysis was restricted to studies that estimated and characterized the WCs frequency of PD in LR. A subclass analysis was utilized to compare the sensitivity of LR persons with and without PD.

Statistical analyses

A dichotomous approach was used, and either a random-effects or fixed-effects model was applied to calculate the odds ratio (OR) and the corresponding 95% confidence interval (95% CI). The I^2 index was assessed on a scale from 0 to 100%. At 0%, 25%, 50%, and 75% of the data, there was no, low, moderate, and significant heterogeneity, respectively.²¹ To validate the suitability of the chosen model, additional frameworks were analyzed, focusing on those demonstrating a high degree of similarity among the included studies. The random effect model was utilized. A subgroup analysis was conducted by dividing the original estimation into the previously defined consequence groups. A p-value of less than 0.05 meant statistical significance of differences among subgroups.

Reporting bias assessment

We employed Egger's regression test and funnel plots – plotting the logarithm of the ORs against their standard errors (SEs) – to assess publication bias both quantitatively and visually. A $p \geq 0.05$ was interpreted as indicative of no significant publication bias.²²

Certainty assessment

Two-tailed testing was employed to analyze each p-value. Graphs and statistical analyses were generated utilizing Reviewer Manager (RevMan) v. 5.3 (The Nordic Cochrane Centre, Cochrane Collaboration, Copenhagen, Denmark).

Results

Out of 757 relevant studies that met the inclusion criteria, 10 papers published between 1993 and 2021 were selected for analysis.^{23–32} The details of these studies are presented in Table 2. At the outset of the included research, a total of 5,459 LR were analyzed, of which 2,918 were drained and 2,541 were not. The sample sizes of the individual studies ranged from 81 to 1,868 patients.

Prophylactic drainage was associated with a significantly higher risk of superficial surgical SSWI, with OR of 1.97 (95% CI: 1.09–3.55, $p = 0.02$), and substantial heterogeneity among studies ($I^2 = 79\%$), as shown in Fig. 2. However, no statistically significant difference was observed between the PD and non-drainage groups in terms of IIACs, with an OR of 3.17 (95% CI: 0.93–10.80, $p = 0.07$) and no heterogeneity ($I^2 = 0\%$), as illustrated in Fig. 3.

The use of stratified models to assess the effects of specific factors – such as age, gender and ethnicity – on comparative outcomes was not feasible due to insufficient data. The quantitative Egger's regression test and visual inspection of the funnel plots (Fig. 4,5) indicated no evidence of publication bias ($p = 0.86$ and 0.92 , respectively). Nonetheless, selective reporting bias was ruled out, although most of the included RCTs exhibited inadequate procedural quality.

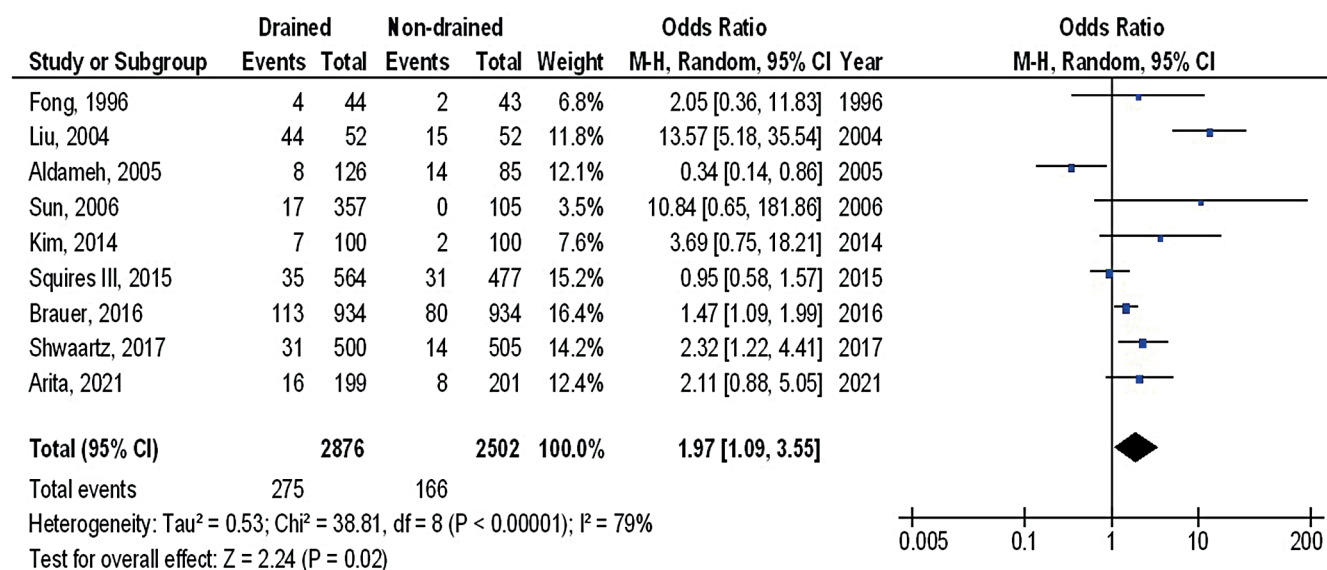


Fig. 2. Forest plot illustrating the effect of prophylactic drainage (PD) compared to no drainage on the incidence of surgical site wound infections (SSWI) following liver resections (LRs)

Table 2. Characteristics of the studies included in the meta-analysis

Research	Country	Total (PD/non-PD)	Major hepatectomy (PD/non-PD)	Ascitic leak (PD/non-PD)	Death (PD/non-PD)	Age [years] (PD/non-PD)
Belghiti et al., 1993 ²³	France	81 (42/39)	14/11	0/1	1/1	47/51
Fong et al., 1996 ²⁴	USA	87 (44/43)	44/43	0/2	2/2	57/57
Liu et al., 2004 ²⁵	China	104 (52/52)	33/29	2/0	0/0	60/58
Aldameh et al., 2005 ²⁶	New Zealand	211 (126/85)	0/0	9/8	3/1	53/52
Sun et al., 2006 ²⁷	China	462 (357/105)	37/44	6/4	0/1	50/49
Kim et al., 2014 ²⁸	South Korea	200 (100/100)	53/55	4/1	0/0	56/54
Squires et al., 2015 ²⁹	USA	1041 (564/477)	190/183	2/3	3/4	54/53
Brauer et al., 2016 ³⁰	USA	1868 (834/934)	200/176	3/2	4/5	60/58
Shwaartz et al., 2017 ³¹	USA	1005 (500/505)	201/210	4/6	3/5	57/60
Arita et al., 2021 ³²	Japan	400 (199/201)	37/44	6/5	6/5	51/50
Total		5,459 (2918/2541)	–	–	–	–

PD – prophylactic drainage.

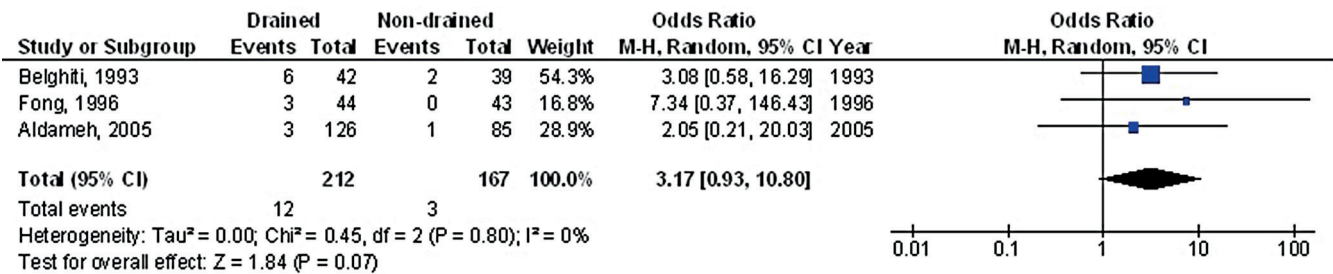


Fig. 3. Forest plot illustrating the effect of prophylactic drainage (PD) compared to no drainage on the incidence of infected intra-abdominal collections (IIACs) following liver resections (LRs)

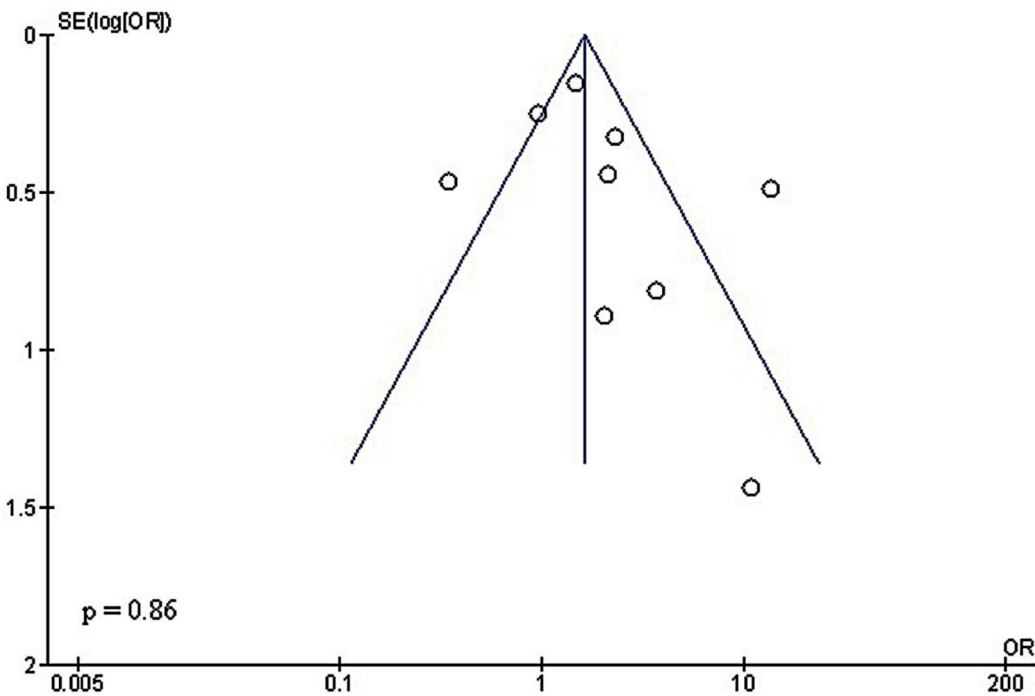


Fig. 4. Funnel plot illustrating the comparison of prophylactic drainage (PD) compared to no drainage on surgical site wound infections (SSWI) following liver resections (LRs)

Discussion

In the studies included in this meta-analysis, a total of 5,459 LR were initially reported. Of these, 2,918

procedures involved the use of PD, while 2,541 were performed without drainage.^{23–32}

Each author employed a closed suction drain inserted through a separate stab incision.^{23–32} The use of surgical

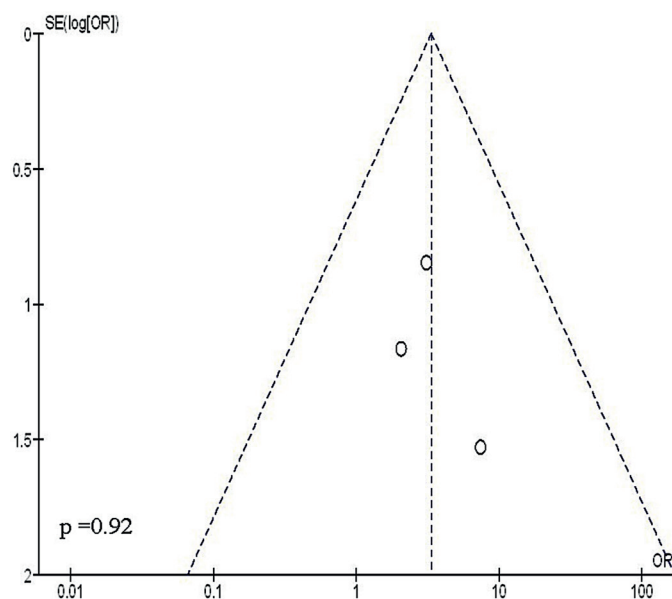


Fig. 5. Funnel plot illustrating the comparison of prophylactic drainage (PD) compared to no drainage on infected intra-abdominal collections (IIACs) following liver resections (LRs)

drains is well-established and based on various assumptions, including the need to monitor potential postoperative complications and to mitigate their effects.³³ Surgeons advocating for routine PD after LR argue that drains can divert ascitic fluid away from the incision, reduce bile leakage, prevent intra-abdominal fluid collections, and enable early detection and quantification of hemorrhage. Nevertheless, a number of authors have expressed concern that drains might raise morbidity.^{29,34} Since some of the research was led prior to the release of the extensively utilized Clavien–Dindo classification, we discovered that the concept of serious problems varies depending on the research.³⁵ Routine ultrasound evaluation of all patients may have contributed to overdiagnosis by detecting clinically insignificant findings that would not have otherwise manifested symptoms or required intervention.³⁶ Only 1 study concluded that ultrasound should be reserved for symptomatic patients, suggesting that routine imaging in asymptomatic individuals may lead to unnecessary interventions or overdiagnosis.³⁶ The findings of this research demonstrated that routine use of drainage did not improve major or secondary outcome measures, and, in fact, was associated with a significantly increased incidence of ascitic leakage. The likelihood of surgical SSWIs varies considerably depending on the type of LR performed, ranging from 9.7% in segmentectomies to 18.3% in trisectionectomies.³⁷ This highlights the importance of maintaining comparable rates of extended LRs across studies. Additionally, the criteria for drain removal varied between studies, further contributing to heterogeneity in outcomes. According to recent research employing the International Study Group of Liver Surgery (ISGLS) standardized definition and grading of bile leakage, drains should be removed on the 3rd postoperative day if the bilirubin concentration

in the drain fluid is less than 3 mg/dL.³⁸ The literature reports that the incidence of bile leakage following LRs ranges from 3.6% to 12%.³⁹ Additionally, another study found no significant difference in bile leakage rates between laparoscopic and open procedures, with reported rates ranging from 4% to 17%.⁴⁰ Given that these conditions could have potentially biased the outcomes in favor of patients who received drains, the absence of a statistically significant difference strongly supports a no-drain strategy.

Limitations

Due to the exclusion of several studies, variability bias may have emerged. However, the eliminated studies failed to satisfy the requisite criteria for inclusion in the meta-analysis. Furthermore, we lacked sufficient information to ascertain whether variables such as gender, race and age impacted the outcomes. The objective of the study was to determine the influence of PD and non-PD on SSWI for LRs management. Bias in this study may have been exacerbated by the inclusion of incomplete or erroneous data from previous research. Additionally, individual factors such as age, gender, race, and nutritional status likely contributed to variability and potential confounding. The absence of data on these variables limits subgroup analysis and may distort the results. Furthermore, the exclusion of unpublished studies and grey literature introduces a risk of publication bias, potentially skewing the overall findings.

Conclusions

Further research is essential. This need has also been emphasized in previous studies that showed comparable effect estimates using similar meta-analytic approaches. Future investigations should aim to address current data limitations, reduce heterogeneity and incorporate standardized methodologies to improve the reliability and generalizability of the findings.^{41–44} People who underwent LRs with PD had a significantly higher rate of SSWIs compared to those without PD. However, there was no statistically significant difference between the PD and non-PD groups in terms of IIACs. It is important to interpret these results cautiously, as the meta-analysis included a limited number of studies for some comparisons. In particular, the low p-value observed for IIACs may affect the reliability and statistical significance of the findings.

Consent for publication

Not applicable.

Use of AI and AI-assisted technologies

Not applicable.

ORCID iDs

Zhiwei Sun  <https://orcid.org/0009-0005-7246-5960>

References

1. Franco D, Karaa A, Meakins JL, Borgonovo G, Smadja C, Grange D. Hepatectomy without abdominal drainage: Results of a prospective study in 61 patients. *Ann Surg*. 1989;210(6):748–750. doi:10.1097/0000658-198912000-00009
2. Noyes LD, Doyle DJ, McSwain NE. Septic complications associated with the use of peritoneal drains in liver trauma. *J Trauma*. 1988;28(3):337–346. doi:10.1097/00005373-198803000-00009
3. Fang Y, Gurusamy KS, Wang Q, et al. Meta-analysis of randomized clinical trials on safety and efficacy of biliary drainage before surgery for obstructive jaundice. *Br J Surg*. 2013;100(12):1589–1596. doi:10.1002/bjs.9260
4. Stroup DF, Berlin JA, Morton SC, et al. Meta-analysis of observational studies in epidemiology: A proposal for reporting. Meta-analysis Of Observational Studies in Epidemiology (MOOSE) group. *JAMA*. 2000;283(15):2008–2012. doi:10.1001/jama.283.15.2008
5. Elshazly H. Effectiveness of postoperative systemic antibiotic prophylaxis following cardiovascular implantable electronic device implantation: A systematic review and meta-analysis. *Int J Clin Med Res*. 2024;2(5):144–154. doi:10.61466/ijcmr2050001
6. Giong Z, Lie N. A meta-analysis of the impact of a phosphate-specific diet on serum phosphate levels in people receiving hemodialysis. *Int J Clin Med Res*. 2024;2(4):135–142. doi:10.61466/ijcmr2040005
7. Jiany L, Xiu W. A meta-analysis evaluated the effectiveness of Chinese herbal medicine as a supplement to conventional care for patients with diabetic foot ulcers. *Int J Clin Med Res*. 2024;2(4):116–123. doi:10.61466/ijcmr2040003
8. Weang Z. A meta-analysis examining the impact of antibiotic prophylaxis on surgical site wound infection during third molar surgery. *Int J Clin Med Res*. 2024;2(4):127–134. doi:10.61466/ijcmr2040004
9. Gu R, Xu G. A meta-analysis looking at the effects of continuous management for complications related to intraoperative pressure wound ulcers in women with breast cancer. *Int J Clin Med Res*. 2024;2(4):100–106. doi:10.61466/ijcmr2040001
10. Liberati A, Altman DG, Tetzlaff J, et al. The PRISMA Statement for Reporting Systematic Reviews and Meta-Analyses of studies that evaluate health care interventions: Explanation and elaboration. *PLoS Med*. 2009;6(7):e1000100. doi:10.1371/journal.pmed.1000100
11. Koang Y. A meta-analysis on the use of photobiomodulation to regulate gingival wound healing in addition to periodontal therapies. *Int J Clin Med Res*. 2024;2(4):107–115. doi:10.61466/ijcmr2040002
12. Guo Y. Effect of resident participation in ophthalmic surgery on wound dehiscence: A meta-analysis. *Int J Clin Med Res*. 2024;2(2):50–56. doi:10.61466/ijcmr2020002
13. Zangeneh A, Zangeneh MM. The application of negative pressure wound treatment in oncoplastic breast surgery. *Int J Clin Med Res*. 2023;2(1):21–26. doi:10.61466/ijcmr2010003
14. Emad M, Osama H, Rabea H, Saeed H. Dual compared with triple antithrombotics treatment effect on ischemia and bleeding in atrial fibrillation following percutaneous coronary intervention: A meta-analysis. *Int J Clin Med Res*. 2023;1(2):77–87. doi:10.61466/ijcmr1020010
15. Osama H, Saeed H, Nicola M, Emad M. Neuraxial anesthesia compared to general anesthesia in subjects with hip fracture surgery: A meta-analysis. *Int J Clin Med Res*. 2023;1(2):66–76. doi:10.61466/ijcmr1020009
16. Sundaresan A. Wound complications frequency in minor technique gastrectomy compared to open gastrectomy for gastric cancer: A meta-analysis. *Int J Clin Med Res*. 2023;1(3):100–107. doi:10.61466/ijcmr1030012
17. Singh RK. A meta-analysis of the impact on gastrectomy versus endoscopic submucosal dissection for early stomach cancer. *Int J Clin Med Res*. 2023;1(3):88–99. doi:10.61466/ijcmr1030011
18. Amin MA. A meta-analysis of the eosinophil counts in the small intestine and colon of children without obvious gastrointestinal disease. *Int J Clin Med Res*. 2023;1(1):1–8. doi:10.61466/ijcmr1010001
19. Shaaban EA, Mohammed IE. Determining the efficacy of N-acetyl cysteine in treatment of pneumonia in COVID-19 hospitalized patients: A meta-analysis. *Int J Clin Med Res*. 2023;1(2):36–42. doi:10.61466/ijcmr1020006
20. Higgins JPT, Thomas J, Chandler J, Cumpston M, Li T, Page MJ, Welch VA, eds. *Cochrane Handbook for Systematic Reviews of Interventions*. 2nd ed. Chichester, UK: Wiley & Sons; 2019. doi:10.1002/9781119536604
21. Perazzo H, Castro R, Luz PM, et al. Effectiveness of generic direct-acting agents for the treatment of hepatitis C: Systematic review and meta-analysis. *Bull World Health Organ*. 2020;98(3):188–197K. doi:10.2471/BLT.19.231522
22. Higgins JPT, Thompson SG, Deeks JJ, Altman DG. Measuring inconsistency in meta-analyses. *BMJ*. 2003;327(7414):557–560. doi:10.1136/bmj.327.7414.557
23. Belghiti J, Kabbej M, Sauvanet A, Vilgrain V, Panis Y, Fekete F. Drainage after elective hepatic resection: A randomized trial. *Ann Surg*. 1993;218(6):748–753. doi:10.1097/0000658-199312000-00008
24. Fong Y, Brennan MF, Brown K, Heffernan N, Blumgart LH. Drainage is unnecessary after elective liver resection. *Am J Surg*. 1996;171(1):158–162. doi:10.1016/S0002-9610(99)80092-0
25. Liu CL, Fan ST, Lo CM, et al. Abdominal drainage after hepatic resection is contraindicated in patients with chronic liver diseases. *Ann Surg*. 2004;239(2):194–201. doi:10.1097/01.sla.0000109153.71725.8c
26. Anweier N, Apaer S, Zeng Q, et al. Is routine abdominal drainage necessary for patients undergoing elective hepatectomy? A protocol for systematic review and meta-analysis. *Medicine (Baltimore)*. 2021;100(6):e24689. doi:10.1097/MD.00000000000024689
27. Sun HC, Qin LX, Lu L, et al. Randomized clinical trial of the effects of abdominal drainage after elective hepatectomy using the crushing clamp method. *Br J Surg*. 2006;93(4):422–426. doi:10.1002/bjs.5260
28. Kim YI, Fujita S, Hwang VJ, Nagase Y. Comparison of abdominal drainage and no-drainage after elective hepatectomy: A randomized study. *Hepatogastroenterology*. 2014;61(131):707–711. PMID:26176061.
29. Squires MH, Lad NL, Fisher SB, et al. Value of primary operative drain placement after major hepatectomy: A multi-institutional analysis of 1,041 patients. *J Am Coll Surg*. 2015;220(4):396–402. doi:10.1016/j.jamcollsurg.2014.12.029
30. Brauer DG, Nywening TM, Jaques DP, et al. Operative site drainage after hepatectomy: A propensity score matched analysis using the American College of Surgeons NSQIP Targeted Hepatectomy Database. *J Am Coll Surg*. 2016;223(6):774–783e2. doi:10.1016/j.jamcollsurg.2016.09.004
31. Shwaartz C, Fields AC, Aalberg JJ, Divino CM. Role of drain placement in major hepatectomy: A NSQIP analysis of procedure-targeted hepatectomy cases. *World J Surg*. 2017;41(4):1110–1118. doi:10.1007/s00268-016-3750-4
32. Arita J, Sakamaki K, Saiura A, et al. Drain placement after uncomplicated hepatic resection increases severe postoperative complication rate: A Japanese multi-institutional randomized controlled trial (ND-trial). *Ann Surg*. 2021;273(2):224–231. doi:10.1097/SLA.00000000000004051
33. Liu X, Chen K, Chu X, Liu G, Yang Y, Tian X. Prophylactic intra-peritoneal drainage after pancreatic resection: An updated meta-analysis. *Front Oncol*. 2021;11:658829. doi:10.3389/fonc.2021.658829
34. Burt BM, Brown K, Jarnagin W, DeMatteo R, Blumgart LH, Fong Y. An audit of results of a no-drainage practice policy after hepatectomy. *Am J Surg*. 2002;184(5):441–445. doi:10.1016/S0002-9610(02)00998-4
35. Dindo D, Demartines N, Clavien PA. Classification of surgical complications: A new proposal with evaluation in a cohort of 6336 patients and results of a survey. *Ann Surg*. 2004;240(2):205–213. doi:10.1097/01.sla.0000133083.54934.ae
36. Gurusamy KS, Samraj K, Davidson BR. Routine abdominal drainage for uncomplicated liver resection. *Cochrane Database Syst Rev*. 2007;3:CD006232. doi:10.1002/14651858.CD006232.pub2
37. Moreno Elola-Olaso A, Davenport DL, Hundley JC, Daily MF, Gedaly R. Predictors of surgical site infection after liver resection: A multicentre analysis using National Surgical Quality Improvement Program data. *HPB (Oxford)*. 2012;14(2):136–141. doi:10.1111/j.1477-2574.2011.00417.x
38. Yamazaki S, Takayama T, Moriguchi M, et al. Criteria for drain removal following liver resection. *Br J Surg*. 2012;99(11):1584–1590. doi:10.1002/bjs.8916
39. Erdogan D, Busch ORC, Van Delden OM, Rauws EAJ, Gouma DJ, Van Gulik TM. Incidence and management of bile leakage after partial liver resection. *Dig Surg*. 2008;25(1):60–66. doi:10.1159/000118024

40. Jin S, Fu Q, Wuyun G, Wuyun T. Management of post-hepatectomy complications. *World J Gastroenterol*. 2013;19(44):7983–7991. doi:10.3748/wjg.v19.i44.7983
41. Hajibandeh S, Hajibandeh S, Raza SS, Bartlett D, Dasari BVM, Sutcliffe RP. Abdominal drainage is contraindicated after uncomplicated hepatectomy: Results of a meta-analysis of randomized controlled trials. *Surgery*. 2023;173(2):401–411. doi:10.1016/j.surg.2022.10.023
42. Mori H, Maehira H, Nitta N, et al. Clinical impact of various drain-fluid data for the postoperative complications after hepatectomy: Criteria of prophylactic drain removal on postoperative day 1. *Langenbecks Arch Surg*. 2024;409(1):209. doi:10.1007/s00423-024-03401-0
43. Dezfouli SA, Ünal UK, Ghamarnejad O, et al. Systematic review and meta-analysis of the efficacy of prophylactic abdominal drainage in major liver resections. *Sci Rep*. 2021;11(1):3095. doi:10.1038/s41598-021-82333-x
44. Gavriilidis P, Hidalgo E, de'Angelis N, Lodge P, Azoulay D. Re-appraisal of prophylactic drainage in uncomplicated liver resections: A systematic review and meta-analysis. *HPB (Oxford)*. 2017;19(1):16–20. doi:10.1016/j.hpb.2016.07.010

Relative qualities of telerehabilitation compared to traditional in-person speech and language treatment for individuals with aphasia: A meta-analysis

Liang Zhang^{A–F}

School of Foreign Studies, China University of Political Science and Law, Beijing, China

A – research concept and design; B – collection and/or assembly of data; C – data analysis and interpretation;
D – writing the article; E – critical revision of the article; F – final approval of the article

Advances in Clinical and Experimental Medicine, ISSN 1899–5276 (print), ISSN 2451–2680 (online)

Adv Clin Exp Med. 2025;34(12):2025–2034

Address for correspondence

Liang Zhang

E-mail: liangzhang_cupl@163.com

Funding sources

None declared

Conflict of interest

None declared

Received on November 23, 2024

Reviewed on January 26, 2025

Accepted on February 19, 2025

Published online on August 26, 2025

Abstract

Background. Stroke is a leading cause of disability and one of the primary causes of death worldwide. Stroke survivors often experience a range of symptoms, including impaired motor function, speech and language abnormalities, swallowing difficulties, cognitive deficits, visual disturbances, and sensory impairments.

Objectives. This meta-analysis was conducted to assess and compare the relative effectiveness of telerehabilitation compared to traditional in-person speech and language therapy for individuals with aphasia.

Materials and methods. A comprehensive literature search was conducted up to October 2024, reviewing 1,185 identified studies. Ultimately, 6 studies were selected that included a total of 168 participants with aphasia at baseline. The meta-analysis examined the relative effectiveness of telerehabilitation compared to traditional in-person speech and language therapy using continuous outcomes, with mean differences (MD) and 95% confidence intervals (95% CIs) calculated. Analyses were performed using either fixed-effect or random-effects models, depending on heterogeneity.

Results. In individuals with aphasia, telerehabilitation demonstrated significantly greater improvements in generalization post-intervention compared to face-to-face treatment (MD = 11.53; 95% CI: 3.64–19.43; $p = 0.004$). However, no significant differences were found between telerehabilitation and face-to-face treatment in naming accuracy post-intervention (MD = 3.09; 95% CI: 1.98–8.16; $p = 0.23$), Western Aphasia Battery (WAB) aphasia quotient (MD = –0.54; 95% CI: –9.96–8.88; $p = 0.91$), auditory comprehension post-intervention (MD = 0.66; 95% CI: –8.83–10.14; $p = 0.89$), or functional communication post-intervention (MD = –0.95; 95% CI: –10.19–8.29; $p = 0.84$).

Conclusions. In individuals with aphasia, telerehabilitation showed significantly greater improvements in generalization post-intervention compared to face-to-face treatment. However, no significant differences were observed between the 2 approaches in naming accuracy, WAB aphasia quotient, auditory comprehension, or functional communication post-intervention. To validate these findings, further research is needed, and caution should be exercised when interpreting the current results due to the limited number of included studies.

Key words: aphasia, telerehabilitation, generalization post-intervention, Western Aphasia Battery (WAB) aphasia quotient, face-to-face treatment

Cite as

Zhang L. Relative qualities of telerehabilitation compared to traditional in-person speech and language treatment for individuals with aphasia: A meta-analysis.

Adv Clin Exp Med. 2025;34(12):2025–2034.

doi:10.17219/acem/202056

DOI

10.17219/acem/202056

Copyright

Copyright by Author(s)

This is an article distributed under the terms of the
Creative Commons Attribution 3.0 Unported (CC BY 3.0)
(<https://creativecommons.org/licenses/by/3.0/>)

Highlights

- A meta-analysis study was done to figure out how to predict the relative qualities of telerehabilitation compared to traditional in-person speech and language treatment for individuals with aphasia.
- In individuals with aphasia, telerehabilitation had significantly higher generalization post-intervention compared to face-to-face treatment.
- No significant difference was found between telerehabilitation and face-to-face treatment in naming accuracy post-intervention, Western Aphasia Battery (WAB) Aphasia Quotient, auditory comprehension post-intervention, and functional communication post-intervention in individuals with aphasia.

Background

Stroke is a leading cause of disability and one of the leading causes of death globally.¹ Stroke survivors frequently have a variety of symptoms, such as reduced motor functions, speech abnormalities, swallowing issues, cognitive deficits, vision impairment, and sensory disturbances.² Aphasia affects about 1/3 of stroke patients.³ Communication problems brought on by aphasia frequently prevent patients and caregivers from engaging in social activities. People with aphasia have a number of deficits in some or all language modalities that can affect speech production and/or comprehension, reading and/or writing, and gesture.⁴ Word-finding difficulties are a sign of mild aphasia, while significant impairment of all language modalities is a sign of global aphasia.⁵ Research indicates that even years after the beginning of aphasia, people might still benefit from rehabilitation programs. However, only some obtain self-tailored treatment, and when they do, it is usually limited to the first few months post-stroke.⁴ Within the first 5 years following the incident, nearly half of stroke survivors express dissatisfaction with the absence of social or clinical assistance.⁶ Stroke survivors, particularly those in rural areas, have limited access to long-term rehabilitation. One of the additional factors is that individuals with brain damage frequently have several comorbidities, which makes it more challenging for them to get to a rehabilitation facility.⁷ Howe et al. investigated the contextual factors that prevent persons with aphasia from engaging in social activities. Individuals with aphasia believed that social integration was hampered by the absence of services following hospital-based speech treatment and the inability to interact with other aphasics. Participants also mentioned having trouble traveling to and from social settings.⁸ Given all of these restrictions, it is vital to offer therapies that guarantee aphasia patients' ongoing care in order to improve their social engagement. Therefore, cutting-edge telecommunications technology appear to be the answer to this problem.

The provision of rehabilitation services through information and communication technology is known as telerehabilitation.⁹ Its main goals is to decrease inpatient hospital stays and boost community services, such as rehabilitation

after hospital ward discharge. Assessment, monitoring, prevention, intervention, supervision, education, consultation, and counseling are some of the specific services that can be included in telerehabilitation. These services are intended to assist people with impairments.¹⁰

Objectives

This study aimed to use a meta-analysis to evaluate the relative effectiveness of telerehabilitation compared to traditional in-person speech and language therapy for individuals with aphasia.¹¹

Methods

Information sources

Figure 1 summarizes the overall study framework. Studies were incorporated when they met the following inclusion criteria^{12,13}: 1) The study was a randomized controlled trial (RCT), observational study, prospective study, or retrospective study; 2) The participants included individuals diagnosed with aphasia; 3) Telerehabilitation was integrated as part of the intervention; 4) The study compared the effects of telerehabilitation with traditional in-person speech and language therapy in individuals with aphasia.

Studies were excluded if they did not assess the relative effectiveness of telerehabilitation compared to traditional in-person speech and language treatment, focused solely on face-to-face interventions, or lacked meaningful comparative significance.^{14,15}

Search strategy

A search protocol was developed using the PICOS framework, defined as follows: the population (P) consisted of patients with aphasia; the intervention (I) was telerehabilitation; the comparison (C) involved comparing telerehabilitation to face-to-face treatment; the outcomes (O) included generalization post-intervention,

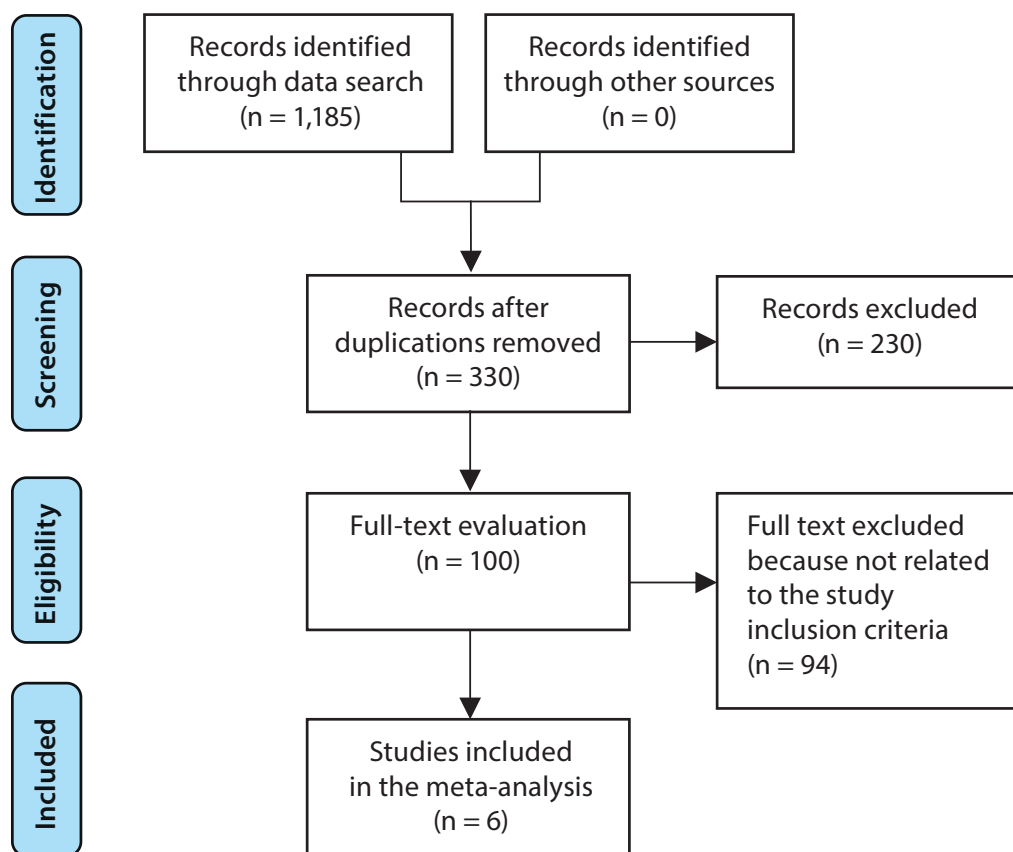


Fig. 1. Preferred Reporting Items for Systematic reviews and Meta-Analyses (PRISMA) flowchart of the study

naming accuracy post-intervention, and Western Aphasia Battery (WAB) Aphasia Quotient scores; and the study design (S) was unrestricted, with no limitations on study type.¹⁶

A thorough search was conducted across the databases Google Scholar, Embase, the Cochrane Library, PubMed, and Ovid up to October 2024, using a set of keywords and additional terms as outlined in Table 1.^{17,18} To avoid including studies that did not address the relative effectiveness of telerehabilitation compared to traditional in-person speech and language therapy for individuals with aphasia, duplicate records were removed. The remaining articles were compiled into an EndNote file (Clarivate, London, UK), and their titles and abstracts were re-assessed for relevance.^{19,20}

Selection process

The meta-analysis method was subsequently used to organize and assess the process in accordance with established epidemiological guidelines.^{21,22}

Data collection process

The data collection process included the following criteria: authors' names, study details, year of publication, country or region, population type, study categories, quantitative and qualitative assessment methods, data sources,

outcome measures, clinical and therapeutic characteristics, and statistical analysis approaches.²³

Data items

When a study yielded multiple values, data related to the evaluation of the relative effectiveness of telerehabilitation compared to traditional in-person speech and language therapy for individuals with aphasia were independently extracted.

Research risk of bias assessment

The risk of bias in the selected studies and the quality of the methods used were carefully assessed. The methodology of each study was objectively reviewed to ensure consistency and rigor.

Effect measures

Sensitivity analysis was restricted to studies that assessed and documented the relative effectiveness of telerehabilitation compared to traditional in-person speech and language therapy for individuals with aphasia. A subgroup analysis was conducted to compare the correlation between telerehabilitation and traditional in-person treatment across different patient variables, examining the sensitivity within aphasia subgroups.

Table 1. Database search strategy for inclusion of studies

Database	Search strategy
Google Scholar	#1 "aphasia" OR "generalization post-intervention" #2 "naming accuracy post-intervention" OR "Western Aphasia Battery Aphasia Quotient" OR "face-to-face treatment" OR "telerehabilitation" #3 #1 AND #2
Embase	#1 "aphasia"/exp OR "generalization post-intervention"/exp OR "face-to-face treatment" #2 "naming accuracy post-intervention"/exp OR "Western Aphasia Battery Aphasia Quotient"/exp OR "telerehabilitation" #3 #1 AND #2
Cochrane Library	#1 (aphasia):ti,ab,kw OR (generalization post-intervention):ti,ab,kw OR (face-to-face treatment):ti,ab,kw (Word variations have been searched) #2 (naming accuracy post-intervention):ti,ab,kw OR (Western Aphasia Battery Aphasia Quotient):ti,ab,kw OR (telerehabilitation):ti,ab,kw (Word variations have been searched) #3 #1 AND #2
PubMed	#1 "aphasia"[MeSH] OR "generalization post-intervention"[MeSH] OR "face-to-face treatment" [All Fields] #2 "naming accuracy post-intervention"[MeSH Terms] OR "Western Aphasia Battery Aphasia Quotient"[MeSH] OR "telerehabilitation" [All Fields] #3 #1 AND #2
Ovid	#1 "aphasia"[All Fields] OR "generalization post-intervention" [All Fields] OR "face-to-face treatment" [All Fields] #2 "naming accuracy post-intervention"[All fields] OR "Western Aphasia Battery Aphasia Quotient"[All Fields] or "telerehabilitation"[All Fields] #3 #1 AND #2

Statistical analyses

Using a conservative approach and a random-effects model, the mean difference (MD) and 95% confidence interval (95% CI) were calculated. The I^2 index was employed to assess heterogeneity, with values ranging from 0 to 100%; thresholds of 0%, 25%, 50%, and 75% indicated no, low, moderate, and high heterogeneity, respectively.²⁴ To ensure that the appropriate model was applied, additional structures demonstrating a high degree of similarity to the relevant inquiry were also examined.²⁴ Subgroup analysis was conducted by dividing the original estimates into the predefined outcome groups. A p -value of less than 0.05 was used to determine the statistical significance of differences across subcategories.

Reporting bias assessment

Both quantitative and qualitative methods were employed to assess bias in the included studies. The Egger regression test and funnel plots, which plot the logarithm of the odds ratios (ORs) against their standard errors (SEs), were utilized. The presence of publication bias was determined using a threshold of $p \geq 0.05$.²⁵

Certainty assessment

Two-tailed tests were applied to examine each p -value. Review Manager v. 5.3 (The Nordic Cochrane Centre, The Cochrane Collaboration, Copenhagen, Denmark) was used to perform the statistical analyses and generate the graphs.

Results

Out of 1,185 identified studies, 6 papers published between 2014 and 2021 met the inclusion criteria and were selected for this meta-analysis.^{7,26–30} The findings from these studies are summarized in Table 2. At baseline, the included studies collectively involved 168 participants with aphasia. The sample sizes of the selected studies ranged from 10 to 40 subjects.

As illustrated in Fig. 2, telerehabilitation resulted in significantly greater generalization post-intervention in individuals with aphasia (MD = 11.53; 95% CI: 3.64–19.43; $p = 0.004$), with no heterogeneity ($I^2 = 0\%$), compared to face-to-face treatment. However, no significant differences were observed between telerehabilitation and face-to-face treatment in naming accuracy post-intervention (MD = 3.09; 95% CI: 1.98–8.16; $p = 0.23$; $I^2 = 0\%$), WAB (MD = -0.54; 95% CI: -9.96–8.88; $p = 0.91$; $I^2 = 0\%$), auditory comprehension aphasia quotient post-intervention (MD = 0.66; 95% CI: -8.83–10.14; $p = 0.89$; $I^2 = 0\%$), or functional communication post-intervention (MD = -0.95; 95% CI: -10.19–8.29; $p = 0.84$; $I^2 = 0\%$), as shown in Fig. 3–6.

The use of stratified models to examine the effects of specific variables was not possible due to the lack of detailed data on factors such as age, gender, severity, and ethnicity in the comparison outcomes. No indication of publication bias was detected based on visual interpretation of the funnel plots or the quantitative Egger regression tests ($p = 0.87, 0.88, 0.89, 0.86$, and 0.85 , respectively), as shown in Fig. 7–9. Nonetheless, it was noted that most of the included RCTs exhibited suboptimal technical quality, although no evidence of selective reporting bias was identified.

Table 2. Characteristics of the studies included in the meta-analysis

Study	Country	Total	Telerehabilitation	Face-to-face treatment	Treatment classification	Length, frequency and duration	Outcome measures
Agostini et al., 2014 ⁷	Italy	10	5	5	Lexical management word finding treatment (face-to-face treatment and telerehabilitation)	8 sessions of equal period for each management program; 3 weeks of wash-out between the 2 managements	Naming accuracy (percent correct) on the treatment set
Woolf et al., 2016 ²⁶	UK	10	5	5	Lexical management word finding treatment (supplied either face to face or remotely (via video conferencing))	1 h, twice a week, total of 8 sessions	Spoken picture naming of comprehensive aphasia test, naming in conversation
Zhou et al., 2018 ²⁷	China	40	20	20	Multimodal management inpatient group and discharge group randomly assigned to computerized speech-language and cognitive training group or control group (which received routine treatment if inpatient, or family topics communication management if discharged).	Inpatient: twice a day for 14 days. Discharged: 30 min/session, 2 times/day for 30 days. Training group: Inpatient: 14 days, twice/day Discharged: 30 min/day for 30 consecutive days.	Western Aphasia Battery, communication activities of daily living
Meltzer et al., 2018 ²⁸	USA	30	15	15	Multimodal management Group 1: In-person management Group 2: Telerehabilitation	Weekly 1 h sessions over 10 weeks	Western Aphasia Battery, Communication Confidence Rating Scale for Aphasia, Communicative Effectiveness Index
Øra et al., 2020 ²⁹	Norway	62	32	30	Multimodal Management Training group: Usual care + telerehabilitation (consisting of augmented language training via videoconference). Control group: Usual care only.	Telerehabilitation: 60 min session, 5 days/week for 4 consecutive weeks. Usual care: Variable.	Norwegian Basic Aphasia Assessment, Verb and Sentence Test, Communicative Effectiveness Index
Peñaloza et al., 2021 ³⁰	USA	16	8	8	Semantic treatment telerehabilitation group in-person therapy group	20 sessions in total (i.e., 2-h sessions twice per week) for both in person and telerehabilitation groups.	Western Aphasia Battery, Boston Naming, Pyramids and Palm Trees Test
Total		168	85	83	–	–	–

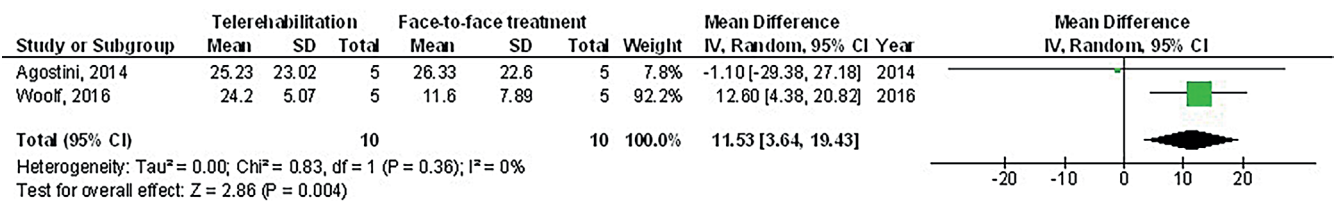


Fig. 2. The telerehabilitation compared to face-to-face treatment’s forest plot influence on generalization post-intervention in participants with aphasia

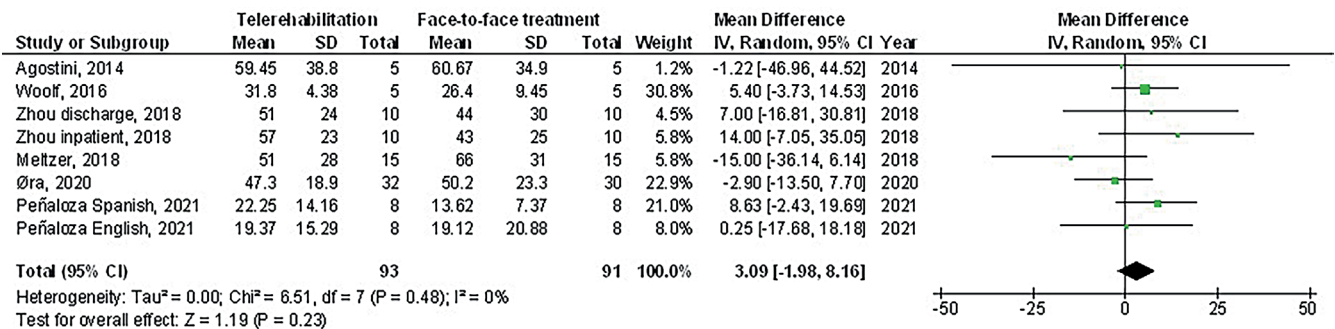


Fig. 3. The telerehabilitation compared to face-to-face treatment’s forest plot influence on naming accuracy post-intervention in participants with aphasia

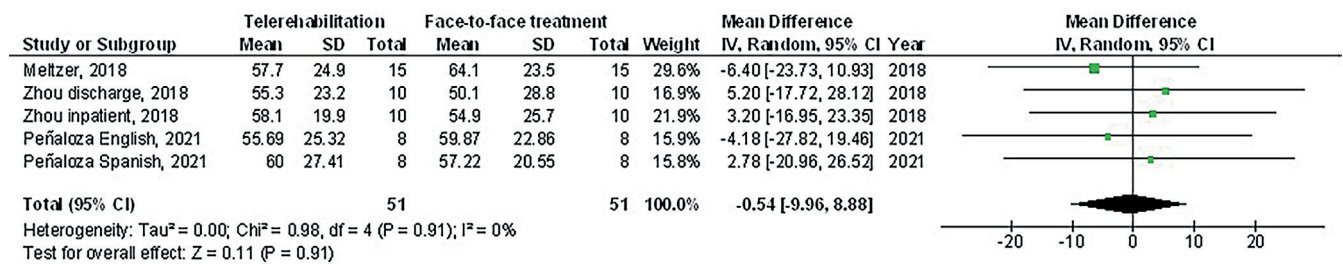


Fig. 4. The telerehabilitation compared to face-to-face treatment's forest plot influence on Western Aphasia Battery aphasia quotient in participants with aphasia

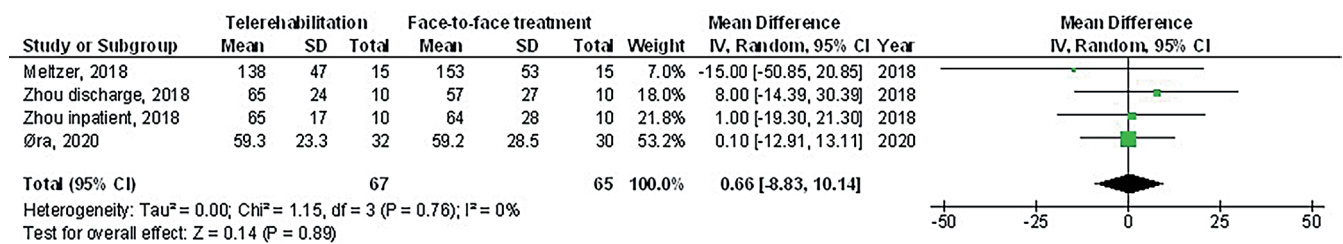


Fig. 5. The telerehabilitation compared to face-to-face treatment's forest plot influence on auditory comprehension post-intervention in participants with aphasia

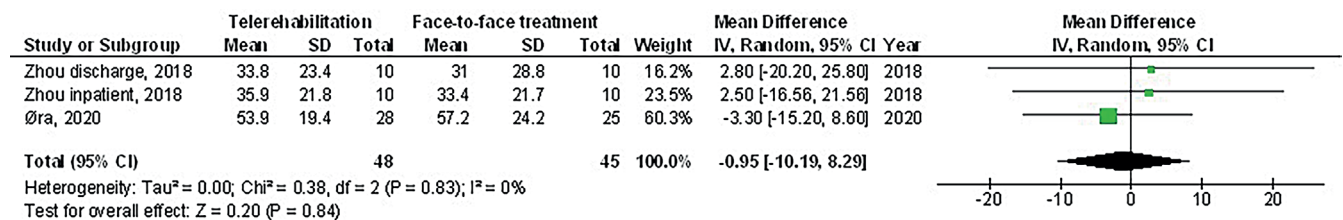


Fig. 6. The telerehabilitation compared to face-to-face treatment's forest plot influence on functional communication post-intervention in participants with aphasia

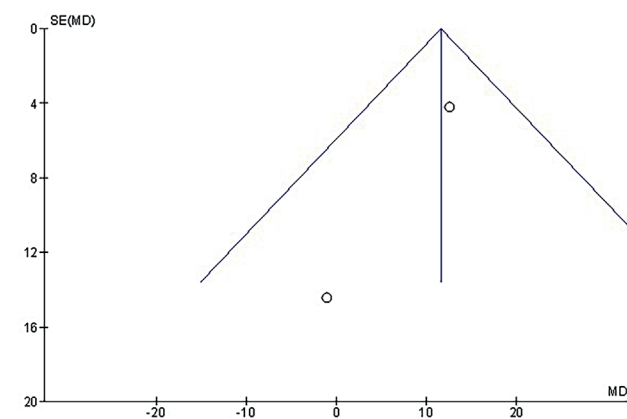


Fig. 7. The telerehabilitation compared to face-to-face treatment's funnel plot influence on generalization post-intervention in participants with aphasia

Discussions

The meta-analysis included 6 studies, which collectively involved 168 participants with aphasia at baseline.^{7,26–30} In individuals with aphasia, telerehabilitation showed significantly greater generalization post-intervention compared to face-to-face treatment. However, no significant differences were found between telerehabilitation and face-to-face treatment in naming accuracy post-intervention,

WAB aphasia quotient, auditory comprehension post-intervention, or functional communication post-intervention. Further research is needed to confirm these findings, and caution should be exercised when interpreting the results, as many of the comparisons were based on a small number of included studies, which may impact the statistical significance and robustness of the assessments.^{31–41}

The validity and reliability of telerehabilitation systems for speech and language disorders are increasingly supported by evidence. Studies have demonstrated the effectiveness of telepractice in the evaluation of acquired language disorders⁴² and in the treatment of these conditions,⁴³ particularly regarding speech and voice impairments in individuals with Parkinson's disease.⁴⁴ Additionally, telerehabilitation has shown promise in addressing fluency disorders, with multiple studies reporting that telerehabilitation is both feasible and effective, leading to positive clinical outcomes in the treatment of stuttering in children,⁴⁵ adolescents⁴⁶ and adults.⁴⁷ However, the effectiveness of telerehabilitation applications specifically targeting aphasic impairments – such as telerehabilitation for anomia⁴⁸ or the evaluation of apraxia of speech⁴⁹ – remains poorly supported and requires further investigation.⁵⁰

Agostini et al. demonstrated the feasibility and efficacy of telerehabilitation for addressing lexical deficiencies

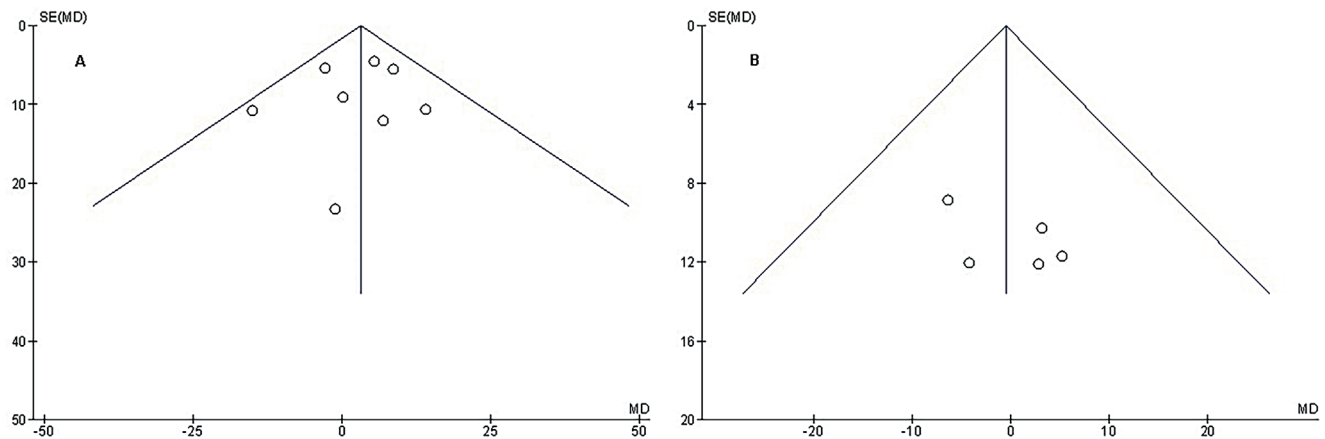


Fig. 8. The telerehabilitation compared to face-to-face treatment's funnel plot influence on naming accuracy post-intervention in participants with aphasia

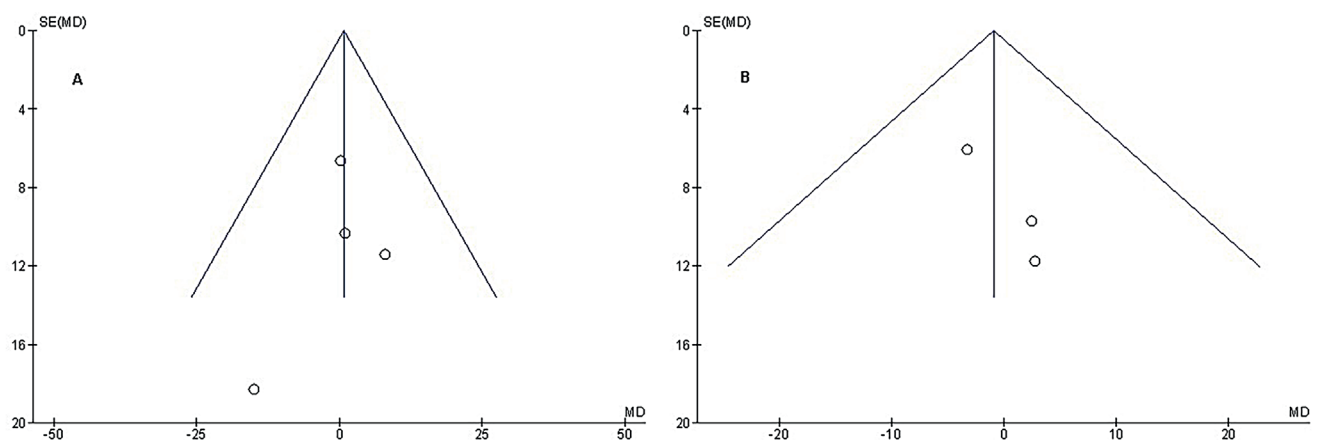


Fig. 9. The telerehabilitation compared to face-to-face treatment's funnel plot influence on Western Aphasia Battery aphasia quotient in participants with aphasia

in chronic stroke patients by showing comparable outcomes between in-person and telerehabilitation settings.⁷ Additionally, Latimer et al. reported that computer-based therapy may reduce the societal costs associated with managing health services for individuals with chronic aphasia.⁵¹ The rationale for telerehabilitation lies in its ability to activate mechanisms similar to those engaged in traditional therapies.⁵² Initial findings from clinical practice suggest that telerehabilitation is well-suited for speech and language therapy and can be effectively applied to lexical retrieval training. For example, interacting with a touchscreen can replicate many of the same therapeutic processes as writing on paper.

Two technological strategies show promise for delivering remote speech and language therapy. The 1st approach, known as asynchronous telerehabilitation, involves self-administered, computer-based activities that allow patients to complete structured training independently, without requiring the immediate presence of a speech-language pathologist. Therapists can later review the patient's progress and adjust the complexity of the exercises based on individual needs.⁵³ Kurland et al. demonstrated that for individuals with chronic aphasia, unsupervised home

practice combined with weekly video teleconferencing support was effective.⁵⁴

The 2nd approach, known as synchronous telerehabilitation, uses two-way videoconferencing, allowing the speech-language pathologist to be present in real time. This method enables therapists to provide live remote treatments while reducing the time and financial burden associated with travel.²⁸

The currently available research indicates that the topic of speech and language telerehabilitation has not been adequately explored through meta-analyses. While telerehabilitation appears to be an acceptable mode of service delivery for individuals with motor impairments following stroke – showing comparable effectiveness to in-person therapy⁵² – such results have not yet been consistently confirmed for individuals with aphasia. To advance therapeutic practice, it is essential to incorporate emerging evidence on the application of telerehabilitation in aphasia treatment. Despite an extensive search strategy, only 6 trials out of 1,185 identified studies met the inclusion criteria for this meta-analysis.

There is a clear need for further research in this field, as the selected studies suggest that speech and language

telerehabilitation is a relatively new approach to aphasia rehabilitation, with the potential for significant improvements. However, because all included studies involved small sample sizes, future research with larger cohorts is necessary to generate more robust and compelling evidence. Additionally, inadequate reporting and a lack of clarification from study authors often made it difficult to determine the risk of bias. For example, Zhou et al. reported that patients were randomly assigned to either the training or control group, but they did not provide details about the randomization process.²⁷

Additionally, the Grading of Recommendations Assessment, Development and Evaluation (GRADE) revealed that the methodological quality of the included studies ranged from extremely low-to-moderate, making it impossible to draw definitive conclusions about the efficacy of telerehabilitation compared to traditional in-person treatment. The certainty assessments were significantly influenced by issues related to indirectness of evidence and risk of bias. Specifically, the quality of evidence was downgraded due to unclear or inadequate methods for patient randomization in RCTs, the nonrandomized allocation of participants between groups, and the lack of reported details on allocation concealment.

Additionally, in accordance with the Core Outcome Set for aphasia research proposed by Wallace et al., evaluations related to the indirectness of evidence were downgraded by 1 level for all outcomes except the WAB.⁵⁵ This downgrade stems from the use of surrogate outcome measures – defined as measures used in place of a true clinical endpoint – since most tests assessing language abilities were conducted within standardized language evaluation settings rather than within natural communication contexts.⁵⁶

Successful communication depends on having language and communication abilities that enable the conveyance of messages through spoken, written, nonverbal, or combined modalities. Formal measures of communication success range from analyzing real-world discourse interactions to sampling conversations during specific activities.⁴ As previously noted by Brady et al., surrogate outcome measures of communicative and linguistic abilities are often employed as formal assessments of receptive and expressive language, typically using standardized language tests. This reliance is largely due to the lack of comprehensive, reliable, valid, and internationally accepted tools for evaluating communication in naturalistic settings.⁴

Due to the considerable variation observed in the results, for which no reasonable explanation could be identified, the certainty rating for the generalization outcome was also downgraded by 1 level for inconsistency. These findings highlight the need for further research and will likely have a significant impact on the ability to predict the treatment's overall effectiveness. As a result, additional high-quality RCTs, as well as data on the cost-effectiveness of telerehabilitation, are needed to strengthen future research in speech and language telerehabilitation.

Although the search strategy included 6 databases and considered studies published in conference proceedings, the grey literature was not explored. In cases where information appeared incomplete or missing, the authors were contacted; however, no responses were received.

Limitations

Although 1,185 studies were initially screened, only 6 ultimately met the inclusion criteria, comprising a total sample size of 168 participants. This small sample size may limit the generalizability and statistical power of the findings. Additionally, the quality of the included studies was uneven, with several methodological flaws that could affect the reliability and validity of the results. Furthermore, inconsistencies in participant characteristics – such as age, gender and cultural background – across the included studies may further limit the external validity and applicability of the conclusions.

Telerehabilitation showed significant improvements in generalization post-intervention; however, no significant differences were observed in naming accuracy, auditory comprehension, or functional communication, which may limit its broader clinical applicability. Additionally, the article does not provide data on the long-term effects of telerehabilitation, making it impossible to evaluate its sustained effectiveness in long-term rehabilitation. Furthermore, the comparison between telerehabilitation and face-to-face treatment did not fully account for specific implementation details or individual patient differences, which may affect the interpretation and applicability of the results.

Conclusions

In individuals with aphasia, telerehabilitation demonstrated significantly greater generalization post-intervention compared to face-to-face treatment. However, no significant differences were observed between telerehabilitation and face-to-face treatment regarding naming accuracy post-intervention, WAB aphasia quotient, auditory comprehension post-intervention, or functional communication post-intervention. Further research is needed to confirm these findings, and caution is warranted when interpreting the results, as many comparisons were based on a limited number of included studies. This limitation may impact the strength and significance of the assessed outcomes.

Use of AI and AI-assisted technologies

Not applicable.

ORCID iDs

Liang Zhang  <https://orcid.org/0009-0004-7391-3991>

References

- Donnan GA, Fisher M, Macleod M, Davis SM. Stroke. *Lancet*. 2008; 371(9624):1612–1623. doi:10.1016/S0140-6736(08)60694-7
- Langhorne P, Bernhardt J, Kwakkel G. Stroke rehabilitation. *Lancet*. 2011;377(9778):1693–1702. doi:10.1016/S0140-6736(11)60325-5
- Engelter ST, Gostynski M, Papa S, et al. Epidemiology of aphasia attributable to first ischemic stroke: Incidence, severity, fluency, etiology, and thrombolysis. *Stroke*. 2006;37(6):1379–1384. doi:10.1161/01.STR.0000221815.64093.8c
- Brady MC, Kelly H, Godwin J, Enderby P, Campbell P. Speech and language therapy for aphasia following stroke. *Cochrane Database Syst Rev*. 2016;2016(6):CD000425. doi:10.1002/14651858.CD000425.pub4
- Code C, Herrmann M. The relevance of emotional and psychosocial factors in aphasia to rehabilitation. *Neuropsychol Rehabil*. 2003; 13(1–2):109–132. doi:10.1080/09602010244000291
- McKevitt C, Fudge N, Redfern J, et al. Self-reported long-term needs after stroke. *Stroke*. 2011;42(5):1398–1403. doi:10.1161/STROKEAHA.110.598839
- Agostini M, Garzon M, Benavides-Varela S, et al. Telerehabilitation in poststroke anomia. *Biomed Res Int*. 2014;2014:06909. doi:10.1155/2014/706909
- Howe TJ, Worrall LE, Hickson LMH. Observing people with aphasia: Environmental factors that influence their community participation. *Aphasiology*. 2008;22(6):618–643. doi:10.1080/02687030701536024
- Winters JM. Telerehabilitation research: Emerging opportunities. *Annu Rev Biomed Eng*. 2002;4(1):287–320. doi:10.1146/annurev.bioeng.4.112801.121923
- Brennan D, Tindall L, Theodoros D, et al. A blueprint for telerehabilitation guidelines. *Int J Telerehabil*. 2010;27(2):31–34. doi:10.5195/ijt.2010.6063
- Stroup DF, Berlin JA, Morton SC, et al. Meta-analysis of observational studies in epidemiology: A proposal for reporting. Meta-analysis Of Observational Studies in Epidemiology (MOOSE) group. *JAMA*. 2000;283(15):2008–2012. doi:10.1001/jama.283.15.2008
- Amin MA. A meta-analysis of the eosinophil counts in the small intestine and colon of children without obvious gastrointestinal disease. *Int J Clin Med Res*. 2023;1(1):1–8. doi:10.61466/ijcmr1010001
- Emad M, Osama H, Rabaa H, Saeed H. Dual compared with triple antithrombotics treatment effect on ischemia and bleeding in atrial fibrillation following percutaneous coronary intervention: A meta-analysis. *Int J Clin Med Res*. 2023;1(2):77–87. doi:10.61466/ijcmr1020010
- Giong Z, Lie N. A meta-analysis of the impact of a phosphate-specific diet on serum phosphate levels in people receiving hemodialysis. *Int J Clin Med Res*. 2024;2(4):135–142. doi:10.61466/ijcmr2040005
- Gu R, Xu G. A meta-analysis looking at the effects of continuous management for complications related to intraoperative pressure wound ulcers in women with breast cancer. *Int J Clin Med Res*. 2024;2(4):100–106. doi:10.61466/ijcmr2040001
- Liberati A, Altman DG, Tetzlaff J, et al. The PRISMA Statement for Reporting Systematic Reviews and Meta-Analyses of studies that evaluate health care interventions: Explanation and elaboration. *PLoS Med*. 2009;6(7):e1000100. doi:10.1371/journal.pmed.1000100
- Guo Y. Effect of resident participation in ophthalmic surgery on wound dehiscence: A meta-analysis. *Int J Clin Med Res*. 2024;2(2):50–56. doi:10.61466/ijcmr2020002
- Jiany L, Xiu W. A meta-analysis evaluated the effectiveness of Chinese herbal medicine as a supplement to conventional care for patients with diabetic foot ulcers. *Int J Clin Med Res*. 2024;2(4):116–123. doi:10.61466/ijcmr2040003
- Koang Y. A meta-analysis on the use of photobiomodulation to regulate gingival wound healing in addition to periodontal therapies. *Int J Clin Med Res*. 2024;2(4):107–115. doi:10.61466/ijcmr2040002
- Osama H, Saeed H, Nicola M, Emad M. Neuraxial anesthesia compared to general anesthesia in subjects with hip fracture surgery: A meta-analysis. *Int J Clin Med Res*. 2023;1(2):66–76. doi:10.61466/ijcmr1020009
- Shaaban MEA, Mohamed AIM. Determining the efficacy of N-acetyl cysteine in treatment of pneumonia in COVID-19 hospitalized patients: A meta-analysis. *Int J Clin Med Res*. 2023;1(2):36–42. doi:10.61466/ijcmr1020006
- Singh RK. A meta-analysis of the impact on gastrectomy versus endoscopic submucosal dissection for early stomach cancer. *Int J Clin Med Res*. 2023;1(3):88–99. doi:10.61466/ijcmr1030011
- Gupta S, Rout G, Patel AH, et al. Efficacy of generic oral directly acting agents in patients with hepatitis C virus infection. *J Viral Hepat*. 2018; 25(7):771–778. doi:10.1111/jvh.12870
- Sheikhabahaei S, Trahan TJ, Xiao J, et al. FDG-PET/CT and MRI for evaluation of pathologic response to neoadjuvant chemotherapy in patients with breast cancer: A meta-analysis of diagnostic accuracy studies. *Oncologist*. 2016;21(8):931–939. doi:10.1634/theoncologist.2015-0353
- Higgins JPT, Thompson SG, Deeks JJ, Altman DG. Measuring inconsistency in meta-analyses. *BMJ*. 2003;327(7414):557–560. doi:10.1136/bmj.327.7414.557
- Woolf C, Cauter A, Haigh Z, et al. A comparison of remote therapy, face to face therapy and an attention control intervention for people with aphasia: A quasi-randomised controlled feasibility study. *Clin Rehabil*. 2016;30(4):359–373. doi:10.1177/0269215515582074
- Zhou Q, Lu X, Zhang Y, Sun Z, Li J, Zhu Z. Telerehabilitation combined speech-language and cognitive training effectively promoted recovery in aphasia patients. *Front Psychol*. 2018;9:2312. doi:10.3389/fpsyg.2018.02312
- Meltzer JA, Baird AJ, Steele RD, Harvey SJ. Computer-based treatment of poststroke language disorders: A non-inferiority study of telerehabilitation compared to in-person service delivery. *Aphasiology*. 2018;32(3):290–311. doi:10.1080/02687038.2017.1355440
- Øra HP, Kirmess M, Brady MC, et al. The effect of augmented speech-language therapy delivered by telerehabilitation on poststroke aphasia: A pilot randomized controlled trial. *Clin Rehabil*. 2020;34(3):369–381. doi:10.1177/0269215519896616
- Peñaloza C, Scimeca M, Gaona A, et al. Telerehabilitation for word retrieval deficits in bilinguals with aphasia: Effectiveness and reliability as compared to in-person language therapy. *Front Neurol*. 2021;12:589330. doi:10.3389/fneur.2021.589330
- Abdelrahim ME, Chrystyn H. Aerodynamic characteristics of nebulized terbutaline sulphate using the Next Generation Impactor (NGI) and CEN method. *J Aerosol Med Pulm Drug Deliv*. 2009;22(1):19–28. doi:10.1089/jamp.2008.0650
- Vecellio L, Abdelrahim ME, Montharu J, Galle J, Diot P, Dubus JC. Disposable versus reusable jet nebulizers for cystic fibrosis treatment with tobramycin. *J Cyst Fibros*. 2011;10(2):86–92. doi:10.1016/j.jcf.2010.10.004
- Ali AMA, Abdelrahim MEA. Modeling and optimization of terbutaline emitted from a dry powder inhaler and influence on systemic bioavailability using data mining technology. *J Pharm Innov*. 2014; 9(1):38–47. doi:10.1007/s12247-014-9171-8
- Elgendy MO, Abdelrahim ME, Salah Eldin R. Potential benefit of repeated MDI inhalation technique counselling for patients with asthma. *Eur J Hosp Pharm*. 2015;22(6):318–322. doi:10.1136/ejhp-2015-000648
- Hassan A, Rabaa H, Hussein RRS, et al. In vitro characterization of the aerosolized dose during non-invasive automatic continuous positive airway pressure ventilation. *Pulm Ther*. 2016;2(1):115–126. doi:10.1007/s41030-015-0010-y
- Hussein RRS, Ali AMA, Salem HF, Abdelrahman MM, Said ASA, Abdelrahim MEA. In vitro/in vivo correlation and modeling of emitted dose and lung deposition of inhaled salbutamol from metered dose inhalers with different types of spacers in noninvasively ventilated patients. *Pharm Dev Technol*. 2017;22(7):871–880. doi:10.3109/10837450.2015.1116567
- Madney YM, Fathy M, Elberry AA, Rabaa H, Abdelrahim MEA. Nebulizers and spacers for aerosol delivery through adult nasal cannula at low oxygen flow rate: An in-vitro study. *J Drug Deliv Sci Technol*. 2017;39:260–265. doi:10.1016/j.jddst.2017.04.014
- Saeed H, Elberry AA, Eldin AS, Rabaa H, Abdelrahim MEA. Effect of nebulizer designs on aerosol delivery during non-invasive mechanical ventilation: A modeling study of in vitro data. *Pulm Ther*. 2017;3(1):233–241. doi:10.1007/s41030-017-0033-7
- Harb HS, Elberry AA, Rabaa H, Fathy M, Abdelrahim ME. Performance of large spacer versus nebulizer T-piece in single-limb noninvasive ventilation. *Respir Care*. 2018;63(11):1360–1369. doi:10.4187/respcare.05976
- Saeed H, Ali AMA, Elberry AA, Eldin AS, Rabaa H, Abdelrahim MEA. Modeling and optimization of nebulizers' performance in non-invasive ventilation using different fill volumes: Comparative study between vibrating mesh and jet nebulizers. *Pulm Pharmacol Ther*. 2018;50:62–71. doi:10.1016/j.pupt.2018.04.005

41. Elgendy MO, Hassan AH, Saeed H, Abdelrahim ME, Eldin RS. Asthmatic children and MDI verbal inhalation technique counseling. *Pulm Pharmacol Ther.* 2020;61:101900. doi:10.1016/j.pupt.2020.101900
42. Theodoros D, Hill A, Russell T, Ward E, Wootton R. Assessing acquired language disorders in adults via the Internet. *Telemed J E Health.* 2008;14(6):552–559. doi:10.1089/tmj.2007.0091
43. Cherney L, Van Vuuren S. Telerehabilitation, virtual therapists, and acquired neurologic speech and language disorders. *Semin Speech Lang.* 2012;33(3):243–258. doi:10.1055/s-0032-1320044
44. Constantinescu G, Theodoros D, Russell T, Ward E, Wilson S, Wootton R. Assessing disordered speech and voice in Parkinson's disease: A telerehabilitation application. *Int J Lang Commun Disord.* 2010;45(6):630–644. doi:10.3109/13682820903470569
45. Wilson L, Onslow M, Lincoln M. Telehealth adaptation of the Lidcombe Program of Early Stuttering Intervention: Five case studies. *Am J Speech Lang Pathol.* 2004;13(1):81–93. doi:10.1044/1058-0360(2004/009)
46. Sicotte C, Lehoux P, Fortier-Blanc J, Leblanc Y. Feasibility and outcome evaluation of a telemedicine application in speech–language pathology. *J Telemed Telecare.* 2003;9(5):253–258. doi:10.1258/135763303769211256
47. O'Brian S, Packman A, Onslow M. Telehealth delivery of the Camperdown Program for adults who stutter: A phase I trial. *J Speech Lang Hear Res.* 2008;51(1):184–195. doi:10.1044/1092-4388(2008/014)
48. Dechène L, Tousignant M, Boissy P, et al. Simulated in-home tele-treatment for anomia. *Int J Telerehabil.* 2011;3(2):3–10. doi:10.5195/ijt.2011.6075
49. Hill AJ, Theodoros D, Russell T, Ward E. Using telerehabilitation to assess apraxia of speech in adults. *Int J Lang Commun Disord.* 2009;44(5):731–747. doi:10.1080/13682820802350537
50. Levy ES, Moya-Galé G, Chang YHM, et al. The effects of intensive speech treatment on intelligibility in Parkinson's disease: A randomised controlled trial. *EClinicalMedicine.* 2020;24:100429. doi:10.1016/j.eclinm.2020.100429.
51. Latimer NR, Dixon S, Palmer R. Cost-utility of self-managed computer therapy for people with aphasia. *Int J Technol Assess Health Care.* 2013;29(4):402–409. doi:10.1017/S0266462313000421
52. Laver KE, Adey-Wakeling Z, Crotty M, Lannin NA, George S, Sherrington C. Telerehabilitation services for stroke. *Cochrane Database Syst Rev.* 2020;2020(1):CD010255. doi:10.1002/14651858.CD010255.pub3
53. Wade J, Mortley J, Enderby P. Talk about IT: Views of people with aphasia and their partners on receiving remotely monitored computer-based word finding therapy. *Aphasiology.* 2003;17(11):1031–1056. doi:10.1080/02687030344000373
54. Kurland J, Liu A, Stokes P. Effects of a tablet-based home practice program with telepractice on treatment outcomes in chronic aphasia. *J Speech Lang Hear Res.* 2018;61(5):1140–1156. doi:10.1044/2018_JSLHR-L-17-0277
55. Wallace SJ, Worrall L, Rose T, et al. A core outcome set for aphasia treatment research: The ROMA consensus statement. *Int J Stroke.* 2019;14(2):180–185. doi:10.1177/1747493018806200
56. Johnston KC. What are surrogate outcome measures and why do they fail in clinical research? *Neuroepidemiology.* 1999;18(4):167–173. doi:10.1159/000026208

Effectiveness of sorafenib in combination with physical thermal ablation for hepatocellular carcinoma: A meta-analysis

*Xiang Wen^{1,B}, *Fuliang Qi^{1,C}, Hailong Qian^{1,B}, Rancen Tao^{2,C}, Jie Li^{1,A}, Liang Wang^{3,D}

¹ Department of Minimally Invasive Interventional Oncology, Baotou Cancer Hospital, China

² Department of Thoracic Oncology Surgery, Baotou Cancer Hospital, China

³ Department of Gastrointestinal Hepatobiliary Surgery, Baotou Cancer Hospital, China

A – research concept and design; B – collection and/or assembly of data; C – data analysis and interpretation;

D – writing the article; E – critical revision of the article; F – final approval of the article

Advances in Clinical and Experimental Medicine, ISSN 1899–5276 (print), ISSN 2451–2680 (online)

Adv Clin Exp Med. 2025;34(12):2035–2043

Address for correspondence

Jie Li

E-mail: 13847293318@163.com

Funding sources

Observation of the clinical efficacy of Hetrupopa on platelets III–IV after solid tumor chemotherapy, Beijing Medical Award Foundation, project No.: YXJL-2022-0791-0082.

Conflict of interest

None declared

* Xiang Wen and Fuliang Qi contributed equally to this work.

Received on November 13, 2024

Reviewed on December 15, 2024

Accepted on February 25, 2025

Published online on August 26, 2025

Abstract

Background. Hepatocellular carcinoma (HCC) is the 6th most common cancer worldwide and claims roughly 700,000 lives each year; nearly 50% of global HCC fatalities occur in China.

Objectives. To conduct a comprehensive meta-analysis identifying predictors of sorafenib efficacy in combination with thermal ablation for HCC treatment.

Materials and methods. A comprehensive literature search was conducted up to October 2024, reviewing 720 identified studies. From these, 19 studies were selected that included a total of 3,341 participants with HCC at baseline. The meta-analysis examined the effects of sorafenib in combination with physical thermal ablation, using odds ratios (ORs) and 95% confidence intervals (95% CIs). Analyses were performed using two-sided methods and either fixed-effect or random-effects models, depending on the level of heterogeneity.

Results. The meta-analysis revealed that combining physical thermal ablation with sorafenib significantly improved outcomes in HCC patients: Overall survival (OS) was more than doubled (OR = 2.03; 95% CI: 1.55–2.67; $p < 0.001$), recurrence rates were significantly reduced (OR = 0.62; 95% CI: 0.39–0.98; $p = 0.04$), and overall treatment efficacy was markedly higher (OR = 2.53; 95% CI: 1.61–3.96; $p < 0.001$) compared with thermal ablation alone.

Conclusions. In individuals with HCC, physical thermal ablation and sorafenib had significantly higher OS, lower recurrence rates, and high overall efficacy compared to physical thermal ablation. To validate this discovery, more research is needed, and caution must be implemented when interacting with its values.

Key words: hepatocellular carcinoma, sorafenib, overall survival, physical thermal ablation, overall efficacy

Cite as

Wen X, Qi F, Qian H, Tao R, Li J, Wang L. Effectiveness of sorafenib in combination with physical thermal ablation for hepatocellular carcinoma: A meta-analysis. *Adv Clin Exp Med*. 2025;34(12):2035–2043. doi:10.17219/acem/202323

DOI

10.17219/acem/202323

Copyright

Copyright by Author(s)

This is an article distributed under the terms of the Creative Commons Attribution 3.0 Unported (CC BY 3.0) (<https://creativecommons.org/licenses/by/3.0/>)

Highlights

- Sorafenib plus thermal ablation doubles survival in HCC patients: Meta-analysis of 3,341 patients shows that combining sorafenib with physical thermal ablation significantly improves overall survival (OR 2.03; $p < 0.001$) in hepatocellular carcinoma (HCC) treatment.
- Combination therapy reduces HCC recurrence risk: Sorafenib and thermal ablation together lower recurrence rates in HCC patients by 38% (OR 0.62; $p = 0.04$), highlighting a strong preventive benefit over ablation alone.
- Enhanced treatment efficacy with sorafenib-based combination strategy: Overall treatment efficacy improved significantly when sorafenib was added to thermal ablation (OR 2.53; $p < 0.001$), indicating superior therapeutic outcomes.
- Meta-analysis supports combined modality for improved HCC outcomes: Evidence from 19 studies suggests that sorafenib-ablation combination offers a powerful approach for improving prognosis in hepatocellular carcinoma, especially in high-burden regions like China.

Background

Globally, hepatocellular carcinoma (HCC) ranks as the 6th most common malignant tumor. Each year, approx. 700,000 people die from HCC worldwide, with China accounting for nearly half of these deaths.^{1,2} Current primary treatment options include liver transplantation, surgical resection, radiofrequency ablation, percutaneous ethanol injection, transarterial chemoembolization, and sorafenib.³ Advances in medical technology and the development of various prognostic scoring systems, such as the Barcelona Clinic Liver Cancer (BCLC) staging system and the Italian Liver Cancer (ITA.LI.CA) tumor staging system, have expanded the range of treatment options available to HCC patients.⁴ Although surgical resection is considered the first-line treatment for HCC, factors such as multiple lesions, unfavorable tumor location, and poor patient condition can render surgery unfeasible.⁵

Because the early symptoms of liver cancer are often subtle or absent, many patients are diagnosed at an advanced stage, missing the optimal window for surgical intervention. The widespread use of liver transplantation is further limited by its high cost and the scarcity of available donor organs. As a result, physical thermal ablation has emerged as a less invasive and effective alternative therapy. Microwave ablation and radiofrequency ablation are the 2 main forms of physical thermal ablation used for liver tumors. Although they rely on different physical principles, both techniques utilize imaging guidance to accurately target the tumor and insert electrodes into the tissue. When the tumor tissue reaches a certain temperature, protein denaturation occurs, leading to tumor destruction and shrinkage. Xu et al. conducted a meta-analysis comparing the effects of radiofrequency ablation and hepatic resection in the treatment of liver cancer.⁶ The study found that, compared to the hepatic resection group, the radiofrequency ablation group had similar 1-year overall survival (OS), lower 5-year OS, a higher

incidence of overall recurrence, shorter hospitalization duration, and a lower complication rate. This suggests that thermal ablation offers the advantages of a shorter treatment time and fewer complications compared to surgery. However, patients with HCC who undergo thermal ablation alone often face poor long-term prognosis and high recurrence rates.⁷ Sorafenib, a multi-targeted kinase inhibitor, addresses some of these challenges by inhibiting key components of the Ras/Raf/MEK/ERK signaling cascade, including B-Raf, Raf-1 and other kinases, thereby suppressing tumor cell growth and differentiation.⁸ Additionally, by blocking receptors such as hepatocyte cytokine receptors (e.g., c-Kit), vascular endothelial growth factor receptors (e.g., VEGFR-2), and platelet-derived growth factor receptors (e.g., PDGFR- β), sorafenib reduces angiogenesis.⁹

According to a meta-analysis of 1,462 patients with advanced HCC, sorafenib reduced the risk of tumor progression and death while improving the disease control rate compared to placebo.¹⁰ Numerous studies have also demonstrated that sorafenib, whether used alone or in combination with other treatments, can extend the survival time of patients with HCC.^{11–13} However, sorafenib may also have adverse effects on normal liver tissue and can delay tissue healing following thermal ablation. Therefore, when considering both the positive and negative effects of sorafenib's therapeutic action, the overall benefit of combining it with physical thermal ablation must be carefully balanced. Meta-analysis, by synthesizing disaggregated data, can provide a higher level of evidence to inform therapeutic decision-making.¹⁴

Objectives

We conducted a meta-analysis to evaluate the effectiveness of sorafenib combined with physical thermal ablation in the treatment of HCC.

Methods

Eligibility criteria

For the purpose of creating a summary, the investigations demonstrating the effectiveness of sorafenib in combination with physical thermal ablation for the treatment of HCC were chosen.¹⁵

Information sources

Figure 1 represents the study selection process. Literature was included when the following inclusion criteria were met^{16,17}:1) The study was a randomized controlled trial (RCT), observational, prospective, or retrospective in design; 2) The participants had been diagnosed with HCC; 3) The intervention included combination therapy with physical thermal ablation and sorafenib; 4) The study specifically evaluated the effectiveness of sorafenib combined with physical thermal ablation for HCC.

Studies were excluded if they did not assess the effectiveness of this combination therapy, focused solely on physical thermal ablation, or lacked meaningful comparative significance.^{18,19}

Search strategy

A search protocol was established using the PICOS framework, defined as follows: the population (P) consisted of individuals with HCC; the intervention or exposure (I) was combination therapy with sorafenib and physical thermal ablation; the comparison (C) involved comparing the combination therapy to physical thermal ablation

alone; the outcomes (O) included OS, recurrence rates and overall efficacy; and the study design (S) was unrestricted, with no limitations placed on study type.²⁰

A thorough search of the Google Scholar, Embase, Cochrane Library, PubMed, and OVID databases was conducted through October 2024, using a predefined set of keywords and additional terms, as detailed in Table 1.^{21,22} To avoid including studies that did not establish a clear link between the effectiveness of sorafenib combined with physical thermal ablation for HCC, duplicate records were removed. The remaining articles were compiled into an EndNote file (Clarivate, London, UK), and their titles and abstracts were reassessed for relevance.^{23,24}

Selection process

The meta-analysis method was then used to organize and assess the process that followed the epidemiological proclamation.^{25,26}

Data collection process

Some of the criteria used for data extraction included the name of the first author, study details, year of publication, country or region, population type, study categories, quantitative and qualitative assessment methods, data sources, outcome measures, clinical and therapeutic characteristics, and statistical analysis approaches.²⁷

Data items

When a study yielded differing values, data related to the evaluation of the effectiveness of sorafenib combined

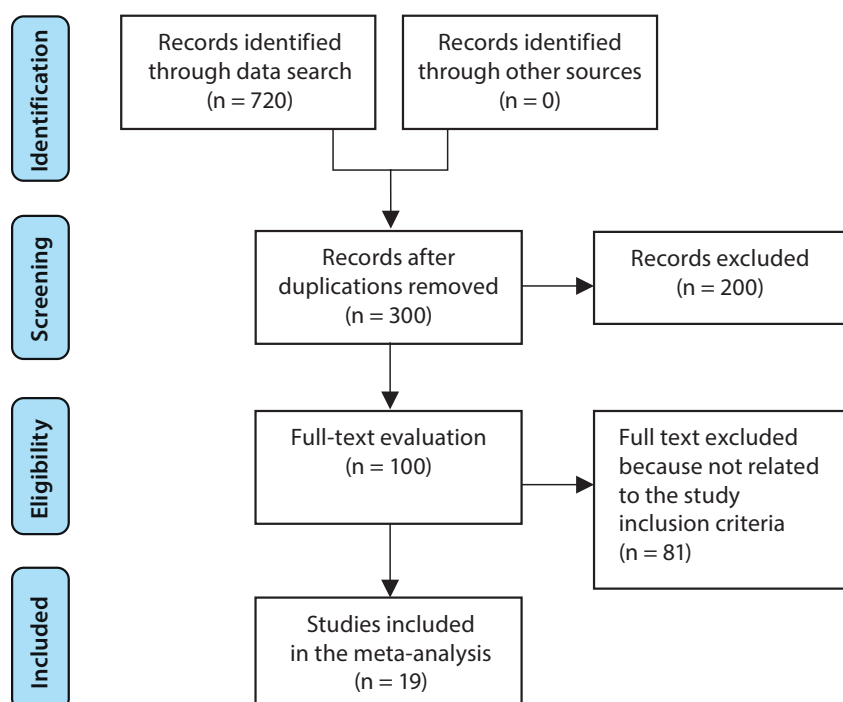


Fig. 1. Workflow of the systematic review and meta-analysis

Table 1. Database search strategy

Database	Search strategy
Google Scholar	#1 "hepatocellular carcinoma" OR "overall survival" #2 "recurrence rates" OR "overall efficacy" OR "physical thermal ablation" OR "sorafenib" #3 #1 AND #2
Embase	#1 "hepatocellular carcinoma"/exp OR "overall survival"/exp OR "physical thermal ablation" #2 "recurrence rates"/exp OR "overall efficacy"/exp OR "sorafenib" #3 #1 AND #2
Cochrane Library	#1 (hepatocellular carcinoma):ti,ab,kw OR (overall survival):ti,ab,kw OR (physical thermal ablation):ti,ab,kw (Word variations have been searched) #2 (recurrence rates):ti,ab,kw OR (overall efficacy):ti,ab,kw OR (sorafenib):ti,ab,kw (Word variations have been searched) #3 #1 AND #2
PubMed	#1 "hepatocellular carcinoma"[MeSH] OR "overall survival"[MeSH] OR "physical thermal ablation"[All Fields] #2 "recurrence rates"[MeSH Terms] OR "overall efficacy"[MeSH] OR "sorafenib"[All Fields] #3 #1 AND #2
OVID	#1 "hepatocellular carcinoma"[All Fields] OR "overall survival"[All Fields] OR "physical thermal ablation"[All Fields] #2 "recurrence rates"[All fields] OR "overall efficacy"[All Fields] or "sorafenib"[All Fields] #3 #1 AND #2

with physical thermal ablation for HCC were independently extracted.

Research risk of bias assessment

Two authors independently assessed the risk of bias in the included studies and evaluated the quality of the methodologies employed in the papers selected for further analysis. An unbiased review of the methods used in each study was conducted by both authors.

Effect measures

Sensitivity analysis was limited to studies that assessed and documented the effectiveness of sorafenib in combination with physical thermal ablation for HCC.

Synthesis methods

Using a dichotomous approach and a random or fixed-effect model, the odds ratio (OR) and a 95% confidence interval (95% CI) were determined. A range of 0–100% was used to determine the I^2 index. Heterogeneity was assessed, with thresholds of 0%, 25%, 50%, and 75% indicating no, low, moderate, and substantial heterogeneity, respectively.²⁸ To ensure that the exact model was used, additional structures that show a high degree of similarity with the related inquiry were also examined. The random effect was used.²⁸ A subclass analysis was performed by splitting the original estimation into the previously specified consequence groups. A p-value of less than 0.05 was utilized in the analysis to define the statistical significance of differences across subcategories.

Reporting bias assessment

Both quantitative and qualitative methods were employed to measure the bias in the investigations: the Egger's

regression test and funnel plots, which display the logarithm of the ORs against their standard errors (SEs). The presence of investigation bias was determined by $p \geq 0.05$.²⁹

Certainty assessment

Each p-value was assessed using two-tailed testing. Graphs and statistical analyses were generated using Review Manager v. 5.3 (The Nordic Cochrane Centre, The Cochrane Collaboration, Copenhagen, Denmark).

Results

Out of 720 identified studies, 19 papers published between 2011 and 2024 met the inclusion criteria and were selected for this analysis.^{30–48} Table 2 presents the findings of these studies. At baseline, the combined studies included a total of 3,341 participants with HCC, with individual study sample sizes ranging from 30 to 1,114 subjects.

As illustrated in Fig. 2–4, in individuals with HCC, combination therapy demonstrated significantly higher OS (OR = 2.03; 95% CI: 1.55–2.67; $p < 0.001$) with moderate heterogeneity ($I^2 = 57\%$), lower recurrence rates (OR = 0.62; 95% CI: 0.39–0.98; $p = 0.04$) with high heterogeneity ($I^2 = 75\%$), and greater overall efficacy (OR = 2.53; 95% CI: 1.61–3.96; $p < 0.001$) with moderate heterogeneity ($I^2 = 44\%$), compared to physical thermal ablation alone.

Due to insufficient data on variables such as age, ethnicity and gender, the application of stratified models to investigate the effects of specific factors was not possible. Using both the quantitative Egger's regression test and visual inspection of the funnel plots, no evidence of publication bias was detected ($p = 0.89, 0.87$ and 0.91 , respectively), as shown in Fig. 5–7. However, it was noted that there was no evidence of selective reporting bias, although the majority of the included RCTs exhibited poor technical quality.

Table 2. Qualities of the studies selected for meta-analysis

Study	Country	Total	Physical thermal ablation and sorafenib	Physical thermal ablation
Sun J, 2011 ³⁰	China	30	15	15
Hua and He, 2012 ³¹	China	90	42	48
Zheng and Li, 2013 ³²	China	94	44	50
Feng et al., 2014 ³³	China	128	64	64
Bruix, et al., 2015 ³⁴	China	1,114	556	558
Kan et al., 2015 ³⁵	China	62	30	32
Guan et al., 2015 ³⁶	China	120	52	68
Wu et al., 2016 ³⁷	China	90	45	45
Gong et al., 2017 ³⁸	China	90	40	50
Yu et al., 2018 ³⁹	China	46	23	23
Zhu et al., 2018 ⁴⁰	China	106	40	66
Sun et al., 2018 ⁴¹	China	90	45	45
Fu and Xi, 2020 ⁴²	China	102	51	51
Li and Song, 2021 ⁴³	China	223	56	167
Abulimiti et al., 2021 ⁴⁴	China	82	36	46
Wei et al., 2022 ⁴⁵	Taiwan	211	103	108
Zhou et al., 2022 ⁴⁶	China	460	185	275
Seidensticker et al., 2023 ⁴⁷	Germany	103	54	49
Yang et al., 2024 ⁴⁸	China	100	50	50
Total		3,341	1,531	1,810

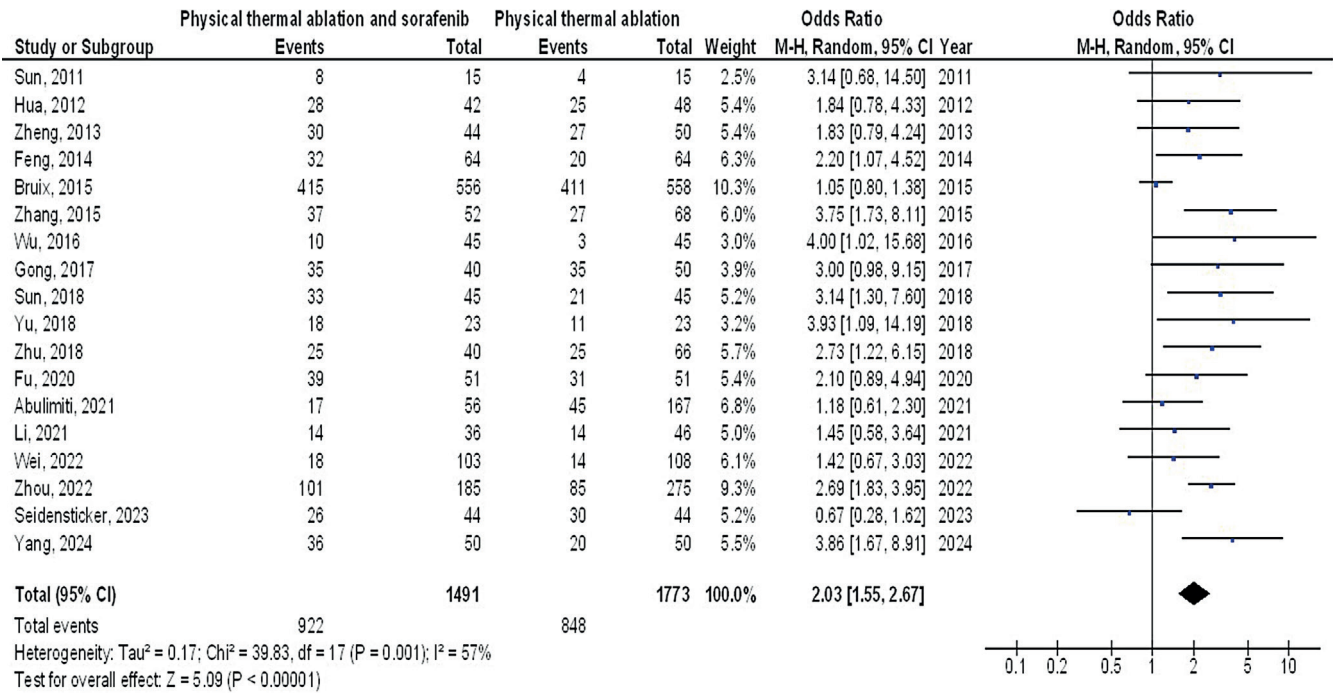


Fig. 2. The combination therapy compared to physical thermal ablation’s forest plot influence on overall survival in hepatocellular carcinoma

Discussions

A total of 3,341 HCC participants were included at baseline across the studies selected for this meta-analysis.^{30–48} In individuals with HCC, combination therapy

demonstrated significantly higher OS, lower recurrence rates, and greater overall efficacy compared to physical thermal ablation alone. However, further studies are required to confirm these findings, and caution should be exercised when interpreting their significance, as they

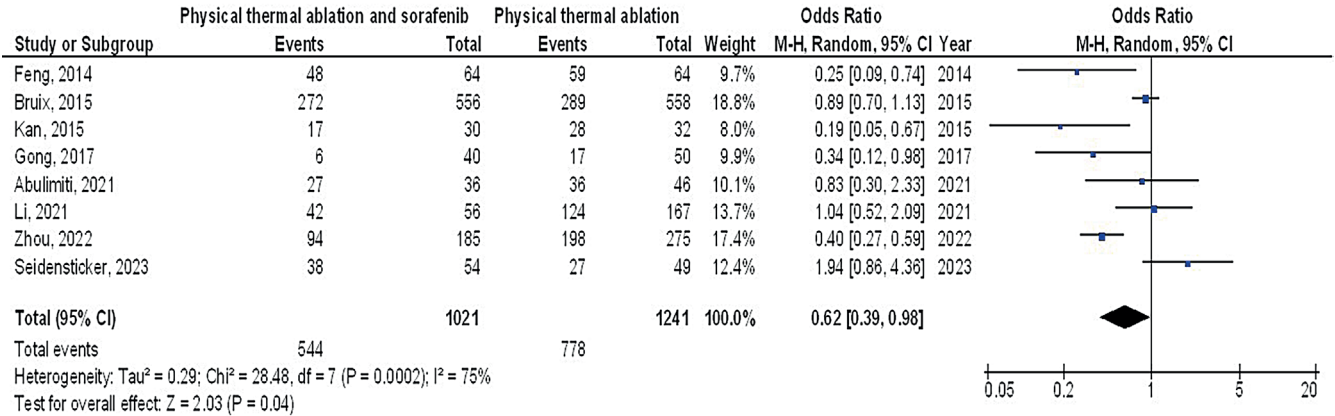


Fig. 3. The combination therapy compared to physical thermal ablation's forest plot influence on recurrence rates in hepatocellular carcinoma

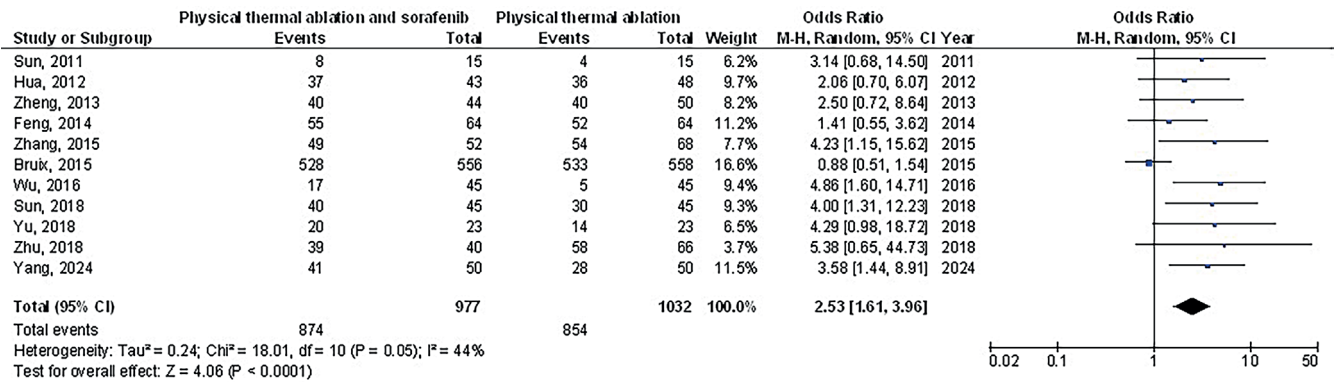


Fig. 4. The combination therapy compared to physical thermal ablation's forest plot influence on overall efficacy in hepatocellular carcinoma

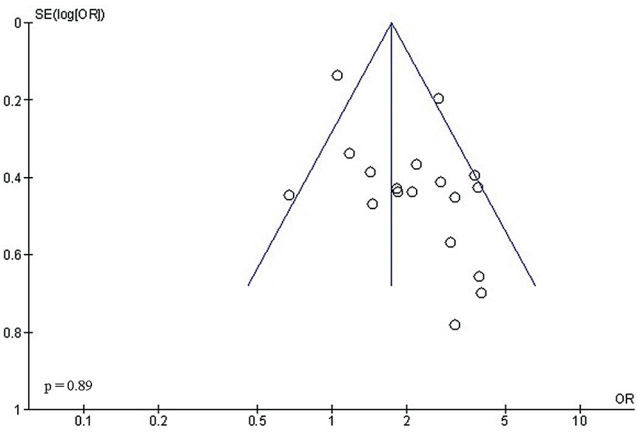


Fig. 5. The combination therapy compared to physical thermal ablation's funnel plot influence on overall survival in hepatocellular carcinoma

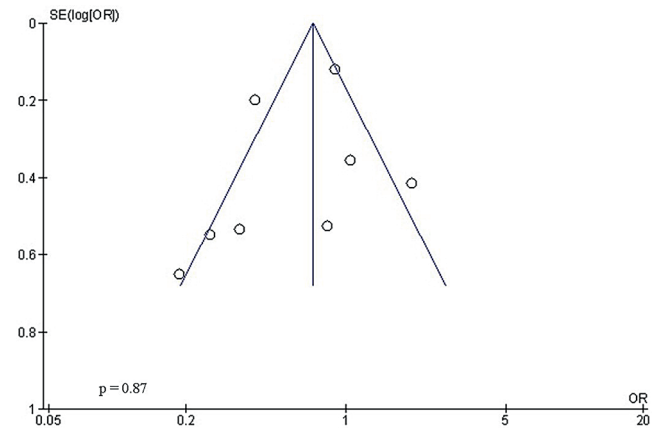


Fig. 6. The combination therapy compared to physical thermal ablation's funnel plot influence on recurrence rates in hepatocellular carcinoma

may affect the robustness and reliability of the reported outcomes.^{49–59}

Chemotherapy and ablation have been employed extensively in the treatment of cancer, including advanced renal cell carcinoma and small cell lung cancer.^{60,61} Physical thermal ablation has the benefits of minimal damage, rapid recovery and repeated application in the treatment of HCC. However, the lesion's size and the presence of heat dissipation make full ablation challenging and increase the chance of local recurrence. Recurrence is more likely when the tumor's

diameter exceeds 3.0 cm.^{62,63} Therefore, the goal of therapy improvement is to lower the rate of tumor recurrence following thermal ablation. Radiofrequency ablation combined with sorafenib achieves greater efficacy and survival, prolongs the radiofrequency interval, and reduces recurrence rates.

It has been demonstrated that radiofrequency ablation and the kinase inhibitor sorafenib work in concert. Its role in tumors is to suppress angiogenesis, which lowers heat loss and indirectly improves ablation. Additionally, sorafenib itself prevents the growth and development of tumor cells.

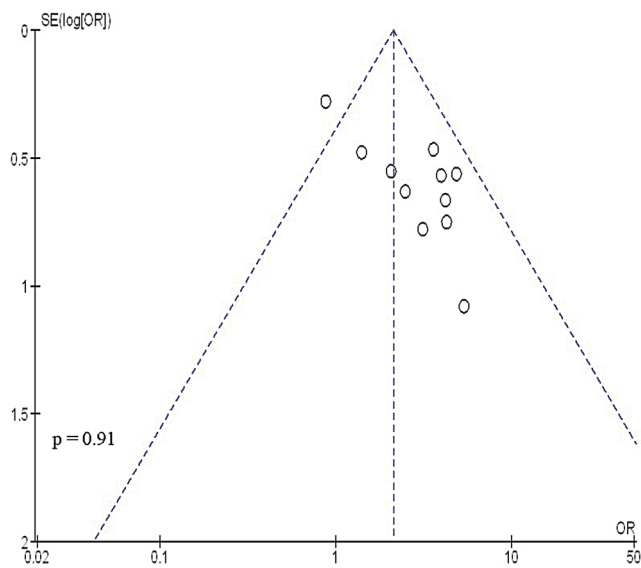


Fig. 7. The combination therapy compared to physical thermal ablation's funnel plot influence on overall efficacy in hepatocellular carcinoma

Millions of people have benefited from the first-line therapy of liver cancer with sorafenib, a tyrosine kinase inhibitor that blocks several receptors, including RAF-1, VEGFR-2 and FLT-3.11 According to studies, sorafenib may cause capillary damage and VEGF and PDGF inhibition as the mechanism of hand-foot skin reaction (HFSR). Direct pressure on the hands and feet causes the vessels to become mechanically injured once more, which causes an inflammatory reaction and the development of blisters.⁶⁴ As is well known, serious side effects might result in treatment suspension and ultimately impact the patient's ability to survive. Studies have also indicated that diarrhea is a predictor of improved OS in individuals with HCC using sorafenib.^{64,65} According to Reig et al., a higher chance of survival was linked to the occurrence of dermatological side effects within 60 days of starting sorafenib.⁶⁶ The quality of life may be impacted, and the anti-tumor efficacy may be limited if the adverse reaction results in a dose adjustment or interruption of sorafenib, regardless of whether it has a direct impact on survival. Therefore, to increase the lifespan and quality of life for patients with HCC, sorafenib dose adjustments and standardized treatment are required.

Not all of the studies included in this meta-analysis were RCTs. The number of original publications was limited, and the retrospective cohort studies were subject to recall and selection biases. Furthermore, the majority of the study populations were Chinese, with only a small proportion of Japanese and Spanish participants, making the overall study cohort racially non-representative and limiting generalizability. Notably, HCC is the 2nd most common cause of cancer-related mortality in China, after lung cancer, with China accounting for approx. 27% of global cancer deaths.⁶⁷

China now has the highest prevalence of liver cancer (about 55% of the global total rate) and the highest number of fatalities due to hepatitis B virus infection, aflatoxin

exposure, alcohol misuse, and environmental pollution.⁶⁸ The fact that the majority of the research participants in this meta-analysis were Chinese may be due in large part to the fact that China still has a long way to go in reducing the incidence and mortality of liver cancer. The heterogeneity of other parameters was noteworthy, with the exception of radiofrequency interval and overall efficacy. Variations in sample size, tumor characteristics (size and number), patient age, and prior treatment history may account for these differences. The effectiveness of radiofrequency ablation in conjunction with sorafenib in patients with HCC has also been meta-analyzed by Chen et al.⁶⁹

The best treatment for HCC is still being investigated. According to a thorough comparative study of HCC scoring systems published in the *World Journal of Hepatology*, a customized approach for patients with HCC should be created, and the appropriate scoring system should be chosen based on the patient's circumstances.⁴ Whether a treatment is curative, palliative, or a combination of both, as in this study (radiofrequency ablation + sorafenib), depends on the patient's characteristics and liver function. Thus, the development of a treatment plan for HCC requires the integration of several fields, including oncology, interventional radiology, and hepatobiliary surgery. Depending on the patient's development, side effects, and complications, customized settings and modifications would be required at any moment. In the treatment of HCC, physical thermal ablation in conjunction with sorafenib is superior to radiofrequency ablation or microwave ablation alone, per the present meta-analysis. Patients receiving combination therapy should be regularly monitored for adverse effects. Despite the use of random-effects models and subgroup analysis in this investigation, the reliability of the findings may still be impacted by study heterogeneity. More high-caliber research is still required to prove that physical thermal ablation plus sorafenib is superior than physical thermal ablation alone.

Limitations

Nevertheless, the excluded studies did not meet the necessary standards to be incorporated into the meta-analysis. Moreover, we did not have enough information to determine whether factors such as race, sex and age had an impact on results. Bias may have increased as a result of the incorporation of incomplete or erroneous data from earlier studies. The individuals' age, gender, nutrition and race were likely sources of bias in addition to their nutritional status. Unintentionally skewed values might arise from incomplete data and unpublished research.

Conclusions

In individuals with HCC, combination therapy demonstrated significantly higher OS, lower recurrence rates, and greater overall efficacy compared to physical thermal

ablation. Further research is needed to confirm these findings, and caution should be taken when interpreting their significance. Further exploration of this issue would have an impact on the significant of the evaluated assessments.

Use of AI and AI-assisted technologies

Not applicable.

ORCID iDs

Jie Li  <https://orcid.org/0009-0001-1121-291X>

References

- Jemal A, Bray F, Center MM, Ferlay J, Ward E, Forman D. Global cancer statistics. *CA Cancer J Clin*. 2011;61(2):69–90. doi:10.3322/caac.20107
- Galle PR, Forner A, Llovet JM, et al. EASL Clinical Practice Guidelines: Management of hepatocellular carcinoma. *J Hepatol*. 2018;69(1):182–236. doi:10.1016/j.jhep.2018.03.019
- Rubin J, Ayoub N, Kaldas F, Saab S. Management of recurrent hepatocellular carcinoma in liver transplant recipients: A systematic review. *Exp Clin Transplant*. 2012;10(6):531–543. PMID:23216564.
- Campigotto M, Giuffrè M, Colombo A, et al. Comparison between hepatocellular carcinoma prognostic scores: A 10-year single-center experience and brief review of the current literature. *World J Hepatol*. 2020;12(12):1239–1257. doi:10.4254/wjh.v12.i12.1239
- Liu PH, Hsu CY, Lee YH, et al. When to perform surgical resection or radiofrequency ablation for early hepatocellular carcinoma? A nomogram-guided treatment strategy. *Medicine (Baltimore)*. 2015;94(43):e1808. doi:10.1097/MD.0000000000001808
- Xu XL, Liu XD, Liang M, Luo BM. Radiofrequency ablation versus hepatic resection for small hepatocellular carcinoma: Systematic review of randomized controlled trials with meta-analysis and trial sequential analysis. *Radiology*. 2018;287(2):461–472. doi:10.1148/radiol.2017162756
- Korkusuz Y, Gröner D, Raczynski N, et al. Thermal ablation of thyroid nodules: Are radiofrequency ablation, microwave ablation and high intensity focused ultrasound equally safe and effective methods? *Eur Radiol*. 2018;28(3):929–935. doi:10.1007/s00330-017-5039-x
- Peng ZW, Zhang YJ, Chen MS, Lin XJ, Liang HH, Shi M. Radiofrequency ablation as first-line treatment for small solitary hepatocellular carcinoma: Long-term results. *Eur J Surg Oncol*. 2010;36(11):1054–1060. doi:10.1016/j.ejso.2010.08.133
- Liu L, Cao Y, Chen C, et al. Sorafenib blocks the RAF/MEK/ERK pathway, inhibits tumor angiogenesis, and induces tumor cell apoptosis in hepatocellular carcinoma model PLC/PRF/5. *Cancer Res*. 2006;66(24):11851–11858. doi:10.1158/0008-5472.CAN-06-1377
- Shen A, Tang C, Wang Y, et al. A systematic review of sorafenib in Child–Pugh A patients with unresectable hepatocellular carcinoma. *J Clin Gastroenterol*. 2013;47(10):871–880. doi:10.1097/MCG.0b013e3182a87cfd
- Wilhelm SM, Adnane L, Newell P, Villanueva A, Llovet JM, Lynch M. Preclinical overview of sorafenib, a multikinase inhibitor that targets both Raf and VEGF and PDGF receptor tyrosine kinase signaling. *Mol Cancer Ther*. 2008;7(10):3129–3140. doi:10.1158/1535-7163.MCT-08-0013
- Wu FX, Chen J, Bai T, et al. The safety and efficacy of transarterial chemoembolization combined with sorafenib and sorafenib monotherapy in patients with BCLC stage B/C hepatocellular carcinoma. *BMC Cancer*. 2017;17(1):645. doi:10.1186/s12885-017-3545-5
- Di Maio M, Daniele B, Perrone F. Role of sorafenib in HCC patients with compromised liver function. *Nat Rev Clin Oncol*. 2009;6(9):505–506. doi:10.1038/nrclinonc.2009.114
- de'Angelis N, Landi F, Nencioni M, et al. Role of sorafenib in patients with recurrent hepatocellular carcinoma after liver transplantation. *Prog Transplant*. 2016;26(4):348–355. doi:10.1177/1526924816664083
- Stroup DF, Berlin JA, Morton SC, et al. Meta-analysis of observational studies in epidemiology: A proposal for reporting. Meta-analysis Of Observational Studies in Epidemiology (MOOSE) group. *JAMA*. 2000;283(15):2008–2012. doi:10.1001/jama.283.15.2008
- Amin MA. A meta-analysis of the eosinophil counts in the small intestine and colon of children without obvious gastrointestinal disease. *Int J Clin Med Res*. 2023;1(1):1–8. doi:10.61466/ijcmr1010001
- Emad M, Osama H, Rabaa H, Saeed H. Dual compared with triple antithrombotics treatment effect on ischemia and bleeding in atrial fibrillation following percutaneous coronary intervention: A meta-analysis. *Int J Clin Med Res*. 2023;1(2):77–87. doi:10.61466/ijcmr1020010
- Giong Z, Lie N. Phosphate-specific diet effect on serum phosphate levels in adults undergoing hemodialysis: A meta-analysis. *Int J Clin Med Res*. 2024;2(4):135–142. doi:10.61466/ijcmr2040005
- Gu R, Xu G. A meta-analysis looking at the effects of continuous management for complications related to intraoperative pressure wound ulcers in women with breast cancer. *Int J Clin Med Res*. 2024;2(4):100–107. doi:10.61466/ijcmr2040001
- Liberati A, Altman DG, Tetzlaff J, et al. The PRISMA Statement for Reporting Systematic Reviews and Meta-Analyses of Studies That Evaluate Health Care Interventions: Explanation and elaboration. *PLoS Med*. 2009;6(7):e1000100. doi:10.1371/journal.pmed.1000100
- Guo Y. Effect of resident participation in ophthalmic surgery on wound dehiscence: A meta-analysis. *Int J Clin Med Res*. 2024;2(2):50–56. doi:10.61466/ijcmr2020002
- Jiany L, Xiu W. Effect of Chinese herbal medicine as an adjunctive technique to standard treatment for personal with diabetic foot ulcers: A meta-analysis. *Int J Clin Med Res*. 2024;2(4):116–123. doi:10.61466/ijcmr2040003
- Koang Y. A meta-analysis on the use of photobiomodulation to regulate gingival wound healing in addition to periodontal therapies. *Int J Clin Med Res*. 2024;2(4):108–117. doi:10.61466/ijcmr2040002
- Osama H, Saeed H, Nicola M, Emad M. Neuraxial anesthesia compared to general anesthesia in subjects with hip fracture surgery: A meta-analysis. *Int J Clin Med Res*. 2023;1(2):66–76. doi:10.61466/ijcmr1020009
- Shaaban MEA, Mohamed AIM. Determining the efficacy of N-acetyl cysteine in treatment of pneumonia in COVID-19 hospitalized patients: A meta-analysis. *Int J Clin Med Res*. 2023;1(2):36–42. doi:10.61466/ijcmr1020006
- Singh RK. A meta-analysis of the impact on gastrectomy versus endoscopic submucosal dissection for early stomach cancer. *Int J Clin Med Res*. 2023;1(3):88–99. doi:10.61466/ijcmr1030011
- Gupta S, Rout G, Patel AH, et al. Efficacy of generic oral directly acting agents in patients with hepatitis C virus infection. *J Viral Hepat*. 2018;25(7):771–778. doi:10.1111/jvh.12870
- Sheikhabaei S, Trahan TJ, Xiao J, et al. FDG-PET/CT and MRI for evaluation of pathologic response to neoadjuvant chemotherapy in patients with breast cancer: A meta-analysis of diagnostic accuracy studies. *Oncologist*. 2016;21(8):931–939. doi:10.1634/theoncologist.2015-0353
- Higgins JPT, Thompson SG, Deeks JJ, Altman DG. Measuring inconsistency in meta-analyses. *BMJ*. 2003;327(7414):557–560. doi:10.1136/bmj.327.7414.557
- Sun J. Impedance-based stability criterion for grid-connected inverters. *IEEE Trans Power Electron*. 2011;26(11):3075–3078. doi:10.1109/TPEL.2011.2136439
- Hua XD, He ZY. Therapeutic effects of sorafenib combined with transcatheter arterial chemoembolization and microwave ablation on postsurgical recurrent hepatocellular carcinoma [in Chinese]. *Zhonghua Zhong Liu Za Zhi*. 2012;34(10):790–792. doi:10.3760/cma.j.issn.0253-3766.2012.10.015
- Zhang S, Zhao BS, Zhou A, et al. m 6 A demethylase ALKBH5 maintains tumorigenicity of glioblastoma stem-like cells by sustaining FOXM1 expression and cell proliferation program. *Cancer Cell*. 2017;31(4):591–606.e6. doi:10.1016/j.ccell.2017.02.013
- Feng X, Xu R, Du X, et al. Combination therapy with sorafenib and radiofrequency ablation for BCLC stage 0–B1 hepatocellular carcinoma: A multicenter retrospective cohort study. *Am J Gastroenterol*. 2014;109(12):1891–1899. doi:10.1038/ajg.2014.343
- Bruix J, Takayama T, Mazzaferro V, et al. Adjuvant sorafenib for hepatocellular carcinoma after resection or ablation (STORM): A phase 3, randomised, double-blind, placebo-controlled trial. *Lancet Oncol*. 2015;16(13):1344–1354. doi:10.1016/S1473-0455(15)00198-9
- Kan X, Jing Y, Wan QY, et al. Sorafenib combined with percutaneous radiofrequency ablation for the treatment of medium-sized hepatocellular carcinoma. *Eur Rev Med Pharmacol Sci*. 2015;19(2):247–255. PMID:25683938.

36. Guan Q, Gu J, Zhang H, Ren W, Ji W, Fan Y. Correlation between vascular endothelial growth factor levels and prognosis of hepatocellular carcinoma patients receiving radiofrequency ablation. *Biotechnol Biotechnol Equip.* 2015;29(1):119–123. doi:10.1080/13102818.2014.981776
37. Wu X, Lu Y, Zhou S, Chen L, Xu B. Impact of climate change on human infectious diseases: Empirical evidence and human adaptation. *Environ Int.* 2016;86:14–23. doi:10.1016/j.envint.2015.09.007
38. Gong Q, Qin Z, Hou F. Improved treatment of early small hepatocellular carcinoma using sorafenib in combination with radiofrequency ablation. *Oncol Lett.* 2017;14(6):7045–7048. doi:10.3892/ol.2017.7174
39. Yu NS, Yan PJ, Zheng YY, Lu BC. Effect of radiofrequency ablation combined with sorafenib on liver function in patients with advanced hepatic carcinoma [in Chinese]. *Chin J Med Pract.* 2018;16(5):754–756. <http://zhqkxyx.net/en/article/doi/10.16766/j.cnki.issn.1674-4152.000205>. March 15, 2025.
40. Zhu K, Huang J, Lai L, et al. Medium or large hepatocellular carcinoma: Sorafenib combined with transarterial chemoembolization and radiofrequency ablation. *Radiology.* 2018;288(1):300–307. doi:10.1148/radiol.2018172028
41. Sun X, Chen B, Li Q, et al. Toxicities of polystyrene nano- and microplastics toward marine bacterium *Halomonas alkaliphila*. *Sci Total Environ.* 2018;642:1378–1385. doi:10.1016/j.scitotenv.2018.06.141
42. Fu Z, Xi S. The effects of heavy metals on human metabolism. *Toxicol Mech Methods.* 2020;30(3):167–176. doi:10.1080/15376516.2019.1701594
43. Li Q, Song T. Association between adjuvant sorafenib and the prognosis of patients with hepatocellular carcinoma at a high risk of recurrence after radical resection. *Front Oncol.* 2021;11:633033. doi:10.3389/fonc.2021.633033
44. Abulimiti M, Li Z, Wang H, Apizajai P, Abulimiti Y, Tan Y. Combination intensity-modulated radiotherapy and sorafenib improves outcomes in hepatocellular carcinoma with portal vein tumor thrombosis. *J Oncol.* 2021;2021:9943683. doi:10.1155/2021/9943683
45. Wei MC, Zhang YJ, Chen MS, Chen Y, Lau WY, Peng ZW. Adjuvant sorafenib following radiofrequency ablation for early-stage recurrent hepatocellular carcinoma with microvascular invasion at the initial hepatectomy. *Front Oncol.* 2022;12:868429. doi:10.3389/fonc.2022.868429
46. Zhou Q, Wang X, Li R, et al. Sorafenib as adjuvant therapy following radiofrequency ablation for recurrent hepatocellular carcinoma within Milan criteria: A multicenter analysis. *J Gastroenterol.* 2022;57(9):684–694. doi:10.1007/s00535-022-01895-3
47. Seidensticker M, Öcal O, Schütte K, et al. Impact of adjuvant sorafenib treatment after local ablation for HCC in the phase II SORAMIC trial. *JHEP Rep.* 2023;5(5):100699. doi:10.1016/j.jhepr.2023.100699
48. Yang LM, Wang HJ, Li SL, et al. Efficacy of radiofrequency ablation combined with sorafenib for treating liver cancer complicated with portal hypertension and prognostic factors. *World J Gastroenterol.* 2024;30(11):1533–1544. doi:10.3748/wjg.v30.i11.1533
49. Abdelrahim ME. Aerodynamic characteristics of nebulized terbutaline sulphate using the Andersen Cascade Impactor compared to the Next Generation Impactor. *Pharm Dev Technol.* 2011;16(2):137–145. doi:10.3109/10837450903511194
50. Vecellio L, Abdelrahim ME, Montharu J, Galle J, Diot P, Dubus JC. Disposable versus reusable jet nebulizers for cystic fibrosis treatment with tobramycin. *J Cyst Fibros.* 2011;10(2):86–92. doi:10.1016/j.jcf.2010.10.004
51. Ali AMA, Abdelrahim MEA. Modeling and optimization of terbutaline emitted from a dry powder inhaler and influence on systemic bioavailability using data mining technology. *J Pharm Innov.* 2014;9(1):38–47. doi:10.1007/s12247-014-9171-8
52. Elgendy MO, Abdelrahim ME, Salah Eldin R. Potential benefit of repeated MDI inhalation technique counselling for patients with asthma. *Eur J Hosp Pharm.* 2015;22(6):318–322. doi:10.1136/ejpharm-2015-000648
53. Hassan A, Rabea H, Hussein RRS, et al. In vitro characterization of the aerosolized dose during non-invasive automatic continuous positive airway pressure ventilation. *Pulm Ther.* 2016;2(1):115–126. doi:10.1007/s41030-015-0010-y
54. Hussein RRS, M A Ali A, Salem HF, Abdelrahman MM, Said ASA, Abdelrahim MEA. In vitro/in vivo correlation and modeling of emitted dose and lung deposition of inhaled salbutamol from metered dose inhalers with different types of spacers in noninvasively ventilated patients. *Pharm Dev Technol.* 2017;22(7):871–880. doi:10.3109/10837450.2015.1116567
55. Madney YM, Fathy M, Elberry AA, Rabea H, Abdelrahim MEA. Nebulizers and spacers for aerosol delivery through adult nasal cannula at low oxygen flow rate: An in-vitro study. *J Drug Deliv Sci Technol.* 2017;39:260–265. doi:10.1016/j.jddst.2017.04.014
56. Saeed H, Elberry AA, Eldin AS, Rabea H, Abdelrahim MEA. Effect of nebulizer designs on aerosol delivery during non-invasive mechanical ventilation: A modeling study of in vitro data. *Pulm Ther.* 2017;3(1):233–241. doi:10.1007/s41030-017-0033-7
57. Harb HS, Elberry AA, Rabea H, Fathy M, Abdelrahim ME. Performance of large spacer versus nebulizer T-piece in single-limb noninvasive ventilation. *Respir Care.* 2018;63(11):1360–1369. doi:10.4187/respcare.05976
58. Saeed H, Ali AMA, Elberry AA, Eldin AS, Rabea H, Abdelrahim MEA. Modeling and optimization of nebulizers' performance in non-invasive ventilation using different fill volumes: Comparative study between vibrating mesh and jet nebulizers. *Pulm Pharmacol Ther.* 2018;50:62–71. doi:10.1016/j.pupt.2018.04.005
59. Elgendy MO, Hassan AH, Saeed H, Abdelrahim ME, Eldin RS. Asthmatic children and MDI verbal inhalation technique counseling. *Pulm Pharmacol Ther.* 2020;61:101900. doi:10.1016/j.pupt.2020.101900
60. Wei Z, Ye X, Yang X, et al. Microwave ablation in combination with chemotherapy for the treatment of advanced non-small cell lung cancer. *Cardiovasc Intervent Radiol.* 2015;38(1):135–142. doi:10.1007/s00270-014-0895-0
61. Gang G, Hongkai Y, Xu Z. Sorafenib combined with radiofrequency ablation in the treatment of a patient with renal cell carcinoma plus primary hepatocellular carcinoma. *J Can Res Ther.* 2015;11(4):1026. doi:10.4103/0973-1482.150405
62. Reuter NP, Woodall CE, Scoggins CR, McMasters KM, Martin RCG. Radiofrequency ablation vs resection for hepatic colorectal metastasis: Therapeutically equivalent? *J Gastrointest Surg.* 2009;13(3):486–491. doi:10.1007/s11605-008-0727-0
63. White RR, Avital I, Sofocleous CT, et al. Rates and patterns of recurrence for percutaneous radiofrequency ablation and open wedge resection for solitary colorectal liver metastasis. *J Gastrointest Surg.* 2007;11(3):256–263. doi:10.1007/s11605-007-0100-8
64. Lacouture ME, Wu S, Robert C, et al. Evolving strategies for the management of hand-foot skin reaction associated with the multitargeted kinase inhibitors sorafenib and sunitinib. *Oncologist.* 2008;13(9):1001–1011. doi:10.1634/theoncologist.2008-0131
65. Koschny R, Gotthardt D, Koehler C, Jaeger D, Stremmel W, Ganten TM. Diarrhea is a positive outcome predictor for sorafenib treatment of advanced hepatocellular carcinoma. *Oncology.* 2013;84(1):6–13. doi:10.1159/000342425
66. Reig M, Torres F, Rodriguez-Lopez C, et al. Early dermatologic adverse events predict better outcome in HCC patients treated with sorafenib. *J Hepatol.* 2014;61(2):318–324. doi:10.1016/j.jhep.2014.03.030
67. Ferlay J, Soerjomataram I, Dikshit R, et al. Cancer incidence and mortality worldwide: Sources, methods and major patterns in GLOBOCAN 2012. *Int J Cancer.* 2015;136(5):E359–E386. doi:10.1002/ijc.29210
68. Llovet JM, Zucman-Rossi J, Pikarsky E, et al. Hepatocellular carcinoma. *Nat Rev Dis Primers.* 2016;2(1):16018. doi:10.1038/nrdp.2016.18
69. Chen L, Ma X, Liu X, Cui X. Sorafenib combined with radiofrequency ablation as treatment for patients with hepatocellular carcinoma: A systematic review and meta-analysis. *J BUON.* 2017;22(6):1525–1532. PMID:29332348.

Revealing the causal relationship between HBV and HCV infection and liver cirrhosis by Mendelian randomization

*Ju-Cun Huang^{A,D–F}, Yu-Wei Feng^{A,D–F}, Kang Zhao^{B,C,F}, *Dan Dai^{A,D–F}

Liver Disease Department of Integrated Traditional Chinese and Western Medicine, Hubei No. 3 People's Hospital of Jiangnan University, Wuhan, China

A – research concept and design; B – collection and/or assembly of data; C – data analysis and interpretation;

D – writing the article; E – critical revision of the article; F – final approval of the article

Advances in Clinical and Experimental Medicine, ISSN 1899–5276 (print), ISSN 2451–2680 (online)

Adv Clin Exp Med. 2025;34(12):2045–2054

Address for correspondence

Yu-Wei Feng

E-mail: yuwei1872601@163.com

Funding sources

This study was supported by the Hubei Provincial Department of Science and Technology (project No. 2023AFC031).

Conflict of interest

None declared

*Ju-Cun Huang and Dan Dai contributed equally to this work.

Received on June 5, 2024

Reviewed on September 24, 2024

Accepted on February 10, 2025

Published online on August 19, 2025

Cite as

Huang JC, Feng YW, Zhao K, Dai D. Revealing the causal relationship between HBV and HCV infection and liver cirrhosis by Mendelian randomization. *Adv Clin Exp Med.* 2025;34(12):2045–2054. doi:10.17219/acem/201226

DOI

10.17219/acem/201226

Copyright

Copyright by Author(s)

This is an article distributed under the terms of the Creative Commons Attribution 3.0 Unported (CC BY 3.0) (<https://creativecommons.org/licenses/by/3.0/>)

Abstract

Background. The chronic progression of viral hepatitis and the terminal stage of cirrhosis impose a long-term disease burden on patients. The assessment of liver damage can be facilitated through the measurement of liver biomarkers.

Objectives. To conduct a comprehensive analysis of the relationship between hepatitis B virus (HBV), hepatitis C virus (HCV), liver biomarkers, and cirrhosis via Mendelian randomization (MR).

Materials and methods. A bidirectional multi-sample MR approach was used to extract data from publicly available genome-wide association studies (GWAS) databases. Information on liver biomarkers and cirrhosis, along with data from 351,885 HBV samples containing 19,079,722 single nucleotide polymorphisms (SNPs) and 176,698 HCV samples comprising 12,454,320 SNPs, were aggregated. The TwoSampleMR 0.5.7 package in R language facilitated the bidirectional MR analysis, utilizing methods such as inverse-variance weighting, weighted median and MR-Egger to investigate the causal relationships between HBV, HCV, liver biomarkers, and cirrhosis.

Results. The MR analysis revealed potential causal relationships between cirrhosis and HBV infection, indicating an increased probability of HBV as cirrhosis escalates (odds ratio (OR) = 1.253; 95% confidence interval (95% CI): 1.037–1.514; $p = 0.019$). Additionally, a potential causal link was observed between HBV and the level of aspartate aminotransferase (AST), with an increase in HBV leading to a gradual decrease in AST levels (OR = 0.972; 95% CI: 0.958–0.986; $p < 0.01$). A similar causal relationship was identified between HCV infection and cirrhosis, where the probability of cirrhosis significantly increases with rising HCV levels (OR = 2.213; 95% CI: 1.752–2.796; $p < 0.01$). The results demonstrated no pleiotropy or heterogeneity within the analysis.

Conclusions. This research highlights a causal relationship between HBV and AST levels, suggesting that monitoring AST levels can indicate the extent of liver damage caused by chronic HBV infection. Additionally, causal connections were established between HBV, HCV and cirrhosis, emphasizing that cirrhosis represents the terminal stage of chronic HBV and HCV infections. By managing the progression of the disease, the risk of cirrhosis can be reduced.

Key words: Mendelian randomization, cirrhosis, viral hepatitis, liver biomarkers, causal relationships

Highlights

- Bidirectional Mendelian randomization (MR) analysis was used to evaluate causal relationships between hepatitis B virus (HBV), hepatitis C virus (HCV), liver biomarkers, and cirrhosis.
- HCV infection is causally linked to an increased risk of liver cirrhosis, confirming its role in liver disease progression.
- Liver cirrhosis may increase susceptibility to HBV infection, suggesting a potential bidirectional or feedback relationship.
- HBV infection is associated with decreased aspartate aminotransferase (AST) levels, indicating a potential protective biomarker effect.
- These findings support the development of biomarker-driven surveillance and personalized interventions for managing chronic viral hepatitis and liver disease.

Background

Viral hepatitis, encompassing hepatitis B (HBV), hepatitis C (HCV) and hepatitis A, among others, represents a spectrum of diseases characterized by chronic inflammation of the liver. Globally, HBV and HCV infections are the predominant causes of chronic liver disease, with an estimated combined carrier population exceeding 350 million individuals.^{1,2} As of 2019, an estimated 295.9 million people were living with chronic HBV infection, and HCV is responsible for an estimated 57.8 million chronic infections worldwide.³ The progression of these infections often results in liver fibrosis, cirrhosis, and ultimately liver failure or hepatocellular carcinoma (HCC), posing significant health and economic burdens. Early diagnosis remains challenging, and treatment options are often costly and limited in efficacy, particularly in low- and middle-income regions.^{4,5} As such, understanding the mechanisms driving HBV and HCV progression is critical for developing more effective prevention and treatment strategies.

In the diagnosis and monitoring of hepatitis, the levels of liver biomarkers undergo substantial changes, including but not limited to aspartate aminotransferase (AST), alanine aminotransferase (ALT), alkaline phosphatase (ALP), gamma-glutamyl transferase (GGT), and total bilirubin. These markers provide critical insights into the degree of liver inflammation, extent of damage and liver function recovery, serving as key indicators for assessing liver function and disease progression. For instance, AST and ALT are sensitive indicators for detecting early stages of liver cell damage.⁶ As the condition progresses, elevated levels of ALP and GGT may indicate damage to the bile system, while an increase in bilirubin levels reflects compromised liver capacity to clear aged red blood cells. Although the role of liver biomarkers in monitoring liver health is widely recognized, their precise causal relationships with HBV and HCV remain to be fully elucidated. A systematic study of liver biomarkers in the progression of cirrhosis in patients with HBV and HCV is crucial for understanding the disease's development mechanisms, improving early diagnosis and monitoring, and evaluating treatment efficacy.

In recent years, several epidemiological studies have explored the genetic and environmental determinants of HBV and HCV susceptibility, progression and treatment outcomes. Notably, genome-wide association studies (GWAS) have identified numerous genetic variants associated with the risk of chronic viral hepatitis.^{7,8} However, the causal relationships between these genetic factors and disease outcomes remain largely unclear. Mendelian randomization (MR) offers a powerful tool to address this gap by using genetic variants as instrumental variables to infer causal relationships between exposures and outcomes.⁹ The MR method is grounded in 3 core assumptions: 1) The genetic variant must be associated with the exposure of interest; 2) The genetic variant should not be associated with confounders; and 3) The genetic variant influences the outcome only through the exposure. By leveraging these assumptions, MR provides an approach that is less prone to confounding and reverse causation compared to traditional observational studies.^{10,11} Mendelian randomization provides a unique perspective by integrating large-scale cohort genetic and phenotypic data, using genetic variation as an instrumental variable to elucidate the causal links between HBV, HCV, liver biomarkers, and cirrhosis. By reducing the interference of confounding factors, this method allows for a clearer understanding of the complex interactions between genetic variations, viral infections and liver diseases, offering new insights and strategies for disease prevention and treatment.^{12,13} For viral hepatitis, MR studies have mainly focused on genetic predispositions to HBV and HCV infection risks rather than exploring the progression to severe outcomes like cirrhosis.^{14,15} By leveraging genetic instruments associated with liver biomarkers and disease phenotypes, MR provides a unique opportunity to investigate whether changes in these biomarkers causally impact the progression from viral hepatitis to liver cirrhosis.

Objectives

This study aims to apply a multi-sample bidirectional MR approach to assess causal relationships between HBV,

HCV, liver biomarkers, and cirrhosis, providing novel insights into the genetic and phenotypic interactions underlying liver disease progression. Unlike previous MR studies that often focus on single biomarkers or outcomes, our approach integrates multiple biomarkers and examines bidirectional causality, allowing for a more comprehensive understanding of the complex pathways involved. By combining data from extensive GWAS and employing robust statistical methods such as inverse-variance weighting (IVW), weighted median and MR-Egger regression, this research seeks to enhance the accuracy and reliability of causal inferences.

Materials and methods

Study design

This study implements a bidirectional multi-sample MR design to investigate the causal relationships between the exposure (HBV, HCV and liver biomarkers, including ALT, AST, GGT, albumin, total bilirubin, and direct bilirubin) and outcomes (cirrhosis). This approach allows for the assessment of whether the exposure has a causal effect on the outcome and vice versa. In this method, 2 independent GWAS datasets were used: 1 for the exposure and 1 for the outcome. The MR analysis was conducted separately for each direction to infer the causal relationship, following the principles of IVW regression, which combines genetic variant-specific estimates into an overall causal estimate. The MR approach is predicated on 3 core assumptions: 1) The chosen genetic variants are strongly associated with the exposure; 2) The genetic variants are independent of any confounding factors that could influence the risk of HBV and HCV; 3) The genetic variants influence the risk of HBV and HCV exclusively through exposure, without any alternative pathways.

Inclusion and exclusion criteria for GWAS data

The GWAS datasets included in this study were selected based on strict inclusion and exclusion criteria to ensure the representativeness and relevance of the data. Only GWAS with large sample sizes, well-documented methods and European ancestry populations were included to minimize population stratification and enhance comparability between datasets. Specifically, studies with sample sizes exceeding 10,000 participants were prioritized to ensure statistical power.

Data were excluded if they had high levels of missingness (>10%) or low-quality control metrics, such as single nucleotide polymorphisms (SNPs) with call rates below 95%, minor allele frequencies below 1% or failure to meet Hardy–Weinberg equilibrium ($p < 1 \times 10^{-6}$). In addition,

datasets with limited phenotypic information or lacking detailed population descriptors were excluded to avoid introducing biases related to unmeasured confounders.

Sources and GWAS samples

The data for this study were sourced from publicly accessible GWAS databases, primarily the GWAS Catalog (<https://gwas.mrcieu.ac.uk/>). The selection focused on information related to liver biomarkers (ALT, AST, GGT, albumin, total bilirubin, and direct bilirubin) and cirrhosis, as well as samples from patients with HBV and HCV infections. Sample information is provided in Supplementary Table 1. The data utilized in this research are publicly available and have previously received ethical approval and informed consent within their original studies.

In this research, the samples for chronic HCV infection included 176,698 cases, covering 12,454,320 SNPs; for chronic HCV infection, there were 351,885 cases, covering 19,079,722 SNPs. Cirrhosis samples numbered 178,726, spanning 12,454,705 SNPs; ALT samples included 437,724 cases involving 4,231,965 SNPs.

Aspartate aminotransferase samples numbered 436,275, totaling 4,231,525 SNPs; GGT samples encompassed 437,651 cases, totaling 4,231,983 SNPs. Albumin samples included 357,968 cases containing 10,783,656 SNPs. Total bilirubin samples covered 342,829 cases, encompassing 19,046,135 SNPs; direct bilirubin samples included 372,420 cases, containing 4,206,076 SNPs.

Data quality control and cleaning process

To ensure the reliability of the results, we implemented a rigorous data cleaning and quality control process. First, missing data were handled using multiple imputations by chained equations (MICE), pooling results across imputed datasets to address uncertainty. Variables with over 10% missing data were excluded. Outliers were identified and removed using z-score analysis. To control for population stratification, principal component analysis (PCA) was used without rotation, selecting components to explain at least 95% of the variance and removing outliers exceeding ± 3 standard deviations (SDs) on key components. Genetic variants were filtered based on stringent criteria: call rates above 95%, minor allele frequencies of at least 1% and Hardy–Weinberg equilibrium at $p > 1 \times 10^{-6}$. Finally, duplicate records were removed, inconsistencies resolved through cross-validation and logical checks, and continuous variables were normalized as necessary. These steps minimized bias and enhanced the robustness of our findings.

Analysis method

The selection of instrumental variables (IV) is based on genetic variants associated with cirrhosis and liver

biomarkers. The filtering criterion for these variables is set at a p-value of less than $5e-08$. Should no instrumental variables meet this threshold, the threshold is adjusted down to a minimum of $5e-6$.^{16,17} These variants are derived from multiple studies targeting specific populations, with strict linkage disequilibrium (LD) filtering applied to ensure the independence of variants, using an LD threshold of $r^2 < 0.001$.^{18,19} The MR analysis is conducted using the TwoSampleMR 0.5.7 package in R language (R Foundation for Statistical Computing, Vienna, Austria), assessing the causal relationship between cirrhosis and liver biomarkers with HBV and HCV. The analysis employs methods such as IVW, weighted median and MR-Egger, integrating various statistical models to enhance the reliability and accuracy of the results. Sensitivity analyses are conducted to assess the robustness of the results. In cases where sensitivity analyses indicate pleiotropy, the MR-PRESSO test is used to investigate horizontal gene pleiotropy, excluding outliers for re-analysis. If pleiotropy persists, such analysis is excluded.

Sensitivity analyses

We also conducted sensitivity analyses, including MR-Egger regression and the weighted median method, to account for potential pleiotropy and assess the robustness of the causal estimates. These techniques helped ensure that the results were not driven by invalid instrumental variables that might affect the outcome through pathways other than the exposure of interest. The bidirectional nature of this analysis provides a comprehensive understanding of the potential feedback loop between genetic variants and liver disease progression.

Statistical analyses

Statistical significance of study results was determined using a combination of criteria. A result was considered statistically significant if the p-value from methods such as IVW, weighted median or MR-Egger regression was less than 0.05. Additionally, positive results required beta-directional consistency across these methods, ensuring that the effect directions observed were consistent. This dual criterion of p-value threshold and beta-directional consistency helped establish the robustness of the causal inferences.²⁰ A $Q_{pval} > 0.05$ indicated no significant heterogeneity among the included studies. In such cases, both fixed-effects and random-effects IVW models are appropriate. Conversely, when heterogeneity is present ($Q_{pval} < 0.05$), either the IVW random-effects model or the weighted median method should be applied.²¹ A $p > 0.05$ in the multivariate test means no multivariate effects. The instrumental variables used in each analysis are summarized, and the last column shows the F-value of the instrumental variable, which is usually considered a strong instrumental variable if $F \geq 10$.

Results

Causal analysis of SNPs related to HBV and HCV

To assess the potential causal effects of cirrhosis and liver biomarkers on HBV and HCV infections, a multi-sample MR analysis was initially conducted, treating cirrhosis and liver biomarkers as the exposures and HBV and HCV infections as the outcomes. Variants demonstrating pleiotropic effects were meticulously identified and subsequently excluded to ensure the integrity and accuracy of the causal inference. The analysis using the IVW model depicted in forest plots indicated a potential causal effect of cirrhosis on HBV infection (odds ratio (OR) = 1.253; 95% confidence interval (95% CI): 1.037–1.514; $p = 0.019$; Fig. 1). Further analysis and visualization suggested that the trends from the IVW, MR-Egger and weighted median methods were consistent and positively correlated, with an OR greater than 1, suggesting that cirrhosis acts as a potential risk factor for HBV infection (Fig. 2). As the level of cirrhosis increases, so does the probability of HBV infection.

Causal analysis of SNPs related to cirrhosis and liver biomarkers

Subsequently, HBV and HCV were considered as exposures, with cirrhosis and liver biomarkers as outcomes, to conduct a reverse MR analysis. This approach further examined the causal relationships between HBV, HCV, cirrhosis, and liver biomarkers. Variants demonstrating pleiotropic effects were meticulously identified and subsequently excluded to ensure the integrity and accuracy of the causal inference. The results indicated a potential causal relationship between HBV and AST, with significant findings from the IVW model (OR = 0.972; 95% CI: 0.958–0.986; $p < 0.01$; Fig. 3). The trends observed in MR-Egger, IVW and weighted median analyses were consistent and negatively correlated, suggesting HBV acts as a potential protective factor for AST levels, with an increasing probability of reduced AST levels as HBV increases (Fig. 4). Similarly, a potential causal relationship was found between HCV and cirrhosis, with significant results from the IVW model (OR = 2.213; 95% CI: 1.752–2.796; $p < 0.01$; Fig. 3) and consistent trends across MR-Egger, IVW and weighted median analyses, indicating a positive correlation (Fig. 5). An OR greater than 1 suggests that HCV is a potential risk factor for cirrhosis, with an increasing probability of cirrhosis as HCV levels rise.

Sensitivity analysis on the relationship between hepatitis, cirrhosis and liver biomarkers

The sensitivity analysis examined the robustness of associations between hepatitis B and C infections (chronic)

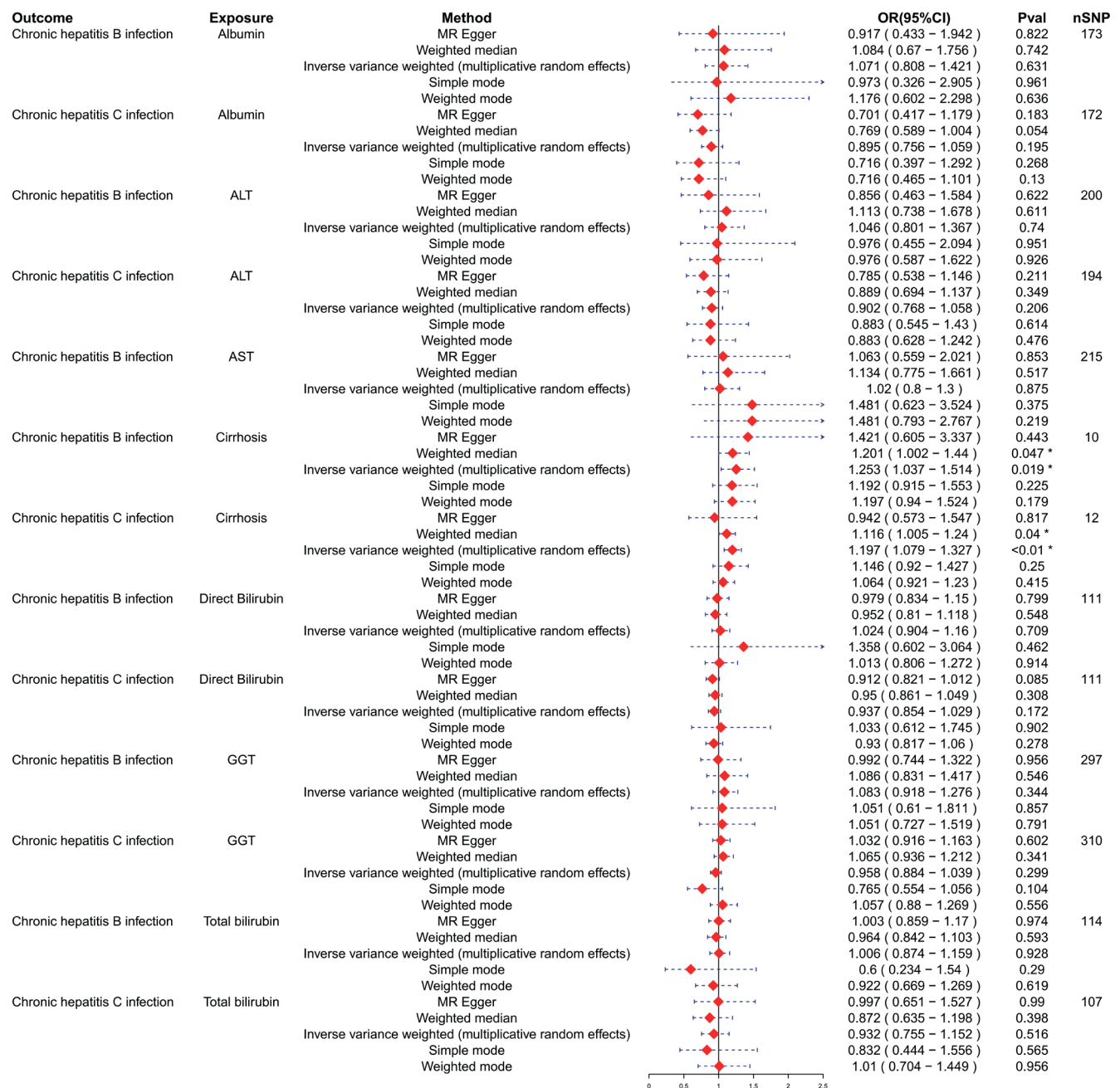


Fig. 1. Forest plot illustrating the causal relationship between cirrhosis and liver biomarkers in the context of HBV and HCV infections. Liver biomarkers include alanine aminotransferase (ALT), aspartate aminotransferase (AST), gamma-glutamyl transferase (GGT), albumin, total bilirubin, and direct bilirubin. Each row represents a distinct outcome or exposure, with red squares indicating odds ratios (ORs) and horizontal lines representing 95% confidence intervals (95% CIs). The number of single nucleotide polymorphisms (SNPs) used in each analysis is listed in the far-right column

and various liver biomarkers. For hepatitis B, the analysis indicated significant heterogeneity in the associations with albumin ($Q_{pval} = 0.0117$) and cirrhosis ($Q_{pval} = 0.135$), but not with other biomarkers. The lack of significant pleiotropy suggests that the associations observed are likely not confounded by unmeasured variables. However, for direct bilirubin, significant heterogeneity was observed without pleiotropic effects (Table 1).

In the context of HCV, there were no significant pleiotropic effects across all biomarkers, indicating robust associations. Some heterogeneity was noted, particularly with

ALT ($Q_{pval} = 0.0014$), cirrhosis ($Q_{pval} = 0.0157$) and total bilirubin ($Q_{pval} = 0.0416$), but it was not deemed substantial as the pleiotropy p-values remained high.

When reversing the analysis by considering HBV and HCV as outcomes and biomarkers as exposures, substantial heterogeneity was found across most biomarkers for both HBV and HCV, indicated by the Q statistic. The Q_{pval} was notably low for cirrhosis with HBV infection ($Q_{pval} = 0.0056$) and for cirrhosis with HCV infection ($Q_{pval} = 0.001$), suggesting significant variability in the results. The p-values for pleiotropy

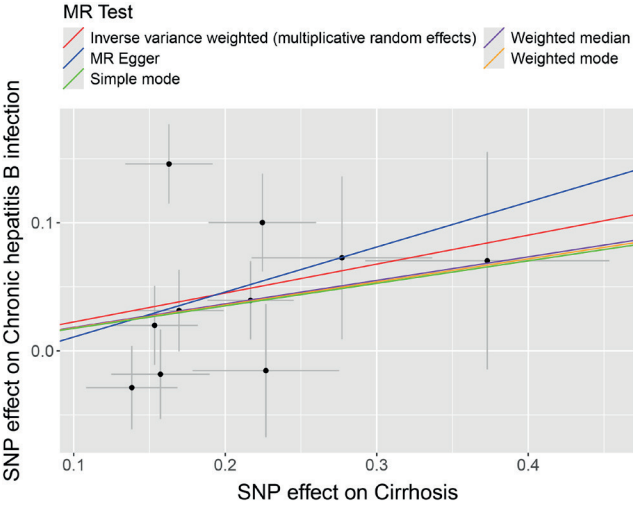


Fig. 2. Scatter plot from a multi-sample Mendelian randomization (MR) analysis illustrating the effect of cirrhosis on HBV infection. The x-axis represents the effect size of each single nucleotide polymorphism (SNP) on cirrhosis, while the y-axis represents the corresponding effect on HBV infection. Each black dot denotes an individual SNP, with vertical and horizontal error bars indicating the 95% confidence intervals (95% CIs) around the SNP effect estimates. The colored lines represent fitted regression lines for different MR methods, visualizing the overall estimated causal effect across analytical approaches

Table 1. Results of sensitivity analysis for hepatitis and cirrhosis in relation to liver biomarkers

Outcome	Exposure	Heterogeneity		Pleiotropy
		Q	Q_pval	
Albumin	chronic hepatitis B infection	18.051	0.0117	0.5875
ALT		0.056	0.9724	0.1489
AST		1.6128	0.4465	0.1968
Cirrhosis		14.9208	0.135	0.0657
Direct bilirubin		28.5295	0	0.8586
GGT		11.3052	0.0035	0.9658
Total bilirubin		19.0879	0.0595	0.7307
Albumin	chronic hepatitis C infection	12.4429	0.1895	0.4511
ALT		19.6837	0.0014	0.5992
AST		9.7142	0.0838	0.3519
Cirrhosis		21.8921	0.0157	0.9961
Direct bilirubin		4.6788	0.4563	0.6284
GGT		16.2286	0.0027	0.4434
Total bilirubin		18.8967	0.0416	0.7776

ALT – alanine transaminase; AST – aspartate aminotransferase; GGT – gamma-glutamyl transferase.

remained high, indicating no substantial pleiotropic influences (Table 2).

Discussion

The degree of liver damage in viral hepatitis can be inferred through the measurement of liver biomarkers. This study employs a bidirectional multi-sample MR approach

Table 2. Results of sensitivity analysis for cirrhosis in relation to liver biomarkers and hepatitis

Outcome	Exposure	Heterogeneity		Pleiotropy
		Q	Q_pval	
Chronic HBV infection	albumin	176.5458	0.3697	0.6619
Chronic HCV infection		175.9681	0.3609	0.3332
Chronic HBV infection	ALT	212.4106	0.2295	0.4788
Chronic HCV infection		208.9291	0.1912	0.4289
Chronic HBV infection	AST	206.2573	0.6171	0.8918
Chronic HBV infection		21.6682	0.0056	0.7747
Chronic HCV infection	cirrhosis	29.5115	0.001	0.3552
Chronic HBV infection		82.1133	0.9745	0.2388
Chronic HCV infection	direct bilirubin	145.4115	0.0113	0.2594
Chronic HBV infection		293.0121	0.5218	0.4654
Chronic HCV infection	GGT	346.742	0.0634	0.0983
Chronic HBV infection		149.5429	0.0103	0.9017
Chronic HCV infection	total bilirubin	115.0825	0.2357	0.7227

HBV – hepatitis B virus; HCV – hepatitis C virus; ALT – alanine transaminase; AST – aspartate aminotransferase; GGT – gamma-glutamyl transferase.

to explore the causal relationships between HBV, HCV, cirrhosis, and liver biomarkers. Key findings include: 1) a potential causal relationship between cirrhosis and HBV, with an increasing likelihood of HBV as cirrhosis levels rise; 2) a potential causal link between HBV and AST, where higher HBV levels correspond to a gradual decrease in AST levels; and 3) a potential causal relationship between HCV and cirrhosis, with an increased probability of cirrhosis as HCV levels rise. Moreover, the MR analysis indicates no horizontal pleiotropy or heterogeneity and does not establish a causal relationship between HBV, HCV and other liver biomarkers. This study’s approach and findings contribute to understanding the genetic factors underlying the progression from viral hepatitis to liver cirrhosis, emphasizing the importance of genetic research in uncovering the mechanisms of disease progression.

During the course of viral hepatitis infections, liver biomarkers such as levels of transaminases and bilirubin, among other inflammation indicators, play a pivotal role. These markers not only serve as indicators of disease progression but may also influence the degree of viral replication and liver damage.²² Previous research into the relationship between HBV and AST has demonstrated a close association between AST levels in the blood and the extent of liver damage. HBV infection damages liver cells, triggering an immune response. This causes inflammation and the release of AST into the bloodstream, raising serum AST levels.²³ In studies exploring liver biomarkers and HCC, including a two-sample MR study based on observational research, while there was no strong evidence to suggest a causal relationship between genetically predicted levels of ALP, ALP and GGT with HCC,

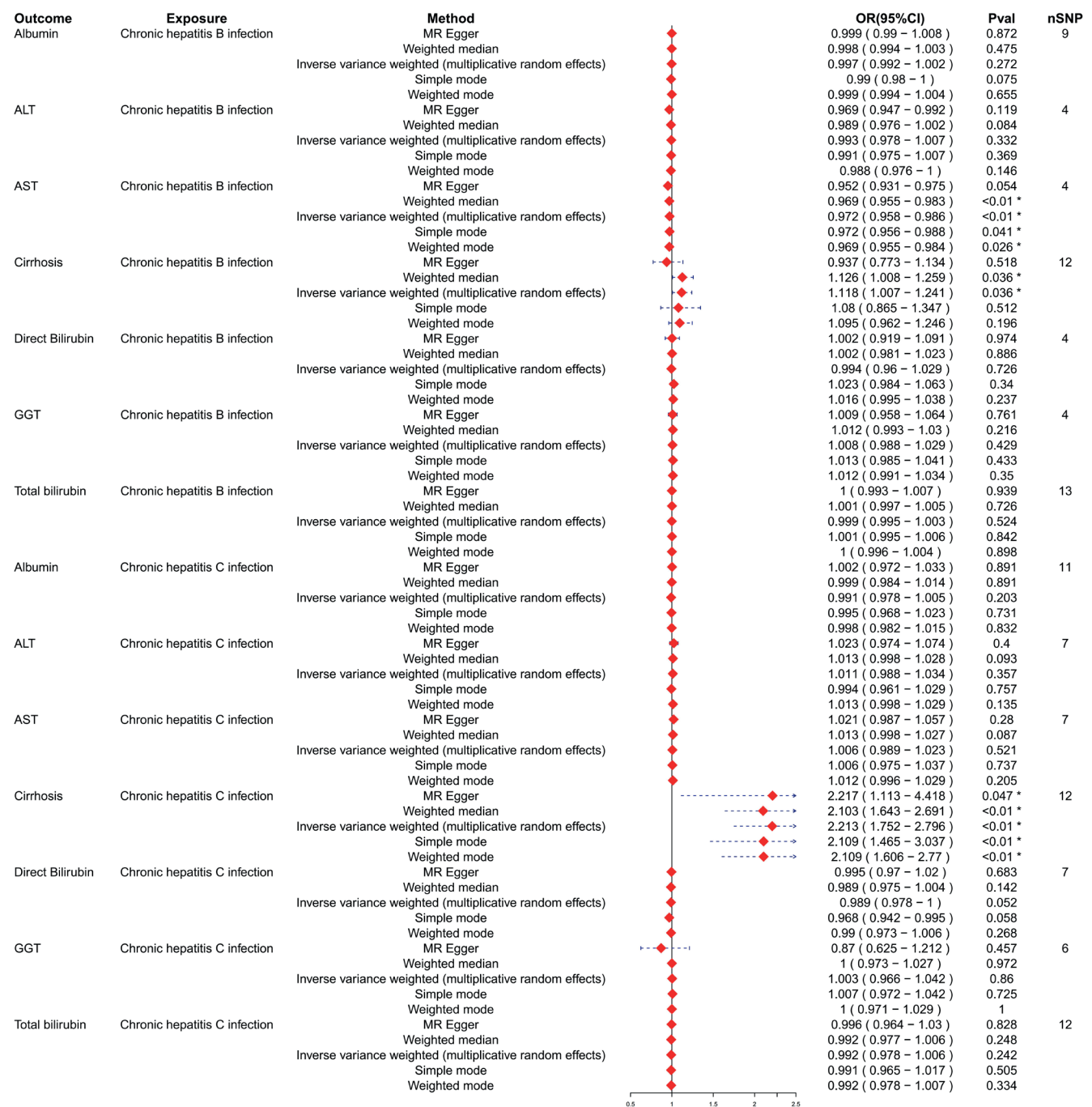


Fig. 3. Forest plot representing the bidirectional Mendelian randomization (MR) analysis between HBV/HCV infections and cirrhosis, as well as associated liver biomarkers

elevated levels of AST were associated with an increased risk of HCC.²⁴ This current study, through MR analysis, identifies a causal relationship between HBV infection and AST levels, suggesting that HBV infection acts as a potential protective factor against elevated AST levels. Considering chronic HBV infection as a significant risk factor for HCC, it is posited that during the acute phase of HBV infection, AST levels rise significantly, but as the infection transitions from acute to chronic, AST levels gradually normalize.¹⁸ This suggests that monitoring AST levels could provide insights into the extent of liver damage and

progression of disease in HBV patients. However, further research is needed to corroborate the causal relationship between HBV and AST.^{25,26}

In the analysis of the causal relationships between HBV, HCV and cirrhosis, this study, employing cirrhosis and liver biomarkers as exposures with HBV and HCV as outcomes, identifies a causal linkage between cirrhosis and both HBV and HCV. These viruses cause persistent damage to liver cells through inflammation, leading to liver fibrosis and, eventually, cirrhosis.²⁷ Previous research, such as the study by Kamiza et al. employing bidirectional MR

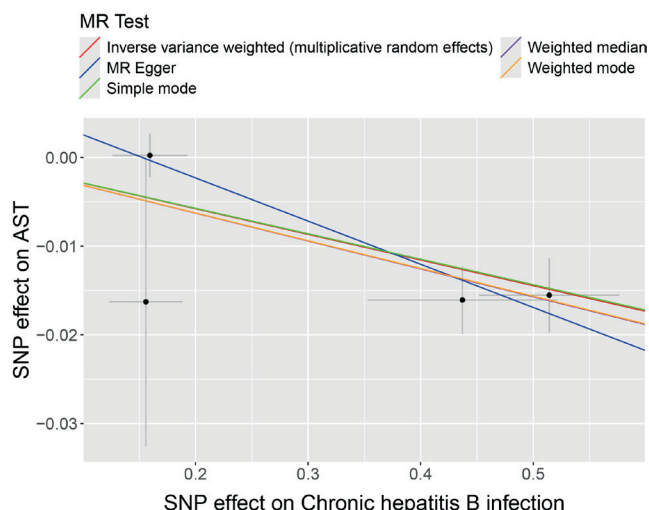


Fig. 4. Scatter plot from a Mendelian randomization (MR) analysis illustrating the relationship between HBV infection and aspartate aminotransferase (AST) levels. The x-axis displays the effect size of each single nucleotide polymorphism (SNP) on HBV infection, while the y-axis shows the corresponding effect on AST levels. Each black dot represents an individual SNP, with error bars indicating the 95% confidence intervals (95% CIs) for the effect estimates. Colored lines represent fitted regression lines for different MR methods. Due to the close similarity of some estimates, the regression lines partially overlap and may not be fully distinguishable in the plot

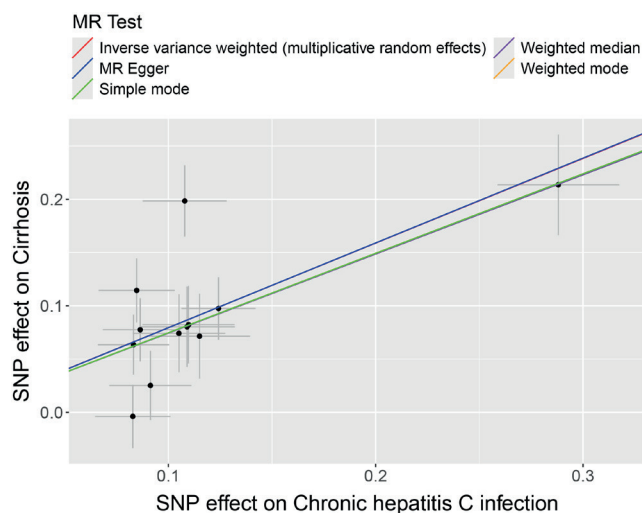


Fig. 5. Scatter plot from a Mendelian randomization (MR) analysis illustrating the relationship between HCV infection and the risk of cirrhosis. The x-axis represents the effect size of each single nucleotide polymorphism (SNP) on HCV infection, while the y-axis indicates the corresponding SNP effect on cirrhosis risk. Each black dot corresponds to an individual SNP, with error bars denoting 95% confidence intervals (95% CIs) for the estimated effects. Colored lines represent regression lines fitted by different MR methods. Due to the proximity of some estimates, the regression lines partially overlap and may not be fully distinguishable in the plot

to investigate individuals of East Asian descent in South Korea, revealed that chronic HBV infection is causally related to HCC and extrahepatic cancers, marking chronic HBV infection as a significant risk factor for HCC.²⁸ Additionally, GWAS highlighted by Zeng et al. have found that genetic loci associated with higher levels of HBV surface antigen increase the risk of cirrhosis, providing

a genetic foundation for the progression of liver disease in HBV-infected individuals.²⁹ The physiological mechanism, which sees prolonged liver inflammation leading to fibrosis and cirrhosis, supports the causal relationship between cirrhosis and HBV and HCV infections. It suggests that controlling the progression of HBV and HCV infections could potentially reduce the risk of cirrhosis.

To ensure the robustness of our findings, we conducted several sensitivity analyses, including MR-Egger regression and the weighted median approach. The results were consistent with the main findings, indicating that the observed associations were reliable. MR-Egger showed no significant directional pleiotropy, suggesting that the genetic instruments did not introduce bias, while the weighted median method provided similar estimates, reinforcing the validity of the results. These findings confirm that potential biases from pleiotropy were minimal, supporting the robustness of the study's conclusions regarding the causal effects of HBV and HCV on liver biomarkers.

Despite the robustness of our analysis, several potential sources of bias must be considered. Population stratification, where genetic differences between populations may confound the results, is a key concern, especially given the use of GWAS data from primarily European populations. Although PCA was employed to adjust for stratification, residual confounding could still be present. Additionally, pleiotropy, where genetic variants influence the outcome through pathways other than exposure, could introduce bias into MR analyses. While sensitivity analyses, including MR-Egger regression, indicated limited pleiotropy in this study, it remains a potential source of bias. Finally, measurement errors in GWAS data, such as inaccuracies in phenotype classification or exposure variables, could affect the precision of the causal estimates. Future studies with more precise phenotypic measurements and larger, more diverse populations will be necessary to validate these findings further.

The causal links between HBV and HCV infections and liver biomarkers, such as AST, observed in this study are supported by well-established physiological mechanisms. Both HBV and HCV infections are known to cause liver inflammation, which leads to elevated AST levels as a result of hepatocellular injury.^{30,31} Aspartate aminotransferase is released into the bloodstream when liver cells are damaged, making it a key marker for liver function and disease progression.³² Chronic viral infections, such as HBV and HCV, can lead to sustained liver damage, cirrhosis and HCC, further contributing to elevated AST levels.³³ Future research should focus on elucidating the precise biological pathways through which HBV and HCV infections affect liver biomarkers, providing deeper insights into potential therapeutic targets and enhancing the scientific basis for the observed causal relationships. Such investigations could pave the way for clinical applications aimed at monitoring and managing liver health in patients with chronic viral hepatitis.

Limitations

Despite the broad data sources used in this study, several limitations need to be acknowledged. First, the reliance on publicly available GWAS databases introduces a potential limitation due to the lack of racial and genetic diversity. As a result, the findings may not be fully generalizable to populations outside of those predominantly represented in these datasets. Future studies should aim to incorporate more diverse populations to assess whether the observed causal relationships are consistent across different genetic backgrounds.

Additionally, MR is primarily focused on genetic factors and does not fully account for the influence of environmental and lifestyle factors, which play a significant role in the development and progression of liver diseases such as HBV and HCV. Factors like alcohol consumption, diet and environmental exposures are crucial contributors to liver health, and their exclusion may limit the comprehensiveness of the findings. Future research should consider incorporating multifactorial approaches that integrate genetic, environmental and lifestyle factors to provide a more complete understanding of the risks associated with liver disease.

Moreover, MR analysis is based on key assumptions, including the strong association between genetic variants and the exposure of interest, as well as the independence of these variants from confounders. In practical applications, these assumptions may not always hold, potentially introducing bias into the results.

Finally, while this study primarily focuses on genetic factors, a more comprehensive approach involving multifactorial models could offer a deeper understanding of the interactions between genetics, environmental factors and lifestyle in the context of HBV, HCV and liver disease progression. These approaches can help identify more nuanced risk factors and inform targeted strategies for prevention and treatment. In future research, expanding the population diversity, incorporating environmental and lifestyle data and using more advanced analytical models will be important steps toward overcoming the limitations identified in this study.

Conclusions

The results from this study may help identify potential therapeutic targets for managing liver diseases in patients with chronic viral hepatitis and contribute to the growing field of precision medicine in hepatology. By employing MR to analyze the causal relationships between HBV, HCV, liver biomarkers, and cirrhosis, this research suggests that monitoring AST levels can evaluate the extent of liver damage due to HBV infection, emphasizing the importance of controlling the progression of HBV and HCV infections in preventing cirrhosis. It provides new insights into the genetic basis of liver disease progression,

paving the way for future genetic research in liver diseases. Monitoring AST levels may serve as a valuable indicator of liver damage progression in chronic HBV infection and could inform treatment strategies aimed at preventing cirrhosis.

Supplementary data

The supplementary materials are available at <https://doi.org/10.5281/zenodo.15086692>. The package includes the following files:

Supplementary Table 1. Information on the samples used for the MR analysis.

Data availability

The datasets generated and/or analyzed during the current study are available from the corresponding author on reasonable request.

Consent for publication


Not applicable.


Use of AI and AI-assisted technologies


Not applicable.

ORCID iDs

Ju-Cun Huang  <https://orcid.org/0000-0003-0009-664X>

Yu-Wei Feng  <https://orcid.org/0000-0002-6486-6247>

Kang Zhao  <https://orcid.org/0000-0002-6199-7428>

Dan Dai  <https://orcid.org/0009-0000-3699-9299>

References

1. He CQ, Sun BH, Yu WT, An SY, Qiao BJ, Wu W. Evaluating the impact of COVID-19 outbreak on hepatitis B and forecasting the epidemiological trend in mainland China: A causal analysis. *BMC Public Health*. 2024;24(1):47. doi:10.1186/s12889-023-17587-3
2. Downs LO, Campbell C, Yonga P, et al. A systematic review of hepatitis B virus (HBV) prevalence and genotypes in Kenya: Data to inform clinical care and health policy. *PLOS Glob Public Health*. 2023;3(1):e0001165. doi:10.1371/journal.pgph.0001165
3. Cui F, Blach S, Manzengo Mingiedi C, et al. Global reporting of progress towards elimination of hepatitis B and hepatitis C. *Lancet Gastroenterol Hepatol*. 2023;8(4):332–342. doi:10.1016/S2468-1253(22)00386-7
4. Wu J, Wang Y, Zhu C, Lin W. Editorial: Diagnosis, treatment, and prognosis of viral hepatitis. *Front Med (Lausanne)*. 2022;9:882878. doi:10.3389/fmed.2022.882878
5. Jagdish RK, Roy A, Kumar K, et al. Pathophysiology and management of liver cirrhosis: From portal hypertension to acute-on-chronic liver failure. *Front Med (Lausanne)*. 2023;10:1060073. doi:10.3389/fmed.2023.1060073
6. Xiang Z, Li J, Lu D, Wei X, Xu X. Advances in multi-omics research on viral hepatitis. *Front Microbiol*. 2022;13:987324. doi:10.3389/fmicb.2022.987324
7. Sanderson E, Glymour MM, Holmes MV, et al. Mendelian randomization. *Nat Rev Methods Primers*. 2022;2:6. doi:10.1038/s43586-021-00092-5
8. Akcay IM, Katrinli S, Ozdil K, Doganay GD, Doganay L. Host genetic factors affecting hepatitis B infection outcomes: Insights from genome-wide association studies. *World J Gastroenterol*. 2018;24(30):3347–3360. doi:10.3748/wjg.v24.i30.3347

9. Wen Q, Lin Q, Chen P, et al. Genetic association of cardiovascular disease related biomarkers with the overall survival of hepatocellular carcinoma: A Mendelian randomization analysis. *Am J Cancer Res*. 2023;13(8):3629–3637. PMID:37693134. PMCID:PMC10492132.
10. Davies NM, Holmes MV, Davey Smith G. Reading Mendelian randomisation studies: A guide, glossary, and checklist for clinicians. *BMJ*. 2018;2018:362. doi:10.1136/bmj.k601
11. Gagliano Taliun SA, Evans DM. Ten simple rules for conducting a Mendelian randomization study. *PLoS Comput Biol*. 2021;17(8):e1009238. doi:10.1371/journal.pcbi.1009238
12. Fu L, Wang Y, Hu Y. Association between homocysteine and nonalcoholic fatty liver disease: Mendelian randomisation study. *Eur J Clin Invest*. 2023;53(3):e13895. doi:10.1111/eci.13895
13. Au Yeung SL, Borges MC, Wong THT, Lawlor DA, Schooling CM. Evaluating the role of non-alcoholic fatty liver disease in cardiovascular diseases and type 2 diabetes: A Mendelian randomization study in Europeans and East Asians. *Int J Epidemiol*. 2023;52(3):921–931. doi:10.1093/ije/dyad212
14. Butler-Laporte G, Farjoun Y, Chen Y, et al. Increasing serum iron levels and their role in the risk of infectious diseases: A Mendelian randomization approach. *Int J Epidemiol*. 2023;52(4):1163–1174. doi:10.1093/ije/dyad010
15. Jin Y, Yu X, Li J, Su M, Li X. Causal effects and immune cell mediators between prescription analgesic use and risk of infectious diseases: A Mendelian randomization study. *Front Immunol*. 2023;14:1319127. doi:10.3389/fimmu.2023.1319127
16. De Silva NMG, Borges MC, Hingorani AD, et al. Liver function and risk of type 2 diabetes: Bidirectional Mendelian randomization study. *Diabetes*. 2019;68(8):1681–1691. doi:10.2337/db18-1048
17. Hou T, Wang Q, Dai H, et al. Interactive association between gut microbiota and thyroid cancer. *Endocrinology*. 2023;165(1):bqad184. doi:10.1210/endo/bqad184
18. Li Y, Zhang Q. Causal associations between liver enzymes and diabetic microvascular complications: A univariable and multivariable Mendelian randomization. *PLoS One*. 2024;19(1):e0296894. doi:10.1371/journal.pone.0296894
19. Fu L, Wang Y, Hu YQ. Bi-directional causal effect between vitamin B12 and non-alcoholic fatty liver disease: Inferring from large population data. *Front Nutr*. 2023;10:1015046. doi:10.3389/fnut.2023.1015046
20. Zhao Y, Li D, Shi H, et al. Associations between type 2 diabetes mellitus and chronic liver diseases: Evidence from a Mendelian randomization study in Europeans and East Asians. *Front Endocrinol (Lausanne)*. 2024;15:1338465. doi:10.3389/fendo.2024.1338465
21. Mao Z, Gao ZX, Ji T, Huan S, Yin GP, Chen L. Bidirectional two-sample mendelian randomization analysis identifies causal associations of MRI-based cortical thickness and surface area relation to NAFLD. *Lipids Health Dis*. 2024;23(1):58. doi:10.1186/s12944-024-02043-x
22. Hayashi S, Nagaoka K, Tanaka Y. Blood-based biomarkers in hepatitis B virus-related hepatocellular carcinoma, including the viral genome and glycosylated proteins. *Int J Mol Sci*. 2021;22(20):11051. doi:10.3390/ijms222011051
23. Mohsen R, Gayadh E, H. Al-azzawi R, Adhiah A. Correlation of chronic viral hepatitis B and liver function tests. *J Univ Anbar Pure Sci*. 2022;16(1):9–12. doi:10.37652/juaps.2022.174819
24. Qin S, Wang J, Yuan H, He J, Luan S, Deng Y. Liver function indicators and risk of hepatocellular carcinoma: A bidirectional Mendelian randomization study. *Front Genet*. 2024;14:1260352. doi:10.3389/fgene.2023.1260352
25. Kim TH, Lee EJ, Choi JH, et al. Identification of novel susceptibility loci associated with hepatitis B surface antigen seroclearance in chronic hepatitis B. *PLoS One*. 2018;13(7):e0199094. doi:10.1371/journal.pone.0199094
26. Rosoff DB, Bell AS, Wagner J, et al. Assessing the impact of PCSK9 and HMGCR inhibition on liver function: Drug-target Mendelian randomization analyses in four ancestries. *Cell Mol Gastroenterol Hepatol*. 2024;17(1):29–40. doi:10.1016/j.jcmgh.2023.09.001
27. Lin C, Kao J. The clinical implications of hepatitis B virus genotype: Recent advances. *J Gastroenterol Hepatol*. 2011;26(Suppl 1):123–130. doi:10.1111/j.1440-1746.2010.06541.x
28. Kamiza AB, Fatumo S, Singini MG, Yeh CC, Chikowore T. Hepatitis B infection is causally associated with extrahepatic cancers: A Mendelian randomization study. *eBioMedicine*. 2022;79:104003. doi:10.1016/j.ebiom.2022.104003
29. Zeng Z, Liu H, Haiying L, et al; the HBVstudy consortium. Genome-wide association study identifies new loci associated with risk of HBV infection and disease progression. *BMC Med Genomics*. 2021;14(1):84. doi:10.1186/s12920-021-00907-0
30. Valva P, Ríos DA, De Matteo E, Preciado MV. Chronic hepatitis C virus infection: Serum biomarkers in predicting liver damage. *World J Gastroenterol*. 2016;22(4):1367–1381. doi:10.3748/wjg.v22.i4.1367
31. Dai YN, Xu CF, Pan HY, Chen MJ, Yu CH. Fatty liver is associated with significant liver inflammation and increases the burden of advanced fibrosis in chronic HBV infection. *BMC Infect Dis*. 2023;23(1):637. doi:10.1186/s12879-023-08632-y
32. Shojaie L, Iorga A, Dara L. Cell death in liver diseases: A review. *Int J Mol Sci*. 2020;21(24):9682. doi:10.3390/ijms21249682
33. Johnson PJ, Kalyuzhnyy A, Boswell E, Toyoda H. Progression of chronic liver disease to hepatocellular carcinoma: Implications for surveillance and management. *BJC Rep*. 2024;2(1):39. doi:10.1038/s44276-024-00050-0

MALAT1 modulates granulosa cells ferroptosis and apoptosis through PAK2 upregulation in polycystic ovary syndrome

Yun Yang^{A,B,F}, Dan Li^{B,C}, Lu Sun^{C,D}, Shasha Liu^{D,E}

Department of Gynecology, Tianjin Central Hospital of Gynecology Obstetrics, China

A – research concept and design; B – collection and/or assembly of data; C – data analysis and interpretation;

D – writing the article; E – critical revision of the article; F – final approval of the article

Advances in Clinical and Experimental Medicine, ISSN 1899–5276 (print), ISSN 2451–2680 (online)

Adv Clin Exp Med. 2025;34(12):2055–2066

Address for correspondence

Yun Yang

E-mail: erff5623@126.com

Funding sources

This study was supported by the Tianjin Health Research Project (grant No. ZC20054) and the Tianjin Key Medical discipline (Specialty) Construction Project (Obstetrics and gynecology) (grant No. TJYXZDXK-043A).

Conflict of interest

None declared

Received on August 8, 2024

Reviewed on January 30, 2025

Accepted on February 26, 2025

Published online on July 31, 2025

Abstract

Background. Polycystic ovary syndrome (PCOS) is a complicated endocrinological disorder.

Objectives. We investigated the ferroptosis-regulated role of MALAT1 and its potential modulatory mechanisms in granulosa cells (GCs).

Materials and methods. Reverse transcripton quantitative polymerase chain reaction (RT-qPCR) was used to measure the relative expression of MALAT1/miR-155-5p/PAK2 in KGN cells after transfection. Online bioinformatic analysis was performed to predict the interactions between MALAT1/PAK2 and miR-155-5p. Dual luciferase assays were performed for relative luciferase activity in cell groups co-transfected with the pmiRGLO plasmids containing wild type (wt) or mutant type (mt) of MALAT1 (MALAT1-wt, MALAT1-mt), siRNA targeting MALAT1 (si-MALAT1) miR-155-5p inhibitor or their control was transfected into KGN cells using Lipofectamine 2000. After 48 h, the transfected cells were collected for the following experiments. Cell viability and apoptosis were measured using Cell Counting Kit-8 (CCK-8) and flow cytometry. Malondialdehyde (MDA) level and reduced glutathione (GSH) / oxidized glutathione disulfide (GSSG) ratio were detected using commercial kits. Western blot was used to measure the relative protein changes in PAK2, SLC7A11 and GPX4.

Results. Knockdown of MALAT1 decreased cell viability, increased apoptosis and ferroptosis, which was reversed by miR-155-5p inhibition. MALAT1 downregulation inhibited PAK2, while miR-155-5p inhibition activated PAK2. The increase of relative luciferase activity in cells transfected with MALAT1-wt or PAK2-wt and miR-155-5p inhibitor suggests the bindings between miR-155-5p and MALAT1 or PAK2.

Conclusions. This study revealed a novel ferroptosis-modulated role of MALAT1 in PCOS in vitro via interactions with miR-155-5p/PAK2. Further in vivo and clinical studies are needed to validate these in vitro findings and fully assess the therapeutic potential of MALAT1 in PCOS.

Key words: PCOS, ferroptosis, MALAT1, PAK2

Cite as

Yang Y, Li D, Sun L, Liu S. MALAT1 modulates granulosa cells ferroptosis and apoptosis through PAK2 upregulation in polycystic ovary syndrome. *Adv Clin Exp Med.* 2025;34(12):2055–2066. doi:10.17219/acem/202385

DOI

10.17219/acem/202385

Copyright

Copyright by Author(s)

This is an article distributed under the terms of the Creative Commons Attribution 3.0 Unported (CC BY 3.0) (<https://creativecommons.org/licenses/by/3.0/>)

Highlights

- MALAT1 controls ferroptosis in KGN granulosa cells, uncovering a novel lncRNA-driven cell-death pathway in ovarian physiology.
- Reduced MALAT1 expression links to polycystic ovary syndrome (PCOS)-associated ovarian dysfunction, highlighting its potential as a biomarker and therapeutic target in PCOS.
- MALAT1 sponges miR-155-5p to upregulate PAK2 in KGN cells, defining a MALAT1/miR-155-5p/PAK2 ceRNA network critical for granulosa-cell function.

Background

Polycystic ovary syndrome (PCOS) is a complex endocrinological disorder affecting 8–13% of reproductive-aged women worldwide, with approx. 70% of cases remaining undiagnosed.^{1,2} As an ovulatory disorder, PCOS is characterized by irregular menstrual patterns, metabolic disturbances and hyperandrogenism. However, the precise causes of PCOS remain unclear, and there is an urgent need for accurate and efficient diagnostic methods.^{3,4} Beyond known risk factors such as obesity, elevated testosterone levels and male-pattern balding, previous studies have reported numerous genetic and protein alterations in patients with PCOS.^{5,6} An increasing body of research suggests that noncoding RNAs may play an important role in the pathogenesis of PCOS.⁷ For example, long non-coding RNA (lncRNA) BBOX1 antisense RNA1 (AS1) has been found to be upregulated in the follicular fluid of PCOS patients and is known to promote the proliferation of granulosa cells (GCs) by downregulating miR-19b.⁸ LncRNA HLA-F-AS1 is downregulated, while microRNA-613 expression is increased in the follicular fluid of PCOS patients; overexpression of HLA-F-AS1 has been shown to promote GC proliferation by inhibiting miR-613.⁹ Metastasis-associated lung adenocarcinoma transcript-1 (MALAT1) has been found to be downregulated in peripheral blood leukocytes from obese PCOS patients¹⁰ and similarly decreased in GCs from PCOS patients.^{11,12} Previous studies have demonstrated that, in vitro, MALAT1 can regulate the viability and apoptosis of GCs and the human granulosa-like tumor cell line (KGN).¹³ In PCOS rat models, MALAT1 is also downregulated in ovarian tissues, and upregulation of MALAT1 has been shown to protect against PCOS via the miR-302d-3p/LIF axis.¹⁴ Mechanistically, MALAT1 modulates KGN cells and GCs in vitro through miR-125b/miR-203a/TGF β signaling pathways.¹² In GCs and KGN cells, MALAT1 promotes the degradation and ubiquitination of p53, thereby regulating cell proliferation and apoptosis.¹⁵ Recently, increased ferroptosis has been identified as being correlated with PCOS.^{7,16} Ferroptosis in PCOS is associated with impaired mitochondrial dynamics, overproduction of proinflammatory cytokines and elevated oxidative stress.¹⁷ In PCOS rat models, inhibition of ferroptosis has

been shown to significantly alleviate PCOS symptoms.^{7,18} However, it remains unknown whether MALAT1 plays a role in mediating ferroptosis in KGN cells or GCs.

Objectives

Interestingly, using online bioinformatic tools, we identified that *PAK2* may be regulated by MALAT1 through competitive binding to miR-155-5p. Downregulation of *PAK2* in PCOS ovarian tissues has been shown to trigger oxidative stress via the Nrf2/HO-1 pathway and mediate apoptosis in KGN cells through the β -catenin/c-Myc/PKM2 signaling axis.¹⁹ Additionally, miR-155-5p has been reported to enhance glycolysis in KGN cells, which may be linked to increased cell proliferation.²⁰ Based on these findings, we hypothesized that MALAT1 may play a regulatory role in the proliferation, apoptosis and ferroptosis of KGN cells through the miR-155-5p/PAK2 axis. This study primarily employed in vitro experiments to validate this hypothesis.

Materials and methods

Bioinformatic analysis

The StarBase online database (<https://rnasysu.com/encori/agoClipRNA.php?source=lncRNA>) was used to predict the binding sites between MALAT1, PAK2 and miR-155-5p. First, the potential binding sites between MALAT1 and miR-155-5p were predicted using the miRNA-Target (lncRNAs) option. Next, the binding sites between miR-155-5p and PAK2 were predicted using the miRNA-Target (mRNA) option.

Cell culture and transfection

The KGN cells (cat. No. CL-0603; Procell, Wuhan, China) were cultured in DMEM/F12 medium supplemented with 10% fetal bovine serum (FBS) in a cell incubator (Thermo Fisher Scientific, Waltham, USA) at 37°C with 5% CO₂. The siRNA targeting MALAT1 (si-MALAT1) and its negative control (si-NC), as well as the miR-155-5p inhibitor and its corresponding control (Ctrl inhibitor), were designed and synthesized by GenePharma (Suzhou, China). Cells

were seeded in 24-well plates, and si-MALAT1, miR-155-5p inhibitor or their respective controls were transfected into KGN cells using Lipofectamine 2000 (cat No. 11668030; Thermo Fisher Scientific). After 48 h, the transfected cells were collected for subsequent experiments.

CCK-8 method

Cells were seeded into 96-well plates at a density of 2,500 cells per well. Each experimental group included at least 3 replicates, along with control wells and blank wells containing culture medium only. On the 2nd day, 10 μ L of Cell Counting Kit-8 (CCK-8) working solution (cat. No. G1613; Sevicebio, Wuhan, China) was added to each well containing 90 μ L of culture medium. The plates were then incubated for an additional 1.5 h in a cell incubator, after which the optical density (OD) values were measured at a wavelength of 450 nm using a microplate reader (MK; Thermo Fisher Scientific).

Apoptosis analysis

After transfection, cells were collected and centrifuged at 500 g for 5 min at 4°C. Apoptosis was assessed using the Annexin V-FITC/PI Apoptosis Kit (cat No. G1511; Servicebio). The binding buffer was precooled to 4°C and used to resuspend the cells at a density of 3×10^6 cells/mL. To each 100 μ L of cell suspension, 5 μ L of Annexin V-FITC and 5 μ L of propidium iodide (PI) were added. After incubating in the dark at room temperature for 10 min, 400 μ L of binding buffer was added. Cell apoptosis was then evaluated using a flow cytometer (CytoFlex; Beckman Coulter, Brea, USA).

RNA extraction

Total RNA was extracted from the cell samples in each group using the TRIzol Kit (cat. No. R0016; Beyotime, Shanghai, China). Briefly, cells were lysed in TRIzol, followed by the addition of 100 μ L of chloroform replacement (cat. No. G3014-01; Servicebio) to every 1 mL of RNA extraction mixture. After vortexing for 15 s, the mixture was left at room temperature for 5 min and then centrifuged at 12,000 g for 15 min at 4°C. The upper colorless aqueous phase was carefully transferred to new centrifuge tubes, and total RNA was precipitated using isopropanol. Subsequently, 75% ethanol was added to remove residual salts and isopropanol. The RNA pellet was dissolved in diethylpyrocarbonate (DEPC)-treated water. The concentration and purity of total RNA were measured with ultraviolet spectrophotometry at A260.

Reverse transcription quantitative polymerase chain reaction

The BeyoFast™ SYBR Green One-Step RT-qPCR Kit (cat. No. D7268S; Beyotime) was used to measure the relative

expression of MALAT1, with GAPDH as the internal reference, using total RNA as the template. According to the manufacturer's protocol, a 20 μ L reaction system was prepared for each well in a 96-well plate, consisting of 10 μ L SYBR Green One-Step Reaction Buffer ($\times 2$), 2 μ L Enzyme Mix ($\times 10$), 2 μ L Primer Mix (3 μ M each), 2 μ L RNA template, and RNase-free water to a final volume of 20 μ L. The reverse transcription quantitative polymerase chain reaction (RT-qPCR) cycling conditions were set as follows: reverse transcription at 50°C for 30 min, pre-denaturation at 95°C for 2 min, followed by 40 cycles of denaturation at 95°C for 15 s and annealing/extension at 60°C for 15–30 s. Primers used in this study were synthesized by Sangon Biotech (Shanghai, China) and included the following sequences:

MALAT1 Forward (F):

5'-GCTCTGTGGTGTGGGATTGA-3';

MALAT1 Reverse (R):

5'-GTGGCAAAATGGCGGACTTT-3';

GAPDH Forward (F):

5'-GGTGGTCTCCTCTGACTTCAACA-3';

GAPDH Reverse (R):

5'-CCAAATTCGTTGTCATACCAGGAAATG-3'.

For miR-155-5p, the RT-qPCR analysis was performed using the miRNA 1st Strand cDNA Synthesis Kit (by stem-loop) (cat. No. MR101-01; Vazyme, Beijing, China) and the miRNA Unimodal SYBR qPCR Master Mix Kit (cat. No. MQ102-C1; Vazyme), with U6 as the internal reference. The cDNA synthesis reaction system included 10 μ L RNA template, 1 μ L RT primer (2 μ M), 2 μ L RT Mix, 2 μ L HiScript II Enzyme Mix, and RNase-free ddH₂O to the final volume. The reaction was carried out under the following conditions: 25°C for 5 min, 50°C for 15 min and 85°C for 5 min. The RT primer used for miR-155-5p was 5'-GTCGTATCCAGTGCAGGGTCCGAGGTATTCGCACTGGATACGACAACCCC-3'. The qPCR primers for miR-155-5p were:

Forward (F): 5'-CGCGTTAATGCTAATCGTGATA-3';

Reverse (R): 5'-AGTGCAGGGTCCGAGGTATT-3'.

The qPCR reaction system consisted of 10 μ L 2 \times miRNA Unimodal SYBR qPCR Master Mix, 0.4 μ L forward primer, 0.4 μ L reverse primer, 2 μ L cDNA template, and RNase-free ddH₂O to the final volume. The qPCR cycling conditions were as follows: 95°C for 10 s, followed by 40 cycles of 95°C for 10 s and 60°C for 30 s. Relative expression levels were analyzed using the $2^{-\Delta\Delta CT}$ method in Microsoft Excel 2013 (Microsoft Corp., Redmond, USA).

Western blot

Total proteins were extracted using RIPA with supplementation of phenylmethylsulfonyl fluoride (PMSF) on ice (cat. No. P0013B; Beyotime). The protein concentration was determined using bicinchoninic acid (BCA) kit (Bioss, Beijing, China). Then 5 \times loading buffer was added and the protein samples were boiled for 20 min. Sodium dodecyl

sulfate–polyacrylamide gel electrophoresis (SDS–PAGE) method was used to separate the proteins. The proteins on the gel were then transferred onto polyvinylidene difluoride (PVDF) membranes. Tris-buffered saline with Tween (TBST) was used to dilute the skim milk to 5%, which was then used to block the membranes for 1 h at 37°C. The primary antibodies were diluted using TBST at 1:1,000, which included the anti-GPX4 (cat. No. bs-3884R; Bioss), anti-SLC7A11 (cat. No. bs-6883R; Bioss) and anti-PAK2 (cat. No. 19979-1-AP; Proteintech, Wuhan, China). The anti-GAPDH was diluted at 1:10,000 (cat. No. bs-10900R; Bioss). The primary antibodies were used to incubate the membranes for 1 h at 37°C. TBST was used to wash the membranes for 3 times, 5 min each time. The secondary antibody (cat. No. AB0101; Abways, Shanghai, China) was diluted at 1 : 20,000 using TBST and was used to incubate the membranes for 1 h at room temperature. The membranes were washed using TBST 3 times, 8 min each time. The electrochemiluminescence (ECL) kit was applied onto the membranes, and the immunoblotting image was taken on an ECL imaging machine (Servicebio). ImageJ (National Institutes of Health (NIH), Bethesda, USA) was used to analyze the grey values.

Dual-luciferase reporter gene assays

Plasmids containing the wild-type and mutant sequences of MALAT1 (MALAT1-wt, MALAT1-mt) and PAK2 (PAK2-wt, PAK2-mt) were constructed using the pmiR-GLO vector (Promega, Madison, USA). The KGN cells were transfected with MALAT1-wt/mt or PAK2-wt/mt along with either the miR-155-5p inhibitor or control inhibitor using Lipofectamine 2000. The Dual Luciferase Reporter Assay Kit (cat. No. RG028; Beyotime) was used following the manufacturer's instructions, and dual luciferase activity was measured using a laboratory luminometer.

Analysis of MDA and GSH/GSSG ratios

The MDA Kit (cat. No. S0131S; Beyotime) and the GSH/GSSG Ratio Detection Kit (cat. No. S0053; Beyotime) were used following the standard procedures provided by the manufacturer. Briefly, malondialdehyde (MDA) levels were measured colorimetrically at 532 nm using a laboratory spectrophotometer, according to the product instructions. Total glutathione levels and reduced glutathione (GSH) levels were measured on a microplate reader at 405 nm. Oxidized GSH levels were calculated by subtracting the measured GSH levels from the total glutathione levels.

Statistical analyses

A non-normal distribution was assumed due to the small sample size. Briefly, the statistical significance of differences was assessed using the Kruskal–Wallis test with Dunn's post hoc analysis for multiple group comparisons

and the Mann–Whitney U test for two-group comparisons, performed using GraphPad Prism 8 (GraphPad Software, San Diego, USA). Statistical analysis results were presented in the supplementary tables. All experiments were performed in triplicate. Basic calculations, including relative expression levels, protein expression, and luciferase activity, were conducted using Microsoft Excel 2013 (Microsoft Corp.). Figures were generated using GraphPad, with triplicate data displayed as scatter plots showing the median and range. A $p < 0.05$ was considered statistically significant.

Results

Downregulation of MALAT1 is associated with increased apoptosis and ferroptosis in KGN cells

We confirmed using RT-qPCR that MALAT1 expression was significantly reduced in KGN cells transfected with siRNA targeting MALAT1, showing a fold change (Fc) of 0.320 ± 0.040 (Fig. 1A). Downregulation of MALAT1 reduced cell viability and induced apoptosis in KGN cells (Fig. 1B–E). Additionally, MALAT1 knockdown increased MDA content and decreased the GSH/GSSG ratio in KGN cells (Fig. 2A,B).

Western blot analysis was performed to assess changes in the relative protein expression levels of the anti-ferroptosis markers SLC7A11 and GPX4. The results showed that knockdown of MALAT1 significantly inhibited the expression of both SLC7A11 and GPX4 in KGN cells (Fig. 2C–E). Taken together, these findings indicate that MALAT1 knockdown induces both apoptosis and ferroptosis while reducing cell viability in KGN cells. Furthermore, MALAT1 was found to modulate PAK2 expression in KGN cells by competitively acting as a molecular sponge for miR-155-5p. Bioinformatic analysis using the StarBase online database predicted the binding sites between MALAT1/PAK2 and miR-155-5p (Fig. 3A,B). Based on the predicted binding sites, pmiR-GLO plasmids containing MALAT1-wt/mt and PAK2-wt/mt were constructed. Dual-luciferase activity assays were performed after KGN cells were transfected with MALAT1-wt/mt or PAK2-wt/mt along with either the miR-155-5p inhibitor or control inhibitor. The results revealed that relative luciferase activity was significantly enhanced in cells transfected with MALAT1-wt and miR-155-5p inhibitor (Fig. 3C) and was similarly increased in cells transfected with PAK2-wt and miR-155-5p inhibitor (Fig. 3D). These findings verified the direct binding interactions between MALAT1/PAK2 and miR-155-5p in KGN cells. Furthermore, downregulation of MALAT1 in KGN cells led to a significant increase in miR-155-5p expression (fold change, 2.39 ± 0.22 ; Fig. 3E). Inhibition of miR-155-5p increased PAK2 mRNA expression (fold change, 1.94 ± 0.15 ; Fig. 3F) as well as PAK2 protein levels

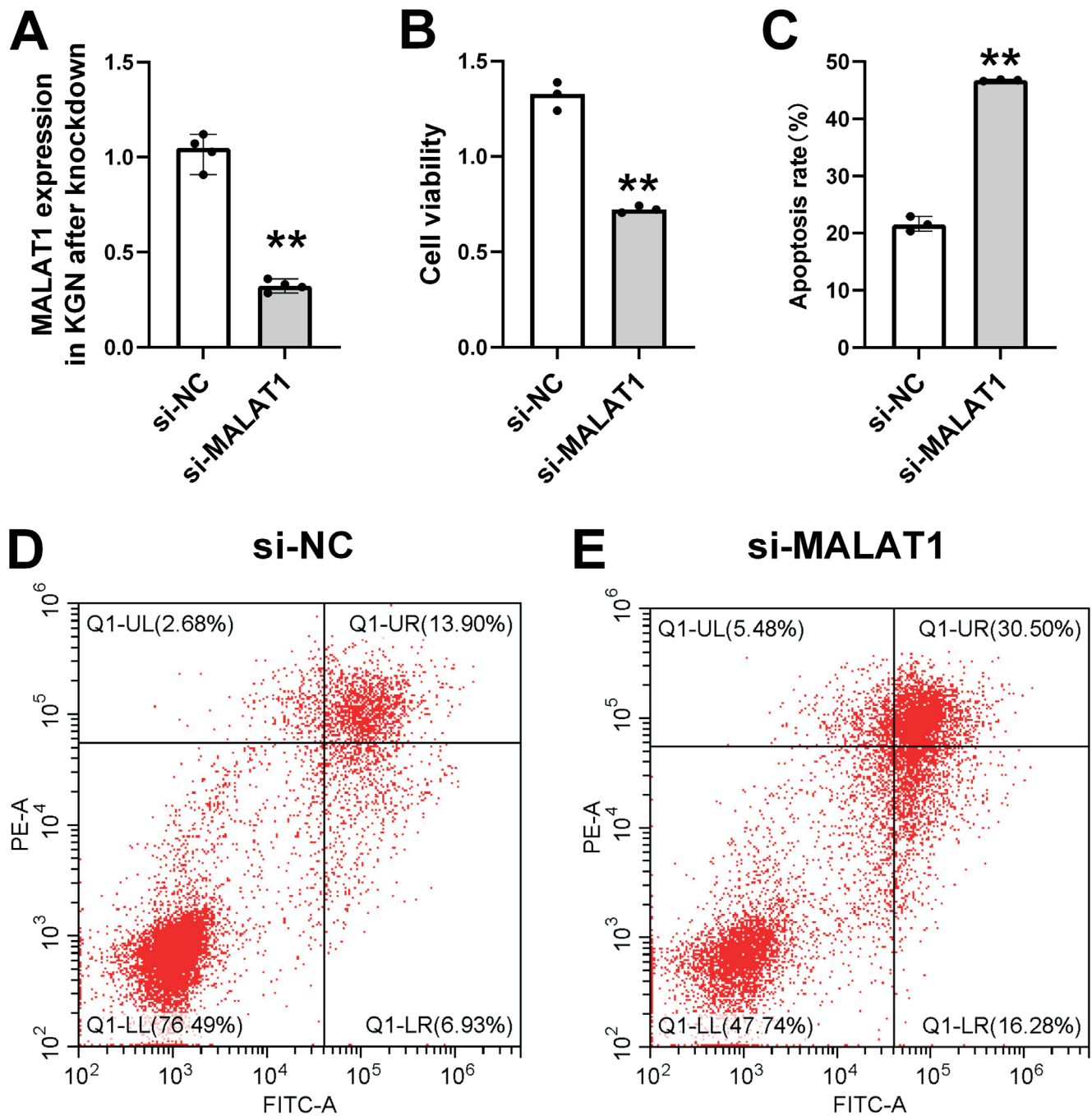


Fig. 1. Downregulation of MALAT1 is associated with apoptosis and ferroptosis in human granulosa cell line (KGN cells). KGN cells were transfected with siRNA targeting MALAT1 (si-MALAT1) and its control (si-NC). A. Cells were collected for reverse transcription quantitative polymerase chain reaction (RT-qPCR) analysis; B. Cell viability assessment; C–E. Apoptosis analysis. The statistical significance of differences was analyzed using the Kruskal–Wallis test with Dunn's post hoc for multiple group comparisons, and the Mann–Whitney U test for comparisons between 2 groups. Data are presented as scatter plots with median and range lines; $p < 0.05$ was considered statistically significant

(Fig. 4B). The mRNA expression level of PAK2 was suppressed by MALAT1 knockdown (fold change, 0.49 ± 0.05) but was restored by co-treatment with the miR-155-5p inhibitor (fold change, 0.92 ± 0.07) in KGN cells (Fig. 4A). Similarly, MALAT1 knockdown reduced PAK2 protein levels, which were reversed upon miR-155-5p inhibition (Fig. 4A,C). Taken together, these results demonstrate that MALAT1 regulates PAK2 expression by competitively binding to miR-155-5p.

miR-155-5p downregulation enhances cell viability and inhibits apoptosis and ferroptosis

Inhibition of miR-155-5p significantly increased cell viability and reduced apoptosis in KGN cells (Fig. 5). Additionally, downregulation of miR-155-5p decreased MDA content, increased the GSH/GSSG ratio, and elevated the protein expression levels of GPX4 and SLC7A11

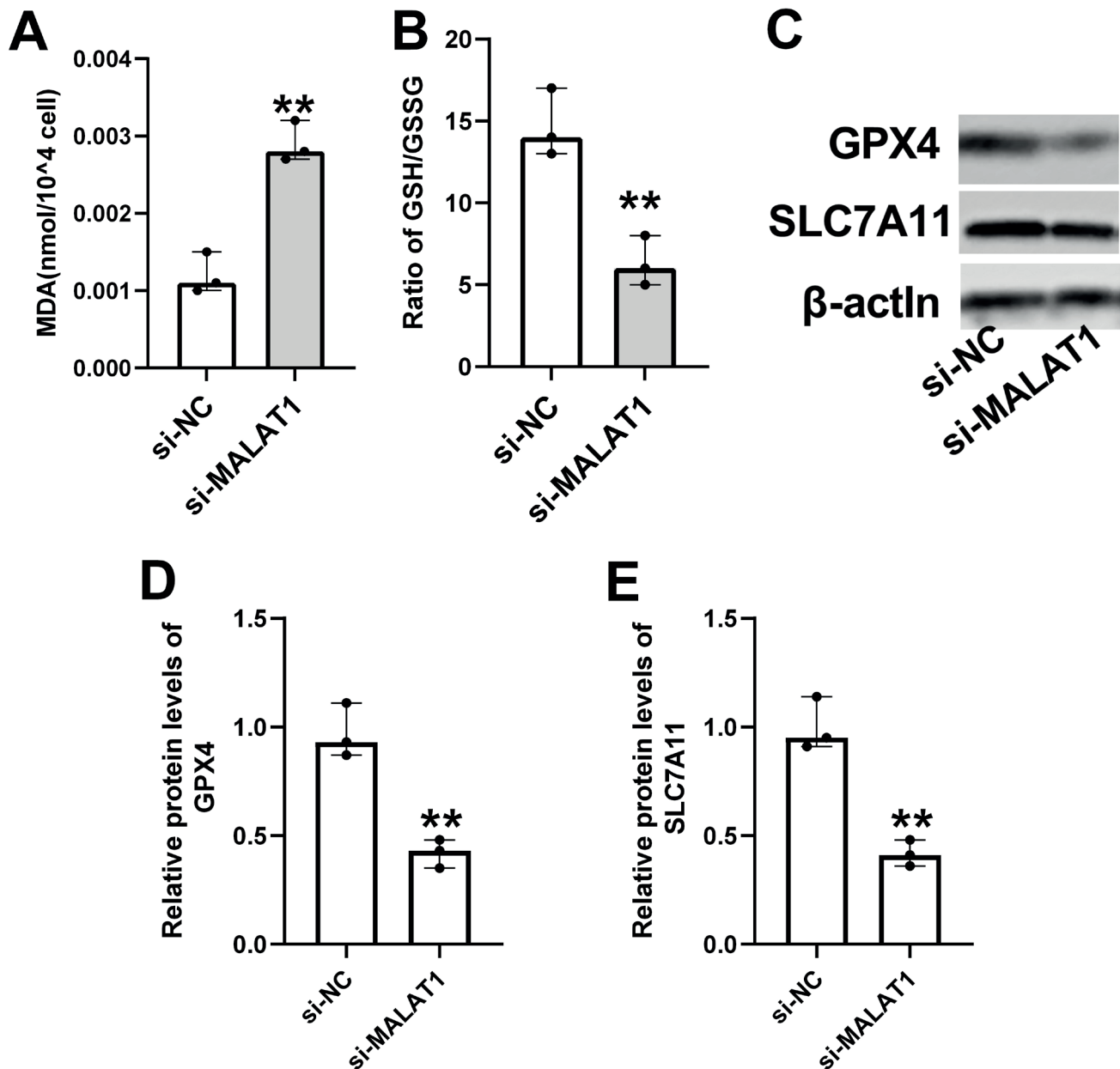


Fig. 2. Downregulation of MALAT1 is associated with ferroptosis in human granulosa cell line (KGN cells). A,B. MDA content and GSH/GSSG ratio; C–E. Western blot experiments and ImageJ analysis were used to assess the protein expression levels of SLC7A11 and GPX4. The statistical significance of differences was analyzed using the Kruskal–Wallis test with Dunn’s post hoc for multiple group comparisons and the Mann–Whitney U test for comparisons between 2 groups. Data are presented as scatter plots with median and range lines; $p < 0.05$ was considered statistically significant

MDA – malondialdehyde; GSH – reduced glutathione; GSSG – oxidized glutathione disulfide.

in KGN cells (Fig. 6), suggesting that miR-155-5p downregulation also reduces ferroptosis in KGN cells.

Downregulation of miR-155-5p reverses the impacts of MALAT1 knockdown in KGN cells

As described above, knockdown of MALAT1 reduced cell viability and induced apoptosis and ferroptosis in KGN cells. We further validated that inhibition of miR-155-5p could reverse the effects of MALAT1 knockdown in these cells (Fig. 7). Specifically, the reduction in cell viability

caused by MALAT1 knockdown was restored by miR-155-5p downregulation (Fig. 7A), and the increase in apoptosis induced by MALAT1 knockdown was reversed by miR-155-5p inhibition (Fig. 7B–E). The increase in MDA content induced by MALAT1 knockdown was reversed by miR-155-5p inhibition (Fig. 8A). Similarly, the reductions in the GSH/GSSG ratio and the relative protein expression levels of GPX4 and SLC7A11 caused by MALAT1 knockdown in KGN cells were restored by downregulation of miR-155-5p (Fig. 8B–E). These findings demonstrate that miR-155-5p inhibition can effectively reverse the impacts of MALAT1 knockdown in KGN cells.

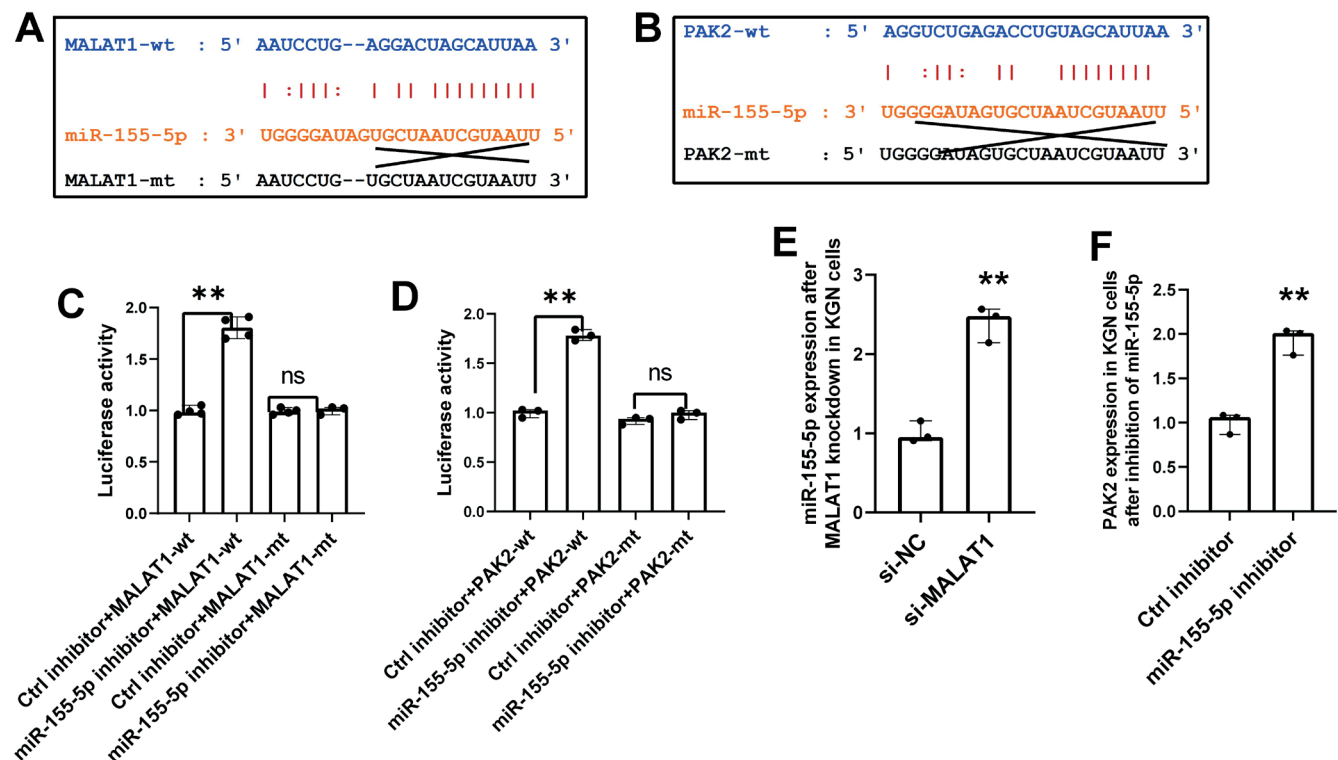


Fig. 3. MALAT1 sponges miR-155-5p and targets PAK2 in human granulosa cell line (KGN cells). A,B. Bioinformatic analysis was conducted using the StarBase online database (<https://rnasysu.com/encori/agoClipRNA.php?source=IncRNA>) to predict the targeting sites between miR-155-5p and MALAT1/PAK2; C,D. Dual-luciferase reporter assays were performed to examine the relative luciferase activity; E. Relative expression of miR-155-5p in KGN cells following MALAT1 knockdown; F. PAK2 expression in KGN cells after inhibition of miR-155-5p

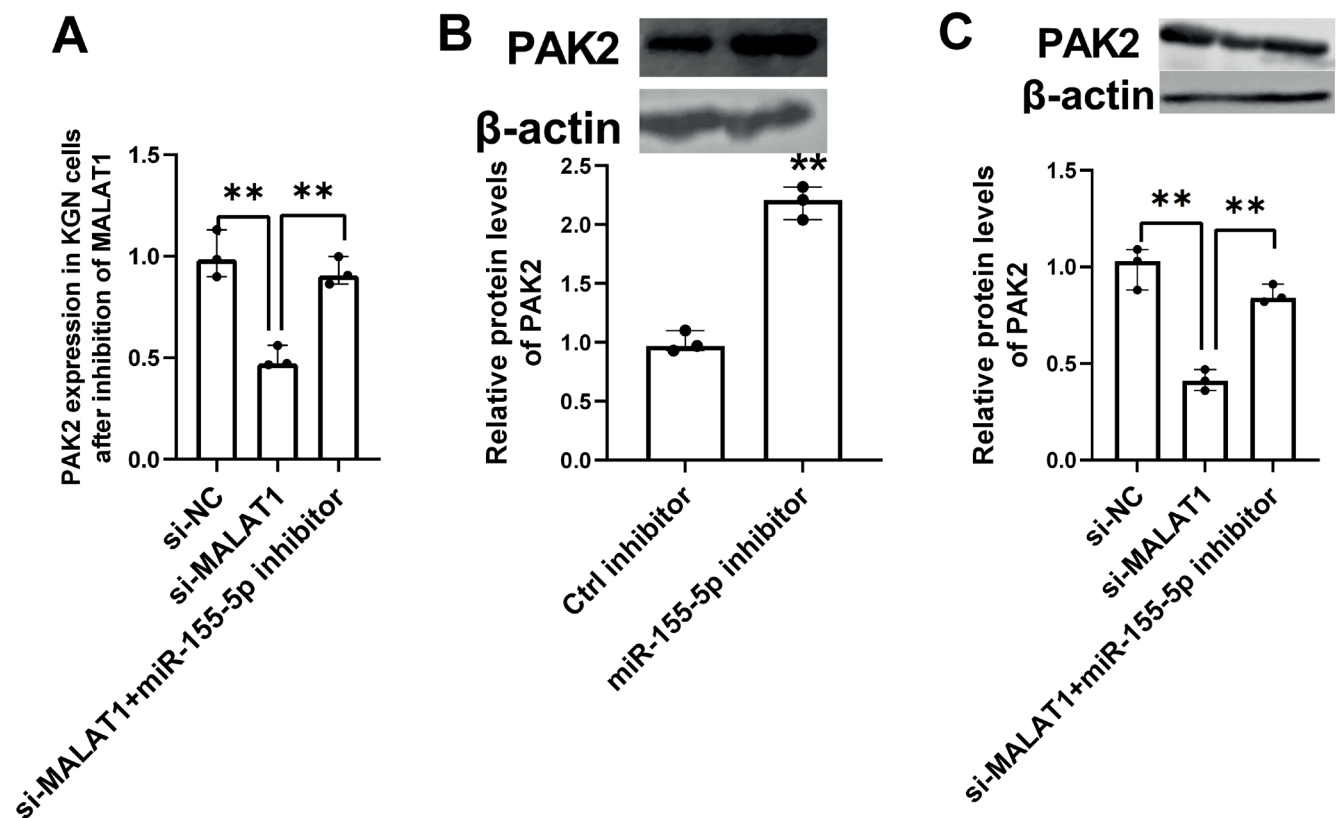


Fig. 4. PAK2 is inhibited by knockdown of MALAT1 and restored by miR-155-5p inhibitor in human granulosa cell line (KGN cells). A. PAK2 expression in KGN cells after MALAT1 knockdown or MALAT1 knockdown combined with miR-155-5p inhibition; B,C. Relative protein expression levels of PAK2; p < 0.05 was considered statistically significant

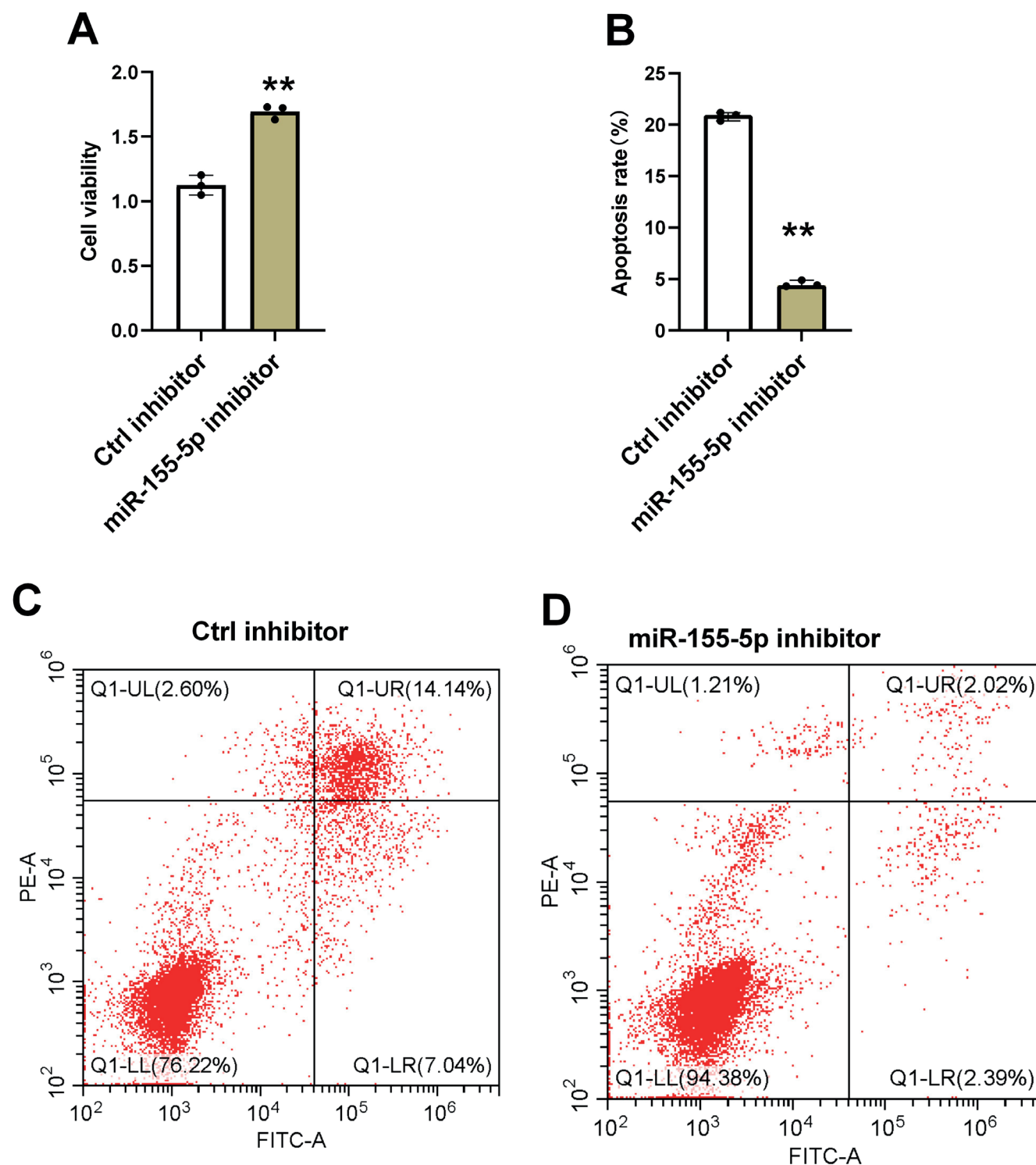


Fig. 5. miR-155-5p downregulation enhances cell viability and inhibits apoptosis and ferroptosis. Human granulosa cell line (KGN cells) were transfected with the miR-155-5p inhibitor or its control (Ctrl inhibitor). A. Cell viability; B–D. Cell apoptosis analysis; $p < 0.05$ was considered statistically significant

Discussion

The significance of this study lies in its investigation of MALAT1's role in regulating apoptosis and ferroptosis in KGN cells, providing new insights into the pathophysiology of PCOS. Prior research has shown that MALAT1

downregulation is associated with increased apoptosis and decreased proliferation in GCs, contributing to ovary dysfunction in PCOS.^{15,21} Abnormal GC death, particularly through apoptosis, has been identified as a key factor driving disrupted folliculogenesis in PCOS, ultimately leading to anovulation and infertility.²² Ferroptosis, a relatively

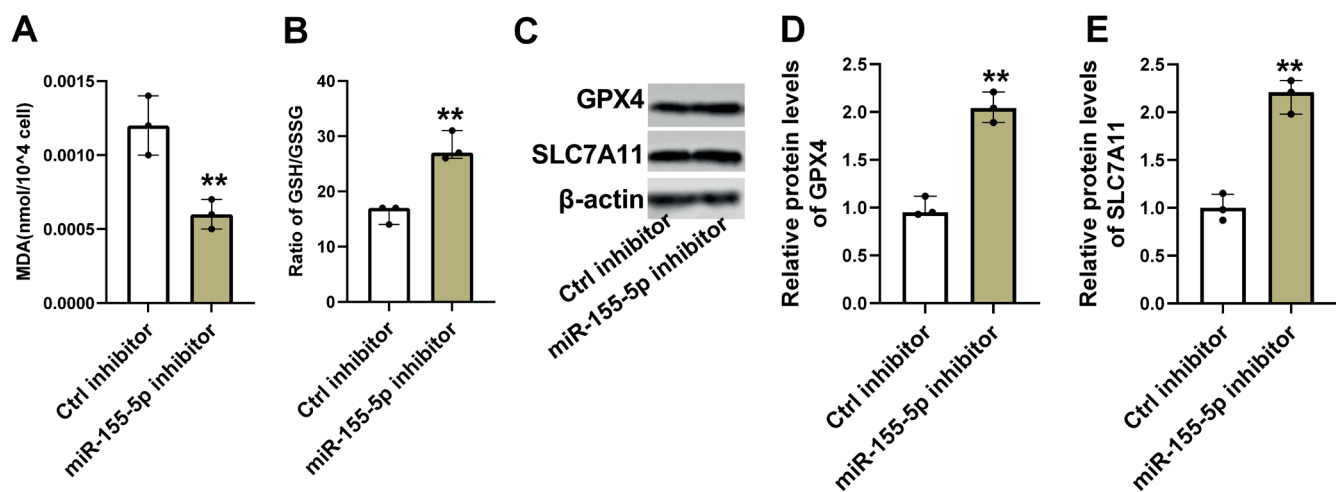


Fig. 6. miR-155-5p downregulation inhibits ferroptosis. A,B. MDA levels and GSH/GSSG ratios; C-E. Relative protein expression of the anti-ferroptosis markers SLC7A11 and GPX4; $p < 0.05$ was considered statistically significant

MDA – malondialdehyde; GSH – reduced glutathione; GSSG – oxidized glutathione disulfide.

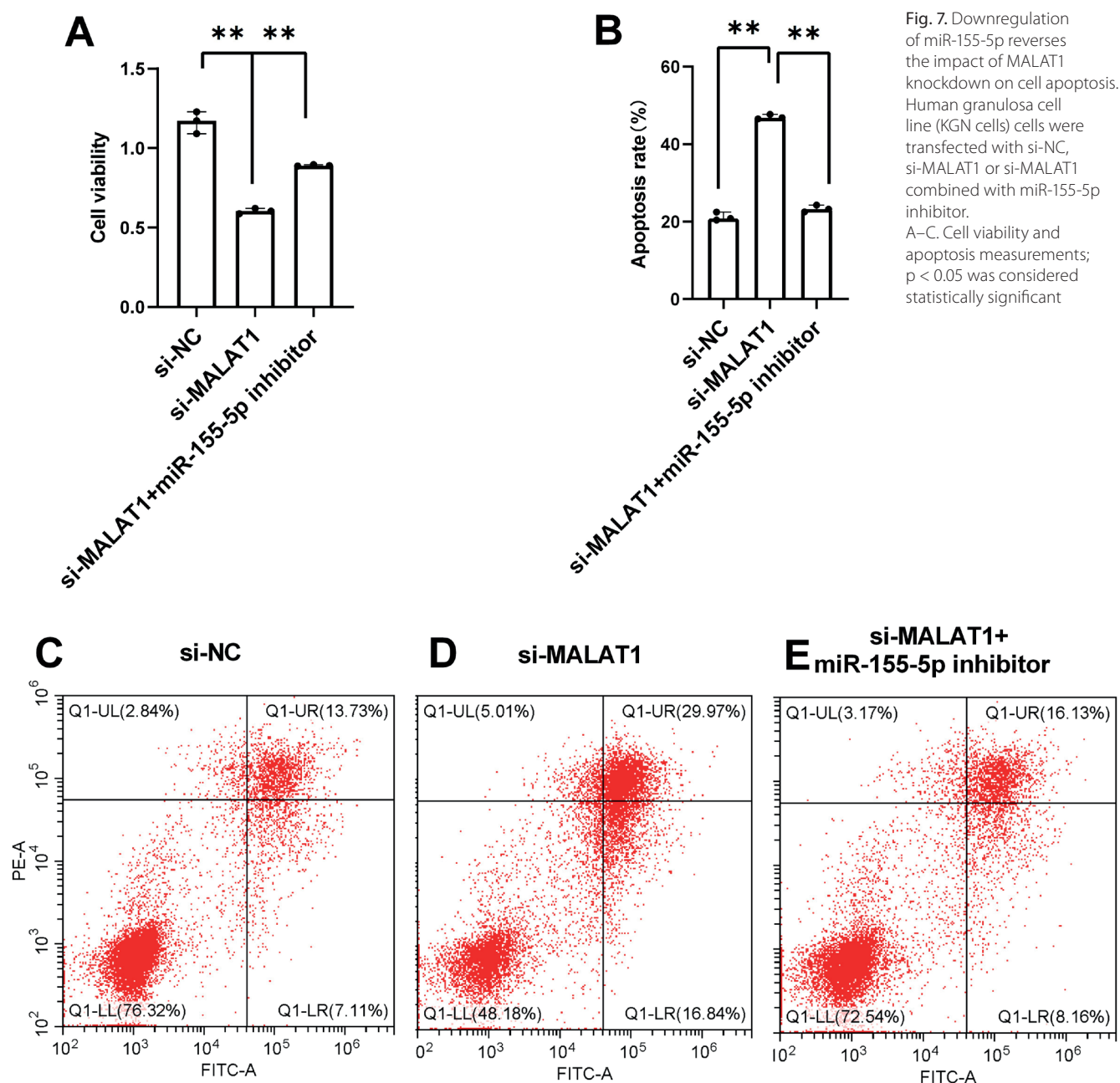


Fig. 7. Downregulation of miR-155-5p reverses the impact of MALAT1 knockdown on cell apoptosis. Human granulosa cell line (KGN cells) cells were transfected with si-NC, si-MALAT1 or si-MALAT1 combined with miR-155-5p inhibitor. A-C. Cell viability and apoptosis measurements; $p < 0.05$ was considered statistically significant

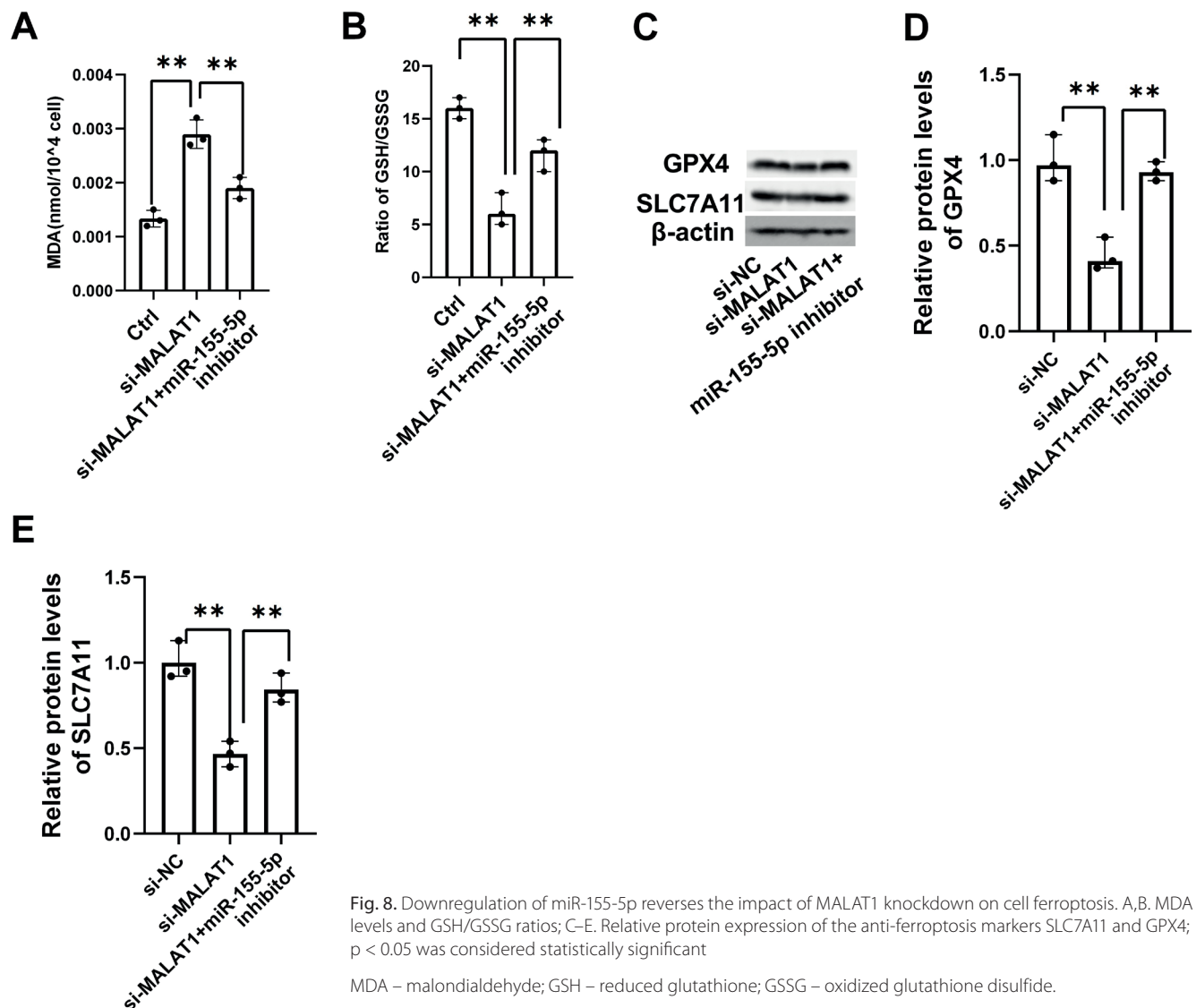


Fig. 8. Downregulation of miR-155-5p reverses the impact of MALAT1 knockdown on cell ferroptosis. A,B. MDA levels and GSH/GSSG ratios; C–E. Relative protein expression of the anti-ferroptosis markers SLC7A11 and GPX4; $p < 0.05$ was considered statistically significant

MDA – malondialdehyde; GSH – reduced glutathione; GSSG – oxidized glutathione disulfide.

newly characterized form of programmed cell death distinct from apoptosis, is marked by iron-dependent lipid peroxidation.^{21,23} In recent years, studies have found that ferroptosis-related genes are dysregulated in GCs from PCOS patients and that inhibition of ferroptosis can alleviate PCOS symptoms in animal models.^{7,21} Interestingly, another study reported that MALAT1 knockdown promotes ferroptosis in ectopic endometrial stromal cells in endometriosis, suggesting a potential connection between MALAT1 and ferroptosis regulation.²⁴

In PCOS, ferroptosis-related genes have been linked to impaired oocyte quality.²⁵ Enhanced ferroptosis in ovarian GCs from PCOS patients is associated with oocyte dysmaturity, increasing the risk of infertility.²⁶ GPX4 acts as a key antioxidant regulator of ferroptosis by reducing reactive oxygen species (ROS) accumulation and enhancing cellular resistance to ferroptosis.²⁷ Additionally, GSH is synthesized from cysteine via the System Xc⁻ (comprising SLC7A11 and SLC3A2) and the transsulfuration pathway, with GSH consumption leading to GPX4 inactivation.²⁸ SLC7A11, an upstream modulator of ferroptosis,

inhibits lipid peroxidation accumulation and protects cells from ferroptosis by increasing cysteine availability and facilitating GSH synthesis.²⁹

Recent studies have begun exploring ferroptosis-related regulatory mechanisms in PCOS using both cell and animal models. For example, PPAR- α has been shown to inhibit ferroptosis in GCs by interacting with FADS2, reducing MDA levels, and increasing GSH and GPX4 expression.²³ miR-93-5p has been identified as a potential target in PCOS, as it can promote apoptosis and ferroptosis in GCs.^{30,31} However, to date, no studies have specifically examined the role of MALAT1 in ferroptosis regulation within the context of PCOS. In this study, we demonstrated that downregulation of MALAT1 in KGN cells reduces GSH, GPX4 and SLC7A11 levels, thereby promoting ferroptosis. This reveals a previously uncharacterized ferroptosis-related function of MALAT1 in the pathophysiology of PCOS in vitro. Furthermore, our research builds on previous findings by elucidating a novel MALAT1/miR-155-5p/PAK2 regulatory axis in KGN cells, expanding the understanding of MALAT1's role as a competing

endogenous RNA (ceRNA). While the ceRNA function of MALAT1 has been established in various biological contexts, e.g., sponging miR-211-5p to regulate FOXO3 in H₂O₂-induced GCs,³² regulating the MALAT1/miR-212-5p/MyD88 axis in osteoarthritis,³³ and controlling the MALAT1/miR-216a-5p/FOXA1 pathway in prostate cancer,³⁴ our study is the first to report MALAT1's modulation of miR-155-5p and its downstream effects on PAK2 in KGN cells.

Previous studies have shown that miR-155-5p is differentially expressed in follicular fluid exosomes from PCOS patients and is involved in glycolysis-related pathways in KGN cells, potentially influencing cell proliferation and apoptosis.²⁰ Additionally, *PAK2* has been shown to upregulate PKM2, a key glycolysis indicator, thereby mediating cell proliferation.³⁰ In the context of PCOS, *PAK2* has been implicated in regulating KGN cell apoptosis and proliferation via the β -catenin/c-Myc/PKM2 signaling pathway.^{19,35} *PAK2* regulates glycolytic processes and cell proliferation through the β -catenin/c-Myc/PKM2 signaling pathway in PCOS, underscoring the importance of altered glucose metabolism in the pathological mechanisms driving PCOS development.

Limitations

This study has several limitations. Obtained in vitro, our findings may not fully capture the complex conditions within the ovary environment in vivo, limiting their direct applicability to PCOS. Additionally, while we examined apoptosis and ferroptosis, other cell death pathways, such as autophagy, might also play roles in GC dysfunction. Lastly, the absence of clinical validation means the relevance of MALAT1 as a therapeutic target remains uncertain. Future studies should use in vivo models and patient samples to confirm these results.

Conclusions

This study reveals that MALAT1 regulates apoptosis and ferroptosis in KGN cells through the miR-155-5p/*PAK2* pathway, providing new insights into GC dysfunction in PCOS. Our findings highlight MALAT1 as a potential therapeutic target, suggesting that targeting the MALAT1/miR-155-5p/*PAK2* axis could mitigate cellular damage in PCOS. Further research in animal models and clinical settings is needed to validate these findings and explore MALAT1's potential as a treatment target.

Supplementary data

The supplementary materials are available at <https://doi.org/10.5281/zenodo.14872220>. The package includes the following files:

Supplementary Table 1. Mann–Whitney U test results.

Supplementary Table 2. Results of Kruskal–Wallis test with Dunn's post hoc test.

Data availability

The datasets generated and/or analyzed during the current study are available from the corresponding author on reasonable request.





Consent for publication

Not applicable.

Use of AI and AI-assisted technologies

Not applicable.

ORCID iDs

Yun Yang  <https://orcid.org/0009-0002-6763-0958>
 Dan Li  <https://orcid.org/0009-0008-2403-4746>
 Lu Sun  <https://orcid.org/0009-0008-5956-2063>
 Shasha Liu  <https://orcid.org/0000-0001-6516-7168>

References

- Wang Z, Jukic AMZ, Baird DD, et al. Irregular cycles, ovulatory disorders, and cardiometabolic conditions in a US-based digital cohort. *JAMA Netw Open*. 2024;7(5):e249657. doi:10.1001/jamanetworkopen.2024.9657
- Teede HJ, Tay CT, Laven JJE, et al. Recommendations from the 2023 International Evidence-based Guideline for the Assessment and Management of Polycystic Ovary Syndrome. *J Clin Endocrinol Metab*. 2023;108(10):2447–2469. doi:10.1210/clinem/dgad463
- Yang J, Chen C. Hormonal changes in PCOS. *J Endocrinol*. 2024;261(1):e230342. doi:10.1530/JOE-23-0342
- Joshi A. PCOS stratification for precision diagnostics and treatment. *Front Cell Dev Biol*. 2024;12:1358755. doi:10.3389/fcell.2024.1358755
- Hesampour A, Jafarabadi M, Rajabi S, Rezayof E, Nezamabadi AG. Dual oxidase 1, 2 gene expression in women with polycystic ovary syndrome (PCOS). *J Fam Reprod Health*. 2023;17(4):205–215. doi:10.18502/jfrh.v17i4.14592
- Zhou J, Liu F, Tian L, et al. Mutational analysis of minichromosome maintenance complex component (*MCM*) family genes in Chinese Han women with polycystic ovarian syndrome. *Gynecol Endocrinol*. 2023;39(1):2206912. doi:10.1080/09513590.2023.2206912
- Li X, Lin Y, Cheng X, et al. Ovarian ferroptosis induced by androgen is involved in pathogenesis of PCOS. *Hum Reprod Open*. 2024;2024(2):hoae013. doi:10.1093/hropen/hoae013
- Zhou Z, Zhang Y, Tan C, et al. The long non-coding RNA BBOX1 antisense RNA 1 is upregulated in polycystic ovary syndrome (PCOS) and suppresses the role of microRNA-19b in the proliferation of ovarian granulosa cells. *BMC Womens Health*. 2023;23(1):508. doi:10.1186/s12905-023-02632-5
- Li X, Zhu L, Luo Y. Long non-coding RNA HLA-F antisense RNA 1 inhibits the maturation of microRNA-613 in polycystic ovary syndrome to promote ovarian granulosa cell proliferation and inhibit cell apoptosis. *Bioengineered*. 2022;13(5):12289–12297. doi:10.1080/21655979.2022.2070965
- ElMonier AA, El-Boghdady NA, Fahim SA, Sabry D, Elsetohy KA, Shaheen AA. LncRNA NEAT1 and MALAT1 are involved in polycystic ovary syndrome pathogenesis by functioning as competing endogenous RNAs to control the expression of PCOS-related target genes. *Noncoding RNA Res*. 2023;8(2):263–271. doi:10.1016/j.ncrna.2023.02.008
- Li S, Li Y, Yan X, et al. MALAT1 expression in granulosa cells in PCOS patients with different phenotypes. *Sci Rep*. 2024;14(1):5019. doi:10.1038/s41598-024-55760-9

12. Zhang D, Tang HY, Tan L, Zhao DM. MALAT1 is involved in the pathophysiological process of PCOS by modulating TGF β signaling in granulosa cells. *Mol Cell Endocrinol.* 2020;499:110589. doi:10.1016/j.mce.2019.110589
13. Tu M, Wu Y, Wang F, et al. Effect of lncRNA MALAT1 on the granulosa cell proliferation and pregnancy outcome in patients with PCOS. *Front Endocrinol (Lausanne).* 2022;13:825431. doi:10.3389/fendo.2022.825431
14. Chen Y, Chen Y, Cui X, He Q, Li H. Down-regulation of MALAT1 aggravates polycystic ovary syndrome by regulating MiR-302d-3p-mediated leukemia inhibitory factor activity. *Life Sci.* 2021;277:119076. doi:10.1016/j.lfs.2021.119076
15. Li Y, Xiang Y, Song Y, Zhang D, Tan L. MALAT1 downregulation is associated with polycystic ovary syndrome via binding with MDM2 and repressing P53 degradation. *Mol Cell Endocrinol.* 2022;543:111528. doi:10.1016/j.mce.2021.111528
16. Peiyin F, Yuxian W, Jiali Z, Jian X. Research progress of ferroptosis in female infertility. *J Ovarian Res.* 2024;17(1):183. doi:10.1186/s13048-024-01508-y
17. Wang M, Zhang BQ, Ma S, et al. Broadening horizons: The role of ferroptosis in polycystic ovary syndrome. *Front Endocrinol (Lausanne).* 2024;15:1390013. doi:10.3389/fendo.2024.1390013
18. Li YY, Peng YQ, Yang YX, et al. Baicalein improves the symptoms of polycystic ovary syndrome by mitigating oxidative stress and ferroptosis in the ovary and gravid placenta. *Phytomedicine.* 2024;128:155423. doi:10.1016/j.phymed.2024.155423
19. Hui M, Hu S, Ye L, Zhang M, Jing X, Hong Y. PAK2/beta-catenin/c-Myc/PKM2 signal transduction suppresses ovarian granulosa cell apoptosis in polycystic ovary syndrome. *Biochem Biophys Res Commun.* 2023;677:54–62. doi:10.1016/j.bbrc.2023.08.004
20. Cao J, Huo P, Cui K, et al. Follicular fluid-derived exosomal miR-143-3p/miR-155-5p regulate follicular dysplasia by modulating glycolysis in granulosa cells in polycystic ovary syndrome. *Cell Commun Signal.* 2022;20(1):61. doi:10.1186/s12964-022-00876-6
21. Yao YY, Wang B, Jiang Y, Guo H, Li Y. The mechanisms crosstalk and therapeutic opportunities between ferroptosis and ovary diseases. *Front Endocrinol (Lausanne).* 2023;14:1194089. doi:10.3389/fendo.2023.1194089
22. Escobar-Morreale HF. Polycystic ovary syndrome: Definition, aetiology, diagnosis and treatment. *Nat Rev Endocrinol.* 2018;14(5):270–284. doi:10.1038/nrendo.2018.24
23. Liu Y, Ni F, Huang J, et al. PPAR- α inhibits DHEA-induced ferroptosis in granulosa cells through upregulation of FADS2. *Biochem Biophys Res Commun.* 2024;715:150005. doi:10.1016/j.bbrc.2024.150005
24. Liang Z, Wu Q, Wang H, et al. Silencing of lncRNA MALAT1 facilitates erastin-induced ferroptosis in endometriosis through miR-145-5p/MUC1 signaling. *Cell Death Discov.* 2022;8(1):190. doi:10.1038/s41420-022-00975-w
25. Huang J, Fan H, Li C, et al. Dysregulation of ferroptosis-related genes in granulosa cells associates with impaired oocyte quality in polycystic ovary syndrome. *Front Endocrinol (Lausanne).* 2024;15:1346842. doi:10.3389/fendo.2024.1346842
26. Ni Z, Li Y, Song D, et al. Iron-overloaded follicular fluid increases the risk of endometriosis-related infertility by triggering granulosa cell ferroptosis and oocyte dysmaturity. *Cell Death Dis.* 2022;13(7):579. doi:10.1038/s41419-022-05037-8
27. Forcina GC, Dixon SJ. GPX4 at the crossroads of lipid homeostasis and ferroptosis. *Proteomics.* 2019;19(18):1800311. doi:10.1002/pmic.201800311
28. Sun Y, Chen P, Zhai B, et al. The emerging role of ferroptosis in inflammation. *Biomed Pharmacother.* 2020;127:110108. doi:10.1016/j.biopha.2020.110108
29. Ye Z, Liu W, Zhuo Q, et al. Ferroptosis: Final destination for cancer? *Cell Prolif.* 2020;53(3):e12761. doi:10.1111/cpr.12761
30. Gupta A, Ajith A, Singh S, Panday RK, Samaiya A, Shukla S. PAK2-c-Myc-PKM2 axis plays an essential role in head and neck oncogenesis via regulating Warburg effect. *Cell Death Dis.* 2018;9(8):825. doi:10.1038/s41419-018-0887-0
31. Tan W, Dai F, Yang D, et al. MiR-93-5p promotes granulosa cell apoptosis and ferroptosis by the NF- κ B signaling pathway in polycystic ovary syndrome. *Front Immunol.* 2022;13:967151. doi:10.3389/fimmu.2022.967151
32. Zhang M, Xing J, Zhao S, et al. Exosomal YB-1 facilitates ovarian restoration by MALAT1/miR-211-5p/FOXO3 axis. *Cell Biol Toxicol.* 2024;40(1):29. doi:10.1007/s10565-024-09871-8
33. Gao Z, Guo C, Xiang S, Zhang H, Wang Y, Xu H. Suppression of MALAT1 promotes human synovial mesenchymal stem cells enhance chondrogenic differentiation and prevent osteoarthritis of the knee in a rat model via regulating miR-212-5p/MyD88 axis. *Cell Tissue Res.* 2024;395(3):251–260. doi:10.1007/s00441-024-03863-0
34. Zeng F, Li D, Kang X, et al. MALAT1 promotes FOXA1 degradation by competitively binding to miR-216a-5p and enhancing neuroendocrine differentiation in prostate cancer. *Transl Oncol.* 2024;39:101807. doi:10.1016/j.tranon.2023.101807
35. Liang A, Zhang W, Wang Q, et al. Resveratrol regulates insulin resistance to improve the glycolytic pathway by activating SIRT2 in PCOS granulosa cells. *Front Nutr.* 2023;9:1019562. doi:10.3389/fnut.2022.1019562

YOLO algorithm improves diagnostic performance of mammography: More than eyes

Heng Zhang^{1,B,C}, Xiao Yang^{2,D}, Leilei Yuan^{3,E}, Haibo Zhao^{3,E}, Pei Jiang^{4,E,F}, Qing-Qing Yu^{5,E,F}

¹ Department of Radiology, Jining No. 1 People's Hospital, China

² Department of Anesthesiology, Affiliated Hospital of Jining Medical University, China

³ Department of Oncology, Jining No. 1 People's Hospital, China

⁴ Translational Pharmaceutical Laboratory, Jining No. 1 People's Hospital, China

⁵ Clinical Research Center, Jining No. 1 People's Hospital, China

A – research concept and design; B – collection and/or assembly of data; C – data analysis and interpretation;

D – writing the article; E – critical revision of the article; F – final approval of the article

Advances in Clinical and Experimental Medicine, ISSN 1899–5276 (print), ISSN 2451–2680 (online)

Adv Clin Exp Med. 2025;34(12):2067–2075

Address for correspondence

Qing-Qing Yu

E-mail: yuqingqing_lucky@163.com

Funding sources

This study was supported by the Key R&D Program of Jining (grant No. 2023YXNS051) and the Medicine and Health Care Science and Technology Development Plan Projects Foundation of Shandong Province (grant No. 202301060260).

Conflict of interest

None declared

Received on June 29, 2024

Reviewed on March 7, 2025

Accepted on March 14, 2025

Published online on November 6, 2025

Abstract

Background. Breast cancer (BC) is now the most common malignancy in women. Early detection and precise diagnosis are essential for improving survival.

Objectives. To develop an integrated computer-aided diagnosis (CAD) system that automatically detects, segments and classifies lesions in mammographic images, thereby aiding BC diagnosis.

Materials and methods. We adopted YOLOv5 as the object-detection backbone and used the Curated Breast Imaging Subset of the Digital Database for Screening Mammography (CBIS-DDSM). Data augmentation (random rotations, crops and flips) increased the dataset to 5,801 images, which were randomly split into training, validation and test sets (7 : 2 : 1). Lesion-classification performance was evaluated with the area under the receiver operating characteristic (ROC) curve (AUC), precision, recall, and mean average precision at a 0.5 confidence threshold (mAP@0.5).

Results. The CAD system yielded an mAP@0.5 of 0.417 and an F1-score of 0.46 for lesion detection, achieved an AUC of 0.90 for distinguishing benign from malignant lesions, and processed images at 65 fps.

Conclusions. The integrated CAD system combines rapid detection and classification with high accuracy, underscoring its strong clinical value.

Key words: machine learning, mammography, diagnosis, breast cancer

Cite as

Zhang H, Yang X, Yuan L, Zhao H, Jiang P, Yu QQ. YOLO algorithm improves diagnostic performance of mammography: More than eyes. *Adv Clin Exp Med.* 2025;34(12):2067–2075. doi:10.17219/acem/202947

DOI

10.17219/acem/202947

Copyright

Copyright by Author(s)

This is an article distributed under the terms of the Creative Commons Attribution 3.0 Unported (CC BY 3.0) (<https://creativecommons.org/licenses/by/3.0/>)

Highlights

- YOLOv5-powered, end-to-end system delivers real-time lesion detection, precise segmentation and malignancy classification in a single pipeline.
- Malignancy classifier posts an area under the curve (AUC) of 0.90 on the independent test set, underscoring strong diagnostic accuracy.
- Precision–recall and F1 curves verify high object-detection performance across a broad spectrum of lesion types.
- Sub-second inference pairs high accuracy with fast processing, making the platform ideal for clinical computer-aided diagnosis.

Background

According to the latest statistics from the World Health Organization (WHO), the number of new breast cancer (BC) cases worldwide has surpassed that of lung cancer, making BC the most prevalent cancer among women and accounting for nearly 15% of female cancer-related deaths in 2020.¹ The etiology of BC encompasses genetic predispositions, environmental exposures and behavioral factors such as reproductive history and lifestyle choices. Early detection and accurate diagnosis are critical for effective treatment and personalized therapeutic strategies.² Breast cancer diagnosis can be classified into invasive and noninvasive approaches. To minimize unnecessary biopsies and reduce patient harm, low-risk imaging modalities such as mammography, breast ultrasound and breast magnetic resonance imaging (MRI) are preferred.³ While breast ultrasound demonstrates high sensitivity for soft tissue masses, it struggles to precisely delineate the margins of small lesions and detect morphological changes in microcalcifications, requiring substantial operator expertise. Although breast MRI provides high-resolution images, its high cost and lengthy examination time limit its utility as a routine screening tool. In contrast, mammography offers advantages such as affordability, rapid examination times and sensitivity in detecting breast masses and calcifications, enabling early identification of small tumors. It is currently recognized as one of the primary early screening methods for BC.⁴ The American Cancer Society (ACS) recommends annual mammographic screening for women aged 45 and older, transitioning to biennial screening at age 55 and beyond.⁵ Despite its advantages, accurate diagnosis with digital mammography is hindered by the lesions' irregular shapes and their subtle density differences from surrounding normal tissue. Moreover, manual review of mammographic images is labor-intensive, time-consuming, and prone to variability based on the professional expertise of different radiologists, potentially leading to misdiagnoses. Studies indicate that approx. 10–30% of BC cases are overlooked during mammography, with miss rates reaching up to 50% depending on lesion type and breast density.⁶ Another study revealed that approx. 50% of prior mammograms could retrospectively identify lesions upon follow-up and diagnosis.⁷

To alleviate the workload of radiologists, enhance screening efficiency and minimize missed or incorrect diagnoses caused by subjective factors, computer-aided diagnostic (CAD) systems have emerged as essential auxiliary tools for radiologists. These systems integrate medical imaging with computer vision techniques to assist in the early detection and precise treatment of breast lesions. Early CAD technologies relied on large-scale data analysis and training based on patients' pathological features, constructing detection and recognition models through statistical inference. However, the diagnostic accuracy of these methods was relatively limited. In recent years, with advancements in technology, numerous studies have incorporated the concept of neural networks into CAD systems, introducing deep learning – a multi-layer neural network-based approach for model training.⁸ Deep learning models possess the capability to directly extract high-level image features from raw input images. Several studies^{9–11} have developed CAD systems tailored for breast lesion detection, segmentation or classification, achieving remarkable success in identifying and categorizing lesions in mammographic images. The models commonly referenced in the literature are predominantly variations of Convolutional Neural Networks (CNNs), such as Region-based Convolutional Neural Networks (R-CNN), Fast R-CNN and Faster R-CNN.¹²

However, these models often struggle to detect small lesions and exhibit limited real-time detection speed, which fails to meet clinical requirements. Rapid detection and accurate classification of lesions in medical images remain a pressing issue that require immediate attention in current research. In 2016, Redmon et al.¹³ introduced the initial version of the You Only Look Once (YOLO) object detection model, and in June 2020, the You Only Look Once v. 5 (YOLOv5) model was released. The YOLO model is categorized as a 1-stage object detection algorithm, which completes recognition in a single pass, contrasting with the 2-stage detection models. YOLOv5 is currently recognized as one of the fastest image recognition algorithms in the field of artificial intelligence (AI) and has been extensively studied in industrial applications.¹⁴ However, its application in the medical field remains relatively underexplored.

Objectives

The aim of our study is to develop an integrated CAD system that incorporates lesion detection, segmentation and classification using the YOLOv5 model. This model performs both detection and classification tasks simultaneously, features low memory requirements and offers fast processing speed, thereby facilitating the clinical application of CAD systems.

Materials and methods

Study design

Considering that the classification problem is generally easier than the object detection problem, we first designed a high-accuracy classification model to directly infer whether the lesion in the image is benign or malignant, and then developed an auxiliary object detection model to provide detailed localization of benign and/or malignant areas within the image. The YOLOv5 model was selected as the base framework due to its efficient architecture and strong performance in object detection tasks. It uses a single neural network to perform both object detection and classification, making it faster and more efficient compared to previous versions of YOLO.

In this study, we utilized the Curated Breast Imaging Subset of the Digital Database for Screening Mammography (CBIS-DDSM) (<https://www.cancerimagingarchive.net/collection/cbis-ddsm>) as our dataset. This dataset represents an updated and standardized version of the DDSM dataset. The DDSM dataset comprises digital mammograms from 2,620 patients, collected across 4 institutions in the USA. It includes images of both left and right breasts, categorized into 4 classes: normal, benign, malignant, and other. Additionally, the dataset provides metadata such as patient age, breast density and lesion type. The CBIS-DDSM collection consists of a curated subset of DDSM data selected by a trained mammographer. The images have been decompressed and converted to the DICOM format. Updated region-of-interest (ROI) segmentations, bounding boxes and pathologic diagnoses for the training data were also included. For this research, we employed the CBIS-DDSM database, which encompasses 1,644 examinations from 1,566 individuals, with 891 cases involving masses and 753 related to calcifications.¹⁵ In our study, we focused exclusively on mammograms with confirmed masses. Among the 891 examinations associated with masses, the majority provided 2 distinct views: the mediolateral oblique (MLO) and the craniocaudal (CC). By incorporating both viewing angles, the total number of mammographic images increased to 1,592.

To implement our method, we first needed to convert the original data format into the form required by YOLO. This involved 3 components: the detection image,

the corresponding object bounding box and the image label. Subsequently, the dataset was divided into 3 parts: the training set, validation set and testing set. The next step involved training the classification and object detection models using the training set data. The validation set data were utilized to select the model with the best performance. Finally, the testing dataset was used to generate the final results. By leveraging our classification and object detection models, breast surgeons can better interpret patient symptoms.

Data preprocess and setting

The CBIS-DDSM dataset was selected as the dataset for the tumor detection model due to its substantial sample size, encompassing both benign and malignant cases of mammograms. However, the original structure of the dataset is complex, with multiple nested folders containing DICOM files for each mammogram and associated tumors. These files are named inconsistently, making it challenging to logically group data based on individual mammograms and their corresponding ROIs. To address this issue, a batch sequential architecture was employed to preprocess the CBIS-DDSM data into a usable format. A metadata file containing relevant information, such as filenames and local file paths, was generated and subsequently used to create a single CSV file for training, testing and validation purposes. The resulting dataset provides all the necessary information for developing a model while simplifying the file structure. Generally, the accuracy of a deep learning model improves with an increase in the number of training samples.

After creating the new data structure, we proceeded to process the data itself. The mammograms in the CBIS-DDSM dataset contain visual noise, such as annotations and tape marks, introduced during the original sampling process. Additionally, the mammograms include large areas of background, which can unnecessarily extend processing time. To improve the quality of the mammograms, we removed unwanted noise using morphological opening and cropped the images around the breast region to eliminate excess background. Furthermore, the mammograms were enhanced to improve the contrast between intense tumor areas and subtle background tissue. Contrast Limited Adaptive Histogram Equalization (CLAHE) was employed to enhance image contrast. This well-established image processing algorithm has proven effective in improving mammogram detection performance.¹⁶ The bounding box coordinates for each tumor in the mammograms were calculated based on the provided ground truth masks.

Generally speaking, providing a larger number of samples to a deep learning model tends to improve its accuracy. However, this relationship is not always strictly linear due to factors such as data quality and model complexity. To prevent overfitting and enhance network performance,

the training images were subjected to data augmentation techniques. Specifically, we augmented the dataset by applying random rotation, random cropping and random flipping. As a result, the total number of samples was increased to 5,801.

Statistical methods and model construction

The classification model and the object detection model in our method share similarities, as both are based on YOLOv5. The network structure of the YOLOv5 classification model is described as follows:

Input layers: The YOLOv5 classification model accepts an image of fixed size as input. The input image undergoes preprocessing and normalization to meet the model's requirements.

Backbone network: The backbone network of YOLOv5 is a CNN designed to extract features from the input image. It consists of several blocks, each containing multiple convolutional layers with batch normalization and activation functions.

Neck: The neck component of YOLOv5 aggregates features extracted by the backbone network across different layers. It comprises multiple upsampling and concatenation operations, which merge features from different scales to enhance multi-scale representation.

Classification head: The classification head of YOLOv5 includes fully connected layers that take the aggregated

features from the neck as input. This head performs the classification task by predicting the probability of the input image belonging to each class.

Output layers: The output layers of YOLOv5 generate the final classification results. These layers apply post-processing operations such as softmax to convert the output scores into probabilities, thereby producing the final class prediction.

Figure 1 presents an overview of the network architecture and components of the YOLOv5 model, clearly illustrating its processing pipeline and utilized modules. The BottleneckCSP module embodies the residual structure of the network, enabling the extraction of deep semantic information from images and integrating feature maps across different scales to enhance network depth. Additionally, the YOLOv5 model incorporates a simplified version of the BottleneckCSP (False) module, which consists of 2 concatenated convolutional layers. The spatial pyramid pooling (SPP) module performs spatial pyramid pooling, involving convolutional operations both before and after the module. At its core, the SPP layer includes 4 branches: 3 branches perform max-pooling operations with kernel sizes of 5×5 , 9×9 and 13×13 , while 1 branch bypasses pooling entirely. The outputs from these 4 branches are concatenated via the Concat module and then passed through a convolutional layer to produce the final output. This design enables the SPP module to extract critical contextual features without compromising the model's speed. In the YOLOv5

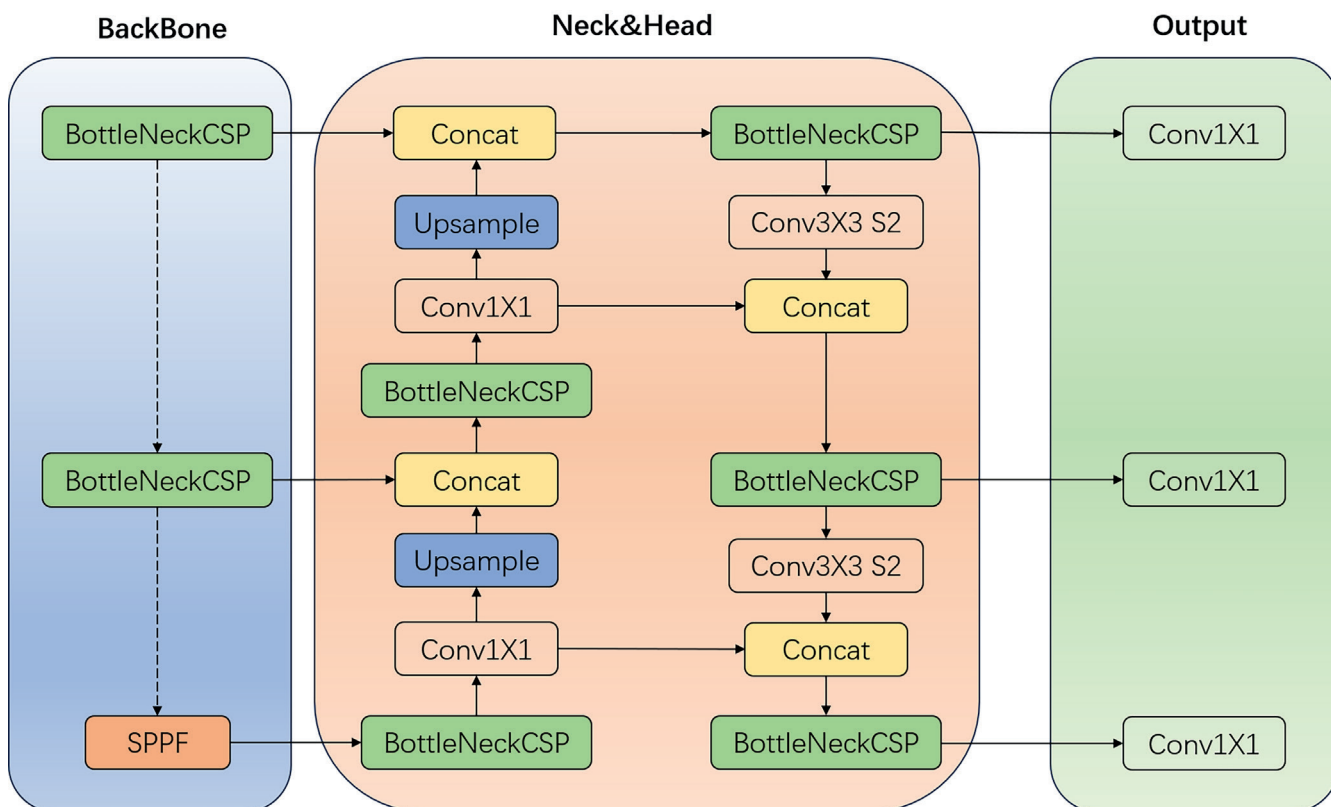


Fig. 1. Overview of the network architecture and key components of the YOLOv5 model

network, the path-aggregation network (PANet) module serves as the header, incorporating 2 upsampling stages followed by 2 downsampling stages post-convolution. This sampling mechanism facilitates the fusion of feature values at various scales, thereby enriching the feature information.

Experiment

The classification and object detection tasks have distinct evaluation measures. In the medical field, classification evaluation often employs the area under the curve (AUC), a widely used metric in machine learning for assessing the performance of binary classification models. Area under the curve quantifies the model's ability to distinguish between positive and negative classes across various classification thresholds.

In a binary classification problem, the model outputs a probability score for each sample, representing the likelihood of it belonging to the positive class. By adjusting the classification threshold (i.e., the cut-off probability score above which a sample is classified as positive), the model can generate different combinations of true positive and false positive rates.

The AUC is computed by determining the area under the receiver operating characteristic (ROC) curve, which plots the true positive rate (on the y-axis) against the false positive rate (on the x-axis) at various classification thresholds. The AUC value ranges from 0 to 1, with higher values indicating superior model performance.

Object-detection models are typically assessed with 4 key metrics: precision (Pr), recall (Rc), mean average precision (mAP), and intersection over union (IoU).

Precision: Precision measures the proportion of true positive detections among all positive predictions. In other words, it indicates the fraction of predicted detections that are actually correct. Precision is calculated as:

$$Pr = TP / (TP + FP).$$

Recall: Recall measures the proportion of true positive detections among all actual positive instances in the dataset. In other words, it indicates the fraction of actual objects that were correctly detected. Recall is calculated as:

$$Rc = TP / (TP + FN).$$

Mean average precision (mAP) is a widely adopted evaluation metric for object detection models, accounting for both precision and recall across various confidence thresholds. Essentially, it quantifies the average precision achieved by a model at different recall levels. A higher mAP score signifies superior performance. It is computed by determining the area under the precision–recall curve. mAP is calculated as:

$$mAP = \frac{1}{N} \sum_{i=1}^n AP_i$$

Results

The YOLOv5-based integrated CAD system we developed for automatic detection, segmentation and classification of breast X-ray masses demonstrates outstanding performance. In the mass-classification task, the system achieves an AUC of 0.90, underscoring its strong ability to distinguish among different mass types (Fig. 2A). The confusion matrix is a critical tool for evaluating classification model performance, enabling us to identify areas where the model struggles with predictions. Each column of the matrix corresponds to an actual category, while each row represents a predicted category. As illustrated in Fig. 2B, the horizontal axis denotes “True” categories, and the vertical axis denotes “Predicted” categories. In this matrix, the values within each cell represent normalized probabilities rather than absolute counts, as column-wise normalization has been applied to transform the raw

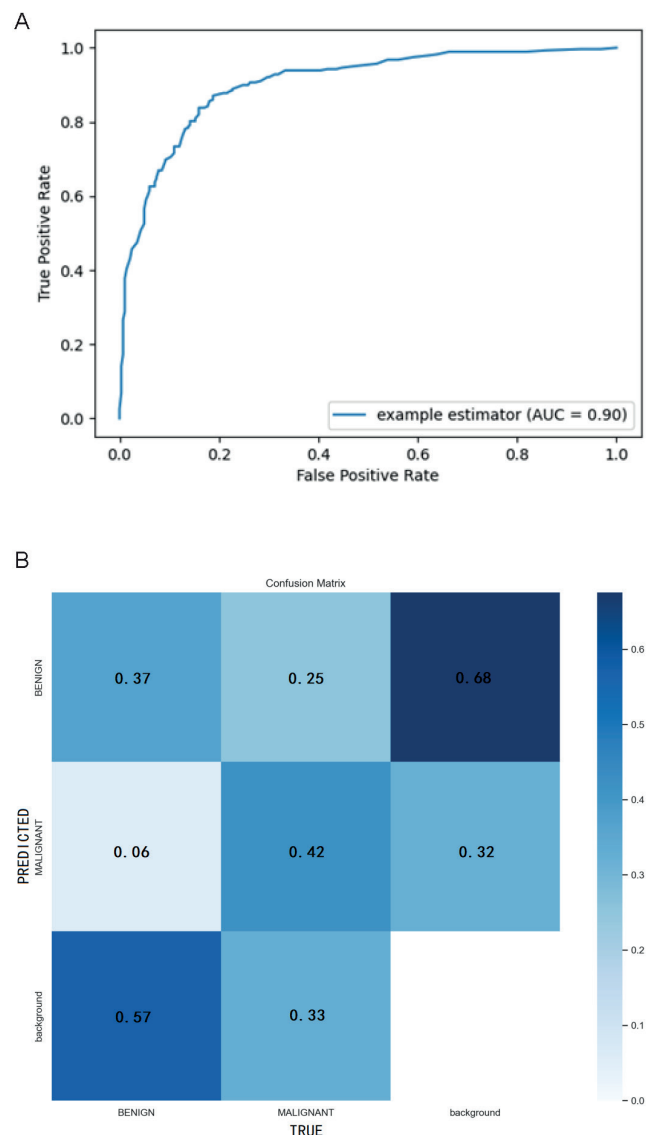


Fig. 2. Area under the curve (AUC) and confusion matrix results for computer-aided diagnostic (CAD) based on YOLOv5. A. Classification AUC plot; B. Object detection confusion matrix

counts into predicted probabilities. These normalized results are automatically generated by the YOLOv5 model during the prediction process. For benign lesions, the Rc is calculated as $0.37/(0.37 + 0.06 + 0.57) = 0.37$, while for malignant lesions, the Rc is $0.42/(0.42 + 0.25 + 0.33) = 0.42$. Notably, the diagonal values of the confusion matrix correspond to the Rc for each category. As evident from the data, the Rc for malignant lesions (0.42) is higher than that for benign lesions (0.37).

In terms of object detection, we employ the F1 curve, precision–confidence curve and precision–recall curve to evaluate the system's performance. The F1 curve in Fig. 3A represents the harmonic mean of precision and recall, providing a comprehensive reflection of the detection system's performance. As shown in Fig. 3A, the F1 score reaches its peak value of 0.46 at a confidence threshold of 0.520. Consequently, this value can be regarded as the optimal confidence threshold. The precision–confidence curve in Fig. 3B depicts the relationship between precision and confidence. Higher precision indicates a greater proportion of true positive samples among those predicted as positive by the model. By analyzing the precision (P) curve, we can assess the model's accuracy across various confidence thresholds. It is evident that as the confidence level increases, the detection accuracy also improves correspondingly. Additionally, the precision–recall curve in Fig. 3C serves as a visual tool to illustrate the trade-off between precision and recall for the classification model. By plotting the precision–recall curve, we can evaluate and compare the model's performance under different classification thresholds and calculate the mAP to measure overall performance. Here, mAP@0.5 denotes the average mAP value when the Intersection over Union (IoU) threshold equals 0.5. As depicted in Fig. 3C, the mAP@0.5 value of our object detection model is 0.417, indicating that the model performs well.

To visually demonstrate the performance of the CAD system, Fig. 4 presents a comparison between predicted results and actual results for several cases. From these comparison figures, it is evident that the CAD system successfully detected masses in most cases and classified them with high accuracy. These results strongly validate the high performance and practicality of our integrated CAD system for automatic detection, segmentation and classification of breast X-ray masses based on YOLOv5.

Discussion

In our study, the integrated CAD system demonstrated excellent performance in the detection, segmentation and classification of breast lesions. Indeed, breast lesion detection is the most critical task in any CAD system, as accurate identification of suspicious lesions significantly enhances diagnostic accuracy. In this study, the YOLOv5 deep learning model, a CNN-based region of interest (ROI) model, utilizes the features of the entire image to predict bounding

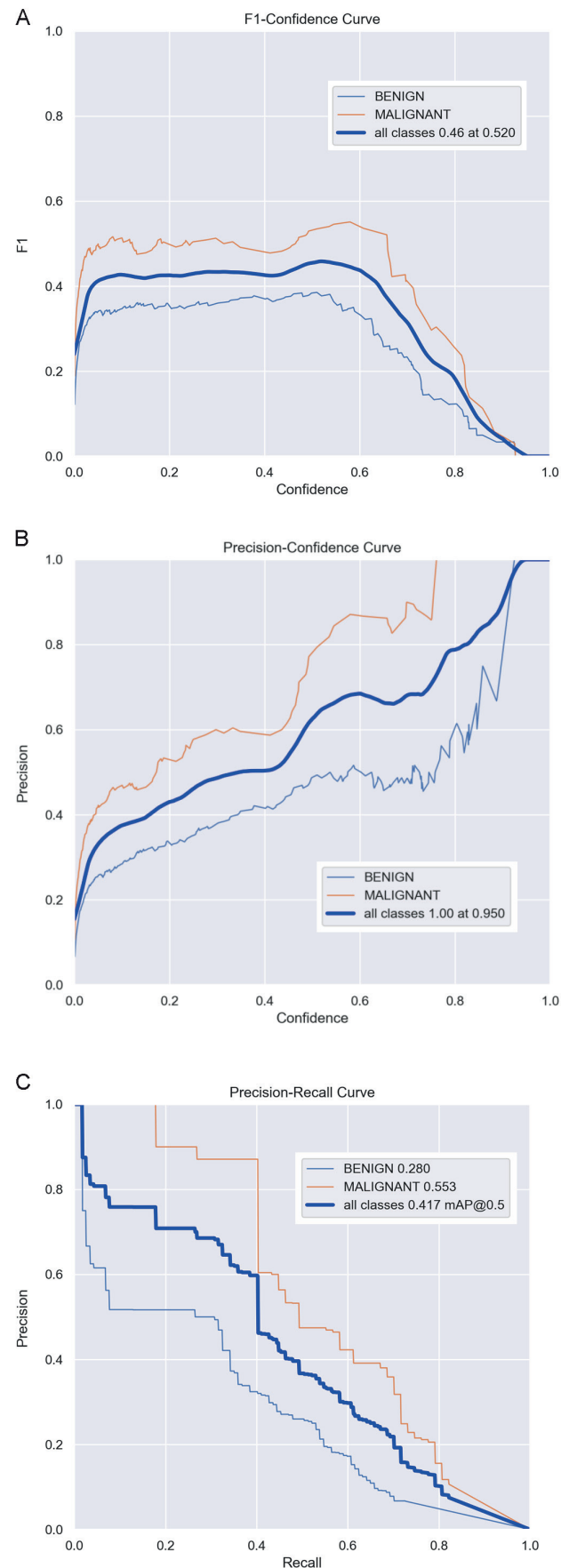


Fig. 3. Performance evaluation of computer-aided diagnostic (CAD) based on YOLOv5. A. F1 curve for object detection; B. Precision (P) curve for object detection; C. Precision-recall (PR) curve for object detection

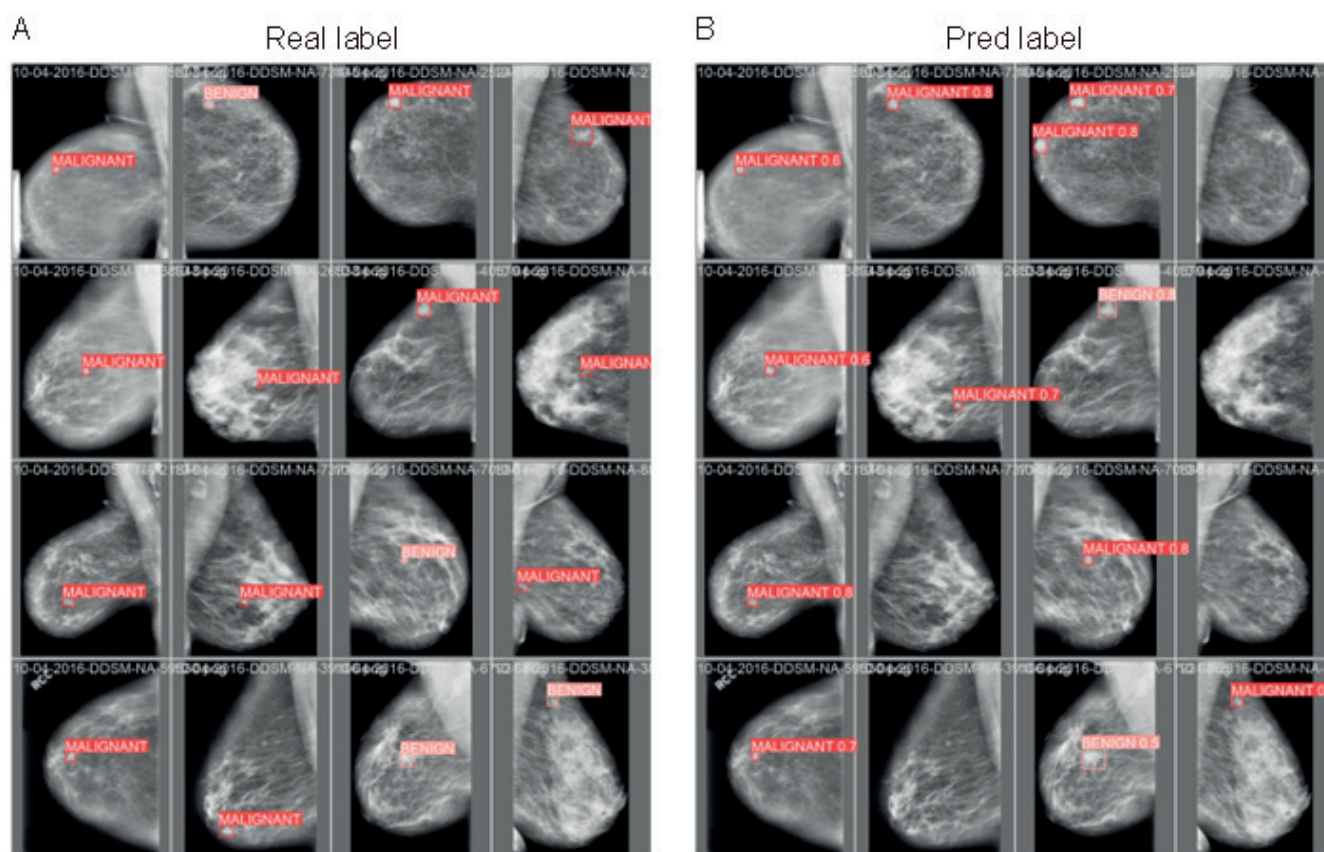


Fig. 4. Predicted results of case studies using YOLOv5. A. Ground truth labels for object detection; B. Predicted labels for object detection

boxes for all target classes, enabling end-to-end training and real-time inference while maintaining high average accuracy.¹⁴ The YOLOv5-based detection model has proven effective for breast lesion detection in the DDSM database, capable of directly detecting lesions and accurately anchoring bounding boxes within mammographic images. One study had shown that YOLO can handle challenging detection tasks, such as identifying lesions located within chest muscles or dense tissues.¹⁷ Compared to other models, the YOLO detection framework demonstrates a lower false positive rate and significantly reduced testing time and memory usage, making it more efficient than more complex deep learning architectures.¹⁸ End-to-end lesion detection and segmentation are essential for reducing false positives and negatives, thereby enhancing CAD system performance.

Breast lesion classification represents the final stage of a CAD system, where the primary objective is to classify breast lesions as either benign or malignant. Deep learning has become the most widely adopted technology for this task. Currently, various architectures of CNN models, along with stacked autoencoders, have been employed for the classification of benign and malignant lesions in mammographic images. Arevalo et al.¹⁹ utilized a CNN combined with a Support Vector Machine (SVM) classifier to classify breast masses in mammographic images, achieving an AUC of 0.86. In contrast, when manually extracted features were combined with an SVM classifier,

the AUC was only 0.799. This demonstrates that deep learning-based feature extraction methods, particularly those based on CNNs, significantly outperform traditional handcrafted feature extraction techniques, resulting in substantially improved classification performance. Ribli et al.²⁰ proposed a CAD system based on Faster R-CNN for the detection and classification of benign and malignant breast lesions. Their model was evaluated and tested using the INbreast database, achieving an overall classification accuracy of 95%. However, there have been relatively few studies exploring the application of YOLO in breast lesion classification. Our developed target classification model, based on YOLOv5, was trained, validated and tested on the CBIS-DDSM database, achieving an AUC value of 0.9 in the test set. This result confirms that YOLOv5 also exhibits excellent classification performance.

In recent years, several studies have developed integrated CAD systems based on deep learning that can simultaneously perform breast lesion detection, segmentation and classification. Kooi et al.²¹ developed a CAD system that integrates deep features with imaging features. This system first employs conditional random fields (CRF) for lesion detection, followed by region growing to segment the lesion boundary, and finally uses a CNN for breast lesion classification. The CAD system demonstrates excellent diagnostic performance, achieving an AUC of 0.941. Another study²² proposed an integrated CAD system for breast masses

that adopts a complex deep learning cascade structure for lesion detection and segmentation. It utilizes a standard feedforward CNN to classify breast lesions as benign or malignant, exhibiting strong diagnostic performance. Despite the success of these CAD systems in breast mass diagnosis, certain limitations remain, such as high storage requirements, long prediction times and challenges in meeting clinical application needs. Our integrated CAD diagnostic system, developed based on YOLOv5, achieves a mAP@0.5 of 0.417 in breast lesion detection, an AUC of 0.9 in breast lesion benign/malignant classification, and a processing speed of 65 fps. It is characterized by high detection accuracy and fast processing speed, making it suitable for clinical applications. YOLO's high recall across most categories can be attributed to its single-stage architecture, grid-based prediction mechanism, utilization of anchor boxes, balanced trade-offs between speed and accuracy, end-to-end training approach, extensive data augmentation techniques, and a carefully designed loss function. These features collectively enhance YOLO's ability to detect objects of various sizes, shapes and positions with high precision and recall. Notably, the YOLO algorithm has demonstrated high recall in the development and application of numerous tumor diagnosis models,^{23–25} which aligns closely with our research findings.

We applied YOLOv5, which demonstrates significant advancements in optimizing and streamlining neural network architectures. These improvements not only enhance the computational efficiency and real-time performance of models but also strengthen their robustness and generalization capabilities. Therefore, we did not further narrow down the neural network structures. In the evolution of the YOLO series of algorithms, optimizations and reductions in neural network architectures are primarily reflected in 3 key areas. First, efficiency improvements through layer reduction: Although the number of layers increased from YOLOv1 to YOLOv5 (e.g., Darknet-53 has more layers than Darknet-19²⁶), overall efficiency and real-time performance were significantly improved by adopting more efficient convolutional layers and feature extraction methods. Second, multi-scale prediction and feature fusion: Starting with YOLOv3 and continuing through YOLOv4, these versions introduced multi-scale prediction and feature fusion techniques, enhancing the model's ability to detect objects of varying sizes and improving detection accuracy.²⁷ Lastly, lightweight design: The YOLO series emphasizes maintaining model performance while reducing complexity and computational load through strategies such as using more efficient convolutional kernels and eliminating redundant layers.²⁸

Limitations

There are still some limitations in this study that warrant discussion. First, the CBIS-DDSM database used in this study comprises traditional film-based mammograms that were

digitized using a scanner. As a result, the images are subject to high noise levels and represent an incomplete spectrum of lesion types. Second, the YOLOv5 model employed in this study was published in 2022. In recent years, the YOLO series algorithms have undergone rapid development, with notable advancements such as YOLOX,²⁹ YOLOR,³⁰ PP-YOLO series,^{31–33} YOLOv6,³⁴ YOLOv7,³⁵ and YOLOv8.³⁶ Whether these newer models can achieve superior performance in BC detection and classification remains unexplored in this paper. Third, the training parameters of YOLOv5 were not fine-tuned in this study, which may limit the model's potential for further performance improvement.

Conclusions

This study developed an integrated CAD system based on YOLOv5, encompassing detection, segmentation and classification tasks, for the automatic diagnosis of breast lesions in mammographic images. The system demonstrates high diagnostic accuracy and fast processing speed. We conclude that the integrated CAD system holds significant potential for breast lesion diagnosis. In the future, the CAD system proposed in this study will undergo practical testing to validate its true effectiveness. Future practical validation will be required to confirm the CAD system's real-world clinical effectiveness.

Data Availability Statement

The datasets analyzed during the current study are available in the Curated Breast Imaging Subset of Digital Database for Screening Mammography (CBIS-DDSM), <https://www.mammoimage.org/databases>.

Consent for publication

Not applicable.

Use of AI and AI-assisted technologies

Not applicable.

ORCID iDs

Qing-Qing Yu  <https://orcid.org/0000-0001-5695-6747>

References

1. Sung H, Ferlay J, Siegel RL, et al. Global cancer statistics 2020: GLOBOCAN estimates of incidence and mortality worldwide for 36 cancers in 185 countries. *CA Cancer J Clin*. 2021;71(3):209–249. doi:10.3322/caac.21660
2. Siegel RL, Miller KD, Jemal A. Cancer statistics, 2017. *CA Cancer J Clin*. 2017;67(1):7–30. doi:10.3322/caac.21387
3. Alabousi M, Wadera A, Kashif Al-Ghita M, et al. Performance of digital breast tomosynthesis, synthetic mammography, and digital mammography in breast cancer screening: A systematic review and meta-analysis. *J Natl Cancer Inst*. 2021;113(6):680–690. doi:10.1093/jnci/djaa205

4. Duffy SW, Tabár L, Yen AMF, et al. Mammography screening reduces rates of advanced and fatal breast cancers: Results in 549,091 women. *Cancer*. 2020;126(13):2971–2979. doi:10.1002/cncr.32859
5. Jin J. Breast cancer screening guidelines in the United States. *JAMA*. 2015;314(15):1658. doi:10.1001/jama.2015.11766
6. Woodard DB, Gelfand AE, Barlow WE, Elmore JG. Performance assessment for radiologists interpreting screening mammography. *Stat Med*. 2007;26(7):1532–1551. doi:10.1002/sim.2633
7. Warren Burhenne LJ, Wood SA, D'Orsi CJ, et al. Potential contribution of computer-aided detection to the sensitivity of screening mammography. *Radiology*. 2000;215(2):554–562. doi:10.1148/radiology.215.2.r00ma15554
8. Chan HP, Samala RK, Hadjiiski LM, Zhou C. Deep learning in medical image analysis. *Adv Exp Med Biol*. 2020;1213:3–21. doi:10.1007/978-3-030-33128-3_1
9. Wimmer M, Sluiter G, Major D, et al. Multi-task fusion for improving mammography screening data classification. *IEEE Trans Med Imaging*. 2022;41(4):937–950. doi:10.1109/TMI.2021.3129068
10. Al-Antari MA, Al-Masni MA, Choi MT, Han SM, Kim TS. A fully integrated computer-aided diagnosis system for digital X-ray mammograms via deep learning detection, segmentation, and classification. *Int J Med Inform*. 2018;117:44–54. doi:10.1016/j.ijmedinf.2018.06.003
11. Shen L, Margolies LR, Rothstein JH, Fluder E, McBride R, Sieh W. Deep learning to improve breast cancer detection on screening mammography. *Sci Rep*. 2019;9(1):12495. doi:10.1038/s41598-019-48995-4
12. Latif J, Xiao C, Imran A, Tu S. Medical imaging using machine learning and deep learning algorithms: A review. In: *2019 2nd International Conference on Computing, Mathematics and Engineering Technologies (ICOMET)*. Sukkur, Pakistan: IEEE; 2019:1–5. doi:10.1109/ICOMET.2019.8673502
13. Redmon J, Divvala S, Girshick R, Farhadi A. You Only Look Once: Unified, real-time object detection. In: *2016 IEEE Conference on Computer Vision and Pattern Recognition (CVPR)*. Las Vegas, USA: IEEE; 2016: 779–788. doi:10.1109/CVPR.2016.91
14. Zhang R, Zhang L, Su Y, Yu Q, Bai G. Automatic vessel plate number recognition for surface unmanned vehicles with marine applications. *Front Neurorobot*. 2023;17:1131392. doi:10.3389/fnbot.2023.1131392
15. Lee RS, Gimenez F, Hoogi A, Miyake KK, Gorovoy M, Rubin DL. A curated mammography data set for use in computer-aided detection and diagnosis research. *Sci Data*. 2017;4:170177. doi:10.1038/sdata.2017.177
16. Pisano ED, Zong S, Hemminger BM, et al. Contrast limited adaptive histogram equalization image processing to improve the detection of simulated spiculations in dense mammograms. *J Digit Imaging*. 1998;11(4):193–200. doi:10.1007/BF03178082
17. Al-Masni MA, Al-Antari MA, Park JM, et al. Simultaneous detection and classification of breast masses in digital mammograms via a deep learning YOLO-based CAD system. *Comput Methods Programs Biomed*. 2018;157:85–94. doi:10.1016/j.cmpb.2018.01.017
18. Carneiro G, Nascimento J, Bradley AP. Automated analysis of unregistered multi-view mammograms with deep learning. *IEEE Trans Med Imaging*. 2017;36(11):2355–2365. doi:10.1109/TMI.2017.2751523
19. Arevalo J, González FA, Ramos-Pollán R, Oliveira JL, Guevara Lopez MA. Representation learning for mammography mass lesion classification with convolutional neural networks. *Comput Methods Programs Biomed*. 2016;127:248–257. doi:10.1016/j.cmpb.2015.12.014
20. Ribli D, Horváth A, Unger Z, Pollner P, Csabai I. Detecting and classifying lesions in mammograms with deep learning. *Sci Rep*. 2018; 8(1):4165. doi:10.1038/s41598-018-22437-z
21. Kooi T, Litjens G, van Ginneken B, et al. Large scale deep learning for computer aided detection of mammographic lesions. *Med Image Anal*. 2017;35:303–312. doi:10.1016/j.media.2016.07.007
22. Dhungel N, Carneiro G, Bradley AP. A deep learning approach for the analysis of masses in mammograms with minimal user intervention. *Med Image Anal*. 2017;37:114–128. doi:10.1016/j.media.2017.01.009
23. Huang J, Ding W, Zhong T, Yu G. YOLO-TumorNet: An innovative model for enhancing brain tumor detection performance. *Alexandria Eng J*. 2025;119:211–221. doi:10.1016/j.aej.2025.01.062
24. Chen A, Lin D, Gao Q. Enhancing brain tumor detection in MRI images using YOLO-NeuroBoost model. *Front Neurol*. 2024;15:1445882. doi:10.3389/fneur.2024.1445882
25. Jia X, Shkolyar E, Laurie MA, Eminaga O, Liao JC, Xing L. Tumor detection under cystoscopy with transformer-augmented deep learning algorithm. *Phys Med Biol*. 2023;68(16):10.1088/1361-6560/ace499. doi:10.1088/1361-6560/ace499
26. Uyar T, Uyar DS. Assessment of using transfer learning with different classifiers in hypodontia diagnosis. *BMC Oral Health*. 2025;25(1):68. doi:10.1186/s12903-025-05451-2
27. Kumar BC, Punitha R, Mohana. YOLOv3 and YOLOv4: Multiple object detection for surveillance applications. In: *2020 Third International Conference on Smart Systems and Inventive Technology (ICSSIT)*. Tirunelveli, India: IEEE; 2020:1316–1321. doi:10.1109/ICSSIT48917.2020.9214094
28. Ali ML, Zhang Z. The YOLO framework: A comprehensive review of evolution, applications, and benchmarks in object detection. *Computers*. 2024;13(12):336. doi:10.3390/computers13120336
29. Ge Z, Liu S, Wang F, Li Z, Sun J. YOLOX: Exceeding YOLO series in 2021 [posted online as a preprint August 6, 2021]. *arXiv*. 2021. doi:10.48550/ARXIV.2107.08430
30. Wang CY, Yeh IH, Liao HYM. You Only Learn One Representation: Unified network for multiple tasks [posted online as a preprint May 10, 2021]. *arXiv*. 2021. doi:10.48550/ARXIV.2105.04206
31. Long X, Deng K, Wang G, et al. PP-YOLO: An effective and efficient implementation of object detector [posted online as a preprint August 3, 2020]. *arXiv*. 2020. doi:10.48550/ARXIV.2007.12099
32. Huang X, Wang X, Lv W, et al. PP-YOLOv2: A practical object detector [posted online as a preprint April 21, 2021]. *arXiv*. 2021. doi:10.48550/ARXIV.2104.10419
33. Xu S, Wang X, Lv W, et al. PP-YOLOE: An evolved version of YOLO [posted online as a preprint December 12, 2022]. *arXiv*. 2022. doi:10.48550/ARXIV.2203.16250
34. Li C, Li L, Jiang H, et al. YOLOv6: A single-stage object detection framework for industrial applications [posted online as a preprint September 7, 2022]. *arXiv*. 2022. doi:10.48550/ARXIV.2209.02976
35. Wang CY, Bochkovskiy A, Liao HYM. YOLOv7: Trainable bag-of-freebies sets new state-of-the-art for real-time object detectors [posted online as a preprint July 6, 2022]. *arXiv*. 2022. doi:10.48550/ARXIV.2207.02696
36. Hussain M. YOLOv5, YOLOv8 and YOLOv10: The go-to detectors for real-time vision [posted online as a preprint July 3, 2024]. *arXiv*. 2024. doi:10.48550/ARXIV.2407.02988

Gender identity stories: Experiences and perspectives of transgender people about healthcare system in Spain

Antonio Martinez-Sabater^{1,2,A,B,F}, Elena Chover-Sierra^{1,3,A,E,F}, Pablo Del Pozo-Herce^{4,A,C,D},
Alberto Tovar-Reinoso^{4,C,D}, Natalia Cano-Ruiz^{1,A,B}, Marta Araujo-Blesa^{5,B,C}, Javier Curto-Ramos^{6,A,D},
Gustavo Mora-Navarro^{7,A,E}, Raquel Martínez-Pascual^{1,A,B}, Raúl Juárez-Vela^{8,E,F}, Eva García Carpintero-Blas^{4,B–D}

¹ Nursing Care and Education Research Group (GRIECE), Department of Nursing, University of Valencia, Spain

² Care Research Group (INCLIVA), University Clinical Hospital in Valencia, Spain

³ Department of Internal Medicine, Consortium General University Hospital of Valencia, Spain

⁴ Research Group on Innovation in Health Care and Nursing Education (INcUIdE), UNIE University, Madrid, Spain

⁵ Department of Health and Biomedical Sciences, Loyola Andalucía University, Sevilla, Spain

⁶ Department of Psychiatry, Clinical Psychology and Mental Health, La Paz University Hospital, Madrid, Spain

⁷ Health Technology Assessment Unit of Madrid, Madrid Health Service, Spain

⁸ Group of Research in Care (GRUPAC), Faculty of Health Sciences, University of La Rioja, Logroño, Spain

A – research concept and design; B – collection and/or assembly of data; C – data analysis and interpretation;

D – writing the article; E – critical revision of the article; F – final approval of the article

Advances in Clinical and Experimental Medicine, ISSN 1899–5276 (print), ISSN 2451–2680 (online)

Adv Clin Exp Med. 2025;34(12):2077–2089

Address for correspondence

Pablo Del Pozo-Herce

E-mail: pablo.delpozo@universidadunie.com

Funding sources

None declared

Conflict of interest

None declared

Acknowledgements

We would like to thank all the participants who contributed to this research.

Received on April 27, 2025

Reviewed on July 2, 2025

Accepted July, 10 2025

Published online on August 19, 2025

Cite as

Martinez-Sabater A, Chover-Sierra E, Del Pozo-Herce P, et al. Gender identity stories: Experiences and perspectives of transgender people about healthcare system in Spain.

Adv Clin Exp Med. 2025;34(12):2077–2089.

doi:10.17219/acem/208133

DOI

10.17219/acem/208133

Copyright

Copyright by Author(s)

This is an article distributed under the terms of the Creative Commons Attribution 3.0 Unported (CC BY 3.0) (<https://creativecommons.org/licenses/by/3.0/>)

Abstract

Background. Despite legal advances and the depathologization of transgender identities, transgender individuals still face significant barriers and discrimination within healthcare systems. A pervasive lack of training in gender diversity among healthcare professionals often results in uncomfortable, even hostile, clinical encounters, exacerbating physical and mental health vulnerabilities. Consequently, fear of stigma and discrimination leads many transgender people to avoid seeking care, placing their wellbeing at further risk due to delayed or foregone medical attention.

Objectives. To explore transgender individuals' perceptions of healthcare professionals' awareness and responsiveness to their care and support needs in the Valencian Community (Spain).

Materials and methods. We conducted a descriptive qualitative study with a phenomenological approach in the Valencian Community. Using convenience sampling, we recruited 14 participants. Data were collected between April and June 2022 via in-depth, semi-structured, open-ended interviews. The study comprised 2 sequential phases: An initial focus group session, followed by individual interviews conducted using a snowball sampling technique.

Results. We identified 3 thematic domains: T1: Experiences of professional care among transgender individuals; T2: Impact of cisgender-centric regulations within the healthcare system; T3: Gender diversity education needs for healthcare professionals.

Conclusions. The transformation of the health system is urgent to ensure inclusive and equitable care for transgender people. According to the interviews, they consider that better training of professionals will improve their care. In addition, they highlight the need to reduce bureaucratic barriers, create specific protocols, and improve access to specialized treatment. Implementing inclusive public policies will contribute to a fairer and more accessible system.

Key words: qualitative research, social determinants of health, transgender, health disparities, gender diversity

Highlights

- Transgender healthcare access in Spain remains restricted: Persistent barriers undermine respectful, equitable services despite progressive legal reforms.
- Healthcare provider gender diversity training gaps compromise care quality: Insufficient education on transgender issues leads to substandard patient experiences.
- Transphobic practices and pathologization persist in the health system: Stereotypes, discriminatory protocols, and the misclassification of trans identities continue to harm outcomes.
- Urgent need for targeted professional development and streamlined protocols: Calls for mandatory gender-diversity curricula, trans-specific clinical guidelines, and reduced bureaucratic hurdles.
- Inclusive public policies and safe care environments are critical: Implementing comprehensive equity-focused policies and fostering respectful clinical settings will enhance transgender health in Spain.

Background

Despite regulatory advances and the depathologization of transgender identities, transgender people continue to face barriers and gaps in access to adequate healthcare.^{1,2} Although the World Health Organization (WHO) eliminated “gender dysphoria” as a mental disorder in its International Classification of Diseases (ICD-11) in 2019, the reality of healthcare shows that transphobic practices and widespread ignorance on the part of healthcare personnel persist.³ The lack of training in sexual and gender diversity issues in health sciences careers translates into poor and sometimes disrespectful care towards this population.⁴

Stigma remains a fundamental barrier in the healthcare environment, where the perception of transgender people as “different” or “problematic” influences the treatment offered. According to reports from organizations such as Lambda and FELGTB (Federación Estatal de Lesbianas, Gays, Transexuales y Bisexuales), many transgender people are questioned about their identity or transition process during medical consultations, which generates an invasive and dehumanizing experience.⁵ In some cases, healthcare professionals refer to patients by their name assigned at birth (or “deadname”), completely ignoring their gender identity and generating an environment of vulnerability and mistreatment.^{6,7} These deficiencies profoundly impact the healthcare system.^{8,9} The lack of trained professionals to address the specific needs of transgender people, such as psychological accompaniment, hormone support, or care during the transition period, leads to insufficient and poorly informed care.^{10,11} From a healthcare approach perspective, addressing the needs of transgender individuals requires not only clinical competence but also an institutional commitment to equity.¹⁰ This involves the integration of inclusive care models that ensure continuity, accessibility, and person-centered services. An affirmative healthcare model recognizes gender diversity, avoids pathologization and fosters safe spaces where people can receive holistic care, including physical, emotional and social wellbeing, without fear of discrimination.¹¹ This situation affects both the quality

of healthcare and the confidence of transgender patients in the healthcare system, who often prefer to avoid medical consultations so as not to expose themselves to situations of discrimination or discomfort.¹² Low adherence to medical treatment becomes therefore a serious risk, as fear of mistreatment or misunderstanding leads to many health problems remaining undiagnosed or untreated.¹³

Given this reality, it would be a priority to design inclusive healthcare protocols and promote the training of healthcare professionals from a trans-inclusive perspective.^{2,13} Transgender people need to be cared for in a respectful and safe environment that recognizes their diversity without questioning or pathologizing them.¹⁴ For healthcare professionals, comprehensive training is essential to improve specific clinical knowledge and to foster attitudes that ensure dignified and empathetic treatment of sexual and gender diversity, including the proper use of inclusive language. It should also provide a basic understanding of the legislation regulating aspects of transgender health, such as Law 4/2023 of February 28, aimed at ensuring the accurate and effective equality of transgender people and safeguarding the rights of LGTBI+ individuals.¹⁵ These actions are essential to build a fairer and more respectful healthcare system capable of adequately serving everyone, regardless of gender identity.¹⁶

The impact of these shortcomings goes beyond the physical. Discrimination and stigma in health services generate a situation of vulnerability that has serious repercussions on the mental health of transgender people.¹⁷ Several studies have shown that constant exposure to transphobia in healthcare settings is related to an increased risk of developing disorders such as anxiety, depression and increased rates of suicide and self-harm.^{18,19} This reality is linked to the phenomenon known as “minority stress”, which refers to the psychological impact experienced by transgender people as a result of social exclusion, discrimination, and lack of support. In addition, fear of rejection, mistreatment, or misinformation from health professionals leads many transgender people to avoid seeking healthcare. This often results in delayed visits and postponed treatment.

This avoidance, motivated by previous experiences of discrimination or the perception that professionals are not prepared to care for them adequately, prevents early detection of diseases, access to crucial treatments⁵ and, in some cases, the recourse of these patients to unsafe centers or resources. In the long term, this reluctance to seek medical care results in a general deterioration of the person's health. It also increases the risk of untreated chronic diseases, complications such as infections, and severe mental health problems.^{20,21}

At the structural level, there are also barriers to access to specialized services and resources.²² Despite attempts by some autonomous communities to implement trans-inclusive protocols, many of these initiatives are insufficient or limited in scope. Transgender people sometimes have to travel long distances to access gender identity units or specialized services, which aggravates the precariousness of their care. Decentralization in the design and implementation of public health policies generates inequalities in the coverage and quality of services, depending on the territory where they reside. It is urgent to design inclusive healthcare protocols and promote the training of health professionals from a trans-inclusive perspective.²³ Transgender people need to be cared for in a respectful and safe environment that recognizes their identities without questioning or pathologizing them.²⁴ For healthcare professionals, comprehensive training is required, encompassing both specific medical knowledge and sensitization to ensure the dignified and empathetic treatment of sexual and gender diversity.²⁵ These actions are essential to build a fairer and more respectful healthcare system capable of adequately caring for all people, regardless of gender identity.

Objectives

To explore the perceptions of transgender people on the awareness of healthcare personnel concerning their care and accompaniment in the Valencian Community, Spain.

Materials and methods

Study design

A descriptive qualitative study with a phenomenological approach was conducted to explore and understand individual human experience within its specific context.²⁶ This study was based on the theory of relativism, which holds that all perspectives are personal and valid, and has been used previously in studies such as Eckstrand et al.²⁷ Under this approach, it is recognized that people with LGBTBI+ identities have diverse experiences, not a single reality.²⁸ This study followed the Consolidated Criteria for Communicating Qualitative Studies (COREQ)²⁹ and the Standards for Communicating Qualitative Research (Supplementary File 1).

Experience or role of researchers

The research team consisted of 5 women and 6 men, including 4 nurses with qualitative research design experience (E.G.C.-B, A.T.-R, P.D.P.-H, and M.A.-B) and 2 researchers with clinical and mental health research experience (P.D.P.-H and J.C.-R). The data were triangulated by 2 external researchers (G.M.-N and R.J.-V). None of the research team members had any previous relationship with the participants. At the start of the study, the position of the researchers was determined based on their beliefs, previous experiences, theoretical framework, and motivation for the study.

Participants and setting

We employed purposive convenience sampling, recruiting volunteer members of the Transgender group from Lambda in the Valencian Community. Data saturation was achieved by the 14th participant, after which no new information emerged, rendering further coding unnecessary.³⁰ Initially, a focus group was conducted with 10 participants. Subsequently, individual interviews were conducted using the snowball method until data saturation was reached. The researchers did not consider it necessary to recruit more participants. Table 1 presents the demographic data of the participants.

Data collection instrument

The data were collected in 2 complementary phases from April to June 2022. First, a focus group was held at the headquarters of Lambda Valencia, facilitated by 2 researchers (M.A.-B and N.C.-R). The session, which lasted 90 min, allowed for a collective exploration of the participants' experiences and perceptions of the study phenomenon. We developed a focus group (FG) discussion guide, informed by existing literature, to address specific topics of interest (Table 2). Given the subject's sensitivity, participants were informed that they could interrupt their participation anytime if they experienced emotional discomfort. In the 2nd phase, semi-structured in-depth interviews were conducted, following the same guide of questions used in the focus group. The interviews were conducted face-to-face, individually, in a comfortable environment for the participants, with an average duration of 49 min. Their flexible nature allowed the interviewees to express themselves freely while the researchers inquired about emerging aspects. Notes were taken during both phases to record contextual observations, interactions and methodological reflections. The transcripts of the focus groups and interviews generated 158,760 written words, providing a substantial volume of data for analysis. The transcripts were returned to the participants for additional comments. Finally, all data were securely stored in a digital location with restricted access, ensuring the confidentiality of the information collected (Table 2).

Table 1. Participant characteristics (n = 14)

Focus group (FG)			Interviews (I)		
participants (P)	gender	age	interviewees	gender	age
P 1	transgender woman	30	–	–	–
P 2	transgender woman	25	I1	transgender woman	35
P 3	transgender woman	45	I2	transgender woman	55
P 4	transgender woman	55	I3	transgender man	25
P 5	transgender man	25	I4	transgender man	25
P 6	transgender woman	25	–	–	–
P 7	transgender man	45	–	–	–
P 8	transgender man	25	–	–	–
P 9	transgender woman	45	–	–	–
P 10	transgender man	25	–	–	–

P – participant; I – interview.

Table 2. Semi-structured question script

Interview questions
<ol style="list-style-type: none"> 1. What word or term do you think best represents your gender identity and why? How has your relationship with that term changed over time? 2. How would you describe your overall experience in the healthcare system? Have you noticed any improvements or changes in care for trans people in recent years? 3. Have you felt respected in terms of your gender identity by healthcare and administrative staff? 4. What difficulties have you faced when trying to access medical services? How do you think these barriers affect the health of the transgender community in general? 5. Have you experienced situations in which you have been questioned about your gender identity unrelated to the reason for the consultation? How does this affect your experience in the healthcare system? 6. If you have been hospitalized, what was the experience like in terms of ward assignment and treatment concerning your gender identity? 7. Do you feel that you have ever been pressured to undergo reassignment surgery or other types of treatment? How did that situation make you think, and how did it impact your perception of the healthcare system? 8. What do you consider essential aspects that healthcare personnel should understand about the reality of transgender people to provide more appropriate care? 9. What aspects would you like to be considered every time you go to a doctor's office? 10. Can you share a time when you felt discriminated against or, on the contrary, supported in a healthcare setting? How do you think that experience influenced your trust in the healthcare system?

Data analysis

An iterative and inductive thematic analysis approach was carried out based on the methodology described by Braun and Clarke.³¹ This process allowed data analysis from focus groups, in-depth interviews and field notes, ensuring the triangulation of information to strengthen the study's validity. First, 2 researchers (M.A.-B and N.C.-R) familiarized themselves with the data by repeatedly listening to the audio and independently reading the focus group transcripts and interviews. In parallel, they reviewed the field notes taken during data collection, which provided additional information about the participants' context, interactions and behaviors. During this initial phase, they made handwritten annotations to identify connections, key phrases and emerging patterns in the participants' discourses, enriching the understanding of the phenomenon studied. They then proceeded to highlight and classify statements that directly addressed the research question, ensuring that the selection of fragments was comprehensive and representative of the various perspectives collected. Statements that directly

addressed the research question were then highlighted and categorized, ensuring that the selection of excerpts was comprehensive and representative of the multiple perspectives collected. These fragments were coded using short phrases or keywords to synthesize their core meaning. For this purpose, the qualitative data analysis software ATLAS-ti.³² was used, facilitating the information's organization and structuring.

In the following analysis stage, the codes generated were grouped into preliminary categories, from which the first themes began to emerge. This process was carried out collaboratively, with the participation of 3 researchers (E.G.C.-B, A.T.-R and P.D.P.-H). The data triangulation between interviews, focus groups and field notes made it possible to identify convergences and divergences in the narratives, providing a more robust and profound vision of the phenomenon being analyzed. To ensure the coherence and validity of the analysis, any discrepancies in the interpretation of the data were discussed within the team until a consensus was reached. This reflective and dynamic process allowed the initial themes to be reorganized and redefined according to the connections and nuances identified

in the data. Finally, a comprehensive review of the identified themes was conducted to verify their relevance and consistency with the research question. Combining multiple data sources and methodological triangulation contributed to an enriched interpretation, ensuring a more complete and nuanced understanding of the phenomenon studied.

A qualitative analysis of each interview and the researchers' field notes was conducted using an inductive thematic approach. Codes were generated to identify the most descriptive content, which was then reduced and grouped to identify common categories representing meaningful content units. This process led to the emergence of thematic areas describing the experiences of study participants.

Three researchers (E.G.C.-B, A.T-R and P.D.P-H) conducted independent double coding of each interview and each field note. They then met to discuss, compare and refine their findings. Subsequently, the same process was carried out with the themes. In addition, joint meetings were held to consolidate the results of the analysis, as well as an external audit with an independent researcher to ensure confirmability. All coding were discussed by the research team until a consensus was reached on the main categories and themes, creating a final matrix of categories.

To control the rigor and reliability of the qualitative data, the criteria of Guba and Lincoln ³⁰ were applied (Table 3).

Ethical approval

This study was conducted in accordance with the Declaration of Helsinki and received approval from the Ethics Committee of the University of Valencia (approval No. UV-INV_ETICA-2662329; verification code S126XGMF60UWV255). All participants were briefed on the study's objectives and signed written informed consent before participating in interviews and focus groups, with assurance of their right to withdraw at any time without penalty. Data collection was anonymous, voluntary and confidential; sessions were audio-recorded with participants' permission and transcribed verbatim, and no personal identifiers were documented. The information obtained was treated anonymously and

confidentially, complying with the General Data Protection Regulation (EU) 2016/679 of the European Parliament and Organic Law 3/2018. The investigators did not declare ethical, moral or legal conflicts, nor did they receive financial compensation, just as the participants did not receive compensation for their collaboration in the study.

Results

Of the 14 focus group participants, 8 (57%) identified as transgender women and 6 (42%) as transgender men. The mean age was 34.6 years (standard deviation (SD) = 12.84).

Three thematic blocks with their categories were identified: (T1) Experience of professional care for transgender people; (T2) Impact of cisgender regulations in the Health System; and (T3) Need for education in gender diversity for health professionals (Table 4).

Theme 1. Experiences of healthcare professionals in caring for transgender people

Quality of treatment received

Healthcare and perceptions of gender identity are critical to the wellbeing of transgender people, but unfortunately, the experience is not always the same for everyone. While some people find adequate and respectful treatment, others face significant obstacles in their interaction with the healthcare system, often due to prejudice or lack of training on gender issues: *I have generally had a good experience in my process because I have gone to the same health center every time, and they have attended to me well, both the one who attends to me on the phone and the family doctor who makes me feel comfortable* (FG_P3). This type of experience shows the importance of longitudinal care that ensures constant and personalized treatment by the same professionals, allowing patients to feel comfortable and safe, ensuring more fluid access

Table 3. Rigor criteria

Criteria	Techniques and procedures used
Credibility	Team meetings were held to compare analyses and identify categories and themes with the rest of the team. Triangulation of data collection methods: focus groups, semi-structured interviews and field notes collected by the researchers were conducted. Validation by participants (member-checking): participants were offered the opportunity to review the audio recordings to confirm their experience. No additional comments were made by any of the participants.
Transferability	Detailed descriptions of the study conducted, specifying the characteristics of the researchers, participants, contexts, sampling strategies, and data collection and analysis procedures.
Reliability/Trustworthiness	External investigator audit: The data were triangulated by 2 external researchers (G.M.-N and R.J.-V), who evaluated the research protocol, focusing on the methods applied and the study design.
Confirmability	Triangulation of researchers, validation by participants and triangulation in data collection.

Table 4. Themes and categories

Themes (T)	Categories
T1: Experience of health professionals' care for transgender people	Quality of treatment received Professional skills and training Access to specialized treatment
T2: Impact of cisgender regulations on the health system	Expectations of gender expression Lack of inclusive spaces Obsolete diagnoses and pathologization
T3: Gender diversity education needs for health professionals	Formal diversity training Empathy and respect in the consultation Strategies for normalization

to the medical care they need. However, some face serious difficulties, and seeking support in these services points to poor or even discriminatory treatment: *One girl I know who went to the Gender Unit encountered a nurse who did not respect her gender identity and did not treat her well at all* (FG_P1). Others emphasize how specialized gender services do not meet the expectations of empathy. They even report situations in which healthcare personnel do not respect the gender identity of transgender people: *I have to say that, curiously, I find better treatment outside the Gender Unit than inside. In fact, I have had awful experiences* (FG_P2). Lack of sensitivity may also be reflected in erroneous or derogatory diagnoses: *I had to change my family doctor. When I went to tell him what was wrong with me and that I wanted to have surgery, his conclusion was that I wanted to remove my boobs because they were too big, and since they were not big enough to have surgery, he was not going to send me to any specialist and that I should go home* (FG_P5).

Bureaucracy, waiting lists, and a lack of resources are persistent barriers within the healthcare system. In contrast, some patients have relatively quick access to the care they need. The reality remains a constant struggle for many others to overcome these obstacles, highlighting the urgent need to reform the system to ensure that all patients, regardless of their situation, receive the care they require without having to wait unnecessarily.

Professional skills and training

The experiences shared by transgender people regarding healthcare reflect a notable disparity in the sensitivity and preparation of the staff. On the one hand, some professionals show an attitude of skepticism toward the gender identity of their patients: *With my family doctor, she kind of denies me, she doubts me all the time asking me if I am really sure* (FG_P6). In contrast, other more empathetic professionals have respected the patient's name and pronouns, showing active support by referring them to safe spaces. For some people, the lack of respect for their identity is perceived as a conscious choice by the professional: *I don't think it's complicated either: 'My name is X, call me X, call me X.' The person knows what you are telling them and when they don't respect it, they know what you are*

telling them. The person knows what you are saying, and when they don't respect it on purpose, it is because they don't feel like it (FG_P2). This lack of understanding can cause transgender people to feel out of place in medical settings: *The truth is that you feel a bit alien* (FG_P10).

Lack of knowledge about the transgender reality and lack of training in gender diversity are significant barriers in healthcare: *Because they have no idea how it affects. It is noticeable that they lack knowledge about the transgender reality, and the gender issue is not deepened in their studies* (FG_P7). Some patients have had to assume the role of educators, instructing the professionals about their needs and experiences: *It is noticeable that they lack knowledge about the transgender reality, the professionals ask many questions, to try to inform the patient directly* (I2). This type of comment not only denotes a clear ignorance of the needs and experiences of transgender people. It is observed that, although some healthcare professionals do not have specialized training in issues related to transgender people, such as the correct use of inclusive language, what makes the difference is their willingness to learn and adapt to the specific needs of these patients. Unfortunately, stereotypes and misunderstandings persist among healthcare personnel, as reflected in this comment: *I've heard it more than once: 'Look, not a man, not a woman.' But the truth is, that's not how it is... I know I'm not what they say* (I4). This type of prejudice perpetuates an unsafe environment for transgender patients.

Access to specialized treatment

Access to healthcare for transgender people continues to be a problem that affects many people: *With the endocrinology part, I have had very poor treatment because you need them to be there, and they are not* (FG_P2). In addition, many people must share the same doctor due to the lack of professionals: *It is that practically all of us have the same doctor* (FG_P1). This situation directly impacts the quality of care and delays necessary treatments. Waiting times can be disproportionately long, affecting the quality of life of those seeking treatment: *The first time I got an appointment, I had to wait 9 months... By the time I started hormone therapy, I was starting university and had to go through all my changes there* (I1). These ideas

reflect the slowness of the process, which can generate distress and frustration in patients. In turn, the lack of access to the public system means that those with economic resources can access the same doctors through private consultations, which raises an ethical question: *Deep down, they're all the same... What really matters is getting money, and that's not ethical* (I2).

Hormone treatment, in addition to being a lifelong process for many people, involves side effects and important decisions: *They told me I wouldn't become infertile until 5 or 10 years later and that I could start hormone therapy and then freeze my eggs... The thing is, everyone said something different* (FG_P8). The side effects of treatment can generate emotional instability and notable physical changes: *Each one affects us differently, but of course it affects us psychologically* (I3).

In some cases, they delay the start of their treatment to preserve their fertility: *Even though they asked me the typical question about whether I want to have kids, and at 20 or 21, I honestly had no idea. That really messed me up, to be honest. Since I was so unsure about what to do, I ended up freezing my eggs to use them when the time comes* (FG_P8). Surgical procedures are also a key point in the transition process, with experiences varying regarding results and recovery: *There are many surgeries because at minimum one operation to construct the penis, another to place the testicular implants, and another surgery so you can have an erection. After all that, if you manage to have some sensitivity* (FG_P5). However, these procedures may involve prolonged pain and discomfort. Voice therapy is also fundamental for many people in their transition process: *There's something about my voice that doesn't feel right – I'm not sure if it should be stronger or softer. I'm working on it... That's why I'm in voice therapy* (I2). The importance of voice in gender identity highlights the need for equal access to this type of therapy.

Many people describe the transition process as an emotional [...] roller coaster: *You always feel a mix of emotions; as a child, I used to cry because I couldn't be who I wanted to be* (FG_P1). However, the support of the environment can make a big difference. While some people have had a favorable environment, others have experienced social rejection and loss of relationships: *There are people who are with you at first, but then disappear... In the end, the ones that matter remain* (I2). Despite the challenges, the shared experiences also reflect the importance of self-determination and personal struggle: *You know something's wrong, but until you name it, you don't understand it. And when you recognize yourself and fight for yourself, it feels amazing* (I3).

Theme 2. Impact of cisgender regulations in the health system

Prevailing cisnormative regulations within the healthcare system impose significant barriers on transgender individuals, compelling them to conform to restrictive

gender-expression standards to access treatment and services. These requirements not only perpetuate discrimination but also undermine both the right to health and the affirmation of one's gender identity.

Expectations of gender expression

One of the main problems faced by transgender people within the healthcare system is the need to conform to a stereotypical image of the gender with which they identify to receive care: *Here, to get something, you have to show that you are a woman; you have to wear long hair, dresses and heels; otherwise, it is very difficult to be referred* (FG_P2). This statement underscores the implicit expectation that individuals conform to conventional standards of femininity in order to attain social recognition. Other participants reinforce this idea by advising other transgender women about the importance of appearing normative gender to be accepted in medical consultations: *I tell all the transgender girls I know to lie on the test and wear the best dress. If you have heels, wear them, if you have makeup, wear it. Until there's a change, that's the way it's going to be* (FG_P1). This statement highlights that, beyond gender identity, validation within the healthcare system depends on the ability to fit into a pre-designed image of femininity or masculinity. Such circumstances place an added burden on transgender individuals, compelling them to alter their appearance and behavior to access essential medical care.

The impact of cisgender normativity also extends to the legal recognition of gender identity, affecting access to adequate medical services: *The trans person still hasn't changed their gender on their ID* (FG_P3). Without documents that correspond to their identity, many transgender people face constant questioning about their gender, which makes healthcare complex. In other cases, despite having updated documents, they face bureaucratic obstacles and resistance from staff.

Lack of inclusive spaces

The existence of significant barriers for people who do not conform to gender binarism is evident, especially in areas where segregation by sex continues to be the norm. This lack of recognition and adaptation to the diversity of identities generates situations of exclusion and discomfort, directly affecting the wellbeing and dignity of the people concerned. One of the main problems pointed out is the invisibilization of non-binary people in environments structured under a strict binary scheme: *If it is already difficult to be accepted when you do not fit into the traditional categories of man and woman, imagine what it means for a non-binary person: They simply stop taking you into account* (FG_P4).

Distributing spaces in institutions such as hospitals or nursing homes poses an additional difficulty. Allocating rooms solely on the basis of legal or biological sex creates

uncomfortable situations and does not respect the identity of many people: *I don't think it's appropriate for rooms to be divided into male and female only. But, if that is how it should be, they should at least allow each person to be in the one that corresponds to their identity* (FG_P5). The absence of inclusive bathrooms represents another essential barrier. The obligation to choose between a male or female restroom can be an unpleasant or even stigmatizing experience for many transgender people. In this sense, one solution suggested by the interviewees would be the implementation of shared bathrooms accessible to all: *The ideal would be to have a common bathroom* (FG_P4). Another problem identified is the constant need to explain and justify one's identity in institutional settings. The lack of clear protocols in many institutions is highlighted, which generates improvisation and resistance on the part of the staff. This situation not only creates uncertainty but also perpetuates discrimination.

Obsolete diagnoses and pathologization

Across many settings, particularly in healthcare, transgender and gender-diverse individuals often encounter arbitrary treatment by providers, resulting in inequitable and distressing experiences: *Something that also makes me very angry is that, in any field, whether this is health or administrative or whatever, in the end, you are exposed to the arbitrariness of the person who touches you* (FG_P1). Medical decisions, diagnoses and treatments can depend more on the beliefs or prejudices of the professional on duty than on a criterion that is really based on the patient's welfare. A clear example of this point is the persistence of obsolete diagnoses in clinical records, which is not only a technical problem but has real consequences for the care and treatment received: *In my medical records from October of last year, they still put 'Dual-role transvestism' as my diagnosis* (FG_P5). This term, in addition to being outdated, reinforces a pathologizing view of transgender and non-binary identities by classifying gender experiences as disorders instead of recognizing them as part of human diversity. Pathologization is especially evident when a transgender individual's gender identity is referenced in clinical contexts where it is irrelevant: *If you go to the emergency because you've dislocated a shoulder, you're going to get: 'Transsexualism'* (FG_P1). This phenomenon illustrates that the lack of updating of healthcare personnel can make transgender identity ubiquitous data, even when it has no relation to the reason for consultation.

Conversely, requiring a formal diagnosis to access certain specialized health services underscores the enduring medicalized, biologist approach: *That is true, and at least you have to have a diagnosis before you can be sent to a specialist. In the Unit, we use the current manual, the ICD-11, I think* (I4). Although ICD-11 has advanced by removing pathologizing terms such as "transsexualism" and replacing them with "gender incongruence", in practice, barriers

still exist: *Ugh, it's all pretty rough, I mean, there are a lot of things that just aren't right...* (FG_P4). This comment suggests that, despite theoretical improvements in the approach to transgender health, in practice, there are still gaps, inconsistencies, and resistance on the part of healthcare personnel.

Theme 3. Gender diversity education needs for health professionals

Formal diversity training

Education on gender diversity is an essential component of healthcare professional training. Healthcare should focus not only on clinical factors but also on empathy and proper treatment of patients, ensuring an inclusive and respectful approach: *Periodic training to health personnel, both on purely medical issues and on issues of empathy and treatment of patients* (FG_P1). Regular training activities must be aimed at healthcare personnel, strictly covering clinical knowledge, communication, and inclusive treatment skills. Including these topics in the curricula and continuing education would improve care for people with diverse gender identities. For example, in Argentina, in some medical universities, "treatment of transgender people" has already been incorporated into the curriculum, which represents a significant advance in the training of future health professionals: *My daughter, who is in her 4th year of medical school in Argentina, told me that just this year they have a part of the subject that is 'Treatment of transgender people'* (FG_P3). This initiative highlights the importance of integrating content on gender diversity in formal education. *Any profession should have basic training in sexual, gender and family diversity, but especially the medical field should have an exclusive subject on that* (FG_P5).

In this sense, all health-related professions require basic training in sexual, gender, and family diversity. In healthcare, this training should be mandatory, integrated across all curricula, and include dedicated modules that comprehensively address gender diversity issues.

And there are many things out there that we still have to cope with, within society, health professionals, at the legal level... (I2). Despite progress, there are still many challenges within society and the healthcare professional community regarding inclusive care and understanding of gender diversity. Ongoing training and the implementation of diversity education policies would significantly reduce discrimination and enhance healthcare quality.

Empathy and respect in the consultation

Treatment in the healthcare environment is a fundamental element in guaranteeing dignified and quality care. Empathetic, respectful medical consultations improve patient experience and foster trust in the healthcare

system. However, the testimonies collected show that practices that generate discomfort still persist, which underlines the need to improve staff training in terms of diversity and sensitization. One of the most relevant aspects pointed out is the importance of asking the person's name and pronouns in a natural way, without assuming information based on official documents or appearance. Asking for this not only avoids uncomfortable situations but also represents an essential gesture of respect and recognition of each patient's identity. *Simply ask for the name, regardless of the name you may have on the registry. Ask for the name and pronouns as a matter of course* (FG_P1).

On the other hand, experiences are mentioned in which healthcare personnel ask unnecessary or invasive questions, such as the previous registry name, anatomy, or surgical procedures that a person may or may not have undergone. Such questions are often irrelevant to the clinical encounter and can be intrusive, leaving patients feeling exposed or vulnerable: *Don't ask me what my name was, don't ask me what I have between my legs, don't ask me if I am going to have surgery, it's none of your business* (FG_P9). In this sense, it is emphasized that the focus should be kept on the real reason for the consultation, without diverting the conversation to personal aspects unrelated to the health problem for which the person comes to the medical center.

Similarly, reports indicate that the inherent dynamics of healthcare settings can cause patient discomfort. For example, in gynecological consultations, a person may feel part of the environment until their name is called out loud. At this point, they experience looks of judgment or surprise from other people present: *Like when you go to the gynecologist, and you are surrounded by women and, while you are sitting down, you may be accompanying a woman, but the moment they call your name, and you stand up, everyone looks at you* (I4). These experiences highlight the need to rethink specific procedures so everyone feels comfortable and safe in these spaces. Finally, although some healthcare professionals show sensitivity and care in their treatment, they sometimes make mistakes or overlook specific fundamental details to ensure respectful care. Insufficient training and awareness of these issues lead to inconsistent patient experiences – some consultations proceed smoothly, while others induce significant stress or anxiety. This anxiety is expressed in experiences about the process of psychological accompaniment in the context of gender transition, which seems to be marked by a mixture of support and pressure, together with institutional bureaucracy. The importance of good information and psychological follow-up is emphasized. However, it is mentioned that this follow-up should not be interpreted as an external validation of a person's identity, but as ongoing support. This perspective reflects a critique of the validation approach, suggesting that accompaniment should be a tool for well-being, not a barrier to personal identity. They reflect how

the process of psychological support for transgender people is an experience that varies greatly depending on the professionals involved and the institutional structures: *Having that psychological support makes me feel much calmer, and for the first time in my life, I can open up and share what I've been through with someone* (I2).

Strategies for normalization

The testimonies collected reflect a consensus on the importance of education as a central axis for normalization. The need to implement courses in companies and healthcare centers to generate knowledge and promote structural changes in society is highlighted: *Regarding education, which we all consider crucial to establish knowledge and standardization, I think we could take advantage of it and give courses in companies and medical centers* (FG_P7).

Despite progress in some regions, such as the Valencian Community, forms of discrimination persist, underscoring the urgency of strengthening education as a key tool for social change. *The Valencian Community is doing well, but there is still discrimination, and we cannot relax; we have to tighten up, and the only way out is education* (FG_P3). In this sense, it is pointed out that the educational system, including the training of medical personnel, continues to reproduce a normative vision that perceives what is different as not acceptable. *The educational system, including education to future medical personnel, maintains a style of society that understands that anything different outside of normativity is dangerous* (FG_P4).

The lack of a unified registry that allows documenting and addressing existing problems in a structured manner was identified, which evidences the need for a shared database to improve the institutional response: *Sure, but it should be registered. So a complaint is that there should be a common database* (I1). Finally, the lack of adequate knowledge in certain areas is highlighted, reinforcing that education is a fundamental factor in advancing standardization. *The truth is, there are terms they've never even heard of they just don't understand them* (I1).

These results reflect the complexity of understanding the experiences of transgender people. Figure 1 allows us to establish the following themes: (T1) Experience of professional care for transgender people; (T2) Impact of cisgender regulations in the healthcare system; (T3) Gender diversity education needs for healthcare professionals. The program ATLAS-ti was used to code and synthesize the data, and a graphic designer prepared the results in the form of a map of agents and interactions, as shown in Fig. 1.³²

Discussion

At the beginning of the study, we set out to learn about the experiences of transgender people in their relationship with the healthcare system. Access to adequate and

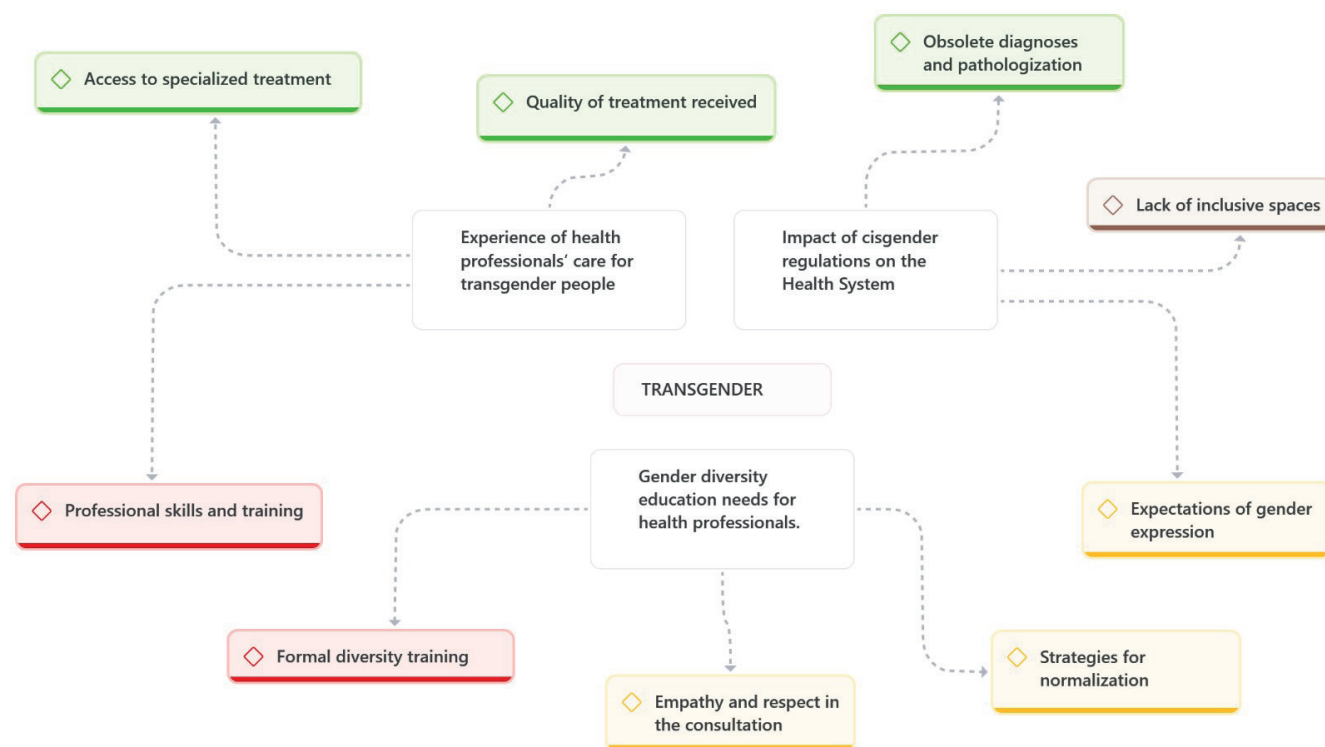


Fig. 1. Qualitative data analysis

respectful healthcare is a fundamental right, especially for transgender people, who often face significant barriers within the healthcare system.³³ These barriers can manifest in healthcare personnel's lack of knowledge about this population's specific needs, explicit or implicit discrimination in health services, and the scarcity of adequate clinical protocols for their care.

The results of this study show contrasting experiences in the healthcare of transgender people, reflecting both advances in awareness and persistent deficiencies in the quality of treatment received. While some professionals have demonstrated greater openness and willingness to provide respectful care, attitudes and practices persist that generate mistrust and discomfort in transgender patients. This, in turn, may discourage their timely access to medical care. Healthcare providers must cultivate a safe, supportive and empathetic environment grounded in clinical expertise, ensuring that transgender individuals receive care free from prejudice and unnecessary barriers. Incorporating gender identity content throughout all stages of healthcare training, including continuing nursing education, is essential for delivering truly inclusive, high-quality care.²⁵ Such training equips healthcare professionals with the competencies to provide comprehensive, respectful care that addresses the unique needs of transgender individuals.³⁴

One key finding is the wide variability in care quality: While some transgender individuals describe encounters with empathetic, eager-to-learn professionals, others recount experiences of discrimination, disrespect and

a lack of awareness regarding their specific needs.³⁵ This finding could be attributed to the influence of stereotype threat in the healthcare setting,³⁶ as well as the fear that, in the medical office, harmful stereotypes about transgender people are reinforced. Additionally, there is concern that an individual's social group identity may influence how healthcare professionals perceive, evaluate and treat them.³⁵ This idea suggests the need to strengthen the training of healthcare personnel in gender diversity and to implement institutional strategies to ensure equitable, human rights-based care.³⁷ Health systems should establish periodic training for professionals to be updated on best practices in inclusive care and to prevent the perpetuation of stereotypes and prejudices in healthcare.³⁸

Another relevant aspect is the impact of bureaucracy and scarcity of resources on the quality of care. A lack of sufficient public resources was identified; transgender people face long waiting lists and difficulties in accessing transgender health specialists. This point reinforces the need to increase investment in specialized health services and ensure timely access without discrimination. In addition, access to hormone treatments and gender-affirming surgeries is often hindered by overly restrictive criteria, prolonging the distress of those seeking professional assistance.³⁹ Allocating additional resources to mental health programs for the transgender community, and supporting research to develop adaptable, evidence-based interventions, is essential for expanding our understanding of clinical efficacy, improving mental health outcomes, and ensuring the long-term sustainability of these initiatives.⁴⁰

Providing culturally competent and gender-affirmative care is a relevant aspect for various disciplines. However, evidence points to insufficient preparation and limited knowledge about the specific needs and challenges of transgender individuals.³⁷ The findings show that healthcare professionals who seek to inform themselves and adapt their practice to the needs of transgender patients generate more positive and satisfying experiences. This finding is consistent with literature highlighting the importance of gender diversity training as an essential tool to improve the relationship between patients and healthcare professionals.^{41,42} Student-led initiatives have effectively enhanced peers' knowledge and confidence in providing transgender-affirming healthcare.⁴³ Encouraging the development of tools tailored to the transgender community that address their unique needs and support an interdisciplinary treatment approach is essential.⁴⁴ Additionally, establishing support networks and safe spaces for transgender individuals can foster more comprehensive, patient-centered care. Implementing these enhancements would not only benefit transgender individuals, but also strengthen the healthcare system's ability to equitably and respectfully address the diverse needs of all users. In the long term, establishing specialized, multidisciplinary units – staffed by experts in endocrinology, mental health, surgery, and social support – could profoundly advance transgender people's right to health.

Limitations

This study offers valuable insights into the healthcare experiences of transgender individuals in Spain, underscoring the challenges they face and the urgent need for more inclusive clinical protocols. Training healthcare personnel in gender diversity, removing bureaucratic barriers, and creating safe spaces are key strategies to improve their access to healthcare. In addition, the expansion of specialized resources and cooperation with organizations working to defend their rights is essential.

Despite these advances, the study has limitations, such as the small sample size and the need for further research to generalize the findings. In addition, the results may not be generalizable to other parts of the world due to cultural complexities. Participants may not have disclosed very sensitive information. Implementing change requires political will, adequate resources, and overcoming resistance from some healthcare sectors. Continued advocacy for public policies that ensure equitable and respectful healthcare for all individuals is essential, guaranteeing that gender identity does not impede access to quality services.

Furthermore, one important limitation noted by the reviewers is the lack of analysis regarding differences in discourse between trans men and trans women. That is, the study does not include a gender perspective within the trans population itself. It is possible that the needs

of both groups differ and that they face distinct challenges, which future research should address to ensure more inclusive and nuanced approaches.

Conclusions

The conclusions of this study highlight the urgent need to transform the healthcare system to guarantee inclusive and equitable care for transgender people. The people interviewed expressed the need for this transformation to feel better cared for and accompanied throughout their entire process. Awareness raising and training of healthcare personnel, the design of specific protocols, and the reduction of bureaucratic barriers are essential to achieve a fairer health system. It is also crucial to improve accessibility to specialized treatment and create safe spaces that respect each person's gender identity. Equally important is training professionals in the care of transgender people, strengthening their knowledge of specific health needs, and facilitating better access to resources. In addition, the development and implementation of inclusive public policies are key to ensuring that healthcare is a guaranteed right, thus promoting wellbeing and equity in access to health.

Data availability statement

The participants of this study did not give written consent for their data to be shared publicly, so due to the sensitive nature of the research, the supporting data are not available.

Supplementary data

The supplementary materials are available at <https://doi.org/10.5281/zenodo.16570654>. The package includes the following files:

Supplementary File 1. COREQ checklist.










Consent for publication

Not applicable.

Use of AI and AI-assisted technologies

Not applicable.

ORCID iDs

Antonio Martinez-Sabater  <https://orcid.org/0000-0002-6440-1431>
Elena Chover-Sierra  <https://orcid.org/0000-0002-4141-6956>
Pablo Del Pozo-Herce  <https://orcid.org/0000-0002-2652-4895>
Alberto Tovar-Reinoso  <https://orcid.org/0000-0003-3348-3232>
Marta Araujo-Blesa  <https://orcid.org/0000-0003-0830-5899>
Javier Curto-Ramos  <https://orcid.org/0000-0003-0480-6530>
Gustavo Mora-Navarro  <https://orcid.org/0000-0002-0604-5205>
Raúl Juárez-Vela  <https://orcid.org/0000-0003-3597-2048>
Eva García Carpintero-Blas  <https://orcid.org/0000-0002-4984-2511>

References

- Estay FG, Valenzuela AV, Cartes V. R. Atención en salud de personas LGBT+: Perspectivas desde la comunidad local penquista. *Rev Chil Obstet Ginecol.* 2020;85(4):351–357. doi:10.4067/s0717-7526202000400351
- Medina-Martínez J, Saus-Ortega C, Sánchez-Lorente MM, Sosa-Palanca EM, García-Martínez P, Mármol-López MI. Health inequities in LGBT people and nursing interventions to reduce them: A systematic review. *Int J Environ Res Public Health.* 2021;18(22):11801. doi:10.3390/ijerph182211801
- Strand N, Gomez DA, Kacel EL, et al. Concepts and approaches in the management of transgender and gender-diverse patients. *Mayo Clin Proc.* 2024;99(7):1114–1126. doi:10.1016/j.mayocp.2023.12.027
- Rzewuski M. One person, two identities: The problem of legal gender recognition of a transgender person in Europe. *Behav Sci Law.* 2025;43(1):149–157. doi:10.1002/bsl.2702
- Pastor Bravo MDM, Linander I. Access to healthcare among transgender and non-binary youth in Sweden and Spain: A qualitative analysis and comparison. *PLoS One.* 2024;19(5):e0303339. doi:10.1371/journal.pone.0303339
- Daniels SL, Melvin JW, Jones Q. Caring for transgender patients. *Nurs Clin North Am.* 2024;59(4):625–635. doi:10.1016/j.cnur.2024.07.015
- Dasso N, Ottonello G, Hayter M, et al. Transgender people's experiences of hospitalization: A qualitative metasynthesis. *J Adv Nurs.* 2025;81(2):550–573. doi:10.1111/jan.16325
- Tangpricha V. Health disparities in transgender people. *Lancet Diabetes Endocrinol.* 2021;9(10):641–643. doi:10.1016/s2213-8587(21)00211-4
- Safer JD, Coleman E, Feldman J, et al. Barriers to healthcare for transgender individuals. *Curr Opin Endocrinol Diabetes Obes.* 2016;23(2):168–171. doi:10.1097/med.0000000000000227
- Nelson LA, Shurpin K. Barriers to healthcare for transgender individuals. *J Doct Nurs Pract.* 2024;17(2):110–116. doi:10.1891/jdnp-2023-0018
- Ross MB, Jahouh H, Mullender MG, Kreukels BPC, Van De Griff TC. Voices from a multidisciplinary healthcare center: Understanding barriers in gender-affirming care. A qualitative exploration. *Int J Environ Res Public Health.* 2023;20(14):6367. doi:10.3390/ijerph20146367
- Ahuja TK, Goel AD, Gupta MK, et al. Health care needs and barriers to care among the transgender population: A study from western Rajasthan. *BMC Health Serv Res.* 2024;24(1):989. doi:10.1186/s12913-024-11010-2
- Eckstrand KL, Lunn MR, Yehia BR. Applying organizational change to promote lesbian, gay, bisexual, and transgender inclusion and reduce health disparities. *LGBT Health.* 2017;4(3):174–180. doi:10.1089/lgbt.2015.0148
- Bhatt N, Cannella J, Gentile JP. Gender-affirming care for transgender patients. *Innov Clin Neurosci.* 2022;19(4–6):23–32. PMID:35958971. PMCID:PMC9341318.
- Government of Spain. Law 4/2023, of February 28, for the real and effective equality of trans persons and for the guarantee of the rights of LGBTI persons. Official State Gazette (BOE), No. 51, of March 1, 2023. Madrid, Spain: Government of Spain; 2023. <https://www.boe.es/eli/es/l/2023/02/28/4>.
- Lovejoy C, Fitzgerald L, Mutch A. Understanding access to healthcare for gender diverse young people: A critical review of the literature. *Cult Health Sex.* 2023;25(1):18–32. doi:10.1080/13691058.2021.2017486
- Serón TD, Catalán MA. Identidad de Género y Salud Mental. *Rev Chil Neuropsiquiatr.* 2021;59(3):234–247. doi:10.4067/s0717-92272021000300234
- Falck F, Bränström R. The significance of structural stigma towards transgender people in health care encounters across Europe: Health care access, gender identity disclosure, and discrimination in health care as a function of national legislation and public attitudes. *BMC Public Health.* 2023;23(1):1031. doi:10.1186/s12889-023-15856-9
- Nunes-Moreno M, Furniss A, Cortez S, et al. Mental health diagnoses and suicidality among transgender youth in hospital settings. *LGBT Health.* 2025;12(1):20–28. PMID:39016468.
- Bermúdez-Pozuelo L, Sordo Del Castillo L, Belza Egozcue MJ, Triviño Caballero R. Healthcare for trans people in primary care. *Med Clin (Barc).* 2024;163(5):253–259. doi:10.1016/j.medcli.2024.01.049
- Cutillas-Fernández MA, Jiménez-Ruiz I, Herrera-Giménez M, Jiménez-Barbero JA. Attitudes and behaviours of mental health professionals in the care of transgender people: A qualitative study. *J Psychiatr Ment Health Nurs.* 2024;31(6):1205–1215. doi:10.1111/jpm.13073
- Berrian K, Exsted MD, Lampe NM, Pease SL, Akré EL. Barriers to quality healthcare among transgender and gender nonconforming adults. *Health Serv Res.* 2025;60(1):e14362. doi:10.1111/1475-6773.14362
- Morenz AM, Goldhammer H, Lambert CA, Hopwood R, Keuroghlian AS. A blueprint for planning and implementing a transgender health program. *Ann Fam Med.* 2020;18(1):73–79. doi:10.1370/afm.2473
- Boutillier AJ, Clark KD, Bosse JD, Jackman KB, Jewell J, Dawson-Rose C. Social-ecological barriers and facilitators to seeking inpatient psychiatric care among transgender and nonbinary people: A qualitative descriptive study. *J Adv Nurs.* 2025;81(4):1937–1952. doi:10.1111/jan.16393
- Milionis C, Koukkou E. Barriers and challenges in caring for transgender people: Implications for clinical practice and the experience from a specialized center. *J Doct Nurs Pract.* 2023;16(1):44–53. doi:10.1891/jdnp-2021-0022
- Doyle L, McCabe C, Keogh B, Brady A, McCann M. An overview of the qualitative descriptive design within nursing research. *J Res Nurs.* 2020;25(5):443–455. doi:10.1177/1744987119880234
- Eckstrand K, Ehrenfeld JM, eds. *Lesbian, Gay, Bisexual, and Transgender Healthcare: A Clinical Guide to Preventive, Primary, and Specialist Care.* Cham, Switzerland: Springer International Publishing; 2016. doi:10.1007/978-3-319-19752-4
- Braun V, Clarke V. *Successful Qualitative Research: A Practical Guide for Beginners.* Los Angeles, USA: SAGE Publications; 2013. ISBN: 978-1-84787-581-5, 978-1-84787-582-2.
- Tong A, Sainsbury P, Craig J. Consolidated criteria for reporting qualitative research (COREQ): A 32-item checklist for interviews and focus groups. *Int J Qual Health Care.* 2007;19(6):349–357. doi:10.1093/intqhc/mzm042
- Creswell JW, Poth CN. *Qualitative Inquiry & Research Design: Choosing Among Five Approaches.* 4th ed. Los Angeles, USA: SAGE Publications; 2018. ISBN:978-1-5063-3020-4.
- Braun V, Clarke V. Thematic analysis. In: Cooper H, Camic CM, Long DL, Panter AT, Rindskopf D, Sher KJ, eds. *APA Handbook of Research Methods in Psychology. Vol. 2: Research Designs: Quantitative, Qualitative, Neuropsychological, and Biological.* Washington D.C., USA: American Psychological Association (APA); 2012:57–71. doi:10.1037/13620-004
- Méndez Romero RA. Qualitative data analysis with ATLAS.ti, por Susanne Frieze. *Qual Res Educ.* 2016;5(2):226–228. doi:10.17583/qre.2016.2120
- Hammond P. Transgender. *Best Pract Res Clin Endocrinol Metab.* 2024;38(5):101933. doi:10.1016/j.beem.2024.101933
- Kattari SK, Call J, Holloway BT, Kattari L, Seelman KL. Exploring the experiences of transgender and gender diverse adults in accessing a trans knowledgeable primary care physician. *Int J Environ Res Public Health.* 2021;18(24):13057. doi:10.3390/ijerph182413057
- Stacey L, Wislar W, Reczek R. The medical institution and transgender health: The role of healthcare barriers and negative healthcare experiences. *Soc Sci Med.* 2025;365:117525. doi:10.1016/j.socscimed.2024.117525
- Saunders RK, Carr DC, Burdette AM. Health care stereotype threat and sexual and gender minority well-being. *J Health Soc Behav.* 2024;65(1):20–37. doi:10.1177/00221465231205549
- Jecke L, Zepf FD. Delivering transgender-specific knowledge and skills into health and allied health studies and training: A systematic review. *Eur Child Adolesc Psychiatry.* 2024;33(5):1327–1354. doi:10.1007/s00787-023-02195-8
- Sparks PJ, Bozigar C, Shah KV, et al. Transgender healthcare: A historical narrative of gender-affirming plastic surgery. *Ann Plast Surg.* 2025;94(1):128–133. doi:10.1097/sap.0000000000004161
- Fowler JA, Warzywoda S, Franks N, et al. Highs, lows, and hormones: A qualitative metasynthesis of transgender individuals' experiences undergoing gender-affirming hormone therapy. *J Homosex.* 2024;71(7):1652–1683. doi:10.1080/00918369.2023.2186759
- Thompson HM, Feasley K, Ortiz R, Reyes K, Seanior A, Karnik NS. An implementation of a community-engaged, group-level mental health pilot for black and Latina transgender women. *Health Promot Pract.* 2024;25(5):895–906. doi:10.1177/15248399231172191

41. Martins RS, Saleh R, Kamal H, et al. The need for transgender health-care medical education in a developing country. *Adv Med Educ Pract*. 2020;11:405–413. doi:10.2147/amep.s255483
42. Matthews JJ, Olszewski A, Petereit J. knowledge, training, and attitudes of students and speech-language pathologists about providing communication services to individuals who are transgender. *Am J Speech Lang Pathol*. 2020;29(2):597–610. doi:10.1044/2020_ajslp-19-00148
43. Grosz AM, Gutierrez D, Lui AA, Chang JJ, Cole-Kelly K, Ng H. A student-led introduction to lesbian, gay, bisexual, and transgender health for first-year medical students. *Fam Med*. 2017;49(1):52–56. PMID:28166581.
44. Xie LY, Kanegi SL, Gbordzoe LA, Marchant LA, Eleazer J. Transgender care is health care: Barriers and proposed model to improve access for transgender adults. *Fam Pract*. 2024;41(4):618–619. doi:10.1093/fampra/cmact125

Reconstruction of outer glycolipid synthesis pathways from *Porphyromonas gingivalis* in *Escherichia coli* for production of a vaccine candidate

Ewa Brzozowska^{1,D}, Wiesław Świętnicki^{1,A–D}, Jordan Sycz^{2,B}, Monika Kołodziejczak^{3,B}, Łukasz Stachowicz^{4,B}, Anna Wzorek^{1,B}, Agnieszka Korzeniowska-Kowal^{1,B}, Michał Skowicki^{5,B,C}, Tomasz Lipiński^{5,A–C}

¹ Department of Immunology of Infectious Diseases, Hirsfeld Institute of Immunology and Experimental Therapy, Polish Academy of Sciences, Wrocław, Poland

² Department of Chemistry, Wrocław University of Environmental and Life Sciences, Poland

³ Department of Biochemistry, Faculty of Chemistry, Wrocław University of Science and Technology, Poland

⁴ Department of Pharmacology, Silesian Medical University, Sosnowiec, Poland

⁵ Laboratory of Nanobioengineering, Lukaszewicz Research Network-Polish Center of Technology Development, Wrocław, Poland

A – research concept and design; B – collection and/or assembly of data; C – data analysis and interpretation;

D – writing the article; E – critical revision of the article; F – final approval of the article

Advances in Clinical and Experimental Medicine, ISSN 1899–5276 (print), ISSN 2451–2680 (online)

Adv Clin Exp Med. 2025;34(12):2091–2103

Address for correspondence

Ewa Brzozowska

E-mail: ewa.brzozowska@hirsfeld.pl

Funding sources

National Science Centre of Poland

(grant No. 016/21/B/NZ6/02028).

Conflict of interest

None declared

Received on December 1, 2024

Reviewed on January 2, 2025

Accepted on February 5, 2025

Published online on July 25, 2025

Cite as

Brzozowska E, Świętnicki W, Sycz J, et al. Reconstruction of outer glycolipid synthesis pathways from *Porphyromonas gingivalis* in *Escherichia coli* for production of a vaccine candidate. *Adv Clin Exp Med*. 2025;34(12):2091–2103. doi:10.17219/acem/200882

DOI

10.17219/acem/200882

Copyright

Copyright by Author(s)

This is an article distributed under the terms of the Creative Commons Attribution 3.0 Unported (CC BY 3.0) (<https://creativecommons.org/licenses/by/3.0/>)

Abstract

Background. *Porphyromonas gingivalis* is a major human oral opportunistic pathogen and a key etiological agent of periodontal disease, contributing to inflammation and bone loss in the oral cavity. Periodontitis is not limited to oral health complications; it has also been associated with a range of systemic conditions, including coronary heart disease (CAD), respiratory disease, rheumatoid arthritis, chronic kidney disease (CKD), and certain types of cancer.

Objectives. Immunization-based prevention of periodontitis appears to be a promising strategy; however, no vaccine is currently available for commercial use. In the present study, a novel vaccine candidate against *P. gingivalis* was proposed, consisting of a *P. gingivalis* protein, gingipain, glycosylated with the carbohydrate moiety of *P. gingivalis* lipopolysaccharide (LPS).

Materials and methods. Glycosylation of gingipain was achieved in *Escherichia coli* by introducing the *Campylobacter jejuni* N-glycosylation system, the *P. gingivalis* LPS biosynthetic pathway and the gingipain gene.

Results. The neoglycoprotein was purified using column chromatography to a purity exceeding 99%, yielding a soluble antigen. The modified protein was recognized by commercial antibodies targeting the protein backbone, the carbohydrate moiety, and a custom monoclonal antibody specific to the purified LPS of *P. gingivalis* American Type Culture Collection (ATCC) 33277. The glycoprotein was used to immunize mice, and the resulting sera were analyzed for their ability to opsonize bacterial cells. The absence of detectable opsonization suggests that the elicited antibodies are more likely directed against the protein component of the vaccine rather than the glycan surface antigen.

Conclusions. The final product was most likely assembled correctly, as it was recognized by LPS-specific antibodies. Further evaluation in an animal model of induced periodontitis is necessary to determine whether the elicited antibodies can effectively inhibit gingipain released by the pathogen. If this vaccine candidate demonstrates protective efficacy, the approach could accelerate and enhance the safety of vaccine design against a wide range of other pathogens.

Key words: vaccine, glycoconjugates, *Porphyromonas gingivalis*, gingipain, periodontosis

Acknowledgements

The authors would like to thank the IT Department, Hirsfeld Institute of Immunology and Experimental Therapy of the Polish Academy of Sciences, Wrocław, Poland, for technical help with setting up computational facilities used during the work, Prof. Anna Pawlik for access to the laboratory equipment needed for experiments conduction, Dr. Marta Świtalska, Dr. Dominika Jakubczyk and Prof. Sabina Górńska for planning and performing mice immunization and opsonization tests, and Bernadeta Szostko for performing the sera titration. Many thanks to the Animal Laboratory Staff for helping with the mice immunization and care during the experiment.

Highlights

- A novel *P. gingivalis* vaccine candidate was engineered by glycosylating gingipain with the O-antigen of *P. gingivalis* LPS in a modified *E. coli* strain.
- The antigen was successfully expressed in *E. coli* and purified to over 99% purity using advanced chromatography techniques.
- Western blot analysis confirmed efficient glycosylation, with the antigen recognized by both anti-gingipain and anti-LPS antibodies.
- This innovative strategy eliminates the need for chemical conjugation, enabling precise, recombinant LPS glycosylation for vaccine development.
- If proven effective in animal models, this approach could accelerate the development of vaccines for periodontitis and other bacterial infections.

Background

Porphyromonas gingivalis is a common human opportunistic pathogen of the oral cavity. The bacterium is a facultative anaerobe responsible for the destruction of dental tissue, leading to periodontitis.¹ It is highly difficult to culture in vitro, which hampers studies on its physiology and virulence. However, with the recent advances in genome sequencing and systems biology, it has been possible to elucidate a large part of its metabolic pathways.² The recently published corrected DNA sequence³ of the original data⁴ on *P. gingivalis* and the other published sequences enabled a comparison with the metabolic pathways of other systems, specifically the well-known *Escherichia coli* genome and metabolome.^{5,6} The analysis identified multiple therapeutic targets and potential prophylactic strategies.⁷ The last aspect of the analysis is important as it is more cost-efficient to prevent the disease than to treat it.

There is no commercially available vaccine against periodontitis or *P. gingivalis*. Existing strategies rely on a combination of gingipains with other components, most likely fimbriae^{8–13} or hemagglutinin adhesion.⁸ A capsular polysaccharide was also tested and was found superior to the pure protein antigens.¹⁴

Analysis of DNA genomes of *P. gingivalis* showed that the pathogen produces at least 2 proteases, the Arg-type gingipain and the Lys-type gingipain.¹⁵ The proteins are highly homologous and used by the bacterium to cleave host proteins, including bone tissue of teeth,¹⁶ leading to the destruction of periodontal tissue.¹⁷ The gingipain protein sequences also contain adhesin motifs, potentially responsible for the recognition and attachment to the host's cell surfaces.¹⁸ Research performed by other groups identified a type IX secretion system (T9SS) responsible for gingipains' secretion.^{19,20} The blockade of this system was proposed as an indirect strategy for the prevention of periodontitis caused by *P. gingivalis*.²¹

Objectives

Systems biology analysis of the metabolic network has identified conserved pathways involved in the lipopolysaccharide (LPS) synthesis in *P. gingivalis*.² The LPS is a major constituent of the outer membrane of Gram-negative bacteria. Glycoconjugates composed of the carbohydrate portion of LPS coupled to carrier protein have been employed as vaccine candidates in numerous studies, while glycoconjugates of capsular polysaccharides of *Hemophilus influenzae* type B, *Neisseria meningitis* and *Streptococcus pneumoniae* are already successfully implemented into vaccination regime. Considering studies on the role of LPS in *P. gingivalis* infection and seroprotection,^{15–17} we commonly reasoned that LPS is a good antigenic target for a vaccine against *P. gingivalis*. We also proposed using gingipain as a dual-function component, serving both as a carrier for the LPS carbohydrate moiety and as a proteinaceous antigen.^{10,22–24} However, the metabolic pathways involved in LPS biosynthesis have not been fully elucidated through experimental studies. The pathogen produces 2 distinct types of LPS, one carrying the O-polysaccharide and the A-LPS containing anionic polysaccharide (APS), with different repeating unit structures.^{25,26} The synthesis pathways of the outer carbohydrate O- and A-antigens are poorly understood. Therefore, a comparison with other systems is used to assign putative roles to genes and assemble operons responsible for the synthesis of similar structures in other pathogens.^{27–29}

Glycans are generally poor antigens, and require conjugation with proteins, most notably the inactivated toxoids from different bacterial species, in order to render T-dependent antigenic character and elicit an effective immune response.³⁰ Currently, 5 carrier proteins are licensed as components of glycoconjugate vaccines: a genetically modified cross-reacting material (CRM) of diphtheria toxin, tetanus toxoid (T), meningococcal outer membrane protein complex (OMPC), diphtheria toxoid (D), and *H. influenzae* protein D (HiD).³¹

In the USA, the only adjuvant approved by the U.S. Food and Drug Administration (FDA) for primary vaccination

is aluminum hydroxide, which significantly limits the effectiveness of carbohydrate-based vaccine components.³² Other adjuvants, based on the synthetic LPS component monolauryl phosphate (MLP) or synthetic cytosine-phosphate-guanine (CpG) nucleotides, have been underrepresented in licensed vaccines.³² Adjuvants based on squalene oil, a natural product derived from marine mammals, are not recommended due to their animal source, despite being used in commercial vaccines against influenza.³³

Standard methods for the formation of glycoconjugates are based on the chemical coupling of carbohydrates with a protein via various chemical strategies. This approach raises many issues that have to be addressed in the production process, like reproducibility, yield, purification from undesired chemical modifications, and others. There is an area for improvement, but addressing these challenges may require innovative strategies beyond traditional approaches.

An alternative strategy to couple carbohydrate antigens to peptide or protein is based on the utilization of *Campylobacter jejuni* undecaprenyl-diphosphooligosaccharide-protein-glycotransferase (PglB) glycosyltransferase.³⁴ The enzyme catalyzes carbohydrate transfer to the side-chain amide of Asparagine (Asn) in the recipient peptide with a defined acceptor sequence D/E-X-N-X-S/T. The transfer process is relatively inefficient, and numerous studies have been conducted to improve its efficiency. Finally, a double mutant (RR → DL) in the original PglB sequence was identified, exhibiting broad transfer specificity for the Asp-Tyr-Asn-Ala-Thr (DYNAT) acceptor sequence.^{35,36} The final step involved removing the competing O-antigen ligase (WaaL in *E. coli*) to eliminate the native pathway responsible for transferring the host-synthesized O-antigen to the lipid core. This strategy has been successfully demonstrated using the *Burkholderia mallei* O-antigen to create a recombinant vaccine covalently linked to a protein.³⁷ Additionally, N-glycan transfer-based technology has been applied in the development of other vaccines.^{38–40}

In the current work, a novel strategy has been used to design a genetic system to produce a vaccine candidate against *P. gingivalis*. The genes synthesizing O-antigen in *P. gingivalis* have been identified computationally using various software, transferred into *E. coli* and co-expressed with a mutated *C. jejuni* *pglB* gene and the *P. gingivalis* antigens, termed pI, fused with the recognition sequence for the PglB transferase. The construct produced a modified antigen which was recognized by antibodies raised to all fragments of the derivatized protein.

Materials and methods

Microbial strains

Campylobacter jejuni strain RM1221⁴¹ was obtained from Prof. Anna Pawlik at the Hirsfeld Institute of Immunology and Experimental Therapy of the Polish Academy

of Sciences, Wrocław, Poland. *Porphyromonas gingivalis* strain DSM 20709 (American Type Culture Collection (ATCC) 33277) was obtained from the Leibniz Institute DSMZ (German Collection of Microorganisms and Cell Cultures GmbH, Braunschweig, Germany). *Escherichia coli* cloning strains were purchased from 2 suppliers (Lab-Jot sp. z o.o., Warsaw, Poland; Life Technologies sp. z o.o., Warsaw, Poland). *Saccharomyces cerevisiae* cloning strain MaV203 was supplied with the GeneArt High-Order Genetic Assembly Kit (Life Technologies sp. z o.o.). The *E. coli* protein expression strains BL21(DE3) and its variants were purchased from Merck (Merck Life Sciences sp. z o.o., Poznań, Poland) or from New England Biolabs (Lab-Jot sp. z o.o.).

Microbial growth media

Bacterial media were purchased from Sigma-Aldrich (Merck Life Sciences sp. z o.o.) or BTL (BTL Sp. z o.o., Łódź, Poland). Antibiotics for bacterial selection were obtained from Merck (Merck Life Sciences sp. z o.o.). Auxotrophic yeast selection medium Complete Supplement Mixture (CSM) was supplied with the GeneArt High-Order Genetic Assembly Kit (Life Technologies sp. z o.o.). Yeast cells were grown on CSM medium supplied with glucose, included in the GeneArt High-Order Genetic Assembly Kit, at 30°C for 3 days.

Culture of *P. gingivalis* for LPS isolation

Porphyromonas gingivalis ATCC 33277 strain was revitalized after lyophilization under anaerobic conditions (BD GasPak EZ Anaerobe Container System, ref. 260678; BD Biosciences, Franklin Lakes, USA) on Columbia Agar (Sigma-Aldrich, Merck Life Sciences sp. z o.o.) plates supplemented with 5% defibrinated sheep blood. The bacterial growth was carried out at 37°C for 5–7 days. Bacterial mass was collected, suspended in Columbia Broth (BioWorld, Dublin, Ireland), centrifuged at 5,000 × g for 30 min (HERMLE Labortechnik Z36HK, Wehingen, Germany) and the bacterial pellet was freeze-dried (Lablyo Freezedrier, York, UK).

Bacteria were typically selected on Miller–Hinton agar plates with appropriate antibiotics: ampicillin (50 µg/L), kanamycin (50 µg/mL), spectinomycin (50 µg/mL), or chloramphenicol (25 µg/L). Bacteria were grown on an appropriate selection plate or in a Luria–Bertani liquid medium supplied with appropriate antibiotics at 37°C for 12–24 h. Longer growth times for bacteria were needed for constructs in the final phases of assembly.

Chemical reagents

Common chemical reagents were purchased from Sigma-Aldrich (Merck Life Sciences sp. z o.o.). Chromatography columns were bought from Sigma-Aldrich (Merck Life Sciences sp. z o.o.) or VWR (VWR sp. z o.o.,

Gdańsk, Poland). Imidazole (p.a.) was purchased from Sigma-Aldrich (Merck Life Sciences sp. z o.o.). TCEP-HCl was obtained from Sigma-Aldrich (Merck Life Sciences sp. z o.o.).

Primary and secondary antibodies

Mouse α -6 \times Histidine (His) monoclonal antibody and biotin-conjugated goat α -mouse IgM secondary antibody were purchased from Life Technologies (Life Technologies sp. z o.o.). Mouse α -*P. gingivalis* strain W83 monoclonal antibody was obtained from Creative Diagnostics (CD Biosciences, Shirley, USA). Rabbit polyclonal α -*P. gingivalis* and α -gingipain R1 (a.a. 228–720) antibodies were purchased from antibodies on-line (antibodies on-line, Aachen, Germany). The streptavidin-HRP conjugate was bought from Sigma Aldrich (Merck Life Sciences sp. z o.o.).

Monoclonal antibodies against *P. gingivalis* LPS were raised using *P. gingivalis* ATCC 33277 strain bacterial mass as an immunogen and a purified LPS as an antigen for screening in enzyme-linked immunosorbent assay (ELISA). The LPS was prepared from a dry mass (35 mg) of *P. gingivalis* via extraction with Trizol reagent according to the protocol described by Yi and Hackett.⁴² The generation of the hybridoma cell lines was performed using a standard procedure,⁴³ with some minor modifications. Briefly: 7-week-old Balb/c mice were immunized 4 times at 2-week intervals with 50 μ g of dry bacterial mass suspended in 100 μ L of phosphate-buffered saline (PBS) and emulsified with an equal volume of Freund's incomplete adjuvant; 2 \times 50 μ L was given into a skin fold in the lumbar region and the remaining portion intraperitoneally. The final boost (4th injection) was administered intraperitoneally without adjuvant. Two days later, the animals were euthanized and spleens harvested for cell isolation. Splenocytes were fused with Sp2/0-Ag14 myeloma cells according to the standard method with polyethylene glycol (PEG). Hybridoma colonies were screened using ELISA on 96-well microtiter plates coated with *P. gingivalis* LPS. Positive wells were subjected to repeated cloning (3 times) using the limiting dilution method to ensure monoclonality. Hybridoma clones were expanded and adapted to grow in hybridoma serum-free medium (CD Hybridoma Medium, CD Biosciences; Thermo Fisher Scientific, Waltham, USA) for antibody production. Antibody class was estimated using the Mouse typer isotyping kit (Bio-Rad, Hercules, USA), indicating IgM class. Finally, a portion of the antibody was purified in an Maltose-binding protein (MBP) agarose column (Pierce, Rockford, USA), according to manufacturer protocol.

Animal experiments obtained approval from the Committee for Animal Experiments at Hirsfeld Institute of Immunology and Experimental Therapy, Polish Academy of Sciences (approval No. 062/2023). *Porphyromonas gingivalis* and *C. jejuni* were grown on Q (a specialized culture medium used for the isolation and growth of *P. gingivalis*) agar plates under anaerobic conditions at 37°C.

Typically, bacteria were grown for 3–4 days and the number of bacteria from 1 agar plate was enough for isolation of genomic DNA.

Cloning vectors

Yeast shuttle cloning vector pYES1 linearized (pYES1L) was supplied with the GeneArt High-Order Genetic Assembly Kit (Life Technologies sp. z o.o.). Bacterial subcloning vectors were obtained from the TOPO XL-2 Cloning Kit (Life Technologies sp. z o.o.) or the NEB PCR Cloning Kit (Lab-Jot sp. z o.o.). Destination vectors: pACYC-DUET-1, pETDUET-1, pRSFDuet-1, and pCDFDuet-1 were purchased from Merck (Merck Life Sciences sp. z o.o.).

Site-directed mutagenesis

The procedure was performed with GeneArt Site-Directed Mutagenesis Kit (Life Technologies sp. z o.o.) on plasmids with size up to 13 kb or with Q5 Site-Directed Mutagenesis Kit (Lab-Jot sp. z o.o.) on longer plasmids.

Bioinformatics analysis

Reconstructed metabolic networks of bacteria were obtained from the BioCyc database.⁵ Pathways involved in cell wall biosynthesis were selected for *E. coli* as a reference and compared with *P. gingivalis* pathways. Due to a later revision of the originally deposited genome assembly for *P. gingivalis* ATCC 33277, the hits were corrected manually. Genes identified as potential hits were analyzed with PathwayTools software available within the BioCyc database to identify operons and other genes potentially involved in LPS biosynthesis in *P. gingivalis*.

Since the database does not have identified pathways for LPS biosynthesis besides for *E. coli*, an additional search was performed within the Prokaryotic Operon Database ProOpDB⁴⁴ to identify genes involved in LPS biosynthesis.

The final assignment was performed by comparing whole genomes with the Mauve tool⁴⁵ using *E. coli* K-12 as a reference strain and *P. gingivalis* W83 strain, in which some genes involved in LPS biosynthesis have already been identified.²⁸

Genomic DNA isolation

Whole genome nucleic acids were isolated from a single Q agar plate using a Genomic Mini kit from A&A Biotechnology (A&A Biotechnology, Gdynia, Poland).

DNA cloning and assembly

Genes assigned as having roles in LPS biosynthesis were amplified with Platinum Superfine (Life Technologies sp. z o.o.) or Q5 Hot Start (Lab-Jot sp. z o.o.) DNA polymerases according to manufacturer's instructions, separated on an agarose gel, excised, and extracted with Monarch

DNA Gel Extraction kit (Lab-Jot sp. z o.o.). Polymerase chain reaction (PCR)-amplified genes were used directly for subassembly of smaller parts or subcloned into appropriate vectors using the TOPO XL-2 Cloning Kit (Life Technologies sp. z o.o.) or the NEB PCR Cloning Kit (Lab-Jot sp. z o.o.).

pACYC/pET/pCDFDuet-1 vectors assembly

Assembly of fragments was performed with the GeneArt High-Order Genetic Assembly System (Life Technologies sp. z o.o.) according to manufacturer's instructions. The 1st assembly was performed in the yeast strain MaV203 with up to 6 inserts/vector and the fragment order was verified with a single colony PCR amplification using primers spanning putative fragment junctions. The product size was selected not to exceed 600–700 bp due to the known restrictions of the PCR approach. In the 2nd round, the fragments were reassembled into the yeast pYES1L vector to obtain a single fragment. The 3rd assembly stage used that fragment and the destination vector. As before, the verification was performed with a single colony PCR. The final construct was verified using Sanger DNA sequencing on fragments amplified by PCR.

The strategy with the yeast shuttle vector created problems at the 3rd assembly stage when moving the constructs into *E. coli*. Therefore, it was decided to use up to 3 fragments per assembly directly in *E. coli* employing the GeneArt Plus Seamless Assembly System (Life Technologies sp. z o.o.). Fragments were amplified directly from genomic DNA with the 2nd fragment typically preceded by an internal ribosome entry sites (IRES) sequence and assembled into the expression vectors according to the manufacturer's instructions. Gene order was verified with PCR of junction sequences and the ends were verified by partial DNA sequencing. Due to the length of constructs and general difficulties with amplification of long DNA fragments, attempts to fully sequence the constructs were not successful. The final strategy was as follows: The gene fragment pl, corresponding to the modified antigen for the pRSFDuet-1 vector, was codon-optimized for *E. coli* and synthesized using GenScript. The *pglB* gene was cloned from *C. jejuni* genomic DNA using NEB PCR cloning kit (New England Biolabs), mutated to contain RR>DL replacement³⁵ and assembled into pRSFDuet-1 using GeneArt Genetic Assembly System (Life Technologies sp. z o.o.) according to the manufacturer's instructions. The remaining genes for pACYC-Duet-1, pCDFDuet-1 and pETDuet-1 vectors were cloned from the genomic DNA of *P. gingivalis* ATCC 33277 strain (gingipain fragments, LPS biosynthetic pathway genes) using standard molecular biology techniques.

Protein expression and purification

Plasmids pACYCDuet-1, pETDuet-1, pRSFDuet-1, and pCDFDuet-1 with cloned inserts were transformed into BL21(DE3) chemically competent cells according

to the manufacturer's instructions. Clones were selected on Luria–Bertani or Miller–Hinton agar plates supplemented with chloramphenicol (25 µg/mL), ampicillin (50 µg/mL), kanamycin (50 g/µmL), and spectinomycin (50 µg/mL).

To express proteins, a single colony from the selection plate was added to 3 mL of lysogeny broth (LB) medium supplemented with antibiotics and grown at 37°C with constant shaking (150 rpm; Excella 24R; Excella, Hamburg, Germany) overnight. The next day, 300 µL of the culture was added to a fresh 30 mL LB medium supplemented with antibiotics and grown at 37°C with constant shaking for about 2–3 h to become visibly turbid (optical density (OD) 600 = 0.4–0.6). The culture was added to 3 L of Terrific Broth (TB; Thermo Fisher Scientific) medium in baffled flasks supplemented with antibiotics and grown as before to reach OD600 = 0.4–0.6. At this point, the culture was cooled down at room temperature for about 30 min and isopropyl β-D-1-thiogalactopyranoside (IPTG) was added to a final concentration of 0.2 mM. The culture was incubated again at 18°C with vigorous shaking (300 rpm; Excella 24R) for 16–20 h. The cells were harvested by centrifugation at 12,000 × g, 4°C for 30 min (Sorvall Lynx 6000 centrifuge, and Fiberlite F12- 6x500 LEX rotor; Thermo Fisher Scientific). The combined cell paste was stored at –80°C for processing.

The frozen cells from a 3L bacterial culture were thawed by warming at room temperature for about 30 min and resuspended in 200 mL of ice-cold extraction buffer (20 mM Tris-HCl, pH = 8.0, 0.5 M NaCl, 10% v/v glycerol, 20 mM imidazole, pH = 8.0, 1 mM tris(2-carboxyethyl) phosphine (TCEP)-HCl, 1 mM ethylenediaminetetraacetic acid (EDTA)) supplemented with Complete EDTA-Free (Roche, Basel, Switzerland) protease inhibitor cocktail according to manufacturer's recommendations. The cells were disrupted by sonication on ice (3 cycles of a 30 s burst followed by a 30-s cooling period; Ultrasonic Disintegrator model UD-11, power level 4; Techpan sp. z o.o., Puławy, Poland) and centrifuged at 50,000 × g at 4°C for 1 h using a Sorvall LYNX 6000 (A27-8x50 rotor; Thermo Fischer Scientific) centrifuge.

The supernatant was collected, and MgCl₂ was added to a final concentration of 5 mM to complex with EDTA. The mixture was loaded directly onto a preequilibrated Ni-agarose column (5 × 5 mL HisTrap crude + 1 × HisPrep FF 16/10) connected to an AKTA START (GE Healthcare, Chicago, USA) system at 1–2 mL/min flow rate of the loading buffer (20 mM Tris-HCl, pH = 8.0, 0.5 M NaCl, 10% v/v glycerol, 20 mM imidazole, pH = 8.0, 1 mM TCEP-HCl), and the column was washed with 5 column volumes (CV) of the loading buffer and developed with a stepwise elution by imidazole: 5 CV of loading buffer with 20, 250 and 500 mM imidazole, pH = 8.0. Fractions were analyzed with sodium dodecyl sulfate–polyacrylamide gel electrophoresis (SDS-PAGE), subjected to rapid buffer exchange on desalting columns (2 × HiPrep 26/20 Desalting) against

buffer A (10 mM Tris-HCl, pH = 8.0, 10% v/v glycerol, 1 mM TCEP-HCl) and loaded onto Q Sepharose anion exchanger (5 × 5 mL HiTrap Q Sepharose HP) at 2 mL/min flow rate. The column was washed with 5 CV of buffer A and developed with a 0–100% gradient of buffer B (buffer A + 1 M NaCl) over 20 CV at 2 mL/min flow rate. Column fractions were examined with SDS-PAGE, and positive fractions, as judged by molecular weight and western blotting results with anti-gingipain and anti-His antibodies, were diluted with an equal volume of hydrophobic interactions chromatography (HIC) buffer A (2 M ammonium sulfate, 10% glycerol v/v, 10 mM Tris-HCl, pH = 8.0, 1 mM TCEP-HCl) and loaded onto HiScreen Phenyl HP column (1 × 4.7 mL; GE Healthcare) at 1 mL/min flow rate. The column was washed with 3 CV of HIC buffer A and developed with a 0–100% gradient of HIC buffer B (HIC buffer A without ammonium sulfate) at 1 mL/min flow rate. Fractions were examined using SDS-PAGE for molecular weight and reactivity with anti-His and anti-gingipain antibodies. Positive fractions were pooled and stored at –20°C for further examinations.

SDS-PAGE and western blotting

The protein electrophoresis was routinely performed on 10% acrylamide gels using the FastCast premixed solutions (Bio-Rad) or MiniProtean TGX precast 4–20% 10-well minigels (Bio-Rad) according to the manufacturer's recommendations. All gels were run under reducing conditions and protein detection was performed with NOVEX Colloidal Blue Staining Kit (Life Technologies sp. z o.o.). To detect proteins by specific antibodies, the gels were transferred to a 0.22-μm Whatman Westran S polyvinylidene difluoride (PVDF) (Sigma-Aldrich, Merck Life Sciences sp. z o.o.) or a 0.45-μm Pierce nitrocellulose (Life Technologies sp. z o.o.) membrane using a MiniProtean Western Blotting wet transfer module (Bio-Rad) either overnight or for 1 h, according to the manufacturer's recommendations.

Western blotting

Following wet transfer, samples were incubated with primary antibodies in blocking buffer (3% non-fat dry milk, 0.05% Tween-20 in 1× Tris-buffered saline, pH 8.0) for at least 2 h at room temperature or overnight at 4 °C. The antibodies were used at the following dilutions: α-His – 1:2,000; α-gingipain – 1:5,000; α-LPS IgG – 1:5,000; and α-LPS IgM – 1:2,000.

After washing 5 times with 10 mL 1 × TBST for 5 min, the membranes were incubated with secondary antibodies coupled to biotin diluted 1:10,000 for 2 h at room temperature, washed again with 1 × Tris-buffered saline with Tween (TBST) as before and incubated with a 1:500,000 diluted streptavidin-horseradish peroxidase (HRP) conjugate for 2–3 h at room temperature. The membranes were washed 7 times with 10 mL of 1 × TBST and additionally 2 times

with 1 × TBS. Drained membranes were overlaid with TMB Enhanced One Component HRP Membrane Substrate (Sigma-Aldrich, Merck Life Sciences sp. z o.o.) or Pierce 1-Step ULTRA Blotting Solution (Life Technologies sp. z o.o.), according to the manufacturer's recommendations. Developed membranes were visualized using an in-house imaging system based on Nikon D7100 camera equipped with an AF-S Micro Nikkor 60 mm 1:2.8 G ED lens (Nikon Corp., Tokyo, Japan). Images were transferred to a laptop with NikonTransfer2 software, converted to a *.tiff format with Adobe CS2 software (Adobe Inc., San Jose, USA) and saved for further manipulation. Due to the overall blue background of the TMB substrate, the images were minimally enhanced to remove the background.

Results

General strategy

The overall concept for the formation of neoglycoconjugate composed of *P. gingivalis* gingipain and O-antigen is presented in Fig. 1. The original biosynthetic pathway responsible for the synthesis of O-specific antigen (Fig. 1A) was identified via systems biology analysis and then transferred into *E. coli*. The host's *waaL* ligase gene was removed and replaced with an engineered *pglB* glycosyltransferase gene from *C. jejuni* (Fig. 1B).

Genome analysis and pathways identification

Analysis of the genome of *P. gingivalis* strain ATCC 33277 was performed with BioCyc software PathwayTools.⁵ The search identified conserved genes based on the putative function assignment according to the Kyoto Encyclopedia of Genes and Genomes (KEGG) database of metabolic pathways.⁴⁶ However, the analysis was limited in scope as the similarity of genes between the BioCyc reference, *E. coli* K-12 strain and the *P. gingivalis* ATCC 33277 genome was too low to have an unambiguous assignment. Therefore, the *P. gingivalis* genome was analyzed again using the prokaryotic operon database ProOpDB⁴⁴ to identify putative operons involved in LPS biosynthesis (KEGG pathway 0540). The performance was verified on known *E. coli* genomes and the cataloged pathways available in EcoCyc⁶ and KEGG databases.⁴⁶ The result of the analysis of the *P. gingivalis* genome was again compared with the genome of *E. coli* K-12 strain to identify genes with a function similar to the *E. coli* genes involved in LPS synthesis (EcoCyc database). The results were compared by whole genome alignment of *E. coli* and *P. gingivalis* W83, W50 and ATCC 33277 genomes to find potential rearrangements. The final results identified 36 genes belonging to 8 metabolic pathways (Table 1). Only 1 gene was identified directly as involved

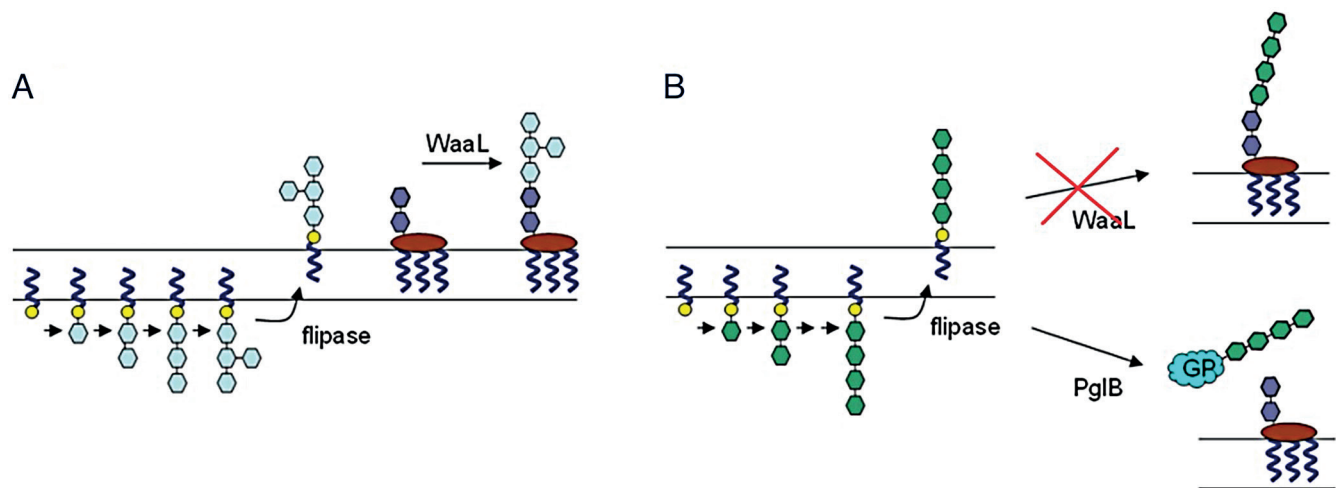


Fig. 1. A simplified scheme of the proposed strategy for genetically engineering *Escherichia coli* to produce recombinant O-antigens of *Porphyromonas gingivalis*. **A.** In the parental *E. coli* strain, lipopolysaccharide (LPS) biosynthesis begins with the assembly of the O-specific polysaccharide unit on the carrier lipid undecaprenyl phosphate. This unit is subsequently transported to the periplasm, where polymerization occurs and the completed O-antigen chain is transferred to the lipid A-core by the endogenous WaaL ligase. **B.** In the engineered *E. coli* strain, the native O-antigen biosynthetic genes are deleted and replaced with a gene cluster encoding the *P. gingivalis* O-antigen. In this modified background, O-antigen chains are no longer transferred to the lipid A-core via WaaL, but instead conjugated to a recombinant gingipain (GP) protein engineered to contain an N-glycosylation motif. This enables transfer of the O-antigen to the protein via the *Campylobacter jejuni* PglB oligosaccharyltransferase, resulting in the formation of a gingipain–O-antigen glycoconjugate

in O-antigen biosynthesis (*pgn0223*) and 2 in capsular antigen biosynthesis (*pgn1524*→*pgn1525*). The Lipid IVA biosynthesis genes (*pgn0206*, *pgn0544*), as well as the dTDP-L-rhamnose biosynthetic pathway I genes (*pgn0546*→*pgn0549*) were also identified. The former is a part of a broader lipid IVA biosynthesis pathway, while the latter is the common enterobacterial antigen biosynthesis pathway identified using the PathwayTools software in the BioCyc database.

The *pgn1243* gene product (Table 1) is involved in O-antigen biosynthesis in many Gram-negative bacteria. The gene is part of a larger operon *pgn1245*→*pgn1240* (BioCyc database, PathwayTools prediction). In *E. coli*, the ortholog of *pgn1243* is involved in the production of colanic acid,⁴⁷ a part of the *E. coli* capsular antigen. Transposon mutagenesis of *P. gingivalis* showed that the gene is essential for LPS biosynthesis.⁴⁸

Gene *pgn1251* has a dual function in type A and type O LPS biosynthesis in *P. gingivalis*.⁴⁹ It is also essential for pathogen growth.^{50,51} Genes *pgn0361*, *pgn1239*→*pgn1240* and *pgn1668* have been shown to be involved in type A LPS biosynthesis.⁵² Due to technical problems with assembling different operons in *E. coli* (described later), the genes *pgn0361* and *pgn1668* are not listed in Table 1 despite having been identified in the ProOpDB search.

Genes *pgn0223*→*pgn0244* form an operon (BioCyc, PathwayTools). The *pgn0223* ortholog is involved in lipid and common enterobacterial antigen biosynthesis in *E. coli*.⁵³ Genes *pgn0224*→*pgn0229* are part of an operon (BioCyc database, PathwayTools software) whose members (WecC, RfaB) have orthologs in *E. coli* genome and are involved in bacterial lipid biosynthesis (KEGG pathways database).

Gene *pgn0234* (Table 1) codes an enzyme involved in the biosynthesis of the common enterobacterial

in *E. coli*.^{54,55} The *E. coli* operon has orthologs corresponding to only 2 genes, *pgn0233* and *pgn0234*, from the *P. gingivalis* ATCC 33277 strain genome (BioCyc database, PathwayTools software).

Gene *pgn0206* is part of a lipid IVA biosynthesis pathway (PGN_RS00965). The pathway is highly conserved in bacteria and could easily be identified in *P. gingivalis* due to the protein sequence similarity (BioCyc database, PathwayTools software).

Antigen identification and engineering

The choice of antigen for the vaccine construct was based on the literature data. *Porphyromonas gingivalis* secretes gingipains, Kgp and Rgp, which have been shown to be responsible for bone destruction and a general host protein proteolysis.¹⁷ Gingipains also contain cell adhesion domains that interact with proteins in the gum matrix, facilitating bacterial colonization.⁵⁶ Since the whole gingipain is too large a protein for seamless recombination, fragments corresponding to the catalytic domain of Rgp gingipain have been used in fusion with the cell adhesion fragments (Fig. 2).

The O-specific antigen is a substrate for the WaaL ligase that transfers the newly synthesized polysaccharide onto lipid A core oligosaccharide, a key step in LPS synthesis (Fig. 1). Short forms of LPS (composed of Lipid A and core oligosaccharide) are present in rough serotypes of Gram-negative bacteria. Therefore, WaaL activity is not requisite for survival. To prevent O-antigen attachment to the LPS, the *waaL* gene was removed. The resulting strain of modified *E. coli* BL21(DE3) exhibited poor growth and was not stable in the presence of ampicillin, despite having an engineered β -lactamase gene as a resistance marker. Since

Table 1. Partial list of genes identified in database searches

Gene ID	Predicted gene function	Predicted pathway
Pgn0545	LTN synthase	none
Pgn0546	glucose-1-phosphate thymidyltransferase rmlA	dTDP-L-rhamnose biosynthesis I
Pgn0547	dTDP-4-dehydrorhamnose 3,5-epimerase	dTDP-L-rhamnose biosynthesis I
Pgn0548	NAD(P)-dependent oxidoreductase	dTDP-L-rhamnose biosynthesis I
Pgn0549	dTDP-glucose 4,6-dehydratase	dTDP-L-rhamnose biosynthesis I
Pgn1239	glycosyltransferase family 2	LPS type A biosynthesis ⁵²
Pgn1240	glycosyltransferase RfaB	LPS type A and type O biosynthesis ⁵²
Pgn1241	MULTISPECIES: hypothetical proteinpgn_RS05960	none
Pgn1242	exopolysaccharide biosynthesis protein (EpsG)	none
Pgn1243	UDG-glucose 6-dehydrogenase	UDP- α -D-glucuronate biosynthesis (from UDP-glucose)
Pgn1244	protein release chain factor B	none
Pgn1245	long-chain-fatty-acid-Co-A ligase	multiple (fatty acids biosynthesis)
Pgn1246	hypothetical protein PGN_RS05985	none
Pgn1250	hypothetical protein PGN_RS05990	none
Pgn1251	glycosyltransferase RfaB	type A and type O LPS biosynthesis ⁴⁹
Pgn1523	polysaccharide export outer membrane protein	polysaccharide transport
Pgn1524	capsule biosynthesis protein (CapM)	capsule biosynthesis
Pgn1525	capsular polysaccharide biosynthesis protein	capsule biosynthesis
Pgn0223	undecaprenyl-phosphate N-acetylglucosamine 1-phosphate transferase WecA	O-antigen biosynthesis/lipid biosynthesis
Pgn0224	UDP-N-acetyl-D-mannosamine dehydrogenaseWecC	UDP-N-acetyl- α -D-mannosaminouronate biosynthesis
Pgn0225	glycosyltransferase	none
Pgn0226	hypothetical protein PGN_RS01085	none
Pgn0227	glycosyltransferase family 1 RfaB	none
Pgn0228	coenzyme F390 synthetase	none
Pgn0229	histidinol phosphate phosphatase	L-histidine biosynthesis
Pgn0230	serine O-acetyltransferase	none
Pgn0231	aminolaevulinic acid dehydrogenase	none
Pgn0232	glycosyltransferase family 2	none
Pgn0233	glycosyltransferase	none
Pgn0234	UDP-N-acetylglucosamine 2-epimerase (non-hydrolyzing)	UDP-N-acetyl- α -D-mannosaminouronate biosynthesis
Pgn0206	lipid-A-disaccharide synthase	lipid IVa biosynthesis
Pgn0376	3-deoxy-8-phosphooctulonate synthase	LPS biosynthesis
Pgn0544	3-deoxy-D-manno-octulosonic acid transferase	lipid IVa biosynthesis
Pgn0696	HAD-IIIa family hydrolase	none
Pgn1750	3-deoxy-manno-octulosonate cytidyltransferase	LPS biosynthesis
Pgn2086	lysophospholipid acyltransferase family protein	lipid A biosynthesis

LTN – lysine-tRNA ligase; rmlA – rhamnose metabolism locus; dTDP – deoxythymidine diphosphate; NAD(P) – nicotinamide adenine dinucleotide (phosphate); LPS – lipopolysaccharide; RfaB – lipopolysaccharide glucosyltransferase I; UDP – uridine diphosphate; WecA – undecaprenyl-phosphate α -N-acetylglucosaminyl 1-phosphate; WecC – UDP-N-acetyl-D-mannosamine dehydrogenase; HAD – haloacid dehalogenase.

the final construct was supposed to have multiple vectors, each with a separate resistance marker and a replication origin, it was decided to abandon the strategy assuming removal of the *waal* gene from *E. coli*. Instead, the protein acceptor was modified with a removable 6xHis affinity tag to facilitate product purification on His tag affinity column.

Attachment of O-antigen was engineered to proceed to a triplicate DYNAT sequence previously used for glycosylation in bacteria. The strategy used here employed a modified *C. jejuni* *pglB* gene having a DL (aspartic acid, leucine) mutation introduced to relax the transfer specificity and increase the efficiency of produced glycoconjugates.^{35,36} Finally, the engineered *E. coli* BL21(DE3)

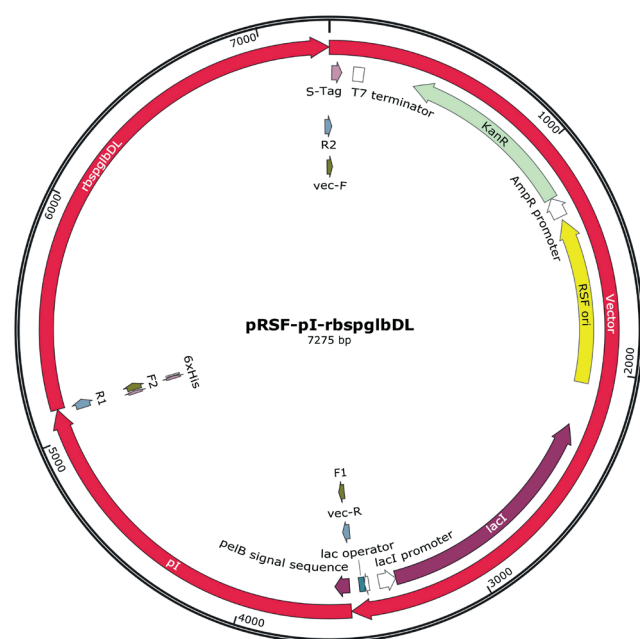


Fig. 2. Map of the pRSFDuet vector containing the cloned *Porphyromonas gingivalis* antigen gene *pl* and the *Campylobacter jejuni* glycosyltransferase gene protein glycosylation locus B (*pglB*). The *pl* gene is a synthetic construct codon-optimized for expression in *Escherichia coli*. The *pglB* gene was cloned from *C. jejuni* genomic DNA and modified by introducing a double RR → DL mutation, as detailed in the Materials and Methods section

R – arginine D – aspartic acid L – leucine.

strain has 2 parallel active pathways for the attachment of O-antigen in the original *E. coli* pathway and the modified pathway from *P. gingivalis* exerted by the mutated PglB protein. Since the PglB is a membrane protein, the original antigen containing gingipain sequence fragments was modified to include a periplasmic secretion signal *pelB* attached to the N-terminus (Fig. 2).

Genetic assembly and pathway reconstruction

The number of genes and the length of the potential construct were not optimal for a single vector. It was decided that the genes would be split into 4 separate vectors: pRSFDuet-1, pETDuet-1, pCDFDuet-1, and pACYCDuet-1. The vectors allow stable co-expression of up to 8 gene fragments under the control of separate T7 promoters⁵⁷ and the strategy has been used in the past by different groups.^{58,59}

The sequences were arranged to conserve transcription order with linkers followed by ribosomal binding sites attached to new reading frames. The final gene arrangements in the pCDFDuet, pETDuet and pACYCDuet vectors, each containing genes involved in *P. gingivalis* LPS biosynthesis, are presented in Fig. 3.

Protein expression, purification and analysis

Assembled plasmids were used for protein expression in *E. coli* BL21(DE3) strain. The presence of all 4 plasmids

significantly reduced bacterial growth. Initial attempts to grow the cells at 37°C during the induction phase were not successful due to protein degradation. Also, the main protein band detected in total cell lysate corresponded to a lower molecular weight species when examined using anti-His antibodies. Therefore, the cells were grown in TB medium at 37°C without induction and cooled down to room temperature before adding IPTG. The growth temperature was also lowered to 18°C to allow for protein induction while preventing protein degradation. The strategy resulted in a soluble protein after the first Ni-agarose purification.

However, the main anti-His band corresponded to a lower molecular weight, most likely the non-glycosylated product. Due to the low sensitivity of anti-LPS antibodies, the potentially derivatized antigen band at around 70 kDa was not visible on the same blot. The main protein fraction eluting at 250 mM imidazole was subsequently dialyzed and further purified using an anion exchange column. At this stage, the protein could be detected in the fractions eluting at around 150 mM NaCl concentration (Fig. 4A).

The pooled fractions were subsequently applied to a high-resolution hydrophobic interaction chromatography (HIC) column – HiScreen Phenyl Sepharose. The protein eluted near the end of the salt gradient (Fig. 4B), indicating a high degree of hydrophobicity. This observation was supported by computational modeling and molecular dynamics (MD) simulations, which suggested that the protein likely forms a stable dimer.

Final protein purity was assessed with SDS-PAGE using the Colloidal Blue Staining Kit (Life Technologies sp. z o.o.). The purified protein exceeded 99% purity (Fig. 4A, G) and displayed an apparent molecular weight of approx. 70 kDa (Fig. 4G). It was also successfully derivatized with the O-antigen from *P. gingivalis* strains W83 (Fig. 4C) and ATCC 33277 (Fig. 4D), and incorporated the fused *pl* antigen (Fig. 4F).

Discussion

Periodontal diseases are an increasingly prevalent health concern influenced by multiple factors. Chief among these are poor oral hygiene and high consumption of refined sugars, especially in children, which together foster the proliferation of pathogenic oral microbiota, ultimately contributing to alveolar bone resorption and dental caries.^{60,61} At least 3 major bacterial pathogens are implicated in human periodontal disease, with *P. gingivalis* emerging as one of the most prominent.⁶² Currently, no commercial vaccine is available, and ongoing research is focused on developing effective vaccination strategies.^{22,63,64} Several protein antigens have been proposed as vaccine targets. Notably, studies on vaccines against other Gram-negative bacteria have demonstrated that bacterial polysaccharides, particularly when conjugated to a protein carrier, can serve

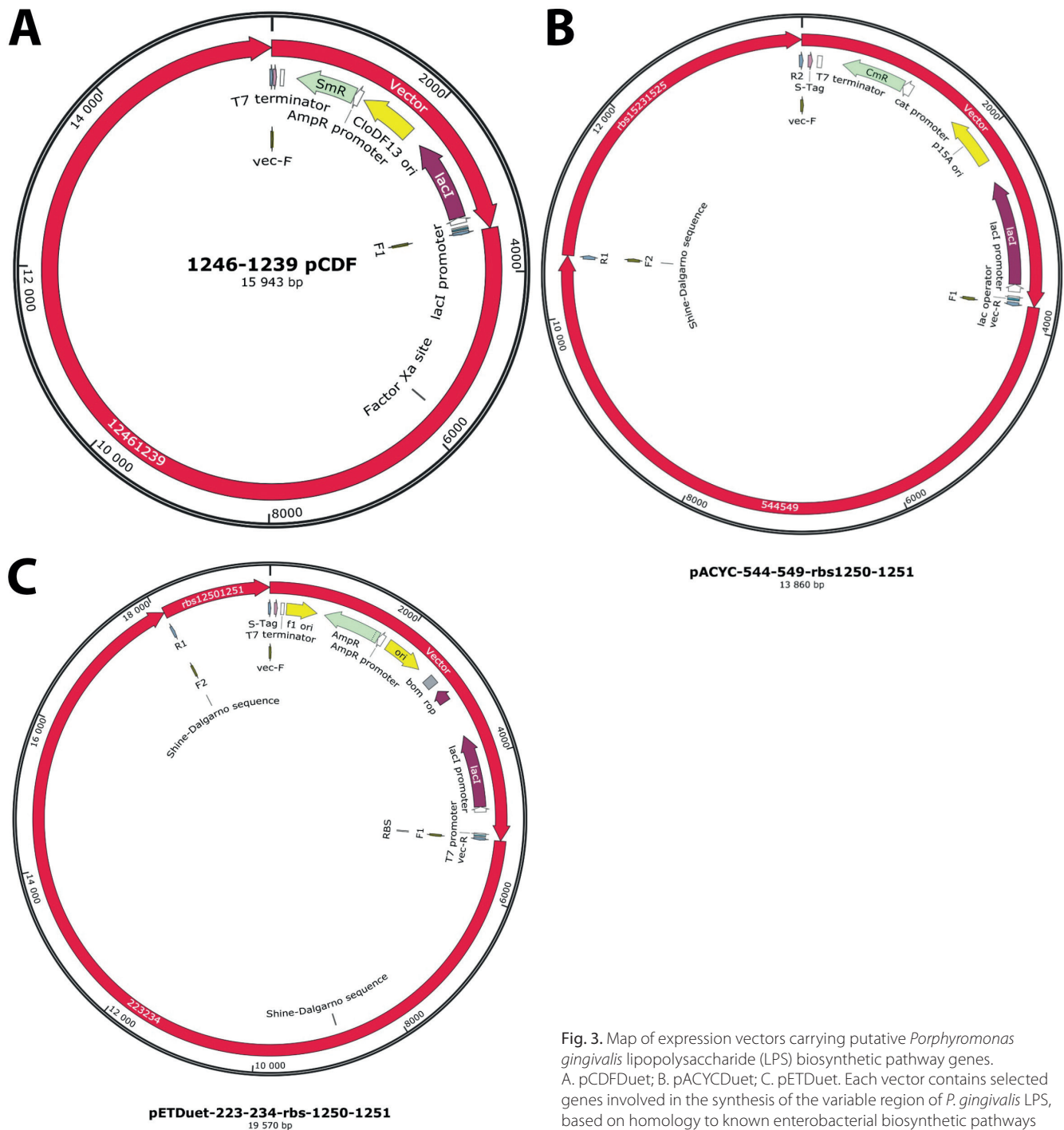


Fig. 3. Map of expression vectors carrying putative *Porphyromonas gingivalis* lipopolysaccharide (LPS) biosynthetic pathway genes. A. pCDFDuet; B. pACYCDuet; C. pETDuet. Each vector contains selected genes involved in the synthesis of the variable region of *P. gingivalis* LPS, based on homology to known enterobacterial biosynthetic pathways

as highly effective immunogens. The O-antigen portion of LPS is particularly preferred, as it is highly strain-specific. Targeting the O-antigen helps minimize the risk of generating antibodies that cross-react with commensal bacterial flora.

Vaccine design strategies based on systems biology approaches to reconstruct putative bacterial pathways remain in the early stages of development. In particular, efforts to map carbohydrate biosynthetic pathways are often constrained by the limited experimental validation of *in silico* predictions, leading to significant gaps in available data.

In silico metabolic reconstruction of *P. gingivalis* polysaccharide biosynthetic pathways began shortly after the organism's genome was sequenced.² These analyses predicted the existence of 3 major extracellular carbohydrate components; however, to date, experimental evidence has confirmed only 2: type A and type O LPS.^{25,26} The identification of additional components involved in LPS biosynthesis has largely been based on gene-level analysis, focusing on genes homologous to those in the well-characterized LPS biosynthetic pathways of enterobacteria (Table 1).

To facilitate the identification of vaccine candidates against *P. gingivalis*, the pathogen's complete metabolome

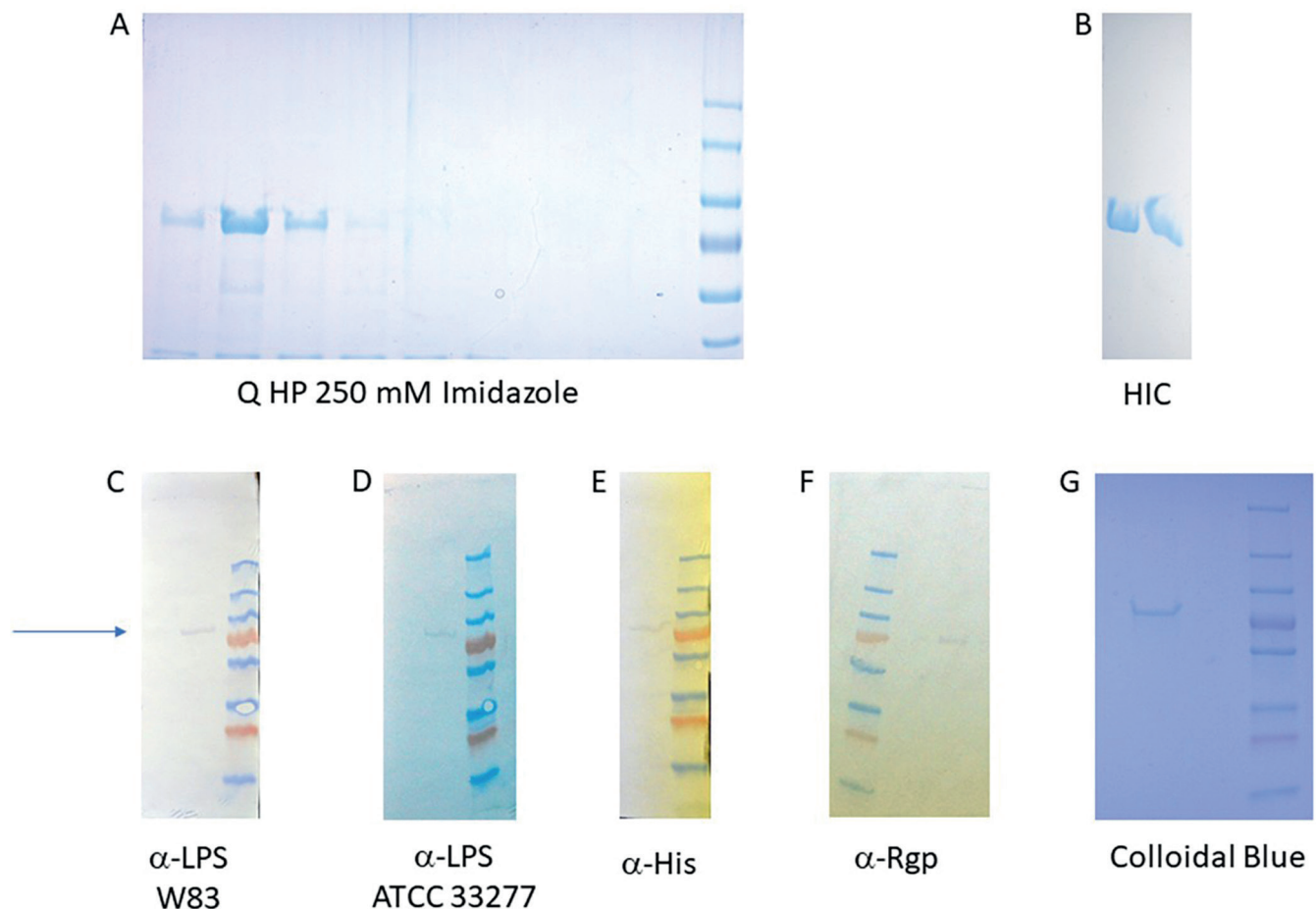


Fig. 4. Purification and immunological characterization of the pl antigen derivatized with carbohydrates from *Porphyromonas gingivalis* American Type Culture Collection (ATCC) 33277. A. Anion exchange chromatography fractions (Sephacel Q HP); B. Hydrophobic interaction chromatography (HIC) fractions (HiScreen Phenyl Sepharose); C–F. Western blot analysis of pooled HIC fractions using the following antibodies: C. α -LPS IgG (raised against *P. gingivalis* W83); D. α -LPS IgM (raised against *P. gingivalis* ATCC 33277); E. α -His tag antibody; F. α -Arg-type gingipain antibody; G. Total protein staining with the Colloidal Blue Kit. Experimental procedures are described in detail in the Materials and Methods section

His – Histidine; Arg – Arginine; LPS – lipopolysaccharide; IgG – immunoglobulin G; Q – quaternary amine, HP – high-performance.

was reconstructed using in silico methods. Genes associated with the synthesis of the variable region of LPS were selected and introduced into *E. coli* (Table 1). Because many biosynthetic components are conserved between *E. coli* and *P. gingivalis*, gene selection was deliberately limited to reduce vector load and maintain plasmid stability (Fig. 2,3). Antigen conjugation was also designed in *E. coli* by the inclusion of a mutated PglB enzyme to couple synthesized carbohydrate coats to the antigen (Fig. 1). Unfortunately, removal of the competing *waaL* ligase gene from *E. coli* was not possible due to its detrimental effect on the survival of the host. Therefore, the mixture of the pl antigen derivatized with *P. gingivalis* and *E. coli* carbohydrates were separated chromatographically to a very high degree and the purified antigen was confirmed to contain the *P. gingivalis* O-antigen (Fig. 4C,D). Due to a low amount of protein, attempts to determine carbohydrate structure were not undertaken.

While experimental verification of the full biosynthetic pathways proposed in this study was not conducted, selected components have been identified by other researchers

(Table 1 and the Results section). The final product was most likely assembled correctly, as it was recognized by LPS-specific antibodies (Fig. 4C,D). This strategy provides a proof-of-concept for designing future vaccine candidates without the need for toxoid conjugation or large-scale cultivation of pathogenic bacteria to isolate LPS. If the candidate demonstrates protective efficacy in an animal model of periodontitis, the approach could enable faster and safer vaccine development for a wide range of pathogens. Preparations for in vivo verification of the proposed periodontitis vaccine candidate are currently underway.

Conclusions

Although we faced some issues during experimentation, the final product was most likely assembled correctly, as the LPS-specific antibodies recognized it. Despite the lack of bacterial opsonization by the generated antibodies, their specificity suggests that the antigenic

presentation was successful, primarily targeting the protein component. If the candidate is confirmed to offer protection in an animal model of periodontitis, the design of future vaccines could be performed faster and more safely for many other pathogens.

Data availability statement

The datasets supporting the findings of the current study are openly available in Zenodo at <https://doi.org/10.6084/m9.figshare.27960216>.

Consent for publication

Not applicable.

Use of AI and AI-assisted technologies

Not applicable.

ORCID iDs

Ewa Brzozowska  <https://orcid.org/0000-0003-0922-3625>
 Wiesław Świętnicki  <https://orcid.org/0000-0002-9354-8184>
 Jordan Sycz  <https://orcid.org/0000-0003-4709-094X>
 Agnieszka Korzeniowska-Kowal  <https://orcid.org/0000-0001-7569-8018>
 Michał Skowicki  <https://orcid.org/0000-0003-1955-5615>
 Tomasz Lipiński  <https://orcid.org/0000-0002-1644-1308>

References

- Nakayama M, Ohara N. Molecular mechanisms of *Porphyromonas gingivalis*-host cell interaction on periodontal diseases. *Jpn Dent Sci Rev*. 2017;53(4):134–140. doi:10.1016/j.jdsr.2017.06.001
- Mazumdar V, Snitkin ES, Amar S, Segre D. Metabolic network model of a human oral pathogen. *J Bacteriol*. 2009;191(1):74–90. doi:10.1128/JB.01123-08
- Acuña-Amador L, Primot A, Cadieu E, Roulet A, Barloy-Hubler F. Genomic repeats, misassembly and reannotation: A case study with long-read resequencing of *Porphyromonas gingivalis* reference strains. *BMC Genomics*. 2018;19(1):54. doi:10.1186/s12864-017-4429-4
- Naito M, Hirakawa H, Yamashita A, et al. Determination of the genome sequence of *Porphyromonas gingivalis* strain ATCC 33277 and genomic comparison with strain W83 revealed extensive genome rearrangements in *P. gingivalis*. *DNA Res*. 2008;15(4):215–225. doi:10.1093/dnares/dsn013
- Karp P, Billington R, Holland T, et al. Computational metabolomics operations at BioCyc.org. *Metabolites*. 2015;5(2):291–310. doi:10.3390/metabo5020291
- Karp PD, Riley M, Paley SM, Pellegrini-Toole A, Krummenacker M. EcoCyc: Encyclopedia of *Escherichia coli* genes and metabolism. *Nucleic Acids Res*. 1997;25(1):43–50. doi:10.1093/nar/25.1.43
- Grover V, Kapoor A, Malhotra R, Kaur G. *Porphyromonas gingivalis* antigenic determinants: Potential targets for the vaccine development against periodontitis. *Infect Dis Drug Targets*. 2014;14(1):1–13. doi:10.2174/1871526514666140827100930
- Yonezawa H, Kato T, Kuramitsu HK, Okuda K, Ishihara K. Immunization by Arg-gingipain A DNA vaccine protects mice against an invasive *Porphyromonas gingivalis* infection through regulation of interferon- γ production. *Oral Microbiol Immunol*. 2005;20(5):259–266. doi:10.1111/j.1399-302X.2005.00220.x
- O'Brien-Simpson NM, Pathirana RD, Paolini RA, et al. An immune response directed to proteinase and adhesin functional epitopes protects against *Porphyromonas gingivalis*-induced periodontal bone loss. *J Immunol*. 2005;175(6):3980–3989. doi:10.4049/jimmunol.175.6.3980
- Zhang P, Yang QB, Balkovetz DF, et al. Effectiveness of the B subunit of cholera toxin in potentiating immune responses to the recombinant hemagglutinin/adhesin domain of the gingipain Kgp from *Porphyromonas gingivalis*. *Vaccine*. 2005;23(39):4734–4744. doi:10.1016/j.vaccine.2005.05.004
- Frazer LT, O'Brien-Simpson NM, Slakeski N, et al. Vaccination with recombinant adhesins from the RgpA–Kgp proteinase–adhesin complex protects against *Porphyromonas gingivalis* infection. *Vaccine*. 2006;24(42–43):6542–6554. doi:10.1016/j.vaccine.2006.06.013
- Puth S, Hong SH, Park MJ, et al. Mucosal immunization with a flagellin-adjuvanted Hgp44 vaccine enhances protective immune responses in a murine *Porphyromonas gingivalis* infection model. *Hum Vaccin Immunother*. 2017;13(12):2794–2803. doi:10.1080/21645515.2017.1327109
- Kim TG, Huy NX, Kim MY, et al. Immunogenicity of a cholera toxin B subunit *Porphyromonas gingivalis* fimbrial antigen fusion protein expressed in *E. coli*. *Mol Biotechnol*. 2009;41(2):157–164. doi:10.1007/s12033-008-9102-3
- Choi JI, Schifferle RE, Yoshimura F, Kim BW. Capsular polysaccharide-fimbrial protein conjugate vaccine protects against *Porphyromonas gingivalis* infection in SCID mice reconstituted with human peripheral blood lymphocytes. *Infect Immun*. 1998;66(1):391–393. doi:10.1128/IAI.66.1.391-393.1998
- Ross BC, Czajkowski L, Hocking D, et al. Identification of vaccine candidate antigens from a genomic analysis of *Porphyromonas gingivalis*. *Vaccine*. 2001;19(30):4135–4142. doi:10.1016/S0264-410X(01)00173-6
- Kadowaki T, Yoneda M, Okamoto K, Maeda K, Yamamoto K. Purification and characterization of a novel arginine-specific cysteine proteinase (argingipain) involved in the pathogenesis of periodontal disease from the culture supernatant of *Porphyromonas gingivalis*. *J Biol Chem*. 1994;269(33):21371–21378. PMID:8063764.
- O'Brien-Simpson N, Veith P, Dashper S, Reynolds E. *Porphyromonas gingivalis* gingipains: The molecular teeth of a microbial vampire. *Curr Protein Pept Sci*. 2003;4(6):409–426. doi:10.2174/1389203033487009
- Boisvert H, Duncan MJ. Clathrin-dependent entry of a gingipain adhesin peptide and *Porphyromonas gingivalis* into host cells. *Cell Microbiol*. 2008;10(12):2538–2552. doi:10.1111/j.1462-5822.2008.01228.x
- Nonaka M, Shoji M, Kadowaki T, et al. Analysis of a Lys-specific serine endopeptidase secreted via the type IX secretion system in *Porphyromonas gingivalis*. *FEMS Microbiol Lett*. 2014;354(1):60–68. doi:10.1111/1574-6968.12426
- Nonaka E, Kiyama-Kishikawa M, Hayakawa M. Identification of 40-kDa outer membrane protein as an aggregation factor of *Porphyromonas gingivalis* to *Streptococcus gordonii*. *J Oral Sci*. 2001;43(4):239–243. doi:10.2334/josnurd.43.239
- Lasica AM, Ksiazek M, Madej M, Potempa J. The type IX secretion system (T9SS): Highlights and recent insights into its structure and function. *Front Cell Infect Microbiol*. 2017;7:215. doi:10.3389/fcimb.2017.00215
- O'Brien-Simpson NM, Holden JA, Lenzo JC, et al. A therapeutic *Porphyromonas gingivalis* gingipain vaccine induces neutralising IgG1 antibodies that protect against experimental periodontitis. *NPJ Vaccines*. 2016;1(1):16022. doi:10.1038/npjvaccines.2016.22
- Yasaki-Inagaki Y, Inagaki S, Yamada S, Okuda K, Ishihara K. Production of protective antibodies against *Porphyromonas gingivalis* strains by immunization with recombinant gingipain domains. *FEMS Immunol Med Microbiol*. 2006;47(2):287–295. doi:10.1111/j.1574-695X.2006.00091.x
- Nakagawa T, Saito A, Hosaka Y, Ishihara K. Gingipains as candidate antigens for *Porphyromonas gingivalis* vaccine. *Keio J Med*. 2003;52(3):158–162. doi:10.2302/kjm.52.158
- Paramonov N, Bailey D, Rangarajan M, et al. Structural analysis of the polysaccharide from the lipopolysaccharide of *Porphyromonas gingivalis* strain W50. *Eur J Biochem*. 2001;268(17):4698–4707. doi:10.1046/j.1432-1327.2001.02397.x
- Rangarajan M, Aduse-Opoku J, Paramonov N, et al. Identification of a second lipopolysaccharide in *Porphyromonas gingivalis* W50. *J Bacteriol*. 2008;190(8):2920–2932. doi:10.1128/JB.01868-07
- Paramonov N, Aduse-Opoku J, Hashim A, Rangarajan M, Curtis MA. Identification of the linkage between A-polysaccharide and the core in the A-lipopolysaccharide of *Porphyromonas gingivalis* W50. *J Bacteriol*. 2015;197(10):1735–1746. doi:10.1128/JB.02562-14

28. Rangarajan M, Aduse-Opoku J, Hashim A, Paramonov N, Curtis MA. Characterization of the α - and β -Mannosidases of *Porphyromonas gingivalis*. *J Bacteriol*. 2013;195(23):5297–5307. doi:10.1128/JB.00898-13
29. Shoji M, Sato K, Yukitake H, Naito M, Nakayama K. Involvement of the Wbp pathway in the biosynthesis of *Porphyromonas gingivalis* lipopolysaccharide with anionic polysaccharide. *Sci Rep*. 2014; 4(1):5056. doi:10.1038/srep05056
30. Costantino P, Rappuoli R, Berti F. The design of semi-synthetic and synthetic glycoconjugate vaccines. *Exp Opin Drug Discov*. 2011;6(10): 1045–1066. doi:10.1517/17460441.2011.609554
31. Pichichero ME. Protein carriers of conjugate vaccines: Characteristics, development and clinical trials. *Hum Vaccin Immunother*. 2013; 9(12):2505–2523. doi:10.4161/hv.26109
32. Shi S, Zhu H, Xia X, Liang Z, Ma X, Sun B. Vaccine adjuvants: Understanding the structure and mechanism of adjuvanticity. *Vaccine*. 2019;37(24):3167–3178. doi:10.1016/j.vaccine.2019.04.055
33. Del Giudice G, Rappuoli R, Didierlaurent AM. Correlates of adjuvanticity: A review on adjuvants in licensed vaccines. *Semin Immunol*. 2018;39:14–21. doi:10.1016/j.smim.2018.05.001
34. Matsumoto S, Shimada A, Nyirenda J, Igura M, Kawano Y, Kohda D. Crystal structures of an archaeal oligosaccharyltransferase provide insights into the catalytic cycle of N-linked protein glycosylation. *Proc Natl Acad Sci USA*. 2013;110(44):17868–17873. doi:10.1073/pnas.1309777110
35. Ihssen J, Haas J, Kowarik M, et al. Increased efficiency of *Campylobacter jejuni* N-oligosaccharyltransferase PglB by structure-guided engineering. *Open Biol*. 2015;5(4):140227. doi:10.1098/rsob.140227
36. Ollis AA, Zhang S, Fisher AC, DeLisa MP. Engineered oligosaccharyltransferases with greatly relaxed acceptor-site specificity. *Nat Chem Biol*. 2014;10(10):816–822. doi:10.1038/nchembio.1609
37. Garcia-Quintanilla F, Iwashiki JA, Price NL, Stratillo C, Feldman MF. Production of a recombinant vaccine candidate against *Burkholderia pseudomallei* exploiting the bacterial N-glycosylation machinery. *Front Microbiol*. 2014;5:381. doi:10.3389/fmicb.2014.00381
38. Marshall LE, Nelson M, Davies CH, et al. An O-antigen glycoconjugate vaccine produced using protein glycan coupling technology is protective in an inhalational rat model of tularemia. *J Immunol Res*. 2018;2018:8087916. doi:10.1155/2018/8087916
39. Wetter M, Kowarik M, Steffen M, Carranza P, Corradin G, Wacker M. Engineering, conjugation, and immunogenicity assessment of *Escherichia coli* O121 O antigen for its potential use as a typhoid vaccine component. *Glycoconj J*. 2013;30(5):511–522. doi:10.1007/s10719-012-9451-9
40. Cuccui J, Thomas RM, Moule MG, et al. Exploitation of bacterial N-linked glycosylation to develop a novel recombinant glycoconjugate vaccine against *Francisella tularensis*. *Open Biol*. 2013;3(5):130002. doi:10.1098/rsob.130002
41. Fouts DE, Mongodin EF, Mandrell RE, et al. Major structural differences and novel potential virulence mechanisms from the genomes of multiple *Campylobacter* species. *PLoS Biol*. 2005;3(1):e15. doi:10.1371/journal.pbio.0030015
42. Yi EC, Hackett M. Rapid isolation method for lipopolysaccharide and lipid A from Gram-negative bacteria. *Analyst*. 2000;125(4):651–656. doi:10.1039/b000368i
43. Mitra S, Tomar PC. Hybridoma technology: Advancements, clinical significance, and future aspects. *J Genet Eng Biotechnol*. 2021;19(1):159. doi:10.1186/s43141-021-00264-6
44. Taboada B, Ciria R, Martinez-Guerrero CE, Merino E. ProOpDB: Prokaryotic Operon DataBase. *Nucleic Acids Res*. 2012;40(D1):D627–D631. doi:10.1093/nar/gkr1020
45. Walker JM, Darling AE, Treangen TJ, Messeguer X, Perna NT. Analyzing patterns of microbial evolution using the Mauve genome alignment system. *Methods Mol Biol*. 2007;396:135–152. doi:10.1007/978-1-59745-515-2_10
46. Kanehisa M, Goto S. KEGG: Kyoto Encyclopedia of Genes and Genomes. *Nucl Acids Res*. 2000;28(1):27–30. doi:10.1093/nar/28.1.27
47. Stevenson G, Andrianopoulos K, Hobbs M, Reeves PR. Organization of the *Escherichia coli* K-12 gene cluster responsible for production of the extracellular polysaccharide colanic acid. *J Bacteriol*. 1996; 178(16):4885–4893. doi:10.1128/jb.178.16.4885-4893.1996
48. Sato K, Kido N, Murakami Y, Hoover CI, Nakayama K, Yoshimura F. Lipopolysaccharide biosynthesis-related genes are required for colony pigmentation of *Porphyromonas gingivalis*. *Microbiology*. 2009; 155(4):1282–1293. doi:10.1099/mic.0.025163-0
49. Yamaguchi M, Sato K, Yukitake H, Noiri Y, Ebisu S, Nakayama K. A *Porphyromonas gingivalis* mutant defective in a putative glycosyltransferase exhibits defective biosynthesis of the polysaccharide portions of lipopolysaccharide, decreased gingipain activities, strong autoaggregation, and increased biofilm formation. *Infect Immun*. 2010;78(9):3801–3812. doi:10.1128/IAI.00071-10
50. Chen J, Ni Y, Liu C, et al. Rapid identification and quantitation for oral bacteria based on short-end capillary electrophoresis. *Talanta*. 2016;160:425–430. doi:10.1016/j.talanta.2016.07.049
51. Klein BA, Tenorio EL, Lazinski DW, Camilli A, Duncan MJ, Hu LT. Identification of essential genes of the periodontal pathogen *Porphyromonas gingivalis*. *BMC Genomics*. 2012;13(1):578. doi:10.1186/1471-2164-13-578
52. Shoji M, Sato K, Yukitake H, et al. Identification of genes encoding glycosyltransferases involved in lipopolysaccharide synthesis in *Porphyromonas gingivalis*. *Mol Oral Microbiol*. 2018;33(1):68–80. doi:10.1111/omi.12200
53. Lehrer J, Vigeant KA, Tatar LD, Valvano MA. Functional characterization and membrane topology of *Escherichia coli* WecA, a sugar-phosphate transferase initiating the biosynthesis of enterobacterial common antigen and O-antigen lipopolysaccharide. *J Bacteriol*. 2007; 189(7):2618–2628. doi:10.1128/JB.01905-06
54. Danese PN, Oliver GR, Barr K, Bowman GD, Rick PD, Silhavy TJ. Accumulation of the enterobacterial common antigen lipid II biosynthetic intermediate stimulates *degP* transcription in *Escherichia coli*. *J Bacteriol*. 1998;180(22):5875–5884. doi:10.1128/JB.180.22.5875-5884.1998
55. Meier-Dieter U, Starman R, Barr K, Mayer H, Rick PD. Biosynthesis of enterobacterial common antigen in *Escherichia coli*: Biochemical characterization of Tn10 insertion mutants defective in enterobacterial common antigen synthesis. *J Biol Chem*. 1990;265(23):13490–13497. PMID:2166030.
56. McAlister AD, Sroka A, Fitzpatrick RE, et al. Gingipain enzymes from *Porphyromonas gingivalis* preferentially bind immobilized extracellular proteins: A mechanism favouring colonization? *J Periodontol Res*. 2009;44(3):348–353. doi:10.1111/j.1600-0765.2008.01128.x
57. Tolia NH, Joshua-Tor L. Strategies for protein coexpression in *Escherichia coli*. *Nat Methods*. 2006;3(1):55–64. doi:10.1038/nmeth0106-55
58. Wu X, You P, Su E, Xu J, Gao B, Wei D. In vivo functional expression of a screened *P. aeruginosa* chaperone-dependent lipase in *E. coli*. *BMC Biotechnol*. 2012;12(1):58. doi:10.1186/1472-6750-12-58
59. Pham SQ, Gao P, Li Z. Engineering of recombinant *E. coli* cells co-expressing P450_{pyr}TM monooxygenase and glucose dehydrogenase for highly regio- and stereoselective hydroxylation of alicycles with cofactor recycling. *Biotech Bioeng*. 2013;110(2):363–373. doi:10.1002/bit.24632
60. Johansson AK, Johansson A, Birkhed D, Omar R, Baghdadi S, Carlsson GE. Dental erosion, soft-drink intake, and oral health in young Saudi men, and the development of a system for assessing erosive anterior tooth wear. *Acta Odontol Scand*. 1996;54(6):369–378. doi:10.3109/00016359609003554
61. Kim S, Park S, Lin M. Permanent tooth loss and sugar-sweetened beverage intake in U.S. young adults. *J Public Health Dent*. 2017;77(2): 148–154. doi:10.1111/jphd.12192
62. Zhang Y, Shi W, Song Y, Wang J. Metatranscriptomic analysis of an in vitro biofilm model reveals strain-specific interactions among multiple bacterial species. *J Oral Microbiol*. 2019;11(1):1599670. doi:10.1080/20002297.2019.1599670
63. Huang N, Shimomura E, Yin G, et al. Immunization with cell-free-generated vaccine protects from *Porphyromonas gingivalis*-induced alveolar bone loss. *J Clin Periodontol*. 2019;46(2):197–205. doi:10.1111/jcpe.13047
64. Muramatsu K, Kokubu E, Shibahara T, Okuda K, Ishihara K. HGP44 induces protection against *Porphyromonas gingivalis*-induced alveolar bone loss in mice. *Clin Vaccine Immunol*. 2011;18(5):888–891. doi:10.1128/CI.00556-10

Assessment of physical performance and muscle function in hemodialysis patients participating in an exercise regimen: A cluster-randomized, single-center study

Łukasz Rogowski^{1,A–E}, Joanna Kowalska^{2,D–F}, Katarzyna Bulińska^{2,B}, Małgorzata Stefańska^{2,C,E}, Agnieszka Zembroń-Łacny^{3,C}, Andrea Mahrová^{4,E}, Jitka Marenčáková^{4,B}, Weronika Pawlaczyk^{5,B}, Tomasz Gołębiowski^{6,B,F}, Witold Wnukiewicz^{7,E}, Mariusz Kuształ^{6,8,A,E,F}, Wioletta Dziubek^{2,A,B,D,F}

¹ Faculty of Health and Physical Culture Sciences, Witelon Collegium State University, Legnica, Poland

² Faculty of Physiotherapy, Wrocław University of Health and Sport Sciences, Poland

³ Department of Applied and Clinical Physiology, Collegium Medicum, University of Zielona Góra, Poland

⁴ Faculty of Physical Education and Sport, Charles University, Prague, Czech Republic

⁵ Lower Silesian Oncology Center, Department of Physiotherapy, Wrocław, Poland

⁶ Department of Nephrology, Transplant Medicine and Internal Medicine, Wrocław Medical University, Poland

⁷ Emkamed Medical Center, Wrocław, Poland

⁸ St. Luke Hospital, Bolesławiec, Poland

Received on September 23, 2024

Reviewed on December 31, 2024

Accepted on March 13, 2025

Published online on June 11, 2025

A – research concept and design; B – collection and/or assembly of data; C – data analysis and interpretation; D – writing the article; E – critical revision of the article; F – final approval of the article

Advances in Clinical and Experimental Medicine, ISSN 1899–5276 (print), ISSN 2451–2680 (online)

Adv Clin Exp Med. 2025;34(12):2105–2118

Address for correspondence

Mariusz Kuształ

E-mail: mariusz.kuształ@umw.edu.pl

Funding sources

The study was conducted as part of the National Science Centre (Poland) project No. 2011/03/B/NZ7/01764 and was registered in the clinical research database under No. ACTRN 12618001870246. Part of the study was funded by the Witelon Collegium State University under internal grant No. DB.406.1.24.

Conflict of interest

None declared

Acknowledgements

We would like to thank the patients, the nurses and the entire team from the Dialysis Center of the University Hospital in Wrocław for their help and support.

Cite as

Rogowski Ł, Kowalska J, Bulińska K, et al. Assessment of physical performance and muscle function in hemodialysis patients participating in an exercise regimen: A cluster-randomized, single-center study. *Adv Clin Exp Med.* 2025;34(12):2105–2118. doi:10.17219/acem/202940

DOI

10.17219/acem/202940

Copyright

Copyright by Author(s)

This is an article distributed under the terms of the Creative Commons Attribution 3.0 Unported (CC BY 3.0) (<https://creativecommons.org/licenses/by/3.0/>)

Abstract

Background. Many studies reported positive effects of physical exercise on the condition of dialysis patients. The insufficient value of those changes makes it difficult to interpret their clinical relevance.

Objectives. This study aimed to assess the influence of selected training (endurance, resistance, tai chi) on cardiopulmonary fitness and muscle function, as well as to analyze the factors having the most significant effect on cardiopulmonary fitness in a group of dialysis patients.

Material and methods. Ninety-eight patients agreed to participate in the study. Selection of the type of training was done by cluster randomization. Group 1 were patients in a cluster with an endurance exercise program, and group 2 in a cluster with resistance exercises. Group 3 consisted of patients who took part in a tai chi program (non-cluster randomization). Exercise programs with each of the 3 groups were conducted for a period of 6 months, 3 times a week (groups 1 and 2) and twice a week (group 3), up to 60 min for 1 session.

Results. The full exercises was completed by 45 patients: group 1 – 16; group 2 – 15; group 3 – 14. The significance of the observed difference in the cardiopulmonary function was confirmed only in endurance group for absolute oxygen consumption (VO_2) and heart rate (HR). Measurements of peak torque (PTQ) and total work (TW) performed at a speed of 60°/s showed a significant increase in the measured values only in the resistance training group. Measurements of PTQ and TW performed at 180°/s showed a significant increase in the measured values in the endurance and resistance group.

Conclusions. The 6 months of training resulted in a slight improvement in cardiopulmonary parameters only in the endurance group. The above results seem to confirm the observed limited potential for improving aerobic capacity in dialysis patients. The results of strength and speed parameters shows the specificity of each training, expressed by selective improvements in isometric and both isokinetic tests.

Key words: hemodialysis, endurance training, strength training, muscle function, spirometry

Highlights

- A 6-month exercise program – aerobic, resistance and tai chi – was conducted in a cohort of end-stage renal disease patients with significantly lower levels of physical capacity.
- After a 6-month exercise program, limited increase in cardiorespiratory function was observed in the aerobic exercise group.
- After a 6-month resistance exercise program, changes in strength and speed parameters, were observed.
- Resistance training demonstrates superior functional relevance in a group of dialysis patients.
- A long-term rehabilitation program can be successfully implemented in a group of dialysis patients.

Background

Chronic kidney disease (CKD) is a rapidly emerging public health concern worldwide and is now recognized as a civilization disease. Over the past 2 centuries, the average human life expectancy has more than doubled, leading to a significant increase of the elderly population. Aging processes contribute to structural and functional changes in all organs, including the kidneys.

The rise in CKD cases can also be attributed to lifestyle factors. The prevalence of CKD is steadily increasing, particularly in rapidly developing countries, likely driven by the concurrent epidemics of diabetes and cardiovascular diseases.^{1,2} These changes are undoubtedly reflected in the epidemiology of kidney disease.^{2,3} Unfortunately, the early stages of kidney disease can be secretive, even latent. The final stage of kidney failure, the end-stage renal disease (ESRD), is often referred to as “silent epidemic”.³

Patients with ESRD show significantly lower levels of physical activity and associated physical capacity than the population average.^{4–6} The process of physical impairment begins with the initial changes in renal function, although it may not be subjectively noticeable in the early stages.⁵ This poses a serious problem because the level of physical activity correlates significantly with physical capacity (oxygen uptake rate) and is independently associated with mortality.^{7,8} The VO_2max index, also known as maximal oxygen consumption or oxygen capacity, is a widely adopted measure of physical fitness used to assess both healthy individuals and patients with various medical conditions. Decreased aerobic capacity levels are evident even in the earlier stages of kidney failure⁹ and become significantly lower in patients with ESRD, averaging 15–21 mL/min/kg, compared to the general population average of 30–40 mL/min/kg.^{9,10}

Adequate muscular strength is essential for maintaining the proper function of the musculoskeletal system, enabling individuals to engage in necessary daily activities, including professional work and fulfilling basic needs, as well as intentional and recreational physical activities. Several studies suggest a significant correlation between muscle strength and various factors influencing individual fitness, particularly gait speed,^{9,10} as well as the incidence of balance disorders, risk of falls and fractures,^{10,12} and

frequency of hospitalization.^{11,12} Consequently, a reduction in muscle strength and power contributes to decreased physical activity^{13–15} and is an important factor in the development of disability.^{11,12,15}

Patients with CKD show a reduction in muscle strength already in the early stages of the disease, correlating with a decrease in the glomerular filtration rate (GFR). The most significant decline in strength occurs in ESRD, potentially hindering physical functioning even after transplantation.^{15,16} The mechanism of these changes can be both primary, due to uremic myopathy, as well as secondary, due to a number of factors: comorbidities, lifestyle and age-related sarcopenia.¹⁷ This combination of the aforementioned variables leads to significant alterations in the muscle tissue structure of dialysis patients. Magnetic resonance imaging (MRI) scans of hemodialysis patients reveal pronounced atrophic changes in the muscles, along with an increased presence of non-contractile muscle elements, which significantly impacts muscle functionality.¹⁸

The recommendations and clinical guidelines established by experts in 2016, including the European Renal Best Practice Guideline (ERBPB) and the expert team of the rehabilitation section of the Polish Society of Nephrology, highlight the importance of evaluating patient's functional status. They emphasize the need to implement individualized physical training programs to enhance the functional capacity of patients with ESRD.^{19,20}

Many studies reported positive effects of physical exercise on the condition of dialysis patients. The evidence supports the integration of structured exercise programs into routine care for dialysis patients, emphasizing the need for healthcare providers to promote physical activity as a vital component of comprehensive CKD management. Despite that, the insufficient value of those changes makes it difficult to interpret their clinical relevance.²¹ There is also no consensus on which form of physical training offers the greatest potential for improving the widest range of physical fitness aspects in this patient group. Tailored exercise programs that consider individual patient capabilities and preferences are essential for maximizing the therapeutic benefits of physical activity in this population.

Objectives

The primary aim of this study was to assess the influence of selected training modalities (endurance, resistance and tai chi) on cardiopulmonary fitness and muscle function in ESRD patients. The secondary aim was to analyze the factors that most significantly impact cardiopulmonary fitness within this group of patients.

Materials and methods

Trial design

This study was designed as a parallel cluster intervention trial. Two care providers delivered specific exercise programs to 3 groups of ESRD patients. Group 1 participated in a cluster with an endurance exercise program, while group 2 engaged in a cluster with resistance exercises. Group 3 (tai chi) consisted of patients who wanted to take a part in workouts on their non-dialysis days (not subject to cluster randomization). All care providers were selected by project leader, based on their experience in their field. Care provider 1, a physiotherapist and instructor in resistance and endurance training, supervised the exercise programs in groups 1 and 2. Care provider 2, a physiotherapist and instructor, who specializes in yoga and tai chi exercise programs, supervised group 3.

This research was conducted in line with the recommendations of the Declaration of Helsinki. The research project received a positive opinion from the Senate Committee on Research Ethics at the Wrocław University of Health and Sport Sciences issued on January 18, 2012.

Participants

Ninety-eight patients with ESRD at the dialysis station of the Department of Nephrology, Transplant Medicine and Internal Medicine of Wrocław Medical University (Poland) agreed to participate in the study. All training participants were qualified by a nephrologist and a cardiologist. Written informed consent was obtained from the patients to participate in the tests and workouts, which was preceded by an explanation of the purpose and conduct of the workouts, assurances of the confidentiality of the data obtained, and information that the patients could withdraw from the project upon request.

Inclusion criteria

- Diagnosed end-stage renal failure;
- renal replacement therapy with hemodialysis for at least 6 months;
- adequate dialysis therapy: dialysis adequacy index $Kt/V > 1.2$ (K – dialyzer clearance of urea, t – dialysis time,

V – volume of distribution of urea, approximately equal to patient's total body water);

- protein catabolism ratio-polymerase chain reaction (PCR) 0.8–1.4 g protein/kg body weight/day;
- age 40–80 years.

Exclusion criteria

- The presence of contraindications to the exercise test and physical training;
- kidney transplant;
- no final tests;
- adherence to training units below 70%;
- malnutrition expressed by hypoalbuminemia (<3 g/dL) and <17 points in the assessment of nutritional status with the Mini Nutritional Assessment (MNA) questionnaire*;
- lack of patient consent.

*The MNA scale is a simple nutrition screening and assessment tool, designed to determine the possibility of malnutrition.

Intervention

Exercise programs with each of the 3 groups were conducted for a period of 6 months, 3 times a week (groups 1 and 2) and twice a week (group 3), up to 60 min for 1 session. Group 1 comprised undergoing controlled endurance training during a hemodialysis procedure. Group 2 consisted of undergoing controlled strength (resistance) training during a hemodialysis procedure. Group 3 were participating in tai chi training 2 times a week on non-dialysis days.

Physical training

The trainings were conducted at the Dialysis Center of the University Hospital in Wrocław and the gym of the Wrocław University of Health and Sport Sciences (tai chi training). The exercises for groups 1 and 2 were conducted during the first 2 h of hemodialysis while the patients remained seated in their dialysis chairs. The workouts took place under the constant supervision of a nephrologist and a physiotherapist. Each training session was divided into 3 parts: 1. The introductory part, which was a short warm-up of about 5 min. It included active exercises of the lower limbs in the supine position. 2. The main part took lasted 10–50 min. In this part, depending on the assigned training, group 1 performed endurance training, and group 2 performed strength (resistance) exercises. 3. The final part, or cool-down, lasted about 5 min and included limb relaxation exercises, as well as breathing exercises.

Endurance training

Group 1 performed endurance training on the Reck MOTomed® letto2 rotor (Reck-Technik, Betzenweiler, Germany), which allows for riding in a supine or semi-recumbent

position. This rotor allows for the adjustment of set parameters to modulate the intensity of the workout: speed of rotation [rpm] and degree of mechanical resistance 1–11 [nm].

Training intensity was assessed using a subjective 10-degree Borg scale. The premise of the training was to achieve load progression from low intensity (1–3 on the Borg scale) in the 1st week, through medium (4–7) to high intensity (>7 on the Borg scale). The aerobic training commenced with a brief 5-min warm-up at a moderate rotation speed, without mechanical resistance, before transitioning to the main session.

During the main session, based on the patient's subjective reaction, as well as the parameter of average power [W], the physiotherapist increased the intensity of the training in 10-min stages, modulating the speed of rotation and mechanical resistance. The training was conducted until participants experienced a clear, subjective feeling of fatigue, followed by a 5-min cooling phase to conclude the session, with a reduction (approx. 50%) of mechanical resistance and rotation, until the patient's breathing calmed down significantly.

After the workout, the physiotherapist wrote down the training parameters from the rotor: training duration [min], speed [rpm], motor power [W], and total work (TW) cost [J]. These formed the basis for determining the training load progression for subsequent workouts. The physiotherapist encouraged patients to progressively increase their workload in each session or, at a minimum, maintain the same level as in the previous workout.

Strength training

Group 2 performed resistance exercises using weights, balls and elastic bands under individual supervision of the physiotherapist (care provider 1). The exercises primarily targeted the lower limbs and the upper limb that was not affected by the arteriovenous fistula. Each movement pattern included 1 exercise, performed in 4–5 sets. The 1st set was light, consisting of 20 repetitions, while sets 2–5 were standard, ranging from 10 to 20 repetitions, continuing until significant fatigue was reached. The intensity was adjusted based on subjective perception, with the appropriate selection of resistance bands' color or the weight of the dumbbells. If the patient demonstrated clear tolerance to the exercise, the training load was increased and maintained at a constant level for at least 3 training sessions (1 week) to allow adaptation to the new load. If the patient demonstrated clear progression, the training load was increased in the following week. The exercise was performed until a clear, subjective feeling of fatigue was achieved (at the beginning of training sessions 5–6 according to the 10-point Borg scale), but not to "muscle breakdown" (to avoid the risk of injuries in the area of tendons, muscle attachments, etc.). The time of exercise unit, intensity (weights and color of elastic bands used) and volume (numbers of repetitions and sets of single exercises) were noted. The duration of the actual part gradually increased from 10 min in the initial training period,

up to 50 min. In addition to the training time, the training intensity and volume increased, depending on the patients' responses to the physical effort.

Tai chi training

Group 3 participated in tai chi training, which took place twice a week for 6 months on non-dialysis days. The training took place under the constant supervision of a physiotherapist (care provider 2) and the attending physician. The training was divided into 3 parts: preliminary – warm-up, main and final. The warm-up and final part lasted about 10 min each, while the main part lasted up to 40 min.

Exercises were conducted in a standing position, requiring no instruments or utensils. Exercises for the lower limbs in "soft" high positions required continuous muscle engagement, stimulating increased lower limb strength. The training intensity and duration were assessed using the subjective 10-point Borg scale. Intensity was adjusted by extending the duration of specific positions and incorporating new exercises. The training protocol aimed for a gradual progression in load intensity, starting from low intensity (1–3 on the Borg scale) in the 1st week, progressing through moderate intensity (4–7) and ultimately reaching high intensity (>7 on the Borg scale).

Outcomes/research methods

Primary outcomes were the changes in cardiopulmonary function expressed with oxygen consumption (peak VO_2max) and muscle force of lower limbs (speed-strength parameters). The secondary outcome was to assess the strongest predictors of oxygen consumption in this patient population.

The primary objective of this study was to assess the potential risks and feasibility of exercise therapies by evaluating adherence, side effects and tolerance. Preliminary and final examinations were carried out at the Mikulicz-Radecki University Hospital in Wrocław and the Functional Research Laboratory of the Department of Rehabilitation in Internal Diseases at the Wrocław University of Health and Sport Sciences. To assess the impact of the intervention, the following tests were performed on each patient at the beginning of the program (pre-test) and the end of the 6-month training program (post-test):

The Cardio-Pulmonary Exercise Test (CPET) was performed on a Cosmed K4b2 ergospirometer (Cosmed, Rome, Italy), on a Kettler cycloergometer, by an experienced exercise physiologist. The following parameters were used for analysis: absolute oxygen consumption – VO_2 [mL/min], relative oxygen uptake – VO_2max [mL/min/kg], and maximum heart rate HR [bpm].

Lower limb strength was assessed using a Biodex Multi-Joint 4 isokinetic test stand by an experienced researcher. Isokinetic testing included the calculation of peak torque

(PTQ) [nm] from 5 repetitions at 60°/s and 20 repetitions at 180°/s, as well as TW [J] at both 60°/s and 180°/s. Isometric testing assessed the maximum peak torque (static PTQ) [nm].

Randomization

The selection of the training type and allocation to groups (1 and 2) was carried out using cluster randomization. A cluster was a group of patients in 1 room on a specific shift of dialysis sessions (e.g., Tuesday 3rd shift). The rule ensured that each cluster (patients in the same room during a specific dialysis shift) received only 1 type of training. Clusters were randomized by evenly selecting and assigning pairs of clusters to either strength or endurance training across all dialysis shifts over a 1-week period. Group 1 consisted of patients assigned to a cluster with an endurance exercise program, while group 2 participated in a cluster with strength exercises. Both groups were supervised by care provider 1. Group 3 (tai chi), supervised by care provider 2, included patients who voluntarily participated in workouts on their non-dialysis days and were not subject to cluster randomization.

Blinding

Blinding was not feasible in this study. Participants were informed that the study aimed to compare the 3 different forms of training, but they were not informed of all the research hypotheses. There was no blinding of care providers, as they were specialists in their field. To limit the bias, data collection, pre- and post-tests and data analysis were performed by a blinded researcher, i.e., a team member who did not provide any intervention to the participants.

Statistical analyses

The normality of the distribution of the analyzed characteristics was evaluated using the Shapiro–Wilk test. For a matched-pair analysis, normality of the distribution was assessed for the differences between the paired values. Descriptive statistics were calculated. Depending on the result of the normality of the distribution test, the mean and standard deviation (SD) or median and quartile range (IQR) were used. For nominal variables, counts and percentages were calculated.

The analysis of differences between the 1st and 2nd studies was conducted using either the Wilcoxon paired rank test or Student's t-test for dependent samples, depending on the distribution of the data. The analysis of differences between groups of subjects was performed depending on the type of variables using analysis of variance. For quantitative variables with a normal distribution, a one-way analysis of variance (ANOVA) was performed. In cases where the distribution was non-normal or the variables were ordinal, the Kruskal–Wallis test was used, followed

by the Dunn–Bonferroni–Holm post hoc test for multiple comparisons. Multivariate regression analysis was also employed. Statistical significance was determined at $p < 0.05$. In the case of multiple comparisons, the Bonferroni correction was applied by dividing the assumed significance level by the number of comparisons ($0.05/4 = 0.0125$). The value of rc ($rc = Z/\sqrt{n}$) was used as the effect size for the Wilcoxon pairwise order test.²² Effect size for the T-test for dependent pairs was calculated using Hedges' g-factor. According to the template, Hedges' g is calculated as follows:

$$g = \frac{\mu_1 - \mu_2}{\sqrt{SD_1^2 + SD_2^2 - 2rSD_1SD_2}}$$

where:

μ_1 and μ_2 – mean values; SD1 and SD2 – standard deviations; r – Pearson correlation coefficient.²³

The effect size for the Kruskal–Wallis ANOVA was determined using η^2 and subsequently converted to Cohen's d coefficient.²⁴ Statistical calculations were performed using Statistica v. 13.1 (TIBCO Software Inc., Palo Alto, USA) and PQstat 1.8.2 (StatSoft Polska, Cracow, Poland).

Results

Ninety-eight patients with ESRD met the inclusion criteria, consented to participate in the study and were assigned to the respective groups: 33 participants in group 1 (endurance), 35 participants in group 2 (resistance) and 30 participants in group 3 (tai chi). Twelve participants were excluded from the study. The trial group comprised 86 patients who engaged in pre-tests and commenced the 6-month exercise intervention as per the prior allocation. The intervention included 45 patients: group 1 had 16 participants, group 2 had 15 and group 3 had 14 (Fig. 1). The characteristics of the patients who completed the exercise program, underwent final examinations and were included in the statistical analysis are presented in shared data.

Spiroergometric test

In the post-training assessment (study 2), all groups, except for group 3, demonstrated an increase in VO_2 , VO_2/kg and heart rate (HR) compared to the baseline assessment (study 1). However, the observed differences were statistically significant only in group 1 for VO_2 and HR. Additionally, a strong effect size was noted in both cases (Table 1). A statistically significant difference in VO_2 levels was observed between group 2 and group 3 in both study 1 and study 2. In study 1, group 2 had a significantly higher average VO_2 value compared to group 3, and this difference became more pronounced in study 2. Also, the HR value in study 2 in group 2 was significantly higher compared to group 3 (Table 1,2).

Measurements of PTQ and TW performed under isokinetic conditions at a movement speed of 60°/s in study 2

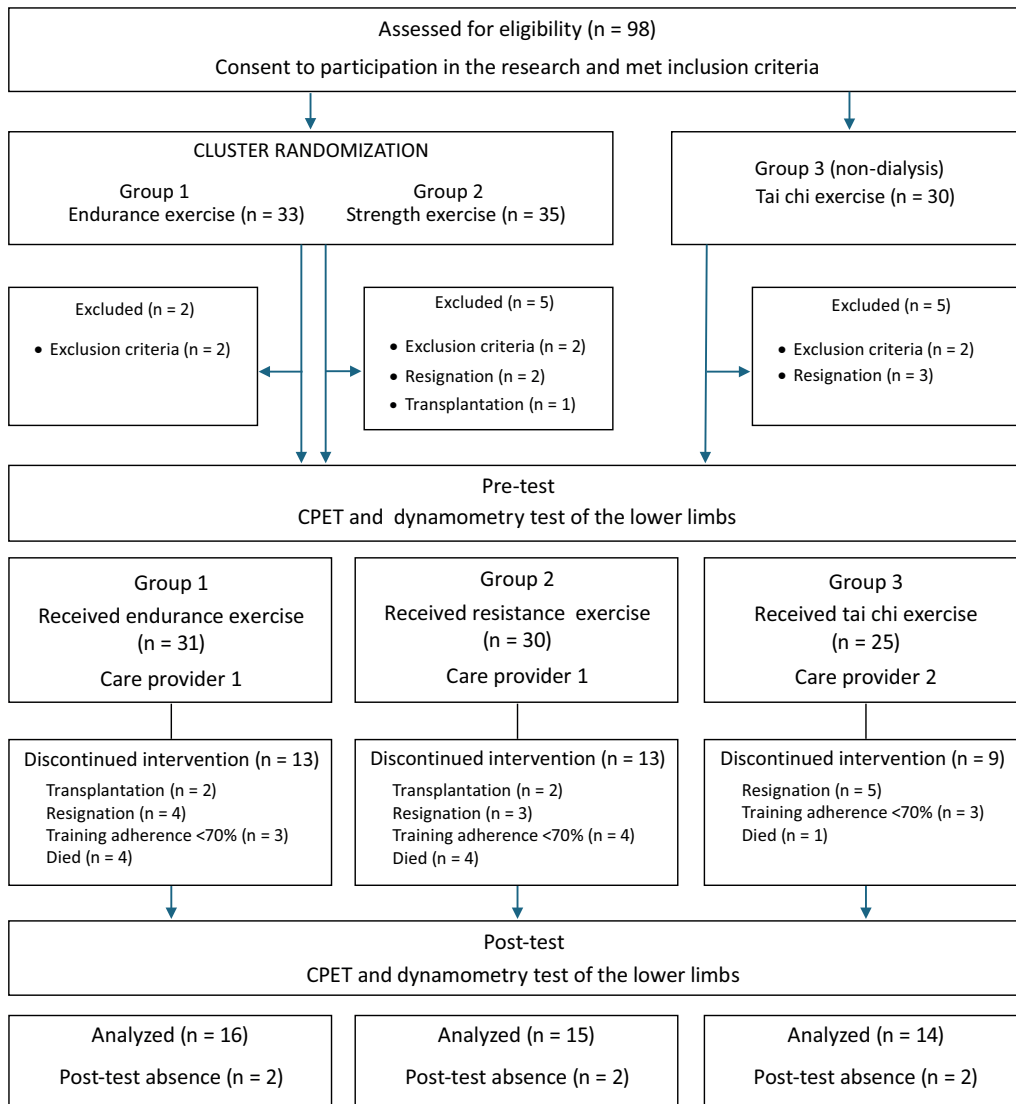


Fig. 1. A detailed process of patient recruitment for the study

CPET – Cardio-Pulmonary Exercise Test.

Table 1. Spiroergometric parameters before and after the training cycle

Group	Variable	Pre-test		Post-test		Wilcoxon test		r_c
		median	IQR	median	IQR	T	p-value	
Group 1	VO ₂ [mL/min]	975.50	394.50	1002.50	445.00	10.000	0.003*	0.75
	VO ₂ /kg [mL/min/kg]	12.84	4.61	13.50	4.13	26.000	0.029	0.54
	HR bpm	101.50	14.50	104.00	10.50	1.500	0.001*	0.80
Group 2	VO ₂ [mL/min]	1403.00	781.00	1585.00	810.00	30.000	0.088	0.44
	VO ₂ /kg [mL/min/kg]	18.20	10.63	19.50	13.18	27.000	0.061	0.48
	HR bpm	109.00	44.00	118.00	30.00	17.000	0.015	0.63
Group 3	VO ₂ [mL/min]	892.00	510.00	875.00	590.00	22.000	0.056	0.51
	VO ₂ /kg [mL/min/kg]	12.75	1.91	12.85	4.65	41.000	0.470	0.19
	HR bpm	99.00	18.00	100.00	18.00	17.500	0.050	0.52

Group 1 – endurance training; group 2 – resistance training; group 3 – tai chi; VO₂ – oxygen consumption; HR – heart rate; IQR – interquartile range; T – Wilcoxon test value; r_c – rank correlation coefficient; *p < 0.012

showed a significant increase in values for both the extensor and flexor muscles of the knee joint, but only in the group that participated in resistance training (group 2). A strong effect size was also observed for these variables (Table 3).

The analysis of results between the subject groups revealed significant differences, particularly in study 2. In the study performed after the end of the training cycle, significantly higher values were observed in group 2

Table 2. Comparison between groups of spiroergometric test results

Research	Variable	Kruskal–Wallis ANOVA		Post hoc test (p-value)			Cohen's d
				group			
		H	p-value	1 vs 2	1 vs 3	2 vs 3	
Pre-test	VO ₂ [mL/min]	9.20	0.010*	0.044	0.511	0.013*	0.91
	VO ₂ /kg [mL/min/kg]	4.03	0.133	0.167	0.712	0.275	0.45
	HR [bpm]	2.32	0.313	0.668	0.668	0.398	0.18
Post-test	VO ₂ [mL/min]	10.31	0.006*	0.023	0.594	0.009*	0.99
	VO ₂ /kg [mL/min/kg]	5.32	0.070	0.125	0.880	0.125	0.59
	HR [bpm]	9.61	0.008*	0.031	0.577	0.012*	0.94

Group 1 – endurance training; group 2 – resistance training; group 3 – tai chi; ANOVA – analysis of variance; VO₂ – oxygen consumption; HR – heart rate; *p < 0.012.

Table 3. Values of peak torque and total work at 60°/s before and after the training cycle

Group	Variable	Pre-test		Post-test		Wilcoxon test		r _c
		median	IQR	median	IQR	T	p-value	
Group 1	PTQ E 60 R [nm]	55.30	16.35	56.90	16.15	66.00	0.918	0.03
	PTQ E 60 L [nm]	60.30	28.40	58.15	30.05	61.00	0.717	0.09
	PTQ F 60 R [nm]	29.80	11.15	28.55	12.00	68.00	1.000	0.00
	PTQ F 60 L [nm]	28.25	11.90	25.90	13.00	56.00	0.535	0.16
	TW E 60 R [J]	287.45	122.70	277.25	124.00	54.00	0.469	0.18
	TW E 60 L [J]	286.35	132.40	276.65	139.30	54.00	0.469	0.18
	TW F 60 R [J]	131.80	74.00	130.65	74.70	46.00	0.255	0.28
	TW F 60 L [J]	130.95	55.75	123.60	61.60	34.50	0.083	0.43
Group 2	PTQ E 60 R [nm]	99.80	46.70	129.90	62.10	0.00	0.001*	0.88
	PTQ E 60 L [nm]	95.60	51.90	120.60	64.70	0.00	0.001*	0.88
	PTQ F 60 R [nm]	44.70	23.80	59.10	28.80	0.00	0.001*	0.88
	PTQ F 60 L [nm]	44.40	18.70	54.30	26.90	0.00	0.001*	0.88
	TW E 60 R [J]	476.40	199.40	543.00	267.80	0.00	0.001*	0.88
	TW E 60 L [J]	432.30	292.90	530.11	256.00	0.00	0.001*	0.88
	TW F 60 R [J]	225.10	91.30	270.50	182.40	0.00	0.001*	0.88
	TW F 60 L [J]	201.20	81.80	251.30	135.20	0.00	0.001*	0.88
Group 3	PTQ E 60 R [nm]	61.90	32.30	66.25	39.40	21.00	0.048	0.53
	PTQ E 60 L [nm]	60.75	49.60	66.20	56.00	28.50	0.132	0.40
	PTQ F 60 R [nm]	29.15	13.00	32.60	20.40	24.00	0.133	0.40
	PTQ F 60 L [nm]	30.75	11.30	33.30	15.20	29.00	0.140	0.39
	TW E 60 R [J]	334.35	149.80	340.05	156.10	14.00	0.016	0.65
	TW E 60 L [J]	300.50	126.00	308.10	129.40	16.00	0.022	0.61
	TW F 60 R [J]	147.15	47.50	147.95	45.60	30.00	0.158	0.38
	TW F 60 L [J]	136.40	89.00	140.30	101.30	24.50	0.079	0.47

Group 1 – endurance training; group 2 – resistance training; group 3 – tai chi; PTQ – peak torque; TW – total work; E – knee extensors; F – knee flexors; R – right limb; L – left limb; 60 – movement velocity 60°/s; IQR – interquartile range; T – Wilcoxon test value; r_c – rank correlation coefficient; *p < 0.012.

compared to group 1. The significance of the differences between the groups was also shown for some of the variables in the preliminary study. In study 2, the magnitude of the differences was increased. Group 2 demonstrated higher results in study 2 compared to group 3. The significance of the differences was confirmed for the PTQ values of the knee flexors and the TW performed by the knee extensor muscles on the right side (Table 3,4).

Measurements of PTQ and TW performed under isokinetic conditions at 180°/s showed in study 2 a significant increase in the values obtained for both the extensor and flexor muscles of the knee joint in the group participating in endurance (group 1) and resistance (group 2) training. In all of those variables, a strong effect size was also noted (Table 5). Analysis of the differences between groups highlighted significant differences between the values

Table 4. Comparison between groups of isokinetic test results (60°/s)

Research	Variable	Kruskal–Wallis ANOVA		Post hoc test (p-value)			Cohen's d
				group			
		H	p-value	1 vs 2	1 vs 3	2 vs 3	
Pre-test	PTQ E 60 R [nm]	10.72	0.005*	0.004*	0.300	0.072	1.02
	PTQ E 60 L [nm]	8.91	0.012*	0.011*	0.403	0.091	0.89
	PTQ F 60 R [nm]	7.68	0.022	0.032	0.782	0.056	0.79
	PTQ F 60 L [nm]	7.44	0.024	0.024	0.484	0.121	0.77
	TW E 60 R [J]	10.92	0.004*	0.005*	0.477	0.035	1.04
	TW E 60 L [J]	8.42	0.015	0.016	0.557	0.070	0.85
	TW F 60 R [J]	8.15	0.017	0.019	0.556	0.077	0.83
	TW F 60 L [J]	8.69	0.013	0.010*	0.220	0.220	0.87
Post-test	PTQ E 60 R [nm]	14.02	0.001*	0.001*	0.283	0.026	1.28
	PTQ E 60 L [nm]	14.86	0.001*	0.001*	0.291	0.019	1.33
	PTQ F 60 R [nm]	16.87	0.001*	0.000*	0.404	0.006*	1.48
	PTQ F 60 L [nm]	16.79	0.001*	0.000*	0.316	0.009*	1.48
	TW E 60 R [J]	14.80	0.001*	0.001*	0.406	0.012*	1.32
	TW E 60 L [J]	13.86	0.001*	0.001*	0.457	0.013	1.26
	TW F 60 R [J]	12.54	0.002*	0.002*	0.407	0.025	1.16
	TW F 60 L [J]	13.25	0.001*	0.001*	0.169	0.064	1.21

Group 1 – endurance training; group 2 – resistance training; group 3 – tai chi; PTQ – peak torque; TW – total work; E – knee extensors; F – knee flexors; R – right limb; L – left limb; 60 – movement velocity 60°/s; H – Kruskal–Wallis test value; ANOVA – analysis of variance; *p < 0.012.

Table 5. Values of peak torque and TW at 180°/s before and after the training cycle

Group	variable	Pre-test		Post-test		Wilcoxon test		r _c
		median	IQR	median	IQR	T	p-value	
Group 1	PTQ E 180 R [nm]	44.30	13.95	49.00	19.15	0.00	0.001*	0.88
	PTQ E 180 L [nm]	39.35	24.90	45.30	25.30	0.00	0.001*	0.88
	PTQ F 180 R [nm]	24.70	9.25	27.35	13.35	0.00	0.001*	0.88
	PTQ F 180 L [nm]	23.90	7.95	28.20	12.05	1.00	0.001*	0.87
	TW E 180 R [J]	671.90	290.20	690.05	301.05	0.00	0.001*	0.88
	TW E 180 L [J]	674.75	414.35	693.50	423.40	0.00	0.001*	0.88
	TW F 180 R [J]	332.35	152.10	342.80	152.95	0.00	0.001*	0.88
	TW F 180 L [J]	313.10	122.55	324.85	134.70	0.00	0.001*	0.88
Group 2	PTQ E 180 R [nm]	59.20	34.10	63.00	35.10	5.00	0.002*	0.81
	PTQ E 180 L [nm]	64.10	29.70	69.40	32.00	9.00	0.004*	0.75
	PTQ F 180 R [nm]	33.80	13.60	35.60	16.00	13.00	0.008*	0.69
	PTQ F 180 L [nm]	27.30	12.30	31.20	13.90	18.00	0.017	0.62
	TW E 180 R [J]	1137.60	314.10	1150.00	333.60	10.00	0.005*	0.73
	TW E 180 L [J]	1070.10	469.40	1103.00	472.60	5.00	0.002*	0.81
	TW F 180 R [J]	575.90	255.60	595.30	249.60	13.00	0.008*	0.69
	TW F 180 L [J]	464.80	308.00	498.70	304.90	12.00	0.006*	0.70
Group 3	PTQ E 180 R [nm]	43.65	19.60	43.05	27.50	40.00	0.433	0.21
	PTQ E 180 L [nm]	39.80	25.60	38.25	30.50	39.00	0.397	0.23
	PTQ F 180 R [nm]	24.95	11.60	24.00	14.90	32.00	0.198	0.34
	PTQ F 180 L [nm]	23.40	7.70	22.55	11.10	25.50	0.090	0.45
	TW E 180 R [J]	779.15	436.00	770.35	441.00	36.00	0.300	0.28
	TW E 180 L [J]	767.20	357.60	749.55	379.80	19.00	0.036	0.56
	TW F 180 R [J]	371.30	173.30	355.15	175.30	27.00	0.109	0.43
	TW F 180 L [J]	372.15	230.30	347.35	223.90	11.00	0.009*	0.70

Group 1 – endurance training; group 2 – resistance training; group 3 – tai chi; PTQ – peak torque; TW – total work; E – knee extensors; F – knee flexors; R – right limb; L – left limb; 180 – movement velocity 180°/s; IQR – interquartile range; T – Wilcoxon test value; r_c – rank correlation coefficient; *p < 0.012.

Table 6. Comparison between groups of isokinetic test results (180°/s)

Research	Variable	Kruskal–Wallis ANOVA		Post hoc test (p-value)			Cohen's d
				group			
		H	p-value	1 vs 2	1 vs 3	2 vs 3	
Pre-test	PTQ E 180 R [nm]	5.19	0.075	0.103	0.794	0.147	0.57
	PTQ E 180 L [nm]	7.82	0.020	0.035	0.897	0.042	0.80
	PTQ F 180 R [nm]	5.38	0.068	0.099	0.839	0.126	0.59
	PTQ F 180 L [nm]	5.92	0.052	0.098	0.992	0.098	0.64
	TW E 180 R [J]	10.80	0.005*	0.003*	0.228	0.098	1.03
	TW E 180 L [J]	10.49	0.005*	0.004*	0.286	0.082	1.01
	TW F 180 R [J]	8.30	0.016	0.015	0.424	0.106	0.84
	TW F 180 L [J]	5.97	0.051	0.044	0.358	0.358	0.65
Post-test	PTQ E 180 R [nm]	7.64	0.022	0.116	0.386	0.022	0.79
	PTQ E 180 L [nm]	7.65	0.022	0.147	0.315	0.020	0.79
	PTQ F 180 R [nm]	6.05	0.049	0.324	0.324	0.043	0.65
	PTQ F 180 L [nm]	7.23	0.027	0.293	0.293	0.022	0.75
	TW E 180 R [J]	9.87	0.007*	0.006*	0.368	0.074	0.86
	TW E 180 L [J]	10.61	0.005*	0.005*	0.417	0.048	1.02
	TW F 180 R [J]	8.23	0.016	0.022	0.695	0.054	0.84
	TW F 180 L [J]	5.49	0.064	0.068	0.542	0.217	0.60

Group 1 – endurance training; group 2 – resistance training; group 3 – tai chi; PTQ – peak torque; TW – total work; E – knee extensors; F – knee flexors; R – right limb, L – left limb; 180 – movement velocity 180°/s; H – Kruskal–Wallis test value; ANOVA – analysis of variance; *p < 0.012.

Table 7. Values of maximum peak torque (static conditions) before and after the training cycle

Group	variable	Pre-test		Post-test		Wilcoxon test		r _c
		median	IQR	median	IQR	T	p-value	
Group 1	static PTQ E R [nm]	76.35	42.85	75.90	44.55	64.50	0.698	0.10
	static PTQ E L [nm]	72.00	30.30	70.65	32.60	61.50	1.000	0.00
	static PTQ F R [nm]	35.20	18.25	33.15	21.55	61.00	0.737	0.08
	static PTQ F L [nm]	31.70	18.20	29.25	18.55	66.00	0.737	0.08
Group 2	static PTQ E R [nm]	112.80	72.80	136.10	69.70	1.00	0.001*	0.87
	static PTQ E L [nm]	103.80	58.40	124.40	73.90	1.00	0.001*	0.87
	static PTQ F R [nm]	53.40	23.30	60.70	24.30	1.00	0.001*	0.87
	static PTQ F L [nm]	46.00	16.50	53.00	25.20	1.00	0.001*	0.87
Group 3	static PTQ E R [nm]	75.45	20.50	79.50	26.50	18.00	0.056	0.51
	static PTQ E L [nm]	76.70	23.90	77.80	28.90	20.00	0.026	0.60
	static PTQ F R [nm]	33.65	14.30	38.00	17.80	30.00	0.052	0.52
	static PTQ F L [nm]	32.65	8.20	37.45	13.00	21.00	0.064	0.50

Group 1 – endurance training; group 2 – resistance training; group 3 – tai chi; static PTQ – maximum peak torque; E – knee extensors; F – knee flexors; R – right limb; L – left limb; IQR – interquartile range; *p < 0.012.

of the TW obtained for the knee joint extensor muscles in both measurements. In group 2, the values obtained were significantly higher compared to group 1 (Table 5,6).

Tests of the PTQ under static conditions showed an increase in the obtained values in study 2 in groups 2 and 3. However, the observed differences proved to be significant in group 2 participating in resistance training. Also, a strong effect size is noted only for group 2 (Table 7). In group 2, the values obtained proved to be the highest in both study 1 and study 2 compared to the results

of groups 1 and 3. Study 2 showed the significance of differences between all static measurements in groups 1 and 2, as well as between the results obtained for the flexor muscles in groups 2 and 3. In study 1, the significance of differences concerned only the maximum PTQ of the right knee flexors (Table 7,8).

Multivariate regression analysis was performed to indicate which variables have a significant effect on personal VO₂/kg. Analysis of the results obtained before the training program indicated a significant effect of age, body

Table 8. Comparison between study groups of static measurement results

Research	Variable	Kruskal–Wallis ANOVA		Post-hoc test p-value			Cohen's d
				group			
		H	p-value	1 vs 2	1 vs 3	2 vs 3	
Pre-test	static PTQ E R [nm]	8.18	0.017	0.020	0.624	0.065	0.83
	static PTQ E L [nm]	8.08	0.018	0.016	0.388	0.128	0.82
	static PTQ F R [nm]	10.53	0.005*	0.012*	0.829	0.012*	1.01
	static PTQ F L [nm]	7.82	0.020	0.035	0.886	0.043	0.80
Post-test	static PTQ E R [nm]	11.54	0.003*	0.003*	0.479	0.028	1.08
	static PTQ E L [nm]	12.37	0.002*	0.002*	0.279	0.045	1.46
	static PTQ F R [nm]	14.90	0.001*	0.001*	0.809	0.003*	1.33
	static PTQ F L [nm]	12.82	0.002*	0.003*	0.726	0.009*	1.18

Group 1 – endurance training; group 2 – resistance training; group 3 – tai chi; static PTQ – maximum peak torque; E – knee extensors; F – knee flexors; R – right limb; L – left limb; ANOVA – analysis of variance; *p < 0.012.

Table 9. Multivariate regression model indicating predictors of VO₂/kg (for study 1)

Dependent variable VO ₂ /kg	b	SE (b)	–95% CI	+95% CI	Student's t-test value	p-value
Gender	–2.1	1.47	–5.09	0.88	–1.43	0.165
Age [years]	–0.2	0.06	–0.32	–0.08	–3.38	0.002*
BMI [kg/m ²]	–0.34	0.13	–0.61	–0.07	–2.53	0.016*
Years of dialysis	–0.02	0.17	–0.36	0.32	–0.13	0.894
Number of comorbidities	–0.43	0.5	–1.44	0.58	–0.87	0.392
1 static PTQ 75 E R [nm]	0.04	0.02	0	0.07	2.03	0.050*
R	0.74	–	–	–	–	–
R ² adjusted	0.47	–	–	–	–	–
Standard error of estimation	3.89	–	–	–	–	–
F	7.58	–	–	–	–	–
p-value	<0.001*	–	–	–	–	–

Gender: female 0; male 1; static PTQ 75 E R – maximum peak torque (test 1), E – extensors; R – right limb; F – F test value; VO₂ – oxygen consumption; SE – standard error; 95% CI – 95% confidence interval; BMI – body mass index; *p < 0.05.

mass index (BMI) and maximum knee extensor torque on VO₂/kg. There was a negative direction of the relationship between age and BMI and a positive static PTQ. According to this model, increasing age by 1 year will decrease VO₂/kg by 0.02, increasing BMI by 1 unit will induce a decrease in VO₂/kg by 0.34, and increasing static PTQ will result in an increase in VO₂/kg by 0.04 (Table 9,10).

A very similar model was obtained for the results of study 2. There was also a negative significant relationship between VO₂/kg, and age and BMI, and a positive one with isokinetic PTQ at 60°/s. However, there was no significant effect of any training model (Table 10).

Discussion

The accumulation of traditional (e.g., age, hypertension, smoking, dyslipidemia) and non-traditional (e.g., hyperphosphatemia, conductance, vascular stiffness, years of dialysis therapy) cardiovascular risk factors in a dialysis

patient with a sedentary lifestyle raises questions about an appropriate (safe and effective) rehabilitation program. Given the challenge of maintaining full attendance in this patient group, the final analysis included only those patients who completed at least 70% of the training sessions. This accounted for 45.9% of the total qualifying group, totaling 45 patients. Adherence serves as a key indicator of the practical efficacy of the rehabilitation approach. However, it is important to acknowledge that this was an extensive 6-month training program conducted among a cohort of patients with a significantly higher average age. Shorter training programs provide higher results and are associated with a lower average age of the patients examined.²⁵

In this research project, the most common reasons for discontinuing training were a lack of motivation and health-related events unrelated to exercise. These factors contributed to inconsistencies in participation and a lack of regularity in the training program. During the first month of the program, the most common reasons for

Table 10. Multivariate regression model indicating others predictors of VO_2/kg (for study 2)

Dependent variable VO_2/kg	b	SE (b)	–95% CI	+95% CI	Student's t-test value	p-value
Gender	–2.22	1.50	–5.27	0.83	–1.47	0.149
Endurance training	–0.29	1.81	–3.97	3.38	–0.16	0.872
Tai chi	–1.73	1.63	–5.03	1.57	–1.06	0.295
Age [years]	–0.22	0.07	–0.36	–0.09	–3.35	0.002*
BMI [kg/m^2]	–0.41	0.16	–0.72	–0.09	–2.61	0.013*
Years of dialysis	–0.06	0.18	–0.42	0.30	–0.34	0.734
Number of comorbidities	–0.27	0.52	–1.32	0.79	–0.51	0.611
PTQ E 60 R [nm]	0.05	0.02	0.00	0.10	2.09	0.044*
R	0.81	–	–	–	–	–
R^2 adjusted	0.58	–	–	–	–	–
Standard error of estimation	3.84	–	–	–	–	–
F	8.61	–	–	–	–	–
p-value	<0.001*	–	–	–	–	–

Endurance training and tai chi compared to resistance training, Gender: female 0, male 1, static PTQ 75ER – max peak torque (test 2); E – extensors; R – right limb; VO_2 – oxygen consumption; SE – standard error; 95% CI – 95% confidence interval; BMI – body mass index.

patient dropout were discomfort with post-exercise fatigue and a low subjective perception of the exercise's appeal. As the program progressed, the group size remained stable, with subsequent dropouts primarily due to health-related events, kidney transplant surgery or death.

Evaluation of spiroergometric parameters

The oxygen uptake capacity (oxygen ceiling; VO_2max) can be viewed as a determinant of the body's ability to perform maximal work.²⁶ After a 6-month exercise program, an increase in minute oxygen uptake (VO_2), VO_2/kg and HR was demonstrated in each of the study groups, compared to study 1. The significance of the observed difference was confirmed only in group 1 for VO_2 and HR, with a strong effect size.

In the available literature, the results vary depending on the training model, duration and anthropometric parameters of the participants, ranging from no significant changes in VO_2max aerobic capacity^{27,28} to substantial improvements of up to 40%.^{29,30} Scapini et al. observed a greater increase in VO_2max , reaching 3.35 mL/kg/min.³¹ Matsuzawa et al. analyzed a population of elderly patients with ESRD and found a statistically significant mean change in VO_2max of 0.62 mL/kg/min after various workout programs, including those following a day-off model.³² Young et al. conducted a meta-analysis evaluating the effects of cycloergometer training during dialysis on spiroergometric parameters. Other authors highlighted the limited potential of this intervention to improve exercise capacity (oxygen uptake), pointing to an unmeasured increase in the VO_2max parameter of only 1.19 mL/kg/min in the entire collected cohort of dialysis patients.²¹ Groussard et al. reported that, following a 3-month

aerobic training program, VO_2max decreased from 14.7 ± 2.1 mL/kg/min to 14.3 ± 2.3 mL/kg/min.²⁸ Reboredo et al., after a 3-month rotor training program ($n = 12$, age 50.7 ± 10.7 years, initial VO_2max 25.8 ± 5.5 mL/kg/min, BMI 22.8 ± 2.3), recorded a significant increase in VO_2max to 29 ± 7 mL/kg/min.³³

The analysis of the cited works indicates the dependence of performance on baseline fitness, age and BMI. This was also confirmed by the results of the regression analysis, which showed that age and BMI had the greatest effect on VO_2/kg in the study group of dialysis patients. Studies on populations with a higher average age and lower initial VO_2max , often accompanied by increased BMI,^{27,28} generally do not report significant changes. However, when conducted on younger patients with higher initial VO_2max values and a normal BMI, the results demonstrate a significant positive effect.^{33,34} Advanced age and prolonged dialysis therapy significantly impair the body's physiological adaptive capacity and exacerbate sarcopenic changes. Reduced aerobic capacity and increased body fat mass (negatively impacting VO_2max) are indicative of reduced physical condition from the outset, which in turn impacts the patient's adaptive capacity and motivation to maintain training intensity and regularity. Older patients are more likely to experience fatigue during dialysis and shortness of breath, which further discourages them from engaging in physical activity.³⁵

Based on the study's findings and those of other researchers, it can be inferred that younger individuals in better physical condition and those with a shorter duration of dialysis therapy benefited the most from the implemented training cycle. In our study, group 3, which participated in tai chi training on non-dialysis days ("day-off"), showed nonsignificant improvements in the assessed fitness parameters.

The minimal gains in fitness indices are likely attributed to the participants' age, as well as the methodology and specific characteristics of tai chi training. The resultant VO_2max following 6 months of endurance training in group 1, considering the individuals' average age and beginning fitness levels, was comparable to findings from previous studies. Hence, the results of our study confirm the reported challenges of rehabilitation and highlight the unique characteristics of this patient group, including the accumulation of both traditional and non-traditional risk factors.³⁵

Evaluation of strength and speed parameters

Endurance training is mainly used to increase fitness and improve cardiovascular function and is not the preferred intervention to induce functional muscle improvement. However, depending on an individual's age, activity level and physical fitness, it can also enhance strength and speed parameters.^{36,37} After 6 months of training on cycle-ergometers, nonsignificant increases in peak force moments of the knee extensors and flexors on isometric testing were recorded in group 1. In contrast, significant observations were noted in the isokinetic test at 180°/s. In group 1, there was a significant overall improvement in force-velocity parameters, with a significant increase in peak force moments for the extensors and flexors of the knee joint. In rehabilitation and biomechanical studies on elderly individuals, a significant reduction in neuromuscular reaction speed during dynamic movements has been observed, which can increase the risk of falls and injuries.³⁸ Improving neuromuscular excitability and PTQ during dynamic movements through simple rotor training may offer potential benefits in injury prevention. Consistent with scientific findings, enhancing muscular endurance, as reflected in TW, could contribute to improved daily functioning.¹¹

Group 2 recorded the greatest changes in strength and speed parameters, both in isometry and isokinetic testing at 60°/s. In contrast, at 180°/s, group 2 had a weaker but significant improvement compared to the endurance group (group 1). To the best of the authors' knowledge, no studies have been conducted using comparable direct dynamometry measurements. Most researchers assess strength using indirect measures and report percentage changes, making direct comparisons unfeasible. Consequently, only general conclusions can be drawn.

Chen et al. reported significant increases in knee extensor muscle strength of $44.9 \pm 26.3\%$ after a 6-month training intervention following a similar model. However, this measurement was conducted using a hand dynamometer under isometric conditions.³⁹ In contrast, Thompson et al., using a similar training methodology but a shorter 12-week program ($n = 7$, age 59.7 (45.9 – 81.4) years), observed no significant improvement in strength. However, strength was assessed using the one-repetition maximum (1RM) method.⁴⁰ Cheema et al., following a similar training

model during dialysis, observed an improvement in muscle strength, including knee extensors, under isometric conditions after 3 months of training.⁴¹ Kirkman et al. reported a 7% increase in isometric muscle strength after 12 weeks of resistance training ($n = 12$; age 48 ± 18 years). It should be noted that Kirkman implemented a high-resistance training program using a specially designed resistance platform mounted to the dialysis chair.⁴² Headley et al. reported a 12.7% improvement in knee extensor strength after 3 months of training in a day-off resistance training model, but only for the slowest speed tested, i.e., 90°/s.⁴³

Group 3 engaged in 6 months of tai chi training, a supervised exercise program that does not require specialized equipment. The key advantage of tai chi lies in its diverse set of movement sequences, with gradually increasing difficulty levels that necessitate the adaptation of muscle strength and motor control. This practice enhances balance, coordination and overall functional stability. The group exhibited a slight improvement in both static and dynamic strength moments, though these changes were not statistically significant. However, it is important to consider that group 3 participated in sessions only twice per week, whereas the other groups followed a 3-times-per-week training model. This difference in training frequency may explain the nonsignificant gains observed in the biomechanical parameters. Currently, there are no published studies on this specific patient group using an analogous method for measuring muscle strength.

Chang et al. conducted a 12-week tai chi program involving 21 ESRD patients (mean age 54.2 ± 15.2 years). Lower limb strength was assessed using the sit-to-stand (STS) test, which included the 5- and 10-repetition tests (STS5 and STS10) measured by time, as well as the 60-second test (STS60) performed for the maximum number of repetitions. After 12 weeks of training, a significant improvement was observed only in the STS60 test, which the authors attributed to enhanced lower limb muscular endurance. The STS5 and STS10 tests, requiring 5 and 10 repetitions of the "stand up/sit down" movement, assess the ability to generate power and muscle speed. In contrast, the STS60 test, performed over 60 s, allows for a slower movement pace with less demand for agonist-antagonist muscle control, making it a better indicator of endurance rather than explosive strength.⁴⁴

Limitations

The main limitation of this study is the lack of a non-exercise control group. This is due to the specificity of this group of patients. The CPET and dynamometry tests are highly demanding assessments. It was not possible to get enough patients to do these tests without a tradeoff in the form of therapy intervention. We used the cluster randomization method which has some drawbacks – it does not give a precise picture of the whole population. The studied groups were relatively small and the results require confirmation using a larger group of patients.

Also, an important aspect of the planned workouts was the tradeoff between maintaining adequate training intensity and its safety for patients and the hemodialysis process. It should be noted that the task of the conducted research was not to determine the maximum adaptive capacity of patients with ESRD (expressed in spirometric and strength-velocity parameters), but to establish an effective, safe and pragmatic model – possibly accessible to all patients. In addition, tai chi training, for organizational reasons, took place twice a week, on a day without dialysis. In contrast, resistance training, for reasons of safety and correctness of execution, requires individual supervision of a physiotherapist during exercise, which could increase the sense of safety and have a motivating effect on the patient, potentially increasing the intensity of training and greater acceptance of the progression being introduced.

Conclusions

The above results seem to confirm the observed limited potential for improving aerobic capacity in patients with ESRD. The strongest determinants of exercise capacity, aside from age and BMI, were the strength of the lower limbs. Enhancing performance in this area is challenging and warrants further research. However, greater potential for improving patients' overall condition is associated with the incorporation of resistance training. The analysis of strength and speed parameters highlights the specificity of each training modality, as evidenced by selective improvements in isometric and isokinetic test performance. These changes could have a protective influence on the risk of falls. Activities of daily living, such as walking, climbing stairs, lifting objects, and performing manual work, require overcoming the resistance of body weight and involve muscle groups of the trunk and upper limbs. In this context, resistance training demonstrates superior functional relevance due to its engagement of nearly the entire muscular system and the notable improvements in muscle strength it produces.

Data availability

The datasets generated and/or analyzed during the current study are available from the Repository for Open Data: <https://doi.org/10.18150/ZZJY3I,RepOD,V1>, and in Zenodo: <https://doi.org/10.5281/zenodo.15024227>.




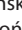







Consent for publication

Not applicable.

Use of AI and AI-assisted technologies

Not applicable.

ORCID iDs

Łukasz Rogowski  <https://orcid.org/0000-0001-9747-3098>
 Joanna Kowalska  <https://orcid.org/0000-0002-5232-1688>
 Katarzyna Bulińska  <https://orcid.org/0000-0002-4233-176X>
 Małgorzata Stefańska  <https://orcid.org/0000-0003-2070-8535>
 Agnieszka Zembroń-Łacny  <https://orcid.org/0000-0001-7596-9850>
 Andrea Mahrová  <https://orcid.org/0000-0001-6303-0627>
 Jitka Marenčáková  <https://orcid.org/0000-0003-1981-818X>
 Tomasz Gołębiowski  <https://orcid.org/0000-0001-5477-2020>
 Witold Wnukiewicz  <https://orcid.org/0000-0003-1165-4651>
 Mariusz Kusztal  <https://orcid.org/0000-0002-6502-0374>
 Wioletta Dziubek  <https://orcid.org/0000-0003-3511-7623>

References

1. Zdrojewski Ł, Zdrojewski T, Rutkowski M, et al. Prevalence of chronic kidney disease in a representative sample of the Polish population: Results of the NATPOL 2011 survey. *Nephrol Dial Transplant*. 2016;31(3):433–439. doi:10.1093/ndt/gfv369
2. Robinson BM, Akizawa T, Jager KJ, Kerr PG, Saran R, Pisoni RL. Factors affecting outcomes in patients reaching end-stage kidney disease worldwide: Differences in access to renal replacement therapy, modality use, and haemodialysis practices. *Lancet*. 2016;388(10041):294–306. doi:10.1016/S0140-6736(16)30448-2
3. Zoccali C, Kramer A, Jager KJ. Epidemiology of CKD in Europe: An uncertain scenario. *Nephrol Dial Transplant*. 2010;25(6):1731–1733. doi:10.1093/ndt/gfq250
4. Sugahara K, Miyatake N, Kondo T, et al. Relationships between various parameters of prolonged sedentary bouts and health-related quality of life (HRQOL) in patients on chronic hemodialysis: A cross-sectional study. *Cureus*. 2024;16(9):e70126. doi:10.7759/cureus.70126
5. Odden MC, Chertow GM, Fried LF, et al. Cystatin C and measures of physical function in elderly adults: The Health, Aging, and Body Composition (HABC) study. *Am J Epidemiol*. 2006;164(12):1180–1189. doi:10.1093/aje/kwj333
6. Navaneethan SD, Kirwan JP, Arragain S, Schold JD. Adiposity measures, lean body mass, physical activity and mortality: NHANES 1999–2004. *BMC Nephrol*. 2014;15(1):108. doi:10.1186/1471-2369-15-108
7. Ross R, Blair SN, Arena R, et al. Importance of assessing cardiorespiratory fitness in clinical practice: A case for fitness as a clinical vital sign. A scientific statement from the American Heart Association. *Circulation*. 2016;134(24):e653–e699. doi:10.1161/CIR.0000000000000461
8. Chu DJ, Ahmed AM, Qureshi WT, et al. Prognostic value of cardiorespiratory fitness in patients with chronic kidney disease: The FIT (Henry Ford Exercise Testing) Project. *Am J Med*. 2022;135(1):67–75.e1. doi:10.1016/j.amjmed.2021.07.042
9. Chinnappa S, White E, Lewis N, et al. Early and asymptomatic cardiac dysfunction in chronic kidney disease. *Nephrol Dial Transplant*. 2018;33(3):450–458. doi:10.1093/ndt/gfx064
10. Johansen KL, Painter P. Exercise in individuals with CKD. *Am J Kidney Dis*. 2012;59(1):126–134. doi:10.1053/j.ajkd.2011.10.008
11. Roshanravan B, Patel KV, Fried LF, et al. Association of muscle endurance, fatigability, and strength with functional limitation and mortality in the health aging and body composition study. *J Gerontol A Biol Sci Med Sci*. 2017;72(2):284–291. doi:10.1093/gerona/glw210
12. Shirai N, Yamamoto S, Osawa Y, et al. Low muscle strength and physical function contribute to falls in hemodialysis patients, but not muscle mass. *Clin Exp Nephrol*. 2024;28(1):67–74. doi:10.1007/s10157-023-02403-4
13. Leblanc A, Taylor BA, Thompson PD, et al. Relationships between physical activity and muscular strength among healthy adults across the lifespan. *SpringerPlus*. 2015;4(1):557. doi:10.1186/s40064-015-1357-0
14. Mitchell WK, Williams J, Atherton P, Larvin M, Lund J, Narici M. Sarcopenia, dynapenia, and the impact of advancing age on human skeletal muscle size and strength: A quantitative review. *Front Physiol*. 2012;3:260. doi:10.3389/fphys.2012.00260
15. Madziarska K, Hap K, Mazanowska O, Sutkowska E. Comprehensive lifestyle modification as complementary therapy to prevent and manage post-transplant diabetes mellitus. *Postepy Hig Med Dosw*. 2021;75(1):238–245. doi:10.5604/01.3001.0014.8311
16. Zhou Y, Hellberg M, Svensson P, Höglund P, Clyne N. Sarcopenia and relationships between muscle mass, measured glomerular filtration rate and physical function in patients with chronic kidney disease stages 3–5. *Nephrol Dial Transplant*. 2018;33(2):342–348. doi:10.1093/ndt/gfw466

17. Moorthi RN, Avin KG. Clinical relevance of sarcopenia in chronic kidney disease. *Curr Opin Nephrol Hypertens*. 2017;26(3):219–228. doi:10.1097/MNH.0000000000000318
18. Heitman K, Alexander MS, Faul C. Skeletal muscle injury in chronic kidney disease: From histologic changes to molecular mechanisms and to novel therapies. *Int J Mol Sci*. 2024;25(10):5117. doi:10.3390/ijms25105117
19. Clinical Practice Guideline on management of older patients with chronic kidney disease stage 3B or higher (eGFR < 45 ml/min/1.73 m²). *Nephrol Dial*. 2017;19(1):207–220. doi:10.28996/1680-4422-2017-1-207-220
20. Dziubek W, Chojak-Fijałka K, Gołębiowski T, et al. Physiotherapy in chronic haemodialysis patients: Recommendations of the Expert Committee of the Rehabilitation Section at the Polish Society of Nephrology. *Med Rehabil*. 2023;26(4):4–20. doi:10.5604/01.3001.0016.2833
21. Young HML, March DS, Graham-Brown MPM, et al. Effects of intradialytic cycling exercise on exercise capacity, quality of life, physical function and cardiovascular measures in adult haemodialysis patients: A systematic review and meta-analysis. *Nephrol Dial Transplant*. 2018;33(8):1436–1445. doi:10.1093/ndt/gfy045
22. Rosnow RL, Rosenthal R. Effect sizes for experimenting psychologists. *Can J Exp Psychol*. 2003;57(3):221–237. doi:10.1037/h0087427
23. Prajzner A. Selected indicators of effect size in psychological research. *Annales Universitatis Mariae Curie-Skłodowska Sectio J Paedagogia-Psychologia*. 2023;35(4):139–157. doi:10.17951/j.2022.35.4.139-157
24. Lenhard W, Lenhard A. Computation of Effect Sizes. *Psychometrica.de*; 2017. doi:10.13140/RG.2.2.17823.92329
25. Deschamps T. Let's programme exercise during haemodialysis (intradialytic exercise) into the care plan for patients, regardless of age. *Br J Sports Med*. 2016;50(22):1357–1358. doi:10.1136/bjsports-2016-096356
26. Myers J, Prakash M, Froelicher V, Do D, Partington S, Atwood JE. Exercise capacity and mortality among men referred for exercise testing. *ACC Curr J Rev*. 2002;11(4):33–34. doi:10.1016/S1062-1458(02)00697-9
27. Bohm C, Stewart K, Onyskie-Marcus J, Esliger D, Kriellaars D, Rigatto C. Effects of intradialytic cycling compared with pedometry on physical function in chronic outpatient hemodialysis: A prospective randomized trial. *Nephrol Dial Transplant*. 2014;29(10):1947–1955. doi:10.1093/ndt/gfu248
28. Groussard C, Rouchon-Isnard M, Coutard C, et al. Beneficial effects of an intradialytic cycling training program in patients with end-stage kidney disease. *Appl Physiol Nutr Metab*. 2015;40(6):550–556. doi:10.1139/apnm-2014-0357
29. Deligiannis A, Kouidi E, Tourkantonis A. Effects of physical training on heart rate variability in patients on hemodialysis. *Am J Cardiol*. 1999;84(2):197–202. doi:10.1016/S0002-9149(99)00234-9
30. Konstantinidou E, Koukouvou G, Kouidi E, Deligiannis A, Tourkantonis A. Exercise training in patients with end-stage renal disease on hemodialysis: Comparison of three rehabilitation programs. *J Rehabil Med*. 2002;34(1):40–45. doi:10.1080/165019702317242695
31. Scapini KB, Bohlke M, Moraes OA, et al. Combined training is the most effective training modality to improve aerobic capacity and blood pressure control in people requiring haemodialysis for end-stage renal disease: Systematic review and network meta-analysis. *J Physiother*. 2019;65(1):4–15. doi:10.1016/j.jphys.2018.11.008
32. Matsuzawa R, Hoshi K, Yoneki K, et al. Exercise training in elderly people undergoing hemodialysis: A systematic review and meta-analysis. *Kidney Int Rep*. 2017;2(6):1096–1110. doi:10.1016/j.ekir.2017.06.008
33. Reboredo MM, Neder JA, Pinheiro BV, Henrique DM, Faria RS, Paula RB. Constant work-rate test to assess the effects of intradialytic aerobic training in mildly impaired patients with end-stage renal disease: A randomized controlled trial. *Arch Phys Med Rehabil*. 2011;92(12):2018–2024. doi:10.1016/j.apmr.2011.07.190
34. Painter P, Moore G, Carlson L, et al. Effects of exercise training plus normalization of hematocrit on exercise capacity and health-related quality of life. *Am J Kidney Dis*. 2002;39(2):257–265. doi:10.1053/ajkd.2002.30544
35. Delgado C, Johansen KL. Barriers to exercise participation among dialysis patients. *Nephrol Dial Transplant*. 2012;27(3):1152–1157. doi:10.1093/ndt/gfr404
36. Dziubek W, Bulińska K, Kusztal M, et al. Evaluation of exercise tolerance in dialysis patients performing tai chi training: Preliminary study. *Evid Based Complement Alternat Med*. 2016;2016(1):5672580. doi:10.1155/2016/5672580
37. Bouaziz W, Schmitt E, Kaltenbach G, Geny B, Vogel T. Health benefits of cycle ergometer training for older adults over 70: A review. *Eur Rev Aging Phys Act*. 2015;12(1):8. doi:10.1186/s11556-015-0152-9
38. Boccia G, Dardanelli D, Rosso V, Pizzigalli L, Rainoldi A. The application of sEMG in aging: A mini review. *Gerontology*. 2015;61(5):477–484. doi:10.1159/000368655
39. Chen JLT, Godfrey S, Ng TT, et al. Effect of intra-dialytic, low-intensity strength training on functional capacity in adult haemodialysis patients: A randomized pilot trial. *Nephrol Dial Transplant*. 2010;25(6):1936–1943. doi:10.1093/ndt/gfp739
40. Thompson S, Klarenbach S, Molzahn A, et al. Randomised factorial mixed method pilot study of aerobic and resistance exercise in haemodialysis patients: DIALY-SIZE! *BMJ Open*. 2016;6(9):e012085. doi:10.1136/bmjopen-2016-012085
41. Cheema B, Abas H, Smith B, et al. Progressive exercise for anabolism in kidney disease (PEAK): A randomized, controlled trial of resistance training during hemodialysis. *J Am Soc Nephrol*. 2007;18(5):1594–1601. doi:10.1681/ASN.2006121329
42. Kirkman DL, Mullins P, Junglee NA, Kumwenda M, Jibani MM, Macdonald JH. Anabolic exercise in haemodialysis patients: A randomised controlled pilot study. *J Cachexia Sarcopenia Muscle*. 2014;5(3):199–207. doi:10.1007/s13539-014-0140-3
43. Headley S, Germain M, Mailloux P, et al. Resistance training improves strength and functional measures in patients with end-stage renal disease. *Am J Kidney Dis*. 2002;40(2):355–364. doi:10.1053/ajkd.2002.34520
44. Chang JH, Koo M, Wu SW, Chen CY. Effects of a 12-week program of tai chi exercise on the kidney disease quality of life and physical functioning of patients with end-stage renal disease on hemodialysis. *Complement Ther Med*. 2017;30:79–83. doi:10.1016/j.ctim.2016.12.002

Next-generation sequencing study of inflammatory spindle cell lesions focused on receptor tyrosine kinase gene rearrangements most frequently occurring in inflammatory myofibroblastic tumor

Krzysztof Siemion^{1,2,A–F}, Joanna Kiśluk^{3,B,D,E}, Natalia Wasilewska^{3,B,D,E},
Joanna Reszec-Gielażyn^{1,D–F}, Anna Korzyńska^{2,D–F}, Tomasz Łysoń^{4,E,F}, Zenon Mariak^{4,E,F}

¹ Department of Medical Pathomorphology, Medical University of Białystok, Poland

² Laboratory of Processing and Analysis of Microscopic Images, Nalecz Institute of Biocybernetics and Biomedical Engineering, Polish Academy of Sciences, Warsaw, Poland

³ Department of Clinical Molecular Biology, Medical University of Białystok, Poland

⁴ Department of Neurosurgery, Medical University of Białystok, Poland

A – research concept and design; B – collection and/or assembly of data; C – data analysis and interpretation;

D – writing the article; E – critical revision of the article; F – final approval of the article

Advances in Clinical and Experimental Medicine, ISSN 1899–5276 (print), ISSN 2451–2680 (online)

Adv Clin Exp Med. 2025;34(12):2119–2135

Address for correspondence

Krzysztof Siemion

E-mail: krzysztof.siemion@ibib.waw.pl

Funding sources

The study was financed from funds of the Medical University of Białystok (grants No. SUB/1/DN/21/002/1194 and No. SUB/1/DN/22/002/1155) and Nalecz Institute of Biocybernetics and Biomedical Engineering Polish Academy of Sciences (grant No. FBW/3.1/23).

Conflict of interest

None declared

Received on January 28, 2024

Reviewed on December 10, 2024

Accepted on March 19, 2025

Published online on July 31, 2025

Cite as

Siemion K, Kiśluk J, Wasilewska N, et al. Next-generation sequencing study of inflammatory spindle cell lesions focused on receptor tyrosine kinase gene rearrangements most frequently occurring in inflammatory myofibroblastic tumor. *Adv Clin Exp Med.* 2025;34(12):2119–2135. doi:10.17219/acem/203097

DOI

10.17219/acem/203097

Copyright

Copyright by Author(s)

This is an article distributed under the terms of the Creative Commons Attribution 3.0 Unported (CC BY 3.0) (<https://creativecommons.org/licenses/by/3.0/>)

Abstract

Background. A group of inflammatory spindle cell lesions (ISCLs) includes many nosological entities with a common histological image consisting of spindle-shaped cells and inflammatory infiltrate. Diverse diseases indicate different prognoses that can be difficult to predict. The most well-known neoplasm from the group is an inflammatory myofibroblastic tumor (IMT) that harbors tyrosine kinase gene rearrangement frequently affecting *ALK*, *ROS1*, *RET*, *PDGFRB*, *NTRK*, and *IGF1R* genes. In contrast, a reactive mass-forming lesion is regarded as an inflammatory pseudotumor (IPT).

Objectives. This study aimed to: 1) investigate the accuracy of the primary diagnosis of IMT and IPT with the diagnostics using extended analysis of clinical data, re-evaluation of histopathological slides and next-generation sequencing (NGS); and 2) to establish prognostic and diagnostic factors.

Materials and methods. Finally, 46 cases of ISCLs were retrieved. The authors revised diagnoses and performed NGS based on ribonucleic acids isolated from selected paraffin blocks. Clinical and paraclinical data were also collected. The final diagnoses were made as a result of available information integration.

Results. The sequencing confirmed 4 IMTs and detected 4 fusion gene types – *EML4-ALK*, *RANBP2-ALK*, and *ETV6-NTRK3*. Additionally, 1 afunctional EGFR-PPARGC1A rearrangement was found in gastric inflammatory fibroid polyp. A subset of reactive lesions also contained some mutations, which is consistent with actual knowledge. Neoplasms with ganglion-like cells, nuclear atypia and increased mitotic activity gave local recurrences. A higher percentage of necrosis indicated IMTs and patients who died in the analyzed period. No relation between genetic alterations and relapse was found.

Conclusions. A final diagnosis can be made based on all clinical and paraclinical data. The prognosis after the treatment is dependent on the pathological diagnosis, disease location and resection completeness, presence of ganglion-like cells, nuclear atypia, mitotic index, and necrosis. Not only neoplastic but also reactive lesions can recur. The presence of gene rearrangements and necrosis can have diagnostic value.

Key words: next-generation sequencing, receptor tyrosine kinase, inflammatory myofibroblastic tumors, inflammatory pseudotumors, inflammatory spindle cell lesions

Highlights

- Inflammatory spindle cell lesions (ISCLs) feature spindle cells mixed with inflammatory infiltrates – hallmark morphology for this rare entity.
- ISCL spectrum ranges from neoplastic inflammatory myofibroblastic tumors (IMTs) to reactive inflammatory pseudotumors (IPTs).
- Neoplastic and reactive ISCLs alike can exhibit aggressive histology, oncogenic mutations and clonal genetic changes.
- Tyrosine receptor kinase gene rearrangement testing (ALK, ROS1, NTRK) is mandatory for a definitive IMT diagnosis.
- Pathology reports should list prognostic and diagnostic markers – ganglion-like cells, cytologic atypia, mitotic index, necrosis, and gene rearrangements.

Background

Inflammatory spindle cell lesions (ISCLs) represent a histologically defined group of disorders. Microscopically, they are characterized by the presence of spindle-shaped cells interspersed with a dense inflammatory infiltrate (Fig. 1). This group is heterogeneous in nature, encompassing a range of distinct pathological entities.^{1–4} Initially, ISCLs were divided into 2 subgroups: 1) a neoplastic lesion – an inflammatory myofibroblastic tumor (IMT); and 2) a reactive lesion – an inflammatory pseudotumor (IPT).¹ Subsequently, the group was gradually expanded.^{3,5–18} Any

secondary inflamed spindle cell neoplasm may be included in this group. However, establishing an accurate diagnosis can be challenging.¹⁹

Inflammatory spindle cell lesions may occur in any region of the human body, with symptoms and signs depending on the location.³ Radiological imaging is often heterogeneous and nonspecific.²⁰ Correlation of histological features, molecular genetic testing, clinical history, and radiological data is essential for accurate diagnosis.

Inflammatory myofibroblastic tumors are intermediate-grade neoplasms characterized by a relatively high recurrence rate and low metastatic potential. Under a light

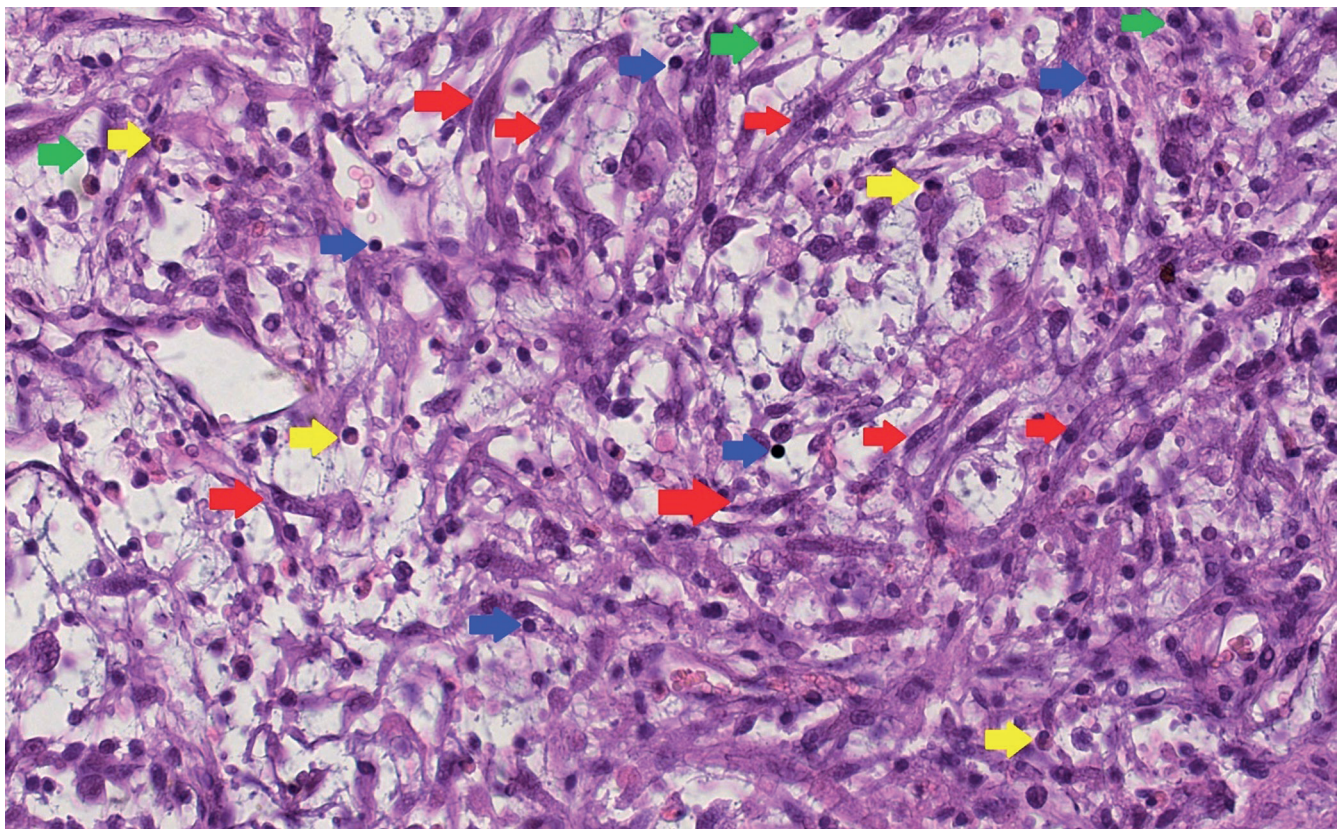


Fig. 1. Histopathological image of an inflammatory spindle cell lesion is composed of spindle cells (red arrows) and inflammatory infiltrate. Blue arrows: lymphocytes, green arrows: plasma cells, yellow arrows: eosinophils

microscope, 3 major histopathological patterns can be distinguished: classical, hypocellular and hypercellular. A hypercellular pattern, high mitotic activity, presence of myxoid stroma, ganglion-like cells, multinucleated giant cells, necrosis, lymphovascular invasion, and infiltrative growth are considered adverse prognostic factors.^{3,21} Approximately 50–60% of IMTs harbor *ALK* gene rearrangements. Other gene fusions – such as *ROS1*, *PDGFRB*, *RET*, *NTRK1/3*, and *IGF1R* – occur less frequently. Prior to the identification of these driver fusion genes, the terms IMT and IPT were sometimes used interchangeably by clinicians.³

Objectives

The aim of the study was to: 1) investigate the accuracy of primary diagnoses of IMT and IPT by incorporating extended clinical data analysis, re-evaluation of histopathological slides and next-generation sequencing (NGS); 2) determine whether pathological diagnoses, disease location, histological features, and genetic changes influence local recurrence of ISCLs.

Materials and methods

Participants

Eighty-five cases of ISCLs, initially diagnosed as IMT or IPT, were retrieved from the Department of Medical Pathomorphology, Medical University of Białystok (Poland) database. After excluding 39 cases, 46 patients were included in the study (22 men and 24 women; most common lesion locations: abdomen and orbit). Based on the final histopathological diagnoses, the cases were classified into 2 groups: neoplastic ($n = 24$) and reactive ($n = 22$). Clinical and paraclinical data collected before and after diagnosis were analyzed for both groups.

Design and settings

The study was approved by Guidelines for Good Clinical Practice by the Bioethical Committee at the Medical University of Białystok (approval No. APK.002.339.2020). First, archival formalin-fixed paraffin-embedded (FFPE) blocks were prepared using the Leica TP1020 tissue processor (Leica Camera AG, Wetzlar, Germany) and the HistoCore Arcadia H + C embedding system (Leica Camera AG) before the study. At this stage, standard reagents, including 10% buffered neutral formalin, xylene (isomeric mixture), ethanol, and paraffin wax, were used. Then, using the HistoCore AUTOCUT microtome (Leica Camera AG), 4–5 μm -thick sections were prepared and placed on SuperFrost Plus base glasses (Thermo Fisher Scientific, Waltham, USA). Hematoxylin and eosin (H&E) staining

was performed using the ST5010 Autostainer XL (Leica Camera AG). Finally, histopathological slides were covered using CV5030 Glass Coverslipper (Leica Camera AG).

The initial evaluation of H&E-stained histopathological slides was performed by the 1st pathologist (K.S.) using a light microscope (Olympus BX43; Olympus Corp., Tokyo, Japan). A second opinion was provided for each case by the 2nd pathologist (J.R.G.). Final assessments were based on consensus between the 2 specialists. The histopathological evaluation included the following criteria:

- overall pattern (classical, hypocellular or hypercellular);
- degree of nuclear atypia, assessed according to the criteria proposed by Weir et al.²²;
- percentage of necrosis;
- mitotic index, defined as the number of mitoses per 10 high-power fields (HPF);
- intensity of the inflammatory infiltrate, graded according to the method presented by Klintrup et al.²³;
- predominant type of inflammatory cells within the infiltrate;
- presence of ganglion-like cells, angioinvasion and perineural invasion.

Two pathology specialists reviewed all cases and selected 46 for the NGS procedure. Genomic RNA was extracted from the macrodissected FFPE material using the AllPrep DNA/RNA FFPE Kit (Qiagen, Hilden, Germany). Quantity and quality of isolated RNA were determined using the NanoDrop 1000 UV Spectrophotometer (Thermo Fisher Scientific) and Qubit Fluorometer (Thermo Fisher Scientific).

Sample analysis was performed by NGS technology with the Archer® Fusion Plex® Lung Kit v. PI028.1 (ArcherDX, Inc, Boulder, USA) on the Illumina MiSeq platform. The NGS-based targeted sequencing assay allows detection of known and novel gene fusions, single nucleotide variations (SNVs), insertion/deletion polymorphism (indels), splicing, and gene expression. The kit contains 163 GSPs targeting 14 genes. The unique molecular on-target is above 93%. The assay targets are presented in Table 1. The recommended number of reads for all targets was 500,000. Data were analyzed using the Lung Target Region File and vendor-supplied software (Archer Analysis v. 6.2.7; Integrated DNA Technologies Inc.). The limit of detection (LoD) was defined as a minimum of 5 reads with at least 3 unique sequencing start sites spanning the breakpoint regions. The read length was paired-end, with a cut-off of 5% for variant allele frequency (VAF). The median coverage for all samples was 1,350.

Criteria

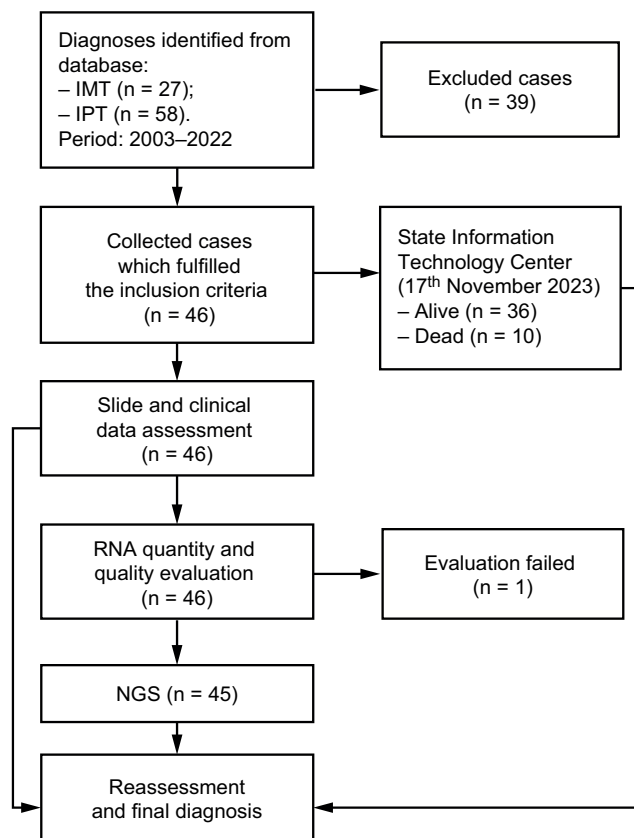
Following the analysis of clinical and paraclinical data, histopathological slide assessments and NGS results, the final diagnoses were established by 2 pathologists based on the World Health Organization (WHO) soft

Table 1. Next-generation sequencing target genes

Gene	Exons
ALK	NM_004304 exon 22, 23, 25 mutations
	NM_004304 exon 2, 4, 6, 10, 16, 17, 18, 19, 20, 21, 22, 23, 26 fusions 5'
BRAF	NM_004333 exon 15 mutation (V600)
	NM_004333 exon 2, 7, 8, 9, 10, 11, 12, 15, 16 fusion 5'
EGFR	NM_004333 exon 1, 3, 7, 8, 10, 13 fusion 3'
	NM_005228 exon 18, 19, 20, 21 mutations
	NM_005228 exon 7, 8, 9, 16, 19, 20, fusion 5'
	NM_005228 8 exon 2–7 skipping (EGFRvIII) 5'
	NM_005228 exon 1, 24, 25 fusion 3'
FGFR1	NM_005228 1 exon 2–7 skipping (EGFRvIII) 3'
	NM_015850 exon 2, 3, 4, 5, 6, 7, 8, 9, 10, 11, 17 fusions 5'
FGFR2	NM_015850 exon 12, 17 fusion 3'
	NM_000141 exon 2, 5, 7, 8, 9, 10 fusion 5'
FGFR3	NM_000141 16, 17 fusion 3'
	NM_000142 exon 3, 5, 8, 9, 10 fusion 5'
KRAS	NM_000142 exon 16, 17, 18 fusion 3'
	NM_004985 exon 2, 3 mutation
MET	NM_000245 exon 2, 4, 5, 6, 13, 14, 15, 16, 17, 21 fusion 5'
	NM_000245 15 exon 14 skipping 5'
	NM_000245 exon 2, 13 fusion 3'
	NM_000245 13 exon 14 skipping 3'
NRG1	NM_013957 exon 1, 8 fusion 5'
	NM_004495 exon 1, 2, 3, 4, 6 fusion 5'
	NM_013962 exon 1 fusion 3'
NTRK1	NM_002529 exon 2, 4, 6, 8, 10, 11, 12, 13 fusion 5'
	NM_006180 exon 5, 7, 9, 11, 12, 13, 14, 15, 16, 17 fusion 5'
NTRK3	NM_002530 exon 4, 7, 10, 12, 13, 14, 15, 16 fusion 5'
	NM_001007156 exon 15 fusion 5'
	NM_002530 exon 13, 14, 15 fusion 3'
RET	NM_020630 exon 15,16 mutation
	NM_020630 exon 2, 4, 6, 8, 9, 10, 11, 12, 13, 14 fusion 5'
ROS1	NM_002944 exon 38 mutation
	NM_002944 exon 2, 4, 7, 31, 32, 33, 34, 35, 36, 37 fusion 5'

ALK – anaplastic lymphoma kinase; BRAF – B-type rapidly accelerated fibrosarcoma; EGFR – epidermal growth factor receptor; FGFR – fibroblast growth factor receptor; KRAS – Kirsten rat sarcoma; MET – mesenchymal-to-epithelial transition factor; NRG1 – neuregulin 1; NTRK – neurotrophic tyrosine receptor kinase; RET – rearranged during transfection; ROS1 – v-ras avian UR2 sarcoma virus oncogene homolog 1.

tissue tumor classification criteria²⁴ (Fig. 2). The inclusion criteria were: 1) primary histopathological diagnosis of IMT or IPT; 2) presence of FFPE blocks; 3) spindle cell morphology with inflammatory infiltrate resembling IMT; and 4) RNA integrity number (RIN) with a minimum value of 2. Cases were excluded if FFPE material was unavailable, if histopathological features differed from the study criteria, or if the RNA integrity number (RIN) was below 2.

**Fig. 2.** Diagram depicting the data collection and work schedule

FFPE – formalin-fixed paraffin-embedded; IMT – inflammatory myofibroblastic tumor; IPT – inflammatory pseudotumor.

Statistical analyses

The statistical parameter formulas and definitions used for diagnostic verification are outlined in Fig. 3. Dichotomous division was used at each stage of the analysis, e.g., neoplasms compared to other diseases, IMTs compared to other ISCLs, recurrent compared to non-recurrent cases, and patients who died compared to those who survived. To assess the impact of the dichotomous classification, odds ratios (ORs) and 95% confidence intervals (95% CIs) for the 2 proportions were calculated using the method described by Tenny et al.²⁵ These statistical parameters were selected because they effectively quantify the strength of association between the 2 groups (with and without events) in retrospective studies.²⁵ Probability values (p-values) were calculated using the MedCalc online calculator (<https://www.medcalc.org>).

All numerical data (e.g., necrosis percentage, mitotic index) obtained through light microscopy represented subjective assessments by the pathologists. While these should be considered continuous variables, they could not be assumed to follow a normal distribution. The data obtained using NGS should be treated similarly. At each stage of the analysis, values were categorized into 1 of 2 groups; therefore, a nonparametric test was selected to account for

a		
Parameter		
sensitivity		$\frac{TP}{TP + FN}$
specificity		$\frac{TN}{TN + FP}$
accuracy		$\frac{TP + TN}{TP + FP + TN + FN}$
precision		$\frac{TP}{TP + FP}$
F1 score		$\frac{2TP}{2TP + FP + FN}$

b		
neoplasm diagnosis correctness	Primary diagnosis	Final diagnosis
TP	neoplasm	neoplasm
TN	other diseases	other diseases
FN	other diseases	neoplasm
FP	neoplasm	other diseases

c		
IMT diagnosis correctness	Primary diagnosis	Final diagnosis
TP	IMT	IMT
TN	other diseases	other diseases
FN	other diseases	IMT
FP	IMT	other diseases

Fig. 3. A. Statistical parameter formulas; B. Definitions used during verification of neoplasm diagnosis correctness; C. Definitions used during verification of inflammatory myofibroblastic tumor diagnosis correctness

FN – false negative; FP – false positive; IMT – inflammatory myofibroblastic tumor; TN – true negative; TP – true positive.

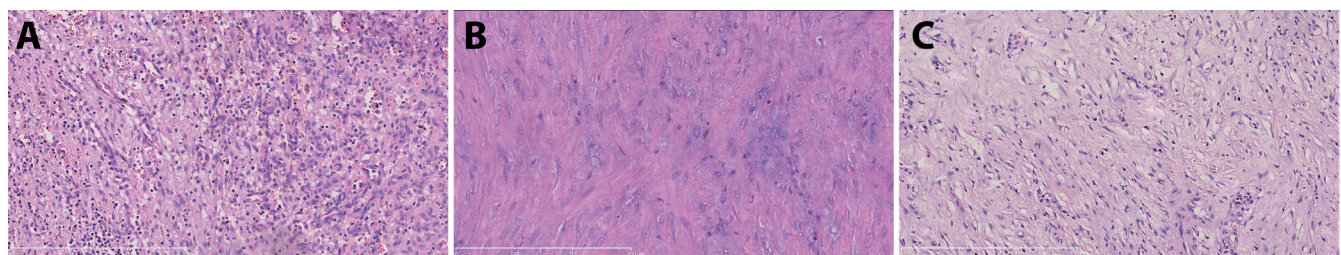


Fig. 4. Tissue pattern. A. Classical (case 4); B. Hypercellular (case 5); C. Hypocellular (case 2). Hematoxylin and eosin (H&E) slides, ×200 magnification

the data distribution. A two-tailed Mann–Whitney U test was conducted at a 5% significance level using the Statistics Kingdom online calculator (<https://www.statskingdom.com>). Outlier values were included in the analysis.

Results

Histopathological assessment

The predominant tissue patterns were classical (41.3%), mixed (30.4%) and hypocellular (17.4%) (Fig. 4). Nuclear atypia was observed in 17 cases (37%), mostly mild, while 3 cases (6.5%) contained ganglion-like cells. Necrosis was present in 26 cases (56.5%). Approximately ⅓ of the lesions showed no mitoses. Chronic inflammatory infiltrates, primarily composed of lymphocytes and plasma cells, dominated among the cases. Angiovascular and perineural invasion were not observed.

The ORs for the presence of atypia and mitoses in neoplastic lesions compared to reactive lesions were statistically significant at the 95% confidence level: OR = 7.48 (95% CI: 1.74–32.17, $p = 0.007$) and OR = 7.14 (95% CI:

1.35–37.75, $p = 0.021$), respectively. These values were calculated using the method described by Tenny et al.²⁵

The estimated necrosis percentage in IMTs (cases 1, 2, 3, 4, and 46) compared to other ISCLs was evaluated using the Mann–Whitney U test ($U = 162.5$, $p = 0.028$). A statistically significant difference was observed, with the 1st group exhibiting a mean value of 34.2% compared to 11.9% in the 2nd group, at the 95% CI (Fig. 5). Based on histopathological features and clinical data, 46 cases were qualified for molecular diagnostics.

Molecular diagnostics

Gene fusions

One sample (case 46) failed RNA quality and quantity control because the RIN value was below 2. Fusion genes were identified in 5 cases. Among them, 4 cases were ultimately diagnosed as IMTs due to the presence of tyrosine kinase rearrangements. Cases 1 and 2 presented an *EML4-ALK* fusion, while case 3 displayed a *RANBP2-ALK* fusion, which led to the diagnosis of epithelioid inflammatory myofibroblastic sarcoma (EIMS) – a more aggressive

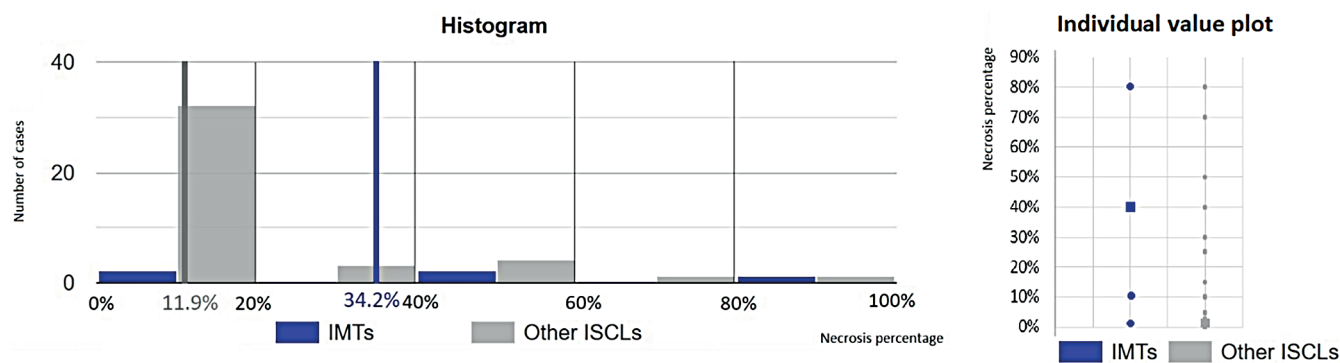


Fig. 5. Histogram (left) depicts the distribution of necrosis percentage values among inflammatory myofibroblastic tumors (IMTs; blue) and other inflammatory spindle cell lesions (ISCLs; grey). The arithmetic mean values are marked with vertical lines. Axes: abscissa – necrosis percentage intervals in the histopathological slides: [0–20%], [20–40%], [40–60%], [60–80%], and [80–100%]; ordinate – number of cases. Individual value plot (right) shows a dot for the actual value of each observation in both groups. The median values are marked with squares. Axes: abscissa – groups of cases (blue: IMTs, grey: other ISCLs); ordinate – necrosis percentage

Table 2. Collective description of fusion genes diagnosed in neoplasms during the study

Case number	Diagnosis	Pattern	Atypia	Necrosis	Inflammatory infiltrate intensity	Dominating inflammatory cells	IHC	Fusion gene	Breakpoints	Recurrence	Observation period
1	IMT of the external nose	C	mild	10%	severe	histiocytes	(+): SMA; (–) S100	EML4-ALK	chr2:42522656 (exon 13) chr2:29446394 (exon 18)	1 year	7 years
2	hepatic IMT	C/↓	none	1%	severe	neutrophils	(+): vim, SMA, CD 99; (–): CK, CD 10, CD31, CD34; Ki67: low	EML4-ALK	chr2:42492091 (exon 6) chr2:29446394 (exon 18)	none	8 years
3	EIMS of the left sphenoid sinus	C	moderate	40%	moderate	lymphocytes, plasma cells, neutrophils	(+): SMA; ALK (focally); (–): CK, CD34; Ki67: 10%	RANBP2-ALK	chr2:110449532 (intron 24) chr2:29443649 (exon 23)	none	7 years
4	IMT of the right orbit	C	mild	80%	moderate	lymphocytes, plasma cells, neutrophils	not performed	ETV6-NTRK3	chr12:12022903 (exon 5) chr15:88483984 (exon 15)	none	1 year
5	gastric IFP	↑	mild	1%	mild	eosinophils	(+): CD34, SMA; (–): desmin, H-caldesmon, ALK, CK, CD117, DOG1	EGFR-PPARGC1A	chr7:55087048 (exon 1) chr4:23926271 (exon 2)	none	4 years

↓ – hypocellular; ↑ – hypercellular; (–) – negative; (+) – positive; ALK – anaplastic lymphoma kinase; C – classical; CD – cluster of differentiation; CK – (pan) cytokeratin; EGFR – epidermal growth factor receptor; EML4 – echinoderm microtubule-associated protein-like 4; ETV6 – ETS variant transcription factor 6; F – female; IFP – inflammatory fibroid polyp; IMT – inflammatory myofibroblastic tumor; IHC – immunohistochemistry; M – male; NTRK – neurotrophic tyrosine receptor kinase; PPARGC1A – peroxisome proliferator-activated receptor gamma, coactivator 1 alpha; RANBP – RAN-binding protein; SMA – smooth muscle actin; vim – vimentin.

variant of IMT. Case 4 was characterized by a translocation involving the *NTRK3* and *ETV6* genes. In case 5, an *EGFR-PPARGC1A* rearrangement, which was deemed nonfunctional due to the absence of a promoter, was identified in a gastric inflammatory fibroid polyp (Table 2).

Gene variants

Eighty-four genetic changes, including substitutions, insertions, duplications, and deletions, were identified across 58 gene variants through RNA NGS analysis. According

to the Varsome database (<https://varsome.com>), these variants were classified as follows: 15 pathogenic, 17 likely pathogenic, 38 of uncertain significance, and 14 benign (Table 3). The most frequently observed pathogenic variants were nucleotide substitutions at positions 34 and 35 of the *KRAS* gene. These mutations were detected in multiple cases, including EIMS (case 3), Langerhans cell histiocytosis (case 11), inflammatory fibroid polyp (case 16), and IPTs (cases 21, 24 and 27).

Additionally, the most commonly identified likely pathogenic variant involved a cytosine-to-thymine substitution at position 2975 of the *MET* gene. The mutation was

Table 3. List of gene variants detected using of NGS and their significance according to the Varsome database (<https://varsome.com/>)

Case number	Diagnosis (fusion gene)	Gene	HGVSp	HGVSc	VAF	Gene variant significance	Recurrence
1	IMT (<i>EML4-ALK</i>)	MET	p.Asn375Ser	c.1124A>G	0.663	benign	1 year
		RET	p.Val25Ala	c.74T>C	0.051	benign	
		RET	p.Leu27Ser	c.80T>C	0.050	uncertain	
2	IMT (<i>EML4-ALK</i>)	none	–	–	–	–	no
3	EIMS (<i>RANBP2-ALK</i>)	EGFR	p.Gln276Ter	c.826C>T	0.090	uncertain	no
		KRAS	p.Gly12Cys	c.34G>T	0.067	pathogenic	
		NTRK3	p.Leu449Phe	c.1345C>T	0.051	uncertain	
4	IMT (<i>ETV6-NTRK3</i>)	none	–	–	–	–	no
5	inflammatory fibroid polyp (<i>EGFR-PPARGC1A</i>)	none	–	–	–	–	no
6	granular cell tumor	FGFR3	p.Val642_Leu645delinsIleHisHisIle	c.1924_1933delinsATTCACCACA	0.956	uncertain	6 years
7	plasma cell myeloma	BRAF	p.Gly315AspfsTer57	c.944del	0.564	likely pathogenic	no
		EGFR	p.Glu746Val	c.2237A>T	0.071	uncertain	
		EGFR	p.Leu747_Pro753delinsSer	c.2240_2257del	0.067	pathogenic	
		RET	p.Leu27Ser	c.80T>C	0.052	uncertain	
8	fibroma	FGFR3	p.Val642_Leu645delinsIleHisHisIle	c.1924_1933delinsATTCACCACA	0.897	uncertain	no
		EGFR	p.Ser768Ile	c.2303G>T	0.569	pathogenic	
		MET	p.Thr992Ile	c.2975C>T	0.552	likely pathogenic	
		EGFR	p.Gly719Ala	c.2156G>C	0.529	pathogenic	
9	anaplastic meningioma	none	–	–	–	–	4 months
10	submucosal fibromatosis	none	–	–	–	–	no
11	Langerhans cell histiocytosis	KRAS	p.Gly12Val	c.35G>T	0.065	pathogenic	no
		ALK	p.Met1199Ile	c.3597G>A	0.063	uncertain	no
12	desmoid fibromatosis	ALK	p.Met1199Ile	c.3597G>A	0.058	uncertain	1 st : 1 year, 2 nd : 6 years
		RET	p.Leu27Ser	c.80T>C	0.051	uncertain	
13	sarcomatoid urothelial carcinoma	EGFR	p.His870Tyr	c.2608C>T	0.063	uncertain	1 st : 1 month, 2 nd : 2 months
14	plexiform fibromyxoma	BRAF	p.Lys591Glu	c.1771A>G	0.065	pathogenic	no
15	angiosarcoma	FGFR3	p.Val642_Leu645delinsIleHisHisIle	c.1924_1933delinsATTCACCACA	1.0	uncertain	no
16	inflammatory fibroid polyp	KRAS	p.Gly12Cys	c.34G>T	0.981	pathogenic	no
		BRAF	p.Ile572Val	c.1714A>G	0.167	uncertain	
		ALK	p.Thr1026Pro	c.3076A>C	0.119	benign	
		BRAF	p.Arg603Ter	c.1807C>T	0.081	likely pathogenic	
17	inflammatory fibroid polyp	BRAF	p.Arg603Ter	c.1807C>T	0.556	likely pathogenic	no
		BRAF	p.Arg444Gln	c.1331G>A	0.357	uncertain	
		BRAF	p.Ser446_Ser447delinsLeuAsn	c.1337_1340delinsTGAA	0.294	uncertain	
		ALK	p.Thr1026Pro	c.3076A>C	0.105	benign	
18	inflammatory fibroid polyp	MET	p.Thr992Ile	c.2975C>T	0.889	likely pathogenic	no

Table 3. List of gene variants detected using of NGS and their significance according to the Varsome database (<https://varsome.com/>) – cont.

Case number	Diagnosis (fusion gene)	Gene	HGVSp	HGVSc	VAF	Gene variant significance	Recurrence
19	GIST	MET	p.Thr992Ile	c.2975C>T	0.060	likely pathogenic	2 years
20	neurofibroma	BRAF	p.Asn581Tyr	c.1741A>T	0.579	pathogenic	no
21	IPT	KRAS	p.Gly12Cys	c.34G>T	0.331	pathogenic	no
		EGFR	p.Gln1020Ter	c.3058C>T	0.082	uncertain	
		NTRK3	p.Pro514Leu	c.1541C>T	0.054	likely pathogenic	
22	IPT	BRAF	p.Gly469Ala	c.1406G>C	0.438	pathogenic	no
		NTRK2	p.Pro50Leu	c.149C>T	0.063	uncertain	no
		FGFR3	p.Arg124Trp	c.370C>T	0.051	uncertain	no
23	IPT (associated with small cell carcinoma)	FGFR1	p.Pro151Ser	c.451C>T	0.056	likely pathogenic	no
24	IPT	KRAS	p.Gly12Val	c.35G>T	0.402	pathogenic	no
		FGFR3	p.Val364TrpfsTer30	c.1090del	0.192	likely pathogenic	
		MET	p.His1079Tyr	c.3235C>T	0.188	uncertain	
25	IPT	ROS1	P.Ser1891LysfsTer18	c.5671dup	0.054	uncertain	no
26	IPT	BRAF	p.Gly315AspfsTer57	c.944del	0.406	likely pathogenic	no
		RET	p.Leu27Ser	c.80T>C	0.068	uncertain	
27	infective IPT	KRAS	p.Gly12Ala	c.35G>C	0.248	pathogenic	no
		BRAF	p.Ser446_Ser447delinsLeuAsn	c.1337_1340delinsTGAA	0.192	uncertain	
		BRAF	p.Arg603Ter	c.1807C>T	0.208	likely pathogenic	
		BRAF	p.Arg444Gln	c.1331G>A	0.179	uncertain	
		FGFR1	p.Thr724Ile	c.2171C>T	0.077	likely pathogenic	
28	IPT – dacryoadenitis	BRAF	p.Asn581Tyr	c.1741A>T	0.579	pathogenic	no
29	IPT	BRAF	p.Ile617Phe	c.1848_1849delinsTT	0.714	uncertain	no
		BRAF	p.Arg603Ter	c.1807C>T	0.24	likely pathogenic	
		BRAF	p.Trp619Cys	c.1857G>T	0.083	pathogenic	
30	infective IPT	RET	p.Arg886Trp	c.2656C>T	0.549	uncertain	no
		MET	p.Thr992Ile	c.2975C>T	0.469	likely pathogenic	
31	infective IPT	FGFR1	p.Gln762Ter	c.2284C>T	0.1	uncertain	1 year
32	IPT	BRAF	p.Pro367Leu	c.1100C>T	0.140	uncertain	no
		NTRK1	p.Thr434Met	c.1301C>T	0.109	benign	
		EGFR	p.Gln40Ter	c.118C>T	0.078	uncertain	
		BRAF	p.Pro301Leu	c.902C>T	0.059	benign	
33	IPT	ALK	p.Thr1026Pro	c.3076A>C	0.086	benign	no
		BRAF	p.Arg603Ter	c.1807C>T	0.076	likely pathogenic	
		ALK	p.His1030Pro	c.3089A>C	0.065	benign	
		BRAF	p.His539Tyr	c.1615C>T	0.058	uncertain	
		BRAF	p.Glu533Ter	c.1597G>T	0.057	uncertain	
		BRAF	p.Phe583Val	c.1747T>G	0.057	uncertain	
		BRAF	p.Phe548Ser	c.1643T>C	0.056	uncertain	
		BRAF	p.Lys591Glu	c.1770_1771delinsGG	0.05	likely pathogenic	

Table 3. List of gene variants detected using of NGS and their significance according to the Varsome database (<https://varsome.com/>) – cont.

Case number	Diagnosis (fusion gene)	Gene	HGVSp	HGVSc	VAF	Gene variant significance	Recurrence
34	IPT	NTRK3	p.Val308Met	c.922G>A	0.559	benign	no
		EGFR	p.Ser229Cys	c.685A>T	0.095	uncertain	
35	IPT – aneurysm wall	ALK	p.Thr1026Pro	c.3076A>C	0.333	benign	no
		ALK	p.His1030Pro	c.3089A>C	0.079	benign	
36	xanthogranulomatous pyelonephritis	BRAF	p.Gly32_Ala33dup	c.95_100dup	0.431	benign	no
		ALK	p.Thr1026Pro	c.3076A>C	0.145	benign	
37	infective IPT	BRAF	p.Ala349del	c.1046_1048del	0.051	uncertain	no
38	ischemic fasciitis (associated with mammary carcinoma)	MET	p.Thr992Ile	c.2975C>T	0.06	likely pathogenic	no
39	IPT	FGFR1	p.Ala411Val	c.1232C>T	0.152	uncertain	no
		KRAS	p.Ser39Phe	c.116C>T	0.096	uncertain	
		FGFR1	p.Arg716Cys	c.2146C>T	0.078	pathogenic	
		EGFR	p.Phe44Ser	c.131T>C	0.073	benign	
		KRAS	p.Gln43Ter	c.127C>T	0.056	uncertain	
40	IPT (associated with colon adenocarcinoma)	FGFR3	p.Ser779Asn	c.2336G>A	0.06	uncertain	no
41	spindle cell SCC	none	–	–	–	–	6 months
42	solitary fibrous tumor	none	–	–	–	–	no
43	leiomyoma	none	–	–	–	–	1 month
44	IPT (after treatment of DLBCL)	none	–	–	–	–	no
45	IPT – sinusitis	none	–	–	–	–	no
46	IMT/PMP	NGS not performed				–	1 month

ALK – anaplastic lymphoma kinase; BRAF – B-type rapidly accelerated fibrosarcoma; DLBCL – diffuse large B-cell lymphoma; EGFR – epidermal growth factor receptor; EIMS – epithelioid inflammatory myofibroblastic sarcoma; FGFR – fibroblast growth factor receptor; GIST – gastrointestinal stromal tumor; HGVSc – Human Genome Variation Society coding sequence name; HGVSp – Human Genome Variation Society protein sequence name; IMT – inflammatory myofibroblastic tumor; IPT – inflammatory pseudotumor; KRAS – Kirsten rat sarcoma; MET – mesenchymal-to-epithelial transition factor; NGS – next-generation sequencing; NTRK – neurotrophic tyrosine receptor kinase; PMP – pseudosarcomatous myofibroblastic proliferation; RET – rearranged during transfection; ROS1 – v-ras avian UR2 sarcoma virus oncogene homolog 1; SCC – squamous cell carcinoma; VAF – variant allele frequency.

found in several cases, including orbital fibroma (case 8), inflammatory fibroid polyp (case 18), gastrointestinal stromal tumor (GIST – case 19), infective IPT (case 30), and ischemic fasciitis (case 38). Substitutions at position 1807 of the *BRAF* gene were also detected in inflammatory fibroid polyps (cases 16 and 17) and IPTs (cases 27, 29 and 33).

Clonality

The NGS gene panel revealed clonality in a majority of the neoplasms studied. At least 1 gene variant with a VAF value greater than 0.5 or a functional gene rearrangement was identified in 50% of the neoplasms. Lower values of VAF and no functional rearrangement were found in 29% of patients. Only 21% of examined neoplasms did not present either mutation or rearrangement. Moreover, genetic alterations were identified in 82% of inflammatory

lesions, cases with VAF values exceeding 0.5 in 18% of inflammatory lesions and with a VAF range of 0–0.5 in 64%. The OR for the presence of at least 1 functional rearrangement or genetic alteration with a VAF of 0.5 or higher in the neoplastic group compared to the reactive group was approx. 5.85. This result was statistically significant at the 95% confidence level (95% CI: 1.50–22.83, $p = 0.011$), calculated using the method described by Tenny et al.²⁵

Clinical follow-up

The maximum observation for the study was 17 years. During this time, 10 patients (21.7%) died within a maximum of 6 years following the surgery. The causes of deaths were related to severe neoplastic diseases, including plasma cell myeloma (case 7), anaplastic meningioma (case 9), desmoid fibromatosis (case 12), angiosarcoma (case 15), and

Table 4. Collective description of histological features of recurrent lesions during the study

Case number	Location	Final diagnosis	Pattern	Ganglion-like cells	Atypia	Necrosis	Mitotic activity	Inflammatory infiltrate intensity	Dominating inflammatory cells	Recurrence	Period of observation	Death
1	external nose	IMT	C	(–)	mild	10%	(–)	severe	histiocytes	1 year	7 years	no
6	right frontal sinus	granular cell tumor	C	(–)	none	none	(–)	severe	lymphocytic	6 years	13 years	no
9	right occipital region	anaplastic meningioma	mixed	(+)	severe	40%	20/10 HPF	mild	lymphocytic	4 months	1 year 4 months	yes
12	right axillary region	desmoid fibromatosis	C	(+)	moderate	40%	1/10 HPF	moderate	histiocytes	1 st : 1 year, 2 nd : 6 years	6 years	yes
13	urinary bladder	sarcomatoid urothelial carcinoma	C	(+)	severe	10%	19/10 HPF	mild	mixed	1 st : 1 month, 2 nd : 2 months	7 years	no
19	small intestine	GIST	↑	(–)	mild	3%	1/10 HPF	mild	lymphocytic	2 years	2 years	yes
31	left orbit	infective IPT	C	(–)	mild	10%	(–)	severe	mixed	6 months	2 years	yes
41	larynx	spindle cell squamous cell carcinoma	mixed	(–)	severe	10%	6/10 HPF	moderate	neutrophils	6 months	1 year	no
43	mesentery	leiomyoma	↑/C	(–)	none	none	(–)	moderate	lymphocytic	1 month	2 years	no
46	urinary bladder	IMT/PMP	C	(–)	mild	40%	1/10 HPF	mild	neutrophils	1 month	12 years	no

↑ – hypocellular; (–) – absent; C – classical; IMT – inflammatory myofibroblastic tumor; IPT – inflammatory pseudotumor; HPF – high-power fields; PMP – pseudosarcomatous myofibroblastic proliferation.

intestinal GIST (case 19). One patient (case 35) died post-surgery due to an abdominal aortic rupture. The overall odds of death were 0.33 in the neoplastic group and 0.22 in the reactive group.

During the surveillance period, which ranged from 1 to 13 years, 10 patients (21.7%) experienced local recurrence of their disease (Table 4). Nine of these cases were neoplastic in origin, including IMT (case 1), granular cell tumor (case 6), anaplastic meningioma (case 9), desmoid fibromatosis (case 12), sarcomatoid urothelial carcinoma (case 13), intestinal GIST (case 19), spindle cell squamous cell carcinoma (case 41), leiomyoma (case 43), and IMT/pseudosarcomatous myofibroblastic proliferation (PMP) (case 46). Episodes of double recurrence were observed in desmoid fibromatosis (case 12) and sarcomatoid urothelial carcinoma (case 13). One reactive lesion, classified as infective IPT (case 31), also presented a recurrence. The overall odds of recurrence were 0.6 in the neoplastic group and 0.048 in the reactive group. The OR for recurrence (12.6) was statistically significant at the 95% confidence level (95% CI: 1.44–10.32, $p = 0.022$), calculated based on method described by Tenny et al.²⁵ Four patients died following local recurrence, including those with anaplastic meningioma (case 9), desmoid-type fibromatosis (case 12), intestinal GIST (case 19), and infective IPT (case 31).

Patients diagnosed with IMTs survived until the end of the study with observation periods lasting between 1 and 8 years. Recurrence was noted in only 1 IMT with

the *EML4-ALK* fusion gene (case 1), occurring 1 year after the initial surgery. No distant metastases were observed during the follow-up period.

Clinicopathological relation

Histopathological features and local recurrence

Ganglion-like cells were identified in specimens from 3 patients with recurrent neoplastic tumors (Table 4), including anaplastic meningioma of the right occipital region (case 9), desmoid fibromatosis of the right axillary region (case 12) and sarcomatoid urothelial carcinoma of the urinary bladder (case 13) (Fig. 6).

The OR for the presence of nuclear atypia in the group with recurrent disease compared to the non-recurrent group was 12, which was statistically significant at the 5% level (95% CI: 2.14–67.24, $p = 0.005$), calculated using the method described by Tenny et al.²⁵ This suggests that nuclear atypia is associated with an adverse prognosis and an increased risk of disease recurrence. Four cases showed severe nuclear atypia (Table 4). Three of them, anaplastic meningioma of the right occipital region (case 9), sarcomatoid urothelial carcinoma of the urinary bladder (case 13) and spindle cell squamous cell carcinoma of the larynx (case 41), presented recurrence. One patient with angiosarcoma of the ileum (case 15) died within 3 days after the operation. Desmoid fibromatosis (case 12) presented moderate atypia and recurred twice.

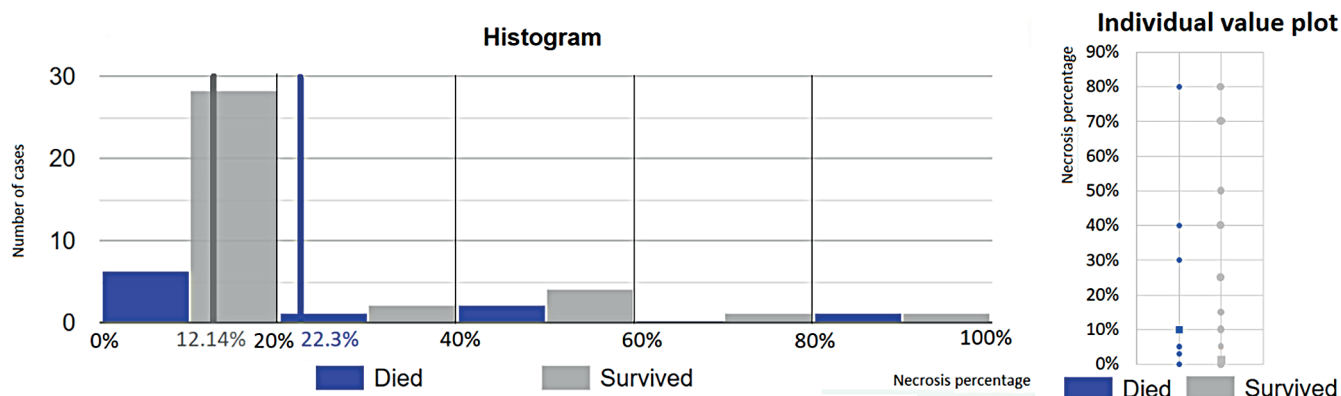


Fig. 8. Histogram (left) depicts the distribution of necrosis among patients who died (blue) and survived (grey) in the analyzed period. The arithmetic mean values are marked with vertical lines. Axes: abscissa – necrosis percentage intervals in the histopathological slides: [0%–20%), [20%–40%), [40%–60%), [60%–80%), and [80%–100%]; ordinate – number of cases. Individual value plot (right) shows a dot for the actual value of each observation in both groups. The median values are marked with squares. Axes: abscissa – groups of patients (blue: who died, grey: who survived); ordinate – necrosis percentage

Table 5. Quantity of diagnosed entities

Neoplastic lesions	Number
Inflammatory myofibroblastic tumor	5
Inflammatory fibroid polyp	4
Leiomyoma	1
Plexiform fibromyxoma	1
Gastrointestinal stromal tumor	1
Desmoid fibromatosis	1
Solitary fibrous tumor	1
Fibroma	1
Angiosarcoma	1
Neurofibroma	1
Anaplastic meningioma	1
Submucosal fibrosis	1
Sarcomatoid urothelial carcinoma	1
Spindle cell squamous cell carcinoma	1
Granular cell tumor	1
Langerhans cell histiocytosis	1
Plasma cell myeloma	1
Reactive lesions	
IPT, not otherwise specified	12
Infective IPT	4
IPT associated with a neoplasm	2
IPT – wall of aneurysm	1
Xanthogranulomatous pyelonephritis	1
Chronic dacryoadenitis	1
Ischemic fasciitis	1

IPT – inflammatory pseudotumor.

Discussion

Inflammatory spindle cell lesions appear to represent an artificial and heterogeneous group of entities, and the term is rarely used in contemporary literature. Many distinct diseases can be differentiated from within this

category.^{1,2,26–28} Establishing an accurate diagnosis is extremely challenging and requires clinicopathological correlation, genetic testing and considerable time, as also demonstrated by the findings of this study. Moreover, making a definitive diagnosis without ancillary tests is nearly impossible, as noted in previous reports.^{13,19,29,30} Unfortunately, such diagnostic tools are typically available only in highly specialized medical centers. Therefore, the term “inflammatory spindle cell lesion” may be appropriately used in pathology departments with limited diagnostic resources, where molecular techniques are unavailable. However, the final diagnosis should ideally be confirmed in specialized soft tissue pathology centers using molecular assays.

Entities from the ISCL group are a rare occurrence, making it difficult to collect a sufficient number of cases to standardize research protocols.²⁰ In this study, we aimed to gather as many tumors as possible and successfully included 46 cases. Inflammatory myofibroblastic tumor (IMT) remains the most representative entity within the ISCL spectrum,¹ which is why our focus was placed on investigating tyrosine kinase gene rearrangements. The final diagnosis of IMT requires a typical histopathological image and the presence of certain fusions. Detection of tyrosine kinase gene fusions using FISH, PCR or NGS plays a crucial role in confirming the diagnosis and assessing the prognosis of IMT.^{20,31} However, only NGS can provide comprehensive information about novel fusion genes.^{32–34}

Interestingly, our cohort was predominantly composed of middle-aged and older adults, which contrasts with the typical age distribution reported for IMT in the existing literature.²⁰ As the population ages, the prevalence of certain diseases increases, some of which can be severe and contribute to higher mortality. In older populations, comparing local recurrence rates is more relevant, as recurrence appears to be influenced by the final pathological diagnosis, anatomical location and type of surgical resection. Literature supports an association between these factors and local recurrence.³⁵

Table 6. Confusion matrices of diagnosis correctness verification

Diagnosis correctness verification					
Neoplasm vs other diseases			IMT vs other diseases		
Predicted condition	actual condition		Predicted condition	Actual condition	
Total population (n = 46)	positive (n = 24)	negative (n = 22)	total population (n = 46)	positive (n = 5)	negative (n = 41)
Positive (n = 21)	TP (n = 17)	FP (n = 4)	positive (n = 22)	TP (n = 3)	FP (n = 19)
Negative (n = 25)	FN (n = 7)	TN (n = 18)	negative (n = 24)	FN (n = 2)	TN (n = 22)

FN – false negative; FP – false positive; IMT – inflammatory myofibroblastic tumor; TN – true negative; TP – true positive.

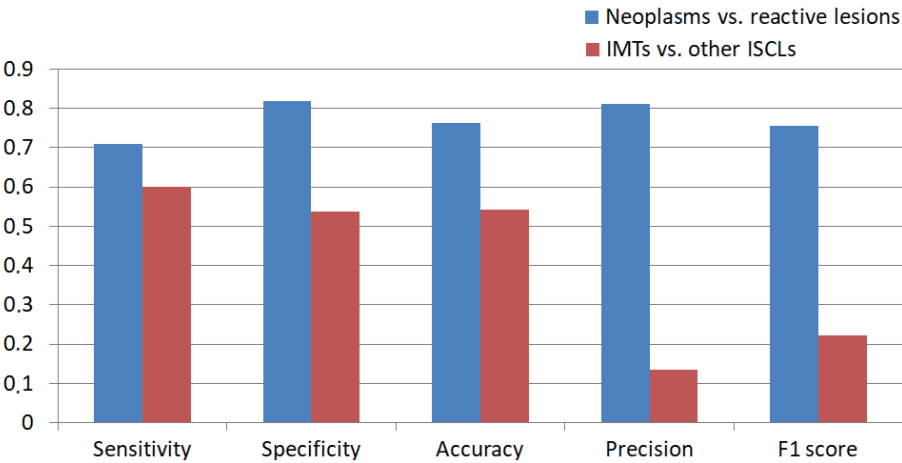


Fig. 9. Column chart presents the diagnosis correctness values of neoplastic lesion (blue) and inflammatory myofibroblastic tumor (IMT; red)

In this study, primary histopathological diagnoses were compared to final diagnoses, which were based on clinical and paraclinical data. The results indicate that histopathological diagnostics are highly satisfactory for distinguishing between neoplastic and reactive lesions. However, primary recognition of IMT was inconsistent with the final diagnosis. The low values of precision, F1 score and sensitivity highlight the risk of diagnostic inaccuracies, even within academic medical centers. This aligns with prior publications highlighting the risk of misdiagnosis in histopathological evaluation of ISCLs.^{10,36–41} Our findings underline the prevalence of this problem.

In IMT histopathological slides, the presence of intercellular mucus, ganglion-like cells, giant cells, necrosis, increased mitotic activity, and high cellularity are considered adverse prognostic factors.^{3,42} In this study, local recurrences were observed in other neoplastic ISCLs containing ganglion-like cells, nuclear atypia and increased mitotic activity (Table 4). Statistical analysis revealed that the OR of these histological features significantly separated neoplastic from reactive groups within a 95% CI. Although no association was found between tissue pattern, necrosis or inflammatory infiltrate intensity and local recurrence as prognostic factors, a higher estimated necrosis percentage was observed in patients who died compared to those who survived with the difference being statistically significant. Thus, the presence of ganglion-like cells, nuclear atypia, increased mitotic activity, and necrosis should be noted in pathological reports as negative prognostic factors.

No relationship between genetic changes and clinical outcomes was identified (Tables 2,3). Consistent with the literature, *ALK* gene fusions were the most frequent,²⁰ present in 75% of IMTs confirmed with sequencing in this study (Table 2). Only 1 neoplasm (case 4) exhibited an *NTRK3*-rearrangement and *EML4-ALK* fusion genes were detected in 2 IMTs (cases 1 and 2). This fusion gene has also been identified in anaplastic large cell lymphoma, as well as colorectal and breast cancers.⁴³ It contributes to tumorigenesis by producing a transcript that includes the intracellular kinase domain of *ALK* and the trimerization domain of *EML4*, enabling constitutive *ALK* activation through oligomerization and autophosphorylation. Tumors harboring this fusion are generally responsive to treatment with tyrosine kinase inhibitors.⁴⁴

RANBP1-ALK, *RANBP2-ALK* and *RRBP1-ALK* rearrangements are characteristic of EIMS, a malignant IMT variant with an aggressive clinical course.^{31,45} These fusions produce distinctive nuclear membrane or perinuclear accentuation patterns in *ALK* immunohistochemical staining.⁴⁵ In case 3, the *RANBP2-ALK* gene was associated with focal nuclear membranous *ALK* positivity. Complete surgical removal of the neoplasm resulted in no recurrence over a 7-year follow-up period.

The *ETV6* gene, a member of the ETS transcription factor family, regulates gene expression by nuclear binding. *NTRK* genes encode tropomyosin receptor kinases, which are crucial for neuronal tissue development and functioning.^{17,28} The *ETV6-NTRK3* fusion gene has been detected in several neoplasms, including *ALK*-negative

IMT, congenital infantile fibrosarcoma, acute myeloblastic leukemia, secretory breast carcinoma, mammary analog secretory carcinoma of the salivary gland, papillary thyroid carcinoma, and congenital mesoblastic nephroma.⁴⁶ Differentiation between IMT and congenital infantile fibrosarcoma can be challenging, as both tumors may exhibit similar behavior. Histopathological features, such as classical pattern, inflammatory infiltrate and patients age above 1 year suggest an IMT rather than congenital infantile fibrosarcoma.⁴⁷ Both tumors may also respond to tyrosine kinase inhibitors, underscoring the overlap in their management. Histologically, the term “inflammatory fibrosarcoma” has even been used synonymously with IMT.³⁰

In the urinary bladder, pseudosarcomatous myofibroblastic proliferations (PMPs) typically present grossly as nodular or polypoid ulcerative masses and exhibit microscopic features that closely resemble those of classical IMTs.⁴⁸ Pseudosarcomatous myofibroblastic proliferations occur mainly in slightly older populations, are more cellular, and have shorter cells and fewer plasma cells than IMTs. While PMP tends to follow a slightly more aggressive course, both lesions can exhibit *ALK* fusions. However, the *ALK* breakpoint differs, being situated in exons 18 or 19 for PMP and exon 20 for IMT.⁹ In this study, differentiation between the 2 entities in case 46 was not possible due to low-quality RNA in the FFPE block. The histopathological findings and *ALK*-positivity in immunohistochemical

assays were consistent with both entities (Fig. 10). Treatment for PMP and IMT is similar,^{20,48} and some authors consider them synonymous.⁴⁹

Case 5 was ultimately diagnosed as a gastric inflammatory fibroid polyp containing the *EGFR-PPARGC1A* fusion gene. This rearrangement has previously been reported only in chronic sun exposure-related cutaneous squamous cell carcinoma.⁵⁰ In this case, the fusion appeared to be nonfunctional due to the absence of the *EGFR* gene promoter kinase domain (exon 20).⁵¹ In certain IMTs, the coexistence of an *EML4-ALK* rearrangement and an activating *EGFR* mutation plays a significant role in resistance to tyrosine kinase inhibitors.⁴⁴ Since the *EGFR* gene is located on the short arm of chromosome 7 and the *PPARGC1A* gene on the short arm of chromosome 4, this fusion may result from a chromosomal translocation.

Indeed, IPT is thought to be a reactive lesion,¹ but it can recur after surgical resection, especially when an incomplete excision is performed.^{51,52} Moreover, if a causative agent persists in the organism, the recurrence may take place, as a result of ineffective antibiotic therapy in infections or insufficient suppressive treatment in autoimmune diseases. Such a situation was also observed in this study (case 31). However, the OR of relapse in our neoplastic compared to reactive group is approx. 12.6 and statistically significant within the 95% CI, which suggests local relapse tends to be more common for neoplasms.

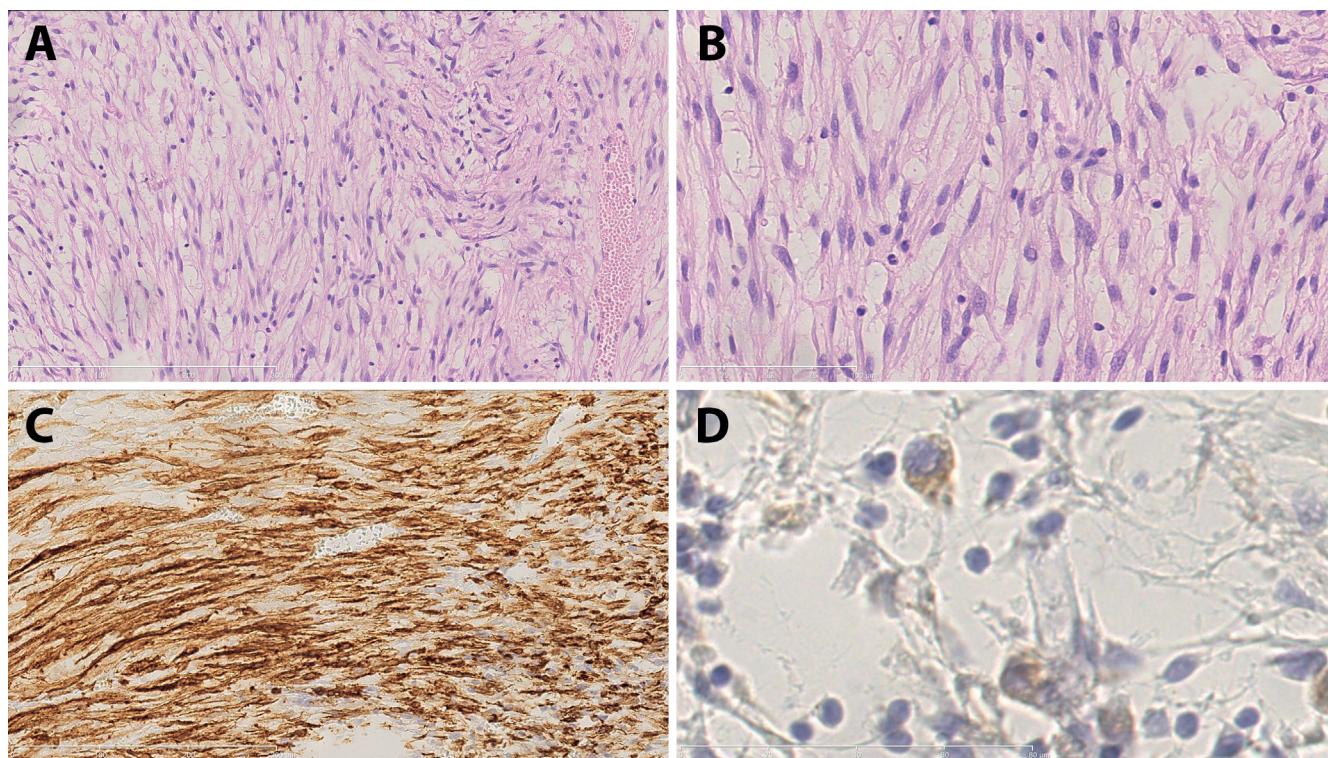


Fig. 10. Case 46. A. Hematoxylin and eosin (H&E) staining, $\times 200$ magnification; B. H&E staining, $\times 400$ magnification; C. Immunohistochemical staining against smooth muscle actin, $\times 200$ magnification; D. Immunohistochemical staining against anaplastic lymphoma kinase (ALK), $\times 1000$ magnification

In this study, neoplasms exhibited features such as ganglion-like cells, atypical cells and mitoses more frequently than reactive lesions. Ganglion-like cells, according to the literature, may occur in benign,⁵³ intermediate and malignant neoplasms,⁵⁴ but are also found in reactive lesions like proliferative myositis and necrotizing fasciitis.⁵⁵ The presence of nuclear atypia is typically associated with a worse prognosis and is more commonly found in neoplastic lesions.⁵⁶ In the neoplastic group, the presence of mitoses is associated with worse outcomes. Also, atypical mitotic figures can be found in neoplasms.⁵⁷ Reactive lesions can also contain multiple mitoses, but are never atypical.⁵⁸

Necrosis, calcifications and extravasated erythrocytes are rare in IMTs.⁵⁹ Höhne et al. noted the presence of necrosis both in IMTs and IPTs but did not define a differentiating percentage.⁶⁰ In this study, IMTs showed a significantly higher necrosis percentage than other ISCLs, as confirmed using the Mann–Whitney U test. Furthermore, a higher necrosis percentage was statistically associated with increased mortality.

Certain benign non-neoplastic lesions with histopathological features, like hypercellularity, cytological atypia and increased mitotic activity, are classified as pseudosarcomas.⁶¹ Integrating clinical and paraclinical data can help avoid misdiagnosing inflammatory lesions as sarcomas.

Interestingly, mutations were also observed in reactive lesions. While genetic clonality is a hallmark of neoplasms,⁴⁷ clonal expansion is possible in non-cancerous lesions. The presence of driver mutations in these tissues may indicate an early tumorigenesis, which does not always progress to neoplasm development.⁶² Factors like aging, chronic inflammation and environmental exposures support clonal expansion.^{62,63} Neoplasm development and progression require the accumulation of genetic mutations and epigenetic alterations, so a single change may not be sufficient to induce a real tumorigenesis.⁶³ In this study, 82% of inflammatory lesions exhibited genetic clonality, which is consistent with this theory. The number of functional fusion genes with frequencies above 50% and variants with VAF values greater than 0.5 distinguished neoplastic from reactive lesions using the Mann–Whitney U test.

Limitations

This study has several limitations: 1) all cases were diagnosed within a single pathology department, potentially limiting generalizability; 2) only cases initially diagnosed as IMT or IPT were included, which may have introduced selection bias; 3) it was not possible to retrieve all FFPE blocks and histological slides; and 4) a limited targeted NGS gene panel was used. Detailed comparisons are provided in Supplementary Table 1.

Conclusions

This study underscores the importance of integrating clinical and paraclinical data to achieve an accurate diagnosis. Prognosis is influenced more significantly by the final pathological diagnosis, anatomical location of the lesion and completeness of surgical resection than by isolated histopathological or genetic findings. However, neoplastic etiology and some of the features, such as the presence of ganglion-like cells, nuclear atypia and increased mitotic activity, can occur in lesions that present local recurrences. The study strongly supports the theory, which assumes that not only neoplasms but also reactive diseases can present worrisome histological features, pathogenic mutations and genetic clonality. However, neoplastic ISCLs more frequently exhibited ganglion-like cells, nuclear atypia, elevated mitotic index, and the presence of functional gene rearrangements or point mutations with a VAF ≥ 0.5 compared to reactive lesions. Notably, both lesion types may recur if the underlying causative factor persists following excision. Among the detected functional gene rearrangements, the most frequent involved ALK and *NTRK3* genes, which are considered key drivers in inflammatory myofibroblastic tumors.

Confirmation of tyrosine receptor kinase gene rearrangements is necessary for diagnosing IMTs, which showed a higher necrosis percentage than other ISCLs. A higher necrosis percentage was also linked to increased mortality. In summary, this study confirms the prognostic significance of a neoplastic diagnosis, presence of ganglion-like cells, nuclear atypia, elevated mitotic index, and increased necrosis percentage. It also highlights the diagnostic value of ganglion-like cells, nuclear atypia, higher mitotic activity, and functional gene rearrangements or point mutations with a VAF ≥ 0.5 . These features should be consistently reported in pathology assessments to support informed clinical decision-making.

Supplementary data

The supplementary materials are available at <https://doi.org/10.5281/zenodo.15034538>. The package includes the following files:

Supplementary Table 1. Full dataset of the study.

Data availability

The datasets generated and/or analyzed during the current study are available from the corresponding author on reasonable request.

Consent for publication

Not applicable.

Use of AI and AI-assisted technologies

Not applicable.

ORCID iDs

Krzysztof Siemion  <https://orcid.org/0000-0003-2354-9891>
 Joanna Kiśluk  <https://orcid.org/0000-0002-1668-0288>
 Natalia Wasilewska  <https://orcid.org/0000-0001-6327-8526>
 Joanna Reszec-Gielazyn  <https://orcid.org/0000-0002-0169-0897>
 Anna Korzyńska  <https://orcid.org/0000-0002-6488-4832>
 Tomasz Łysoń  <https://orcid.org/0000-0002-9757-8276>
 Zenon Mariak  <https://orcid.org/0000-0003-4132-9278>

References

- Kutok JL, Pinkus GS, Dorfman DM, Fletcher CDM. Inflammatory pseudotumor of lymph node and spleen: An entity biologically distinct from inflammatory myofibroblastic tumor. *Hum Pathol*. 2001;32(12):1382–1387. doi:10.1053/hupa.2001.29679
- Irani S, Rabbani Anari M, Yazdani Bioki F, Nasirmohammadi S, Kaedi Z, Alipour S. Inflammatory myofibroblastic tumor: Two cases in head and neck region. *Indian J Otolaryngol Head Neck Surg*. 2022;74(Suppl 3):6394–6399. doi:10.1007/s12070-022-03119-9
- Siemion K, Reszec-Gielazyn J, Kiśluk J, Roszkowiak L, Zak J, Korzyńska A. What do we know about inflammatory myofibroblastic tumors? A systematic review. *Adv Med Sci*. 2022;67(1):129–138. doi:10.1016/j.advms.2022.02.002
- Chávez-Peón Berle E, Hallman C, Kleinhenz K, Plattner BL. Multifocal spinal inflammatory myofibroblastic tumors in a juvenile paraparetic dog. *Vet Radiol Ultrasound*. 2023;64(2):E14–E18. doi:10.1111/vru.13195
- Moro A, De Angelis P, Gasparini G, et al. Orbital desmoid-type fibromatosis: A case report and literature review. *Case Rep Oncol Med*. 2018;2018:1684763. doi:10.1155/2018/1684763
- Hu G, Chen H, Liu Q, et al. Plexiform fibromyxoma of the stomach: A clinicopathological study of 10 cases. *Int J Clin Exp Pathol*. 2017;10(11):10926–10933. PMID:31966436. PMID:PMC6965819.
- Kai K, Miyoshi A, Aishima S, et al. Granulomatous reaction in hepatic inflammatory angiomyolipoma after chemoembolization and spontaneous rupture. *World J Gastroenterol*. 2015;21(32):9675–9682. doi:10.3748/wjg.v21.i32.9675
- Hornick JL, Sholl LM, Dal Cin P, Childress MA, Lovly CM. Expression of *ROS1* predicts *ROS1* gene rearrangement in inflammatory myofibroblastic tumors. *Modern Pathol*. 2015;28(5):732–739. doi:10.1038/modpathol.2014.165
- Acosta AM, Demicco EG, Dal Cin P, Hirsch MS, Fletcher CDM, Jo VY. Pseudosarcomatous myofibroblastic proliferations of the urinary bladder are neoplasms characterized by recurrent FN1–ALK fusions. *Modern Pathol*. 2021;34(2):469–477. doi:10.1038/s41379-020-00670-0
- Völker HU, Scheich M, Höller S, et al. Differential diagnosis of laryngeal spindle cell carcinoma and inflammatory myofibroblastic tumor: Report of two cases with similar morphology. *Diagn Pathol*. 2007;2:1. doi:10.1186/1746-1596-2-1
- Lopez-Beltran A, Montironi R, Raspollini MR, Cheng L, Netto GJ. Iatrogenic pathology of the urinary bladder. *Semin Diagn Pathol*. 2018;35(4):218–227. doi:10.1053/j.semdp.2018.03.001
- Arsalan ME, Li H, Fu Z, Jennings TA, Lee H. Plexiform fibromyxoma: Review of rare mesenchymal gastric neoplasm and its differential diagnosis. *World J Gastrointest Oncol*. 2021;13(5):409–423. doi:10.4251/wjgo.v13.i5.409
- Croce S, Hostein I, McCluggage WG. *NTRK* and other recently described kinase fusion positive uterine sarcomas: A review of a group of rare neoplasms. *Genes Chromosomes Cancer*. 2021;60(3):147–159. doi:10.1002/gcc.22910
- Tariq MU, Din NU, Abdul-Ghafar J, Park YK. The many faces of solitary fibrous tumor: Diversity of histological features, differential diagnosis and role of molecular studies and surrogate markers in avoiding misdiagnosis and predicting the behavior. *Diagn Pathol*. 2021;16(1):32. doi:10.1186/s13000-021-01095-2
- Zhang BX, Chen ZH, Liu Y, Zeng YJ, Li YC. Inflammatory pseudotumor-like follicular dendritic cell sarcoma: A brief report of two cases. *World J Gastrointest Oncol*. 2019;11(12):1231–1239. doi:10.4251/wjgo.v11.i12.1231
- Khatir A, Agrawal A, Sikachi R, Mehta D, Sahni S, Meena N. Inflammatory myofibroblastic tumor of the lung. *Adv Respir Med*. 2018;86(1):27–35. doi:10.5603/ARM.2018.0007
- Antonescu CR. Emerging soft tissue tumors with kinase fusions: An overview of the recent literature with an emphasis on diagnostic criteria. *Genes Chromosomes Cancer*. 2020;59(8):437–444. doi:10.1002/gcc.22846
- Dall Bello AG, Severo CB, Guazzelli LS, Oliveira FM, Hochegger B, Severo LC. Histoplasmosis mimicking primary lung cancer or pulmonary metastases. *J Bras Pneumol*. 2013;39(1):63–68. doi:10.1590/S1806-37132013000100009
- Armstrong V, Khazeni K, Rosenberg A, Swain SK, Moller M. Inflammatory pseudotumor secondary to urachal cyst: A challenging clinical case report. *Int J Surg Case Rep*. 2020;66:360–364. doi:10.1016/j.ijscr.2019.12.029
- Gros L, Dei Tos AP, Jones RL, Digkila A. Inflammatory myofibroblastic tumour: State of the art. *Cancers (Basel)*. 2022;14(15):3662. doi:10.3390/cancers14153662
- Coffin CM, Hornick JL, Fletcher CDM. Inflammatory myofibroblastic tumor: Comparison of clinicopathologic, histologic, and immunohistochemical features including ALK expression in atypical and aggressive cases. *Am J Surg Pathol*. 2007;31(4):509–520. doi:10.1097/01.pas.0000213393.57322.c7
- Weir MM, Rosenberg AE, Bell DA. Grading of spindle cell sarcomas in fine-needle aspiration biopsy specimens. *Am J Clin Pathol*. 1999;112(6):784–790. doi:10.1093/ajcp/112.6.784
- Klintrup K, Mäkinen JM, Kauppila S, et al. Inflammation and prognosis in colorectal cancer. *Eur J Cancer*. 2005;41(17):2645–2654. doi:10.1016/j.ejca.2005.07.017
- World Health Organization (WHO). Soft Tissue and Bone Tumours. 5th ed. Geneva, Switzerland: World Health Organization (WHO); 2020. ISBN: 978-92-832-4502-5, 978-92-832-4503-2.
- Tenny S, Hoffman MR. Odds ratio. In: *StatPearls*. Treasure Island, USA: StatPearls Publishing; 2025:Bookshelf ID: NBK431098. <http://www.ncbi.nlm.nih.gov/books/NBK431098>. Accessed March 19, 2025.
- Shah A, Pey E, Achonu JU, Bai JDK, Khan F. Inflammatory myofibroblastic tumor 12 years after treatment for synovial sarcoma: A case report. *Orthop Res Rev*. 2021;13:163–169. doi:10.2147/ORR.S333124
- Hisaoka M, Shimajiri S, Matsuki Y, et al. Inflammatory myofibroblastic tumor with predominant anaplastic lymphoma kinase-positive cells lacking a myofibroblastic phenotype. *Pathol Int*. 2003;53(6):376–381. doi:10.1046/j.1440-1827.2003.01484.x
- Yamamoto H, Nozaki Y, Kohashi K, Kinoshita I, Oda Y. Diagnostic utility of pan-Trk immunohistochemistry for inflammatory myofibroblastic tumours. *Histopathology*. 2020;76(5):774–778. doi:10.1111/his.14010
- Tauziède-Espariat A, Duchesne M, Baud J, et al. *NTRK*-rearranged spindle cell neoplasms are ubiquitous tumours of myofibroblastic lineage with a distinct methylation class. *Histopathology*. 2023;82(4):596–607. doi:10.1111/his.14842
- Al Shenawi H, Al-Shaibani SA, Al Saad SK, et al. An extremely rare case of malignant jejunal mesenteric inflammatory myofibroblastic tumor in a 61-year-old male patient: A case report and literature review. *Front Med (Lausanne)*. 2022;9:1042262. doi:10.3389/fmed.2022.1042262
- Giannaki A, Doganis D, Giamarelou P, Konidari A. Epithelioid inflammatory myofibroblastic sarcoma presenting as gastrointestinal bleed: Case report and literature review. *JPGN Rep*. 2021;2(1):e019. doi:10.1097/PJG.0000000000000019
- Antonescu CR, Suurmeijer AJH, Zhang L, et al. Molecular characterization of inflammatory myofibroblastic tumors with frequent *ALK* and *ROS1* gene fusions and rare novel *RET* rearrangement. *Am J Surg Pathol*. 2015;39(7):957–967. doi:10.1097/PAS.0000000000000404
- Strom SP. Current practices and guidelines for clinical next-generation sequencing oncology testing. *Cancer Biol Med*. 2016;13(1):3–11. doi:10.28092/j.issn.2095-3941.2016.0004
- Drilon A, Jenkins C, Iyer S, Schoenfeld A, Keddy C, Davare MA. *ROS1*-dependent cancers: Biology, diagnostics and therapeutics. *Nat Rev Clin Oncol*. 2021;18(1):35–55. doi:10.1038/s41571-020-0408-9
- Cantin J, McNeer GP, Chu FC, Booher RJ. The problem of local recurrence after treatment of soft tissue sarcoma. *Ann Surg*. 1968;168(1):47–53. doi:10.1097/0000658-196807000-00005

36. Agaimy A, Märkl B. Inflammatory angiomyolipoma of the liver: An unusual case suggesting relationship to IgG4-related pseudotumor. *Int J Clin Exp Pathol*. 2013;6(4):771–779. PMID:23573326. PMCID:PMC3606869.
37. Taylor MS, Chougule A, MacLeay AR, et al. Morphologic overlap between inflammatory myofibroblastic tumor and IgG4-related disease: Lessons from next-generation sequencing. *Am J Surg Pathol*. 2019;43(3):314–324. doi:10.1097/PAS.0000000000001167
38. Tran TAN, Chang KTE, Kuick CH, Goh JY, Chang CC. Local ALK-positive histiocytosis with unusual morphology and novel *TRIM33-ALK* gene fusion. *Int J Surg Pathol*. 2021;29(5):543–549. doi:10.1177/1066896920976862
39. Lee J, Singh A, Ali SM, Lin DI, Klempner SJ. TNS1-ALK fusion in a recurrent, metastatic uterine mesenchymal tumor originally diagnosed as leiomyosarcoma. *Acta Med Acad*. 2019;48(1):116. doi:10.5644/ama2006-124.248
40. Carballo EV, Pham TV, Turashvili G, Hanley K, Starbuck KD, Meisel JL. Recurrent uterine inflammatory myofibroblastic tumor previously managed as leiomyosarcoma has sustained response to alectinib. *Gynecol Oncol Rep*. 2022;43:101062. doi:10.1016/j.gore.2022.101062
41. Kojima M, Nakamura S, Ohno Y, Sugihara S, Sakata N, Masawa N. Hepatic angiomyolipoma resembling an inflammatory pseudotumor of the liver: A case report. *Pathol Res Pract*. 2004;200(10):713–716. doi:10.1016/j.prp.2004.08.001
42. Choi M, Kim W, Cheon MG, Lee CW, Kim JE. Polo-like kinase 1 inhibitor BL2536 causes mitotic catastrophe following activation of the spindle assembly checkpoint in non-small cell lung cancer cells. *Cancer Lett*. 2015;357(2):591–601. doi:10.1016/j.canlet.2014.12.023
43. Roskoski R. Anaplastic lymphoma kinase (ALK): Structure, oncogenic activation, and pharmacological inhibition. *Pharmacol Res*. 2013;68(1):68–94. doi:10.1016/j.phrs.2012.11.007
44. Hunt AL, Nutchareon A, Randall J, et al. Integration of multi-omic data in a molecular tumor board reveals EGFR-associated ALK-inhibitor resistance in a patient with inflammatory myofibroblastic cancer. *Oncologist*. 2023;28(8):730–736. doi:10.1093/oncolo/oyad129
45. Lee JC, Li CF, Huang HY, et al. ALK oncoproteins in atypical inflammatory myofibroblastic tumours: Novel *RRBP1-ALK* fusions in epithelioid inflammatory myofibroblastic sarcoma. *J Pathol*. 2017;241(3):316–323. doi:10.1002/path.4836
46. Takahashi A, Kurosawa M, Uemura M, Kitazawa J, Hayashi Y. Anaplastic lymphoma kinase-negative uterine inflammatory myofibroblastic tumor containing the *ETV6-NTRK3* fusion gene: A case report. *J Int Med Res*. 2018;46(8):3498–3503. doi:10.1177/0300060518780873
47. Lindberg MR, ed. *Diagnostic Pathology: Soft Tissue Tumors*. 3rd ed. Philadelphia, USA: Elsevier; 2019. ISBN:978-0-323-71149-4.
48. Harik LR, Merino C, Coindre JM, Amin MB, Pedeutour F, Weiss SW. Pseudosarcomatous myofibroblastic proliferations of the bladder: A clinicopathologic study of 42 cases. *Am J Surg Pathol*. 2006;30(7):787–794. doi:10.1097/01.pas.0000208903.46354.6f
49. Tanaka T, Ueda T, Yokoyama T, Harada S, Hatakeyama K, Yoshimura A. Pseudosarcomatous myofibroblastic proliferation of the appendix with an abdominal abscess due to diverticulum perforation: A case report. *Surg Case Rep*. 2020;6(1):144. doi:10.1186/s40792-020-00901-1
50. Egashira S, Jinnin M, Ajino M, et al. Chronic sun exposure-related fusion oncogenes *EGFR-PPARGC1A* in cutaneous squamous cell carcinoma. *Sci Rep*. 2017;7(1):12654. doi:10.1038/s41598-017-12836-z
51. Wang F, Li C, Wu Q, Lu H. EGFR exon 20 insertion mutations in non-small cell lung cancer. *Transl Cancer Res*. 2020;9(4):2982–2991. doi:10.21037/tcr.2020.03.10
52. Goto T, Akanabe K, Maeshima A, Kato R. Surgery for recurrent inflammatory pseudotumor of the lung. *World J Surg Oncol*. 2011;9(1):133. doi:10.1186/1477-7819-9-133
53. Coffin CM, Alaggio R. Fibroblastic and myofibroblastic tumors in children and adolescents. *Pediatr Dev Pathol*. 2012;15(1 Suppl):127–180. doi:10.2350/10-12-0944-PB.1
54. Barak S, Wang Z, Miettinen M. Immunoreactivity for calretinin and keratins in desmoid fibromatosis and other myofibroblastic tumors: A diagnostic pitfall. *Am J Surg Pathol*. 2012;36(9):1404–1409. doi:10.1097/PAS.0b013e3182556def
55. Domanski HA, Qian X, Åkerman M, Stanley DE. Soft tissue. In: Domanski HA, ed. *Atlas of Fine Needle Aspiration Cytology*. Cham, Switzerland: Springer International Publishing; 2019:465–551. doi:10.1007/978-3-319-76980-6_14
56. Hunis AP, Hunis M. Soft tissue sarcomas. *J Inter Med Emer Res*. 2022;3(3):1–51. doi:10.37191/Mapsci-2582-7367-3(3)-049
57. Kallen ME, Hornick JL. The 2020 WHO classification: What's new in soft tissue tumor pathology? *Am J Surg Pathol*. 2021;45(1):e1–e23. doi:10.1097/PAS.0000000000001552
58. Gobbi H, Tse G, Page DL, Olson SJ, Jensen RA, Simpson JF. Reactive spindle cell nodules of the breast after core biopsy or fine-needle aspiration. *Am J Surg Pathol*. 2000;113(2):288–294. doi:10.1309/RPW4-CXCC-1JHM-OTL7
59. Surabhi VR, Chua S, Patel RP, Takahashi N, Lalwani N, Prasad SR. Inflammatory myofibroblastic tumors. *Radiol Clin North Am*. 2016;54(3):553–563. doi:10.1016/j.rcl.2015.12.005
60. Höhne S, Milzsch M, Adams J, Kunze C, Finke R. Inflammatory pseudotumor (IPT) and inflammatory myofibroblastic tumor (IMT): A representative literature review occasioned by a rare IMT of the transverse colon in a 9-year-old child. *Tumori J*. 2015;101(3):249–256. doi:10.5301/tj.5000353
61. Rosenberg AE. Pseudosarcomas of soft tissue. *Arch Pathol Lab Med*. 2008;132(4):579–586. doi:10.5858/2008-132-579-POST
62. Kakiuchi N, Ogawa S. Clonal expansion in non-cancer tissues. *Nat Rev Cancer*. 2021;21(4):239–256. doi:10.1038/s41568-021-00335-3
63. Hibino S, Kawazoe T, Kasahara H, et al. Inflammation-induced tumorigenesis and metastasis. *Int J Mol Sci*. 2021;22(11):5421. doi:10.3390/ijms22115421

Comparative study of the protective effects of adenosine triphosphate and resveratrol against amiodarone-induced potential liver damage and dysfunction in rats

Muhammed Talha Karadogan^{1,A,D–F}, Bulent Yavuzer^{2,B–F}, Cebirail Gursul^{3,B–D,F}, Gulbaniz Huseynova^{4,A,D,F}, Gulce Naz Yazici^{5,B–D,F}, Mine Gulaboglu^{6,B–D,F}, Furkan Yilmaz^{7,A,C,D,F}, Ali Sefa Mendil^{8,B–D,F}, Halis Suleyman^{2,A,C–F}

¹ Department of Pediatrics, Faculty of Medicine, Erzincan Binali Yildirim University, Turkey

² Department of Pharmacology, Faculty of Medicine, Erzincan Binali Yildirim University, Turkey

³ Department of Physiology, Faculty of Medicine, Erzincan Binali Yildirim University, Turkey

⁴ Department of Pharmacology, Azerbaijan Medical University, Baku, Azerbaijan

⁵ Department of Histology and Embryology, Faculty of Medicine, Erzincan Binali Yildirim University, Turkey

⁶ Department of Biochemistry, Faculty of Pharmacy, Atatürk University, Erzurum, Turkey

⁷ Department of Pediatrics, Esenyurt Necmi Kadioglu State Hospital, Istanbul, Turkey

⁸ Department of Pathology, Faculty of Veterinary Medicine, Erciyes University, Kayseri, Turkey

A – research concept and design; B – collection and/or assembly of data; C – data analysis and interpretation;

D – writing the article; E – critical revision of the article; F – final approval of the article

Advances in Clinical and Experimental Medicine, ISSN 1899–5276 (print), ISSN 2451–2680 (online)

Adv Clin Exp Med. 2025;34(12):2137–2152

Address for correspondence

Halis Suleyman

E-mail: halis.suleyman@gmail.com

Funding sources

None declared

Conflict of interest

None declared

Received on April 14, 2024

Reviewed on October 14, 2024

Accepted on February 18, 2025

Published online on August 19, 2025

Cite as

Karadogan MT, Yavuzer B, Gursul C, et al. Comparative study of the protective effects of adenosine triphosphate and resveratrol against amiodarone-induced potential liver damage and dysfunction in rats. *Adv Clin Exp Med.* 2025;34(12):2137–2152. doi:10.17219/acem/202011

DOI

10.17219/acem/202011

Copyright

Copyright by Author(s)

This is an article distributed under the terms of the Creative Commons Attribution 3.0 Unported (CC BY 3.0) (<https://creativecommons.org/licenses/by/3.0/>)

Abstract

Background. Amiodarone is the most commonly used class III antiarrhythmic drug with antiarrhythmic and vasodilator properties. Adenosine triphosphate (ATP) serves as a crucial source of intracellular energy, while resveratrol is known for its potent antioxidant activity.

Objectives. This study aimed to biochemically, histopathologically and immunohistochemically evaluate the effects of ATP, resveratrol and their combination on potential liver damage and dysfunction induced by amiodarone in rats.

Materials and methods. The rats were divided into 6 groups: healthy control (HG), amiodarone alone (ADG), amiodarone + ATP at 2 mg/kg (AAG-2), amiodarone + ATP at 5 mg/kg (AAG-5), resveratrol + amiodarone (RAG), and resveratrol + amiodarone + ATP at 2 mg/kg (RAA-2). Amiodarone (50 mg/kg, orally), ATP (2 mg/kg and 5 mg/kg, intraperitoneally) and resveratrol (25 mg/kg, orally) were administered once daily for 14 days. Following treatment, liver tissues were excised for biochemical analysis. Oxidative stress was assessed by measuring malondialdehyde (MDA) levels, while antioxidant status was evaluated through total glutathione (GSH), superoxide dismutase (SOD) and catalase (CAT) levels. To assess liver function, alanine aminotransferase (ALT) and aspartate aminotransferase (AST) activities were measured in serum samples collected from the animals' tail veins. In addition, liver tissues were subjected to histopathological and immunohistochemical examination to evaluate structural and molecular changes associated with treatment.

Results. Amiodarone administration led to a significant increase in oxidative stress markers and a reduction in antioxidant levels in rat liver tissue. Additionally, serum levels of ALT and AST were elevated, indicating liver dysfunction. Histopathological and immunohistochemical analyses revealed severe (grade 3) oxidative damage in the liver tissue. All biochemical parameters in the 5 mg/kg ATP and resveratrol + 2 mg/kg ATP treatment groups were comparable to those observed in the HG group. Histopathological and immunohistochemical evaluations showed a reduction in liver damage severity to grade 2 in the groups treated with ATP (2 mg/kg) and resveratrol alone, and to grade 1 in the groups receiving ATP (5 mg/kg) or the combination of resveratrol + ATP (2 mg/kg).

Conclusions. The results of the present study suggest that adjusting the ATP dosage or using a combination of ATP and resveratrol may be effective strategies for minimizing amiodarone-induced liver damage.

Key words: rats, resveratrol, amiodarone, adenosine triphosphate, oxidative liver damage

Highlights

- Amiodarone as a leading class III antiarrhythmic agent combines antiarrhythmic and vasodilator effects but carries a risk of hepatotoxicity.
- Amiodarone induces severe oxidative liver damage in rats, confirmed by biochemical, histopathological, and immunohistochemical analyses.
- Mitochondrial dysfunction underlies hepatocyte injury, with reduced ATP content and elevated ROS levels driving oxidative stress.
- Exogenous ATP and resveratrol supplementation mitigate liver damage, with resveratrol enhancing intracellular ATP production.
- Optimizing ATP dosing or combining ATP with resveratrol may offer a protective strategy against amiodarone-induced hepatic injury.

Background

Amiodarone, a benzofuran derivative with antiarrhythmic and vasodilator properties, is the most commonly used Vaughan–Williams class III antiarrhythmic drug today.¹ Amiodarone is approved by the U.S. Food and Drug Administration (FDA) for the treatment of ventricular arrhythmias. However, it is also used off-label for the treatment of supraventricular tachyarrhythmias, such as atrial fibrillation (AF), and for the prevention of ventricular tachyarrhythmias in high-risk patients.² According to the European Society of Cardiology's (ESC) 2020 guideline, amiodarone is recommended in addition to β -blockers to prevent AF following cardiac surgery, regardless of risk factors.³ Although β -blockers are often used as first-line antiarrhythmic therapy, amiodarone may be needed in some cases.¹ Amiodarone's ability to block sodium, potassium and calcium channels as well as adrenergic receptors⁴ may be an important reason for its need. However, serious and potentially life-threatening side effects can occur with long-term treatment with amiodarone.⁵ It is known to be toxic to organs and tissues such as the thyroid, lungs, heart, liver, eyes, skin, and central and peripheral nervous system.^{6,7} Previous studies have suggested that the formation of reactive oxygen species (ROS) leading to lipid peroxidation (LPO) and oxidative stress is an important component of amiodarone toxicity.⁸ In addition, mitochondrial adenosine triphosphate (ATP) content in hepatocytes was found to decrease in parallel with the amiodarone-induced increase in mitochondrial ROS.⁹ However, amiodarone has been shown to significantly reduce cellular ATP levels and cell viability even at low concentrations.¹⁰ Adenosine triphosphate is recognized as one of the most vital molecules for cellular function, playing critical roles both intracellularly and extracellularly. It is a crucial component in the biosynthesis of nucleic acids and a significant source of intracellular energy.¹¹ The literature suggests that amiodarone-induced tissue damage may be linked to increased production of ROS caused by ATP deficiency. Adenosine triphosphate is known to play a role in the synthesis of antioxidants that scavenge and neutralize ROS.¹² Adenosine triphosphate also acts as an energy source for the antioxidants

synthesis.¹³ Additionally, resveratrol – a natural polyphenol – is included in this study to evaluate its potential protective effect against amiodarone-induced liver damage.¹⁴ Resveratrol was first extracted from the *Vera oleifera* root by the Japanese scientist Takaoka in 1939.¹⁴ Resveratrol can currently be obtained from over 70 different plants, including peanuts, grapes, *Polygonum cuspidatum*, and mulberries.^{14,15} It has demonstrated a wide range of biological activities, including anti-inflammatory, antioxidant, cardioprotective, anti-carcinogenic, anti-diabetic, anti-obesity, neuroprotective, and anti-aging effects.¹⁶ Resveratrol is also known to enhance intracellular ATP production.¹⁷

Objectives

The literature suggests that oxidative liver damage induced by amiodarone may be related to increased production of ROS due to ATP deficiency. In addition, the literature suggests that ATP, resveratrol, and their combination – referred to as ATP-resveratrol combinations (ARCs) – may offer therapeutic benefits in the treatment of amiodarone-induced oxidative liver injury. Furthermore, there are no available data on the protective effects of ATP, resveratrol and ARCs against oxidative liver damage induced by amiodarone. Therefore, the aim of our study was to investigate and compare the protective effects of ATP, resveratrol and ARCs against potential amiodarone-induced liver damage and dysfunction in rats.

Materials and methods

Animals

The experiment involved 60 male albino Wistar-type rats weighing 280–292 g and aged 9–10 weeks. Animals were purchased from the Experimental Animals Application and Research Centre (Erzincan Binali Yıldırım University, Erzincan, Turkey). The animals were randomized into 6 groups

so that the average body weight of each group was similar to the others. Prior to the experiment, the rats were housed in groups of 10 in wire cages under laboratory conditions, maintained at 22°C with 30–70% humidity and a 12-h light/dark cycle. Animals were given tap water and standard pellet feed (Experimental Animal Feed; Bayramoglu Co., Erzurum, Turkey) *ad libitum*. All experiments were carried out according to the guidelines of Directive 2010/63/EU of the European Parliament and Council (approval No. 2016-24-199) and the Animal Research: Reporting of In Vivo Experiments (ARRIVE) guidelines.¹⁸ All procedures were carried out with the approval of Erzincan Binali Yıldırım University Animal Experiments Local Ethics Committee (meeting date: November 30, 2023, meeting No. 2023/11, decision No. 39).

Chemical substances

The chemicals used in the experiment were thiopental sodium supplied by IE Ulagay (Istanbul, Turkey), ATP purchased from Zdorove Narodu (Kharkiv, Ukraine) and resveratrol obtained from Sigma-Aldrich (St. Louis, USA).

Experimental design

The minimum number of animals was selected in accordance with the Reduction, Refinement, Replacement, Responsibility (4R) guidelines to ensure ethical and responsible use of experimental subjects.¹⁹ Animals displaying signs such as hunched posture, reduced movement or injury caused by other animals were excluded from the experiment and corresponding data points were omitted from the analysis. There were no exclusions during the experiment. A random numbers table was used to generate the randomization sequence. Cages and animals were numbered to minimize potential confounding factors.

Experimental groups

Six groups of rats were used in the experiment: healthy control (HG), amiodarone alone (ADG), amiodarone + 2 mg/kg ATP (AAG-2), amiodarone + 5 mg/kg ATP (AAG-5), amiodarone + resveratrol (RAG), and amiodarone + resveratrol + 2 mg/kg ATP (RAA-2).

Experimental procedure

The AAG-2 group ($n = 10$) was administered an intraperitoneal (i.p.) injection of ATP at a dose of 2 mg/kg, while the AAG-5 group ($n = 10$) was administered the same injection at a dose of 5 mg/kg. The RAG group ($n = 10$) received resveratrol at a dose of 25 mg/kg orally via gastric gavage. The RAA-2 group ($n = 10$) was administered resveratrol (25 mg/kg) and ATP (2 mg/kg) as described above. Distilled water was used as the solvent for both the HG ($n = 10$) and ADG ($n = 10$) groups. One hour after the administration of ATP, resveratrol, or distilled water, amiodarone was

administered orally by gastric gavage to the ADG, AAG-2, AAG-5, RAG, and RAA-2 groups at a dose of 50 mg/kg. Over a period of 14 days, the procedures were repeated once a day. Animals were sacrificed under high-dose thiopental sodium anesthesia (50 mg/kg), and liver tissues were excised at the end of this period. In the excised liver tissues, levels of malondialdehyde (MDA), total glutathione (tGSH), superoxide dismutase (SOD), and catalase (CAT) were measured. Blood samples were collected from the tail veins of the animals prior to euthanasia, and the activities of alanine aminotransferase (ALT) and aspartate aminotransferase (AST) were measured to assess liver function. Additionally, histopathological and immunohistochemical examinations were conducted on liver tissues from 6 rats randomly selected from each experimental group of 10 animals. The biochemical, histopathologic and immunohistochemical results of the experiment were compared and evaluated between groups.

Biochemical analyses

Preparation of samples

Initially, the tissue samples were rinsed with physiological saline, then pulverized in liquid nitrogen and subsequently homogenized. The protein levels of MDA, tGSH, SOD, and CAT were determined in the supernatants.

Determination of the protein levels of MDA, tGSH, SOD and CAT

Commercially available rat enzyme-linked immunosorbent assay kits (MDA product No. 10009055; tGSH product No. 703002; SOD product No. 706002; Cayman Chemical Co., Ann Arbor, USA) were purchased for the measurement of MDA, tGSH and SOD parameters. The method suggested by Góth was applied to perform CAT determination.²⁰ Protein concentration was determined using the Bradford method, with absorbance measured spectrophotometrically at 595 nm.²¹

Measurement of ALT and AST activities

Venous blood samples were collected into anticoagulant-free tubes for serum separation. Serum was separated by centrifuging after blood clotting and kept at -80°C until the assay was performed. Liver function tests were performed by measuring serum ALT and AST activities spectrophotometrically using commercially available kits on a Cobas® 8000 auto-analyzer (Roche Diagnostics GmbH, Mannheim, Germany).

Histopathological examination

Tissue samples were fixed in 10% formaldehyde solution for 72 h. After fixation, the tissues were placed

in cassettes and rinsed under running water for 24 h. They were then dehydrated by passing through a series of increasing degrees of alcohol (70%, 80%, 90%, and 100%). The xylol-transparent liver tissues were embedded in paraffin blocks, and 4–5- μ m-thick sections were taken. The sections were stained with hematoxylin and eosin (H&E) double stain and evaluated and photographed using the Olympus DP2-SAL firmware program (Olympus Corp., Tokyo, Japan). In the serial sections obtained, six areas (1 central and 5 peripheral) were selected per section for each experimental group. At a $\times 100$ magnification, deviations from normal histological structure were scored based on hepatocyte vacuolization, necrosis, vascular dilatation/congestion, and polymorphonuclear leukocyte (PMNL) infiltration. Each of the above criteria was scored on a scale from 0 to 3 (0 – none, 1 – mild, 2 – moderate, 3 – severe). Histopathological evaluations were performed by a histologist who was blinded to the experimental group assignments.

Immunohistochemical examination

Briefly, 4 μ m-thick sections mounted on polylysine-coated slides were deparaffinized in xylene and rehydrated through a graded alcohol series. After rinsing with phosphate-buffered saline (PBS), endogenous peroxidase activity was blocked by incubating the sections in 3% hydrogen peroxide (H_2O_2) for 10 min. In order to reveal the antigen in the tissues, it was treated with antigen retrieval solution at 500 W for 2×5 min. Later, cleaved *caspase-3* (product No. E-AB-30004; Elabscience, Houston, USA) and tumor necrosis factor alpha (*TNF- α* ; product No. sc-133192; Santa Cruz Biotechnology, Inc., Santa Cruz, USA) were incubated overnight with primary antibodies (dilution 1/200). Large Volume Detection System (anti-polyvalent, horseradish peroxidase (HRP); product No. TP-125-HL; Thermo Fisher Scientific Inc., Waltham, USA) was applied as recommended by the manufacturer. Subsequently, 3-amino-9-ethylcarbazole (AEC) was used as the chromogen. The sections were then counterstained with Mayer's hematoxylin, mounted with an aqueous mounting medium, and examined under a light microscope. Immunoreactivities were semi-quantitatively evaluated as none (0), mild (1), moderate (2), and severe (3).

Statistical analyses

All statistical analyses were carried out using IBM SPSS v. 27.0 (IBM Corp., Armonk, USA). Figures were generated using GraphPad Prism v. 8.0.1 (GraphPad Software, San Diego, USA). All biochemical results are expressed as mean \pm standard deviation (mean \pm SD) along with the 95% confidence interval (95% CI) of the mean. The assumption of normality was evaluated with Shapiro–Wilk test and the assumption of homogeneity of variances was

evaluated with Levene's test. One-way analysis of variance (ANOVA) or Welch's ANOVA test was used to assess differences in means between groups. Pairwise comparisons regarding these tests were made with Tukey's honestly significant difference (HSD) and Games–Howell test, respectively. All histopathological and immunohistochemical results are presented as median and minimum and maximum. In the histopathological and immunohistochemical evaluation, the difference between the groups in terms of median values was determined using the Kruskal–Wallis test, a nonparametric test. Dunn's test with Bonferroni correction was used for pairwise comparisons between groups, and adjusted p-values are presented. A $p < 0.05$ was deemed statistically significant.

Results

Biochemical findings

MDA analysis results of liver tissue

The MDA levels in liver tissue were higher in the amiodarone-treated group than in the healthy group, as shown in Fig. 1 and Table 1,2. The difference in the levels of MDA in the liver tissue between the healthy group and the group treated with amiodarone was statistically significant. In addition, ATP 2 mg/kg and 5 mg/kg, resveratrol, and resveratrol + ATP 2 mg/kg treatment significantly suppressed the amiodarone-induced rise in MDA levels in liver tissue. In the groups treated with ATP 2 mg/kg and resveratrol, a statistically significant difference in MDA levels was found in the liver tissues compared to the healthy group. However, the difference in MDA levels between the healthy group and the groups treated with ATP 5 mg/kg and resveratrol + ATP 2 mg/kg was not statistically significant.

tGSH analysis results of liver tissue

As shown in Fig. 1 and Table 1,2, the levels of tGSH in the liver tissue were lower in the group treated with amiodarone than in the HG. The difference in liver tGSH levels between the HG and the amiodarone-treated group was statistically significant. Furthermore, the amiodarone-induced reduction in liver tGSH levels was significantly attenuated by treatment with ATP at 2 mg/kg and 5 mg/kg, resveratrol alone, and the combination of resveratrol + ATP at 2 mg/kg. In the ATP 2 mg/kg and resveratrol-treated groups, a statistically significant difference in tGSH levels was found in liver tissue compared to HG. However, the difference in tGSH levels between the HG and the groups treated with ATP 5 mg/kg and resveratrol + ATP 2 mg/kg was not statistically significant.

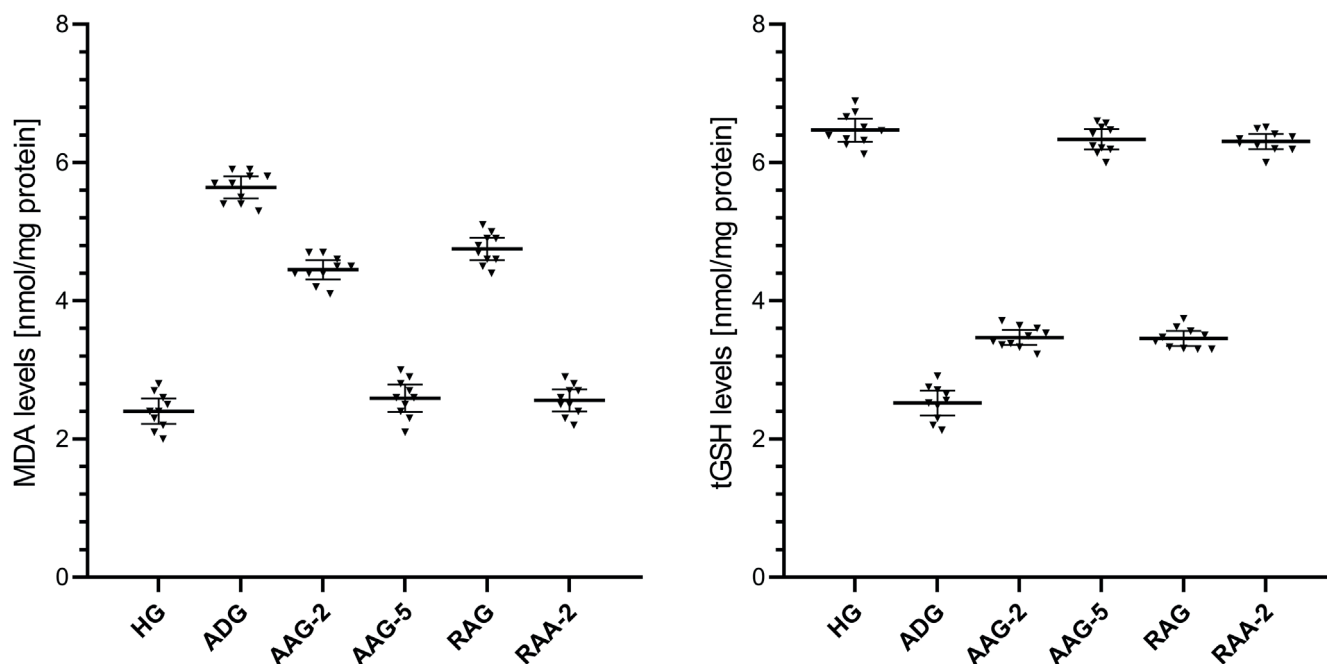


Fig. 1. Effects of amiodarone, adenosine triphosphate and resveratrol on MDA and tGSH levels in rat liver tissue. Data are presented as mean values and 95% confidence intervals (95% CIs). Statistical analyses were performed using one-way analysis of variance (ANOVA) test followed by Tukey's honestly significant difference (HSD) test as post hoc test. For all groups $n = 10$

HG – healthy group; ADG – amiodarone alone-administered group; AAG-2 – 2 mg/kg adenosine triphosphate + amiodarone-administered group; AAG-5 – 5 mg/kg adenosine triphosphate + amiodarone-administered group; RAG – resveratrol + amiodarone-administered group; RAA-2 – resveratrol + 2 mg/kg adenosine triphosphate + amiodarone-administered group; MDA – malondialdehyde; tGSH – total glutathione.

Table 1. Effects of amiodarone, adenosine triphosphate and resveratrol on oxidant and antioxidant levels in rat liver tissue and liver enzyme activities in blood serum

Groups and 95% CI for mean			Biochemical variables					
			MDA (nmol/mg protein)	tGSH (nmol/mg protein)	SOD (U/mg protein)	CAT (U/mg protein)	ALT (U/L)	AST (U/L)
Groups	HG		2.40 ±0.26	6.47 ±0.23	8.31 ±0.16	7.45 ±0.23	23.20 ±2.66	27.10 ±3.98
	ADG		5.64 ±0.22	2.52 ±0.25	3.22 ±0.10	3.28 ±0.09	76.70 ±4.67	191.90 ±6.61
	AAG-2		4.45 ±0.20	3.47 ±0.15	4.23 ±0.09	4.61 ±0.33	52.00 ±3.33	107.90 ±7.85
	AAG-5		2.59 ±0.28	6.34 ±0.20	8.11 ±0.25	7.30 ±0.21	27.60 ±4.06	30.20 ±6.36
	RAG		4.75 ±0.23	3.45 ±0.15	4.22 ±0.14	3.23 ±0.10	67.80 ±7.47	175.40 ±4.50
	RAA-2		2.56 ±0.22	6.30 ±0.15	8.15 ±0.06	7.34 ±0.35	26.70 ±2.41	31.90 ±4.36
95% CI for mean	HG	lower	2.2153	6.3004	8.1978	7.2820	21.30	24.25
		upper	2.5847	6.6356	8.4202	7.6160	25.10	29.95
	ADG	lower	5.4811	2.3419	3.1498	3.2132	73.36	187.17
		upper	5.7989	2.7001	3.2962	3.3488	80.04	196.63
	AAG-2	lower	4.3099	3.3592	4.1717	4.3699	49.62	102.28
		upper	4.5901	3.5768	4.2943	4.8441	54.38	113.52
	AAG-5	lower	2.3921	6.1885	7.9307	7.1482	24.70	25.65
		upper	2.7879	6.4815	8.2933	7.4498	30.50	34.75
	RAG	lower	4.5874	3.3451	4.1120	3.1578	62.46	172.18
		upper	4.9126	3.5629	4.3180	3.2982	73.14	178.62
	RAA-2	lower	2.4011	6.1938	8.1088	7.0925	24.98	28.78
		upper	2.7189	6.4142	8.1932	7.5875	28.42	35.02

The results are presented as mean ± standard deviation (SD). For all groups $n = 10$. HG – healthy group; ADG – amiodarone alone-administered group; AAG-2 – 2 mg/kg adenosine triphosphate + amiodarone-administered group; AAG-5 – 5 mg/kg adenosine triphosphate + amiodarone-administered group; RAG – resveratrol + amiodarone-administered group; RAA-2 – resveratrol + 2 mg/kg adenosine triphosphate + amiodarone-administered group; MDA – malondialdehyde; tGSH – total glutathione; SOD – superoxide dismutase; CAT – catalase; ALT – alanine aminotransferase; AST – aspartate aminotransferase; 95% CI – 95% confidence interval.

Table 2. Effects of amiodarone, adenosine triphosphate and resveratrol on oxidant and antioxidant levels in rat liver tissue and liver enzyme activities in blood serum; comparison of p-values

Group comparisons	Post hoc test p-values					
	MDA*	tGSH*	SOD**	CAT**	ALT**	AST*
HG vs ADG	<0.001	<0.001	<0.001	<0.001	<0.001	<0.001
HG vs AAG-2	<0.001	<0.001	<0.001	<0.001	<0.001	<0.001
HG vs AAG-5	0.470	0.653	0.340	0.664	0.098	0.836
HG vs RAG	<0.001	<0.001	<0.001	<0.001	<0.001	<0.001
HG vs RAA-2	0.652	0.428	0.092	0.958	0.060	0.440
ADG vs AAG-2	<0.001	<0.001	<0.001	<0.001	<0.001	<0.001
ADG vs AAG-5	<0.001	<0.001	<0.001	<0.001	<0.001	<0.001
ADG vs RAG	<0.001	<0.001	<0.001	0.818	0.055	<0.001
ADG vs RAA-2	<0.001	<0.001	<0.001	<0.001	<0.001	<0.001
AAG-2 vs AAG-5	<0.001	<0.001	<0.001	<0.001	<0.001	<0.001
AAG-2 vs RAG	0.064	>0.999	0.999	<0.001	<0.001	<0.001
AAG-2 vs RAA-2	<0.001	<0.001	<0.001	<0.001	<0.001	<0.001
AAG-5 vs RAG	<0.001	<0.001	<0.001	<0.001	<0.001	<0.001
AAG-5 vs RAA-2	>0.999	0.999	0.996	0.999	0.989	0.986
RAG vs RAA-2	<0.001	<0.001	<0.001	<0.001	<0.001	<0.001
F-value	348.705	845.219	5227.768 ^a	1222.962 ^a	288.257 ^a	1721.094
df (df1/df2)	5/54	5/54	5/24.453	5/24.288	5/24.827	5/54
p-value	<0.001	<0.001	<0.001 ^b	<0.001 ^b	<0.001 ^b	<0.001

* Statistical analyses were performed using the one-way analysis of variance (ANOVA) test followed by Tukey's honestly significant difference (HSD) test as post hoc. ** Statistical analyses were performed using the Welch's ANOVA test followed by Games–Howell test as post hoc test.

^a means of asymptotically F distributed. ^b means of Welch's ANOVA p-values. HG – healthy group; ADG – amiodarone alone-administered group; AAG-2 – 2 mg/kg adenosine triphosphate + amiodarone-administered group; AAG-5 – 5 mg/kg adenosine triphosphate + amiodarone-administered group; RAG – resveratrol + amiodarone-administered group; RAA-2 – resveratrol + 2 mg/kg adenosine triphosphate + amiodarone-administered group; MDA – malondialdehyde; tGSH – total glutathione; SOD – superoxide dismutase; CAT – catalase; ALT – alanine aminotransferase; AST – aspartate aminotransferase; df – degree of freedom.

SOD analysis results of liver tissue

The activities of SOD in the liver tissue were lower in the group treated with amiodarone than in the HG, as shown in Fig. 2 and in Table 1,2. The difference in liver SOD activities between the HG and the group treated with amiodarone was statistically significant. In addition, ATP 2 mg/kg, ATP 5 mg/kg, resveratrol and resveratrol + ATP 2 mg/kg treatment significantly suppressed the amiodarone-induced decrease in SOD activities in liver tissue. In the groups treated with ATP at 2 mg/kg and resveratrol, liver SOD activity showed a statistically significant difference compared to the HG group. However, the difference in SOD activity between the HG and the ATP 5 mg/kg and resveratrol + ATP 2 mg/kg treatment groups was not statistically significant.

CAT analysis results of liver tissue

As shown in Fig. 2 and Table 1,2, the activities of CAT in the liver tissue were lower in the group treated with amiodarone than in the HG group. The difference in liver CAT activities between the HG group and the amiodarone-treated group was statistically significant. Treatment with ATP at 2 mg/kg, ATP at 5 mg/kg, and the combination

of resveratrol + ATP at 2 mg/kg significantly suppressed the amiodarone-induced decrease in CAT activity in liver tissue, whereas resveratrol alone did not produce a significant effect. In the groups treated with ATP 2 mg/kg and resveratrol, a statistically significant difference in liver CAT activities was observed compared to the HG group. However, the difference in CAT activity between the HG and the ATP 5 mg/kg and resveratrol + ATP 2 mg/kg treatment groups was not statistically significant.

ALT and AST analysis results of blood serum

The ALT activity in blood serum was higher in the amiodarone-treated group than in the HG group, as shown in Fig. 3 and Table 1,2. The difference in serum ALT activity between the HG group and the amiodarone-treated group was statistically significant. Notably, treatment with ATP at 2 mg/kg, ATP at 5 mg/kg, and the combination of resveratrol + ATP at 2 mg/kg significantly attenuated the amiodarone-induced increase in serum ALT levels, whereas resveratrol alone did not produce a significant effect. A statistically significant difference in blood serum ALT activity was observed in the groups treated with ATP 2 mg/kg and resveratrol compared to the HG group.

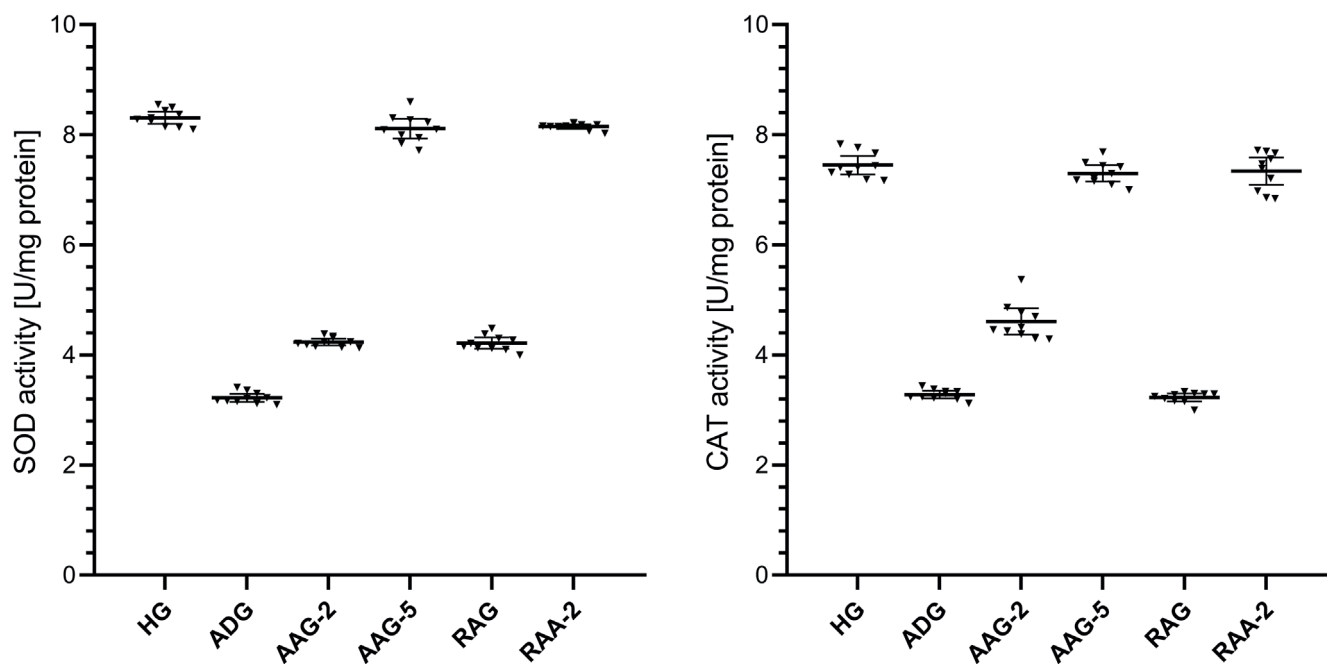


Fig. 2. Effects of amiodarone, adenosine triphosphate and resveratrol on SOD and CAT activities in rat liver tissue. Data are presented as mean values and 95% confidence intervals (95% CIs). Statistical analyses were performed using Welch's analysis of variance (ANOVA) test followed by Games–Howell test as post hoc test. For all groups $n = 10$

HG – healthy group; ADG – amiodarone alone-administered group; AAG-2 – 2 mg/kg adenosine triphosphate + amiodarone-administered group; AAG-5 – 5 mg/kg adenosine triphosphate + amiodarone-administered group; RAG – resveratrol + amiodarone-administered group; RAA-2 – resveratrol + 2 mg/kg adenosine triphosphate + amiodarone-administered group; SOD – superoxide dismutase; CAT – catalase.

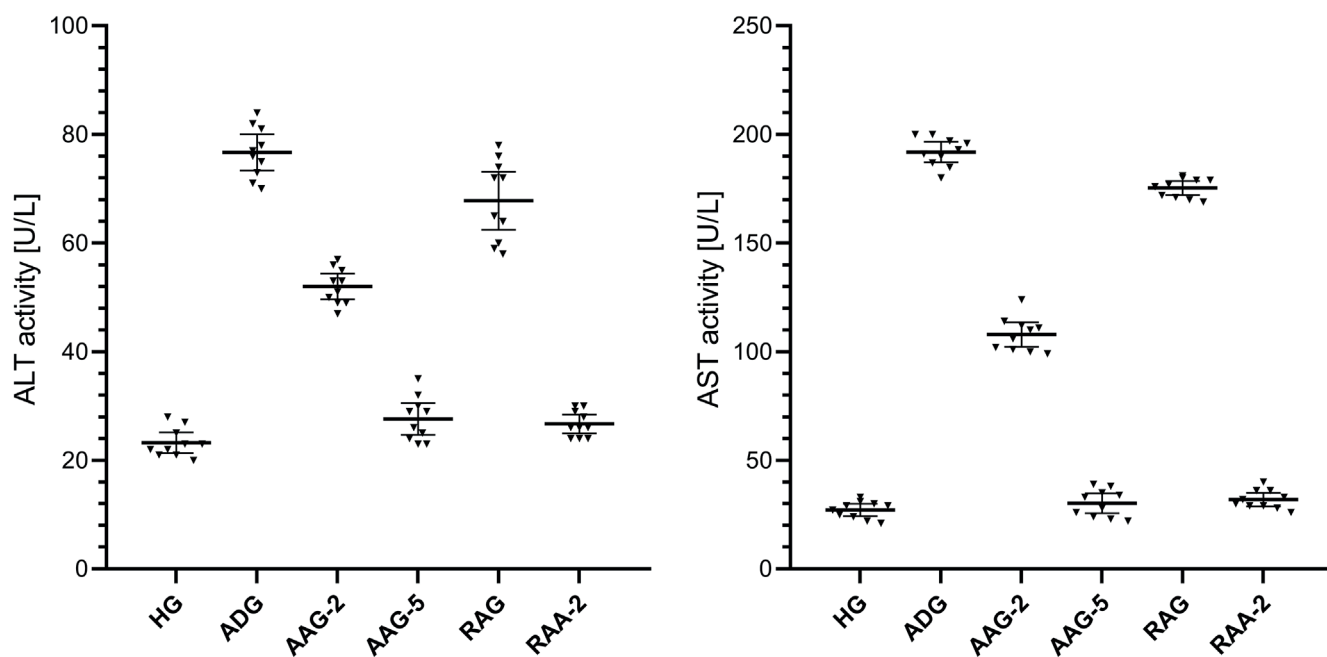


Fig. 3. Effects of amiodarone, adenosine triphosphate and resveratrol on ALT and AST activities in rat blood serum. Data are presented as mean values and 95% confidence intervals (95% CIs). Statistical analyses were performed using a Welch's analysis of variance (ANOVA) test, followed by a Games–Howell post-hoc test for ALT, and a one-way ANOVA test, followed by a Tukey's honestly significant difference (HSD) post-hoc test, for AST. For all groups $n = 10$

HG – healthy group; ADG – amiodarone alone-administered group; AAG-2 – 2 mg/kg adenosine triphosphate + amiodarone-administered group; AAG-5 – 5 mg/kg adenosine triphosphate + amiodarone-administered group; RAG – resveratrol + amiodarone-administered group; RAA-2 – resveratrol + 2 mg/kg adenosine triphosphate + amiodarone-administered group; ALT – alanine aminotransferase; AST – aspartate aminotransferase.

However, the difference in ALT activity between the HG and the treatment groups with ATP 5 mg/kg and resveratrol + ATP 2 mg/kg was not statistically significant.

As shown in Fig. 3 and Table 1,2, the activity of AST in the blood serum was higher in the group treated with amiodarone than in the HG group. The difference in serum

AST activities between the HG and the amiodarone treatment group was statistically significant. In addition, treatment with ATP 2 mg/kg, ATP 5 mg/kg, resveratrol and resveratrol + ATP 2 mg/kg significantly suppressed the amiodarone-induced increase in serum AST activity. In the groups treated with ATP 2 mg/kg and resveratrol, a statistically significant difference in blood serum AST activity was observed compared to the HG group. However, the difference in AST activity between the HG and the ATP 5 mg/kg and resveratrol + ATP 2 mg/kg treatment groups was not statistically significant.

Histopathological findings

The liver tissue sections of the HG group exhibited normal hepatic cords with radial arrangement in the hepatic lobule, with a central vein in the center. The general tissue arrangement of the liver was also normal (Fig. 4A). Histopathological damage was classified as grade 3 in the group treated with amiodarone alone. Upon analysis of the liver tissue from this group, severe dilatation and congestion were observed in both the central artery and the surrounding blood vessels. It was observed that the hepatic cords lost their radial arrangement and became irregular and spiralized cords. Severe lipid infiltration was observed in the irregularly arranged hepatocyte cords around the central vein, with the cell content almost completely filled with lipid and becoming vacuolized. The liver tissue exhibited necrosis in some of the hepatocytes, and there was PMNL infiltration throughout the tissue, along with other accompanying findings (Fig. 4B). The histopathological damage was grade 2 in the group that received

amiodarone and 2 mg/kg ATP. In this group, while necrotic nuclei were decreased compared to the amiodarone group, the hepatic cords remained disorganized, hepatocytes were severely vacuolized. Vascular structures showed severe dilation and congestion, and PMNL infiltration was seen in the areas surrounding the vessels (Fig. 5A). In the group administered amiodarone and ATP at a dose of 5 mg/kg, hepatic damage was evaluated as grade 1. The liver tissue of this group showed a decrease in lipid infiltration in hepatocytes forming irregular hepatic cords, a decrease in necrotized nuclei compared to the previous group, and the presence of mild PMNL infiltration was remarkable. Vessels were moderately dilated but did not show congestion (Fig. 5B). The liver damage severity in the group treated with amiodarone and resveratrol was classified as grade 2. When the liver tissues of this group were examined, it was observed that the lipid infiltration of the hepatocytes was at a moderate level and the hepatic cords were arranged in a regular pattern. The amount of necrotic cell nuclei and the distribution of PMNLs were similar to the ADG group, while there was severe dilatation and congestion in the vessels (Fig. 5C). The liver tissue of the group treated with amiodarone, 2 mg/kg ATP, and resveratrol showed similarities to that of the HG group (grade 0–1). Mild lipid accumulation was observed in the hepatocytes, forming regular hepatic cords in this group. Necrotized cells and PMNLs were not observed throughout the tissue. However, moderate dilatation of the vascular structures was observed, but they were not congested (Fig. 5D). Histopathological grading data obtained from rat liver tissue and comparison of p-values are presented in Table 3,4.

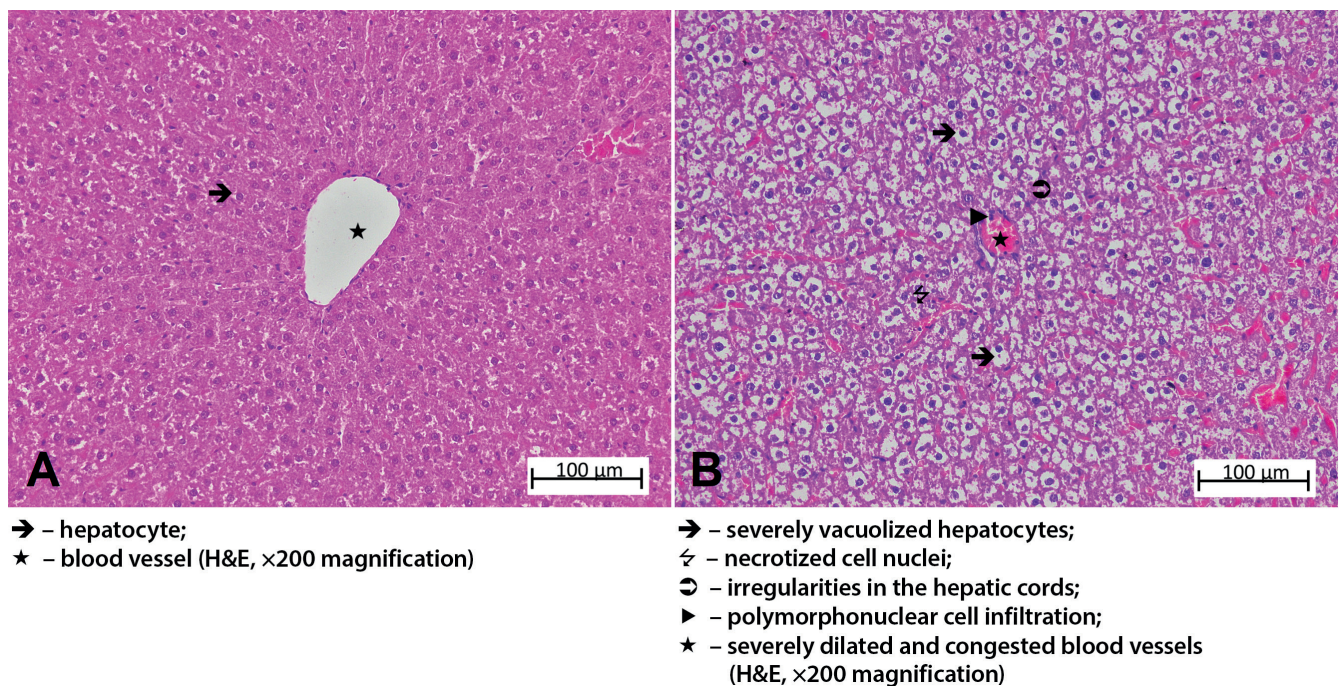


Fig. 4. Hematoxylin and eosin (H&E)-labeled liver tissue. A. In the healthy control group (HG); B. In the group receiving amiodarone alone (ADG). For all groups n = 6

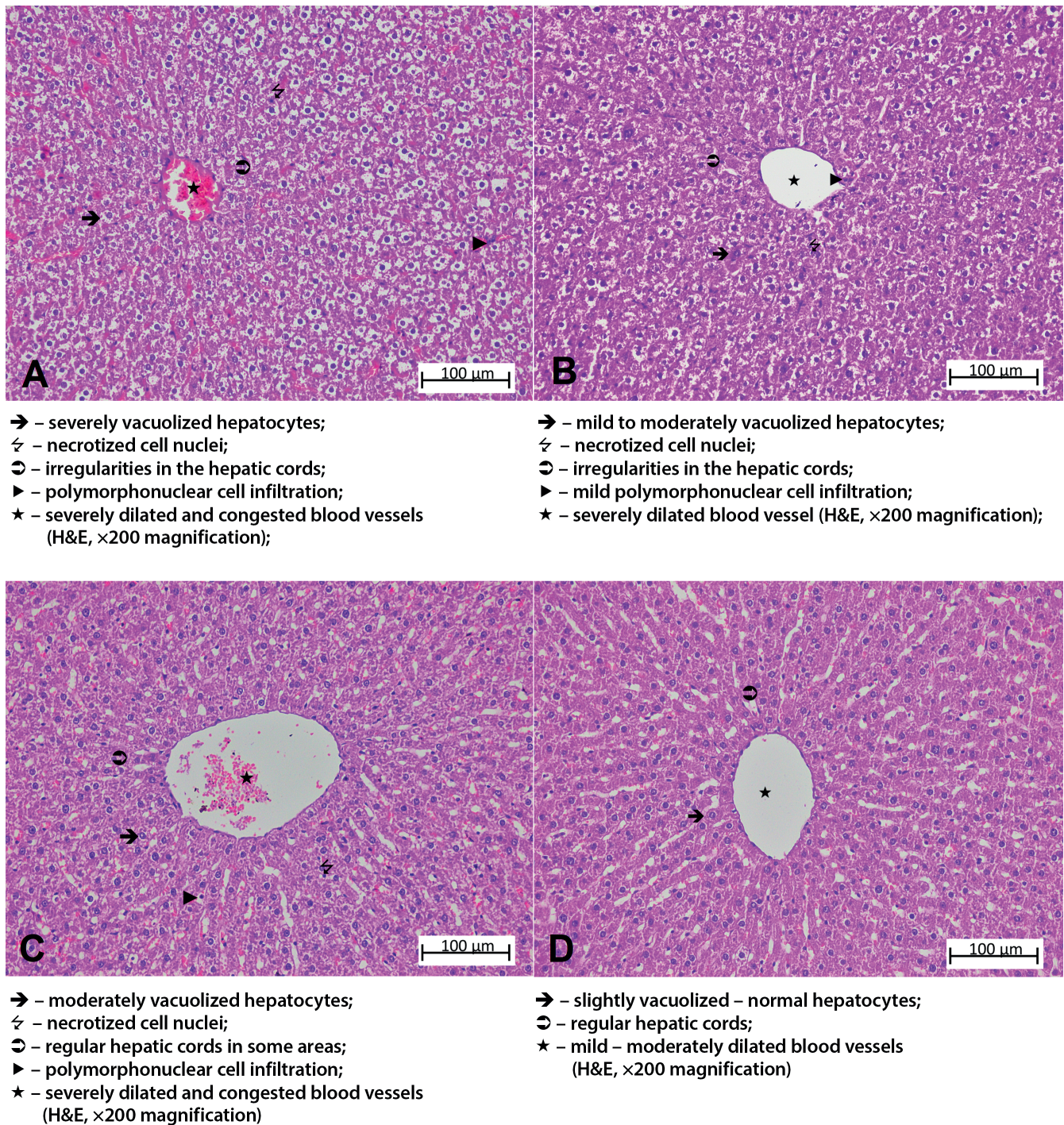


Fig. 5. Hematoxylin and eosin (H&E)-labeled liver tissue. A. In the 2 mg/kg ATP + amiodarone-administered group (AAG-2); B. In the 5 mg/kg ATP + amiodarone-administered group (AAG-5); C. In the resveratrol + amiodarone-administered group (RAG); D. In the resveratrol + 2 mg/kg ATP + amiodarone-receiving group (RAA-2). For all groups $n = 6$

Immunohistochemical findings

Immunohistochemical examinations for *caspase-3* (Fig. 6) and *TNF-α* (Fig. 7) revealed statistically significant differences between the groups (Table 5,6; $p < 0.05$). No significant *caspase-3* and *TNF-α* immunopositivity was found in the HG group. Among the treatment groups, strong *caspase-3* and *TNF-α* immunopositivity was observed in the ADG group, moderate immunopositivity

in the AAG-2 and RAG groups, and mild immunopositivity in the AAG-5 and RAA-2 groups.

Discussion

This study investigates the protective effects of ATP, resveratrol and their combination (ARCs) against amiodarone-induced liver injury and dysfunction in rats, using

Table 3. Analysis of histopathological grading data from rat liver tissue

Groups	Histopathological grading data			
	lipid infiltration/vacuolization	necrosis	vascular dilatation /congestion	PMNL infiltration
HG	0 (0–0)	0 (0–0)	0 (0–0)	0 (0–0)
ADG	3 (2–3)	3 (2–3)	3 (2–3)	2 (1–3)
AAG-2	2 (2–3)	2 (1–3)	3 (2–3)	2 (0–3)
AAG-5	2 (2–3)	2 (1–3)	2 (1–3)	2 (1–3)
RAG	2 (2–3)	2 (1–3)	2 (2–3)	2 (0–3)
RAA-2	2 (0–2)	1 (0–2)	1 (1–2)	0 (0–1)

The results are presented as median (minimum–maximum). Values indicate histopathological damage grades: 0 – none, 1 – mild, 2 – moderate, and 3 – severe. For all groups n = 6. HG – healthy group; ADG – amiodarone alone-administered group; AAG-2 – 2 mg/kg adenosine triphosphate + amiodarone-administered group; AAG-5 – 5 mg/kg adenosine triphosphate + amiodarone-administered group; RAG – resveratrol + amiodarone-administered group; RAA-2 – resveratrol + 2 mg/kg adenosine triphosphate + amiodarone-administered group; PMNL – polymorphonuclear leukocyte.

Table 4. Comparison of p-values of histopathologic grading data obtained from rat liver tissue

Group comparisons	Post hoc test p-values			
	lipid infiltration/vacuolization	necrosis	vascular dilatation/congestion	PMNL infiltration
HG vs ADG	<0.001	<0.001	<0.001	<0.001
HG vs AAG-2	<0.001	<0.001	<0.001	<0.001
HG vs AAG-5	<0.001	<0.001	<0.001	<0.001
HG vs RAG	<0.001	<0.001	<0.001	<0.001
HG vs RAA-2	<0.001	0.281	0.004	>0.999
ADG vs AAG-2	>0.999	0.769	>0.999	>0.999
ADG vs AAG-5	0.104	0.034	0.014	0.018
ADG vs RAG	0.953	0.269	0.313	>0.999
ADG vs RAA-2	<0.001	<0.001	<0.001	<0.001
AAG-2 vs AAG-5	>0.999	>0.999	0.104	0.206
AAG-2 vs RAG	>0.999	>0.999	>0.999	>0.999
AAG-2 vs RAA-2	<0.001	<0.001	<0.001	<0.001
AAG-5 vs RAG	>0.999	>0.999	>0.999	0.037
AAG-5 vs RAA-2	0.017	<0.001	0.012	<0.001
RAG vs RAA-2	0.001	<0.001	<0.001	<0.001
KW	140.283	155.641	155.106	152.433
p-value	<0.001	<0.001	<0.001	<0.001

All statistical analyses were performed using the Kruskal–Wallis (KW) test followed by Dunn's test with Bonferroni correction. For all groups n = 6. HG – healthy group; ADG – amiodarone alone-administered group; AAG-2 – 2 mg/kg adenosine triphosphate + amiodarone-administered group; AAG-5 – 5 mg/kg adenosine triphosphate + amiodarone-administered group; RAG – resveratrol + amiodarone-administered group; RAA-2 – resveratrol + 2 mg/kg adenosine triphosphate + amiodarone-administered group; PMNL – polymorphonuclear leukocyte.

biochemical, histopathological and immunohistochemical approaches. Previous studies have reported a decrease in ATP content in parallel with the increase in mitochondrial ROS associated with amiodarone.⁹ Furthermore, it has been emphasized that amiodarone causes a significant decrease in cellular ATP and cell viability.¹⁰ The results of our biochemical analyses revealed that amiodarone treatment led to an increase in MDA, tGSH, SOD, and CAT levels in liver tissue. It is well established that MDA is a byproduct of the oxidation of polyunsaturated fatty acids, including arachidonic acid.²² In simpler terms, MDA serves as a marker of LPO and is widely used as a reliable indicator of oxidative damage severity.²³ Literature data and

our experimental results suggest that amiodarone treatment increases ROS production and induces LPO reaction in liver tissue. Previous studies have indicated that amiodarone-induced toxicity is primarily driven by the generation of ROS, leading to oxidative stress and LPO.⁸

As previously stated, amiodarone has been linked to toxic effects in various organs and tissues, including the liver.^{6,7} Furthermore, long-term use of amiodarone may result in life-threatening side effects.⁵ However, Jiang et al. reported that acute liver injury can occur due to parenteral administration of amiodarone and that antioxidant treatment was effective in relieving the hepatotoxicity.²⁴ Akbay et al. reported a decrease in glutathione (GSH),

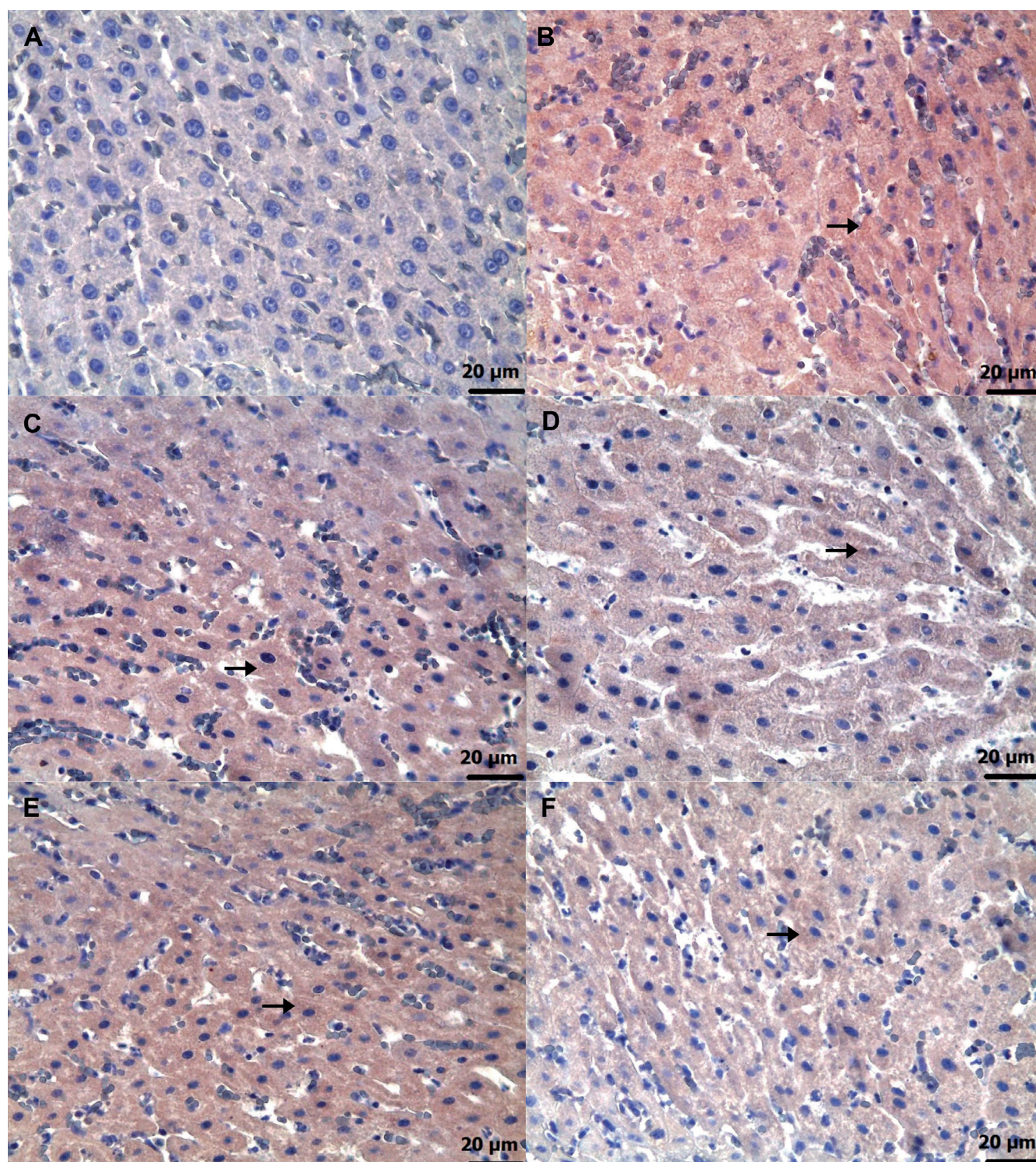


Fig. 6. A. HG group, *caspase-3* immune negativity in healthy liver tissue, immunohistochemistry (IHC); B. ADG group, severe *caspase 3* immunopositivity (arrow) in liver tissue, IHC; C. AAG-2 group, moderate *caspase-3* immunopositivity (arrow) in liver tissue, IHC; D. AAG-5 group, mild *caspase-3* immunopositivity (arrow) in liver tissue, IHC; E. RAG group, moderate *caspase-3* immunopositivity (arrow) in liver tissue, IHC; F. RAA-2 group, mild *caspase-3* immunopositivity (arrow) in liver tissue, IHC. For all groups $n = 6$

HG – healthy group; ADG – amiodarone alone-administered group; AAG-2 – 2 mg/kg adenosine triphosphate + amiodarone-administered group; AAG-5 – 5 mg/kg adenosine triphosphate + amiodarone-administered group; RAG – resveratrol + amiodarone-administered group; RAA-2 – resveratrol + 2 mg/kg adenosine triphosphate + amiodarone-administered group.

a key endogenous antioxidant, in cases of amiodarone-induced hepatotoxicity, and demonstrated that antioxidant supplementation alleviated the resulting liver injury.²⁵ Amiodarone hepatotoxicity has been assessed using tGSH,

an endogenous antioxidant composed of 3 amino acids.²⁶ Furthermore, GSH serves as a key marker of cellular redox status in various diseases and cell death processes, and plays a critical role in regulating numerous cellular

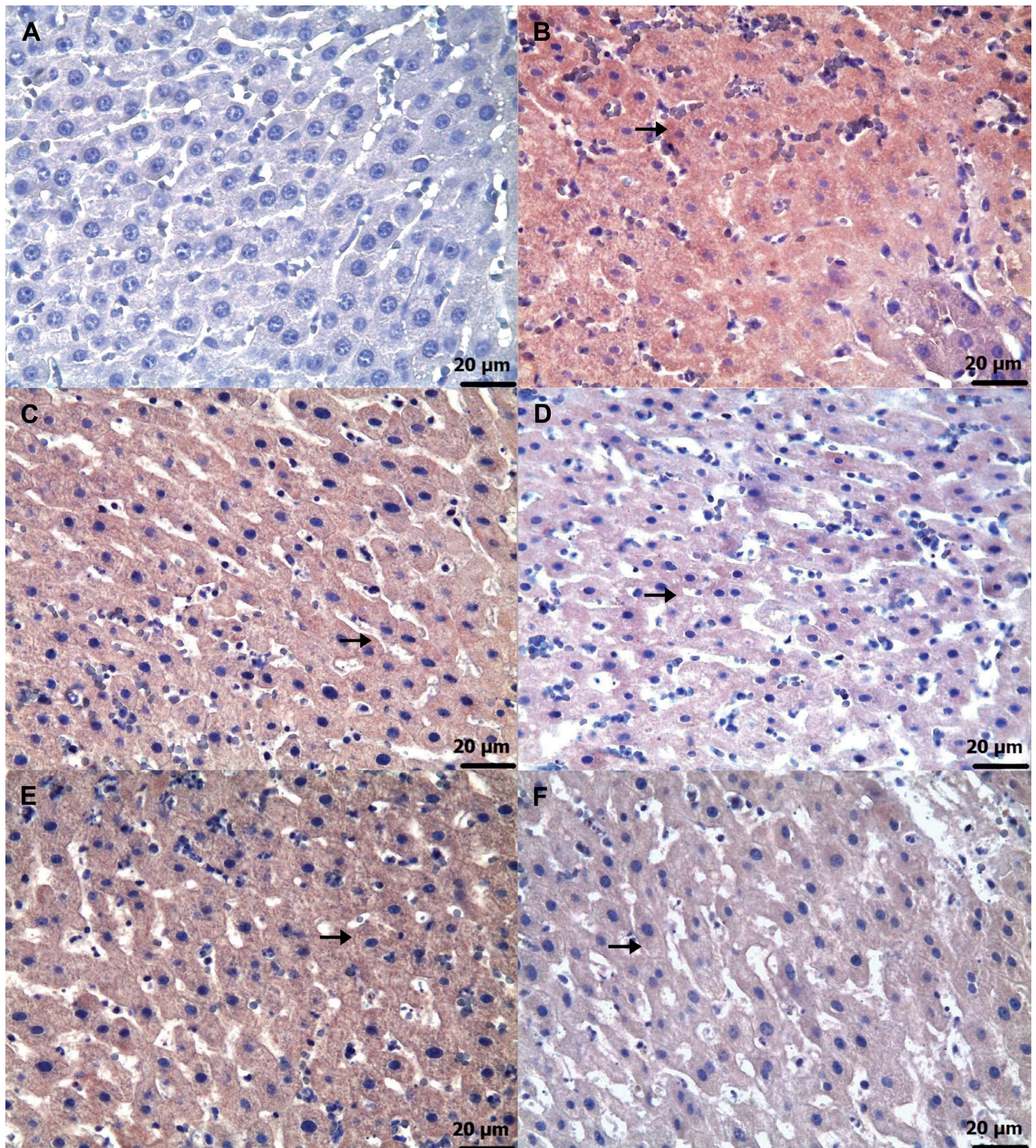


Fig. 7. A. HG group, *TNF-α* immune negativity in healthy liver tissue, immunohistochemistry (IHC); B. ADG group, severe *TNF-α* immunopositivity (arrow) in liver tissue, IHC; C. AAG-2 group, moderate *TNF-α* immunopositivity (arrow) in liver tissue, IHC; D. AAG-5 group, mild *TNF-α* immunopositivity (arrow) in liver tissue, IHC; E. RAG group, moderate *TNF-α* immunopositivity (arrow) in liver tissue, IHC; F. RAA-2 group, mild *TNF-α* immunopositivity (arrow) in liver tissue, IHC. For all groups $n = 6$

HG – healthy group; ADG – amiodarone alone-administered group; AAG-2 – 2 mg/kg adenosine triphosphate + amiodarone-administered group; AAG-5 – 5 mg/kg adenosine triphosphate + amiodarone-administered group; RAG – resveratrol + amiodarone-administered group; RAA-2 – resveratrol + 2 mg/kg adenosine triphosphate + amiodarone-administered group; *TNF-α* – tumor necrosis factor alpha.

functions.²⁷ Similar to the findings of the literature, our study showed a significant reduction in the amount of tGSH in the liver tissue of amiodarone-treated animals.

In liver tissue treated with amiodarone, the enzymatic defense systems, including SOD and CAT, showed a decrease in their antioxidant activity. Superoxide dismutase

Table 5. Analysis of immunohistochemical grading data from rat liver tissue

Groups	Immunohistochemical grading data	
	<i>caspase-3</i>	<i>TNF-α</i>
HG	0 (0–1)	0 (0–1)
ADG	3 (2–3)	3 (2–3)
AAG-2	2 (2–2)	2 (1–2)
AAG-5	1 (1–2)	1 (1–2)
RAG	2 (2–2)	2 (1–2)
RAA-2	1 (1–2)	1 (1–1)

The results are presented as median (minimum–maximum). Values indicate immunohistochemical damage grades: 0 – none, 1 – mild, 2 – moderate, and 3 – severe. For all groups $n = 6$. HG – healthy group; ADG – amiodarone alone-administered group; AAG-2 – 2 mg/kg adenosine triphosphate + amiodarone-administered group; AAG-5 – 5 mg/kg adenosine triphosphate + amiodarone-administered group; RAG – resveratrol + amiodarone-administered group; RAA-2 – resveratrol + 2 mg/kg adenosine triphosphate + amiodarone-administered group; *TNF-α* – tumor necrosis factor alpha.

Table 6. Comparison of p-values of immunohistochemical grading data obtained from rat liver tissue

Group comparisons	Post hoc test p-values	
	<i>caspase-3</i>	<i>TNF-α</i>
HG vs ADG	<0.001	<0.001
HG vs AAG-2	0.012	0.013
HG vs AAG-5	0.968	>0.999
HG vs RAG	0.012	0.013
HG vs RAA-2	>0.999	>0.999
ADG vs AAG-2	>0.999	>0.999
ADG vs AAG-5	0.035	0.048
ADG vs RAG	>0.999	>0.999
ADG vs RAA-2	0.009	0.013
AAG-2 vs AAG-5	>0.999	>0.999
AAG-2 vs RAG	>0.999	>0.999
AAG-2 vs RAA-2	0.877	0.751
AAG-5 vs RAG	>0.999	>0.999
AAG-5 vs RAA-2	>0.999	>0.999
RAG vs RAA-2	0.877	0.751
KW	29.866	28.657
p-value	<0.001	<0.001

All statistical analyses were performed using the Kruskal–Wallis (KW) test followed by Dunn's test with Bonferroni correction. For all groups $n = 6$. HG – healthy group; ADG – amiodarone alone-administered group; AAG-2 – 2 mg/kg adenosine triphosphate + amiodarone-administered group; AAG-5 – 5 mg/kg adenosine triphosphate + amiodarone-administered group; RAG – resveratrol + amiodarone-administered group; RAA-2 – resveratrol + 2 mg/kg adenosine triphosphate + amiodarone-administered group; PMNL – polymorphonuclear leukocyte. *TNF-α* – tumor necrosis factor alpha.

enzymes are recognized as the first line of defense against ROS, catalyzing the dismutation of superoxide radicals into oxygen and hydrogen peroxide.²⁸ Superoxide dismutase catalyzes the transformation of the superoxide

anion free radical ($O_2^{\cdot-}$) to hydrogen peroxide (H_2O_2) and molecular oxygen (O_2). Subsequently, CAT enzyme reduces H_2O_2 to water.²⁹ Therefore, SOD is used in various pathologies to neutralize ROSs. Some studies have reported that amiodarone may exhibit gastroprotective effects by mitigating the reduction of SOD activity and limiting the increase of CAT activity under certain conditions.³⁰ However, it has also been reported that amiodarone decreases SOD and CAT activities in the optic nerve, leading to optic neuropathy.³¹

In this study, we found that the group administered amiodarone alone had significantly higher levels of ALT and AST in their blood serum compared to the HG group. It is important to note that in healthy individuals, the circulating levels of liver enzymes are primarily due to cytoplasmic leakage.³² While ALT is typically found in the hepatocyte cytoplasm, AST is present in both the hepatocyte cytoplasm and mitochondria.^{33,34} The literature and our experimental results suggest that the amiodarone group experienced damage to both hepatocyte cytoplasm and mitochondria. These findings are consistent with the results of the study by Nagata et al. on amiodarone-induced hepatotoxicity.³⁵ Felser et al. reported that amiodarone induced toxic effects, including a reduction in intracellular ATP levels, accumulation of ROS in hepatocyte mitochondria, and inhibition of mitochondrial function.¹³ Furthermore, it has been demonstrated that the amiodarone-associated increase in mitochondrial H_2O_2 production correlates with a reduction in ATP levels.³⁶

As previously stated, amiodarone has been shown to increase ROS production in hepatocyte mitochondria, leading to a significant decrease in ATP content and cell viability.^{9,10} The literature suggests that ATP may be a potential treatment for hepatotoxicity induced by amiodarone. The experimental results show that ATP at a dose of 5 mg/kg was more effective in inhibiting the amiodarone-induced rise in MDA and reduction in tGSH, SOD and CAT, in liver tissue compared to 2 mg/kg. No studies investigating the effect of ATP on amiodarone-induced liver damage were found in the literature. However, literature reports indicate that ATP may protect rat liver tissue from acetaminophen-induced damage by preventing an increase in oxidants and a decrease in antioxidants.³⁷

Drug-induced hepatotoxicity is commonly caused by mitochondrial damage and dysfunction, which can lead to hepatocellular damage. As a result, ALT and AST levels are used to determine the extent of hepatocellular damage.³⁸ In accordance with the literature, our biochemical results revealed that ATP inhibited the amiodarone-induced increase in serum ALT and AST levels in rats. Previous studies have indicated that elevated serum ALT and AST levels in liver injury are associated with decreased hepatocellular ATP content.³⁹ Koç et al.³⁷ reported that ATP administration prevented the elevation of serum ALT and AST levels in rats treated with paracetamol. They also found

that ATP protected the normal structure of the liver from paracetamol-induced damage.

The literature suggests that not only exogenous ATP but also drugs that increase intracellular ATP production may be beneficial in the treatment of amiodarone-induced hepatotoxicity. In our study, we investigated the effect of resveratrol on amiodarone-induced hepatotoxicity. Resveratrol is a well-known antioxidant that has been shown to exert beneficial effects on various organs and tissues.¹⁶ It has also been shown to be an enhancer of intracellular ATP production.¹⁷ Consistent with previous studies, our experimental results demonstrate that resveratrol significantly attenuated amiodarone-induced increases in oxidative stress markers, as well as serum ALT and AST levels. No information investigating the effect of resveratrol on amiodarone-induced hepatotoxicity was found in recent studies. However, it has been reported that resveratrol prevents vancomycin-induced increases in oxidative stress and reductions in antioxidant levels in liver tissue, as well as elevations in serum ALT and AST levels.⁴⁰

In this study, the biochemical findings in amiodarone, ATP, resveratrol, ARCs, and the healthy rat group were consistent with the histopathologic findings. In the amiodarone-only group, characterized by elevated oxidant, ALT, and AST levels and reduced antioxidant levels, liver tissue showed severely dilated and congested blood vessels, irregular hepatocytes with lipid-filled vacuoles and necrosis, as well as widespread infiltration of PMNLs. However, the histopathological damage caused by amiodarone was evaluated as grade 2 in the 2 mg/kg ATP group (AAG-2), grade 1 in the 5 mg/kg ATP group (AAG-5), grade 2 in the resveratrol group (RAG), and grade 1 in the 2 mg/kg ATP + resveratrol group (RAA-2). Previous studies have reported the presence of lipid droplets of different sizes in patients treated with amiodarone,³⁵ supporting our histopathological findings. Furthermore, elevated oxidant levels have been reported to induce hepatocyte apoptosis and/or necrosis.¹³ In addition to hepatocyte necrosis, liver tissue has been reported to show signs of lymphocytic cell infiltration, hepatocyte enlargement, vacuolization, and nuclear hypertrophy.³⁵

Furthermore, the biochemical and histopathological findings observed in the amiodarone, ATP, resveratrol, ARC, and healthy rat groups were consistent with the corresponding immunohistochemical results. Grade 3 level *caspase-3* and *TNF- α* immunopositivity was detected in the liver of the group receiving amiodarone alone. It was observed that this *caspase-3* and *TNF- α* immunopositivity was alleviated to grade 2 in the 2 mg/kg ATP and resveratrol groups, and to grade 1 in the 5 mg/kg ATP and 2 mg/kg ATP + resveratrol groups. A recent study reported that amiodarone induces apoptosis by causing *caspase-3* activation in liver cells.⁴¹ These literature data support our immunohistochemical *caspase-3* findings. Amiodarone decreases intracellular ATP and Ca_2^+ in hepatocytes, causing endoplasmic reticulum stress

and lipid accumulation.⁴² The toxic effects of amiodarone on the liver consist of mitochondrial toxicity, apoptosis and necrosis. Mitochondrial damage leads to activation of *caspase-9*, and binding of death receptors activates *caspase-8*. Activation of both *caspase-9* and *caspase-8* leads to propagation of the cascade of downstream effector caspases, including *caspase-3*. In conclusion, amiodarone induces apoptosis in hepatocytes by activating the mitochondrial apoptotic pathway, involving *caspase-2*, *-3* and *-9*.^{42,43} It has been previously demonstrated that amiodarone causes immune dysregulation in liver tissue, which leads to an increase in the proportion of Th17 and Th1 cells and causes a significant increase in inflammatory factors such as *TNF- α* .⁴⁴ In hepatocytes, mitochondria play a central role in linking *caspase-8* activation to *caspase-9*, ultimately leading to the activation of effector caspases such as *caspase-3* and *caspase-7*. Loss of mitochondrial membrane potential, generation of ROS, formation of the mitochondrial permeability transition pore and release of cytochrome C are critical for *TNF- α* -induced hepatocyte apoptosis.⁴⁵

Limitations

The effectiveness of the combination of 5 mg/kg ATP and resveratrol against amiodarone-induced hepatotoxicity was not assessed in this study. Future research should investigate this combination to determine whether it offers enhanced protective effects compared to individual or lower-dose treatments.

Conclusions

Biochemical, histopathological and immunohistochemical evidence demonstrates that amiodarone causes severe oxidative damage to liver tissue of rats. Damage severity was graded as follows: grade 2 in the 2 mg/kg ATP + amiodarone group (AAG-2), grade 1 in the 5 mg/kg ATP + amiodarone group (AAG-5), grade 2 in the resveratrol + amiodarone group (RAG) and grade 1 in the 2 mg/kg ATP + resveratrol + amiodarone group (RAA-2). The experimental results indicate that adjusting the ATP dose or using the combination of ATP and resveratrol is necessary to minimize amiodarone-induced liver damage.

Supplementary data

The supplementary materials are available at <https://doi.org/10.5281/zenodo.14881625>. The package includes the following files:

Supplementary Table 1. Assumption of normality for biochemical variables assessed with Shapiro–Wilk test.

Supplementary Table 2. The assumption of homogeneity of variance was assessed for the MDA, tGSH, SOD, CAT, ALT, and AST values.

Data availability

The datasets generated and/or analyzed during the current study are available from the corresponding author on reasonable request.





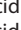

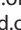


Consent for publication

Not applicable.

Use of AI and AI-assisted technologies

Not applicable.

ORCID iDs

Muhammed Talha Karadogan  <https://orcid.org/0000-0001-5588-0162>
 Bulent Yavuzer  <https://orcid.org/0000-0001-7576-0678>
 Cebrail Gursul  <https://orcid.org/0000-0001-6521-6169>
 Gulbaniz Huseynova  <https://orcid.org/0009-0003-1698-1093>
 Gulce Naz Yazici  <https://orcid.org/0000-0002-6989-997X>
 Mine Gulaboglu  <https://orcid.org/0000-0002-3248-1502>
 Furkan Yilmaz  <https://orcid.org/0000-0001-6459-9647>
 Ali Sefa Mendil  <https://orcid.org/0000-0003-2722-3290>
 Halis Suleyman  <https://orcid.org/0000-0002-9239-4099>

References

- Jørgensen AEM, Hermann TS, Christensen HR, Dalhoff KP. Use of therapeutic drug monitoring in amiodarone treatment: A systematic review of recent literature. *Ther Drug Monit.* 2023;45(4):487–493. doi:10.1097/FTD.0000000000001079
- Florek JB, Lucas A, Girzadas D. Amiodarone. In: *StatPearls*. Treasure Island, USA: StatPearls Publishing; 2025:Bookshelf ID: NBK482154. <http://www.ncbi.nlm.nih.gov/books/NBK482154>. Accessed February 18, 2025.
- Polintan ET, Monsalve R, Menghrajani RH, et al. Combination prophylactic amiodarone with β -blockers versus β -blockers in atrial fibrillation after cardiac surgery: A systematic-review and meta-analysis. *Heart Lung.* 2023;62:256–263. doi:10.1016/j.hrtlng.2023.08.006
- Nademanee K, Singh BN, Stevenson WG, Weiss JN. Amiodarone and post-MI patients. *Circulation.* 1993;88(2):764–774. doi:10.1161/01.CIR.88.2.764
- Newgaard OR, Chaudhry R, Schutte JA, et al. Amiodarone pharmacovigilance through an intelligent electronic health record application. *WMJ.* 2023;122(4):280–283. PMID:37768770.
- Türk U, Türk B, Yılmaz S, Tuncer E, Alioglu E, Dereli T. Amiodarone-induced multiorgan toxicity with ocular findings on confocal microscopy. *Middle East Afr J Ophthalmol.* 2015;22(2):258. doi:10.4103/0974-9233.154411
- Hamilton D, Nandkeolyar S, Lan H, et al. Amiodarone: A comprehensive guide for clinicians. *Am J Cardiovasc Drugs.* 2020;20(6):549–558. doi:10.1007/s40256-020-00401-5
- Jamshidzadeh A, Baghban M, Azarpira N, Bardbori AM, Niknahad H. Effects of tomato extract on oxidative stress induced toxicity in different organs of rats. *Food Chem Toxicol.* 2008;46(12):3612–3615. doi:10.1016/j.fct.2008.09.006
- Felser A, Blum K, Lindinger PW, Bouitbir J, Krähenbühl S. Mechanisms of hepatocellular toxicity associated with dronedarone: A comparison to amiodarone. *Toxicol Sci.* 2013;131(2):480–490. doi:10.1093/toxsci/kfs298
- Fromenty B, Letteron P, Fisch C, Berson A, Deschamps D, Pessayre D. Evaluation of human blood lymphocytes as a model to study the effects of drugs on human mitochondria. *Biochem Pharmacol.* 1993;46(3):421–432. doi:10.1016/0006-2952(93)90518-2
- Suwara J, Radzikowska-Cieciura E, Chworos A, Pawlowska R. The ATP-dependent pathways and human diseases. *Curr Med Chem.* 2023;30(11):1232–1255. doi:10.2174/0929867329666220322104552
- Saquet AA, Streif J, Bangerth F. Changes in ATP, ADP and pyridine nucleotide levels related to the incidence of physiological disorders in 'Conference' pears and 'Jonagold' apples during controlled atmosphere storage. *J Horticult Sci Biotechnol.* 2000;75(2):243–249. doi:10.1080/14620316.2000.11511231
- Yi C, Jiang Y, Shi J, et al. ATP-regulation of antioxidant properties and phenolics in litchi fruit during browning and pathogen infection process. *Food Chem.* 2010;118(1):42–47. doi:10.1016/j.foodchem.2009.04.074
- Li W, Yuan H, Liu Y, et al. Current analytical strategies for the determination of resveratrol in foods. *Food Chem.* 2024;431:137182. doi:10.1016/j.foodchem.2023.137182
- Acuña-Avila PE, Vázquez-Murrieta MS, Franco Hernández MO, López-Cortéz Del Socorro M. Relationship between the elemental composition of grapeyards and bioactive compounds in the Cabernet Sauvignon grapes *Vitis vinifera* harvested in Mexico. *Food Chem.* 2016;203:79–85. doi:10.1016/j.foodchem.2016.02.031
- Zhou DD, Luo M, Huang SY, et al. Effects and mechanisms of resveratrol on aging and age-related diseases. *Oxid Med Cell Longev.* 2021;2021(1):9932218. doi:10.1155/2021/9932218
- Zhang Y, Li T, Ding X, et al. F-53B disrupts energy metabolism by inhibiting the V-ATPase-AMPK axis in neuronal cells. *J Hazard Mater.* 2025;487:137111. doi:10.1016/j.jhazmat.2025.137111
- Percie Du Sert N, Hurst V, Ahluwalia A, et al. The ARRIVE guidelines 2.0: Updated guidelines for reporting animal research. *PLoS Biol.* 2020;18(7):e3000410. doi:10.1371/journal.pbio.3000410
- Kiani AK, Pheby D, Henahan G, et al; International Bioethics Study Group. Ethical considerations regarding animal experimentation. *J Prev Med Hyg.* 2022;63(2 Suppl 3):E255–E266. doi:10.15167/2421-4248/jpmh2022.63.253.2768
- Góth L. A simple method for determination of serum catalase activity and revision of reference range. *Clin Chim Acta.* 1991;196(2–3):143–151. doi:10.1016/0009-8981(91)90067-M
- Bradford MM. A rapid and sensitive method for the quantitation of microgram quantities of protein utilizing the principle of protein-dye binding. *Anal Biochem.* 1976;72(1–2):248–254. doi:10.1016/0003-2697(76)90527-3
- Tsikis D. Acetazolamide and human carbonic anhydrases: Retrospect, review and discussion of an intimate relationship. *J Enzyme Inhib Med Chem.* 2024;39(1):2291336. doi:10.1080/14756366.2023.2291336
- Mohideen K, Chandrasekar K, Ramsridhar S, Rajkumar C, Ghosh S, Dhungel S. Assessment of oxidative stress by the estimation of lipid peroxidation marker malondialdehyde (MDA) in patients with chronic periodontitis: A systematic review and meta-analysis. *Int J Dent.* 2023;2023:6014706. doi:10.1155/2023/6014706
- Jiang Z, Zhao C, Li X, Yi W, Yan R. Liver failure caused by intravenous amiodarone and effective intervention measures: A case report. *J Clin Pharm Ther.* 2022;47(8):1293–1296. doi:10.1111/jcpt.13647
- Akbay E, Erdem B, Ünlü A, Durukan AB, Onur MA. Effects of N-acetyl cysteine, vitamin E and vitamin C on liver glutathione levels following amiodarone treatment in rats. *Pol J Cardiothorac Surg.* 2019;16(2):88–92. doi:10.5114/kitp.2019.86361
- Mirończuk-Chodakowska I, Witkowska AM, Zujko ME. Endogenous non-enzymatic antioxidants in the human body. *Adv Med Sci.* 2018;63(1):68–78. doi:10.1016/j.advms.2017.05.005
- Vásková J, Kočan L, Vaško L, Perjési P. Glutathione-related enzymes and proteins: A review. *Molecules.* 2023;28(3):1447. doi:10.3390/molecules28031447
- Campos-Shimada LB, Hideo Gilgioni E, Fernandes Garcia R, Rizzato Martins-Maciel E, Luzia Ishii-Iwamoto E, Luzia Salgueiro-Pagadigorria C. Superoxide dismutase: A review and a modified protocol for activities measurements in rat livers. *Arch Physiol Biochem.* 2020;126(4):292–299. doi:10.1080/13813455.2018.1520891
- Rosa AC, Corsi D, Cavi N, Bruni N, Dosio F. Superoxide dismutase administration: A review of proposed human uses. *Molecules.* 2021;26(7):1844. doi:10.3390/molecules26071844
- Dengiz GO, Odabasoglu F, Halici Z, Suleyman H, Cadirci E, Bayir Y. Gastroprotective and antioxidant effects of amiodarone on indomethacin-induced gastric ulcers in rats. *Arch Pharm Res.* 2007;30(11):1426–1434. doi:10.1007/BF02977367

31. Bayrakçeken K, Ucgul RK, Coban T, Yazıcı G, Suleyman H. Effect of adenosine triphosphate on amiodarone-induced optic neuropathy in rats: Biochemical and histopathological evaluation. *Cutan Ocul Toxicol.* 2023;42(3):162–167. doi:10.1080/15569527.2023.2227265
32. Zoppini G, Cacciatori V, Negri C, et al. The aspartate aminotransferase-to-alanine aminotransferase ratio predicts all-cause and cardiovascular mortality in patients with type 2 diabetes. *Medicine (Baltimore).* 2016;95(43):e4821. doi:10.1097/MD.00000000000004821
33. Glinghammar B, Rafter I, Lindström AK, et al. Detection of the mitochondrial and catalytically active alanine aminotransferase in human tissues and plasma. *Int J Mol Med.* 2009;23(5):621–631. doi:10.3892/ijmm_00000173
34. Jiang X, Chang H, Zhou Y. Expression, purification and preliminary crystallographic studies of human glutamate oxaloacetate transaminase 1 (GOT1). *Protein Expr Purif.* 2015;113:102–106. doi:10.1016/j.pep.2015.05.010
35. Nagata T, Takata K, Shakado S, Hirai F. Amiodarone-induced hepatotoxicity. *BMJ Case Rep.* 2023;16(11):e256679. doi:10.1136/bcr-2023-256679
36. Serviddio G, Bellanti F, Giudetti AM, et al. Mitochondrial oxidative stress and respiratory chain dysfunction account for liver toxicity during amiodarone but not dronedarone administration. *Free Radic Biol Med.* 2011;51(12):2234–2242. doi:10.1016/j.freeradbiomed.2011.09.004
37. Koç A, Gazi M, Sayar AC, et al. Molecular mechanism of the protective effect of adenosine triphosphate against paracetamol-induced liver toxicity in rats. *Gen Physiol Biophys.* 2023;42(2):201–208. doi:10.4149/gpb_2022055
38. Neuman MG. Hepatotoxicity: Mechanisms of liver injury. In: Radu-Ionita F, Pyrsopoulos NT, Jinga M, Tintoiu IC, Sun Z, Bontas E, eds. *Liver Diseases.* Cham, Switzerland: Springer International Publishing; 2020:75–84. doi:10.1007/978-3-030-24432-3_7
39. Mihajlovic M, Vinken M. Mitochondria as the target of hepatotoxicity and drug-induced liver injury: Molecular mechanisms and detection methods. *Int J Mol Sci.* 2022;23(6):3315. doi:10.3390/ijms23063315
40. Alshehri FS, Alorfi NM. Protective role of resveratrol against VCM-induced hepatotoxicity in male Wistar rats. *Front Pharmacol.* 2023;14:1130670. doi:10.3389/fphar.2023.1130670
41. Wandrer F, Frangež Ž, Liebig S, et al. Autophagy alleviates amiodarone-induced hepatotoxicity. *Arch Toxicol.* 2020;94(10):3527–3539. doi:10.1007/s00204-020-02837-9
42. Erez N, Hubel E, Avraham R, et al. Hepatic amiodarone lipotoxicity is ameliorated by genetic and pharmacological inhibition of endoplasmic reticulum stress. *Toxicol Sci.* 2017;159(2):402–412. doi:10.1093/toxsci/kfx143
43. Özkaya AK, Dilber E, Gürgen SG, Kutlu Ö, Cansu A, Gedik Y. Effects of chronic amiodarone treatment on rat testis. *Acta Histochem.* 2016;118(3):271–277. doi:10.1016/j.acthis.2016.02.003
44. Yuting G, Daqing M, Dasheng X, Yi L. Amiodarone aggravates liver toxicity in mice by inducing immune dysregulation. *Asian J Ecotoxicol.* 2024;19(1):54–64. doi:10.7524/AJE.1673-5897.20231010001
45. Lu J, Miyakawa K, Roth RA, Ganey PE. Tumor necrosis factor- α potentiates the cytotoxicity of amiodarone in Hepa1c1c7 cells: Roles of caspase activation and oxidative stress. *Toxicol Sci.* 2013;131(1):164–178. doi:10.1093/toxsci/kfs289

Combined CB1 antagonist AM6545 and NOP agonist SCH221510 worsen DSS-induced colitis in mice

Adam Fabisiak^{1,A–E}, Maria R. Wołyniak^{1,2,A–D}, Fabiana Piscitelli^{3,B,C,E}, Roberta Verde^{3,B,E}, Vincenzo Di Marzo^{3,4,A,E}, Marta Zielińska^{5,E,F}, Weronika Machelak^{5,B,E}, Ewa Małecka-Wojcieszko^{1,E,F}

¹ Department of Digestive Tract Diseases, Medical University of Lodz, Poland

² Department of Biostatistics and Translational Medicine, Medical University of Lodz, Poland

³ Endocannabinoid Research Group, Consiglio Nazionale Delle Ricerche, Institute of Biomolecular Chemistry, Pozzuoli, Italy

⁴ Canada Research Excellence Chair on the Microbiome-Endocannabinoidome Axis in Metabolic Health (CERC-MEND), Université Laval, Québec City, Canada

⁵ Department of Biochemistry, Medical University of Lodz, Poland

A – research concept and design; B – collection and/or assembly of data; C – data analysis and interpretation;

D – writing the article; E – critical revision of the article; F – final approval of the article

Advances in Clinical and Experimental Medicine, ISSN 1899–5276 (print), ISSN 2451–2680 (online)

Adv Clin Exp Med. 2025;34(12):2153–2162

Address for correspondence

Adam Fabisiak

E-mail: adam.fabisiak@umed.lodz.pl

Funding sources

This work was supported by the National Science Centre, Poland (grant No. 2020/37/N/NZ5/01478 awarded to Adam Fabisiak) and by the Medical University of Lodz, Poland (grant No. 503/1-002-01/503-11-001-19-00 awarded to Ewa Małecka-Wojcieszko).

Conflict of interest

None declared

Received on July 4, 2024

Reviewed on August 31, 2024

Accepted on March 27, 2025

Published online on July 2, 2025

Cite as

Fabisiak A, Wołyniak MR, Piscitelli F, et al. Co-administration of a cannabinoid receptor 1 antagonist, AM6545 and a nociceptin receptor agonist, SCH221510 increases the severity of DSS-induced colitis in mice. *Adv Clin Exp Med.* 2025;34(12):2153–2162. doi:10.17219/acem/203426

DOI

10.17219/acem/203426

Copyright

Copyright by Author(s)

This is an article distributed under the terms of the Creative Commons Attribution 3.0 Unported (CC BY 3.0) (<https://creativecommons.org/licenses/by/3.0/>)

Abstract

Background. Despite the broad range of treatment options available for intestinal inflammation, the development of novel therapeutics remains essential due to the diminishing effectiveness of current therapies over time. Both the endocannabinoid system (ECS) and nociceptin/orphanin FQ peptide (NOP) receptors have been implicated in the pathogenesis of diseases associated with intestinal inflammation, highlighting their potential as therapeutic targets.

Objectives. We hypothesized that an interaction exists between cannabinoid receptors 1 and 2 (CB1 and CB2) and the NOP receptor, which may hold therapeutic relevance for the treatment of colitis.

Materials and methods. In this study, we used 3 selective ligands: a CB1 antagonist (AM6545), a CB2 antagonist (AM630) and a NOP agonist (SCH221510) in a mouse model of colitis induced by 3% dextran sulfate sodium (DSS). Quantification of several secondary messengers was conducted using western blot analysis. Real-time quantitative polymerase chain reaction (qPCR) was employed to assess CB1 expression levels in colonic tissue, while liquid chromatography–mass spectrometry (LC-MS) was used to evaluate the concentrations of endocannabinoids and related lipid mediators.

Results. We observed a statistically significant increase in the macroscopic score and a nonsignificant increase in the microscopic score in inflamed mice treated with both AM6545 and SCH221510 compared to those treated with SCH221510 alone. Additionally, the combination-treated group exhibited significantly lower levels of extracellular signal-regulated kinases 1/2 (ERK1/2) and significantly higher levels of phosphorylated protein kinase B (p-AKT) and β-arrestin relative to the SCH221510-only group.

Conclusions. Our study offers novel insights into the interaction between the ECS and the NOP receptor, which may inform the development of new therapeutic strategies for inflammatory conditions such as colitis.

Key words: nociceptin, colitis, cannabinoid

Highlights

- The study explores interactions between the endocannabinoid system (ECS) and nociceptin receptors (NOP) in dextran sulfate sodium-induced colitis.
- Co-administration of a CB1 antagonist (AM6545) and a NOP agonist (SCH221510) exacerbates colitis severity in mice.
- The treatment combination alters key signaling pathways, reducing ERK1/2 while increasing β -arrestin and phospho-AKT levels.
- CB1 receptor expression is upregulated in inflamed colonic tissue following NOP agonist treatment.
- Findings suggest a complex interplay between endogenous cannabinoid system and NOP, providing insights for future colitis therapies.

Background

Despite the wide variety of treatment options for intestinal inflammation, novel therapeutics is still under development due to the loss of efficacy and adverse effects of the current therapies. Both the endocannabinoid (eCB) system (ECS) and the nociceptin receptor (NOP) are implicated in the pathogenesis of diseases associated with intestinal inflammation, such as inflammatory bowel disease (IBD). The ECS consists of receptors, endogenous cannabinoid ligands (eCBs) and enzymes that metabolize the ligands. The “classical” endocannabinoid receptors consist of 2 G protein-coupled receptors: cannabinoid receptor 1 (CB1) and cannabinoid receptor 2 (CB2). The ECS is part of a larger network of lipid molecules (the endocannabinoidome (eCBome)), which partly share receptors and, particularly, biosynthetic and catabolic pathways with eCBs.¹ Cannabinoid receptor 1 (CB1) is primarily expressed in the central nervous system, whereas cannabinoid receptor 2 (CB2) is predominantly located in peripheral tissues, including immune cells and the mucosa of the gastrointestinal (GI) tract. Within the GI tract, CB1 is mainly localized in the enteric plexus,² while CB2 expression is largely restricted to the lamina propria.³

Modulation of cannabinoid receptors has proven highly effective in alleviating intestinal inflammation in animal models.^{4,5} In a study by Massa et al.⁶ using a 2,4-dinitrobenzene sulfonic acid (DNBS)-induced colitis model in mice, treatment with the CB1 agonist HU210 provided significant protection against colitis, while administration of the CB1 antagonist SR141716A worsened inflammation. Additionally, Singh et al.⁷ demonstrated that the CB2 agonist JWH-133 markedly reduced inflammation in both a dextran sodium sulfate (DSS)-induced colitis model and in interleukin (IL)-10-deficient mice, compared to controls.

The ECS has been shown to engage in crosstalk with other signaling systems, including the endogenous opioid system (endorphins). The opioid receptor family consists of 4 major subtypes: delta (DOP), kappa (KOP), mu (MOP), and nociceptin/orphanin FQ peptide receptor (NOP). The interaction between the ECS and opioid

receptors occurs at multiple levels, including direct receptor–receptor interactions and shared signal transduction pathways, as extensively reviewed by Scavone et al.⁸ Notably, most studies have focused on the interaction between the endocannabinoid system and the classical opioid receptors, i.e., DOP, KOP and MOP. Despite its structural similarity to other opioid peptides,⁹ nociceptin exclusively binds to NOP and does not interact with DOP, KOP or MOP receptors. Accordingly, no classical opioid ligand – such as dynorphin, β -endorphin or enkephalins – has been found to bind to the NOP receptor,¹⁰ which is now frequently excluded from the classical opioid receptor group. NOP has been extensively studied in the context of inflammatory conditions, including intestinal inflammation.¹¹ Moreover, a functional connection between the ECS and NOP has been demonstrated in several studies. For example, Rawls et al.¹² showed that activation of the NOP receptor is essential for cannabinoid agonists to induce hypothermia in rats. Similarly, Cannarsa et al.¹³ reported that Δ^9 -tetrahydrocannabinol (THC) reduced NOP expression in the SH-SY5Y neuroblastoma cell line, an effect that was blocked by the selective CB1 antagonist AM251.

Objectives

Given the functional similarities between the eCB and NOP systems, as well as their reported anti-inflammatory properties, we hypothesized that interactions between CB1, CB2 and NOP receptors may offer therapeutic potential for the treatment of IBD. Therefore, we investigated the possible reciprocal actions between ECS and NOP in an animal model of colitis. We utilized AM6545, a peripherally restricted neutral antagonist for the CB1 receptor, chosen for its demonstrated efficacy in other inflammation-related models.^{14,15} AM630 was selected as the CB2 receptor ligand, based on its demonstrated effectiveness in various studies, including its ability to reverse the anti-inflammatory effects of the CB2 agonist JWH-133 in chronic colitis observed in IL-10^{-/-} mice.⁷

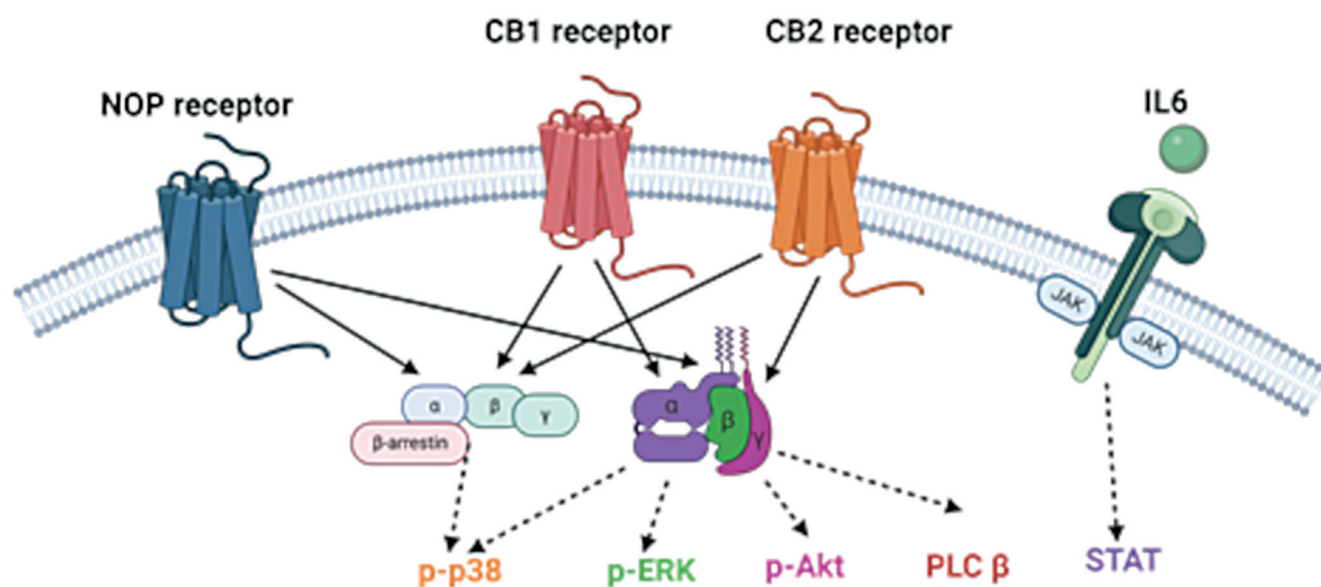


Fig. 1. Potential overlap in signaling pathways activated by cannabinoid 1 (CB1), cannabinoid 2 (CB2) and nociceptin (NOP) receptors. Illustration created with BioRender.com

p-p38 – phosphorylated-p38 mitogen-activated proteins kinases; p-ERK – phosphorylated extracellular signal-related kinase; p-AKT – phosphorylated protein kinase B; PLC β – phospholipase C β; STAT – signal transducer and activator of transcription; JAK – Janus-activated kinase.

SCH221510 was selected as a selective NOP receptor ligand based on the findings of Sobczak et al.¹⁶, who demonstrated that systemic administration of this compound significantly reduced inflammation in mice with 2,4,6-trinitrobenzene sulfonic acid (TNBS)-induced colitis – an effect that was reversed by the selective NOP antagonist J-113397. Figure 1 shows the biological roles of CB1, CB2 and NOP in inflammatory pathways.

Materials and methods

Animals

Male BALB/c mice were sourced from the vivarium at the University of Lodz, Poland. The mice weighed approx. 22 g and were 6–8 weeks old. They were housed in plastic cages lined with sawdust, maintained at a constant temperature of 22°C, under a 12-h light/dark cycle (lights on at 5:00 AM). The mice had free access to chow pellets (Agropol S.J., Motycz, Poland) and tap water. All animal procedures were approved by the Animal Care Committee of the Medical University of Lodz (protocol No. 2/LB191/2021) and conducted in accordance with the European Communities Council Directive of 22 September 2010 (2010/63/EU). Measures were taken to minimize animal suffering and reduce the number of animals used. Each in vivo experiment involved groups of 4–10 mice. The colitis induction and procedures were performed in Animal Research Facility at the Medical University of Lodz. All sections of this project adhered to the Animal Research: Reporting of In Vivo Experiments (ARRIVE) guidelines for animal research.¹⁷

Induction of colitis and evaluation of macro- and microscopic score

Experimental colitis was induced by administering 3% DSS in the drinking water for 5 days, as previously described.¹⁸ On day 5, DSS was replaced with tap water. Treatments were administered from day 3 to day 6. SCH221510 (Tocris Bioscience, Bristol, UK) was selected as a selective NOP receptor agonist. AM6545 and AM630 (both from Tocris Bioscience) were used as selective antagonists for CB1 and CB2, respectively. The control group received vehicle administration, while the following ligand doses were used: SCH221510 at 3 mg/kg, AM6545 at 3 mg/kg and AM630 at 5 mg/kg.^{16,19,20} All compounds were administered intraperitoneally (i.p.) twice daily for 4 consecutive days.

On day 7, animals were sacrificed by cervical dislocation, and macroscopic assessments were performed, including evaluation of colon length, degree of inflammation, and the presence of erythema, ulceration, necrosis, as well as the depth and surface area of lesions. Colonic samples for histological evaluation and further tests were collected and respective analyses were performed. Sections of the distal colon were flattened with the mucosal side up, stapled onto cardboard strips and fixed in 10% neutral-buffered formalin for at least 24 h at 4°C. After fixation, the tissues were dehydrated, embedded in paraffin, cut into 5-μm sections, mounted onto slides, and stained with hematoxylin and eosin (H&E). The slides were reviewed in a blinded manner using a Zeiss Axio Imager 2 microscope (Carl Zeiss AG, Jena, Germany). Images were captured with a digital camera connected to an image analysis software system. The microscopic total damage score was assessed using an established scoring system,²¹ evaluating

parameters such as muscle thickening, cellular infiltration, destruction of mucosal architecture, goblet cell depletion, and the presence of crypt abscesses.

Western blot analyses

Colonic tissue was homogenized using the Precellys Evolution tissue homogenizer (Bertin Instruments, Montigny-le-Bretonneux, France) in 10 volumes of lysis buffer containing 150 mM sodium chloride (NaCl), 0.1% sodium dodecyl sulfate (SDS), 2 mM Tris-EDTA (ethylenediaminetetraacetic acid), 1% Igepal, 2.5% deoxycholic acid, and 10 μ L of 1 \times Protease Inhibitor Cocktail (Sigma-Aldrich, Poznań, Poland). The homogenate was centrifuged at 12,000 rpm for 15 min at 4°C. Protein concentration in supernatants was then quantified using Pierce 660 nm Protein Assay Reagent (Thermo Fisher Scientific, Waltham, USA). Separation of proteins (20 mg/well) was performed on 7.5% SDS-polyacrylamide gel electrophoresis (PAGE) (20–40 mA/gel) in electrophoretic buffer (0.1% SDS, 192 mM glycine, 25 mM Tris, pH 8.3). Proteins separated by electrophoresis were transferred to Invitrolon membranes using a semi-dry electroblotting system (pore size, 0.45 mm; Thermo Fisher Scientific) in transfer buffer containing 20% (v/v) methanol, 192 mM glycine and 25 mM Tris, with a pH 8.3. The membranes were incubated for 1 h at room temperature in 5% non-fat dry milk Tris-buffered saline with Tween 20 (TBST; 150 mM NaCl, 0.05% Tween 20, 100 mM Tris-HCl, pH 7.4) to saturate non-specific protein binding sites. Membranes were then incubated with primary antibodies specific to the following proteins: anti-extracellular signal-regulated kinases 1/2 (ERK1/2) (ab86299; Abcam, Cambridge, UK), anti-signal transducer and activator of transcription 3 (STAT3) (sc-8019; Santa Cruz, Dallas, USA) and anti- β -arrestin-1 (ab31868; Abcam), at 4–8°C. An anti- β -actin antibody (sc-47778; Santa Cruz) was used as a loading control. Appropriate peroxidase-conjugated secondary antibody was applied for 1 h at room temperature and then the bands were visualized using a Super-Signal™ West Femto Maximum Sensitivity Substrate (Thermo Fisher Scientific) as a substrate for the localization of horseradish peroxidase (HRP) activity. Qualitative and quantitative analysis was performed by measuring integrated optical density (IOD) using GelProAnalyze v. 3.0 for Windows™ program (Media Cybernetics, Rockville, USA).

RNA isolation, reverse transcription and real-time polymerase chain reaction

RNA was extracted according to the manufacturer's protocol using the Total RNA Mini Plus Kit (A&A Biotechnology, Gdynia, Poland). Briefly, tissue samples were homogenized in 400 μ L of lysis buffer containing FenoZol Plus reagent. The homogenates were subsequently centrifuged, and the supernatants were collected and washed.

The purified RNA was subsequently eluted into collection tubes using 50 μ L of diethyl pyrocarbonate (DEPC)-treated water. The quantity and purity of the isolated RNA were measured using a spectrophotometer (BioPhotometer; Eppendorf, Hamburg, Germany). For complementary deoxyribonucleic acid (cDNA) synthesis, 1 μ g of total RNA was reverse transcribed using the Maxima cDNA kit (Thermo Fisher Scientific) with the following incubation conditions: 10 min at 25°C, 120 min at 37°C and 5 min at 85°C. Quantitative analysis was performed using TaqMan fluorescent probes on a Mastercycler® ep realplex⁴ S system (Eppendorf) to assess the expression of mouse CBI (*cnr1*), with hypoxanthine phosphoribosyltransferase 1 (*hprt1*) used as the endogenous control. All experiments were conducted in triplicate. The threshold cycle (*Ct*) values of the target genes were normalized to the *Ct* values of the housekeeping gene *hprt1*. The relative messenger ribonucleic acid (mRNA) levels were calculated using the formula $2^{(-\Delta Ct)} \times 1000$.

Quantitative analysis of eCBs and eCB-like mediators

The extraction, purification and quantification of eCBs from tissues were conducted following previously established procedure.²² In summary, tissues were homogenized and subjected to extraction with a mixture of chloroform, methanol and Tris-HCl (50 mmol/L, pH 7.5) in a 2:1:1 (vol/vol) ratio. The extraction solvent contained 15 internal standards: d8-arachidonylethanolamide (d8-AEA) at 5 pmol, d5-2-arachidonoylglycerol (d5-2-AG), d4-palmitoylethanolamide (PEA) and d2-oleoylethanolamide (OEA) at 50 pmol each, and d4-docosahexaenoyl ethanolamide (DHA-EA) and d4-eicosapentaenoic ethanolamide (EPA-EA) at 10 pmol each (all standards were obtained from Cayman Chemical, Ann Arbor, USA). The lipid-containing organic phase obtained after extraction was dried down, weighed and subjected to pre-purification through open-bed chromatography on silica gel. Fractions were collected by eluting the column with chloroform/methanol mixtures in ratios of 99:1, 90:10 and 50:50 (v/v). The 90:10 fraction was utilized for the quantification of 2-AG, AEA, DHA-EA, EPA-EA, OEA, and PEA using liquid chromatography–atmospheric pressure chemical ionization–mass spectrometry (LC/APCI-ITMS). This involved using a Shimadzu high-performance liquid chromatography apparatus (LC10ADVP) coupled to a Shimadzu (LCMS-2020) quadrupole mass spectrometry through a Shimadzu atmospheric pressure chemical ionization interface (Shimadzu, Tokyo, Japan). Mass spectrometry detection was performed with the following *m/z* values: 356 and 348 (molecular ions + 1 for d8-AEA and AEA), 304 and 300 (molecular ions + 1 for d4-PEA and PEA), 330 and 326 (molecular ions + 1 for d4-OEA and OEA), 376 and 372 (molecular ions + 1 for d4-DHA-EA and DHA-EA), 384 and 379 (molecular ions + 1 for d5-2-AG and 2-AG), and 346 and 350 (molecular ions + 1 for d4-EPA-EA and EPA-EA).

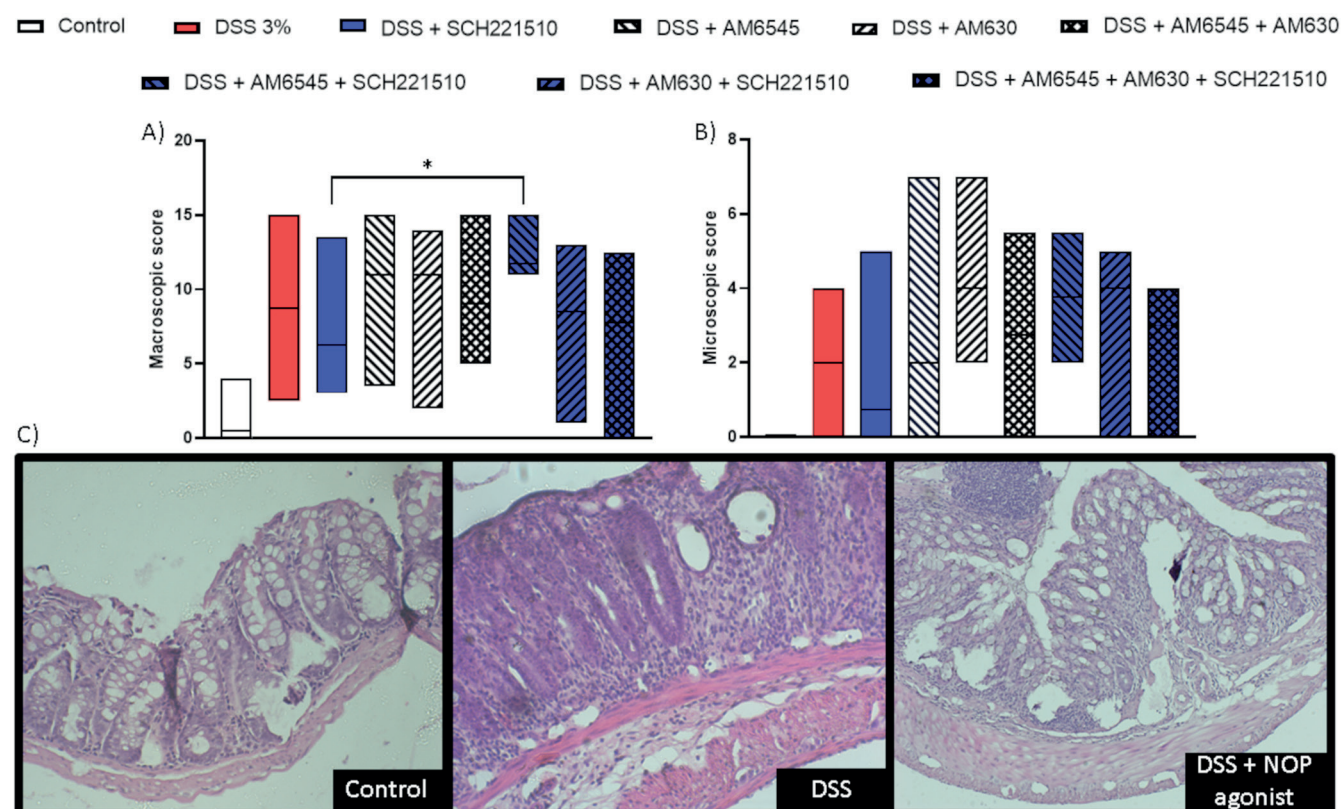


Fig. 2. Effect of the NOP agonist SCH221510 (3 mg/kg), CB1 antagonist AM6545 (3 mg/kg) and CB2 antagonist AM630 (5 mg/kg), each administered intraperitoneally (i.p.; 100 μ L/animal, twice daily on days 3–6 following colitis induction), on (A) macroscopic and (B) microscopic scores in a semi-chronic DSS-induced colitis model, given alone or in combination. Statistical analysis was performed using the Kruskal–Wallis test followed by Dunn's post hoc test. Data are presented as medians with ranges ($n = 5$ –10 mice per group; $p < 0.05$ compared to the DSS + SCH221510 group; C. Representative microphotographs of hematoxylin and eosin (H&E)-stained colon sections

DSS – dextran sulfate sodium; NOP – nociceptin receptor; CB1 – cannabinoid receptor 1; CB2 – cannabinoid receptor 2.

Liquid chromatography analysis was conducted in the isocratic mode using a Discovery C18 column (Supelco, Sigma-Aldrich, Prague, Czech Republic) (15 cm \times 4.6 mm, 5 μ m) with methanol/water/acetic acid (85:15:1 by vol) as the mobile phase at a flow rate of 1 mL/min. The levels of eCBs and eCB-like compounds in tissues were quantified using isotope dilution with the deuterated standards mentioned earlier, and results were expressed as pmol per mg of tissue weight.

Statistical analyses

Statistical analysis was conducted using GraphPad Prism v. 8.0 software (GraphPad Software Inc., La Jolla, USA). Due to the small sample size per group, which limited the ability to reliably assess normality, the Kruskal–Wallis test was employed for multiple group comparisons. Results are presented as the χ^2 test statistic (H), including degrees of freedom (df) and p -value, with post hoc analysis performed using Dunn's test. Data are presented as median values with corresponding minimum and maximum ranges. Outliers were identified and excluded using the Robust Regression and Outlier Removal (ROUT) method. A p -value < 0.05 was considered statistically significant.

Results

First, we performed a mouse semi-chronic model of colitis induced using DSS with selective ligands of CB1, CB2 and NOP receptors (AM6545, AM630 and SCH221510, respectively) given alone or in combination. A statistically significant increase in the macroscopic score was observed in inflamed mice treated with SCH221510 + AM6545, but not with SCH221510 + AM630, when compared to mice treated with SCH221510 alone ($H(8) = 35.52$, $p < 0.001$; Dunn's test: 11.75 (11.00–15.00) vs 6.25 (3.00–13.50), $p = 0.032$; Fig. 2A, Table 1).

Concurrently, only a nonsignificant increase in the microscopic score was found in mice treated with SCH221510 + AM6545 compared to mice treated only with SCH221510 ($H(8) = 16.33$, $p = 0.03$; Dunn's test: 3.75 (2.00–5.50) vs 0.75 (0.00–5.00), $p > 0.083$; no significance between groups was achieved as assessed with Dunn's test; Fig. 2B,C, Table 1). Thus, for further experiments, we chose AM6545.

Next, we investigated the protein levels of a few secondary messengers in mice treated with SCH221510, AM6545 (alone or with combination) or vehicle (Fig. 3A–D, Table 1). We found a reduction in the levels of ERK 1/2 in mice treated with SCH221510 + AM6545 compared

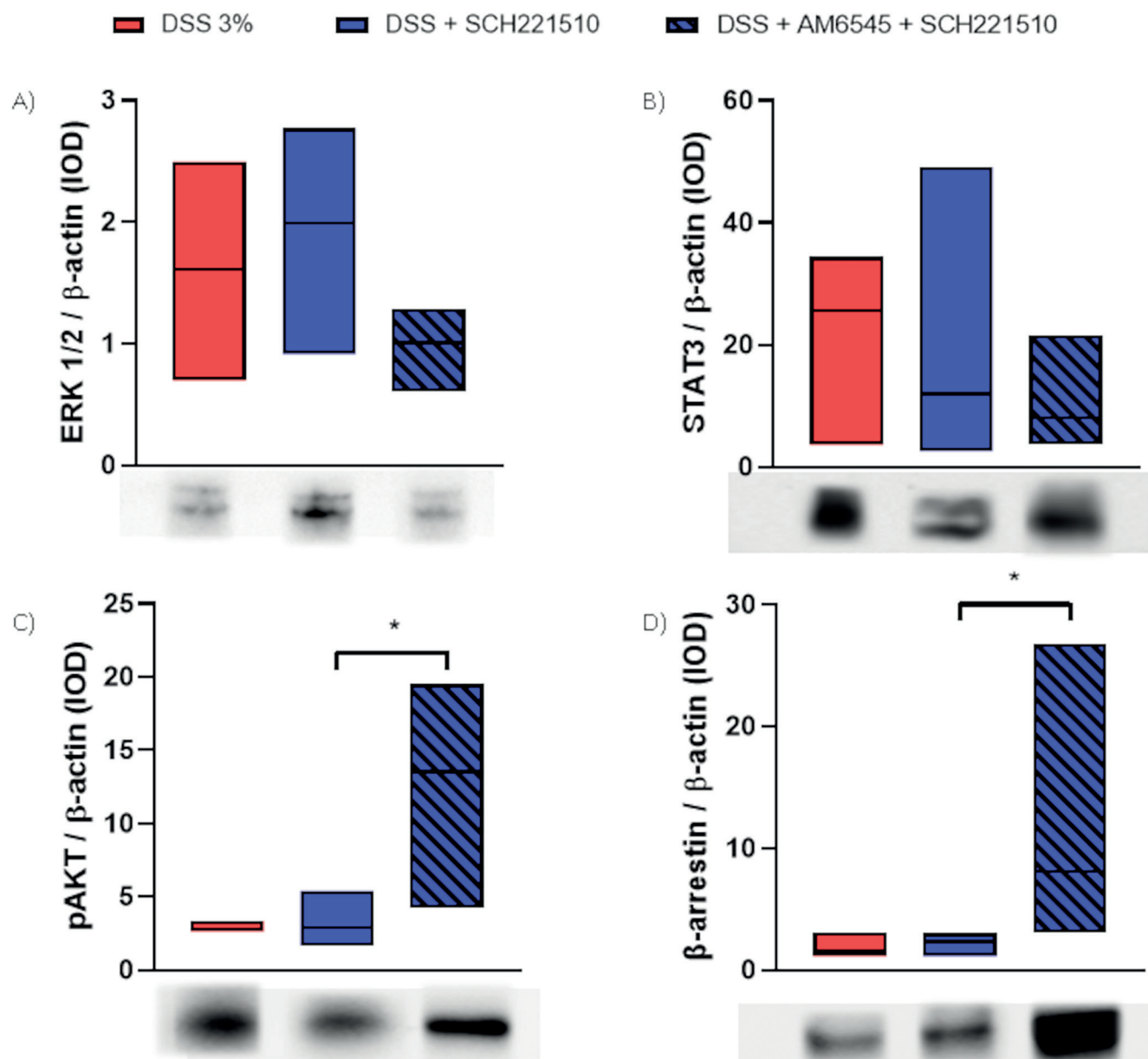


Fig. 3. Effect of the NOP agonist SCH221510 and the CB1 antagonist AM6545 (3 mg/kg, 100 μ L/animal, intraperitoneally (i.p.)), administered twice daily on days 3–6 following DSS-induced colitis on the relative expression of (A) ERK1/2, (B) STAT3, (C) phosphorylated AKT (p-AKT), and (D) β -arrestin in colonic tissue samples. Statistical analysis was performed using the Kruskal–Wallis test followed by Dunn's post hoc test. Data are presented as medians with ranges from 6 randomly selected mice per group. Representative western blot images are shown below the corresponding bars; $p < 0.05$ compared to the DSS + SCH221510 group

DSS – dextran sulfate sodium; NOP – nociceptin receptor; CB1 – cannabinoid receptor 1; ERK1/2 – extracellular signal-regulated kinases 1/2; STAT3 – signal transducer and activator of transcription 3; AKT – protein kinase B.

to mice treated with SCH221510 solely ($H(2) = 2.99$, $p = 0.23$; Dunn's test: 1.01 (0.61–1.28) vs 1.99 (0.91–2.77), $p > 0.252$). A similar trend was noticed when we assessed STAT3 ($H(2) = 1.52$, $p = 0.50$; Dunn's test: 8.04 (3.70–21.61) vs 11.97 (2.65–49.12), $p > 0.999$) in mice treated with SCH221510 + AM6545 or SCH221510 only, respectively. Conversely, we observed a significant increase in the levels of β -arrestin in mice treated with SCH221510 + AM6545 compared to mice treated with SCH221510 only ($H(2) = 7.47$, $p = 0.01$; Dunn's test: 8.07 (3.00–26.77) vs 2.35 (1.14–3.01), $p = 0.047$), as well as in the levels

of phospho-AKT (pAKT) ($H(2) = 8.23$, $p = 0.006$; Dunn's test: 13.52 (4.19–19.52) vs 2.91 (1.67–5.40), $p = 0.031$).

Next, we proceeded to examine the relative expression of CB1 receptor in the studied groups. We found that SCH221510 increased the relative expression of CB1 in inflamed mouse colon compared to mice treated with vehicle ($H(2) = 1.74$, $p = 0.42$; Dunn's test: 10736 (448–50738) vs 2888 (807–8282), $p > 0.999$), although in statistically non-significant manner (Fig. 4, Table 1)

Lastly, we investigated the levels of eCBs and eCBome mediators in mice administered with DSS and treated with

Table 1. Dunn's test results

Compared groups	Mean rank difference	Adjusted p-value
Macroscopic scoring		
DSS 3% vs DSS 3% + SCH221510	8.350	>0.999
DSS 3% vs DSS 3% + AM6545	−10.45	>0.999
DSS 3% vs DSS 3% + AM630	−6.500	>0.999
DSS 3% vs DSS 3% + AM6545 + AM60	−5.406	>0.999
DSS + SCH221510 vs DSS 3% + AM6545 + SCH221510	−33.51	0.032
DSS + SCH221510 vs DSS 3% + AM630 + SCH221510	−3.311	>0.999
DSS + SCH221510 vs DSS 3% + AM6545 + AM630 + SCH221510	2.400	>0.999
Microscopic scoring		
DSS 3% vs DSS 3% + SCH221510	8.903	>0.999
DSS 3% vs DSS 3% + AM6545	7.000	>0.999
DSS 3% vs DSS 3% + AM630	−24.02	0.130
DSS 3% vs DSS 3% + AM6545 + AM60	−6.172	>0.999
DSS + SCH221510 vs DSS 3% + AM6545 + SCH221510	−26.53	0.083
DSS + SCH221510 vs DSS 3% + AM630 + SCH221510	−14.57	>0.999
DSS + SCH221510 vs DSS 3% + AM6545 + AM630 + SCH221510	−12.53	>0.999
ERK 1/2 WB		
DSS 3% vs DSS 3% + SCH221510	−2.000	>0.999
DSS 3% vs DSS 3% + AM6545 + SCH221510	2.850	0.929
DSS 3% + SCH221510 vs DSS 3% + AM6545 + SCH221510	4.850	0.252
STAT3 WB		
DSS 3% vs DSS 3% + SCH221510	2.800	0.967
DSS 3% vs DSS 3% + AM6545 + SCH221510	3.200	0.774
DSS 3% + SCH221510 vs DSS 3% + AM6545 + SCH221510	0.400	>0.999
β-arrestin WB		
DSS 3% vs DSS 3% + SCH221510	0.0500	>0.999
DSS 3% vs DSS 3% + AM6545 + SCH221510	−6.350	0.071
DSS 3% + SCH221510 vs DSS 3% + AM6545 + SCH221510	−6.400	0.047
pAKT WB		
DSS 3% vs DSS 3% + SCH221510	0.250	>0.999
DSS 3% vs DSS 3% + AM6545 + SCH221510	−6.550	0.059
DSS 3% + SCH221510 vs DSS 3% + AM6545 + SCH221510	−6.800	0.031
CB1 RT-PCR		
DSS 3% vs DSS 3% + SCH221510	−8.518	0.719
DSS 3% vs DSS 3% + AM6545 + SCH221510	−1.893	>0.999
DSS 3% + SCH221510 vs DSS 3% + AM6545 + SCH221510	6.625	>0.999

DSS – dextran sulfate sodium; CB1 – cannabinoid receptor 1; ERK1/2 – extracellular signal-regulated kinases 1/2; STAT3 – signal transducer and activator of transcription 3; AKT – protein kinase B; pAKT – phosphorylated AKT; WB – western blot; RT-PCR – real-time polymerase chain reaction.

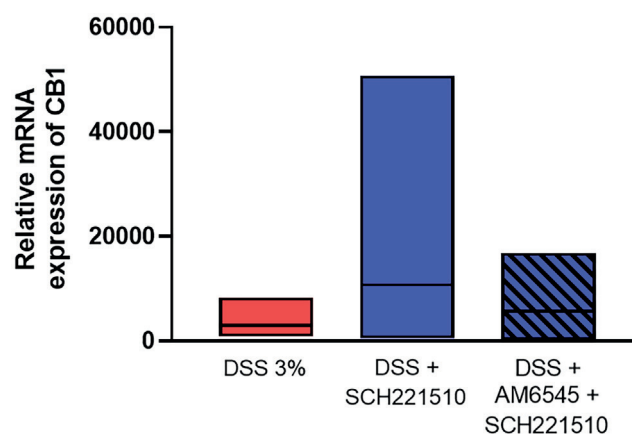


Fig. 4. Effect of the NOP agonist SCH221510 and the CB1 antagonist AM6545 (3 mg/kg, 100 µL/animal, intraperitoneally (i.p.)), administered twice daily on days 3–6 following DSS-induced colitis) on the relative expression of CB1 in a semi-chronic mouse model of colitis. Statistical analysis was performed using the Kruskal–Wallis test followed by Dunn's post hoc test. Data are presented as medians with ranges; n = 7–9 mice per group

NOP – nociceptin receptor; CB1 – cannabinoid receptor 1; DSS – dextran sulfate sodium; mRNA – messenger RNA.

SCH221510 and SCH221510 + AM6545. We found no statistically significant difference comparing mice treated with SCH221510, alone or in combination with AM6545 (Fig. 5, Supplementary Table 1).

Discussion

This is the first study to address the *in vivo* crosstalk between the components of the eCB and NOP systems. We showed that selective blockade of the CB1 receptor in combination with SCH221510, a selective NOP ligand, unlike the latter agonist alone, exacerbates inflammation in a semi-chronic model of colitis induced with DSS assessed macro- and microscopically. The interaction probably occurs at the cellular level as the extent of activation of 2 assessed secondary messengers (ERK1/2 and β-arrestin) was found to be different between the mice treated with NOP agonist + CB1 antagonist and the NOP agonist only. ERK-dependent signaling was shown to be a major signaling pathway regulating nociceptin and its receptor in human peripheral leukocytes, as selective blockade of ERK prevented the phor-bol-12-myristate-13-acetate induced downregulation of NOP mRNA.²³ ERK1/2 is also one of the major players in CB1-related signaling pathways as acute stimulation with THC increases ERK1/2 activation in the dorsal striatum²⁴ and hippocampus.²⁵ β-arrestin is also a crucial messenger in NOP²⁶ and CB1²⁷ signaling. In our study, we observed a decrease in ERK1/2 levels and a significant increase in β-arrestin levels after the administration of AM6545. Both effects may result from AM6545 counteracting the endocannabinoid-mediated activity of CB1, potentially contributing to the exacerbation

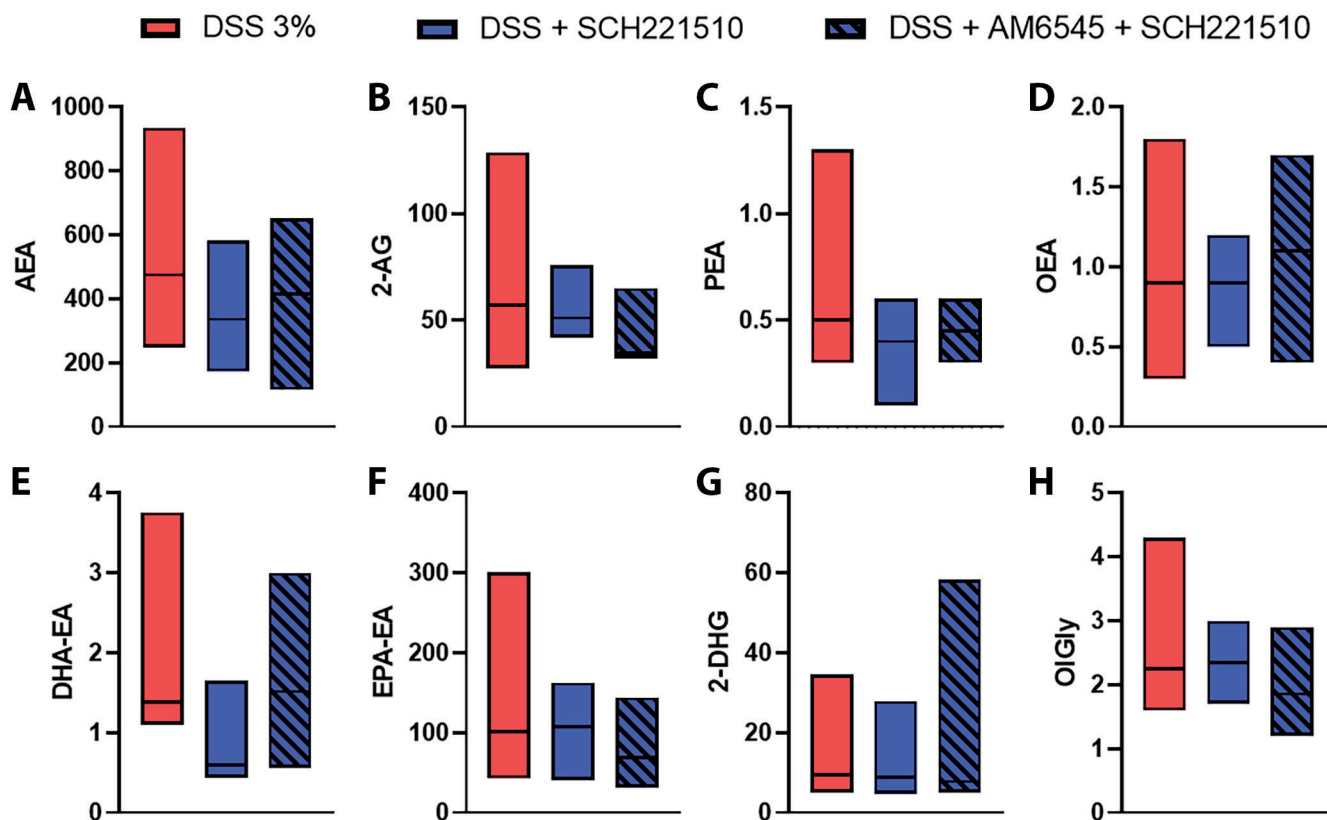


Fig. 5. Effect of the nociceptin receptor (NOP) agonist SCH221510 and cannabinoid receptor 1 (CB1) antagonist AM6545 (3 mg/kg, 100 μ L/animal, intraperitoneally (i.p.)), administered twice daily on days 3–6 following colitis induction) in a semi-chronic dextran sulfate sodium (DSS)-induced colitis model on the levels of endocannabinoids and endocannabinoid-like mediators: anandamide (AEA) (A), 2-arachidonoylglycerol (2-AG) (B), oleylethanolamide (OEA) (C), palmitoylethanolamide (PEA) (D), docosahexaenoyl ethanolamide (DHA-EA) (E), eicosapentaenoyl ethanolamide (EPA-EA) (F), 2-docosahexaenoyl glycerol (2-DHG) (G), and oleoyl glycine (OIGly) (H) in colonic tissue. Results are expressed as pmol/mg of tissue weight. Statistical analysis was performed using the Kruskal–Wallis test followed by Dunn's post hoc test. Data are presented as medians with ranges; $n = 5$ mice per group

of inflammation observed with the antagonist. This antagonistic action may also interfere with the protective effects of SCH221510 in inflamed mice. Additionally, co-administration of SCH221510 and the CB1 antagonist was associated with increased Akt phosphorylation, further supporting this interaction.

Although we did not observe a statistically significant difference, the increase in relative mRNA expression of CB1 in inflamed mice treated with the NOP receptor agonist was evident. The levels of CB1 expression in inflamed mice receiving vehicles were similar to those treated with a combination of NOP agonist and CB1 antagonist. The results are contrary to the effects reported in the literature, which consistently show an increase in CB1/2 expression in active disease and downregulation of these receptors in quiescent disease.^{28,29} In 1 study, a dose-dependent downregulation of NOP expression was found after treatment with THC, and the effect was abolished by the co-administration of AM251, a potent CB1 antagonist.¹³ Taken together, a dependency between the assessed receptors on CB1 mRNA levels is evident but further *in vitro* studies are warranted to fully elucidate this phenomenon, which: 1) in view of the anti-inflammatory effects of CB1 receptors mentioned above, might contribute to the exacerbation

of inflammation-counteraction of SCH221510 protective effect, observed with the CB1 antagonist, and 2) would be in agreement with the reduction of ERK1/2 activity and increase of β -arrestin levels observed here.

Conflicting results regarding the expression levels of CB1/CB2 and eCBs in patients with IBD are evident in the literature. For instance, Di Sabatino et al.³⁰ reported increased CB1 expression and stable levels of 2-AG and PEA in inflamed and uninfamed tissue of patients with ulcerative colitis and Crohn's disease, while the level of AEA was decreased in inflamed tissue. Conversely, Grill et al.³¹ found that CB1 transcripts in IBD are downregulated compared to healthy controls. D'Argenio et al.⁴ presented results indicating an increase in AEA levels in the inflamed rectum or the most inflamed area in patients with UC. We concluded our project by thoroughly evaluating the level of eCBs and eCB-like mediators using high-performance liquid chromatography. Our aim was to assess whether the results observed in the previous experiments are influenced by the level of eCBs. No statistically significant differences were observed, suggesting that the anti-inflammatory effects of NOP receptor activation, either alone or in combination with CB1 blockade, are not mediated by changes in the colonic levels of these inflammatory markers.

Limitations

We acknowledge the limitations of our study, with the primary drawback being the difficulty in specifically elucidating the interaction between the ECS and the NOP receptor. The complexity of the ECS, encompassing both classical and non-classical cannabinoid receptors, a diverse range of ligands, and multiple enzymes involved in their synthesis and degradation, posed a significant challenge in the absence of prior detailed research in this area. Thus, the primary goal of the study was to assess the level at which the interaction between cannabinoid receptors and NOP occurs. By conducting experiments fully in vivo, we succeeded in demonstrating significant differences in secondary messengers in the chosen model. One possible explanation for our observation is that CB1 and NOP form heterodimers under certain conditions, exhibiting distinct biological effects. Importantly, it has been demonstrated that opioid receptors, NOP and CB1, can heterodimerize with other receptors. For instance, Evans et al.³² showed that prolonged NOP activation in cells expressing either opioid receptors or NOP results in the internalization of opioid receptors, while activation of opioid receptors leads to the internalization of NOP receptors. Interaction of μ -opioid receptor/NOP heterodimers with N-type calcium channels and their internalization. This phenomenon occurred exclusively in the presence of NOP. On the other hand, in the case of CB1/ μ -opioid heterodimer, activation of either receptor alone within the heterodimer elicited effective Gi signaling. Conversely, the co-activation of both receptors led to the inhibition of their Gi-mediated responses.³³ Advanced methods such as immunofluorescence, crytallography, molecular docking, and molecular dynamics simulations^{34,35} are the next steps to reveal the structural features responsible for this reciprocal activity between CB1 and NOP, and the possibility for heterodimerization of both receptors.

Conclusions

Our study offers new insights into the interaction between the ECS and NOP system in the context of intestinal inflammation. We hope that the present results will help pave the way to further specific research in this field and to reconsider the ECS as a possible therapeutic target for intestinal inflammation. Indeed, targeting this system in IBD was originally regarded as a promising approach in preclinical studies, but it ultimately failed as results in patients with IBD were unsatisfactory.³⁶ This was due, at least in part, to central nervous system adverse effects observed following treatment with CB1 receptor agonists, which consequently have a narrow therapeutic window in this and other disorders. A deeper understanding of the pathophysiology of the ECS in IBD may lead

to the development of more effective therapeutics. For example, the use of endocannabinoid degradation inhibitors or peripherally restricted CB1 agonists, either indirectly enhancing CB1 receptor activation or selectively targeting peripheral CB1 receptors, offers the potential to avoid the central nervous system side effects associated with brain-penetrant CB1 agonists.

Supplementary data

The supplementary materials are available at <https://doi.org/10.5281/zenodo.14176773>. The package includes the following files:

Supplementary Table 1. Results of Dunn's post hoc test for multiple comparisons, performed following the Kruskal–Wallis test, to analyze group differences in endocannabinoid level analyses.

Data availability

The datasets generated and/or analyzed during the current study are available from the corresponding author on reasonable request.



Consent for publication

Not applicable.

Use of AI and AI-assisted technologies

Not applicable.

ORCID iDs

Adam Fabisiak  <https://orcid.org/0000-0002-6997-4925>
 Maria R. Wołyniak  <https://orcid.org/0009-0003-0459-0642>
 Fabiana Piscitelli  <https://orcid.org/0000-0001-9343-4622>
 Roberta Verde  <https://orcid.org/0000-0002-8103-6616>
 Vincenzo Di Marzo  <https://orcid.org/0000-0002-1490-3070>
 Marta Zielińska  <https://orcid.org/0000-0001-5939-791X>
 Weronika Machelak  <https://orcid.org/0000-0001-5251-0713>
 Ewa Małecka-Wojcieszko  <https://orcid.org/0000-0002-1825-1807>

References

1. Iannotti AF, Piscitelli F. Endocannabinoidome. In: *Encyclopedia of Life Sciences*. Hoboken, USA: Wiley; 2018:1–10. doi:10.1002/9780470015902.a0028301
2. Wright K, Rooney N, Feeney M, et al. Differential expression of cannabinoid receptors in the human colon: Cannabinoids promote epithelial wound healing. *Gastroenterology*. 2005;129(2):437–453. doi:10.1016/j.gastro.2005.05.026
3. Wright KL, Duncan M, Sharkey KA. Cannabinoid CB₂ receptors in the gastrointestinal tract: A regulatory system in states of inflammation. *Br J Pharmacol*. 2008;153(2):263–270. doi:10.1038/sj.bjp.0707486
4. D'Argenio G, Valenti M, Scaglione G, Cosenza V, Sorrentini I, Di Marzo V. Up-regulation of anandamide levels as an endogenous mechanism and a pharmacological strategy to limit colon inflammation. *FASEB J*. 2006;20(3):568–570. doi:10.1096/fj.05-4943fje
5. Sałaga M, Mokrowiecka A, Zakrzewski PK, et al. Experimental colitis in mice is attenuated by changes in the levels of endocannabinoid metabolites induced by selective inhibition of fatty acid amide hydrolase (FAAH). *J Crohns Colitis*. 2014;8(9):998–1009. doi:10.1016/j.crohns.2014.01.025

6. Massa F, Marsicano G, Hermann H, et al. The endogenous cannabinoid system protects against colonic inflammation. *J Clin Invest*. 2004;113(8):1202–1209. doi:10.1172/JCI200419465
7. Singh UP, Singh NP, Singh B, Price RL, Nagarkatti M, Nagarkatti PS. Cannabinoid receptor-2 (CB2) agonist ameliorates colitis in IL-10^{-/-} mice by attenuating the activation of T cells and promoting their apoptosis. *Toxicol Appl Pharmacol*. 2012;258(2):256–267. doi:10.1016/j.taap.2011.11.005
8. Scavone JL, Sterling RC, Van Bockstaele EJ. Cannabinoid and opioid interactions: Implications for opiate dependence and withdrawal. *Neuroscience*. 2013;248:637–654. doi:10.1016/j.neuroscience.2013.04.034
9. Lapalu S, Moisan C, Mazarguil H, Cambois G, Mollereau C, Meunier JC. Comparison of the structure-activity relationships of nociceptin and dynorphin A using chimeric peptides. *FEBS Lett*. 1997;417(3):333–336. doi:10.1016/S0014-5793(97)01318-5
10. Reinscheid RK, Nothacker HP, Bourson A, et al. Orphanin FQ: A neuropeptide that activates an opioidlike G protein-coupled receptor. *Science*. 1995;270(5237):792–794. doi:10.1126/science.270.5237.792
11. Sobczak M, Saaga M, Storr M, Fichna J. Nociceptin/orphanin FQ (NOP) receptors as novel potential target in the treatment of gastrointestinal diseases. *Curr Drug Targets*. 2013;14(10):1203–1209. doi:10.2174/13894501113149990174
12. Rawls SM, Schroeder JA, Ding Z, Rodriguez T, Zaveri N. NOP receptor antagonist, JTC-801, blocks cannabinoid-evoked hypothermia in rats. *Neuropeptides*. 2007;41(4):239–247. doi:10.1016/j.npep.2007.03.001
13. Cannarsa R, Carretta D, Lattanzio F, Candeletti S, Romualdi P. Δ^9 -tetrahydrocannabinol decreases NOP receptor density and mRNA levels in human SH-SY5Y cells. *J Mol Neurosci*. 2012;46(2):285–292. doi:10.1007/s12031-011-9552-0
14. Eid B, Neamatallah T, Hanafy A, et al. Interference with TGF β 1-mediated inflammation and fibrosis underlies reno-protective effects of the CB1 receptor neutral antagonists AM6545 and AM4113 in a rat model of metabolic syndrome. *Molecules*. 2021;26(4):866. doi:10.3390/molecules26040866
15. Wiley MB, Bobardt SD, Nordgren TM, Nair MG, DiPatrizio NV. Cannabinoid receptor subtype-1 regulates allergic airway eosinophilia during lung Helminth infection. *Cannabis Cannabinoid Res*. 2021;6(3):242–252. doi:10.1089/can.2020.0167
16. Sobczak M, Mokrowiecka A, Cygankiewicz AI, et al. Anti-inflammatory and antinociceptive action of an orally available nociceptin receptor agonist SCH 221510 in a mouse model of inflammatory bowel diseases. *J Pharmacol Exp Ther*. 2014;348(3):401–409. doi:10.1124/jpet.113.209825
17. Percie Du Sert N, Hurst V, Ahluwalia A, et al. The ARRIVE guidelines 2.0: Updated guidelines for reporting animal research. *BMJ Open Sci*. 2020;44(11):e100115. doi:10.1136/bmjopen-2020-100115
18. Ko WC, Wang SJ, Hsiao CY, et al. Pharmacological role of functionalized gold nanoparticles in disease applications. *Molecules*. 2022;27(5):1551. doi:10.3390/molecules27051551
19. Cluny N, Vemuri V, Chambers A, et al. A novel peripherally restricted cannabinoid receptor antagonist, AM6545, reduces food intake and body weight, but does not cause malaise, in rodents. *Br J Pharmacol*. 2010;161(3):629–642. doi:10.1111/j.1476-5381.2010.00908.x
20. Krohn RM, Parsons SA, Fichna J, et al. Abnormal cannabidiol attenuates experimental colitis in mice, promotes wound healing and inhibits neutrophil recruitment. *J Inflamm*. 2016;13(1):21. doi:10.1186/s12950-016-0129-0
21. Fichna J, Diczay M, Lewellyn K, et al. Salvinorin A has antiinflammatory and antinociceptive effects in experimental models of colitis in mice mediated by KOR and CB1 receptors. *Inflamm Bowel Dis*. 2012;18(6):1137–1145. doi:10.1002/ibd.21873
22. Bisogno T, Sepe N, Melck D, Maurelli S, Petrocellis LD, Marzo VD. Biosynthesis, release and degradation of the novel endogenous cannabinimetic metabolite 2-arachidonoylglycerol in mouse neuroblastoma cells. *Biochem J*. 1997;322(2):671–677. doi:10.1042/bj3220671
23. Zhang L, Stüber F, Lippuner C, Schiff M, Stamer UM. ERK and p38 contribute to the regulation of nociceptin and the nociceptin receptor in human peripheral blood leukocytes. *Mol Pain*. 2019;15:1744806919828921. doi:10.1177/1744806919828921
24. Valjent E, Pagès C, Rogard M, Besson M, Maldonado R, Caboche J. Δ^9 -tetrahydrocannabinol-induced MAPK/ERK and Elk-1 activation in vivo depends on dopaminergic transmission. *Eur J Neurosci*. 2001;14(2):342–352. doi:10.1046/j.0953-816x.2001.01652.x
25. Derkinderen P, Valjent E, Toutant M, et al. Regulation of extracellular signal-regulated kinase by cannabinoids in hippocampus. *J Neurosci*. 2003;23(6):2371–2382. doi:10.1523/JNEUROSCI.23-06-02371.2003
26. Donica CL, Awwad HO, Thakker DR, Standifer KM. Cellular mechanisms of nociceptin/orphanin FQ (N/OFQ) peptide (NOP) receptor regulation and heterologous regulation by N/OFQ. *Mol Pharmacol*. 2013;83(5):907–918. doi:10.1124/mol.112.084632
27. Delgado-Peraza F, Ahn KH, Nogueras-Ortiz C, et al. Mechanisms of biased β -arrestin-mediated signaling downstream from the cannabinoid 1 receptor. *Mol Pharmacol*. 2016;89(6):618–629. doi:10.1124/mol.115.103176
28. Salaga M, Polepally PR, Zielinska M, et al. Salvinorin A analogues PR-37 and PR-38 attenuate compound 48/80-induced itch responses in mice. *Br J Pharmacol*. 2015;172(17):4331–4341. doi:10.1111/bph.13212
29. Marquéz L, Suárez J, Iglesias M, Bermudez-Silva FJ, Rodríguez De Fonseca F, Andreu M. Ulcerative colitis induces changes on the expression of the endocannabinoid system in the human colonic tissue. *PLoS One*. 2009;4(9):e6893. doi:10.1371/journal.pone.0006893
30. Di Sabatino A, Battista N, Biancheri P, et al. The endogenous cannabinoid system in the gut of patients with inflammatory bowel disease. *Mucosal Immunol*. 2011;4(5):574–583. doi:10.1038/mi.2011.18
31. Grill M, Högenauer C, Blesl A, et al. Members of the endocannabinoid system are distinctly regulated in inflammatory bowel disease and colorectal cancer. *Sci Rep*. 2019;9(1):2358. doi:10.1038/s41598-019-38865-4
32. Evans RM, You H, Hameed S, et al. Heterodimerization of ORL1 and opioid receptors and its consequences for N-type calcium channel regulation. *J Biol Chem*. 2010;285(2):1032–1040. doi:10.1074/jbc.M109.040634
33. Rios C, Gomes I, Devi LA. μ opioid and CB1 cannabinoid receptor interactions: Reciprocal inhibition of receptor signaling and neuritogenesis. *Br J Pharmacol*. 2006;148(4):387–395. doi:10.1038/sj.bjp.0706757
34. Pantiora P, Furlan V, Matiadis D, et al. Monocarbonyl curcumin analogues as potent inhibitors against human glutathione transferase P1-1. *Antioxidants*. 2022;12(1):63. doi:10.3390/antiox12010063
35. Furlan V, Bren U. Insight into inhibitory mechanism of PDE4D by dietary polyphenols using molecular dynamics simulations and free energy calculations. *Biomolecules*. 2021;11(3):479. doi:10.3390/biom11030479
36. Naftali T, Mechulam R, Marii A, et al. Low-dose cannabidiol is safe but not effective in the treatment for Crohn's disease, a randomized controlled trial. *Dig Dis Sci*. 2017;62(6):1615–1620. doi:10.1007/s10620-017-4540-z

Psychometric properties and cultural adaptation of the Spanish version of the Lesbian, Gay, Bisexual, and Transgender Development of Clinical Skills Scale (LGBT-DOCSS-ES)

Piotr Karniej^{1,2,A–F}, Raúl Juárez-Vela^{2,D–F}, Anthony Disen^{3,D–F}, Antonio Martinez-Sabater^{4,5,D–F}, Pablo Del Pozo-Herce^{6,D–F}, Vicente Gea-Caballero^{7,D–F}, Emmanuel Echániz-Serrano^{8,D–F}, Elena Chover-Sierra^{4,9,D–F}, Ruben Perez-Elvira^{10,D–F}, Michał Czapla^{11,2,B–F}

¹ The WSB Merito University, Wrocław, Poland

² Group of Research in Care (GRUPAC), Faculty of Health Sciences, University of La Rioja, Logroño, Spain

³ School of Health Sciences, Stockton University, Galloway, USA

⁴ Faculty of Nursing, Nursing Care and Education Research Group (GRIECE), Nursing Department, University of Valencia, Spain

⁵ Care Research Group (INCLIVA), University Hospital, Valencia, Spain

⁶ Research Group on Innovation in Health Care and Nursing Education (INClUdE), UNIE University, Madrid, Spain

⁷ Faculty of Health Sciences, Research Group Community Health and Care, International University of Valencia, Spain

⁸ Faculty of Health Sciences, University of Zaragoza, Spain

⁹ Internal Medicine Department, Consortium General University Hospital of Valencia, Spain

¹⁰ Faculty of Psychology, Pontifical University of Salamanca, Spain

¹¹ Department of Emergency Medical Service, Faculty of Nursing and Midwifery, Wrocław Medical University, Poland

A – research concept and design; B – collection and/or assembly of data; C – data analysis and interpretation;

D – writing the article; E – critical revision of the article; F – final approval of the article

Advances in Clinical and Experimental Medicine, ISSN 1899–5276 (print), ISSN 2451–2680 (online)

Adv Clin Exp Med. 2025;34(12):2163–2174

Address for correspondence

Michał Czapla

E-mail: michal.czapla@umw.edu.pl

Funding sources

None declared

Conflict of interest

None declared

Received on January 26, 2025

Reviewed on March 11, 2025

Accepted on March 27, 2025

Published online on April 11, 2025

Cite as

Karniej P, Juárez-Vela R, Disen A, et al. Psychometric properties and cultural adaptation of the Spanish version of the Lesbian, Gay, Bisexual, and Transgender Development of Clinical Skills Scale (LGBT-DOCSS-ES). *Adv Clin Exp Med.* 2025;34(12):2163–2174. doi:10.17219/acem/203430

DOI

10.17219/acem/203430

Copyright

Copyright by Author(s)

This is an article distributed under the terms of the Creative Commons Attribution 3.0 Unported (CC BY 3.0) (<https://creativecommons.org/licenses/by/3.0/>)

Abstract

Background. Healthcare systems can present unique challenges for individuals in the lesbian, gay, bisexual, and transgender (LGBT) community, often making it difficult for them to access suitable and respectful care.

Objectives. The aim of this study was to perform a transcultural adaptations and to evaluate psychometric properties of the Spanish version of the Lesbian, Gay, Bisexual, and Transgender Development of Clinical Skills Scale (LGBT-DOCSS-ES). This adaptation is intended for application within Spanish-speaking healthcare settings.

Materials and methods. The LGBT-DOCSS was translated and adapted from the original English version into Spanish using a standardized process, including forward translation, back-translation, and expert panel review. Psychometric properties were tested on a sample of 270 participants from Spain. Internal consistency was evaluated using confirmatory factor analysis (CFA), Cronbach's alpha, the discriminative power index, and McDonald's omega (ω).

Results. The study included 270 participants, with 58.9% being female and 38.9% male. Of the respondents, 52.2% identified as heterosexual, 32.6% as homosexual and 13% as bisexual. The internal consistency of the Spanish version and its domains was good with an overall Cronbach's alpha of 0.746. The alpha ranges for each subscale domains were between 0.769 and 0.822. The McDonald's ω coefficient was 0.808.

Conclusions. The Spanish version of the LGBT-DOCSS-ES has good properties of factorial validity. This tool is a valuable resource for assessing cultural competence and clinical skills among healthcare providers in Spanish-speaking settings.

Key words: interdisciplinary, international, self-assessment, LGBT competence

Highlights

- This is the first tool adapted to assess clinical skills related to LGBT healthcare in Spanish-speaking professionals.
- The Spanish adaptation of the LGBT clinical skills scale shows good consistency and validity, comparable to the original.
- The tool supports research and analysis of areas requiring strengthened competencies among healthcare professionals.
- Its implementation promotes the development of inclusive and culturally competent healthcare for LGBT patients in Spain.

Background

In 2023, 14% of the Spanish population identified themselves as lesbian, gay, bisexual, transgender, queer, questioning, or other (LGBT+), making Spain the country with the second-highest percentage of self-identified LGBT+ individuals globally, just behind Brazil at 15%.¹ Despite this, LGBT+ individuals frequently experience significant disparities in healthcare, primarily due to stigma and discrimination.² Stigma within the healthcare system continues to be a significant barrier, preventing LGBT+ individuals from accessing the care they require.^{3,4}

Spain consistently ranks among the leading European countries in LGBT+ equality, as noted in the International Lesbian, Gay, Bisexual, Trans and Intersex Association (ILGA) 2023 report for Europe. The country's progressive legislation, including the prohibition of conversion therapy practices and advancements in transgender healthcare, reinforces its position as a regional leader. Spain's commitment to equality is also reflected in its participation in European initiatives to counter anti-LGBT+ measures in other nations.⁵

Healthcare professionals often lack sufficient training on LGBT+ specific health issues, which can contribute to the perpetuation of stereotypes and discriminatory practices.⁶ Existing literature highlights the importance of LGBT+-specific assessment tools in healthcare to improve cultural competence among healthcare providers. Research shows that culturally competent care enhances trust, satisfaction and health outcomes for LGBT+ individuals.^{7,8} Such tools are crucial in providing inclusive and non-discriminatory care, addressing health disparities within LGBT+ populations and ensuring compliance with international guidelines on equality in healthcare services.⁹ This deficiency results in negative experiences for LGBT+ patients, fostering mistrust in the healthcare system and its professionals and ultimately leading some individuals to avoid seeking care altogether.^{10,11} Such barriers can further exacerbate the physical and mental health challenges faced by LGBT+ populations.¹² Studies such as Lattanner et al. indicate that structural stigma related to LGBT+ health issues has an effect size comparable to other well-established risk factors for poor health, including income inequality, racial or cultural segregation,

and socioeconomic status.¹³ The World Health Organization (WHO) emphasizes that healthcare services should be accessible to all and free from discrimination. The adoption of the 2030 Agenda for Sustainable Development, with its commitment to “leave no one behind”, further underscores the need to address and improve the health and wellbeing of LGBT+ individuals.¹⁴

Research has demonstrated that healthcare professionals with greater cultural competence and specific clinical skills are crucial for providing inclusive and effective care to the LGBT+ community.^{15–18} Increasing healthcare professionals' competencies significantly enhances patient satisfaction and bolsters trust in the healthcare system.^{6,19} Similarly, LGBT+ cultural competency training programs have improved healthcare providers' knowledge, attitudes and behaviors, increasing satisfaction and better health outcomes for LGBT+ patients.⁸ These programs typically focus on increasing awareness of LGBT health disparities, addressing unconscious biases and developing practical communication skills to ensure more inclusive and patient-centered care. Continuous education and training in LGBT+ cultural competency are essential for improving healthcare professionals' attitudes and practices, promoting inclusive care, reducing health disparities and building trust within the LGBT+ community.^{6,20,21} It is therefore necessary to implement and promote research on the health of LGBT+ individuals to mitigate health inequities, provide inclusive healthcare services and improve the health of this population.²²

A cross-cultural study comparing 7 European countries, including Spain, highlighted significant training needs related to LGBT+ health issues, particularly in areas such as understanding sexual orientation, gender identity, and discrimination against LGBT+ individuals. These training needs were especially pronounced among Spanish health professionals, underscoring the critical role of targeted education in addressing health disparities.²³ The concept of LGBT cultural competence refers to the ability of healthcare professionals to provide respectful, informed, and inclusive care to LGBT patients. It encompasses 3 key domains: Knowledge (understanding the unique health needs and disparities faced by LGBT individuals), Attitudes (awareness of biases and commitment to non-discriminatory care) and Clinical Preparedness (confidence

in addressing LGBT health concerns in practice).^{8,24,25} Various frameworks have been proposed to measure LGBT cultural competence, including self-assessment tools, patient-reported experiences and structured evaluations of provider training.^{8,26,27} The Lesbian, Gay, Bisexual, and Transgender Development of Clinical Skills Scale (LGBT-DOCSS) is one of the few validated instruments designed specifically to assess these competencies in healthcare settings, focusing on the readiness of professionals to engage with LGBT patients in a culturally sensitive manner.²⁵ It has been widely used to evaluate the competencies of diverse healthcare professionals, including physicians, nurses, medical students, and allied health practitioners, making it a versatile tool for assessing LGBT-inclusive clinical skills across different medical and educational contexts.^{28–30} Unlike other instruments, such as the Sexual Orientation Counselor Competency Scale (SOCCSS),²⁶ which primarily assesses counseling-related skills, or the Gay Affirmative Practice Scale (GAP),²⁷ which focuses on affirmative attitudes rather than Clinical Preparedness, the LGBT-DOCSS is specifically tailored for healthcare professionals. Its structured 3-domain model allows for a more targeted assessment of both attitudinal and practical dimensions of LGBT patient care.²⁵ This specificity, along with its strong psychometric properties, was the key reason for selecting LGBT-DOCSS as the basis for this study.

As no comparable tool is currently available in Spain, this study aimed to perform a cross-cultural adaptation and evaluate the psychometric properties of the Spanish version of the LGBT-DOCSS (LGBT-DOCSS-ES).

Materials and methods

Adaptation process

The linguistic and cross-cultural adaptation of the LGBT-DOCSS followed the standardized 6-step approach proposed by Beaton et al., ensuring methodological rigor in its adaptation to Spanish.³¹ The adaptation process involved 6 stages: 1) initial translation, 2) synthesis of translations, 3) back translation, 4) expert committee review, 5) pre-testing of the translated version, and 6) final evaluation.

The initial translation of the LGBT-DOCSS-ES into Spanish was conducted independently by 2 bilingual translators with expertise in healthcare terminology. Following this, these translations were synthesized to ensure consistency and conceptual clarity. This Spanish version was back-translated into English by bilingual translators blind to the original English content. A native English speaker reviewed the back-translated version to check for discrepancies.

Additionally, an expert committee, consisting of native speakers with clinical backgrounds, compared both the original and back-translated versions

of the LGBT-DOCSS. Through consensus, the committee established the final Spanish version, ensuring that it preserved the conceptual intent of the original tool. The expert committee included a diverse group of professionals: a public health specialist, a psychologist, a medical doctor, a nurse, and a paramedic. Each committee member had at least 5 years of experience in their respective fields and specific familiarity with the LGBT community. This collective expertise ensured that the adapted version was culturally and clinically relevant. Specific linguistic adjustments were made to enhance accessibility for Spanish-speaking healthcare professionals.

In the final phase, cognitive interviews were conducted with a convenience sample of 35 healthcare professionals to assess the translated version's clarity, cultural applicability and linguistic accuracy. Participants were selected based on their current employment in healthcare and ability to provide feedback on language and cultural relevance. No significant issues were identified, but based on minor observations, small adjustments were made to enhance readability and relevance. These adjustments ensured that the scale is both linguistically accessible and conceptually appropriate; however, the primary aim of this study was to validate the psychometric properties of the Spanish version for use in Spanish-speaking healthcare settings.

Procedure

A cross-sectional study was conducted between May 2024 and December 2024, enrolling 270 participants through convenience sampling via social media platforms such as Instagram and a dedicated Facebook group for healthcare professionals. The convenience sampling approach was chosen to maximize accessibility and participation among healthcare professionals actively engaged on social media platforms. This method enabled the recruitment of a diverse sample representing various healthcare professions, including nurses, medical doctors and health sciences students. For the calculation, the recommendations for this type of study were considered, which indicated recruiting between 5 to 10 participants per item, with a minimum of 180 (18 items), according to Argimon-Pallás.³²

All participants who met the inclusion criteria, i.e., being medical and/or healthcare students or professionals and voluntarily agreed to participate, completed an anonymous survey after receiving comprehensive study information and giving their informed consent. The inclusion criteria ensured that participants were either medical or healthcare students or active professionals, allowing us to capture perspectives from individuals at different stages in their careers.

The data were collected, and sample access was controlled via the Webankieta platform, which utilized IP filtering for enhanced security. This filtering mechanism ensured that if multiple questionnaires were submitted from the same IP address, only the first completed response

was considered, minimizing the risk of duplicate entries. No such instances were detected during data collection.

A convenience sampling approach was employed due to its feasibility and accessibility in reaching healthcare professionals actively engaged on social media platforms. This method allowed for rapid recruitment of a diverse group of participants from various healthcare fields, including nurses, medical doctors and health sciences students. While convenience sampling offers practical advantages, such as ease of implementation and cost-effectiveness, it also introduces limitations regarding the representativeness of the sample. Participants who voluntarily responded to the survey may have had a greater pre-existing interest in LGBT+ healthcare issues, which could introduce a selection bias. Additionally, the sample may not fully reflect the broader population of Spanish-speaking healthcare professionals, particularly those who are less active on digital platforms. However, efforts were made to include individuals from diverse geographic locations, professional backgrounds and demographic groups, as reflected in Table 1. The potential impact of these limitations on the generalizability of the findings is further addressed in the Limitations section.

Psychometric evaluation

To validate the psychometric properties of the LGBT-DOCSS-ES, internal consistency and factorial validity were assessed. The factorial structure was examined using confirmatory factor analysis (CFA), employing the Diagonally Weighted Least Squares (DWLS) estimation method, which is appropriate for ordinal data. Model fit was evaluated using the Hu–Bentler 2-index strategy, incorporating standardized root mean square residual (SRMR), root mean square error of approximation (RMSEA), comparative fit index (CFI), and Tucker–Lewis index (TLI) indices. The criteria for acceptable model fit were set as $SRMR < 0.09$, along with at least one of the following: $CFI > 0.96$, $TLI > 0.96$ or $RMSEA < 0.06$. Internal consistency was assessed using Cronbach's alpha (α) and McDonald's omega (ω) to evaluate the reliability of the total scale and its factors. In addition, the discriminative power index was employed to determine the contribution of individual items to the internal consistency of each factors. The interpretation of α values followed conventional thresholds: $\alpha \geq 0.9$ was considered excellent, $0.8 \leq \alpha < 0.9$ good, $0.7 \leq \alpha < 0.8$ acceptable, $0.6 \leq \alpha < 0.7$ questionable, $0.5 \leq \alpha < 0.6$ poor, and $\alpha < 0.5$ unacceptable. R v. 4.4.1 (R Foundation for Statistical Computing, Vienna, Austria) was used along with RStudio³³ GUI and psy,³⁴ lavaan,³⁵ psych,³⁶ and diagram packages.³⁷

Measures

The survey consisted of 2 sections: 1. Demographic questionnaire: This section collected information on age,

Table 1. Sociodemographic characteristics of participants

Parameter	Total (n = 270)
Gender	cisgender female
	159 (58.89%)
	cisgender male
	105 (38.89%)
	nonbinary
Place of residence	3 (1.11%)
	transgender man
	2 (0.74%)
	transgender woman
	1 (0.37%)
Sexual orientation	city of more than 500,000 inhabitants
	89 (32.96%)
	city of between 100,000 and 500,000 inhabitants
	54 (20.00%)
	city of between 20,000 and 100,000 inhabitants
Marital/relationship status	52 (19.26%)
	city of up to 20,000 inhabitants
	14 (5.19%)
	village
	61 (22.59%)
Medical profession	heterosexual
	141 (52.22%)
	homosexual
	88 (32.59%)
	bisexual
Courses on LGBT patient issues in the last 5 years	35 (12.96%)
	other
	3 (1.11%)
	i prefer not to respond
	3 (1.11%)
Courses on LGBT patient issues in the last 5 years	single
	63 (23.33%)
	in marriage
	76 (28.15%)
	in a (formal) partnership
Courses on LGBT patient issues in the last 5 years	107 (39.63%)
	in a non-formalised relationship
	12 (4.44%)
	divorce/separation
	10 (3.70%)
Courses on LGBT patient issues in the last 5 years	widowed
	2 (0.74%)
	clinical psychologist
	6 (2.22%)
	doctors
Courses on LGBT patient issues in the last 5 years	58 (21.48%)
	nurses and their specialties (midwife, etc.)
	178 (65.93%)
	opticians
	2 (0.74%)
Courses on LGBT patient issues in the last 5 years	pharmacists
	1 (0.37%)
	physiotherapists
	2 (0.74%)
	student
Courses on LGBT patient issues in the last 5 years	15 (5.56%)
	other health profession
	8 (2.96%)
	never
	163 (60.37%)
Courses on LGBT patient issues in the last 5 years	1–2
	69 (25.56%)
	3–5
	26 (9.63%)
	more than 5
	12 (4.44%)

Demographic characteristics of the study sample (n = 270), including gender identity, age, place of residence, sexual orientation, relationship status, medical profession, and previous LGBT-related training.

gender identity, sexual orientation, place of residence, relationship status, medical occupation, and prior participation in LGBT-related training. The phrasing of demographic questions regarding gender identity and sexual orientation followed international recommendations to ensure inclusivity and accuracy. Gender identity was assessed with the options: cisgender female, cisgender male, nonbinary, transgender man, and transgender woman. Sexual orientation was measured using the categories: heterosexual, homosexual, bisexual, other, and “I prefer not to respond”.

Table 2. Overview of LGBT-DOCSS scores

LGBT-DOCSS [points]	N	Mean	SD	Median	Min	Max	Q1	Q3
Total LGBT-DOCSS score	270	5.19	0.72	5.22	3	7	4.72	5.71
Clinical preparedness	270	4.16	1.36	4.21	1.29	7	3.29	5.14
Attitudinal Awareness	270	6.77	0.59	7	1.43	7	6.86	7
Basic Knowledge	270	4.23	1.58	4.25	1	7	3	5.5

Descriptive statistics (mean; standard deviation (SD); median, min–max, quartile Q1–Q3) for the total Lesbian, Gay, Bisexual, and Transgender Development of Clinical Skills Scale (LGBT-DOCSS) score and its subscales: Clinical Preparedness, Attitudes and Knowledge.

LGBT-DOCSS – The LGBT-DOCSS, which assessed healthcare practitioners’ clinical skills in LGBT patient care, was developed and validated by Bidell in the USA.²⁵ It consists of 18 items and is categorized into three factors: Clinical Preparedness, Attitudinal Awareness and Basic Knowledge. Respondents use a 7-point Likert scale, rating their agreement with each statement from 1 (strongly disagree) to 7 (strongly agree). Eight of the items are scored inversely to ensure that higher scores consistently reflect more affirmative attitudes, greater knowledge and a higher willingness to engage with LGBT patients. The total LGBT-DOCSS score is derived by averaging the scores of all items. Additionally, factors scores are calculated by averaging the items related to Basic Knowledge, Attitudinal Awareness and Clinical Preparedness. Higher points on the factors and overall indicate better Clinical Preparedness, more positive attitudes and greater knowledge of LGBT healthcare.

Ethical consideration

The research adhered to the principles outlined in the Declaration of Helsinki and received ethical approval from the Bioethics Committee at Wroclaw Medical University in Poland (approval No. KB 976/2022) as well as from the University of Valencia (approval No. 2024-EN-FPOD-3314668). This study is a component of the Health Exclusion Research in Europe (HERE) initiative. This study followed the Strengthening the Reporting of Observational Studies in Epidemiology (STROBE) guidelines to ensure the reliability and clarity of the observational study reporting.

Results

Participants

The study included 270 participants, with 58.89% identifying as female, 38.89% as male and 2.22% as nonbinary, transgender men, or transgender women. The median age of participants was 34 years (range: 18–67). Regarding residence, 32.96% lived in cities with more than 500,000 inhabitants, 20.00% in cities between 100,000 and 500,000, 19.26% in cities between 20,000 and 100,000, 5.19% in cities with up to 20,000 inhabitants, and 22.59% in villages.

In terms of sexual orientation, 52.22% identified as heterosexual, 32.59% as homosexual and 12.96% as bisexual. Most participants were in a formal relationship (39.63%), including 28.15% who were married and approx. 11% who were in other legally recognized unions, such as registered partnerships or civil unions. Additionally, 23.33% of participants were single. Nurses and their specialties, including midwives, represented the largest professional group (65.95%). In the past 5 years, 39.63% of participants reported attending courses on LGBT patient issues, while 60.37% stated that they had not participated in such training. Sociodemographic characteristics are presented in Table 1.

LGBT-DOCSS-ES results

The mean total score was 5.19 (standard deviation (SD) = 0.72), with a range from 3 to 7. The mean score for Clinical Preparedness was 4.16 (SD = 1.36), with scores ranging from 1.29 to 7. The Attitudinal Awareness factors showed the highest mean score of 6.77 (SD = 0.59), with a range from 1.43 to 7. The Basic Knowledge factors had a mean score of 4.23 (SD = 1.58), ranging from 1 to 7. Detailed descriptive statistics for each factors and the total score are provided in Table 2.

Analysis of individual questionnaire items

Table 3 illustrates the results for individual questionnaire items, emphasizing a notable ceiling effect observed in items 3, 5, 7, 9, 12, 17, and 18.

Confirmatory factor analysis

As the LGBT-DOCSS-ES questionnaire items are measured on an ordinal scale, the DWLS approach was utilized for CFA. The initial 3-factor model exhibited suboptimal fit indices. To improve model fit, a correlation between items 10 and 11 was incorporated, following recommendations from modification indices. This adjustment resulted in improved fit indices, meeting recommended thresholds (SRMR < 0.09, RMSEA < 0.06). The added correlations linked items within the same factor, ensuring consistency in measurement. This adjustment preserved the original factor structure of the LGBT-DOCSS. Detailed results are shown in Table 4.

Table 3. Analysis of the individual questionnaire items

Item	Floor effect	Ceiling effect
1	10.7%	32.6%
2	18.1%	13.3%
3	1.5%	82.6%
4	1.1%	58.9%
5	1.1%	94.1%
6	24.4%	14.4%
7	1.9%	85.6%
8	22.6%	20.0%
9	0.7%	94.8%
10	51.9%	5.2%
11	40.7%	10.4%
12	0.7%	96.3%
13	12.2%	33.3%
14	8.9%	33.0%
15	13.3%	21.9%
16	24.8%	17.4%
17	0.7%	94.4%
18	1.5%	93.7%

Floor and ceiling effects for each item in the Lesbian, Gay, Bisexual, and Transgender Development of Clinical Skills Scale (LGBT-DOCSS) scale, indicating response distribution patterns.

Internal consistency analysis of the LGBT-DOCSS-ES

The factor loadings for individual items ranged from 0.33 to 0.851, all of which were statistically significant ($p < 0.05$). The Cronbach's alpha coefficients for the 3 factors demonstrated acceptable internal consistency: Clinical Preparedness ($\alpha = 0.822$), Attitudinal Awareness ($\alpha = 0.781$) and Basic Knowledge ($\alpha = 0.769$). The overall reliability of the scale was satisfactory, with a total Cronbach's alpha of 0.746. McDonald's ω index ($\omega = 0.808$) further confirmed the strong internal consistency of the scale. Detailed results for factor loadings and internal consistency are presented in Table 5.

An additional reliability analysis examined whether removing individual items would significantly impact internal consistency. While minor increases in Cronbach's alpha were observed (e.g., excluding Item 4 slightly raised α for

Clinical Preparedness to 0.830), these changes were negligible and did not justify item deletion. Full results of this analysis are presented in Table 6. The path diagram for the CFA of the LGBT-DOCSS-ES is illustrated in Fig. 1. The final version of the LGBT-DOCSS-ES is presented in Table 7.

Discussion

The results suggest that the LGBT-DOCSS-ES demonstrates good psychometric properties, indicating that it is a reliable tool for assessing clinical skills in Spanish-speaking healthcare professionals. This finding supports the scale's applicability in evaluating LGBT cultural competence in diverse linguistic and healthcare contexts. Only minor adjustments to certain expressions were made to ensure cultural appropriateness, but the primary focus remained on evaluating the scale's psychometric properties. Findings from this study align with previous research on the LGBT-DOCSS, supporting its cross-cultural applicability.

The internal consistency of the Spanish version of the Lesbian, Gay, Bisexual, and Transgender Development of Clinical Skills Scale (LGBT-DOCSS-ES) aligns with findings from other adaptations of the scale, including the Polish (LGBT-DOCSS-PL) and Japanese (LGBT-DOCSS-JP) versions, which have demonstrated stable psychometric properties across different cultural contexts.^{25,38,39} While some variations exist between language adaptations, previous research suggests that the scale maintains its reliability, supporting its use in evaluating LGBT clinical skills among healthcare professionals.²⁵ These results indicate that the Spanish version maintains the scale's reliability, confirming its utility for assessing LGBT clinical skills.

In each version, the 2 original factors, such as Clinical Preparedness, Attitudinal Awareness and Basic Knowledge, consistently demonstrated strong internal reliability across different language adaptations.³⁸ The findings from the LGBT-DOCSS-ES align closely with those reported for the Polish version, further supporting the scale's stability in diverse healthcare settings.³⁸ In contrast, the original validation by Bidell reported slightly higher reliability scores across all factors.²⁵ Notably, the Japanese adaptation introduced an additional factor related to Clinical Training, which was not observed in the Polish or Spanish versions.³⁹ This suggests that, in certain cultural contexts,

Table 4. Results of fit indices

Model	χ^2 test			RMSEA	CFI	TLI	SRMR
	χ^2	df	p-value				
I	627.299	131	<0.001	0.118	0.771	0.732	0.096
II	207.754	130	<0.001	0.047	0.952	0.943	0.081

Model fit indices for confirmatory factor analysis (CFA) models tested in the study, including χ^2 root mean square error of approximation (RMSEA), comparative fit index (CFI), Tucker–Lewis index (TLI), and standardized root mean square residual (SRMR). χ^2 represents the goodness-of-fit test comparing the hypothesized model to the observed data. RMSEA estimates the discrepancy between the model and the population covariance matrix. CFI and TLI assess the relative improvement of the tested model compared to a null model. SRMR measures the average difference between observed and predicted correlations.

Table 5. The analysis of the internal consistency of the LGBT-DOCSS-ES

Domain	Item	Loading	p-value	Cronbach's alpha
Clinical Preparedness	4	0.386	< 0.001	0.822
	10	0.417	< 0.001	
	11	0.351	< 0.001	
	13	0.674	< 0.001	
	14	0.851	< 0.001	
	15	0.835	< 0.001	
	16	0.722	< 0.001	
Attitudinal Awareness	3	0.561	< 0.001	0.781
	5	0.330	0.021	
	7	0.617	< 0.001	
	9	0.728	< 0.001	
	12	0.730	< 0.001	
	17	0.809	< 0.001	
	18	0.504	0.005	
Basic Knowledge	1	0.753	< 0.001	0.769
	2	0.785	< 0.001	
	6	0.413	< 0.001	
	8	0.467	< 0.001	
Total:				0.746

Factor loadings of each item within the three subscales of LGBT-DOCSS-ES, along with Cronbach's alpha values for internal consistency assessment.

Table 6. Cronbach's alpha values after excluding individual items

Domain	Item	Cronbach's alpha if item deleted	Domain	Item	Cronbach's alpha if item deleted
Total	1	0.735	Clinical Preparedness	4	0.830
	2	0.736		10	0.803
	3	0.750		11	0.816
	4	0.735		13	0.796
	5	0.750		14	0.773
	6	0.736		15	0.774
	7	0.745		16	0.789
	8	0.726	Attitudinal Awareness	3	0.773
	9	0.744		5	0.790
	10	0.730		7	0.761
	11	0.743		9	0.735
	12	0.742		12	0.729
	13	0.718		17	0.735
	14	0.710		18	0.753
	15	0.710	Basic Knowledge	1	0.746
	16	0.713		2	0.731
	17	0.740		6	0.686
	18	0.750		8	0.685

Cronbach's alpha values if individual items were deleted, showing their impact on overall scale reliability.

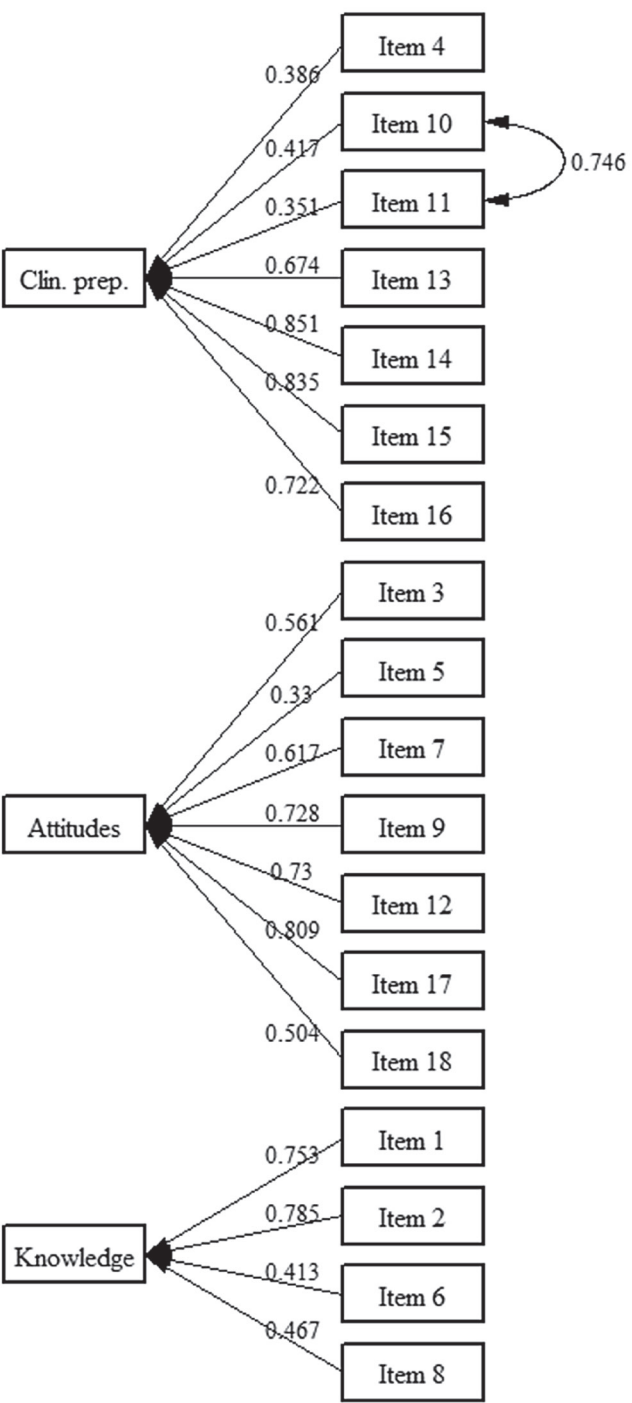


Fig. 1. Path diagram for confirmatory factor analysis (CFA) of the Spanish version of the Lesbian, Gay, Bisexual, and Transgender Development of Clinical Skills Scale (LGBT-DOCSS-ES)

formalized clinical training may play a more distinct role in shaping LGBT competency, whereas in other regions, the original 3-factor structure remains sufficient.

This difference in factor structure could be attributed to variations in healthcare education systems and the emphasis placed on LGBT-related training. In Japan, where formalized LGBT medical education remains limited, a separate “Clinical Training” factor may reflect the necessity of structured instruction in LGBT patient care. Conversely, in Spain and Poland, where LGBT topics are

Table 7. Spanish Version of The Lesbian, Gay, Bisexual, and Transgender Development of Clinical Skills Scale (LGBT- DOCSS-ES)

Versión en español de la Escala de Desarrollo de Habilidades Clínicas para Lesbianas, Gays, Bisexuales y Personas Transgénero (LGBT-DOCSS-ES)						
Instrucciones:						
Los ítems de esta escala están diseñados para medir la preparación clínica, las actitudes y los conocimientos básicos en relación con las pacientes lesbianas, gay, bisexuales y transgénero (LGBT). Utilice la escala adjunta para valorar su grado de acuerdo o desacuerdo con cada punto. Tenga en cuenta que los ítems de esta escala se refieren principalmente a la orientación sexual (LGB = lesbiana, gay, bisexual) o a la identidad de género (transgénero). Dos preguntas están combinadas y se refieren a pacientes lesbianas, gays, bisexuales y transgénero (LGBT).						
1. Soy consciente de las barreras institucionales que pueden impedir que las personas transgénero accedan a los servicios sanitarios.						
Definitivamente no está de acuerdo			En cierta medida de acuerdo/en desacuerdo			Totalmente de acuerdo
1	2	3	4	5	6	7
2. Conozco las barreras institucionales que pueden impedir que las personas LGB accedan a los servicios sanitarios.						
Definitivamente no está de acuerdo			En cierta medida de acuerdo/en desacuerdo			Totalmente de acuerdo
1	2	3	4	5	6	7
3. Creo que ser transgénero es un trastorno mental.						
Definitivamente no está de acuerdo			En cierta medida de acuerdo/en desacuerdo			Totalmente de acuerdo
1	2	3	4	5	6	7
4. No me sentiría preparado para hablar con un paciente/cliente LGBT sobre temas relacionados con su orientación sexual o identidad de género.						
Definitivamente no está de acuerdo			En cierta medida de acuerdo/en desacuerdo			Totalmente de acuerdo
1	2	3	4	5	6	7
5. Una relación del mismo sexo entre dos hombres o dos mujeres no es tan fuerte y comprometida como una relación entre un hombre y una mujer.						
Definitivamente no está de acuerdo			En cierta medida de acuerdo/en desacuerdo			Totalmente de acuerdo
1	2	3	4	5	6	7
6. Conozco las investigaciones que indican que las personas LGB experimentan niveles desproporcionadamente altos de problemas de salud y de salud mental en comparación con las personas heterosexuales.						
Definitivamente no está de acuerdo			En cierta medida de acuerdo/en desacuerdo			Totalmente de acuerdo
1	2	3	4	5	6	7
7. Las personas LGB deben ser discretas sobre su orientación sexual cuando están con niños.						
Definitivamente no está de acuerdo			En cierta medida de acuerdo/en desacuerdo			Totalmente de acuerdo
1	2	3	4	5	6	7
8. Conozco las investigaciones que indican que las personas transgénero experimentan niveles desproporcionadamente altos de problemas de salud y salud mental en comparación con las personas cisgénero.						
Definitivamente no está de acuerdo			En cierta medida de acuerdo/en desacuerdo			Totalmente de acuerdo
1	2	3	4	5	6	7
9. En lo que respecta a las personas transgénero, considero que son moralmente desviadas.						
Definitivamente no está de acuerdo			En cierta medida de acuerdo/en desacuerdo			Totalmente de acuerdo
1	2	3	4	5	6	7
10. He recibido la formación clínica y la supervisión adecuadas para trabajar con pacientes/clientes transgénero.						
Definitivamente no está de acuerdo			En cierta medida de acuerdo/en desacuerdo			Totalmente de acuerdo
1	2	3	4	5	6	7

Table 7. Spanish Version of The Lesbian, Gay, Bisexual, and Transgender Development of Clinical Skills Scale (LGBT- DOCSS-ES) – cont.

Versión en español de la Escala de Desarrollo de Habilidades Clínicas para Lesbianas, Gays, Bisexuales y Personas Transgénero (LGBT-DOCSS-ES)						
11. He recibido la formación y supervisión clínicas adecuadas para trabajar con pacientes/clientes lesbianas, gays y bisexuales (LGB).						
Definitivamente no está de acuerdo			En cierta medida de acuerdo/en desacuerdo			Totalmente de acuerdo
1	2	3	4	5	6	7
12. Un estilo de vida LGB es antinatural o inmoral.						
Definitivamente no está de acuerdo			En cierta medida de acuerdo/en desacuerdo			Totalmente de acuerdo
1	2	3	4	5	6	7
13. Tengo experiencia de trabajo con pacientes/clientes LGB						
Definitivamente no está de acuerdo			En cierta medida de acuerdo/en desacuerdo			Totalmente de acuerdo
1	2	3	4	5	6	7
14. Me siento competente para evaluar a una persona LGB en un entorno terapéutico.						
Definitivamente no está de acuerdo			En cierta medida de acuerdo/en desacuerdo			Totalmente de acuerdo
1	2	3	4	5	6	7
15. Me siento competente para evaluar a una persona transgénero en un entorno terapéutico.						
Definitivamente no está de acuerdo			En cierta medida de acuerdo/en desacuerdo			Totalmente de acuerdo
1	2	3	4	5	6	7
16. Tengo experiencia en el trabajo con pacientes/clientes transgénero.						
Definitivamente no está de acuerdo			En cierta medida de acuerdo/en desacuerdo			Totalmente de acuerdo
1	2	3	4	5	6	7
17. Las personas que visten de forma opuesta a su sexo biológico tienen una perversión.						
Definitivamente no está de acuerdo			En cierta medida de acuerdo/en desacuerdo			Totalmente de acuerdo
1	2	3	4	5	6	7
18. No me sentiría moralmente cómodo trabajando con un pacientes/clientes LGBT.						
Definitivamente no está de acuerdo			En cierta medida de acuerdo/en desacuerdo			Totalmente de acuerdo
1	2	3	4	5	6	7

Instrucciones de puntuación para LGBT-DOCSS-ES

- Anule la puntuación de las 8 preguntas entre paréntesis: (3), (4), (5), (7), (9), (12), (17) i (18). Utilice la puntuación inversa en una escala de Likert (1 = 7, 2 = 6, 3 = 5, 4 = 4, 5 = 3, 6 = 2, 7 = 1).
- Calcular la puntuación media total LGBT-DOCSS: Suma todos los ítems del test (utilizando la puntuación inversa para los ítems entre paréntesis) y divide entre 18.
La puntuación media total LGBT-DOCSS es igual a: 1 + 2 + (3) + (4) + (5) + 6 + (7) + 8 + (9) + 10 + 11 + (12) + 13 + 14 + 15 + 16 + (17) + (18) = Puntuación bruta total LGBT-DOCSS. Divida por 18 para obtener la puntuación media.
- Cálculo de las puntuaciones de las subescalas: Para cada subescala, sume las puntuaciones de las preguntas enumeradas (utilizando la puntuación inversa para los elementos entre paréntesis) y divídalas por el número de preguntas de cada subescala.
Subescala de preparación clínica: (4) + 10 + 11 + 13 + 14 + 15 + 16 = Puntuación bruta total de la subescala de preparación clínica LGBT-DOCSS. Divide por 7 para obtener la puntuación media.
Subescala de actitud: (3) + (5) + (7) + (9) + (12) + (17) + (18) = Subescala de actitud LGBT-DOCSS Puntuación bruta total. Divide por 7 para obtener la puntuación media.
Conocimientos: 1 + 2 + 6 + 8 = Subescala de conocimientos LGBT-DOCSS Puntuación bruta total. Divide por 4 para obtener la puntuación media.
- Las puntuaciones más altas indican un mayor nivel de preparación clínica y conocimientos rudimentarios y una menor conciencia de los prejuicios en relación con los pacientes LGBT.

increasingly integrated into broader medical education, Clinical Preparedness, Attitudinal Awareness and Basic Knowledge appear to be conceptualized as more interrelated dimensions. This highlights the importance of contextualizing LGBT competency assessment within specific cultural and educational frameworks. Cultural differences may influence the factor structure of the LGBT-DOCSS-ES by shaping perceptions of competencies like Clinical Preparedness, Attitudinal Awareness and Basic Knowledge within different healthcare contexts. For instance, societal attitudes towards LGBT individuals and varying healthcare training standards across cultures can lead to different emphases on specific items within these factors. These variations suggest that while core competencies remain consistent, cultural context may shift the relative importance or interpretation of certain items. Norms and values can significantly impact how respondents interpret survey items, influencing the overall findings.^{40,41}

This factorial structure of the instrument reflects the content that some authors suggest should be included in a competency training program aimed at healthcare professionals to improve care for individuals in the LGBT community.⁴² The linguistic adaptation process in all versions involved minor modifications to ensure cultural relevance. In the Spanish version, expressions were slightly adjusted to ensure they resonated with local healthcare professionals, a practice similarly observed in the Polish and Japanese adaptations. Notably, while all adaptations followed a standardized translation process, differences in healthcare terminology and cultural attitudes towards LGBT healthcare led to nuanced linguistic adjustments. The Polish and Japanese versions required additional refinements to align with their respective medical and social frameworks, illustrating the flexibility needed when implementing competency assessments across diverse populations. Significantly, these modifications did not impact the core structure or reliability of the scale.

The LGBT-DOCSS-ES provides a reliable and valid tool for assessing Clinical Preparedness, Attitudinal Awareness and Basic Knowledge of healthcare professionals regarding LGBT patient care. Its application can support scientific research exploring healthcare disparities, educational programs aimed at improving LGBT-related competencies among medical students and practitioners, and workforce training initiatives designed to enhance inclusive healthcare practices. In Spain, this instrument can be particularly valuable for identifying knowledge gaps among healthcare professionals, informing curriculum development in medical and nursing schools, and guiding policy recommendations to improve LGBT healthcare inclusion. Future studies can further explore its use in longitudinal assessments to evaluate the effectiveness of interventions and training programs focused on LGBT competency development.

Limitations

While the sample size was adequate to address the primary objectives, expanding the participant pool could provide deeper insights, especially for subgroups such as non-binary individuals. Additionally, relying exclusively on online data collection may have excluded individuals without stable internet access, potentially reducing the inclusivity of the sample. While convenience sampling effectively recruited a diverse group of healthcare professionals, it may have introduced selection bias, as individuals with a preexisting interest in LGBT+ healthcare were more likely to participate. This could have influenced the overall results by overrepresenting respondents with greater knowledge or more positive Attitudinal Awareness toward LGBT+ patients. Furthermore, the reliance on digital recruitment strategies may have limited participation from healthcare professionals who are less engaged with online platforms, affecting the representativeness of the sample. Finally, relying on self-reported data may have introduced response bias, as participants might have given socially desirable answers, especially considering the sensitive nature of LGBT healthcare topics. Future research should consider employing stratified or random sampling methods to enhance the generalizability of findings to the broader population of Spanish-speaking healthcare professionals.

Conclusions

The findings of this study on the translation and cultural adaptation of the Spanish version of the LGBT-DOCSS-ES indicate that the tool demonstrates acceptable internal consistency and validity. The LGBT-DOCSS-ES holds potential value for research. Compared to the original instrument, the psychometric properties and outcomes of the transcultural adaptation were consistent with those of the original English-language validated version of the LGBT-DOCSS.

Data availability statement

The datasets supporting the findings of the current study are openly available in [repository name] at <https://doi.org/10.5281/zenodo.14741597>.

Consent for publication

Not applicable.

Use of AI and AI-assisted technologies

Not applicable.

ORCID iDs

Piotr Karniej  <https://orcid.org/0000-0002-6489-2525>
 Raúl Juárez-Vela  <https://orcid.org/0000-0003-3597-2048>
 Anthony Dissen  <https://orcid.org/0000-0003-0828-387X>
 Antonio Martínez-Sabater  <https://orcid.org/0000-0002-6440-1431>
 Pablo Del Pozo-Herce  <https://orcid.org/0000-0002-2652-4895>
 Vicente Gea-Caballero  <https://orcid.org/0000-0001-8607-3195>
 Emmanuel Echaniz Serrano  <https://orcid.org/0000-0002-4753-630X>
 Elena Chover-Sierra  <https://orcid.org/0000-0002-4141-6956>
 Rubén Pérez-Elvira  <https://orcid.org/0000-0001-9606-3791>
 Michał Czapla  <https://orcid.org/0000-0002-4245-5420>

References

- Ipsos. Pride month 2023. Paris, France: Institut Public de Sondage d'Opinion Secteur (Ipsos); 2023. <https://www.ipsos.com/en/pride-month-2023-9-of-adults-identify-as-lgbt>. Accessed September 13, 2024.
- Mamede S, Van Gog T, Van Den Berge K, et al. Effect of availability bias and reflective reasoning on diagnostic accuracy among internal medicine residents. *JAMA*. 2010;304(11):1198. doi:10.1001/jama.2010.1276
- Sileo KM, Baldwin A, Huynh TA, et al. Assessing LGBTQ+ stigma among healthcare professionals: An application of the health stigma and discrimination framework in a qualitative, community-based participatory research study. *J Health Psychol*. 2022;27(9):2181–2196. doi:10.1177/13591053211027652
- Nair JM, Waad A, Byam S, Maher M. Barriers to care and root cause analysis of LGBTQ+ patients' experiences: A qualitative study. *Nurs Res*. 2021;70(6):417–424. doi:10.1097/NNR.0000000000000541
- International Lesbian, Gay, Bisexual, Trans and Intersex Association (ILGA)-Europe. Annual Review 2024. Brussels, Belgium: International Lesbian, Gay, Bisexual, Trans and Intersex Association (ILGA)-Europe; 2024. <https://www.ilga-europe.org/report/annual-review-2024/>. Accessed August 25, 2024.
- Donisi V, Amaddeo F, Zakrzewska K, et al. Training healthcare professionals in LGBTI cultural competencies: Exploratory findings from the Health4LGBTI pilot project. *Patient Educ Couns*. 2020;103(5):978–987. doi:10.1016/j.pec.2019.12.007
- Morris M, Cooper RL, Ramesh A, et al. Training to reduce LGBTQ-related bias among medical, nursing, and dental students and providers: A systematic review. *BMC Med Educ*. 2019;19(1):325. doi:10.1186/s12909-019-1727-3
- Yu H, Flores DD, Bonett S, Bauermeister JA. LGBTQ+ cultural competency training for health professionals: A systematic review. *BMC Med Educ*. 2023;23(1):558. doi:10.1186/s12909-023-04373-3
- Patel AU, Nowaskie DZ. Affirmation of LGBTQ+ healthcare providers: A dynamic process, requiring ongoing education and training. *J Gay Lesbian Mental Health*. 2024;28(3):415–423. doi:10.1080/19359705.2023.2197848
- Committee on Understanding the Well-Being of Sexual and Gender Diverse Populations; Committee on Population, Division of Behavioral and Social Sciences and Education; National Academies of Sciences, Engineering, and Medicine. *Understanding the Well-Being of LGBTQI+ Populations*. Patterson CJ, Sepúlveda MJ, White J, eds. Washington, D.C., USA: National Academies Press; 2020:25877. doi:10.17226/25877
- Casey LS, Reisner SL, Findling MG, et al. Discrimination in the United States: Experiences of lesbian, gay, bisexual, transgender, and queer Americans. *Health Serv Res*. 2019;54(Suppl 2):1454–1466. doi:10.1111/1475-6773.13229
- Ortelli TA. Improving LGBTQ health and well-being. *Am J Nurs*. 2020;120(6):1–4. doi:10.1097/01.NAJ.0000668780.88139.1c
- Lattanner MR, McKetta S, Pachankis JE, Hatzembuehler ML. State of the science of structural stigma and LGBTQ+ health: Meta-analytic evidence, research gaps, and future directions [published online as ahead of print on November 12, 2024]. *Ann Rev Publ Health*. 2024. doi:10.1146/annurev-publhealth-071723-013336
- World Health Organization (WHO). Improving LGBTQI+ health and well-being with consideration for SOGIESC. Geneva, Switzerland: World Health Organization (WHO); 2024. <https://www.who.int/activities/improving-lgbtqi-health-and-well-being-with-consideration-for-sogiesc>. Accessed September 13, 2024.
- Okeke UG, Akdemir D, Rabbi I, Kulakow P, Jannink J. Regional heritability mapping provides insights into dry matter content in African white and yellow cassava populations. *Plant Genome*. 2018;11(1):170050. doi:10.3835/plantgenome2017.06.0050
- Liu M, Patel VR, Sandhu S, Reisner S, Keuroghlian AS. Health care discrimination and care avoidance due to patient-clinician identity discordance among sexual and gender minority adults. *Ann Fam Med*. 2024;22(4):329–332. doi:10.1370/afm.3130
- Lampe NM, Barbee H, Tran NM, Bastow S, McKay T. Health disparities among lesbian, gay, bisexual, transgender, and queer older adults: A structural competency approach. *Int J Aging Hum Dev*. 2024;98(1):39–55. doi:10.1177/00914150231171838
- Hash KM, Rogers A. Clinical practice with older LGBT clients: Overcoming lifelong stigma through strength and resilience. *Clin Soc Work J*. 2013;41(3):249–257. doi:10.1007/s10615-013-0437-2
- Ferreira DC, Vieira I, Pedro MI, Caldas P, Varela M. Patient satisfaction with healthcare services and the techniques used for its assessment: A systematic literature review and a bibliometric analysis. *Healthcare*. 2023;11(5):639. doi:10.3390/healthcare11050639
- Hofmann MC, Mulligan NF, Bell KA, et al. LGBTQIA+ cultural competence in physical therapy: An exploratory qualitative study from the clinician's perspective. *Phys Ther*. 2024;104(4):pzae010. doi:10.1093/ptj/pzae010
- Long A, Jennings J, Bademosi K, et al. Storytelling to improve healthcare worker understanding, beliefs, and practices related to LGBTQ+ patients: A program evaluation. *Eval Program Plann*. 2022;90:101979. doi:10.1016/j.evalprogplan.2021.101979
- Ponjoan A, García-Gil MM, Alves-Cabrata L, Martí-Lluch R, Ramos R. Public funding of health research on LGBTIQ+ population in Spain [in Spanish]. *Gac Sanit*. 2022;36(2):106–110. doi:10.1016/j.gaceta.2020.12.034
- Baiocco R, Pezzella A, Pistella J, et al. LGBT+ training needs for health and social care professionals: A cross-cultural comparison among seven European countries. *Sex Res Soc Policy*. 2022;19(1):22–36. doi:10.1007/s13178-020-00521-2
- Bass B, Nagy H. Cultural competence in the care of LGBTQ patients. In: *StatPearls*. Treasure Island, USA: StatPearls Publishing; 2025; Bookshelf ID: NBK563176. <http://www.ncbi.nlm.nih.gov/books/NBK563176>. Accessed March 27, 2025.
- Bidell MP. The Lesbian, Gay, Bisexual, and Transgender Development of Clinical Skills Scale (LGBT-DOCSS): Establishing a new interdisciplinary self-assessment for health providers. *J Homosex*. 2017;64(10):1432–1460. doi:10.1080/00918369.2017.1321389
- Bidell M. Using the Sexual Orientation Counselor Competency Scale (SOCCS) in mental health and healthcare settings: An instructor's guide. *MedEdPORTAL*. 2015;11(1):10040. doi:10.15766/mep_2374-8265.10040
- Crisp C. The Gay Affirmative Practice Scale (GAP): A new measure for assessing cultural competence with gay and lesbian clients. *Social Work*. 2006;51(2):115–126. doi:10.1093/sw/51.2.115
- Elboim-Gabyzon M, Klein R. Lesbian, gay, bisexual, and transgender clinical competence of physiotherapy students in Israel. *BMC Med Educ*. 2024;24(1):729. doi:10.1186/s12909-024-05679-6
- Salter RO, Barham L, Young DL, McIntosh C, Butler CJ. Integrating lesbian, gay, bisexual, transgender, and queer (LGBTQ) competency into the dental school curriculum. *J Dent Educ*. 2024;88(6):823–831. doi:10.1002/jdd.13476
- Nowaskie DZ, Dauterman JW, Dauterman LC, Menez O. U.S. pediatric residents' preparedness, attitudes, and knowledge in LGBTQ+ health care. *J Pediatr Health Care*. 2024;38(2):140–147. doi:10.1016/j.pedhc.2023.12.002
- Beaton DE, Bombardier C, Guillemin F, Ferraz MB. Guidelines for the Process of Cross-Cultural Adaptation of Self-Report Measures. *Spine (Phila Pa 1976)*. 2000;25(24):3186–3191. doi:10.1097/00007632-200012150-00014
- Argimon Pallás JM. *Métodos de Investigación Clínica y Epidemiológica*. 4th ed. Barcelona, Spain: Elsevier España, S.L.; 2012. ISBN:978-84-8086-941-6.
- Allaire JJ. RStudio: Integrated Development Environment for R. Comprehensive R Archive Network (CRAN); 2011. <https://www.r-project.org/conferences/useR-2011/abstracts/180111-allairejj.pdf>. Accessed April 1, 2024.
- Falissard B. psy: Various Procedures Used in Psychometrics. Comprehensive R Archive Network (CRAN); 2022. <https://cran.r-project.org/web/packages/psy/index.html>. Accessed April 1, 2024.

35. Rosseel Y. lavaan: An R Package for Structural Equation Modeling. *J Stat Soft.* 2012;48(2):1–36. doi:10.18637/jss.v048.i02
36. Revelle W. psych: Procedures for Psychological, Psychometric, and Personality Research. Comprehensive R Archive Network (CRAN); 2024. <https://cran.r-project.org/web/packages/psych/index.html>. Accessed April 1, 2024.
37. Soetaert K. diagram: Functions for Visualising Simple Graphs (Networks), Plotting Flow Diagrams. Comprehensive R Archive Network (CRAN); 2020. <https://cran.r-project.org/web/packages/diagram/index.html>. Accessed April 1, 2024.
38. Karniej P, Dissen A, Juarez-Vela R, Gea-Caballero V, Echániz-Serrano E, Czaplá M. Psychometric properties and cultural adaptation of the Polish version of the Lesbian, Gay, Bisexual, and Transgender Development of Clinical Skills Scale (LGBT-DOCSS-PL). *J Homosex.* 2025;72(1):45–59. doi:10.1080/00918369.2024.2302970
39. Kanakubo Y, Sugiyama Y, Yoshida E, et al. Development and validation of the Japanese version of the Lesbian, Gay, Bisexual, and Transgender Development of Clinical Skills Scale. *PLoS One.* 2024;19(3): e0298574. doi:10.1371/journal.pone.0298574
40. Behling O, Law K. *Translating Questionnaires and Other Research Instruments.* Thousand Oaks, USA: SAGE Publications, Inc.; 2000. doi:10.4135/9781412986373
41. Van De Vijver F, Tanzer NK. Bias and equivalence in cross-cultural assessment: An overview. *Eur Rev Appl Psychol.* 2004;54(2):119–135. doi:10.1016/j.erap.2003.12.004
42. Dullius WR, Martins LB, Cesnik VM. Systematic review on health care professionals' competencies in the care of LGBT+ individuals. *Estud Psicol (Campinas).* 2019;36:e180171. doi:10.1590/1982-0275201936e180171

Progress in stem cells mitochondrial proteomics research: A review

Weidong Yao^{B,C,D}, Xinyi Yu^{B,C,E}, Yameng Wang^E, Liang Xia^{A,E,F}

Department of Clinical Medicine, School of Medicine, Hangzhou City University, China

A – research concept and design; B – collection and/or assembly of data; C – data analysis and interpretation;
D – writing the article; E – critical revision of the article; F – final approval of the article

Advances in Clinical and Experimental Medicine, ISSN 1899–5276 (print), ISSN 2451–2680 (online)

Adv Clin Exp Med. 2025;34(12):2175–2186

Address for correspondence

Liang Xia
E-mail: 407928215@qq.com

Funding sources

This work was supported by the Scientific Research Fund of the Zhejiang Provincial Education Department (grant No. Y2023S1164).

Conflict of interest

None declared

Received on August 15, 2024
Reviewed on March 31, 2025
Accepted on April 8, 2025

Published online on August 19, 2025

Abstract

This review summarizes the latest advancements in stem cell (SC) mitochondrial proteomics. With the rapid development of biotechnology, mitochondrial proteomics has emerged as a pivotal area in SC research. The research methods used in mitochondrial proteomics include mass spectrometry (MS), with pre-MS sample processing, MS data acquisition employing both qualitative and quantitative approaches, and bioinformatics analysis to annotate and explore protein functions. In recent years, mitochondrial proteomics research has contributed to the establishment and expansion of our understanding of the roles of various mitochondrial proteins involved in regulating SC differentiation, metabolism and aging, including Drp1, Mfn1/2, OPA1, SIRT3, Bcl-2, YME1L, and PGC-1α. This multidisciplinary approach, combining qualitative and quantitative proteomics with bioinformatics, sheds light on the intricate regulatory mechanisms of mitochondrial proteins in SC. These findings provide a scientific basis for developing novel therapeutic targets and strategies, thereby advancing the field of regenerative medicine and personalized treatment paradigms.

Key words: stem cells, proteomics, mass spectrometry, mitochondria, bioinformatics

Cite as

Yao W, Yu X, Wang Y, Xia L. Progress in stem cells mitochondrial proteomics research: A review. *Adv Clin Exp Med.* 2025;34(12):2175–2186. doi:10.17219/acem/203862

DOI

10.17219/acem/203862

Copyright

Copyright by Author(s)
This is an article distributed under the terms of the Creative Commons Attribution 3.0 Unported (CC BY 3.0) (<https://creativecommons.org/licenses/by/3.0/>)

Highlights

- Advanced mitochondrial purification and quantitative mass spectrometry power high-resolution stem cell (SC) mitochondrial proteomics, delivering unprecedented protein coverage.
- Bioinformatics-driven analysis of mitochondrial proteomes reveals key regulators of SC differentiation, energy metabolism, aging processes, and reactive oxygen species (ROS) homeostasis.
- Stem cell mitochondrial proteomics uncovers novel disease biomarkers and therapeutic targets, accelerating precision diagnostics in metabolic and degenerative disorders.
- Translational impact in regenerative medicine and drug development: Integrating mitochondrial proteomics supports personalized therapy design, biomarker validation, and optimized cell-based treatment strategies.

Introduction

Stem cells (SCs) are undifferentiated cells with self-renewal characteristics.^{1,2} They can be classified by potency. Pluripotent SCs (e.g., embryonic SCs) can form tissues from all 3 germ layers.³ Multipotent SCs, such as hematopoietic SCs (HSCs), can differentiate into a restricted range of cell types within a specific lineage.⁴ Oligo-/unipotent SCs (e.g., spermatogonial SCs) generate only 1 or a few specific cell types.⁵ Biologically, their differentiation and proliferation are regulated by both genetic factors and external signals.^{6,7} They can migrate to sites where they are needed, crucial for development and tissue repair. Additionally, many SCs can survive long-term, remaining in a quiescent state until activated. Due to their ability to generate diverse functional cells, SCs have become a major focus in modern biological and medical research. For example, in the treatment of Alzheimer's disease, SC therapy has shown the effects of promoting neural regeneration, repairing damaged nerves, inhibiting inflammatory responses, and reducing neuronal apoptosis.⁸ For myocardial infarction, SCs succeed in reducing infarct size, abrogating adverse heart remodeling, and improving cardiac function.^{9,10} In addition, the impressive therapeutic effects of SCs on vascular injury, corneal damage, osteoarthritis, acute respiratory distress syndrome, and sepsis are also reported.^{5,10–14}

Mitochondria are the dynamic cytoplasmic organelles with double-membrane structure. In addition to functioning as the cell's "energy factory", mitochondria play a crucial role in regulating calcium homeostasis, responding to oxidative stress, and controlling cell death. It is also the signal center for inducing gene transcription and post-translational regulation.¹⁵ Mitochondrial dysfunctions can occur due to a variety of factors. Mutations in mitochondrial DNA (mtDNA) are a common cause of dysfunction. Since mtDNA encodes several essential proteins involved in the electron transport chain (ETC), which is critical for adenosine triphosphate (ATP) production, these mutations can lead to reduced ATP synthesis and an increase in the production of reactive oxygen species (ROS).¹⁶ Another contributor to mitochondrial dysfunction is defects in nuclear-encoded proteins, which constitute the majority of mitochondrial

components. For instance, mutations in genes involved in mitochondrial protein import can prevent the proper assembly of mitochondrial complexes.¹⁷ Mitochondrial dysfunction can lead to the occurrence of various diseases. Congenital mitochondrial dysfunction is often manifested as mitochondrial myopathy or chronic progressive external ophthalmoplegia (CPEO) in adults (where mitochondrial respiratory chain defects lead to muscle weakness due to energy deficiency^{18,19}) and Leigh syndrome in children with predominant central nervous system (CNS) symptoms. Beyond these, mitochondrial dysfunctions are also implicated in diseases related to the aging process. In Alzheimer's disease, mitochondrial abnormalities lead to impaired bioenergetics and increased ROS production in neurons, which contribute to the accumulation of amyloid- β plaques and tau tangles.^{20,21} In Parkinson's disease, mitochondrial complex I deficiency is commonly observed, leading to dopaminergic neuron death.^{22,23} Furthermore, the relationship between the SCs' mitochondria and neurodegenerative diseases has been noticed by recent studies, which indicate the role of mitochondria as a main regulator of neural SC fates through redox modulation. Meanwhile, mitochondrial biogenesis, dynamics, or ROS scavenging can be impaired by abnormal metabolic products, such as amyloid- β peptide, which compromises SCs' commitment, thereby exacerbating disease progression.^{24–26}

Mitochondrial proteomics provides a holistic view of changes in protein composition, post-translational modifications and expression patterns. Through techniques such as two-dimensional (2D) gel electrophoresis and mass spectrometry (MS), changes in the abundance of mitochondrial proteins can be detected. These findings can help elucidate the underlying molecular mechanisms of the disease. Proteomics can also identify post-translational modifications (PTMs) of mitochondrial proteins, such as phosphorylation, acetylation, and ubiquitination. For instance, altered phosphorylation patterns of mitochondrial proteins have been associated with changes in mitochondrial dynamics and bioenergetics.^{27,28} By mapping these PTMs, proteomics can provide insights into how SCs mitochondrial functions are disrupted. Mitochondrial proteomics can also help in understanding the interactions between mitochondrial

proteins. Proteomic techniques such as co-immunoprecipitation followed by MS can identify interacting proteins and how these interactions are affected in disease states. This knowledge may contribute to a more comprehensive understanding of the molecular events underlying mitochondrial dysfunction in SCs and could facilitate the identification of novel therapeutic targets.

Objectives

This review summarizes the latest advancements in SC mitochondrial proteomics studies, including progress in sample processing, MS, data acquisition, and bioinformatics analysis. We aimed to advance our understanding of mitochondrial protein profiling technology and promote its applications in regenerative medicine and personalized therapy.

Research methods of mitochondrial proteomics

Mass spectrometry is an essential technology in proteomics research. It has become one of the most commonly used discovery and verification tools in the field of life sciences. The research methods of the MS-based technology mainly include pre-MS sample processing (mitochondrial extraction and purification), MS data acquisition and post-MS bioinformatics.

Sample processing

The conventional method for extracting mitochondria is differential centrifugation. During the extraction of mitochondria, it is necessary to pre-cool the equipment and maintain low temperatures throughout the homogenization process of tissues or cells to prevent protein denaturation and aggregation. Undissolved cells, cellular debris, and nuclei will first be removed by low-speed centrifugation ($600 \times g$ or $1,000 \times g$). Since mitochondria may be present in the flaky precipitate, resuspending the precipitate and performing 1 additional low-speed centrifugation can improve the mitochondrial yield. High-speed centrifugation ($3,500 \times g$ or $10,000 \times g$) was performed on the supernatant obtained from the low-speed centrifugation steps,^{29,30} resulting in a crudely extracted mitochondrial precipitate, which has low purity and contains contaminants such as peroxisomes, endoplasmic reticulum and microsomes. Therefore, it can only be used for simpler applications, including analyzing the activity of certain mitochondrial enzymes and detecting mitochondrial morphology and apoptosis.

For mitochondrial proteomics, further purification is required. The sucrose density gradient centrifugation method has become a common method for mitochondrial

purification due to its simple operation and low cost. It uses a sucrose buffer solution, which has a similar dispersion to the cytoplasm phase as the suspension medium and separates cell components of different densities in cell or tissue homogenates through gradient centrifugation.^{31–34} However, sucrose of high concentrations has a high viscosity and high osmotic pressure, which can easily lead to repeated contraction and swelling of mitochondria. Several new density gradient media can purify mitochondria with intact morphology but are generally more expensive. Due to its low diffusion constant, Percoll® forms a very stable gradient that usually does not penetrate the biological membranes. Therefore, it minimizes the rupture of organelles and is commonly used for separating platelet mitochondria.^{35–37} Nycodenz contains sorbitol as an osmotic stabilizer. Due to its high density, low viscosity and minimal impact on osmotic pressure, the yield of intact mitochondria is significantly higher.^{38–40} As a dimer of Nycodenz, OptiPrep has the advantage of forming an automatic gradient in a short period.^{41–43}

The disadvantages of traditional methods include: 1) reliance on costly ultracentrifugation equipment; 2) prolonged centrifugation causing mechanical damage to mitochondrial membrane; and 3) unavoidable contamination from cytoplasmic organelles, cellular debris and gradient medium, resulting in low sample purity. These shortcomings have brought about many limitations to mitochondrial proteomic research. Therefore, some researchers have attempted to use magnetic beads to sort mitochondria. Bousardon et al. used transgenic technology to induce the expression of biotinylated outer membrane protein OM64 in *Arabidopsis thaliana* mitochondria. After the plant tissue was lysed, it was incubated with streptavidin-coated magnetic beads for 1 min, exposed to a magnetic field for 2 min, and then washed 5 times after discarding the supernatant. The success rate, purity and integrity of mitochondrial sorting were significantly higher than those of density gradient centrifugation.⁴⁴ Chen et al. achieved rapid sorting of mitochondria using immunomagnetic beads by constructing a fusion protein of mitochondrial outer membrane protein and tag protein, and detected the high-purity mitochondrial metabolites.⁴⁵ However, these methods are only applicable to cell models and cannot be used for tissues and cells directly from humans or animals. Moreover, the knock-in of tag protein genes is time-consuming and labor-intensive, with a low success rate. Therefore, there is still a need to develop simpler, faster, less damaging and highly purified mitochondrial separation methods.

Mass spectrometry data acquisition

Qualitative mass spectrometric analysis

“Bottom-up” is a proteomic qualitative method that analyzes small peptide fragments directly. The basic process is to digest protein samples into a mixture of peptide segments and separate them with chromatography. Then,

the peptide segments are fragmented using MS, and the ion peak data from the fragmentation spectra is obtained to perform bioinformatics analysis. The identified peptide segments are then assembled into proteins through database matching to achieve protein identification. "Top-down" is another qualitative analysis experiment that enables global analysis on fragmented proteins. The intact proteins are separated from complex biological samples using separation techniques such as liquid chromatography (LC) or 2D gel electrophoresis. Then, techniques such as electron capture dissociation (ECD) are employed to allow low-energy free electrons to interact with protonated multi-charged protein or peptide ions. This interaction generates fragmentation during the exothermic phase. Protein identification is then achieved based on the fragmentation spectrum information and protein mass. Unlike enzymatic digestion-based methods, it can achieve high sequence coverage and retain the correlation information between multiple post-translational modifications. "Top-down" also has some drawbacks, such as difficulties in analyzing fragmented proteins in the gas phase. In contrast, "Bottom-up" involves enzymatically digesting proteins into peptide segments, making them easier to separate, ionize and fragment in the gas phase. As a result, "bottom-up" has become a more widely used method for proteomic qualitative analysis.

Quantitative mass spectrometric analysis

Quantitative proteomics is a method for precisely identifying and quantifying all proteins expressed by the genome or all proteins within a complex mixture system. It can be used to screen and identify the differentially expressed proteins between samples. Common quantitative methods include MS quantification, immunoassay and gene expression analysis.⁴⁶ Mass spectrometry-based protein quantification methods can generally be divided into labeling and non-labeling techniques.⁴⁷

The labeling method obtains peptide or protein quantification from the primary mass spectrometry (MS1) peaks of mixed samples with differential labeling.⁴⁸ Currently, labeled quantitative proteomics methods can be divided into chemical labeling and metabolic labeling. Common chemical labeling methods include Tandem Mass Tag (TMT) isobaric tags for relative and absolute quantification (iTRAQ) and other isobaric peptide labeling methods.^{49,50} These methods can generate isobaric MS1 peaks for multi-channel labeling. After the fragmentation of the isobaric peaks, different reporter ions are released during secondary mass spectrometry (MS2) and tertiary mass spectrometry (MS3) scans for relative quantitative analysis. Tandem Mass Tag labels the amino groups of peptides with 2, 6 or 10 isotopes. It compares the protein expression levels in different sample groups simultaneously by detecting the label intensities in MS. It has recently become a commonly used high-throughput screening technique in quantitative

proteomics.⁴⁹ Tandem Mass Tag allows multiple samples to be processed, labeled and analyzed in 1 batch with small errors, high parallelism and good stability. The iTRAQ refers to the use of 4 or 8 isotopic specific labels for the amino groups of peptides and the use of MS to detect label intensity for relative quantification of protein content.⁵⁰ It offers strong separation capability, wide applicability, quantitative labeling, and high automation and accuracy. Billing et al. used iTRAQ-based MS to analyze the mitochondrial proteome of pluripotent FDCP-Mix cells and identify stage- and lineage-specific mitochondrial changes in hematopoietic progenitor cells. They linked the proteins in cellular differentiation with mitochondrial transport, fatty acid degradation and oxidative phosphorylation. This approach improved the efficiency of peptide identification.⁵¹

The metabolic labeling method Stable Isotope Labeling with Amino Acids in Cell Cultures (SILAC) uses 2 different isotopes, light or heavy, to label essential amino acids, which will be incorporated metabolically into cellular proteins. The protein is then identified and quantified using MS analysis.⁵² It can label living cells *in vivo* with a stable labeling effect and high efficiency. The requirement on sample amounts is low, and multiple proteins can be identified and quantified synchronously with small errors. However, it cannot be applied on tissue or fluid samples. Labeling in animal models is usually too costly to perform.

Label-free technology is a protein quantification method that does not rely on isotopic labeling. Based on the intensity of the parent ion of the peptides, it calculates the signal intensity of each peptide segment on liquid chromatography tandem MS (LC-MS-MS) for relative quantification.⁵³ First, the sample to be tested is digested into peptide segments. Then, the digested sample is analyzed using a mass spectrometer to quantify the protein by detecting the mass and abundance of the peptide segments in the sample. In label-free technology, the capturing frequency of peptides in MS is considered to be positively correlated with the abundance in the mixture. Therefore, an appropriate mathematical formula can link the count of peptide segments in MS to the amount of protein in samples. Compared with traditional labeling methods, label-free technology has the advantages of simple operation, high throughput, high sensitivity, and high applicability,⁵³ and thus has been widely used in proteomic research.

Additionally, based on the Data Independent Acquisition (DIA) mode, sequential windowed acquisition of all theoretical fragment ions (SWATH) has become a new technology that can also perform on label-free samples.⁵⁴ It divides the entire scanning range of MS into several intervals, sequentially performs high-speed MS1 scans on all peptide precursor ions within each mass range, and then collects MS2 fragment ion data for relative or absolute protein quantification.⁵⁴ Detection accuracy of SWATH surpasses traditional label-free approaches. It has superior identification performance on low-abundance proteins and peptides, fewer restrictions on sample quantity, complete

and comprehensive data retention, good reproducibility, and high traceability. However, SWATH has much higher requirements for analysis algorithms than labeled techniques.

Bioinformatics

Based on qualitative and quantitative proteomics techniques, bioinformatics research can explore the potentially related processes and involved mechanisms by annotating differentially expressed proteins in samples with Gene Ontology (GO; <http://www.geneontology.org>), Kyoto Encyclopedia of Genes and Genomes (KEGG; <https://www.kegg.jp>) pathway, and Protein–Protein Interaction Networks (PPI; <https://cn.string-db.org>).

Gene Ontology is an internationally standardized gene function classification system that provides a dynamic and controllable vocabulary to comprehensively describe the attributes of genes and gene products in organisms. It consists of a set of predefined GO terms that define and describe the functions of gene products. The GO annotations library mainly provides annotations for GO terms. The KEGG database is a database that systematically analyzes the metabolic pathways of gene products in cells and the functions of these gene products. This database helps to study genes and expression information as a whole network. It integrates data from genomes, chemical molecules and biochemical systems, including metabolic pathways (PATHWAY), drugs (DRUG), diseases (DISEASE), gene sequences (GENES), and genomes (GENOME). The PPI is formed by proteins interactions that participate in various aspects of life processes such as signaling, gene expression, energy metabolism, and cell cycle regulation. Constructing an interaction network of differentially expressed proteins can help us discover the trends of change and key protein nodes at the proteomic level.

The comprehensive utilization of qualitative and quantitative strategies in mitochondrial proteomics, combined with in-depth bioinformatics analysis, possesses significant scientific value in research. It can help discover the influence of mitochondrial proteins on SC biological processes, including self-renewal, differentiation and aging, thereby providing insights into the relationship between mitochondria and clinical status, such as cancer, cardiovascular and neurological disease.⁵⁵ Based on the establishment of a SC mitochondrial protein database, this multi-faceted research approach will not only unravel the functional architecture underlying mitochondrial proteome complexity but also promote the new therapeutic strategies development for personalized and regenerative medicine.^{56–58}

The role of mitochondrial proteins in stem cell differentiation

Mitochondrial dynamics is an important part of SC physiology and can have a profound impact on SC fate

by regulating mitochondrial morphology and function. Some key proteins related to mitochondrial dynamics are members of the dynamin-related protein family that function as GTPase. They have large molecular weights and include dynamin-related protein 1 (Drp1), mitofusin 1/2 (Mfn1/2) and optic atrophy protein 1 (OPA1).^{59,60} Drp1, as a key mitochondrial fission protein, plays an important role in modulating mitochondrial morphology and function. Studies have shown that Drp1 inhibition will lead to mitochondrial elongation and increase its bioenergetic efficiency.⁶¹ Mfn1/2 is a key protein for mitochondrial outer and inner membrane fusion. Lack of Mfn1/2 leads to decreased ATP levels and slower SC growth. The OPA1 is an inner mitochondrial membrane protein that plays a central role in the precise regulation of mitochondrial fusion and fission. It exists in 2 main forms: transmembrane long form (L-OPA1) and soluble short form (S-OPA1). The long form of OPA1 anchors to the inner mitochondrial membrane, while the short form is released from the inner membrane via proteolysis. The OPA1 responds to changes in membrane potential through the ratio of its isoforms, and this isoform cleavage behavior is activated under depolarization conditions, leading to the transition from L-OPA1 to S-OPA1. This process is crucial for maintaining the stability and morphology of the mitochondrial network.⁶² In addition, OPA1 also directly participates in the regulation of mitochondrial cristae morphology, which further regulates the function of the ETC and ATP synthesis capacity by affecting the structure and number of cristae, thereby affecting the energy state and differentiation potential of SCs.⁶³

Besides Drp1, Mfn1/2 and OPA1, there are some other mitochondrial proteins and related transcription factors that play important roles in regulating SC energetics and influencing cellular lineage commitment.^{64,65} As a mitochondrial deacetylase, SIRT3 can affect SC differentiation by directly regulating a variety of key enzymes involved in mitochondrial energy metabolism through deacetylation.⁶⁶ PGC-1 α is a transcriptional co-activator that can induce mitochondrial biogenesis and respiration, thereby improving cellular metabolic reprogramming. In pluripotent SCs, overexpression of PGC-1 α has been shown to activate transcription factors such as Nrf-1 and 2, which can promote mitochondrial protein synthesis and functional optimization, thereby increasing mitochondrial gene expression and respiratory chain activity, inducing differentiation into specific cell types, such as neural precursor cells.⁶⁵

Mitochondrial proteins that induce apoptosis also play an important role in SC development reprogramming. During the self-renewal of SCs, anti-apoptotic proteins in the Bcl-2 family (e.g., Bcl-2, Bcl-xl, and Mcl-1) are highly expressed.⁶⁷ These proteins inhibit apoptosis by preserving mitochondrial membrane integrity.⁶⁷ This mechanism maintains stemness and supports cellular diversity. On the other hand, Bax, as a pro-apoptotic protein in the BCL-2 family, is generally present in the cytoplasm.

After being activated, it will translocate to the surface of mitochondria to form a pore across the membrane, leading to a decrease in mitochondrial membrane potential, an increase in membrane permeability, and the release of apoptotic factors.⁶⁸ These changes ultimately promote SC apoptosis, eliminating redundant or misprogrammed cells during development.

Mitochondrial proteomics can provide important help for us to better understand the differentiation regulation mechanism of SCs. Researchers used proteomics and metabolomics approaches to reveal the key role of mitochondrial proteins in the differentiation process of neural SCs and progenitor cells.⁶⁹ By analyzing the state transitions of neural stem and progenitor cells (NSPCs) between rest and activation, researchers found that significant changes in 5 mitochondrial proteases (including YME1L, PITRM1, METAP1D, LACTB, and HTRA2) have a significant impact on cellular energetics. Particularly, YME1L plays a crucial role in maintaining the resting state with fatty acid oxidation as the main energy source. The deletion of YME1L triggers differentiation programs, leading to irreversible transitions to other metabolic states. These findings provide a new perspective for understanding the fate determination of SCs and provide potential targets for future therapeutic strategies. Shekari et al. used subcellular proteomic methods that combined subcellular separation with MS techniques to identify 3,183 proteins associated with mitochondria, rough endoplasmic reticulum, nucleus, and microsomes in human embryonic SCs (hESCs).⁷⁰ Among these proteins, a total of 160 differentially expressed proteins were enriched in multiple signaling pathways. Meanwhile, it was also found that Bax protein has a specific localization in the subcellular structure Golgi apparatus in hESCs, and can rapidly translocate to mitochondria and initiate apoptosis programs when hESCs DNA is damaged.⁷⁰ Therefore, Bax's rapid response and translocation ability may be a key factor in regulating apoptosis in hESCs, and may directly affect the self-renewal and differentiation potential of SCs.

Mitochondrial proteins and energy metabolism of stem cells

Mitochondria are the main sites of cellular energy metabolism. In undifferentiated SCs, mitochondria usually exhibit immature morphology, featuring the spherical structure and short cristae of mitochondria, which can provide a much larger surface area to increase the efficiency of ATP synthesis to meet the energy requirements of SCs. At this time, glycolysis is the main metabolic pathway for mitochondria. Some key mitochondrial proteins play a crucial role in the energy metabolism and stemness maintenance of SCs: 1) Uncoupling protein 2 (UCP2) protects SCs from ROS-induced damage by establishing proton leakage across the inner mitochondrial membrane and

reducing oxidative phosphorylation efficiency⁷¹; 2) ATPase inhibitor (IF1) directly inhibits the activity of ATP synthase to ensure that SCs maintain a high rate of glycolysis⁷²; 3) Pyruvate dehydrogenase kinase (PDK) inhibits the phosphorylation of pyruvate dehydrogenase (PDH) to convert pyruvate into acetyl-CoA, effectively limiting pyruvate's entry into the tricarboxylic acid cycle.⁷³ These mitochondrial proteins synergistically provide energy and maintain stemness through metabolic regulation.

In differentiated SCs, mitochondria have a complex inner membrane system and abundant cristae structures. The mitochondrial permeability transition pore (mPTP) is a protein complex between the inner and outer mitochondrial membranes, and its subunits are primarily composed of pore-forming proteins such as voltage-dependent anion channel (VDAC), adenine nucleotide translocator (ANT) and cyclophilin D (CyP-D). Some specific physiological or pathological conditions, such as Ca^{2+} concentration stimulation and oxidative stress, can activate CyP-D and cause the mPTP channel to open, which leads to a sharp increase in mitochondrial membrane permeability and activating oxidative phosphorylation.^{74,75} Appropriate mPTP opening can help maintain the stability of the intracellular environment and promote the smooth differentiation of SCs into specific cell types. Hu et al. reported that transferring functional mitochondria via extracellular vesicles from mouse mesenchymal stem cells (MSCs) to damaged pancreatic cells restored mPTP-related protein function, cellular energy metabolism and ATP supply.⁷⁴ However, excessive mPTP opening may lead to SC apoptosis and affect the differentiation process. In the induced pluripotent SC-derived cardiomyocytes (iPSC-CMs) from patients with hypoplastic left heart syndrome (HLHS), mPTP was found to have excessive opening and related to the upregulated oxidative stress.⁷⁵ By suppressing excessive mPTP opening, the cellular energetics of iPSC-CM can be improved with alleviate oxidative stress.⁷⁵

Mitochondrial Lon protease 1 (LONP1) is a mitochondrial matrix protease that plays an important role in mitochondrial function maintenance and protein quality control. It is involved in fatty acid oxidation and degradation of damaged or misfolded mitochondrial proteins. In addition, LONP1 regulates mitochondrial DNA replication and transcription, affects respiratory chain protein synthesis, and is essential for energy metabolism in human iPSCs.⁷⁶ During the process of iPSCs differentiation into cardiomyocytes, the upregulation of LONP1 activity helps to orchestrate the metabolic shift from glycolysis to fatty acid oxidation, ensuring the balance between glucose and fatty acid oxidation. LONP1 deficiency may induce mitochondrial dysfunction, impairing cardiomyocytes' energy production and cardiac function.⁷⁶ These findings highlight the importance of LONP1 in maintaining energy metabolism and mitochondrial function during SC differentiation and help to understand the underlying mechanisms of mitochondrial dysfunction-related diseases.

Mitochondrial proteomics is of great significance for studying the relationship between mitochondrial proteins and SC bioenergetics. Retinoblastoma 1 (RB1) is one of the best known tumor suppressor genes.⁷⁷ Recent studies have shown that it promotes mitochondrial energy metabolism through the oxidative phosphorylation (OXPHOS) pathway during the differentiation of iPSCs into cardiomyocytes.⁷⁸ Using specific *RB1* gene knockout and TMT-labeled quantitative proteomics techniques, researchers analyzed the effects of RB1 deletion on mitochondrial proteins in adult mouse colon and lung tissues. By analyzing samples from 6 mice of each genotype, a total of 8,063 proteins were identified. Among them, mitochondrial proteins associated with the respiratory chain and OXPHOS were significantly downregulated. Moreover, the mitochondrial oxygen consumption rate, mitochondrial mass and the mitochondrial-to-nuclear DNA ratio all decreased.⁷⁹ This result unveils a new role of RB1 in maintaining mitochondrial function and energy metabolism, which could inform the development of therapeutic strategies for mitochondrial dysfunction-related diseases.

Mitochondrial protein and stem cell aging

With age, the function of SCs gradually declines. Mitochondrial proteins play an important role in this process. Some studies have shown that oxidative damage and abnormal expression of mitochondrial proteins are closely related to SC aging. For example, with the help of cofactor nicotinamide adenine dinucleotide (NAD⁺), SIRT3 can catalyze the deacetylation of mitochondrial proteins, coordinate metabolic responses to oxidative stress and fluctuating energy demands, and maintain mitochondrial health.⁸⁰ In HSCs, SIRT3 is highly expressed, whereas in differentiated hematopoietic cells, its expression is suppressed. Studies have shown that the loss of SIRT3 may cause the loss of quiescent state in HSCs, while overexpression of SIRT3 may improve aging HSCs function. Therefore, SIRT3 may become a potential target for anti-aging therapy in SCs.⁸¹

There are multiple critical connections between mitochondrial homeostasis and SC aging, involving multiple proteins and signaling pathways. Autophagy-related proteins, such as Beclin1, p62 and LC3, play a key role in maintaining mitochondrial function and SC vitality by clearing damaged mitochondrial components.⁸² Mitochondrial fusion and fission-related proteins, such as Mfn1/2, and Drp1, are crucial for maintaining the normal morphology and function of mitochondria.⁸³ Mitochondrial transcription factor A (TFAM) is involved in maintaining the stability of mitochondrial DNA, which has an important impact on SC aging.⁸⁴ Additionally, the ROS scavenging system, as well as the mTOR signaling pathway, also plays key roles in regulating SC growth, metabolism, survival, and function by affecting mitochondrial protein homeostasis.⁸⁵

Mitochondrial proteome analysis can help us further evaluate the role of the above proteins and pathways in SC aging and may provide new strategies for delaying SC aging. Cytoplasmic polyadenylation element binding protein 4 (CPEB4) is an RNA binding protein that can bind to the polyadenylation element sequence of target RNA to regulate the translation. Through immunoprecipitation combined with RNA sequencing technology, researchers found that CPEB4 can specifically bind to messenger RNA encoding mitochondrial proteins in SC,⁸⁶ indicating that CPEB4 may regulate mitochondrial proteomic activity by regulating mitochondrial translation. By performing low-input mass spectrometric analysis of adult muscle SCs at different aging stages in mice, 368 mitochondrial proteins associated with CPEB4 were identified, revealing their significance in SC energetics and aging. To test whether the restoration of CPEB4 expression can reverse the cell cycle stagnation in aged SC, researchers conducted experiments in a mouse muscle transplantation model and demonstrated that increasing CPEB4 levels in aged SCs alone was sufficient to rescue their regenerative capacity and promote the formation of new muscle fibers.⁸⁶

Mitochondrial proteins and ROS

Reactive oxygen species are a class of oxygen-containing substances with high reactive activity that play a role in signal transduction between mitochondrial and cellular communication. During oxidative phosphorylation under physiological conditions, electrons are transferred through the ETC on the inner membrane of mitochondria, and some electrons leak out before reaching the terminal oxidase and reducing oxygen molecules to produce ROS. Maintaining appropriate levels of ROS is crucial for the function of SCs. Suppressing ROS in neural or hematopoietic SCs below physiological levels can significantly reduce their regenerative potential, manifested by impaired proliferation, differentiation and self-renewal abilities.^{61,87}

When cells are under various pathological conditions, such as hypoxia, aging or chemical inhibition of mitochondrial respiration, the rate of mitochondrial ROS production increases, inducing mitophagy and affecting SC signaling pathways.⁸⁸ The KEAP1-Nrf2 pathway is important for antioxidation. By detecting the binding site of KEAP1, Zeb et al. found that only phosphoglycerate mutase 5 (PGAM5), a mitochondrial serine-threonine protein phosphatase, responded to moderate mitochondrial ROS production and accumulated to induce PINK1-Parkin-mediated mitochondrial autophagy.⁸⁸ Nrf2 protects the heart from oxidative damage and plays an antioxidant stress role in skin diseases.⁸⁹ Koch et al. demonstrated impaired Nrf2-mediated oxidative stress response and reduced mitochondrial protein abundance in atopic dermatitis.⁹⁰ These findings suggest that KEAP1-mediated regulation on cellular ROS

levels acts as a negative feedback mechanism, enabling excessive ROS to be cleared by mitochondrial autophagy.

Mitochondrial proteomic research helps to further understand the pathogenesis of oxidative stress injury and reveal potential intervention targets. Ginsenoside Rb1 (GRb1) is a protopanaxadiol isolated from the root of *Panax ginseng*, which plays an important role in inhibiting apoptosis and stabilizing mitochondrial function. In a proteomic analysis of ischemic myocardial SCs, the NADH dehydrogenase subunit of mitochondrial complex I was identified as a GRb1-regulated effector protein, primarily through reduced complex I-dependent oxygen consumption and inhibited enzyme activity.⁷⁶ Furthermore, Venkatesh et al. found that GRb1 binds to the NADH-ubiquinone oxidoreductase chain 3 (ND3) subunit, trapping mitochondrial complex I in an inactive form. This interaction reduces NADH dehydrogenase activity and ROS production, significantly alleviating myocardial ischemia/reperfusion (I/R) injury.⁷⁶

Clinical application of stem cell mitochondrial proteomics

Regenerative medicine and stem cell therapy

Regenerative medicine is an emerging field in health science research that focuses on generating and developing specific functional biological substitutes to restore, replace, or improve tissue and organ function. With no immune suppression and reduced toxicity, it can avoid the huge costs incurred by lifelong anti-rejection therapy. Recently, organoid culture technology has gradually emerged. It can construct three-dimensional (3D) cellular structures resembling real human organs, providing a valuable platform for disease modeling and drug screening.

Stem-cell-based therapies, including human PSCs and MSCs, are central to regenerative medicine. The mechanism of SC-mediated mitochondrial transfer shows clinical potential. For example, iPSC-derived mesenchymal SCs have been shown to treat neuronal damage post-cerebral infarction through the mitochondrial delivery mechanism.⁹¹ In addition, MS and bioinformatics analysis are now used to study traditional Chinese medicine's (TCM) effects on mitochondrial proteomics in lung MSCs, aiming to identify new targets and approaches for pulmonary fibrosis.^{92,93}

Mitochondrial proteomics also contributes a lot to the identification of key biomarkers of signaling pathways and is crucial for understanding the behavior of cells and organoids in various therapeutic environments. In a COVID-19 study, RNA sequencing and proteomic analysis of severe acute respiratory syndrome coronavirus 2 (SARS-CoV-2) proteins revealed a differential protein: The mitochondrial antiviral-signaling protein (MAVS).⁹⁴ Enhancing MAVS expression in MSCs via electroporation

(to improve plasmid transfection efficiency) increased interferon production and innate immune response, reduced viral distribution, and offered a potential new COVID-19 treatment strategy.⁹⁴

Drug development and disease treatment

The study of mitochondrial proteome can also provide new ideas for drug development and disease treatment. By analyzing the role of mitochondrial proteins in the occurrence and development of diseases, we can not only screen potential therapeutic drugs and reveal their mechanisms of action but also evaluate drug efficacy and safety. Using proteomic technology, clinicians can monitor the changes in mitochondrial proteome in patients after treatment, and judge the efficacy of drugs and potential adverse reactions. This process is crucial for drug selection and dose adjustment in personalized medicine. For example, the proteomic analysis identified a new acute myeloid leukemia subtype (Mito-AML) dependent on mitochondrial complex I and sensitive to venetoclax, a small molecule Bcl-2 inhibitor that disrupts mitochondrial OXPHOS to induce apoptosis.⁹⁵ Studies based on mitochondrial proteomics also highlight endogenous/exogenous mitochondrial-targeted molecules, which show promising hope for clinical application. Resveratrol, e.g., enhances SC survival under oxidative stress by regulating mitochondrial biogenesis and autophagy.^{96,97} Understanding these molecules' effect on mitochondrial function and cellular biological processes aids in the design of more effective drugs.

Anti-aging treatment

Mitochondrial proteomics is a powerful tool for anti-aging research, especially for studying SC energetic disorders and aging-related diseases. It not only helps to reveal the mechanism of targeted mitochondrial proteins (e.g., CPEB4), but also provides new strategies for mitochondrial transfer and anti-aging drug development. Through untargeted proteomics analysis, Zhao et al. revealed that mitochondrial proteins spontaneously released by NSCs were significantly enriched in extracellular vesicles (EVs).⁸⁴ Morphological and functional analysis confirmed the presence of ultrastructurally intact mitochondria in EVs, maintaining membrane potential and respiratory activity. Transferring these mitochondria from EVs to NSCs with mitochondrial DNA defects can rescue mitochondrial function and increase the survival rate of SC.⁸⁴ This mechanism provides a new therapeutic strategy for multiple sclerosis and neural degeneration diseases. Other proteomic studies have found the potential of bone marrow MSC-derived EVs in anti-aging therapy, especially in preserving mitochondrial function. All these findings underscore the critical role of proteomics in understanding SC anti-aging mechanisms and advancing SC-based therapeutic strategies, especially for diseases involving mitochondrial damage.

Personalized medicine

Personalized medicine, also known as precision medicine, is a medical model that integrates multi-dimensional biological information (e.g., genomics, proteomics and metabolomics) to design optimal treatment plans tailored to individual patients. Its goal is to maximize the therapeutic effect and minimize the adverse effects. The core principles include precise diagnostic testing and customized interventions based on patient's unique molecular profiles.

Current applications of personalized medicine primarily focus on identifying genetic variations and developing personalized treatment strategies, particularly in oncology.^{57,98} It also encompasses omics-based approaches for disease risk assessment, drug response prediction, and treatment outcome optimization.

Cancer stem cells (CSCs) have attracted wide attention as a distinct cell population within tumors, critically involved in tumorigenesis, progression, recurrence, and treatment resistance. Integrating multi-omics analysis, especially mitochondrial proteomics, provides new insights into the intrinsic molecular mechanisms of CSCs. In a study by Skvortsov et al., CSCs were isolated and enriched from patient tumor tissues using fluorescence-activated cell sorting (FACS), magnetic-activated cell sorting (MACS), laser microdissection, and 3D culture methods.⁹⁸ Subsequent proteomic profiling of mitochondrial protein expression identified specific surface markers (e.g., CD44, CD24, CD133, ALDH), which reflect the energy metabolism and functional status of tumor cells.⁹⁸ This approach is crucial for understanding tumor heterogeneity and microenvironment dynamics.

In clinical practice, SC mitochondrial proteomics shows promise for disease diagnosis and classification. Analysis of patient mitochondrial proteomes can enhance early diagnosis and accuracy, refine disease subtyping, and guide personalized treatment. Diseases-specific alterations in the mitochondrial proteome (e.g., in neurodegenerative diseases,⁹⁹ cardiovascular diseases⁴ and cancers⁵⁷) can serve as biomarkers. For instance, detecting mitochondrial proteins linked to proliferation, apoptosis or metabolic abnormalities in SCs can aid clinicians in diagnosing disease subtypes, assessing disease severity, and tailoring treatment more accurately. This can help improve therapeutic outcomes, reduce adverse reaction risks, and optimize patient care. Thus, SC mitochondrial proteomics holds significant potential in personalized medicine and may become a cornerstone of future clinical practice.

Limitations

First, it remains unclear whether different sample preparation techniques (e.g., density gradient centrifugation vs magnetic beads isolation) or protein quantification methods (e.g., TMT, iTRAQ and SILAC) exhibit different efficiency in detecting signaling pathway proteins in SCs.

Second, the sensitivity of current techniques may not be sufficient to detect low-abundance proteins that might be involved in key processes such as SC self-renewal, differentiation and apoptosis. This limitation could result in an incomplete characterization of the mitochondrial proteome. Third, standardized protocols for SC mitochondrial proteomics are lacking. Most research groups employ custom methods for sample collection, preparation and data analysis, leading to inconsistencies that hinder cross-study comparisons and impede comprehensive understanding. Fourth, future studies should critically compare existing SC proteomics datasets to assess the presence or absence of specific signaling pathway proteins. Finally, clinical studies are needed to verify the biological roles of specific proteins implied by the SC mitochondrial proteomics. Addressing these limitations is essential to establish the methodology's applicability in answering specific biological questions and advancing SC research.

Conclusions


As a focal point in current life sciences, mitochondrial proteomics provides critical insights into the roles of mitochondrial proteins in SC differentiation, energy metabolism, and aging. These discoveries drive progress in regenerative medicine, anti-aging therapies, drug development, and bioengineering innovations. Advances in protein detection technology, deeper mechanistic studies of SC signaling pathways, expanded clinical trials and interdisciplinary collaborations will accelerate the clinical translation of mitochondrial proteomics.


Use of AI and AI-assisted technologies

Not applicable.

ORCID iDs

Weidong Yao  <https://orcid.org/0009-0009-2088-4310>

Xinyi Yu  <https://orcid.org/0009-0007-6509-0317>

Yameng Wang  <https://orcid.org/0000-0002-9626-3029>

Liang Xia  <https://orcid.org/0000-0003-1195-9375>

References

1. Zakrzewski W, Dobrzyński M, Szymonowicz M, Rybak Z. Stem cells: Past, present, and future. *Stem Cell Res Ther.* 2019;10(1):68. doi:10.1186/s13287-019-1165-5
2. Mishra VK, Shih HH, Parveen F, et al. Identifying the therapeutic significance of mesenchymal stem cells. *Cells.* 2020;9(5):1145. doi:10.3390/cells9051145
3. Gonzales KAU, Polak L, Matos I, et al. Stem cells expand potency and alter tissue fitness by accumulating diverse epigenetic memories. *Science.* 2021;374(6571):eabh2444. doi:10.1126/science.abh2444
4. Maged G, Abdelsamed MA, Wang H, Lotfy A. The potency of mesenchymal stem/stromal cells: Does donor sex matter? *Stem Cell Res Ther.* 2024;15(1):112. doi:10.1186/s13287-024-03722-3
5. Murphy C, Mobasheri A, Tancos Z, Kobolák J, Dinnyés A. The potency of induced pluripotent stem cells in cartilage regeneration and osteoarthritis treatment. *Adv Exp Med Biol.* 2017;1079:55–68. doi:10.1007/5584_2017_141

6. Babenko VA, Silachev DN, Danilina TI, et al. Age-related changes in bone-marrow mesenchymal stem cells. *Cells*. 2021;10(6):1273. doi:10.3390/cells10061273
7. Vining KH, Mooney DJ. Mechanical forces direct stem cell behaviour in development and regeneration. *Nat Rev Mol Cell Biol*. 2017;18(12):728–742. doi:10.1038/nrm.2017.108
8. Wang ZB, Wang ZT, Sun Y, Tan L, Yu JT. The future of stem cell therapies of Alzheimer's disease. *Ageing Res Rev*. 2022;80:101655. doi:10.1016/j.arr.2022.101655
9. Houtgraaf JH, de Jong R, Kazemi K, et al. Intracoronary infusion of allogeneic mesenchymal precursor cells directly after experimental acute myocardial infarction reduces infarct size, abrogates adverse remodeling, and improves cardiac function. *Circ Res*. 2013;113(2):153–166. doi:10.1161/CIRCRESAHA.112.300730
10. Müller P, Lemcke H, David R. Stem cell therapy in heart diseases: Cell types, mechanisms and improvement strategies. *Cell Physiol Biochem*. 2018;48(6):2607–2655. doi:10.1159/000492704
11. Shen X, Wang M, Bi X, et al. Resveratrol prevents endothelial progenitor cells from senescence and reduces the oxidative reaction via PPAR- γ /HO-1 pathways. *Mol Med Rep*. 2016;14(6):5528–5534. doi:10.3892/mmr.2016.5929
12. Wang X, Yao W, Wang M, Zhu J, Xia L. TLR4-SIRT3 mechanism modulates mitochondrial and redox homeostasis and promotes EPCs recruitment and survival. *Oxid Med Cell Longev*. 2022;2022:1282362. doi:10.1155/2022/1282362
13. Ghiasi M, Jadidi K, Hashemi M, Zare H, Salimi A, Aghamollaei H. Application of mesenchymal stem cells in corneal regeneration. *Tissue Cell*. 2021;73:101600. doi:10.1016/j.tice.2021.101600
14. Lin KC, Fang WF, Yeh JN, et al. Outcomes of combined mitochondria and mesenchymal stem cells-derived exosome therapy in rat acute respiratory distress syndrome and sepsis. *World J Stem Cells*. 2024;16(6):690–707. doi:10.4252/wjsc.v16.i6.690
15. Khacho M, Harris R, Slack RS. Mitochondria as central regulators of neural stem cell fate and cognitive function. *Nat Rev Neurosci*. 2019;20(1):34–48. doi:10.1038/s41583-018-0091-3
16. Stanga S, Caretto A, Boido M, Vercelli A. Mitochondrial dysfunctions: A red thread across neurodegenerative diseases. *Int J Mol Sci*. 2020;21(10):3719. doi:10.3390/ijms21103719
17. Chacinska A, Koehler CM, Milenkovic D, Lithgow T, Pfanner N. Importing mitochondrial proteins: Machinery and mechanisms. *Cell*. 2009;138(4):628–644. doi:10.1016/j.cell.2009.08.005
18. Lu JQ, Tarnopolsky MA. Mitochondrial neuropathy and neurogenic features in mitochondrial myopathy. *Mitochondrion*. 2021;56:52–61. doi:10.1016/j.mito.2020.11.005
19. Pereira CV, Peralta S, Arguello T, Bacman SR, Diaz F, Moraes CT. Myopathy reversion in mice after restoration of mitochondrial complex I. *EMBO Mol Med*. 2020;12(2):e10674. doi:10.15252/emmm.201910674
20. Bhatia S, Rawal R, Sharma P, Singh T, Singh M, Singh V. Mitochondrial dysfunction in Alzheimer's disease: Opportunities for drug development. *Curr Neuropsychopharmacol*. 2022;20(4):675–692. doi:10.2174/1570159X19666210517114016
21. D'Alessandro MCB, Kanaan S, Geller M, Praticò D, Daher JPL. Mitochondrial dysfunction in Alzheimer's disease. *Ageing Res Rev*. 2025;107:102713. doi:10.1016/j.arr.2025.102713
22. Song L, Cortopassi G. Mitochondrial complex I defects increase ubiquitin in substantia nigra. *Brain Res*. 2015;1594:82–91. doi:10.1016/j.brainres.2014.11.013
23. Almikhlaifi MA, Karami MM, Jana A, et al. Mitochondrial medicine: A promising therapeutic option against various neurodegenerative disorders. *Curr Neuropsychopharmacol*. 2023;21(5):1165–1183. doi:10.2174/1570159X20666220830112408
24. Ribeiro MF, Genebra T, Rego AC, Rodrigues CMP, Solá S. Amyloid β peptide compromises neural stem cell fate by irreversibly disturbing mitochondrial oxidative state and blocking mitochondrial biogenesis and dynamics. *Mol Neurobiol*. 2019;56(6):3922–3936. doi:10.1007/s12035-018-1342-z
25. Coelho P, Fão L, Mota S, Rego AC. Mitochondrial function and dynamics in neural stem cells and neurogenesis: Implications for neurodegenerative diseases. *Ageing Res Rev*. 2022;80:101667. doi:10.1016/j.arr.2022.101667
26. Scandella V, Petrelli F, Moore DL, Braun SMG, Knobloch M. Neural stem cell metabolism revisited: A critical role for mitochondria. *Trends Endocrinol Metab*. 2023;34(8):446–461. doi:10.1016/j.tem.2023.05.008
27. Gao Q, Tian R, Han H, et al. PINK1-mediated Drp1S616 phosphorylation modulates synaptic development and plasticity via promoting mitochondrial fission. *Sig Transduct Target Ther*. 2022;7(1):103. doi:10.1038/s41392-022-00933-z
28. Graier WF, Malli R, Kostner GM. Mitochondrial protein phosphorylation: Instigator or target of lipotoxicity? *Trends Endocrinol Metab*. 2009;20(4):186–193. doi:10.1016/j.tem.2009.01.004
29. Lin YT, Chen ST, Chang JC, Teoh RJ, Liu CS, Wang GJ. Green extraction of healthy and additive free mitochondria with a conventional centrifuge. *Lab Chip*. 2019;19(22):3862–3869. doi:10.1039/C9LC00633H
30. Liao PC, Bergamini C, Fato R, Pon LA, Pallotti F. Isolation of mitochondria from cells and tissues. *Methods Cell Biol*. 2020;155:3–31. doi:10.1016/bs.mcb.2019.10.002
31. Chandra K, Kumar V, Werner SE, Odom TW. Separation of stabilized MOPS gold nanostars by density gradient centrifugation. *ACS Omega*. 2017;2(8):4878–4884. doi:10.1021/acsomega.7b00871
32. Chen BY, Sung CWH, Chen C, et al. Advances in exosomes technology. *Clin Chim Acta*. 2019;493:14–19. doi:10.1016/j.cca.2019.02.021
33. Ććija-Arenas Á, Román-Pizarro V, Fernández-Romero JM. Luminescence continuous flow system for monitoring the efficiency of hybrid liposomes separation using multiphase density gradient centrifugation. *Talanta*. 2021;222:121532. doi:10.1016/j.talanta.2020.121532
34. Hu P, Fabyanic E, Kwon DY, Tang S, Zhou Z, Wu H. Dissecting cell-type composition and activity-dependent transcriptional state in mammalian brains by massively parallel single-nucleus RNA-Seq. *Mol Cell*. 2017;68(5):1006–1015.e7. doi:10.1016/j.molcel.2017.11.017
35. Léger JL, Jouglaux JL, Savadogo F, Pichaud N, Boudreau LH. Rapid isolation and purification of functional platelet mitochondria using a discontinuous Percoll gradient. *Platelets*. 2020;31(2):258–264. doi:10.1080/09537104.2019.1609666
36. Hassani M, Hellebrekers P, Chen N, et al. On the origin of low-density neutrophils. *J Leukoc Biol*. 2020;107(5):809–818. doi:10.1002/JLB.5HR0120-459R
37. Shi W, Wang Y, Zhang C, et al. Isolation and purification of immune cells from the liver. *Int Immunopharmacol*. 2020;85:106632. doi:10.1016/j.intimp.2020.106632
38. Grist TM, Canon CL, Fishman EK, Kohi MP, Mossa-Basha M. Short-, mid- and long-term strategies to manage the shortage of iohexol. *Radiology*. 2022;304(2):289–293. doi:10.1148/radiol.221183
39. Liang S, Su M, Liu B, et al. Evaluation of blood induced influence for high-definition intravascular ultrasound (HD-IVUS). *IEEE Trans Ultrason Ferroelect Freq Contr*. 2022;69(1):98–105. doi:10.1109/TUFFC.2021.3108163
40. Warwick J, Holness J. Measurement of glomerular filtration rate. *Semin Nucl Med*. 2022;52(4):453–466. doi:10.1053/j.semnuclmed.2021.12.005
41. Elgamel S, Cocucci E, Sass EJ, et al. Optimizing extracellular vesicles' isolation from chronic lymphocytic leukemia patient plasma and cell line supernatant. *JCI Insight*. 2021;6(15):e137937. doi:10.1172/jci.insight.137937
42. Inoue T, Kusumoto S, Iio E, et al. Clinical efficacy of a novel, high-sensitivity HBcrAg assay in the management of chronic hepatitis B and HBV reactivation. *J Hepatol*. 2021;75(2):302–310. doi:10.1016/j.jhep.2021.02.017
43. Veerman RE, Teeuwen L, Czarnewski P, et al. Molecular evaluation of five different isolation methods for extracellular vesicles reveals different clinical applicability and subcellular origin. *J Extracell Vesicles*. 2021;10(9):e12128. doi:10.1002/jev2.12128
44. Boussard C, Keech O. Cell type-specific isolation of mitochondria in arabidopsis. *Methods Mol Biol*. 2022;2363:13–23. doi:10.1007/978-1-0716-1653-6_2
45. Chen WW, Freinkman E, Sabatini DM. Rapid immunopurification of mitochondria for metabolite profiling and absolute quantification of matrix metabolites. *Nat Protoc*. 2017;12(10):2215–2231. doi:10.1038/nprot.2017.104
46. Ichibangase T, Imai K. Application of fluorogenic derivatization-liquid chromatography-tandem mass spectrometric proteome method to skeletal muscle proteins in fast thoroughbred horses. *J Proteome Res*. 2009;8(4):2129–2134. doi:10.1021/pr801004s
47. Ludwig C, Gillet L, Rosenberger G, Amon S, Collins BC, Aebersold R. Data-independent acquisition-based SWATH-MS for quantitative proteomics: A tutorial. *Mol Syst Biol*. 2018;14(8):e8126. doi:10.15252/msb.20178126

48. Bai B, Vanderwall D, Li Y, et al. Proteomic landscape of Alzheimer's Disease: Novel insights into pathogenesis and biomarker discovery [Erratum in: *Mol Neurodegener.* 2021;16(1):72. doi:10.1186/s13024-021-00493-w]. *Mol Neurodegener.* 2021;16(1):55. doi:10.1186/s13024-021-00474-z
49. Erdjument-Bromage H, Huang FK, Neubert TA. Sample preparation for relative quantitation of proteins using tandem mass tags (TMT) and mass spectrometry (MS). *Methods Mol Biol.* 2018;1741:135–149. doi:10.1007/978-1-4939-7659-1_11
50. Zhu Y, Bian JF, Lu DQ, et al. Alteration of EIF2 signaling, glycolysis, and dopamine secretion in form-deprived myopia in response to 1% atropine treatment: Evidence from interactive iTRAQ-MS and SWATH-MS proteomics using a guinea pig model. *Front Pharmacol.* 2022;13:814814. doi:10.3389/fphar.2022.814814
51. Billing C, Walker M, Noack N, et al. Features of lineage-specific hematopoietic metabolism revealed by mitochondrial proteomics. *Proteomics.* 2017;17(15–16):1700053. doi:10.1002/pmic.201700053
52. Balas MM, Porman AM, Hansen KC, Johnson AM. SILAC-MS profiling of reconstituted human chromatin platforms for the study of transcription and RNA regulation. *J Proteome Res.* 2018;17(10):3475–3484. doi:10.1021/acs.jproteome.8b00395
53. Klykov O, Kopylov M, Carragher B, Heck AJR, Noble AJ, Scheltema RA. Label-free visual proteomics: Coupling MS- and EM-based approaches in structural biology. *Mol Cell.* 2022;82(2):285–303. doi:10.1016/j.molcel.2021.12.027
54. Vidova V, Spacil Z. A review on mass spectrometry-based quantitative proteomics: Targeted and data independent acquisition. *Anal Chim Acta.* 2017;964:7–23. doi:10.1016/j.aca.2017.01.059
55. Sabatier P, Beusch CM, Saei AA, et al. An integrative proteomics method identifies a regulator of translation during stem cell maintenance and differentiation. *Nat Commun.* 2021;12(1):6558. doi:10.1038/s41467-021-26879-4
56. Aly KA, Moutaoufik MT, Phanse S, Zhang Q, Babu M. From fuzziness to precision medicine: On the rapidly evolving proteomics with implications in mitochondrial connectivity to rare human disease. *iScience.* 2021;24(2):102030. doi:10.1016/j.isci.2020.102030
57. Raghavan S, Mehta P, Ward MR, et al. Personalized medicine-based approach to model patterns of chemoresistance and tumor recurrence using ovarian cancer stem cell spheroids. *Clin Cancer Res.* 2017;23(22):6934–6945. doi:10.1158/1078-0432.CCR-17-0133
58. Xu H, Jiao D, Liu A, Wu K. Tumor organoids: applications in cancer modeling and potentials in precision medicine. *J Hematol Oncol.* 2022;15(1):58. doi:10.1186/s13045-022-01278-4
59. Alexander C, Votruba M, Pesch UEA, et al. OPA1, encoding a dynamin-related GTPase, is mutated in autosomal dominant optic atrophy linked to chromosome 3q28. *Nat Genet.* 2000;26(2):211–215. doi:10.1038/79944
60. Chen H, Detmer SA, Ewald AJ, Griffin EE, Fraser SE, Chan DC. Mitofusins Mfn1 and Mfn2 coordinately regulate mitochondrial fusion and are essential for embryonic development. *J Cell Biol.* 2003;160(2):189–200. doi:10.1083/jcb.200211046
61. Khacho M, Clark A, Svoboda DS, et al. Mitochondrial dynamics impacts stem cell identity and fate decisions by regulating a nuclear transcriptional program. *Cell Stem Cell.* 2016;19(2):232–247. doi:10.1016/j.stem.2016.04.015
62. Gilkerson R, De La Torre P, St. Vallier S. Mitochondrial OMA1 and OPA1 as gatekeepers of organellar structure/function and cellular stress response. *Front Cell Dev Biol.* 2021;9:626117. doi:10.3389/fcell.2021.626117
63. Baker N, Wade S, Triolo M, et al. The mitochondrial protein OPA1 regulates the quiescent state of adult muscle stem cells. *Cell Stem Cell.* 2022;29(9):1315–1332.e9. doi:10.1016/j.stem.2022.07.010
64. Diao Z, Ji Q, Wu Z, et al. SIRT3 consolidates heterochromatin and counteracts senescence [Erratum in: *Nucleic Acids Res.* 2021;49(15):9004–9006. doi:10.1093/nar/gkab698]. *Nucl Acids Res.* 2021;49(8):4203–4219. doi:10.1093/nar/gkab161
65. Sancho P, Burgos-Ramos E, Tavera A, et al. MYC/PGC-1 α balance determines the metabolic phenotype and plasticity of pancreatic cancer stem cells. *Cell Metab.* 2015;22(4):590–605. doi:10.1016/j.cmet.2015.08.015
66. Zhang Q, Siyuan Z, Xing C, Ruxiu L. SIRT3 regulates mitochondrial function: A promising star target for cardiovascular disease therapy. *Biomed Pharmacother.* 2024;170:116004. doi:10.1016/j.biopha.2023.116004
67. Martinou JC, Youle RJ. Mitochondria in apoptosis: Bcl-2 family members and mitochondrial dynamics. *Dev Cell.* 2011;21(1):92–101. doi:10.1016/j.devcel.2011.06.017
68. Youle RJ, Strasser A. The BCL-2 protein family: Opposing activities that mediate cell death. *Nat Rev Mol Cell Biol.* 2008;9(1):47–59. doi:10.1038/nrm2308
69. Wani GA, Sprenger HG, Ndoci K, et al. Metabolic control of adult neural stem cell self-renewal by the mitochondrial protease YME1L. *Cell Rep.* 2022;38(7):110370. doi:10.1016/j.celrep.2022.110370
70. Shekari F, Nezari H, Larijani MR, et al. Proteome analysis of human embryonic stem cells organelles. *J Proteomics.* 2017;162:108–118. doi:10.1016/j.jprot.2017.04.017
71. Liang KX, Kristiansen CK, Mostafavi S, et al. Disease-specific phenotypes in iPSC-derived neural stem cells with *POLG* mutations. *EMBO Mol Med.* 2020;12(10):e12146. doi:10.15252/emmm.202012146
72. Sánchez-Aragó M, García-Bermúdez J, Martínez-Reyes I, Santacatterina F, Cuezva JM. Degradation of IF1 controls energy metabolism during osteogenic differentiation of stem cells. *EMBO Rep.* 2013;14(7):638–644. doi:10.1038/embor.2013.72
73. Sebastian C, Ferrer C, Serra M, et al. A non-dividing cell population with high pyruvate dehydrogenase kinase activity regulates metabolic heterogeneity and tumorigenesis in the intestine. *Nat Commun.* 2022;13(1):1503. doi:10.1038/s41467-022-29085-y
74. Hu Z, Wang D, Gong J, et al. MSCs deliver hypoxia-treated mitochondria reprogramming acinar metabolism to alleviate severe acute pancreatitis injury. *Adv Sci (Weinh).* 2023;10(25):2207691. doi:10.1002/advs.202207691
75. Xu X, Jin K, Bais AS, et al. Uncompensated mitochondrial oxidative stress underlies heart failure in an iPSC-derived model of congenital heart disease. *Cell Stem Cell.* 2022;29(5):840–855.e7. doi:10.1016/j.stem.2022.03.003
76. Venkatesh S, Baljinnyam E, Tong M, et al. Proteomic analysis of mitochondrial biogenesis in cardiomyocytes differentiated from human induced pluripotent stem cells. *Am J Physiol Regul Integr Comp Physiol.* 2021;320(4):R547–R562. doi:10.1152/ajpregu.00207.2020
77. Jiang L, Yin X, Chen YH, et al. Proteomic analysis reveals ginsenoside Rb1 attenuates myocardial ischemia/reperfusion injury through inhibiting ROS production from mitochondrial complex I. *Theranostics.* 2021;11(4):1703–1720. doi:10.7150/thno.43895
78. Nicolay BN, Danielian PS, Kottakis F, et al. Proteomic analysis of pRb loss highlights a signature of decreased mitochondrial oxidative phosphorylation. *Genes Dev.* 2015;29(17):1875–1889. doi:10.1101/gad.264127.115
79. Takebayashi S, Tanaka H, Hino S, et al. Retinoblastoma protein promotes oxidative phosphorylation through upregulation of glycolytic genes in oncogene-induced senescent cells. *Aging Cell.* 2015;14(4):689–697. doi:10.1111/acer.12351
80. Wang Y, Barthez M, Chen D. Mitochondrial regulation in stem cells. *Trends Cell Biol.* 2024;34(8):685–694. doi:10.1016/j.tcb.2023.10.003
81. Qiu X, Brown K, Hirschey MD, Verdin E, Chen D. Calorie restriction reduces oxidative stress by SIRT3-mediated SOD2 activation. *Cell Metab.* 2010;12(6):662–667. doi:10.1016/j.cmet.2010.11.015
82. Su L, Zhang J, Gomez H, Kellum JA, Peng Z. Mitochondria ROS and mitophagy in acute kidney injury. *Autophagy.* 2023;19(2):401–414. doi:10.1080/15548627.2022.2084862
83. König T, Nolte H, Aaltonen MJ, et al. MIROs and DRP1 drive mitochondrial-derived vesicle biogenesis and promote quality control. *Nat Cell Biol.* 2021;23(12):1271–1286. doi:10.1038/s41556-021-00798-4
84. Zhao M, Liu S, Wang C, et al. Mesenchymal stem cell-derived extracellular vesicles attenuate mitochondrial damage and inflammation by stabilizing mitochondrial DNA. *ACS Nano.* 2021;15(1):1519–1538. doi:10.1021/acsnano.0c08947
85. Zhang S, Xie Y, Yan F, et al. Negative pressure wound therapy improves bone regeneration by promoting osteogenic differentiation via the AMPK-ULK1-autophagy axis. *Autophagy.* 2022;18(9):2229–2245. doi:10.1080/15548627.2021.2016231
86. Zeng W, Zhang W, Tse EHY, et al. Restoration of CPEB4 prevents muscle stem cell senescence during aging. *Dev Cell.* 2023;58(15):1383–1398.e6. doi:10.1016/j.devcel.2023.05.012
87. Yuan S, Wei C, Liu G, et al. Sorafenib attenuates liver fibrosis by triggering hepatic stellate cell ferroptosis via HIF-1 α /SLC7A11 pathway. *Cell Prolif.* 2022;55(1):e13158. doi:10.1111/cpr.13158

88. Zeb A, Choubey V, Gupta R, Veksler V, Kaasik A. Negative feedback system to maintain cell ROS homeostasis: KEAP1-PGAM5 complex senses mitochondrially generated ROS to induce mitophagy. *Autophagy*. 2022;18(9):2249–2251. doi:10.1080/15548627.2021.2024702
89. Baird L, Yamamoto M. The molecular mechanisms regulating the KEAP1-NRF2 pathway. *Mol Cell Biol*. 2020;40(13):e00099–20. doi:10.1128/MCB.00099-20
90. Koch M, Kockmann T, Rodriguez E, et al. Quantitative proteomics identifies reduced NRF2 activity and mitochondrial dysfunction in atopic dermatitis. *J Invest Dermatol*. 2023;143(2):220–231.e7. doi:10.1016/j.jid.2022.08.048
91. Yang Y, Ye G, Zhang YL, et al. Transfer of mitochondria from mesenchymal stem cells derived from induced pluripotent stem cells attenuates hypoxia-ischemia-induced mitochondrial dysfunction in PC12 cells. *Neural Regen Res*. 2020;15(3):464. doi:10.4103/1673-5374.266058
92. Ke S, Yue X, Zhu W. Treatment of pulmonary fibrosis by whole course warming from the perspective of mitochondria of pulmonary mesenchymal stem cells [in Chinese]. *China Journal of Traditional Chinese Medicine and Pharmacy*. 2020;35(5):2491–2494.
93. Mo L, Xiu M, Zhu G, et al. Effect of Wenfei Huaxian decoction on aerobic glycolysis of hydrogen peroxide-induced oxidative stress injury of lung mesenchymal stem cells in mice [in Chinese]. *SinoMed*. 2022;63(3):262–268.
94. Suman S, Domingues A, Ratajczak J, Ratajczak MZ. Potential clinical applications of stem cells in regenerative medicine. *Adv Exp Med Biol*. 2019;1201:1–22. doi:10.1007/978-3-030-31206-0_1
95. Jayavelu AK, Wolf S, Buettner F, et al. The proteogenomic subtypes of acute myeloid leukemia. *Cancer Cell*. 2022;40(3):301–317.e12. doi:10.1016/j.ccell.2022.02.006
96. Mestareehi A, Li H, Zhang X, et al. Quantitative proteomics reveals transforming growth factor β receptor targeted by resveratrol and hesperetin coformulation in endothelial cells. *ACS Omega*. 2023;8(18):16206–16217. doi:10.1021/acsomega.3c00678
97. Baur JA, Pearson KJ, Price NL, et al. Resveratrol improves health and survival of mice on a high-calorie diet. *Nature*. 2006;444(7117):337–342. doi:10.1038/nature05354
98. Skvortsov S, Debbage P, Skvortsova I. Proteomics of cancer stem cells. *Int J Radiat Biol*. 2014;90(8):653–658. doi:10.3109/09553002.2013.873559
99. Trushina E, Trushin S, Hasan MF. Mitochondrial complex I as a therapeutic target for Alzheimer's disease. *Acta Pharm Sin B*. 2022;12(2):483–495. doi:10.1016/j.apsb.2021.11.003

The evolution of transanal approaches in rectal cancer surgery

Sara Lauricella^{1,A,D–F}, Francesco Brucchi^{2,D,E}, Roberto Cirocchi^{3,E,F}

¹ Colorectal Surgery Division, Department of Surgery, Fondazione IRCCS Istituto Nazionale dei Tumori, Milan, Italy

² General Surgery Residency Program, University of Milan, Italy

³ Digestive and Emergency Surgery Unit, Santa Maria Hospital Trust, Terni, Italy

A – research concept and design; B – collection and/or assembly of data; C – data analysis and interpretation;

D – writing the article; E – critical revision of the article; F – final approval of the article

Advances in Clinical and Experimental Medicine, ISSN 1899–5276 (print), ISSN 2451–2680 (online)

Adv Clin Exp Med. 2025;34(12):2187–2196

Address for correspondence

Sara Lauricella

E-mail: lauricella3008@gmail.com

Funding sources

None declared

Conflict of interest

None declared

Received on February 25, 2025

Reviewed on March 30, 2025

Accepted on March 31, 2025

Published online on August 19, 2025

Abstract

Minimally invasive techniques are progressively transforming colorectal (CRC) surgery. Given the high mortality and morbidity rates associated with conventional surgical treatments for CRC, the development of less invasive alternatives is crucial. The long-established use of transanal platforms for local excision of early-stage rectal cancers paved the way for the development of a transanal approach to total mesorectal excision (TME). Transanal total mesorectal excision (taTME) has emerged as a novel technique for treating low CRC, offering superior and more accurate visualization of the presacral mesorectal plane compared to the abdominal approach, and providing particular advantages in the narrow male pelvis. The current data on oncological and functional outcomes are promising. The transanal transection and single-stapled anastomosis (TTSS) approach represents the latest advancement in transanal techniques for treating low CRC. Evolving from taTME, it provides a more controlled and potentially safer anastomotic technique. However, the data are still preliminary, and larger studies are needed to validate its effectiveness. This review explores the evolution of minimally invasive and transanal surgical techniques for low CRC treatment, comparing outcomes across various approaches with a focus on patient selection criteria and oncological results.

Key words: rectal cancer, transanal excision, transanal endoscopic surgery, transanal total mesorectal excision (taTME), transanal transection and single-stapled anastomosis (TTSS)

Cite as

Lauricella S, Brucchi F, Cirocchi R. The evolution of transanal approaches in rectal cancer surgery. *Adv Clin Exp Med.* 2025;34(12):2187–2196. doi:10.17219/acem/203579

DOI

10.17219/acem/203579

Copyright

Copyright by Author(s)

This is an article distributed under the terms of the Creative Commons Attribution 3.0 Unported (CC BY 3.0) (<https://creativecommons.org/licenses/by/3.0/>)

Highlights

- Advanced transanal surgical techniques boost precision in rectal cancer care: Innovations over recent decades have refined minimally invasive approaches, reducing patient morbidity and improving surgical accuracy.
- Evolution from TAE to taTME and TTSS expands early-stage rectal cancer options: Transitioning from traditional transanal local excision (TAE) to transanal total mesorectal excision (taTME) and transanal transection with single-stapled anastomosis (TTSS) offers more effective resections.
- taTME and TTSS enhance mesorectal plane dissection and specimen quality: These cutting-edge methods for low rectal tumors deliver superior oncological outcomes by preserving critical pelvic anatomy.
- Strategic patient selection maximizes transanal surgery success: Matching individual tumor characteristics to the optimal transanal technique is essential, since expertise in taTME, TTSS, and TAE drives best-practice results.

Introduction

Colorectal cancer (CRC) poses a significant global health challenge due to its high incidence and mortality rates,¹ making it one of the leading causes of cancer-related deaths worldwide. Effective management of CRC requires a coordinated, multidisciplinary approach to ensure the best possible outcomes for patients. Recently, the management of early CRC has progressed considerably, driven by advancements in diagnostics, surgical techniques and multimodal therapies.² When treated appropriately, the prognosis for patients diagnosed with stage I rectal cancer is generally favorable, with 5-year survival rates exceeding 90%.³

Local excision has been fundamental for select early-stage rectal tumors. Transanal local excision (TAE) was initially used as a minimally invasive method to remove small lesions. However, as technology advanced, novel approaches such as transanal endoscopic microsurgery (TEM), transanal endoscopic operation (TEO) and transanal minimally invasive surgery (TAMIS) emerged. These techniques build upon TAE and have significantly enhanced surgical precision, visualization and access, while reducing patient morbidity and improving postoperative outcomes.^{4–8} By combining the benefits of local excision with oncological results comparable to those of more radical surgeries, these techniques offer a promising alternative for select patients with early-stage CRC.⁹ However, these advanced techniques require highly specialized training and expertise, and not all centers have the necessary equipment or experienced surgeons to perform these procedures effectively. Additionally, appropriate patient selection remains crucial for achieving optimal outcomes.

Natural orifice transluminal endoscopic surgery (NOTES) has further pushed the boundaries of minimally invasive surgery by eliminating external incisions and reducing associated risks such as wound infections and hernias.¹⁰ Initially developed in animal models, NOTES has been explored through various natural orifice routes.^{11,12} Although its clinical application is still considered experimental, it holds considerable potential for future therapeutic use. Meanwhile, hybrid approaches like transanal

total mesorectal (taTME), which builds on the principles of the Transanal Abdominal Transanal Proctosigmoidectomy (TATA) technique, have shown promise in offering safe, precise and minimally invasive alternatives for CRC surgery.¹³ The development of taTME has been driven by the need to enhance visualization and access within the deep and narrow pelvic cavity – an anatomical region that poses significant challenges for traditional laparoscopic or open surgical approaches. The pioneering work of Sylla et al.¹⁴ has paved the way for a more targeted and effective approach to CRC resection. By combining transanal and transabdominal approaches for mesorectal dissection (the precise removal of rectal tissue and surrounding lymphatics), taTME addresses limitations of conventional transabdominal total mesorectal excision (TME). This dual approach enables more precise dissection, improved visualization of critical pelvic anatomy and tighter control of distal resection margins (the cut edge closest to the anus).¹⁵

A recent advancement in transanal approaches for low rectal tumors is transanal transection and single-stapled anastomosis (TTSS). Introduced in 2019, TTSS was designed to overcome the limitations of earlier transanal methods by balancing oncological efficacy with functional outcomes. Although TTSS appears promising, the available data remain preliminary.

Objectives

The objectives of this study are twofold. First, to map the historical evolution of transanal surgical techniques used in the management of rectal tumors. Second, to compare contemporary transanal approaches – including TEM, TEO, TAMIS, taTME, and TTSS – with respect to morbidity, recurrence rates and survival outcomes.

Methodology

A comprehensive search was conducted in PubMed, Embase and Cochrane Library databases. The search strategy

used a combination of free-text terms and MeSH terms. Key search terms included: “transanal,” “rectal cancer,” “early-stage rectal cancer,” “transanal excision,” “transanal endoscopic surgery,” “TEM,” “TEO,” “TAMIS,” “taTME,” and “TTSS.” Boolean operators (AND, OR) were applied to combine these terms. No date limit was applied, and studies published up to January 2025 were included. Studies were included if they were original research, written in English and focused on transanal surgical management of CRC. There were no limitations on the number of participants or the age of patients. Exclusion parameters included studies on non-surgical treatments, studies not available in full text and articles unrelated to the topic of transanal surgical techniques for CRC. Two authors independently screened the titles and abstracts and reviewed full texts to assess eligibility based on predefined criteria. Any disagreements were resolved through discussion or, if necessary, by consulting a 3rd reviewer. Data were collected on various aspects, including general disease information, surgical details (e.g., type of procedure, surgical approach, instrumentation) and outcomes (e.g., morbidity, complication rates, recurrence rates, etc.). The most pertinent articles were selected for inclusion in this review.

Transanal local excision

The TAE, first introduced by Parks in 1970, was a pioneering endoluminal approach for the resection of select rectal tumors.¹⁶ At its inception, TAE provided a less invasive alternative to traditional abdominal procedures, offering key benefits such as reduced recovery times, shorter length of stay (LOS) and lower complication rates for carefully selected patients.^{17,18} Transanal local excision can be performed for selected early tumors that lack adverse prognostic factors, such as poor differentiation or lymphovascular invasion.² The American Radium Society also supports the use of TAE for stage cT1N0 CRC, as defined by endorectal ultrasound or magnetic resonance imaging, provided specific patient selection criteria are met.¹⁹ The tumor should be smaller than 3 cm in size and well or moderately differentiated. It must be located in the low rectum and involve <30% of the rectal circumference. There should be no evidence of nodal involvement. Negative margins (greater than 3 mm) are required, and the excision must be feasible as a full-thickness procedure.

This technique is relatively straightforward and can be performed with ease. It does not require specialized equipment or an extensive learning curve; rather, anal retractors are used to facilitate access and visualization, making it a more cost-effective treatment option. One of the key advantages of TAE is its minimal impact, if any, on anorectal and urogenital function. However, one limitation is that visualization during the procedure can be suboptimal, potentially affecting the quality of the oncologic resection margins. This issue is further compounded by concerns about the high rates of tumor fragmentation and

recurrence associated with TAE, which are likely linked to margin positivity – reported in over 10% of cases, even in the most experienced centers.^{20,21} In a prospective Norwegian study, patients with T1 CRC treated with TAE had significantly higher 5-year local recurrence rates, reduced survival rates and lower disease-free survival (DFS) rates compared to those who underwent radical surgery.²²

For T2 tumors, TAE may be considered in highly selected patients, particularly those who are not optimal candidates for more radical surgery due to comorbid conditions. However, the risk of locoregional recurrence is higher for T2 tumors, and neoadjuvant chemoradiation may be used to downstage the tumor before considering TAE.^{23,24}

Transanal endoscopic surgery: TEM, TAO, TAMIS

A decade later, several anorectal surgical techniques incorporating various instruments were developed. Transanal endoscopic surgery (TES) refers collectively to techniques – including TEM, TEO and TAMIS – that employ endoscopic platforms to excise rectal lesions.

Transanal endoscopic surgery platforms are currently employed for the treatment of endoscopically unresectable rectal adenomas, as well as for early-stage rectal cancers (T1 lesions).^{5,7} They are also employed in cases where previous resections have been incomplete or performed piecemeal,²⁵ and in selected cases of more advanced rectal cancers, typically in palliative or experimental settings. Beyond selected early-stage rectal cancers, TES has been successfully applied for the removal of various other types of tumors. It has also proven effective in treating benign conditions, including stricturoplasty, repair of complex urogenital fistulas and anastomotic leakage.^{26–30}

The TEM platform, originally developed by Gerald Buess in 1982, was introduced as an advanced endoscopic tool for the local resection of rectal tumors.³¹ Transanal endoscopic microsurgery has emerged as an effective technique for the treatment of early-stage CRC and large sessile adenomas that cannot be removed locally or through conventional colonoscopic resection. The procedure employs a specialized rigid operating rectoscope, typically ranging from 12 to 20 cm in length, which is introduced transanally to provide enhanced visualization and precision during excision. This rectoscope features an optical system that offers a magnified, three-dimensional (3D) view of the surgical area, enabling precise full-thickness resections perpendicularly through the bowel wall into the perirectal fat, and is paired with endoscopic instruments. Transanal endoscopic microsurgery is particularly advantageous for tumors located in the mid and upper rectum, which are difficult to access with conventional transanal excision techniques. The procedure maintains a stable pneumorectum using carbon dioxide insufflation, which enhances visibility and facilitates meticulous dissection and suturing.^{6,32}

Transanal endoscopic microsurgery has been shown to provide superior oncological outcomes compared to TAE for T1 rectal lesions. It is associated with lower rates of positive surgical margins and a reduced risk of local recurrence. Research by Christoforidis et al. demonstrated that TEM resulted in fewer positive margins (2% vs 16%, $p = 0.017$) and better DFS for tumors located ≥ 5 cm from the anal verge.³³ Sgourakis et al. also found that TEM significantly lowered the chances of positive margins and local recurrences compared to TAE.³⁴ These findings were further supported by a more recent meta-analysis, which showed that TEM achieved a higher rate of negative microscopic margins, a lower rate of specimen fragmentation and a reduced rate of lesion recurrence, with no significant difference in postoperative complications when compared to TAE.³⁵ These findings collectively suggest that TEM offers oncological superiority over TAE.

A more cost-effective alternative to TEM was introduced a few years later: the TEO platform by Karl Storz (Tuttlingen, Germany). This innovative and more straightforward tool has gained widespread adoption. The TEO platform utilizes a rigid rectoscope (working length: 7.5–15 cm), curved laparoscopic operating instruments and a two-dimensional (2D) visualization system.³⁶ The indications for TEO are comparable to those of TEM, although, like TEM, it presents challenges in excising lesions close to the anal verge. Transanal endoscopic operation benefits from lower costs associated with standard laparoscopic instruments, equipment and setup, making it more accessible to surgeons with prior laparoscopic experience.

Both TEM and TEO utilize rigid platforms, with the telescope fixed to a rigid steel proctoscope. Initially, these rigid platforms provided a stable surgical field but were limited by their lack of flexibility and the restricted field of view they offered. These limitations often resulted in prolonged setup times and difficulties in maneuvering instruments, especially in the distal rectum.³⁷

Due to the significant costs associated with TEM and the extensive learning curve required to master the technique, an alternative transanal approach utilizing a single, disposable, multichannel port was introduced in 2010 by Atallah et al., now known as TAMIS.³⁸ This advancement has contributed to the wider implementation of TES techniques, with a range of ports now available. The development of flexible platforms, in contrast to the rigid operating rectoscope, has resulted in reduced setup times and operative times,³⁹ atraumatic retraction, and better compatibility with standard laparoscopic instruments and conventional CO₂ insufflator, which are more accessible and cost-effective compared to the specialized, high-cost equipment required for TEM.^{38,40} Additionally, TAMIS requires a less steep learning curve compared to TEM, as it utilizes familiar laparoscopic instruments and techniques, making it easier for surgeons with existing laparoscopic expertise to adopt the procedure.⁴⁰ It also provides more flexibility in patient positioning; unlike TEM, which often necessitates

specific positioning depending on the tumor's location, TAMIS can be performed with the patient in a standard position.⁴¹ However, it poses challenges in suturing due to its narrower operative field and more frequent instrument conflicts compared to TEM.^{37,42} The longer channels of the TEM and TEO systems, on the other hand, facilitate intraluminal retraction of the rectum, allowing for better access and visibility during resection. In contrast, TAMIS often requires an assistant to maneuver the laparoscope, increasing complexity, and can be more difficult to access and removing rectal lesions behind a haustral valve.

While TAMIS is particularly effective for lesions in the mid to upper rectum, it has also been successfully used for lesions in the lower rectum.⁴³ Furthermore, TAMIS has been associated with lower overall complication rates and fewer 30-day readmissions compared to rigid platforms like TEM, potentially leading to improved short-term postoperative outcomes for patients.⁴⁴

Transanal endoscopic surgery offers several advantages over radical surgery, including lower morbidity and mortality rates, as well as faster recovery.² While some studies comparing TEM to radical surgery for early-stage CRC have reported comparable outcomes in terms of local recurrence and overall survival (OS),^{45,46} a more recent meta-analysis demonstrated a significantly increased risk of local recurrence following TEM. The analysis reported a risk ratio (RR) of 2.51 with a 95% confidence interval (95% CI) of 1.53–4.21, indicating a more than twofold increase in recurrence compared to radical surgery. This highlights the importance of careful patient selection to optimize treatment outcomes.⁴⁷ The local recurrence rates for T1 early-stage rectal tumors treated with TES vary widely across studies, ranging from 2.4% to 26%.⁴⁸ This variability may be attributed to the substantial risk of occult lymph node metastasis in T1 tumors, particularly when unfavorable histopathological features are present. For instance, a study by O'Neill et al. reported a 3-year local recurrence rate of 2.4% for T1 rectal tumors treated with TEM,⁴⁹ while Stipa et al. found a higher rate of 11.6%.⁵⁰ Additionally, a meta-analysis by Dekkers et al. reported an overall pooled recurrence incidence of 9.1% for T1 CRC treated with local resection techniques, including TEM.⁵¹ These variations highlight the importance of patient selection and the need for careful postoperative surveillance to detect and manage recurrences early.

T1 tumors larger than 4 cm, involving more than 30% of the bowel circumference, and exhibiting high-risk histological features are associated with an increased risk of local recurrence following local excision. In these cases, the TES approach should be avoided.^{52–56} For T2 or more advanced lesions, TME, with or without neoadjuvant therapy, is the standard treatment.

Importantly, studies have not shown any long-term complications related to continence or anorectal function resulting from the transanal placement of ports in TES, further supporting its safety profile in both oncologic and benign applications.^{57–59}

Natural orifice transluminal endoscopic surgery

Natural orifice transluminal endoscopic surgery (NOTES) is a minimally invasive approach that accesses the abdominal cavity via natural orifices. Initially performed on humans in 2008, NOTES introduced the potential for “scarless surgery”.⁶⁰ This technique involves the controlled puncture of an organ (e.g., stomach, rectum, vagina, etc.) with an endoscope to gain access to the abdominal cavity.^{61,62}

This technique has been explored for a variety of procedures, including cholecystectomy, appendectomy and peritoneoscopy. Various access routes have been tested, such as transgastric, transvaginal, transvesical, and transcolonic approaches.^{61,63} The primary advantages of NOTES include reduced postoperative pain, faster recovery, fewer wound infections, and improved cosmetic outcomes due to the absence of external scars.^{63,64}

Despite its promising potential, NOTES remains an experimental technique with several challenges. These include the risk of infection, the need for reliable closure of viscerotomy sites and the development of specialized instruments tailored to the procedure.^{62,63} Society of American Gastrointestinal and Endoscopic Surgeons (SAGES) and American Society for Gastrointestinal Endoscopy (ASGE) have highlighted critical goals and obstacles that must be addressed before NOTES can be widely adopted in clinical practice.⁶²

While NOTES represents an exciting advancement in minimally invasive surgery, further research and technological development are essential to ensure its safety and efficacy before it becomes standard practice in clinical settings.

Transanal natural orifice specimen extraction

Transanal natural orifice specimen extraction (*ta*-NOSE) combines the benefits of laparoscopic techniques with the natural orifice approach for specimen removal. The method enables for the complete resection of the colon or rectum laparoscopically, followed by the extraction of the resected specimen via a natural orifice, usually the anus, without the need for a traditional mini-laparotomy. This eliminates some of the risks associated with conventional open surgery, such as larger incisions and subsequent complications like infections, hernias, postoperative pain, and prolonged recovery. At first, transvaginal and *ta*-NOSE were used for benign diseases,^{65–69} but over time, both techniques were explored for CRC treatment.^{70–73}

Cheung et al. conducted the first trial of laparoscopic colectomy with *ta*-NOSE in 2009.⁷⁰ The study involved 10 patients with left-sided CRC (4 cm or less in size) who underwent laparoscopic resection followed by transanal

specimen retrieval using the TEO device setup. The authors showed that the technique is feasible for carefully selected patients with left-sided CRC.

The largest cohort study on NOSE for CRC was conducted by Franklin et al., who usually employed transanal specimen extraction during laparoscopic anterior resection (LAR).⁷³ In their prospective study involving 179 patients, they reported successfully performing laparoscopic TME, followed by transanal specimen retrieval using specialized instruments. The study found a low overall complication rate (5.0%), with an anastomotic leak rate of 1.7% and rectal stenosis occurring in 2.0% of cases.

Additionally, several studies have shown that *ta*-NOSE is both feasible and safe. For instance, Ng et al. demonstrated that *ta*-NOSE, when combined with LAR for sigmoid and CRC, resulted in lower operative blood loss and shorter LOS compared to conventional LAR.⁷⁴ Similarly, Xu et al. found that laparoscopic-assisted NOSE colectomy for left-sided CRC resulted in lower postoperative pain and faster recovery of gastrointestinal function compared to conventional laparoscopic colectomy.⁷⁵ The technique consists of standard laparoscopic dissection and vascular control, followed by specimen extraction through the rectum using specialized instruments designed to protect the rectal and anal tissues.

Studies have shown that, in addition to benefits such as reduced postoperative pain, shorter LOS, and improved cosmetic outcomes, *ta*-NOSE maintains oncological safety by ensuring adequate lymph node retrieval and clear resection margins.^{76,77}

Transanal total mesorectal excision

For patients with rectal cancer who are not eligible for local surgery, transabdominal resection is recommended. Total mesorectal excision is a cornerstone in the surgical treatment of CRC,⁷⁸ aiming to achieve complete removal of the mesorectum, which contains lymph nodes and potential sites of tumor spread, while preserving key anatomical structures.⁷⁹ In 1982, Prof. Richard Heald revolutionized CRC surgery by identifying that cancer primarily spreads through lymphatic and venous pathways rather than distally along the rectum. He emphasized the importance of the “holy plane”, an avascular space between the mesorectum and its surrounding structures, as the key to precise dissection.⁸⁰ Heald’s concept demonstrated that incomplete resection within this “danger zone” could explain high local recurrence rates, making proper TME within this plane a critical factor in reducing recurrence and improving outcomes. Initially performed as an open procedure, TME quickly became the standard of care in rectal cancer treatment.^{81,82}

The introduction of laparoscopic total mesorectal excision (LaTME) brought the benefits of minimally invasive surgery, such as reduced postoperative pain and shorter LOS. However, concerns emerged regarding its

oncological safety. The COLOR II trial⁸³ demonstrated that LaTME offered similar oncological outcomes to open surgery while enhancing recovery. Despite these benefits, LaTME presented significant challenges, including a 17% conversion rate to open surgery, particularly in anatomically difficult cases such as patients with a narrow pelvis.^{83,84} To address these limitations, robotic TME (RoTME) was introduced, offering improved dexterity, enhanced 3D visualization and better ergonomics. While studies like the ROLARR trial showed similar oncological outcomes between robotic and laparoscopic approaches, robotic surgery has been linked to increased costs and longer procedure times.⁸⁵

To tackle the challenges of achieving optimal distal mesorectal dissection, taTME was developed. By initiating dissection from the anus, surgeons could achieve better visualization and precision when accessing the distal rectum. In the late 2000s, experimental work by Mark Whiteford, Patricia Sylla, et al. demonstrated the feasibility of NOTES transanal rectosigmoid resection in swine and cadaveric models, laying the groundwork for clinical application.^{86,87} The first clinical description of taTME was published in 2010, marking a significant advancement in minimally invasive colorectal surgery.¹⁴ Transanal TME employs a “bottom-up” approach, combining the principles of precise oncological resection, minimally invasive techniques and enhanced visualization.⁸⁸ This comprehensive technique integrates key advancements from the last 3 decades of rectal cancer surgery.

Transanal TME offers several potential advantages for mid and low rectal cancers, particularly in anatomically challenging cases such as those involving obesity, a narrow pelvis or previous pelvic irradiation. By combining transanal and abdominal approaches, the technique enhances visualization, facilitates precision in dissecting the mesorectal plane and ensures improved specimen quality.⁸⁹ Early studies reported promising results, with low occurrences of positive circumferential resection margins and improved oncological radicality.⁹⁰ Registry data have further informed the discussion around taTME. The International taTME registry compiled data from 720 cases and reported high rates of intact TME specimens (85%), low positive margin rates (2.7%) and low rates of anastomotic leakage (5.5%) when performed by experienced surgeons.⁹¹ However, concerns over the complexity of the technique and the need for structured training programs have tempered its adoption. Following an initial wave of enthusiasm supported by promising outcomes from expert centers,⁹² data from national studies in Norway⁹³ and the Netherlands⁹⁴ raised concerns about the procedure's safety. These studies revealed significantly higher local recurrence rates for taTME compared to the laparoscopic approach, prompting questions about its risks. The Norwegian moratorium, released in 2019, reported an initial recurrence rate of 9.5% following a median follow-up period of 11 months.⁹⁵ A nationwide audit in Norway

raised concerns about the long-term oncological results of taTME, reporting a local recurrence rate of 11.6% after 2 years in 157 patients who had undergone the procedure. This contrasted with a recurrence rate of 2.4% in a cohort from the Norwegian CRC Registry.⁹³

To further support the oncologic safety of taTME, Roodbeen et al. published findings from the International taTME Registry.⁹⁶ Among 2,803 patients undergoing primary taTME, the 2-year local recurrence rate was 4.8%. The 2-year DFS and OS rates were 77% and 92%, respectively. Additionally, taTME has shown functional outcomes and quality of life similar to those achieved with LaTME.^{97,98} Despite these promising findings, the broad implementation of taTME has been hindered by a demanding learning curve^{99,100} and concerns over oncological and functional outcomes.^{101–104} Studies suggest that a center must perform at least 20–30 cases to achieve proficiency, underscoring the need for structured training programs such as cadaveric workshops and proctorships.¹⁰⁵ It is widely agreed that taTME should only be performed by well-trained colorectal surgeons in high-volume centers to minimize complications and ensure oncological adequacy.⁹⁰

In summary, taTME marks a major progress in rectal cancer surgery, providing enhanced visualization and access to the distal rectum. While early results are promising, caution must guide its adoption, with emphasis on rigorous training, adherence to oncological principles and ongoing evaluation of outcomes. Future studies and registry data will continue to refine its role within the spectrum of surgical options for rectal cancer.

Transanal transection and single-stapled anastomosis

The TTSS approach represents the latest and most promising advancement in transanal techniques for the treatment of low rectal cancers. The TTSS technique seeks to integrate the strengths of 2 well-established surgical strategies. From traditional TME, it draws upon the long-established dissection technique, honed over generations, and has been proven to be both safe and effective in both conventional open surgeries and minimally invasive approaches. From taTME, it incorporates the concept of transanal transection (TT) and the single-stapled (SS) anastomosis, though with significant technical variations.¹⁰⁶

The technique, introduced by Spinelli et al. in 2019, was initially tested on a small cohort of patients undergoing low rectal surgery. The complications consisted of 1 grade IIIa and 3 grade I events, as defined by the Clavien–Dindo classification. The proof-of-concept study demonstrated that TTSS is both safe and feasible in all patients.¹⁰⁷

In contrast to taTME, the TTSS technique involves placing the transanal purse string only after the full peri-mesorectal dissection is completed, performed from

above through either a conventional or less invasive abdominal approach. After fully mobilizing the lower rectum and mesorectum from the pelvic floor muscles, a full-thickness, circumferential rectotomy is performed using electrocautery.

In TTSS, the rectal cuff below the transection site is fully detached from the pelvic floor before sectioning. This enables the surgeon to place the lower purse string for the anastomosis without the need for further complex or risky maneuvers to mobilize it. Following the transection, a single-stapled anastomosis is created to connect the remaining rectal stump with the proximal bowel (colon or ileum). The single-stapled method eliminates some of the complications associated with double-stapled anastomosis, such as uneven cuff lengths and potential weak points.

Clinical studies have demonstrated that TTSS is linked to reduced rates of anastomotic leakage (AL) and improved functional outcomes compared to double-stapled (DS) techniques.^{106,108}

In the study by Spinelli et al.,¹⁰⁶ both SS techniques – taTME and TTSS – resulted in considerably lower AL rates than the DS technique. The reintervention rate was also reduced in the TTSS group compared to DS, with a significant difference observed (2% vs 12%). These findings suggest that the TTSS approach offers greater safety regarding AL, with fewer patients needing re-intervention for leaks. While overall 30-day complication rates were similar across all 3 techniques (DS, taTME and TTSS), the TTSS group had significantly fewer complications at 90 days compared to the DS group. Additionally, the operative time was notably longer in the taTME group when compared to both TTSS and DS.

Similarly, Harji et al. noted a considerable decrease in AL rates with TTSS in CRC surgery compared to the DS technique.¹⁰⁹ Interestingly, no significant difference was found in the low anterior resection syndrome (LARS) scores between patients who underwent TTSS and those who received the DS technique ($p = 0.228$).

The taTME technique is recognized for being linked to longer operative times and higher procedural costs, primarily due to the requirement for specialized transanal equipment. These factors contribute to taTME being a more expensive surgical option overall. On the other hand, the TTSS is more cost-efficient, utilizing only a single circular stapler (of any available type) in conjunction with basic, low-cost instruments. As a result, TTSS represents a more affordable alternative to taTME, particularly in resource-limited settings, while still preserving the benefits of transanal surgery.

Although the precise number of cases needed to master TTSS remains unclear, initial results suggest that TTSS may be less complex than taTME, potentially requiring fewer cases to achieve comparable outcomes.¹⁰⁷ However, larger, comparative, and multicenter studies are necessary to confirm and further support these results.

Limitations

First, the inclusion of heterogeneous studies, differing in research scope, study design, participant demographics, and contexts, introduces variability that may affect the generalizability of the findings. Additionally, no date limit was applied, and studies published up until January 2025 were included, which may result in the inclusion of studies with varying levels of methodological rigor and relevance to current practices. Although the study aimed to cover a broad range of research, the inclusion criteria were limited to original studies written in English, which could exclude relevant data published in other languages.

Conclusions

Over the past few decades, transanal surgical techniques for rectal cancer have evolved significantly. The progression from TAE to more advanced methods, such as TEM, TEO, and later TAMIS, has resulted in notable advancements in treatment options for patients with early-stage rectal cancer. These techniques offer greater precision, less invasive surgery and improved functional outcomes. More recent approaches, such as taTME and TTSS, are particularly effective for low rectal tumors that are not suitable for local excision. These newer methods enhance precision in mesorectal plane dissection, ensure better specimen quality and show promising oncological results.


In conclusion, appropriate patient selection is crucial for achieving optimal outcomes. Surgeons must be well-informed about the various available treatment options. Furthermore, as these techniques continue to evolve, further research and larger studies are needed to refine patient selection and validate long-term outcomes.


Use of AI and AI-assisted technology

Not applicable.

ORCID iDs

Sara Lauricella  <https://orcid.org/0000-0002-3295-6264>

Francesco Brucchi  <https://orcid.org/0000-0003-3191-4369>

Roberto Cirotchi  <https://orcid.org/0000-0002-2457-0636>

References

- Eng C, Jácome AA, Agarwal R, et al. A comprehensive framework for early-onset colorectal cancer research. *Lancet Oncol*. 2022;23(3): e116–e128. doi:10.1016/S1470-2045(21)00588-X
- Benson AB, Venook AP, Al-Hawary MM, et al. Rectal Cancer, Version 2.2018, NCCN Clinical Practice Guidelines in Oncology. *J Natl Compr Canc Netw*. 2018;16(7):874–901. doi:10.6004/jnccn.2018.0061
- Alrahawy M, Aker M, Issa M, et al. Textural analysis as a predictive biomarker in rectal cancer. *Cureus*. 2022;14(2):e32241. doi:10.7759/cureus.32241
- Park S, Min Y, Shin J, et al. Endoscopic submucosal dissection or transanal endoscopic microsurgery for nonpolypoid rectal high grade dysplasia and submucosa-invasive rectal cancer. *Endoscopy*. 2012;44(11): 1031–1036. doi:10.1055/s-0032-1310015

5. García-Flórez LJ. Local excision by transanal endoscopic surgery. *World J Gastroenterol*. 2015;21(31):9286. doi:10.3748/wjg.v21.i31.9286
6. Saclarides TJ, Smith L, Ko ST, Orkin B, Buess G. Transanal endoscopic microsurgery. *Dis Colon Rectum*. 1992;35(12):1183–1191. doi:10.1007/BF02251975
7. Allaix ME, Arezzo A, Caldart M, Festa F, Morino M. Transanal endoscopic microsurgery for rectal neoplasms: Experience of 300 consecutive cases. *Dis Colon Rectum*. 2009;52(11):1831–1836. doi:10.1007/DCR.0b013e3181b14d2d
8. Neary P, Makin GB, White TJ, et al. Transanal endoscopic microsurgery: A viable operative alternative in selected patients with rectal lesions. *Ann Surg Oncol*. 2003;10(9):1106–1111. doi:10.1245/ASO.2003.01.441
9. Bach SP, Hill J, Monson JRT, et al. A predictive model for local recurrence after transanal endoscopic microsurgery for rectal cancer. *Br J Surg*. 2009;96(3):280–290. doi:10.1002/bjs.6456
10. Emile SH, Lacy FBD, Keller DS, et al. Evolution of transanal total mesorectal excision for rectal cancer: From top to bottom. *World J Gastrointest Surg*. 2018;10(3):28–39. doi:10.4240/wjgs.v10.i3.28
11. Kalloo AN, Singh VK, Jagannath SB, et al. Flexible transgastric peritoneoscopy: A novel approach to diagnostic and therapeutic interventions in the peritoneal cavity. *Gastrointest Endosc*. 2004;60(1):114–117. doi:10.1016/S0016-5107(04)01309-4
12. Autorino R, Yakoubi R, White WM, et al. Natural orifice transluminal endoscopic surgery (NOTES): Where are we going? A bibliometric assessment. *BJU Int*. 2013;111(1):11–16. doi:10.1111/j.1464-410X.2012.11494.x
13. Marks JH, Myers EA, Zeger EL, Denittis AS, Gummadi M, Marks GJ. Long-term outcomes by a transanal approach to total mesorectal excision for rectal cancer. *Surg Endosc*. 2017;31(12):5248–5257. doi:10.1007/s00464-017-5597-7
14. Sylla P, Rattner DW, Delgado S, Lacy AM. NOTES transanal rectal cancer resection using transanal endoscopic microsurgery and laparoscopic assistance. *Surg Endosc*. 2010;24(5):1205–1210. doi:10.1007/s00464-010-0965-6
15. Penna M, Buchs NC, Bloemendaal AL, Hompes R. Transanal total mesorectal excision for rectal cancer: The journey towards a new technique and its current status. *Exp Rev Anticancer Ther*. 2016;16(11):1145–1153. doi:10.1080/14737140.2016.1240040
16. Parks AG, Stuart AE. The management of villous tumours of the large bowel. *J Br Surg*. 1973;60(9):688–695. doi:10.1002/bjs.1800600908
17. Baxter NN, García-Aguilar J. Organ preservation for rectal cancer. *J Clin Oncol*. 2007;25(8):1014–1020. doi:10.1200/JCO.2006.09.7840
18. You YN, Hardiman KM, Bafford A, et al. The American Society of Colon and Rectal Surgeons Clinical Practice Guidelines for the Management of Rectal Cancer. *Dis Colon Rectum*. 2020;63(9):1191–1222. doi:10.1097/DCR.0000000000001762
19. Russo S, Anker CJ, Abdel-Wahab M, et al. Executive Summary of the American Radium Society Appropriate Use Criteria for Local Excision in Rectal Cancer. *Int J Radiat Oncol Biol Phys*. 2019;105(5):977–993. doi:10.1016/j.ijrobp.2019.08.020
20. Paty PB, Nash GM, Baron P, et al. Long-term results of local excision for rectal cancer. *Ann Surg*. 2002;236(4):522–530. doi:10.1097/00000658-200210000-00015
21. García-Aguilar J, Mellgren A, Sirivongs P, Buie D, Madoff RD, Rothenberger DA. Local excision of rectal cancer without adjuvant therapy: A word of caution. *Ann Surg*. 2000;231(3):345–351. doi:10.1097/00000658-200003000-00007
22. Endreseth BH, Myrvold HE, Romundstad P, Hestvik UE, Bjerkeset T, Wibe A. Transanal excision vs major surgery for T1 rectal cancer. *Dis Colon Rectum*. 2005;48(7):1380–1388. doi:10.1007/s10350-005-0044-6
23. Nair RM, Siegel EM, Chen DT, et al. Long-term results of transanal excision after neoadjuvant chemoradiation for T2 and T3 adenocarcinomas of the rectum. *J Gastrointest Surg*. 2008;12(10):1797–1806. doi:10.1007/s11605-008-0647-z
24. Stamos MJ, Murrell Z. Management of early rectal T1 and T2 cancers. *Clin Cancer Res*. 2007;13(22):6885s–6889s. doi:10.1158/1078-0432.CCR-07-1150
25. Arolfo S, Allaix ME, Migliore M, Cravero F, Arezzo A, Morino M. Transanal endoscopic microsurgery after endoscopic resection of malignant rectal polyps: A useful technique for indication to radical treatment. *Surg Endosc*. 2014;28(4):1136–1140. doi:10.1007/s00464-013-3290-z
26. Albert MR, Atallah SB, deBeche-Adams TC, Izfar S, Larach SW. Transanal minimally invasive surgery (TAMIS) for local excision of benign neoplasms and early-stage rectal cancer: Efficacy and outcomes in the first 50 patients. *Dis Colon Rectum*. 2013;56(3):301–307. doi:10.1097/DCR.0b013e31827ca313
27. Kanehira E, Tanida T, Kamei A, Nakagi M, Iwasaki M, Shimizu H. Transanal endoscopic microsurgery for surgical repair of rectovesical fistula following radical prostatectomy. *Surg Endosc*. 2015;29(4):851–855. doi:10.1007/s00464-014-3737-x
28. Tielen R, Bremers AJA, Graaf WTAVD, Flucke UE, Wilt JHWD. Transanal endoscopic microsurgery following treatment with imatinib: A case report of a patient with a rectal gastrointestinal stromal tumor. *Acta Chir Belg*. 2015;115(2):166–169. doi:10.1080/00015458.2015.11681089
29. Duek SD, Gilshtein H, Khoury W. Transanal endoscopic microsurgery: Also for the treatment of retrorectal tumors. *Minim Invasive Ther Allied Technol*. 2014;23(1):28–31. doi:10.3109/13645706.2013.872663
30. Serra-Aracil X, Mora-Lopez L, Alcantara-Moral M, Corredra-Cantarín C, Gomez-Diaz C, Navarro-Soto S. Atypical indications for transanal endoscopic microsurgery to avoid major surgery. *Tech Coloproctol*. 2014;18(2):157–164. doi:10.1007/s10151-013-1040-9
31. Buess G, Theiss R, Hutterer F, et al. Transanal endoscopic surgery of the rectum: Testing a new method in animal experiments [in German]. *Leber Magen Darm*. 1983;13(2):73–77. PMID:6621245.
32. De Graaf EJR, Doornebosch PG, Stassen LPS, Debets JMH, Tetteroo GWM, Hop WCJ. Transanal endoscopic microsurgery for rectal cancer. *Eur J Cancer*. 2002;38(7):904–910. doi:10.1016/S0959-8049(02)00050-3
33. Christoforidis D, Cho HM, Dixon MR, Mellgren AF, Madoff RD, Finne CO. Transanal endoscopic microsurgery versus conventional transanal excision for patients with early rectal cancer. *Ann Surg*. 2009;249(5):776–782. doi:10.1097/SLA.0b013e3181a3e54b
34. Sgourakis G, Lanitis S, Gockel I, et al. Transanal endoscopic microsurgery for T1 and T2 rectal cancers: A meta-analysis and meta-regression analysis of outcomes. *Am Surg*. 2011;77(6):761–772. PMID:21679648.
35. Clancy C, Burke JP, Albert MR, O'Connell PR, Winter DC. Transanal endoscopic microsurgery versus standard transanal excision for the removal of rectal neoplasms: A systematic review and meta-analysis. *Dis Colon Rectum*. 2015;58(2):254–261. doi:10.1097/DCR.00000000000000309
36. Nieuwenhuis DH, Draaisma WA, Verberne GHM, Van Overbeeke AJ, Consten ECJ. Transanal endoscopic operation for rectal lesions using two-dimensional visualization and standard endoscopic instruments: A prospective cohort study and comparison with the literature. *Surg Endosc*. 2009;23(1):80–86. doi:10.1007/s00464-008-9918-8
37. Kim MJ, Park JW, Ha HK, et al. Initial experience of transanal total mesorectal excision with rigid or flexible transanal platforms in cadavers. *Surg Endosc*. 2016;30(4):1640–1647. doi:10.1007/s00464-015-4398-0
38. Atallah S, Albert M, Larach S. Transanal minimally invasive surgery: A giant leap forward. *Surg Endosc*. 2010;24(9):2200–2205. doi:10.1007/s00464-010-0927-z
39. Stipa F, Tierno SM, Russo G, Burza A. Trans-anal minimally invasive surgery (TAMIS) versus trans-anal endoscopic microsurgery (TEM): A comparative case-control matched-pairs analysis. *Surg Endosc*. 2022;36(3):2081–2086. doi:10.1007/s00464-021-08494-y
40. Maglio R, Muzi GM, Massimo MM, Masoni L. Transanal minimally invasive surgery (TAMIS): New treatment for early rectal cancer and large rectal polyps. Experience of an Italian center. *Am Surg*. 2015;81(3):273–277. PMID:25760203.
41. McLemore EC, Coker A, Jacobsen G, Talamini MA, Horgan S. eTAMIS: Endoscopic visualization for transanal minimally invasive surgery. *Surg Endosc*. 2013;27(5):1842–1845. doi:10.1007/s00464-012-2652-2
42. Rimonda R, Arezzo A, Arolfo S, Salvai A, Morino M. TransAnal Minimally Invasive Surgery (TAMIS) with SILS™ Port versus Transanal Endoscopic Microsurgery (TEM): A comparative experimental study. *Surg Endosc*. 2013;27(10):3762–3768. doi:10.1007/s00464-013-2962-z
43. deBeche-Adams T, Nassif G. Transanal minimally invasive surgery. *Clin Colon Rectal Surg*. 2015;28(3):176–180. doi:10.1055/s-0035-1555008
44. Garoufalia Z, Rogers P, Meknarit S, et al. Trans-anal minimally invasive surgery (TAMIS) versus rigid platforms for local excision of early rectal cancer: A systematic review and meta-analysis of the literature. *Surg Endosc*. 2024;38(8):4198–4206. doi:10.1007/s00464-024-11065-6

45. Hershman MJ, Mohammad H, Hussain A, Ahmed A. Local excision of rectal tumours by minimally invasive transanal surgery. *Br J Hosp Med*. 2013;74(7):387–390. doi:10.12968/hmed.2013.74.7.387
46. Sajid MS, Farag S, Leung P, Sains P, Miles WFA, Baig MK. Systematic review and meta-analysis of published trials comparing the effectiveness of transanal endoscopic microsurgery and radical resection in the management of early rectal cancer. *Colorectal Dis*. 2014;16(1):2–14. doi:10.1111/codi.12474
47. Li W, Xiang XX, Da Wang H, Cai CJ, Cao YH, Liu T. Transanal endoscopic microsurgery versus radical resection for early-stage rectal cancer: A systematic review and meta-analysis. *Int J Colorectal Dis*. 2023;38(1):49. doi:10.1007/s00384-023-04341-9
48. Whitehouse PA, Armitage JN, Tilney HS, Simson JNL. Transanal endoscopic microsurgery: Local recurrence rate following resection of rectal cancer. *Colorectal Dis*. 2008;10(2):187–193. doi:10.1111/j.1463-1318.2007.01291.x
49. O'Neill CH, Platz J, Moore JS, Callas PW, Cataldo PA. Transanal endoscopic microsurgery for early rectal cancer: A single-center experience. *Dis Colon Rectum*. 2017;60(2):152–160. doi:10.1097/DCR.0000000000000764
50. Stipa F, Giaccaglia V, Burza A. Management and outcome of local recurrence following transanal endoscopic microsurgery for rectal cancer. *Dis Colon Rectum*. 2012;55(3):262–269. doi:10.1097/DCR.0b013e318241ef22
51. Dekkers N, Dang H, Van Der Kraan J, et al. Risk of recurrence after local resection of T1 rectal cancer: A meta-analysis with meta-regression. *Surg Endosc*. 2022;36(12):9156–9168. doi:10.1007/s00464-022-09396-3
52. Heidary B, Phang TP, Raval MJ, Brown CJ. Transanal endoscopic microsurgery: A review. *Can J Surg*. 2014;57(2):127–138. doi:10.1503/cjs.022412
53. Morino M, Arezzo A, Allaix ME. Transanal endoscopic microsurgery. *Tech Coloproctol*. 2013;17(Suppl 1):55–61. doi:10.1007/s10151-012-0936-0
54. Serra-Aracil X, Mora-Lopez L, Alcantara-Moral M, Caro-Tarrago A, Gomez-Diaz CJ, Navarro-Soto S. Transanal endoscopic surgery in rectal cancer. *World J Gastroenterol*. 2014;20(33):11538–11545. doi:10.3748/wjg.v20.i33.11538
55. You YN. Local excision: Is it an adequate substitute for radical resection in T1/T2 patients? *Semin Radiat Oncol*. 2011;21(3):178–184. doi:10.1016/j.semradonc.2011.02.003
56. Guerrieri M, Gesuita R, Ghiselli R, Lezoche G, Budassi A, Baldarelli M. Treatment of rectal cancer by transanal endoscopic microsurgery: Experience with 425 patients. *World J Gastroenterol*. 2014;20(28):9556–9563. doi:10.3748/wjg.v20.i28.9556
57. Allaix ME, Rebecchi F, Giaccone C, Mistrangelo M, Morino M. Long-term functional results and quality of life after transanal endoscopic microsurgery. *Br J Surg*. 2011;98(11):1635–1643. doi:10.1002/bjs.7584
58. Kreis ME, Jehle EC, Ohlemann M, Becker HD, Starlinger MJ. Functional results after transanal rectal advancement flap repair of transphincteric fistula. *J Br Surg*. 1998;85(2):240–242. doi:10.1046/j.1365-2168.1998.00557.x
59. Kennedy ML, Lubowski DZ, King DW. Transanal endoscopic microsurgery excision: Is anorectal function compromised? *Dis Colon Rectum*. 2002;45(5):601–604. doi:10.1007/s10350-004-6252-7
60. Rao GV, Reddy DN, Banerjee R. NOTES: Human experience. *Gastroenterol Endosc Clin North Am*. 2008;18(2):361–370. doi:10.1016/j.giec.2008.01.007
61. Pearl JP, Ponsky JL. Natural orifice transluminal endoscopic surgery: A critical review. *J Gastrointest Surg*. 2008;12(7):1293–1300. doi:10.1007/s11605-007-0424-4
62. Whang SH. Natural orifice transluminal endoscopic surgery: Where are we going? *World J Gastroenterol*. 2010;16(35):4371. doi:10.3748/wjg.v16.i35.4371
63. Fuchs KH, Meining A, Von Renteln D, et al. Euro-NOTES Status Paper: From the concept to clinical practice. *Surg Endosc*. 2013;27(5):1456–1467. doi:10.1007/s00464-013-2870-2
64. Huang C. Natural orifice transluminal endoscopic surgery: New minimally invasive surgery come of age. *World J Gastroenterol*. 2011;17(39):4382. doi:10.3748/wjg.v17.i39.4382
65. Lacy AM, Delgado S, Rojas OA, Almenara R, Blasi A, Llach J. MA-NOS radical sigmoidectomy: Report of a transvaginal resection in the human. *Surg Endosc*. 2008;22(7):1717–1723. doi:10.1007/s00464-008-9956-2
66. Awad ZT, Qureshi I, Seibel B, Sharma S, Dobbettien MA. Laparoscopic right hemicolectomy with transvaginal colon extraction using a laparoscopic posterior colpotomy: A 2-year series from a single institution. *Surg Laparosc Endosc Percutan Tech*. 2011;21(6):403–408. doi:10.1097/SLE.0b013e31823945ac
67. Fuchs KH, Breithaupt W, Varga G, Schulz T, Reinisch A, Josipovic N. Transanal hybrid colon resection: From laparoscopy to NOTES. *Surg Endosc*. 2013;27(3):746–752. doi:10.1007/s00464-012-2534-7
68. Franklin ME, Liang S, Russek K. Natural orifice specimen extraction in laparoscopic colorectal surgery: Transanal and transvaginal approaches. *Tech Coloproctol*. 2013;17(Suppl 1):63–67. doi:10.1007/s10151-012-0938-y
69. Torres RA, Orban RD, Tocaimaza L, Vallejos Pereira G, Arévalo JR. Transvaginal specimen extraction after laparoscopic colectomy. *World J Surg*. 2012;36(7):1699–1702. doi:10.1007/s00268-012-1528-x
70. Cheung HYS, Leung ALH, Chung CC, Ng DCK, Li MKW. Endo-laparoscopic colectomy without mini-laparotomy for left-sided colonic tumors. *World J Surg*. 2009;33(6):1287–1291. doi:10.1007/s00268-009-0006-6
71. Park JS, Choi GS, Kim HJ, Park SY, Jun SH. Natural orifice specimen extraction versus conventional laparoscopically assisted right hemicolectomy. *Br J Surg*. 2011;98(5):710–715. doi:10.1002/bjs.7419
72. Leung ALH, Cheung HYS, Fok BKL, Chung CCC, Li MKW, Tang CN. Prospective randomized trial of hybrid NOTES colectomy versus conventional laparoscopic colectomy for left-sided colonic tumors. *World J Surg*. 2013;37(11):2678–2682. doi:10.1007/s00268-013-2163-x
73. Franklin ME, Liang S, Russek K. Integration of transanal specimen extraction into laparoscopic anterior resection with total mesorectal excision for rectal cancer: A consecutive series of 179 patients. *Surg Endosc*. 2013;27(1):127–132. doi:10.1007/s00464-012-2440-z
74. Ng HL, Sun WQ, Zhao XM, et al. Outcomes of trans-anal natural orifice specimen extraction combined with laparoscopic anterior resection for sigmoid and rectal carcinoma: An observational study. *Medicine (Baltimore)*. 2018;97(38):e12347. doi:10.1097/MD.00000000000012347
75. Xu SZ, Ding ZJ, Zhang SF, et al. Clinical outcomes of laparoscopic-assisted natural orifice specimen extraction colectomy using a Cai tube for left-sided colon cancer: A prospective randomized trial. *Surg Endosc*. 2023;37(1):749–758. doi:10.1007/s00464-022-09435-z
76. Nishimura A, Kawahara M, Suda K, Makino S, Kawachi Y, Nikkuni K. Totally laparoscopic sigmoid colectomy with transanal specimen extraction. *Surg Endosc*. 2011;25(10):3459–3463. doi:10.1007/s00464-011-1716-z
77. Han FH. Transanal natural orifice specimen extraction for laparoscopic anterior resection in rectal cancer. *World J Gastroenterol*. 2013;19(43):7751. doi:10.3748/wjg.v19.i43.7751
78. Heald RJ, Husband EM, Ryall RDH. The mesorectum in rectal cancer surgery: The clue to pelvic recurrence? *J Br Surg*. 1982;69(10):613–616. doi:10.1002/bjs.1800691019
79. Salerno G, Sinnatambay C, Branagan G, Daniels IR, Heald RJ, Moran BJ. Defining the rectum: Surgically, radiologically and anatomically. *Colorectal Dis*. 2006;8(Suppl 3):5–9. doi:10.1111/j.1463-1318.2006.01062.x
80. Heald RJ. The 'Holy Plane' of rectal surgery. *J R Soc Med*. 1988;81(9):503–508. doi:10.1177/014107688808100904
81. Quirke P, Steele R, Monson J, et al. Effect of the plane of surgery achieved on local recurrence in patients with operable rectal cancer: A prospective study using data from the MRC CR07 and NCIC-CTG C016 randomised clinical trial. *Lancet*. 2009;373(9666):821–828. doi:10.1016/S0140-6736(09)60485-2
82. Heald R, Santiago I, Pares O, Carvalho C, Figueiredo N. The perfect total mesorectal excision obviates the need for anything else in the management of most rectal cancers. *Clin Colon Rectal Surg*. 2017;30(5):324–332. doi:10.1055/s-0037-1606109
83. Van Der Pas MH, Haglind E, Cuesta MA, et al. Laparoscopic versus open surgery for rectal cancer (COLOR II): Short-term outcomes of a randomised, phase 3 trial. *Lancet Oncol*. 2013;14(3):210–218. doi:10.1016/S1470-2045(13)70016-0
84. Bonjer HJ, Deijen CL, Abis GA, et al. A randomized trial of laparoscopic versus open surgery for rectal cancer. *N Engl J Med*. 2015;372(14):1324–1332. doi:10.1056/NEJMoa1414882

85. Jayne D, Pigazzi A, Marshall H, et al. Effect of robotic-assisted vs conventional laparoscopic surgery on risk of conversion to open laparotomy among patients undergoing resection for rectal cancer: The ROLARR randomized clinical trial. *JAMA*. 2017;318(16):1569. doi:10.1001/jama.2017.7219
86. Whiteford MH, Denk PM, Swanström LL. Feasibility of radical sigmoid colectomy performed as natural orifice transluminal endoscopic surgery (NOTES) using transanal endoscopic microsurgery. *Surg Endosc*. 2007;21(10):1870–1874. doi:10.1007/s00464-007-9552-x
87. Sylla P, Willingham FF, Sohn DK, Gee D, Brugge WR, Rattner DW. NOTES rectosigmoid resection using transanal endoscopic microsurgery (TEM) with transgastric endoscopic assistance: A pilot study in swine. *J Gastrointest Surg*. 2008;12(10):1717–1723. doi:10.1007/s11605-008-0637-1
88. Atallah S. Transanal total mesorectal excision: Full steam ahead. *Tech Coloproctol*. 2015;19(2):57–61. doi:10.1007/s10151-014-1254-5
89. Deijen CL, Velthuis S, Tsai A, et al. COLOR III: A multicentre randomised clinical trial comparing transanal TME versus laparoscopic TME for mid and low rectal cancer. *Surg Endosc*. 2016;30(8):3210–3215. doi:10.1007/s00464-015-4615-x
90. Lacy AM, Tasende MM, Delgado S, et al. Transanal total mesorectal excision for rectal cancer: Outcomes after 140 patients. *J Am Coll Surg*. 2015;221(2):415–423. doi:10.1016/j.jamcollsurg.2015.03.046
91. Penna M, Hompes R, Arnold S, et al. Transanal total mesorectal excision: International registry results of the first 720 cases. *Ann Surg*. 2017;266(1):111–117. doi:10.1097/SLA.0000000000001948
92. Lacy AM, García-Valdecasas JC, Delgado S, et al. Laparoscopy-assisted colectomy versus open colectomy for treatment of non-metastatic colon cancer: A randomised trial. *Lancet*. 2002;359(9325):2224–2229. doi:10.1016/S0140-6736(02)09290-5
93. Wasmuth HH, Færden AE, Myklebust TÅ, et al. Transanal total mesorectal excision for rectal cancer has been suspended in Norway. *J Br Surg*. 2020;107(1):121–130. doi:10.1002/bjs.11459
94. Oostendorp SE, Belgers HJ, Bootsma BT, et al. Locoregional recurrences after transanal total mesorectal excision of rectal cancer during implementation. *Br J Surg*. 2020;107(9):1211–1220. doi:10.1002/bjs.11525
95. Larsen SG, Pfeffer F, Kørner H. Norwegian moratorium on transanal total mesorectal excision. *Br J Surg*. 2019;106(9):1120–1121. doi:10.1002/bjs.11287
96. Roodbeen SX, Penna M, Van Dieren S, et al. Local recurrence and disease-free survival after transanal total mesorectal excision: Results from the international TaTME registry. *J Natl Compr Canc Netw*. 2021;19(11):1232–1240. doi:10.6004/jnccn.2021.7012
97. Lauricella S, Brucchi F, Carrano FM, Cassini D, Cirocchi R, Sylla P. Quality of life and functional outcomes after laparoscopic total mesorectal excision (LaTME) and transanal total mesorectal excision (taTME) for rectal cancer: An updated meta-analysis. *Int J Colorectal Dis*. 2024;39(1):129. doi:10.1007/s00384-024-04703-x
98. Donovan KF, Lee KC, Ricardo A, et al. Functional outcomes after transanal total mesorectal excision (taTME) for rectal cancer: Results from the phase II North American multicenter prospective observational trial. *Ann Surg*. 2024;280(3):363–373. doi:10.1097/SLA.0000000000006374
99. Palter VN, De Montbrun SL. Implementing new surgical technology: A national perspective on case volume requirement for proficiency in transanal total mesorectal excision. *Can J Surg*. 2020;63(1):E21–E26. doi:10.1503/cjs.001119
100. Atallah SB, DuBose AC, Burke JP, et al. Uptake of transanal total mesorectal excision in North America: Initial assessment of a structured training program and the experience of delegate surgeons. *Dis Colon Rectum*. 2017;60(10):1023–1031. doi:10.1097/DCR.0000000000000823
101. Koedam TWA, Van Ramshorst GH, Deijen CL, et al. Transanal total mesorectal excision (TaTME) for rectal cancer: Effects on patient-reported quality of life and functional outcome. *Tech Coloproctol*. 2017;21(1):25–33. doi:10.1007/s10151-016-1570-z
102. Veltcamp Helbach M, Van Oostendorp SE, Koedam TWA, et al. Structured training pathway and proctoring: Multicenter results of the implementation of transanal total mesorectal excision (TaTME) in the Netherlands. *Surg Endosc*. 2020;34(1):192–201. doi:10.1007/s00464-019-06750-w
103. Caycedo-Marulanda A, Patel S, Merchant S, Brown C. Introduction of new techniques and technologies in surgery: Where is transanal total mesorectal excision today? *World J Gastrointest Surg*. 2020;12(5):203–207. doi:10.4240/wjgs.v12.i5.203
104. Bjoern MX, Nielsen S, Perdawood SK. Quality of life after surgery for rectal cancer: A comparison of functional outcomes after transanal and laparoscopic approaches. *J Gastrointest Surg*. 2019;23(8):1623–1630. doi:10.1007/s11605-018-4057-6
105. Francis N, Penna M, Mackenzie H, Carter F, Hompes R. Consensus on structured training curriculum for transanal total mesorectal excision (TaTME). *Surg Endosc*. 2017;31(7):2711–2719. doi:10.1007/s00464-017-5562-5
106. Spinelli A, Foppa C, Carvello M, et al. Transanal transection and single-stapled anastomosis (TTSS): A comparison of anastomotic leak rates with the double-stapled technique and with transanal total mesorectal excision (TaTME) for rectal cancer. *Eur J Surg Oncol*. 2021;47(12):3123–3129. doi:10.1016/j.ejso.2021.08.002
107. Spinelli A, Carvello M, D'Hoore A, Foppa C. Integration of transanal techniques for precise rectal transection and single-stapled anastomosis: A proof of concept study. *Colorectal Dis*. 2019;21(7):841–846. doi:10.1111/codi.14631
108. Foppa C, Carvello M, Maroli A, et al. Single-stapled anastomosis is associated with a lower anastomotic leak rate than double-stapled technique after minimally invasive total mesorectal excision for MRI-defined low rectal cancer. *Surgery*. 2023;173(6):1367–1373. doi:10.1016/j.surg.2023.02.018
109. Harji D, Fernandez B, Boissieras L, Celerier B, Rullier E, Denost Q. IDEAL stage 2a/b prospective cohort study of transanal transection and single-stapled anastomosis for rectal cancer. *Colorectal Dis*. 2023;25(12):2346–2353. doi:10.1111/codi.16789